JAERI-Conf
2002-009

JP0250413

PROCEEDINGS OF FUEL SAFETY RESEARCH SPECIALISTS' MEETING
MARCH 4-5, 2002, TOKAI

August 2002

Fuel Safety Research Laboratory

日本原子力研究所
Japan Atomic Energy Research Institute

本レポートは、日本原子力研究所が不定期に公刊している研究報告書です。
入手の問合わせは、日本原子力研究所研究情報部研究情報課（〒319-1195　茨城県那珂郡東海村）あて、お申し越し下さい。なお、このほかに財団法人原子力弘済会資料センター（〒319-1195　茨城県那珂郡東海村日本原子力研究所内）で複写による実費頒布を行っております。

This report is issued irregularly.
Inquiries about availability of the reports should be addressed to Research Information Division, Department of Intellectual Resources, Japan Atomic Energy Research Institute, Tokai-mura, Naka-gun, Ibaraki-ken 〒319-1195, Japan.

© Japan Atomic Energy Research Institute, 2002
編集兼発行　日本原子力研究所

JAERI－Conf 2002－009

Proceedings of Fuel Safety Research Specialists' Meeting

March 4-5, 2002, Tokai,

Fuel Safety Research Laboratory※

Department of Reactor Safety Research
Nuclear Safety Research Center
Tokai Research Establishment
Japan Atomic Energy Research Institute
Tokai-mura, Naka-gun, Ibaraki-ken

(Received June 5, 2002)

Fuel Safety Research Specialists' Meeting, which was organized by Japan Atomic Energy Research Institute, was held on March 4-5, 2002 at JAERI in Tokai Establishment.

Purposes of the Meeting are to exchange information and views on LWR fuel safety topics among the specialist participants from domestic and foreign organizations, and to discuss the recent and future fuel research activities in JAERI. In the Meeting, presentations were given and discussions were made on general report of fuel safety research activities, fuel behaviors in normal operation and accident conditions, FP release behaviors in severe accident conditions, and JAERI's "Advanced LWR Fuel Performance & Safety Research Program". A poster exhibition was also carried out. The Meeting significantly contributed to planning future program and cooperation in fuel research. This proceeding integrates all the pictures and papers presented in the Meeting.

Keywords: LWR, Fuel, Safety, Fuel Behavior, High Burnup, Normal Operation, RIA, LOCA, Severe Accident, FP Release, Analysis Code

---

※ Hiroshi UETSUKA, Takehiko NAKAMURA, Akihide HIDAKA, Jinchi NAKAMURA, Fumihisa Nagase, Motoe SUZUKI, Hideo SASAJIMA, Tamotsu KUDO, Misao FUJITA, Takashi OTOMO, Makio YOSHINAGA, Kazuyuki KUSAGAYA[1], Masataka TANIMOTO[2], Tooru TAKEDA[3], Sadayuki UCHIKAWA[4], Tooru KANAZAWA[5].

1. Visiting researcher (currently GNF, Ltd.) 2. Visiting researcher (currently Mitsubishi Heavy Industry, Ltd.) 3.-5. Visiting researchers. (Editor: Motoe SUZUKI)

JAERI－Conf 2002－009

燃料安全研究専門家会合報告集

2002年3月4日－5日、東海

日本原子力研究所東海研究所安全性試験研究センター原子炉安全工学部

燃料安全研究室※

(2002年6月5日受理)

2002年3月4、5日に、東海研究所で燃料安全研究専門家会合が原研主催で開催された。この会合の目的は、軽水炉の燃料安全に係る諸課題について、国内外の関係機関から参加した専門家との間で情報交換及び意見交換を行うこと、および、原研における最近の燃料安全研究の成果及び今後の研究計画について討論することである。

会合では、燃料研究の全般的状況、通常運転時および事故時ふるまいの研究、シビアアクシデント時のFP放出ふるまい、および「高度化軽水炉燃料試験計画」についての報告と討論がされた。あわせてポスター展示も行われた。会合は今後の燃料研究の展開にとって、また研究協力を推進する上で非常に有益であった。本報告集は、これらすべての研究報告を取りまとめたものである。

東海研究所：　〒319-1195　茨城県那珂郡東海村白方白根2-4

※上塚寛、中村武彦、日高昭秀、中村仁一、永瀬文久、鈴木元衛、笹島栄夫、工藤　保、藤田　操、大友　隆、吉永真希夫、草ヶ谷和幸[1]、谷本政隆[2]、武田　透[3]、内川貞之[4]、金沢　徹[5]、

1.外来研究員（現GNF）　2.外来研究員（現三菱重工）　3.-5. 外来研究員　（編集：鈴木元衛）

Contents

1. **Session 1: General Report of Activities**
1-1. Outline of Fuel Safety Research at JAERI (H.Uetsuka) ····· 1
1-2. Fuel Research at the OECD Halden Reactor Project (W.Wiesenack) ····· 7
1-3. The CABRI International Programme for RIA Research and Development Studies (J.C.Melis) ····· 16
1-4. Fuel Safety Research Activities in Spain (J.Conde) ····· 26
1-5. IPSN Future Programmes in the Phebus Facility (A.Mailliat) ····· 37

2. **Session 2a: RIA Experimental Research on High Burnup Fuel**
2a-1. NSRR RIA Tests on PWR/BWR and MOX Fuels (T.Nakamura) ····· 71
2a-2. NSRR Test Results under Simulated Power Oscillation Conditions of BWRs (J.Nakamura)····· 84
2a-3. Temperature Effect on BWR Cladding Failure under Mechanically Simulated RIA Conditions (V.Grigoriev) ····· 97
2a-4. Studies on Fracture Behavior and Mechanical Properties of Cladding
Part1: Influence of Radial Hydride on Fracture Behavior of Zry-2 Fuel Cladding Tube (T.Takeda) ····· 107
Part2: Mechanical Properties of Hydrided Cladding in Hoop Direction (Uchikawa) ····· 107
2a-5. Influence of Hydrogen on the Integrity of Zircaloy Cladding under Accidental Conditions (S.Yamanaka) ····· 122

3. **Session 2b: RIA Analytical Code and Modelling**
2b-1. Numerical Simulation of the Expansion-due-to-Compression Test (A.Varias) ····· 142
2b-2. Three Dimensional Analysis of RIA in PWR and BWR with High Burnup Fuel (T.Nakajima) ····· 163
2b-3. RIA Modeling - a Comparison between TRANSURANUS and FREY (C.Hellwig) ·· 182

4. **Session 3: LOCA-related Research on High Burnup Fuel**
3-1. Thermo-mechanical Behaviour of Irradiated Zr-1% Nb Alloys Claddings in LOCA Simulating Conditions (L.Andreeva) ····· 200
3-2. Status of LOCA Research in the High Burnup Cladding Performance Program (M.Billone) ····· 219
3-3. Results from JAERI Research Program on High Burnup Fuel Behavior under LOCA Conditions (F.Nagase) ····· 234

5. **Session 4: FP Release from Fuel under Severe Accident**
4-1. Overview of VEGA Program on Radio-nuclide Release from Fuel under Severe Accident Conditions and Effect of Pressure on Release Behavior (A.Hidaka) ····· 247
4-2. Effect of Temperature and Atmosphere on Release of Nuclides Including Short-life FPs –Results of Recent VEGA-3 through -5 Tests – (T.Kudo) ····· 263
4-3. FP Releases from CANDU Fuel at 1650℃: the HCE4 Experiment (R.Dickson) ····· 273

4-4. Fission-product Release and Transport Analysis in Severe Accident Conditions: Strategy and Illustrations (M.Kissane) ····· 285
4-5. Overview of Fission Product Behaviour in the Phebus FP Tests, Including Latest Experimental Results on the FPT2 Tests (M.Zabiego) ····· 295
4-6. Analysis of Phebus FPT1 Samples Carried out at ITU, Karlsruhe (P.D.W.Bottomley) ····· 316

6. **Session 5a: Fuel Behavior under Normal Operation Condition**
5a-1. NOK High Burnup Fuel Surveillance Programme (C.Ott) ····· 354
5a-2. BWR-fuel Performance at High-burnup (G.Ledergerber) ····· 364
5a-3. Fuel Irradiation Experiments for an Advanced PWR Fuel Development in the HANARO (YH.Kang) ····· 376
5a-4. Development of PIE Apparatuses and Techniques in RFEF (R.Yasuda) ····· 383

7. **Session 5b: Fuel Behavior Modelling under Normal Operation Condition**
5b-1. Fission Gas Release Modelling at High Burn-up (P.Tempest) ····· 399
5b-2. Development of Fuel Analysis Codes FEMAXI-6 and FURBEL (M.Suzuki) ····· 426
5b-3. UO_2 Fuel Rod Performance Analysis Code, INFRA Development (CB.Lee) ····· 438

8. **Session 6: Discussion on JAERI's Future Program**
Outline of ALPS Program (T.Nakamura, H.Uetsuka, and J.Nakamura) ····· 459

9. **Poster Session**
· NSRR/High Burnup PWR Fuel Test Results (H.Sasajima) ····· 473
· NSRR/High Burnup BWR Fuel Test Results (T.Nakamura) ····· 474
· NSRR/MOX Fuel Test Results (H.Sasajima) ····· 475
· NSRR/Rock-like Oxide Fuel Test Results (K.Kusagaya and T.Nakamura) ····· 476
· NSRR Test Results under Simulated Power Oscillation Conditions of BWRs (J.Nakamura) ····· 477
· Studies on Fracture Behavior and Mechanical Properties of Cladding (T.Takeda and S.Uchikawa) ····· 478
· LOCA-related Studies at JAERI -Overview of the Research Program- (F.Nagase) ····· 479
· LOCA-related Studies at JAERI -Integral Thermal Shock Test- (F.Nagase) ····· 480
· LOCA-related Studies at JAERI -High Temperature Oxidation of Cladding Tube- (F.Nagase) ····· 481
· LOCA-related Studies at JAERI -Mechanical Property of Cladding- (F.Nagase) ····· 482
· Fuel Behavior Study during Normal Operation (J.Nakamura) ····· 483
· Development of Fuel Analysis Code (M.Suzuki) ····· 484
· Verification Experiments of Radio-nuclides Gas/Aerosol Release-1 (A.Hidaka) ····· 485
· Verification Experiments of Radio-nuclides Gas/Aerosol Release-2 (T.Kudo) ····· 486

Appendix 1 Program of FSRSM ····· 487
Appendix 2 List of Participants ····· 489

1. Session 1 : General Report of Activities

Session 1-1

Outline of Fuel Safety Research at JAERI

Hiroshi UETSUKA
JAERI

ABSTRACT

Fuel safety research at Japan Atomic Energy Research Institute is conducted in response to the five years' national program of safety research on nuclear installations which was decided by the Nuclear Safety Commission of Japan. The tendency of LWR fuel use and development, i.e. higher burn-up use of UO2 fuel and the utilization of MOX fuel, is reflected to the national program.

Various types of experimental and analytical researches are being conducted in the Fuel Safety Research Laboratory by using some unique facilities such as the Nuclear Safety Research Reactor (NSRR), the Japan Material Testing Reactor (JMTR), the VEGA apparatus and equipments in hot cells at JAERI. The emphasis of research is on the fuel behavior under accident conditions of which results can be used for the technical basis of future nuclear regulation. The laboratory has following research programs.

1. NSRR/RIA Program
2. LOCA Program
3. JMTR/BOCA Irradiation Program and Code Development
4. VEGA Program

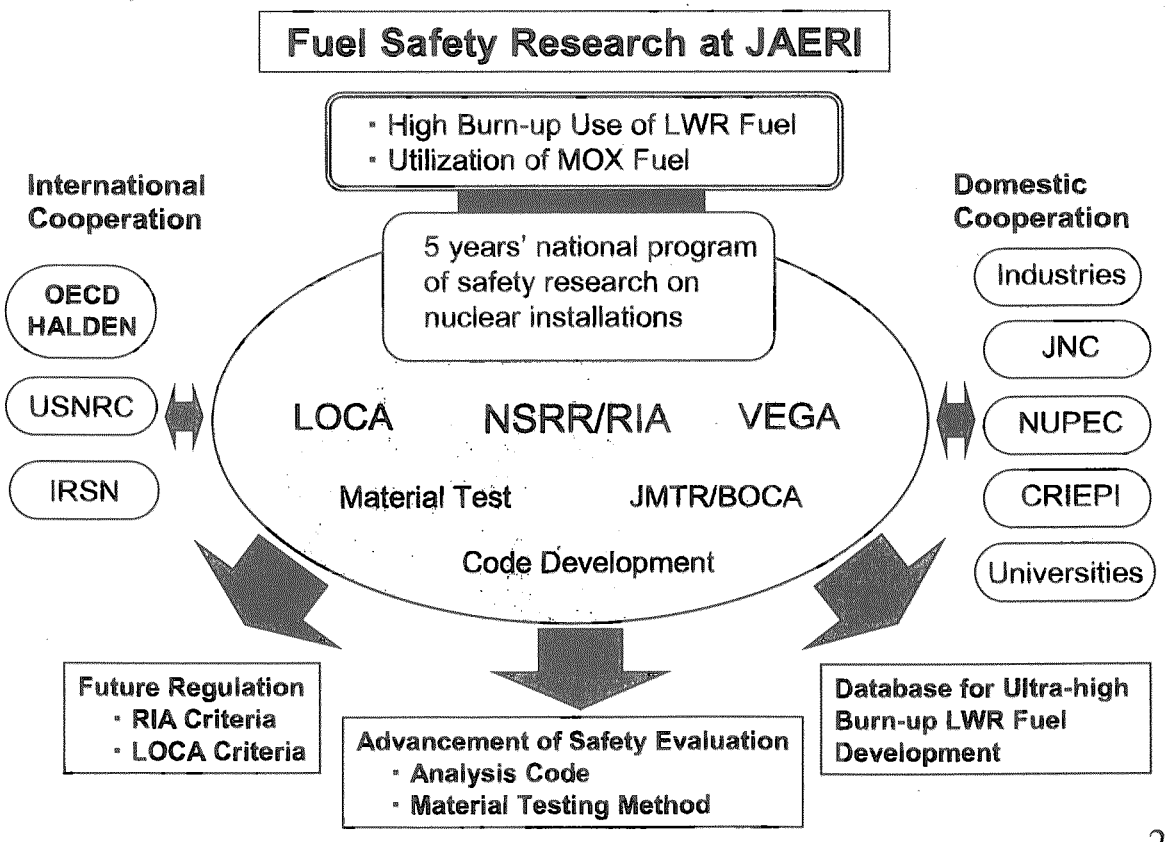
These research programs are supported by both domestic and international cooperation. JAERI has many cooperative research agreements with Japanese industries, JNC, NUPEC, CRIEPI and universities. The cooperation with utilities is especially important to promote the NSRR/RIA experiments on irradiated LWR fuels. International cooperation is also essential for JAERI to proceed the programs efficiently. The wide range technical information and analysis codes from the OECD/Halden program, USNRC and IRSN are helpful for model development and analysis of experiments.

The paper summarizes fuel safety research at JAERI.

Outline of Fuel Safety Research at JAERI

Hiroshi UETSUKA

Fuel Safety Research Laboratory
JAERI



2

Background of Research

- High Burn-up Use of LWR Fuel
  55GWd/t (maximum BU of assembly) in practical use
  next target(～65GWd/t) under development
- Utilization of MOX Fuel
  40-45GWd/t is now ready to start
  higher BU use is intended

★ *understand fuel behavior, fuel rod failure and its consequence during transient,*

★ *provide data base for the development and verification of analytical model,*

★ ***establish technical basis for future regulation***

3

Fuel Safety Research Programs at JAERI

★ **Fuel Behavior under RIA, LOCA Conditions**
- ***NSRR Program,***
- ***LOCA Program,***
- ***Related Mechanical Testing of Cladding***

★ **Fuel Behavior under Normal Operation Condition**
- ***JMTR/BOCA Irradiation,***
- ***Analysis Code Development***
- ***PIE of High Burn-up Fuels***

★ **FP Release and Transport under SA Condition**
- ***VEGA Program***

4

NSRR Program

NSRR Irradiation Experiment

Fuel Behavior under RIA Condition

Samples

- *High Burn-up PWR and PWR Fuels (up to 61GWd/t)*
- *ATR/MOX Fuels (20GWd/t), ROX Fuel, TRIGA Fuel*

Fuel Behavior under BWR Power Oscillation

Samples: *56GWd/t BWR, 26GWd/t JMTR Pre-irradiated*

Separate Effect Tests etc.

- *Tube Burst Test, Modified Ring Tensile Test*
- *Development of Sensor, High Temp.-High Press. Capsule*

Model Development and Verification

Transient Fuel Behavior Analysis

- *FRAPTRAN (supplied by USNRC), FEMAXI-6*

Code Development

- *FEMAXI-based Code*

5

LOCA Program

Experiment

Fracture Threshold of Cladding Tube by Thermal Shock

- *Integral Tests of Rod-burst, Oxidation and Quenching by Flooding Water*

Oxidation Kinetics

- *Isothermal Oxidation Tests*

Burst Behavior

- *Cladding Burst*

Test Samples : *pre-oxidized, pre-hydrided Zry-4*
Zry-4 irradiated in JRR-3
spent fuel from PWRs

Model Development

- *FURBEL(FEMAXI-based Code)*

6

BOCA Irradiation Program and Code Development

JMTR/BOCA Irradiation

Re-irradiation Tests of Spent LWR Fuel

- *Fission gas release during power change*
- *Thermal property and FGR of gadolinia added fuel*
- *Thermal property and FGR of high burn-up fuel*

Code Development and Verification

FEMAXI-6 : High Burnup Fuel Behavior Analysis Code

—for Quantitative Analysis and Cross-check —

- *Main Code: FEMAXI-6*
- *Sub-codes: RODBURN and PLUTON for Burning Analysis*
- *Verification by Halden Data and LWR fuels data*

7

VEGA Program

VEGA Experiment

Release/Transport of FP and Actinides from irradiated Fuel

- *3100K, 1MPa, various atmosphere, re-irradiation of sample*
- *Test VEGA-1 through VEGA-5 successfully conducted*

Thoria Components Development

- *Fabrication techniques developed*

Model Development and Verification

- *VICTORIA & THALES-ART*

8

Cooperation of Research

★ International

- *OECD Halden Reactor Programme*
- *JAERI-IRSN(NSRR, VEGA, LOCA)*
- *JAERI-USNRC*

★ Domestic

- *Industries (TEPCO, KEPCO, MHI, NFI, GNF)*
- *JNC, NUPEC, CRIEPI*
- *OSAKA Univ.*

★ Cooperation for Future Program

Advanced LWR Fuel Performance and Safety Research Program

9

Session 1-2

Fuel Research at the OECD Halden Reactor Project

W. Wiesenack

OECD Halden Reactor Project

ABSTRACT

The fuels testing programme conducted in the Halden reactor (HBWR) is aimed at providing data for a mechanistic understanding of phenomena which may affect fuel performance and safety parameters. The investigations focus on implications of high burnup and in particular address thermal property changes, fission gas release as influenced by power level and operation mode, fuel swelling, and pellet-clad interaction. Relevant burnup levels (>50 MWd/kgU) are provided through long term irradiation in the HBWR and through utilisation of re-instrumented fuel segments from commercial light water reactors (LWR).

For the agreement period 2000 – 2002, the Joint Programme of the Halden Reactor Project encompasses fourteen experiments related to testing the performance of fuels. Many of these experiments contain ex-LWR fuels which have been refabricated and instrumented with sensors such as fuel centre thermocouple, pressure transducer (fission gas release) and cladding elongation detector. In conjunction with burnup extension programmes, the possibility to increase the burnup from the LWR level to a higher values is also being pursued.

The thermal behaviour of urania (with and without Gd) and MOX fuel as a function of burnup is investigated with a number of experiments which constitute a basis for assessing UO_2 conductivity degradation. At the same time, most of these experiments also address fission gas release. Regulation usually requires that rod overpressure due to fission gas release does not lead to increased fuel temperatures because of clad lift-off and gap opening. Experiments are therefore conducted to assess the cladding creep behaviour at different stress levels and to establish the overpressure below which the combination of fuel swelling and cladding creep does not cause increasing fuel temperatures.

Pellet-clad mechanical interaction (PCMI) is manifested with clad elongation measurements which provide information on the strain during a power increase, the relaxation behaviour, and the extent of a possible ratcheting effect during consecutive start-ups. Data are obtained from low and medium burnup fuel as well as from high burnup fuel with bonding between fuel and cladding.

An overview of these investigations is given along with examples of results which have been obtained.

Fuels Research at the OECD Halden Reactor Project



Fuel Safety Research Specialists Meeting
at JAERI/Tokai
March 4 – 5, 2002

W. Wiesenack
OECD Halden Reactor Project
Norway

JAERI–Conf 2002–009

FSRSM-2002
2

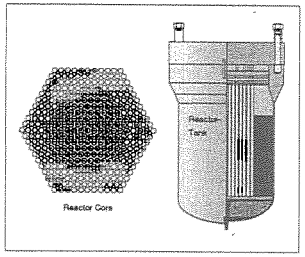
institutt for energiteknikk
OECD HALDEN REACTOR PROJECT

Presentation Overview

- Programme scope and resources
  - Objectives and scope
  - What can be measured?
  - Re-fabrication and instrumentation of ex-LWR fuels
- Fuel capabilities studies
  - Thermal performance
  - Pellet-clad interaction
  - Fission gas release and rod overpressure
  - Creep of zirconium alloy cladding materials
- Overview programme 2003 - 2005

FSRSM-2002
3

institutt for energiteknikk
OECD HALDEN REACTOR PROJECT



Nuclear Safety and Reliability

- **Fuel High Burnup Capabilities in Normal Operating Conditions**
- **Fuel Response to Transients**
- **Fuel Reliability Issues**
- **Plant Lifetime Assessment**

International research co-operation between 20 nations

FSRSM-2002
4

institutt for energiteknikk
OECD HALDEN REACTOR PROJECT

Objectives of the Halden Reactor Project Fuels Testing Programme

Address safety and economy of power generation in present and future nuclear power plants:

- Demonstrate reliability and operational flexibility of current and new fuel designs, in particular for high burnup applications
- Show compliance with safety criteria and assess safety margins

FSRSM-2002
5

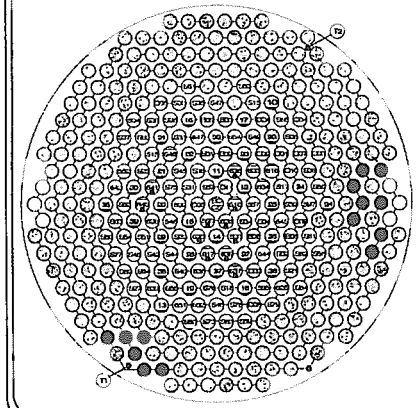
institutt for energiteknikk
OECD HALDEN REACTOR PROJECT

Scope of the HRP Fuels Testing Programme

- Fuel behaviour and properties
- Cladding behaviour and properties
- Various fuel types:
  - standard and modified UO_2
  - MOX and inert matrix fuel
  - UO_2 with gadolinia
  - VVER fuel
- Different modes of operation

FSRSM-2002
6

institutt for energiteknikk
OECD HALDEN REACTOR PROJECT



HBWR Core Configuration

- More than 300 positions individually accessible
- About 110 positions in central core
- About 30 positions for experimental purposes (any of 110/300)
- Height of active core 80cm
- Usable length within moderator about 160cm
- Experimental channel Ø:
  - 70mm in HBWR moderator
  - 35-45mm in pressure flask
- Loop systems for simulation of BWR/PWR conditions

FSRSM-2002
7

institutt for energiteknikk
OECD HALDEN REACTOR PROJECT

What Can be Measured?

- Fuel temperature
- Rod pressure
- Fuel stack length change
- Clad elongation
- Clad diameter
- Crack growth
- Water chemistry parameters
- Neutron flux / power

Give me a fixed point and I shall move the world
- Archimedes -

FSRSM-2002
8

institutt for energiteknikk
OECD HALDEN REACTOR PROJECT

Re-fabrication and instrumentation of ex-LWR fuels

Many of the experiments use high burnup fuel retrieved from LWR assemblies. Instrumentation that can be fitted:

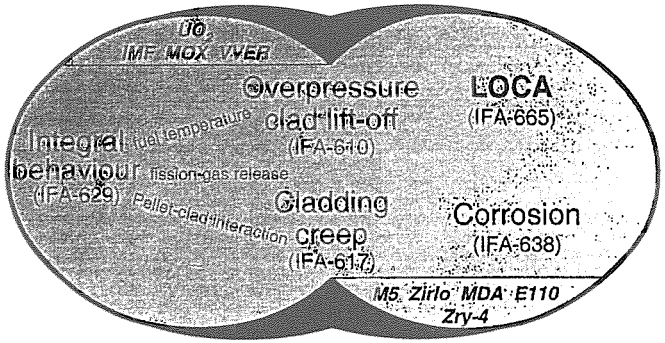
- Fuel centre thermocouple
- Rod pressure transducer (fission gas release)
- Cladding elongation detector (PCMI)
- Gas line for control of rod pressure, gas composition and gamma spectroscopy
- Diameter gauge

It is possible to extend the burnup in BWR/PWR operational conditions, at the same time gaining data from the applied instrumentation.

FSRSM-2002
9

institutt for energiteknikk
OECD HALDEN REACTOR PROJECT

Integrated Testing



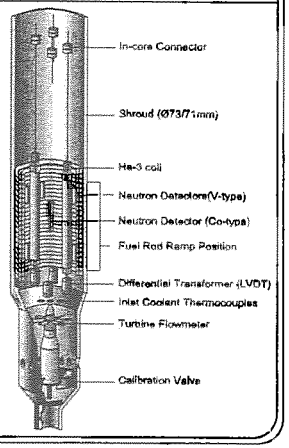
The same or similar fuel and cladding materials are employed in different types of experiments. The data provide a comprehensive picture of performance in different conditions.

FSRSM-2002
10

Institutt for energiteknikk
OECD HALDEN REACTOR PROJECT

IFA-629 Series

- 1- 4 fuel rods can be loaded and subjected to controlled power increase (He-3)
- Instrumentation allows to assess thermal performance, fission gas release, and PCMI
- Emphasis on high burnup fuels, both UO_2 and MOX
- Envisaged continuation with BWR/PWR fuels provided for LOCA test



FSRSM-2002
11

Institutt for energiteknikk
OECD HALDEN REACTOR PROJECT

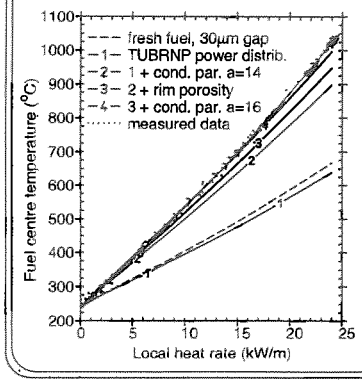
Fuel Temperature / Thermal Conductivity

- Provide data for model development and validation to envisaged burnup limits (75 MWd/kg) and beyond
- Compare temperature behaviour of different types of fuel (UO_2, MOX, $(U,Gd)O_2$, inert matrix)
- Determine effect of burnup-induced conductivity degradation
- Investigate integral behaviour including effect of
  - conductivity degradation
  - rim formation
  - gap closure and fuel-clad bonding
  - fission gas release feed-back on temperature

FSRSM-2002
12

Institutt for energiteknikk
OECD HALDEN REACTOR PROJECT

Thermal behaviour of high burnup BWR fuel

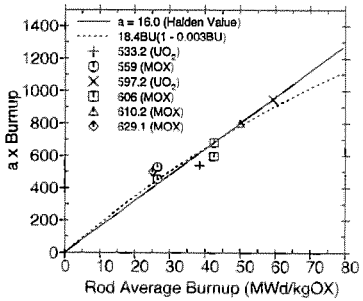


- Appreciable difference to temperatures of fresh fuel
- Important factors:
  - conductivity degradation
  - power distribution
  - rim porosity
- The model for UO_2 conductivity degradation derived from other in-pile temperature data is suitable for explaining the differences

FSRSM-2002
13

Institutt for energiteknikk
OECD HALDEN REACTOR PROJECT

Conductivity change of MOX fuel



Principal conductivity degradation parameter, a, multiplied by burnup

- BOL data indicate lower conductivity of MOX fuel compared to UO_2 fuel:

$$\lambda_{MOX} \approx 0.92 \times \lambda_{UO_2}$$

- Conductivity degradation is qualitatively and quantitatively comparable
- Saturation effect not apparent or masked by data scatter

FSRSM-2002
14

institutt for energiteknikk
OECD HALDEN REACTOR PROJECT

Strain Level / PCMI

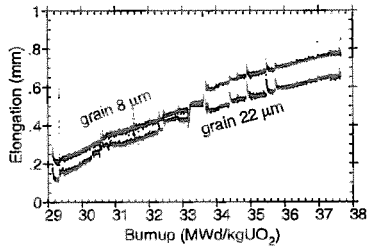
Numerous experiments with measurements of cladding diametral and axial strain. Recent investigations encompass:

- Re-instrumented high burnup segments with bonding between fuel and cladding
- Assessment of fuel swelling through cladding elongation measurements (bonding)
- Evaluation of power changes with respect to PCMI level and possible ratcheting

FSRSM-2002
15

institutt for energiteknikk
OECD HALDEN REACTOR PROJECT

PCMI Behaviour of PWR Fuel



Cladding elongation response of re-instrumented PWR fuel (40 MWd/kgU) with different grain size during steady state periods.

- *Permanent elongation*
  clad elongation increase indicates irradiation growth, no plastic strain
- *Ratcheting*
  elongation peaks associated with shut-down / start-up (release/onset mismatch)
- *Relaxation*
  stress caused by ratcheting is relaxed by fuel creep within a few days

FSRSM-2002
16

institutt for energiteknikk
OECD HALDEN REACTOR PROJECT

Fission Gas Release

The potential for reaching high inner rod pressure increases with burnup. Fission gas release studies explore limiting and mitigating factors through on-line measurement of rod pressure and if possible fuel temperature at different operating conditions:

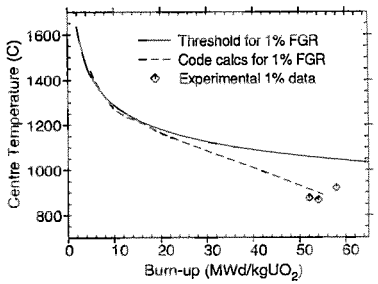
- Establish onset of significant FGR (>1%) as a function of burnup
- Provide data on short and long-term release kinetics
- Investigate effect of microstructure on release properties
- Utilise fuel of different types (UO_2, MOX, $(U,Gd)O_2$) and exposure levels

FSRSM-2002
17

institutt for energiteknikk
OECD HALDEN REACTOR PROJECT

Onset of Fission Gas Release at High Burnup

- Original 1% FGR release criterion overestimates release onset temperature for Bu > 30 MWd/kgUO_2
- FGR code benchmarked against 1% release threshold (Halden data)
- Empirical modifications:
  - resolution parameter
  - burnup dependent diffusion coefficient
- Engineering criterion



Comparison of original and revised criterion for fission gas release onset

FSRSM-2002
18

institutt for energiteknikk
OECD HALDEN REACTOR PROJECT

Rod Overpressure - Clad Lift-off

Excessive fission gas release can cause the rod pressure to rise beyond system pressure and effect the fuel temperature via gap opening. Accelerated FGR may result and eventually impair the cladding integrity. Rod overpressure / clad lift-off studies aim to:

- Establish the overpressure leading to onset of increasing fuel temperature
- Investigate the temperature response at different overpressure levels
- Include different combinations of fuel and cladding

FSRSM-2002
19

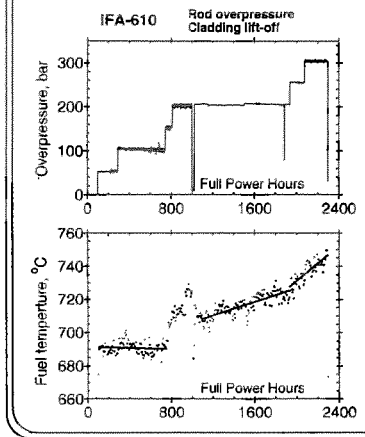
institutt for energiteknikk
OECD HALDEN REACTOR PROJECT

Rod Overpressure Test Overview IFA-610

1. UO_2, 52 MWd/kg, Gösgen NPP
2. MOX, 59 MWd/kg, Gravelines 4 NPP
3. UO_2, 55 MWd/kg, Gravelines 5 NPP
4. repeat/continuation of loading 2
5. repeat/continuation of loading 3
6. BWR and PWR fuel of LOCA test series

FSRSM-2002
20

institutt for energiteknikk
OECD HALDEN REACTOR PROJECT

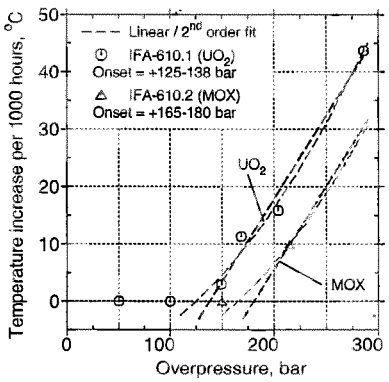


Rod overpressure

- The fuel segment is subjected to externally controlled over-pressure of up to 400 bar (above PWR system pressure)
- Small temperature drift over days and weeks detectable
- Substantial overpressure required to produce tempera-ture increase (>130 bar)

FSRSM-2002
21

institutt for energiteknikk
OECD HALDEN REACTOR PROJECT



Summary of response to overpressure

Rod overpressure summary

- Temperature increase due to lift-off measurable with fuel centre thermocouple
- Overpressure for lift-off >130 bar
- MOX seems to sustain more overpressure before lift-off
- Combination of fuel and clad properties and possibly pre-history → evaluation by fuel modelling codes

FSRSM-2002
22

institutt for energiteknikk
OECD HALDEN REACTOR PROJECT

Creep and Growth of Zr-based Materials

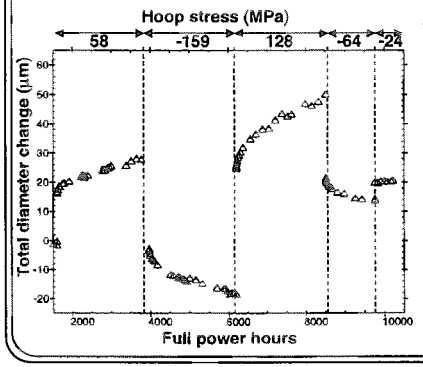
Provide engineering data on creep and growth of zirconium alloys caused by various operating conditions:

- clad creep-down (compressive, BOL)
- clad creep-out (tensile, MOL to EOL)
- guide tube creep and growth (axially compressive)

FSRSM-2002
23

institutt for energiteknikk
OECD HALDEN REACTOR PROJECT

Halden Creep Test Series

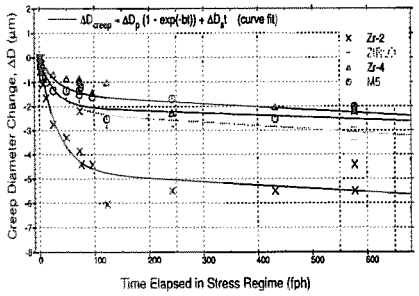


- IFA-585
  - 1992 – 1997 (~15,000 fph)
  - high fluence Zr-2, fresh + pre-irradiated Zr-4
- IFA-617
  - 1999 – 2000 (~3500 fph)
  - pre-irradiated M5, ZIRLO, Zr-4, Zr-2
- IFA-663
  - new test 2001 – M5, Zirlo, Zr1Nb, GE-P5

FSRSM-2002
24

institutt for energiteknikk
OECD HALDEN REACTOR PROJECT

Creep of Zirconium Alloys



Segment	Primary strain ΔD_p (µm)	Primary strain $\varepsilon_p \times 10^{-4}$	Secondary creep rate $\varepsilon_s \times 10^{-7}\ h^{-1}$
M5	2	2.1	1.0
Zr-4	1.5	1.6	1.4
ZIRLO	2.2	2.3	1.6
Zr-2	4.7	4.9	1.5

FSRSM-2002
25

institutt for energiteknikk
OECD HALDEN REACTOR PROJECT

Programme 2003 - 2005

The programme being prepared for the period 2003 - 2005 builds on the experience and capabilities acquired during previous programme periods. While continuing long-term experiments related to the performance of various fuel types with high burnup, emphasis is increased for life extension issues as well as fuel performance in transients.



Institutt for energiteknikk
OECD HALDEN REACTOR PROJECT

Programme 2003 - 2005

Fuel High Burnup Capabilities in Normal Operating Conditions

- Performance of gadolinia fuel
- Thermal and fission gas release behaviour of MOX fuel
- Investigations on inert matrix fuel
- Performance of VVER fuel
- Power cycling behaviour of high burnup fuel
- Fission gas release from fuel with high initial rating
- Iodine release and gap inventory
- Tolerable internal pressure in PWR and BWR rods
- Cladding creep under variable loading conditions

Fuel Response to Transients

- Rim fuel investigations
- Loss of Coolant Studies
- BWR power oscillations without scram
- Axial gas transport in high burnup fuel

Fuel Reliability Issues

- Cladding corrosion and hydriding
- CRUD deposition and axial offset effects
- Localised corrosion

Plant Lifetime Assessment

- Crack growth rate studies in PWR cond.
- BWR crack growth rate test
- Crack initiation (time to failure)
- Dry irradiation programmes
- Out-of-pile CERT tests on irradiated mat.
- Characterisation of IASCC test materials
- Pressure vessel integrity studies

Session 1-3

THE CABRI INTERNATIONAL PROGRAMME FOR RIA RESEARCH AND DEVELOPMENT STUDIES

JC Melis, J Papin, J Lewi

IPSN

ABSTRACT:

Currently, most fuel manufacturers and utilities in the world plan to increase the maximum fuel burn-up used in light water nuclear power plants, both for UO_2 and MOX fuel. As past data have been acquired at rather low burn-up values, a number of safety authorities and technical support organizations feel it today necessary to acquire new experimental evidence in the area of fuel behavior for reactivity induced accidents, in order to assess current safety criteria and/or to elaborate new relevant criteria for future fuel management strategies. In this context, the French Institute for Nuclear Protection and Safety has initiated Research and Development studies in order to investigate high burn up fuel behavior under reactivity transients.

As a first step, the CABRI REP Na experimental program has been launched in the sodium loop of the CABRI reactor in which only the initial phase of the transient, which is almost adiabatic, could be studied.

In parallel to the REP Na experiments, the SCANAIR code was developed in order to interpret the test results, perform sensitivity studies and translate the results to reactor conditions.

Separate-effects tests are also being conducted for the study of the cladding mechanical properties (PROMETRA), the clad-fluid heat transfer under fast transients (PATRICIA) and the transient behaviour of fission gases (SILENE-RIA).

As a first outcome, the REP Na tests which showed potential for rod failure at low fuel enthalpy levels underlined the lack of adequacy of the present safety criteria for high burnup UO2 and MOX fuel. Similar conclusion was derived from tests performed in the NSRR facility in Japan .

On the other hand, the detailed analysis and interpretation of the first REP Na tests allowed to identify the physical mechanisms and key parameters influencing the fuel behaviour. However, questions are still pending on the fuel rod behaviour under prototypical RIA conditions such as rod behaviour after boiling crisis, influence of rod internal pressure and possible fuel-coolant interaction after failure.

These aspects and the need of safety evaluation of the high burnup fuels and future fuel concepts including MOX, led to define the new CABRI International Program (CIP) devoted to the study of fuel behavior, under fully representative conditions (coolant, temperature, pressure, pulse duration), using a new water loop implemented in CABRI.

This program has been extensively presented in different international meetings. The two first tests of this program (CIP0-1 and CIP0-2) are planned in 2002 and will use high burn-up fuel (75 GWd/t local) and advanced cladding materials (Zirlo and M5). They will be performed in the present Na loop and will be the basis for comparison with tests in the water loop.

The first test in the water loop is foreseen in 2005 and will serve to qualify the new loop (CIPQ). The rest of the program (9 tests) will be realized between 2005 and 2007.

The program will include

- test fuel preparation and characterization ;
- post-test examination and measurements analysis ;
- access to separate effects test programs (clad mechanical characterization,...)

At present time, nine organizations representing seven countries have signed an agreement. Discussions with five other organizations are under finalization.

The proposed new International CABRI Water Loop Program aims to gather international specialists, in order to:

- optimize the test program ;
- share the necessary effort ;
- establish a comprehensive and diversified database ;
- elaborate consensus on test results relevance for improved safety criteria.

A specific motivation for the French-Japanese cooperation is the strong complementarity between CABRI tests and the tests performed in the NSRR reactor. Indeed, NSSR offers the possibility to perform sensitivity studies on a broad range of physical parameters, while the modified CABRI reactor will reproduce reactor transients in a fully realistic way. Cooperation between the two programs is therefore highly desirable.

THE CABRI PROGRAMME

ORIGIN OF THE PROGRAM

* Beginning of the 90ths, EDF requested to increase fuel discharge burn-up from 47 GWd/t to 52 Gwd/t

* Some NSRR tests (JM4, JM5) exhibited clad failure by PCMI

* Use of the availability of CABRI in which a FBR program was conducted in a Na loop

* **IPSN was, since the beginning, fully aware of the limitations of such tests to the PCMI phase**

THE CABRI PROGRAMME

IPSN METHODOLOGY

* IN-PILE EXPERIMENTS
  - Display physical phenomena
  - Coupling between physical phenomena
  - Representativity

* SEPARATE EFFECT TESTS
  - PATRICIA: out-of pile study of DNB in water conditions -completed
  - PROMETRA : clad mechanical characterization in RIA conditions – Zr4+M5/5 cycles
  - SILENE : fission gas dynamics study – in progress

* CODE DEVELOPMENT (SCANAIR)
  - Validation on in-pile and out-of-pile tests and extrapolation to rector case

THE CABRI PROGRAMME

PRESENT STATUS OF THE REP Na PROGRAMME

* 12 TESTS PERFORMED

  - 8 with UO2 fuel : 3 test with clad failure

  - 4 with MOX fuel : 1 test with clad failure

* **Extra test with MOX fuel under study**

* **REP Na synthesis foreseen mid 2002**

THE CABRI PROGRAMME

CONTEXT OF THE WATER LOOP

+ Most utilities in the world want to increase the fuel discharge burn-up

+ MOX fuel is introduced in the reactors (especially in France)

+ Key points :

  - improve clad resistance to corrosion
  - improve MOX microstructure

THE CABRI PROGRAMME

OBJECTIVES OF WATER LOOP

+ Evaluate adequacy of the present safety criteria

+ If not adequate, propose more appropriate ones

+ Evaluate safety margins

+ Assess MOX fuel behavior

THE CABRI PROGRAMME

KEY FEATURES OF THE PROGRAM (1/2)

+ Fuel vendors (Framatome, Westinghouse, Siemens) have accepted to test their advanced fuel in the same conditions :

- out of pile clad mechanical characterization
- integral in pile CABRI tests in representative conditions

+ Very high burn up fuel(> 80 GWd/t) and MOX fuel anticipated

+ Few Na loop tests combined with Water loop tests

THE CABRI PROGRAMME

KEY FEATURES OF THE PROGRAM (2/2)

+ 13 countries have expressed their intention to participate

+ For each country, participation of both safety organizations and industry

+ Flexible agreements :

- Umbrella agreement (OECD)
- Bilateral agreements

THE CABRI PROGRAMME

TEST MATRIX (12 tests)

- CIP0 : 2 reference tests in the sodium loop, advanced fuels (Zirlo, M5 cladding)
- CIPQ : qualification test of the water loop
- CIP1 : 2 reference tests in the water loop , similar to CIP0 tests
- CIP2 : ultra high burnup (80-100 GWd/t)
- CIP3 : improvement of physical understanding of RIA : NSRR coupling
- CIP4 : MOX fuel , high burnup
- CIP5 : complementary tests (open)

THE CABRI PROGRAMME

PLANNING

- 2002 : end of 1 st phase of reniewal + 2 first tests of WLP

- 2003-2004 : 2 nd phase of reniewal + WL installation

- 2005 : 1 st test in WL environment

- 2005-2007 : 10 WLP tests

THE CABRI PROGRAMME

INTEREST IN INTERNATIONAL COOPERATION

Gather specialists in order to:

+ optimize the test program

+ share the necessary effort

+ establish a comprehensive and diversified database

+ elaborate consensus on test results relevance for improved safety criteria

THE CABRI PROGRAMME

FRENCH-JAPANESE COOPERATION

Specific motivation:

+ NSRR offers the possibility to perform studies on a broad range of physical parameters

+ CABRI, with the Water Loop, offers the possibility to reproduce reactor transients in a fully representative environment

+ Both expert teams have a broad and recognized knowledge

STRONG COMPLEMENTARITY BETWEEN NSRR AND CABRI

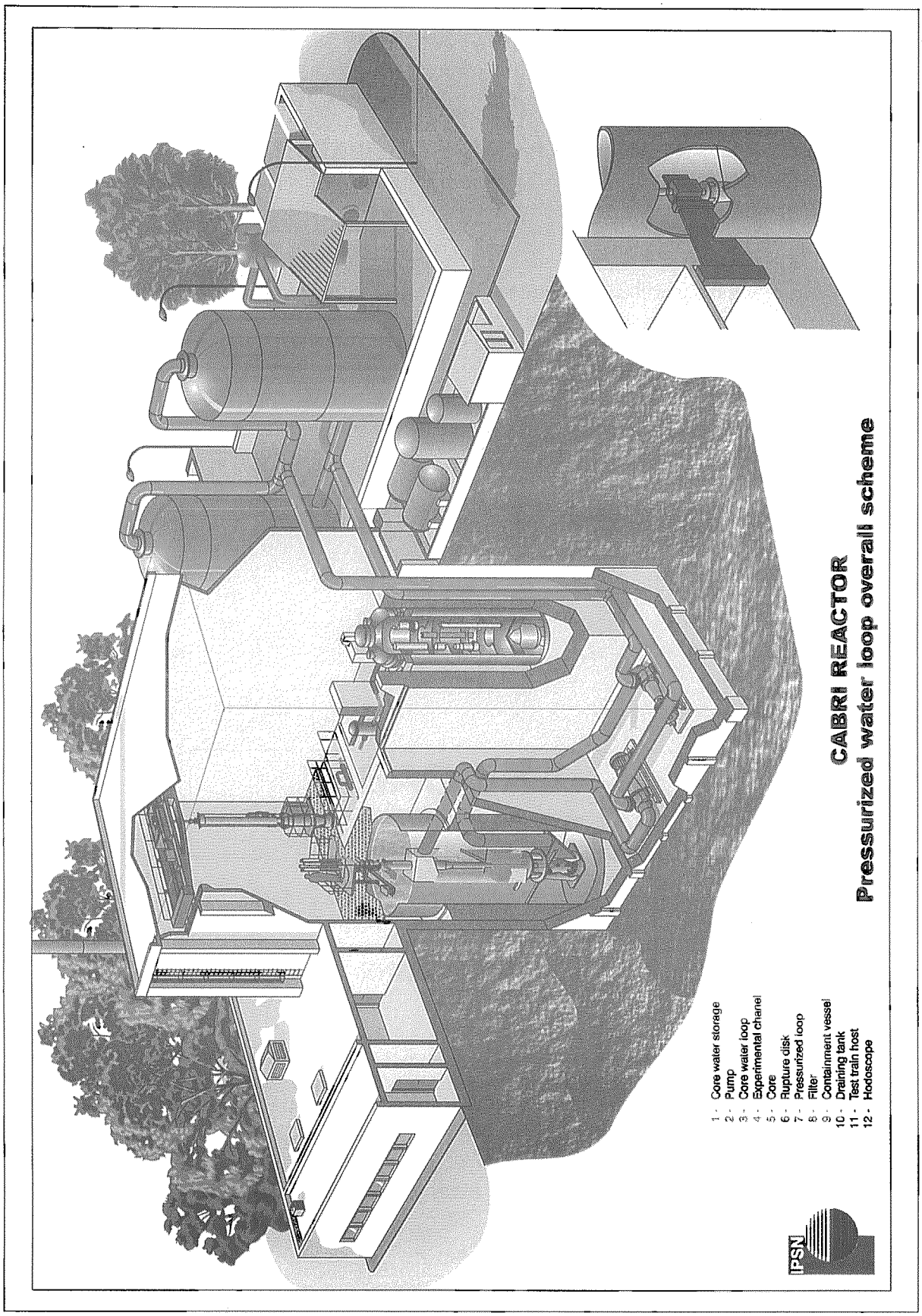
THE CABRI PROGRAMME

CONCLUSIONS

- CABRI and NSRR programs have, in the passed, strongly improved the knowledge in the RIA field and have demonstrated that present safety criteria are no longer adequate

- CABRI and NSRR have, for the future, already committed important programs (in-pile and separate effects)

Cooperation between programs is therefore highly desirable


CABRI REACTOR
Pressurized water loop overall scheme
1 - Core water storage
2 - Pump
3 - Core water loop
4 - Experimental channel
5 - Core
6 - Rupture disk
7 - Pressurized loop
8 - Filter
9 - Containment vessel
10 - Draining tank
11 - Test train hoist
12 - Hodoscope
IPSN

The RIA Test Device: Measurement locations

Session 1-4

FUEL SAFETY RESEARCH ACTIVITIES IN SPAIN

José M. Conde
Consejo de Seguridad Nuclear
jmcl@csn.es

Manuel Quecedo
ENUSA Industrias Avanzadas
mqg@enusa.es

Pedro González Arjona
ENDESA
pgonzalez@endesa.es

ABSTRACT

Spain is currently represented in most of the international programs in fuel research, both regulatory and industry-based. The participation is direct in many cases (CABRI, NFIR, Robust, Halden...), while in others access to the program results has been obtained through bi-lateral research agreements (NRC program at ANL).

Several Lead Test Assemblies programs have been carried out in Spain during the last decade aimed to demonstrate the correct behaviour of new fuel products under real operating conditions. In the PWR side, three programs have been performed in Vandellós II NPP under a partnership of Japanese and Spanish utilities and vendors, namely: Segmented Fuel Rod Program (1991-2001), Irradiation Extension Program (1999-2001) and High Burnup Demonstration Program (to be finished in 2005).

These programs have provided well-characterised irradiated fuel, with a verified behaviour under normal operating conditions. In particular, the rods coming from the irradiation extension program have been characterised during fabrication, pool-side inspected during irradiation and PIE data are available. The rod average burnup reached is in the order of 68 MWd/kgU. This nuclear material constitutes a good candidate for fuel safety research, and is already being used in two programs:

CABRI Water Loop Program. Segments from two rods with Zirlo cladding, with a burnup of 74 MWd/kgU, will be used for the reference tests in the sodium and water loops. These are 4.5% enrichment rods, with high corrosion. The RIA integral tests will be performed at high levels of deposited enthalpy in 2002 and 2005.

High burnup fuel isotopic composition project. The objective of this domestic project is to measure the isotopic composition of six samples of 4.5% enriched fuel at burnup levels up to 80 MWd/kgU. The measurements are being carried out at the Studsvik laboratories since February 2002.

The Spanish organisations continue to make efforts to use the available nuclear material in fuel safety research projects, in order to take profit of the synergies coming from the existence of ample information on the characterisation and behaviour under normal operating conditions of this fuel.

FUEL SAFETY RESEARCH ACTIVITIES IN SPAIN

José M. Conde - Consejo de Seguridad Nuclear
Manuel Quecedo - ENUSA
Pedro González Arjona - ENDESA

Fuel Research

- Research requirements:
  - Fuel characterisation
  - Fuel irradiation
  - On-site inspections during reload shutdowns
  - Fuel transport to the experimental laboratory
  - Fuel testing: Hot-cell PIE, power ramping, power transients in experimental reactors,...
- Expensive process:
  - International programs
  - Co-operative efforts

International Programs

- Spain is present in most of the fuel research international programs:
  - Halden Reactor Project
  - CABRI Water Loop Program
  - ALPS
  - NRC Program at Argonne National Laboratory
  - NFIR
  - Robust Fuel Program
- Participation:
  - Direct participation (CABRI, NFIR, Robust, Halden...)
  - Access to the program through bi-lateral research agreements (NRC-ANL)

3

LTA Programs in Spain

- The objective is to demonstrate the correct behaviour of new fuel products under real operating conditions
- R&D Projects performed together with Japanese industry at Vandellós II reactor:
  - Segmented Fuel Rod Program (1991-2001)
  - Irradiation Extension Program (1999-2001)
  - High Burnup Demonstration Program (2000-2005)

4

Segmented Rod Program

- Sponsored by NUPEC
- Participation: Kansai, ENDESA, MHI and ENUSA
- Contents:
  - Four fuel assemblies
  - 32 segmented rods and 80 full length rods
  - Different combinations of advanced cladding alloys and pellets
  - Burnup reached at Vandellós II: 55 MWd/kgU
  - Fully characterised rods
  - Inspected on-site and hot cell PIE

5

Irradiation Extension

- Participation: Kansai, ENDESA, MHI and ENUSA
- Contents: 12 full length rods from the Segmented Rod Program were re-inserted for an extra cycle of irradiation
- Burnup reached: 74 MWd/kgU (rod average)
- PIE under way

6

High Burnup Program

- Co-operative effort:
  - Japanese utilities represented by Kansai
  - Fuel vendors: MHI, NFI
  - Cladding manufacturers: ZP, MMNF
  - Spanish industry: ENDESA
  - Spanish and USA vendors: ENUSA and Westinghouse
- Four fuel assemblies with advanced material cladding will reach 75 MWd/kgU (rod average)
- Irradiation ongoing

7

Importance for Safety Research

- Irradiated fuel with high burnup is available for safety research
- The fuel performance under normal operating conditions is well known:
  - Well characterised
  - Pool-side inspected during irradiation and at discharge
  - PIE examination in hot cell
- The material is suitable for safety research: it is already being used in two projects

8

CABRI Water Loop Project

- The CABRI WLP has already been described in a prior presentation by IPSN
- Participation of Spain:
  - Direct involvement of CSN
  - Technical support by a National Laboratory
  - Technical collaboration with ENUSA
  - Use of rods from the Irradiation Extension Program for RIA tests: safety research with well characterised fuel under normal operating conditions
  - Clad mechanical properties determination in PROMETRA: will confirm and complete the data already available

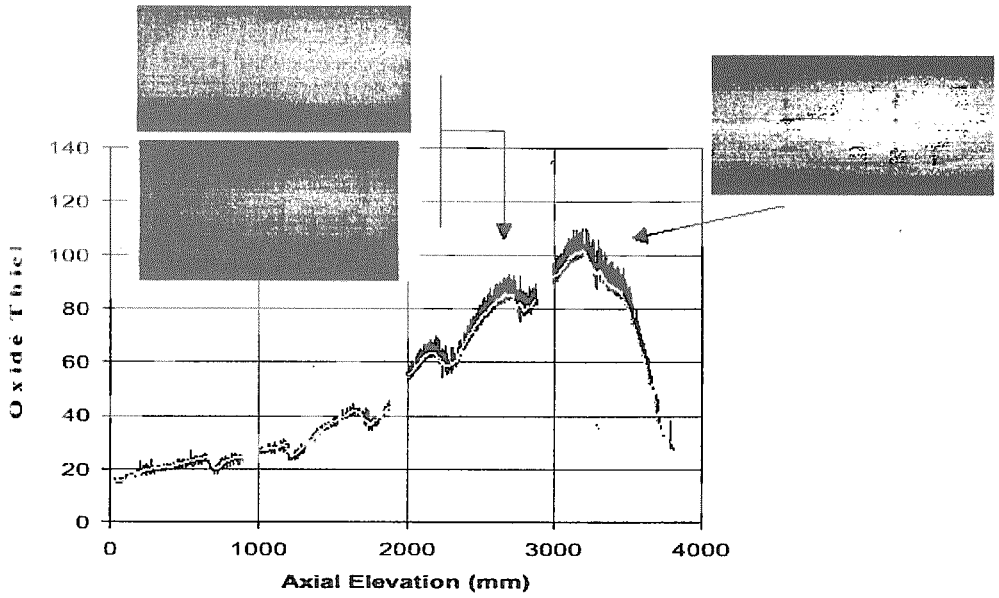
9

Vandellós II Rods in CABRI

- Two rods are being used for the reference experiments, together with two M5 rods:
  - Last experiments in the Sodium loop (2002)
  - First experiments in the water loop (2005)
- Rod description:
  - 17x17 design
  - 4.5% enrichment
  - Zirlo cladding
  - 68 MWd/kgU average burnup
  - 74 Mwd/kgU rodlet burnup
  - Corrosion thickness close to the design limits used by the industry

10

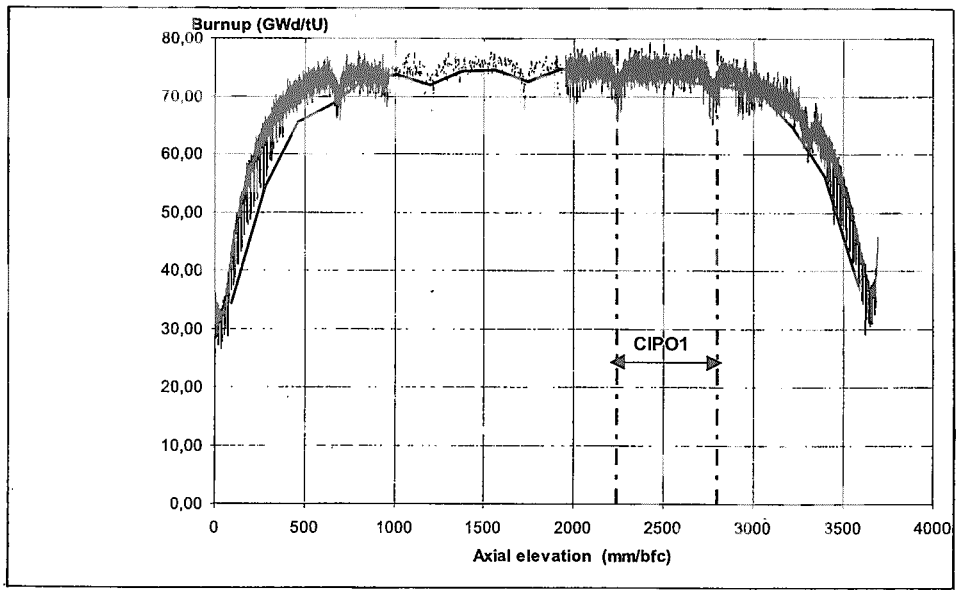
CIP0-1 Test (Na Loop)



11

CIP0-1 Test

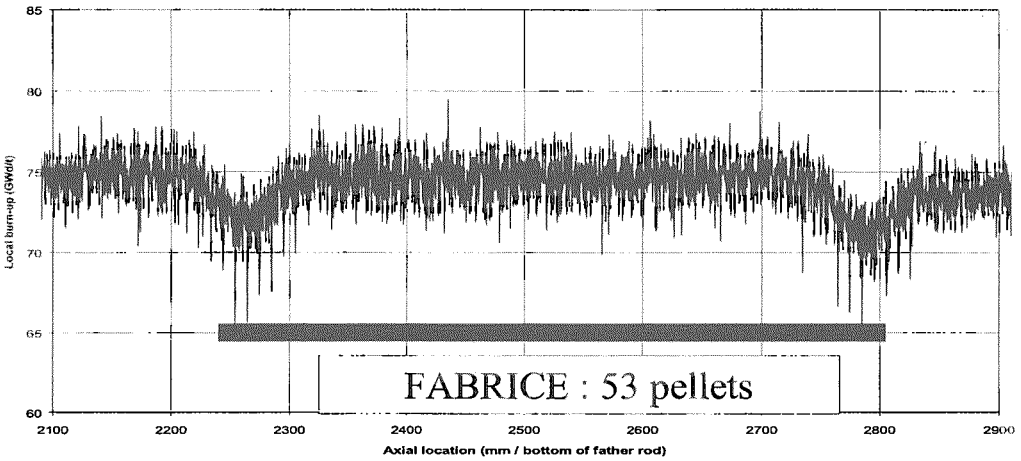
- Rod cutting positions:



12

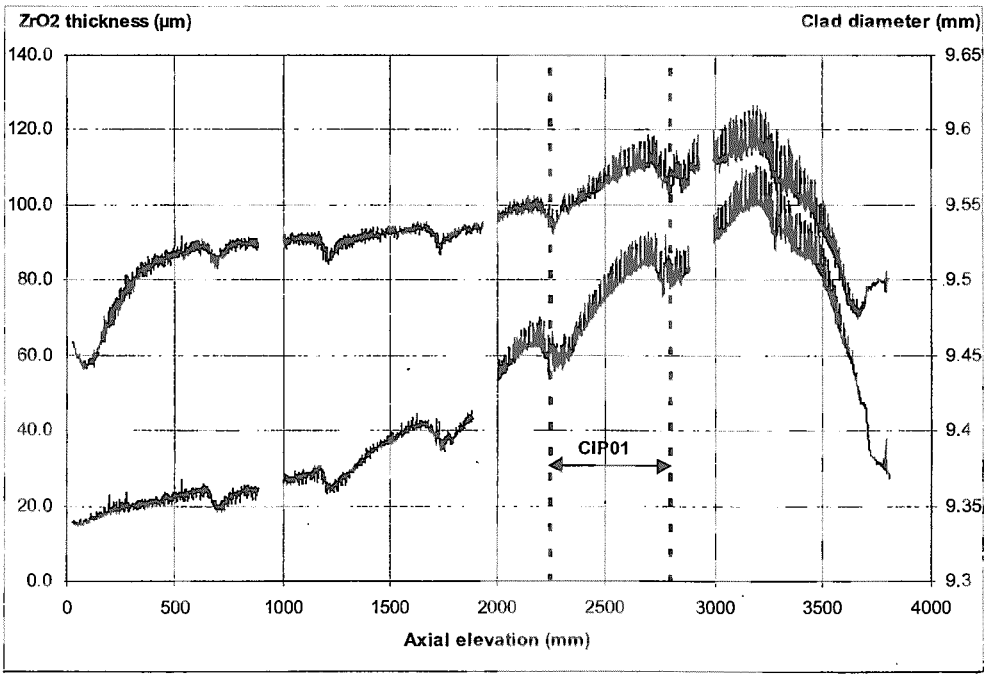
CIP0-1 Test

- Rodlet burnup



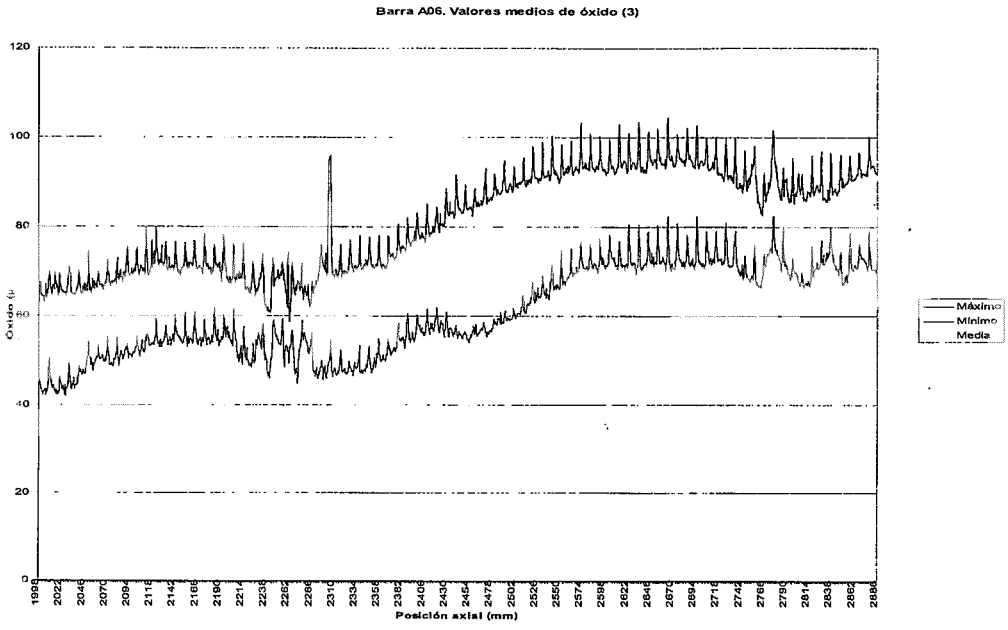
13

CIP0-1 Test



14

CIP0-1 Test



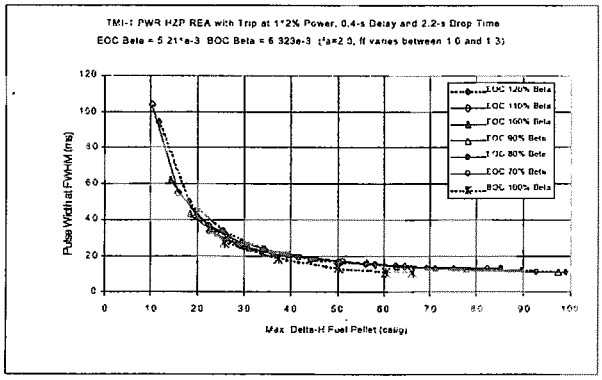
15

Reference tests

- RIA test conditions:
  - Pulse width representative of commercial PWR cores: 30 ms
  - High deposited enthalpy in order to bound the calculated enthalpy: around 90 cal/g

-High enthalpy is reached with narrow pulses in PWR cores

- One test in the water loop will be made with a 10 ms pulse (Zirlo?)



16

High Burnup Fuel Isotopics

- There is a lack of experimental data on the isotopic composition of fuel with high initial enrichment and high burnup
  - Needed to validate fuel burnup codes
  - Specially important for applications such as credit to burnup for criticality safety (storage and transport)
- A co-operative research project has been started in February 2002:
  - CSN
  - ENRESA (Company responsible for nuclear waste management in Spain)
  - ENUSA itself, and as representative of the Irradiation Extension Program partners

17

Project Description

- Two rods from the Irradiation Extension Program will be used:
  - The composition of 6 fuel samples will be measured
  - Five different burnup values up to 80 MWd/kgU
- Project scope: isotopes relevant for criticality, shielding and residual heat
  - Gamma scan
  - Rod puncturing
  - Sample burnup determination
  - Chemical dilution
  - Analytical work with different calculation codes: evaluation of the experimental results and code validation

18

Isotopes

- U 234, 235, 236, 238
- Pu 238, 239, 240, 241, 242
- Am 241, 243
- Np 237
- Cs 133, 134, 135, 137
- Sm 147, 149, 150, 151, 152
- Nd 143, 145
- Eu 151, 153
- Gd 155
- Ba-137m
- Pr-144
- Rh-106
- Eu-154
- Cm-244, 246
- Kr-85
- Ru-103, 106 Ce-140, 142 Nd-146, 148

19

Conclusions

- Irradiation programs have provided high burnup PWR fuel
  - Well characterised: inspections and PIE data
  - Correct behaviour under normal operating conditions, including power ramps
- Efforts are being made to use the material for fuel safety research
  - CABRI
  - Isotopics
- Important synergies can be obtained if tested in other safety programs
  - Different testing conditions
  - CABRI, ANL, ALPS...

20

JP0250414

JAERI－Conf 2002－009

Session 1-5

IPSN FUTURE PROGRAMMES IN THE PHEBUS FACILITY

Alain MAILLIAT

Institut de Protection et de Sûreté Nucléaire
Département de Recherches en Sécurité
C.E. CADARACHE, France

ABSTRACT

In many countries, the production and distribution of electric power has experienced a dual evolution over the last decade. Firstly, the construction and commissioning of nuclear power plants virtually came to a complete stop. Secondly, the liberalisation and deregulation of the sector introduced a harsh competition. In order to improve effectiveness, operators are considering a variety of means to enhance plant performance and reduce costs, introducing measures such as burn-up extension, power up-rates and plant life extension. This trend has taken place in the last several years and is likely to continue in the long term. In fact, it can be seen as a continuation of an evolution that has taken place over a long time and that for light water reactors started already three decades ago.

As a consequence of this evolution, there is a permanent need to reassess the reactor safety studies, in order to ensure that this progress takes place without detriment to safety. This implies improving the associated knowledge and upgrading the corresponding calculation tools. In particular, regulatory bodies will be faced with the need to qualify models and codes applicable to new materials, new designs and validated to cover an extended range of operational conditions. Amongst others, regulators will need to continuously review and if necessary update the technical basis and the assumptions made for the analysis of design basis and severe accidents. Reviews of safety criteria can only be made on the basis of experimental data from tests carried out in representative conditions.

Another aspect to consider is the margin associated to safety criteria. Formerly, nuclear safety models were designed with wide margins. This enabled to cope with the uncertainties both in the database and in the knowledge of the phenomena prevailing in safety transients. Further, conservative scenarios were taken as a basis and standard setting for regulatory deliberations. The margins provided by this conservative approach, however, risk of being gradually eroded by more aggressive demands on plant and core operation posed by the industry. This will require not only that the database for accident analyses is extended to broader conditions and materials, but also that the uncertainties associated with such database and its use for specific applications is adequately quantified.

Considering fuel safety aspects, licensing guidelines for nuclear design are primarily directed toward ensuring that various fuel design limits or acceptance criteria are not exceeded during normal operation or during anticipated operational transients. As designs and operational requirement evolve, these guidelines need continuous update through experiments devised to improve or extend the database. This might involve small-scale, out-of-pile examinations or experiments, normally intended to provide materials property data. However, this is largely insufficient for most safety (and reliability) applications, which do require representative reactor conditions. To this end, experiments must be conducted in test reactors. For fuel safety tests, single or multiple test arrangements can be considered depending on the type of investigation. In general, integral in-pile experiments run with representative materials and at representative conditions are essential for accident analyses. But equally important is the analytical effort that should always accompany the experimental work, thanks to separate effects tests. The results allow the final code assessment in terms of reactor applicability and simulation completeness.

According to this context, IPSN is preparing new experimental programmes in the CABRI and PHEBUS facilities. Regarding PHEBUS facility the IPSN future programmes consist in a two aspects.

- ✓ The High Burnup Fuel LOCA experimental programme. One of the important aspect of this programme is in-Pile experiments involving bundle geometries .
- ✓ The Phébus-2000 programme Its aim is to provide new information about the impact of high burn-up and MOX fuels and of reflooding of a degraded core on core additional degradation, potential threat to containment and Source Term.

IRSN FUTURE PROGRAMMES IN THE PHEBUS FACILITY

Alain MAILLIAT

Institut de Radioprotection et de Sûreté Nucléaire
Département de Recherches en Sécurité
CADARACHE, BP3, 13115 St Paul Lez Durance - France

INTRODUCTION

In many countries, the production and distribution of electric power has experienced a dual evolution over the last decade. Firstly, the construction and commissioning of nuclear power plants virtually came to a complete stop. Secondly, the liberalisation and deregulation of the sector introduced a harsh competition. In order to improve effectiveness, operators are considering a variety of means to enhance plant performance and reduce costs, introducing measures such as burn-up extension, power up-rates and plant life extension. This trend has taken place in the last several years and is likely to continue in the long term. In fact, it can be seen as a continuation of an evolution that has taken place over a long time and that for light water reactors started already three decades ago. Among others, this evolution consisted in:

- ✓ Increasing the reactor power: from 900 MWe to 1,400 MWe;
- ✓ Increasing the fuel burn-up: from ~30 to 50-60 MWd/kg
- ✓ Introducing new types of fuel - including MOX in some countries - and new cladding materials
- ✓ Adopting new fuel assembly and new control rod designs;
- ✓ Fuel cycle lengthening from 1 year up to 1.5 or even 2 years;
- ✓ U5 enrichment increases, poison additions, etc.

As a consequence of this evolution, there is a permanent need to update the reactor safety studies, in order to ensure that this progress takes place without detriment to safety. The regulators require the operators to justify their requests. Such justifications impose to qualify models and codes applicable to new materials, new designs and to validate them to cover an extended range of operational conditions. They impose also to verify the adequacy of the criteria or to define their modifications, keeping in mind the need to maintain sufficient margins. For satisfying the regulator requirements, both the utilities and safety organisations working in support of the regulators -like IRSN- have to engage the studies and the experimental programmes which will make possible to continuously review and if necessary update the technical basis and the assumptions made for the analysis of design basis and severe accidents.

One aspect to consider is the margin associated to safety criteria. Formerly, nuclear safety models were designed with wide margins. This enabled to cope with the uncertainties both in the database and in the knowledge of the phenomena prevailing in safety transients. The margins provided by this conservative approach, however, risk of being gradually reduced by continuous demands on plant and core operation and the increasing tendency of the operators to use "best estimate codes" and more realistic conditions for reactor accident analyses. This will require not only that the database for accident analyses is extended to

broader conditions and materials, but also that the uncertainties associated with such database and its use for specific applications is adequately quantified. Burn-up extension, for instance, is likely to require that both analytical tools and safety criteria be modified in order to account for the profound property changes that occur at high burn-up. Reviews of safety criteria can only be made on the basis of experimental data from tests carried out in representative conditions.

Considering fuel safety aspects, licensing guidelines for nuclear design are primarily directed toward ensuring that various fuel design limits or acceptance criteria are not exceeded during normal operation, during anticipated operational transients or design basis accidents. As designs and operational requirement evolve, these guidelines need continuous update through experiments devised to improve or extend the database. This might involve small-scale, out-of-pile examinations or experiments, normally intended to provide materials property data. However, this is largely insufficient for most safety (and reliability) applications, which do require representative reactor conditions. To this end, experiments must be conducted in test reactors. For fuel safety tests, single or multiple test arrangements can be considered depending on the type of investigation. Nearly forty years experience in reactor safety at IRSN provide a clear evidence that integral in-pile experiments run with representative materials and at representative conditions are essential for accident analyses. But equally important is the analytical effort that should always accompany the experimental work, thanks to separate effects tests. The results allow the final code assessment in terms of reactor applicability and simulation completeness.

According to this context, IRSN is preparing new experimental programmes in the CABRI and PHEBUS facilities. A companion paper (see : The CABRI International Program for Research and Development Studies) is devoted to the IRSN researches on the Reactivity Initiated Accidents The present paper provides an overview of the IRSN future programmes in the PHEBUS facility which consist in a two aspects.

- ✓ Loss Of Coolant Accident (LOCA)
- ✓ Severe accidents.

LOSS OF COOLANT ACCIDENTS

In LWRs, loss of coolant transients normally consists of a blowdown, a cladding heat-up in steam cooling conditions provoking a clad burst and oxidation, a quench and a post-quench phase

The current regulatory safety criteria for LOCA, still in use in most countries, are derived from the ECCS acceptance criteria that were issued by USAEC in December 1973 and published in the Code of Federal Regulations (10.CFR50, part 50.46). The criteria are stated as 5 requirements, concerning the calculated performance of the cooling system under the most severe loss-of-coolant accident conditions :

- ✓ the peak cladding temperature (PCT) shall not exceed 1204°C,

- ✓ the maximum cladding oxidation rate, defined through an equivalent cladding reacted (ECR), shall nowhere exceed 17% of the cladding thickness before oxidation but after cladding swelling with or without rupture,
- ✓ the maximum hydrogen generation total amount shall not exceed 1% of the hypothetical amount generated by the reaction of all the metal in the cladding surrounding fuel,
- ✓ the last two requirements are related with core cooling after changes in core geometry during and after any operation of the ECCS.

CURRENT STATUS AND PENDING ISSUES

CURRENT STATUS

In the aftermath of the AEC LOCA criteria release, numerous studies were undertaken world-wide in order to improve the basic knowledge of the physical phenomena intervening in LOCA transients, so as to allow a better prediction with realistic models. Beyond the numerous experimental investigations that were conducted on unirradiated rods or cladding, either in-pile or out-of-pile, there exists a few number of available results of such experiments with irradiated material. Following is a very short review of the current knowledge on clad and fuel rod behaviour gained from experiments on irradiated material, that will introduce the pending questions and critical issues for irradiated fuel behaviour in LOCA.

CLAD BEHAVIOUR

An important progress in knowledge relative to irradiated clad behaviour has been obtained from the results of the French EDF/IRSN [1,2] program (TAGCIR and HYDRAZIR tests), addressing the oxidation kinetics and quench bearing capability of irradiated zircaloy. The main outcome concern :

- the protective effect of corrosion oxide scale ;
- the oxidation kinetics of irradiated zircaloy ;
- the resistance to quench loads of irradiated zircaloy ;
- the effect of high hydrogen content, as a result of internal hydriding during LOCA transient.

Relative to oxidation kinetics and quench behaviour, a comprehensive understanding of all involved phenomena and of their inter-related influences is not yet achieved and leaves still pending questions, most of them being not specific to high BU fuel. One important question is the influence on clad quenching resistance of axial constraints that may result from differential contractions upon quench between guide tubes and a fuel rod blocked in spacer grids as a result of ballooning or metallurgical interaction. Such blockage consequences had been evidenced on past tests at JAERI [3] on unirradiated rods and should therefore be expected to some extent on irradiated rods.

ROD BEHAVIOUR

There exists a few number of available results from experiments with irradiated fuel rods under LOCA conditions. The main outcome were found in results from the PBF-LOC tests[4,5] in the USA, the FR2 tests[6] in Germany, and the FLASH5 test[7] in France. They concern the fuel relocation process and an increased cladding deformation.

FUEL RELOCATION

All the available tests performed with irradiated fuel rods experiencing LOCA conditions have shown an accumulation of fuel debris in the swollen region –called balloon- of the burst cladding which resulted from fuel fragments slumping from upper locations (see figures 1 and 2 below from FR2 results).

This process, here after called fuel relocation, is initiated at the.time of the cladding burst, as demonstrated by the FR2-E3 and E4 tests. It is thought that the driving forces are both gravity and the pressure difference between the rod upper plenum and the channel.

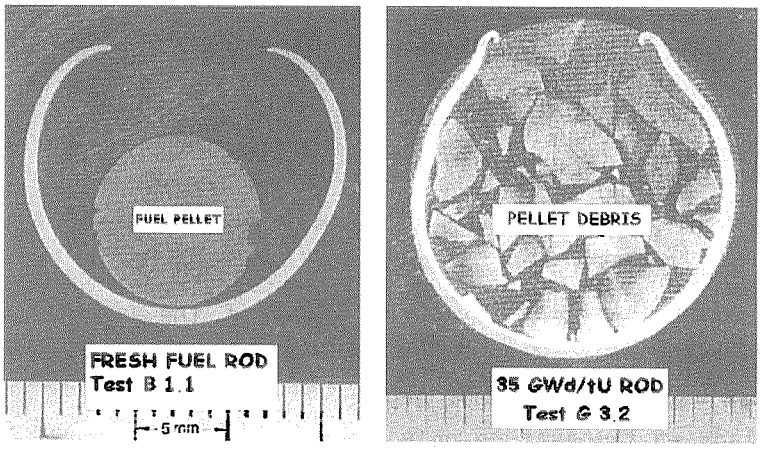


Figure 1

This fuel relocation is not counteracted by the fuel-clad tight bounding which exists with high burnup fuel. Indeed, the process was observed in the FLASH-5 test with 50GWd/t fuel in spite of a rather low clad strain (not higher than 16%). It is thought that the cladding temperature increase combined with its ballooning suppress –at less partly- the bounding making possible the fuel relocation. Finally, fuel relocation process is not specific of high burnup fuel. It was also observed for fuel rod having a burnup as low as 48MWd/t (LOC5-7B test)

AN INCREASED CLADDING DEFORMATION

In PBF-LOC experiments 2 couples of rods (2 unirradiated + 2 irradiated) were simultaneously tested in the same test train. Available data for comparison, although in very limited number due to technical problems, clearly indicate significant differences in the deformation behaviour of irradiated versus unirradiated rods.

- A higher circumferential rupture strain for irradiated rods (a factor greater than 2 relatively to unirradiated rod strain for maximum values) and more axially extended ;
- A wall thinning affecting almost all the circumference of irradiated rods, thus indicating low azimuthal temperature differences as compared to unirradiated rods .

These differences in behaviour have been attributed to the lower temperature differences on the clad of irradiated rods, circumferentially and axially, as a result of the pellet-clad gap reduction due to clad creepdown during rod irradiation.

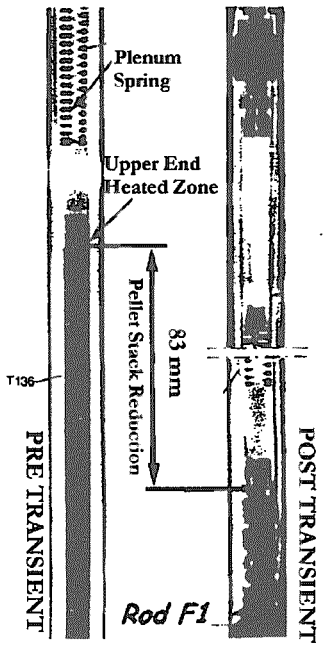


Figure 2

THE PENDING ISSUES

A better understanding of the specific phenomena shortly mentionned above leads to raise a list of some complementary questions related with rod behaviour, fuel relocation process and coolability issue during LOCA transients.

ROD BEHAVIOUR

The question mark about rod behaviour is related with the influence of hydrogen pick-up and other irradiation effects on ballooning, burst behaviour and embrittlement during reflooding which were not considered when 10CFR50, part 50.46 was released.

FUEL RELOCATION

Several questions are induced by the relocation process. The first ones concern the process itself. The needed data are the following ones.

- Instant of fuel movement at high burn-up, with possible delay due to fuel-clad bonding.
- Filling ratio of clad balloon at high burn-up, with fragmentation of UO2 rim or MOX clusters
- Impact of the relocated material on steam access inside the balloon and hydrogen uptake rate.

The second set of question marks concerns the consequences of the relocation process. Which are the effects on peak clad temperature and final oxidation ratio of the local increase in lineic and surfacic powers and of the local decrease in fuel-clad gap resulting from fuel accumulation ?

Note that these last issues are particularly important for end-of-life MOX fuel for which power generation is not reduced, unlike for UO2 fuel.

COOLABILITY

Related questions should be considered additionally, relative to flow blockage behaviour of highly deformed cladding with possibly relocated fuel and the embrittlement potentials associated to fuel fragmentation. The 90% value for flow blockage still coolable, as derived from results of flooding experiments (FEBA, SEFLEX et al) on unirradiated rods arrays is

questionable since these experiments did not take account of any fuel relocation and associated effects. The needed information are the following.

- ✓ What is the maximum flow blockage ratio that leaves coolable an irradiated rods bundle ?
- ✓ Does the maximum flow blockage ratio attainable with an irradiated rods array remain below the maximum coolable value indicated above ?
- ✓ There is presently a complete lack of data allowing to answer these questions.
- ✓ what flow blockage configuration would be worst coolable with occurrence of fuel relocation ?

In other words, is the coplanar flow blockage still the worst coolable case ?

LOCA FUTURE EXPERIMENTAL NEEDS

Regarding the LOCA issue, the current testing programmes dealing with irradiated material only involve out-of-pile experiments : separate effect quench tests on irradiated cladding (TAGCIR tests) in France ; tests on irradiated cladding and integral type experiments (ballooning / burst / oxidation / quench) on irradiated rods at ANL (USA) [8] and JAERI (Japan) [9] with the support of an important programme of mechanical tests. In addition , OECD has planned an in-pile programme consisting of some single rod geometry tests with irradiated fuel. The programme should be conducted in the Halden reactor and should provide information about the relocated fuel characteristics.
But these programmes will not solve all the previously mentioned uncertainties because these ones are mainly associated with the combined behaviour of fuel and cladding under representative conditions of the reactor evolution during the LOCA transient. Based on the long fruitful experiences of a three-tier method, A programme, providing the in-pile experiments third tier, should provide the missing part of the data bases required for code assessments in terms of reactor applicability and simulation completeness. IRSN, taking advantages of its experience in the field of LOCA tests due it former programme [11, 12, 13, 14], is preparing such an High Burnup fuel LOCA project [15]. This one is prepared in a coherent way with the present international efforts in order to validate, and possibly update, the results obtained from separate effects tests and previous limited in-pile tests.

THE MAIN EXPERIMENTAL OBJECTIVES

The main objectives of the in-pile experiments will be to investigate the behaviour of fuel and cladding with conditions representative of the reactor during LOCA sequences. The main factors that will be accounted for are :

- the nature of fuel (UO2, MOX, Burn-up),
- the fuel-clad thermomechanical coupling (i.e. fuel relocation)
- thermal azimuthal gradients (main factor affecting cladding strain and blockage ratio)
- thermal-hydraulic aspects (i.e. quenching, coolability of blocked arrays)

TEST DEFINITION RATIONALE

The following analysis provides the rationale for the *LOCA* programme characteristics. It is shown that the conditions for having representative data for reactor applications are both in-pile tests and bundle geometry.

NEEDS FOR IN-PILE TESTS

The in-pile test need results from three reasons.

Neutron flux provides the unique way to produce the correct heat generation in the fuel fragments, corresponding to the residual power, whatever are the relocations induced by the ballooning and/or the burst of the rod. Both the exact amount of heat generation in the balloon and the heat exchanges with the rod channel depend on the characteristics of the relocated fuel fragments, their size, shapes, compaction ratio. This heat generation correctness is one of the main conditions for having realistic estimates of the relocation consequences in terms of equivalent clad reacted, peak clad temperature and hydrogen uptake inside the balloon. All these aspects impact the strength of the rod during the quenching phase and the residual ductility of the rod after the LOCA transient.

During the blowdown phase of the LOCA transient, there is much less heat generation in the fuel and the clad coolant heat transfer is drastically reduced. Therefore, the fuel stored energy is redistributed in the pellet and the cladding. Simultaneously, within a few seconds, this redistribution produces a decrease of the pellet center-line temperature from 1500°C down to, say, 1000°C and an increase of both the pellet rim and clad temperatures from 300°C up to 1000°C. Due to these temperature transients, the central part of the pellet will experience a contraction while the rim and the clad will undergo an expansion. Fuel mechanical stresses and fragmentation could be induced by these adverse effects. It has to be kept in mind that during usual experiments, for which a blowdown phase is not reproduced, clad and fuel temperatures are simultaneously increased or decreased without producing any comparable thermomechanical transient. in-pile tests including a blowdown phase provide the way to get a definitive answer regarding the additional fuel fragmentation prior to the relocation and how much this refragmentation process affects the amount and the characteristics of the relocated fuel.

Finally, during reflooding and quench process studies, in-pile tests allow to maintain the heat generation in the fuel corresponding to the residual power. By this way, more representative conditions of the thermomechanical loads of the rods are provided. Without such a power during the reflooding phase, steam production and cladding oxidation are reduced, the temperature transients experienced by the rods are less severe. Consequently, under estimates of core embrittling during reflooding could be obtained.

NEEDS FOR BUNDLE GEOMETRY

In addition to the requirement associated to heat generation mentioned above, a bundle geometry is an second important condition to produce realistic data. Relocation being closely associated with the volume which is made free by the rod burst, it is clear that a correct amount of relocated fuel will be produced only if the sizes of the balloons are representative of the reactor conditions. Such balloon sizes can be obtained –as explained below- only with a bundle geometry. This is the reason why these tests are essential and complementary of single rod tests. During the early stage of the LOCA transient the fuel rods experience the ballooning and burst processes.

For such phenomena, a bundle geometry is a necessity to get a correct azimuthal temperature field around the fuel rods since this field is crucial to produce a realistic balloon size.

An illustration of the impact of the azimuthal temperature field on the stain at burst is given by the results of single rod tests with heated or non shroud.

An uniformly heated shroud reduces the azimuthal temperature variation around the rod. For such tests a higher rod deformation is obtained.

Conversely, an unheated shroud tends to increase the azimuthal gradient and, therefore, leads to small rod deformation at strain (see figure 3).

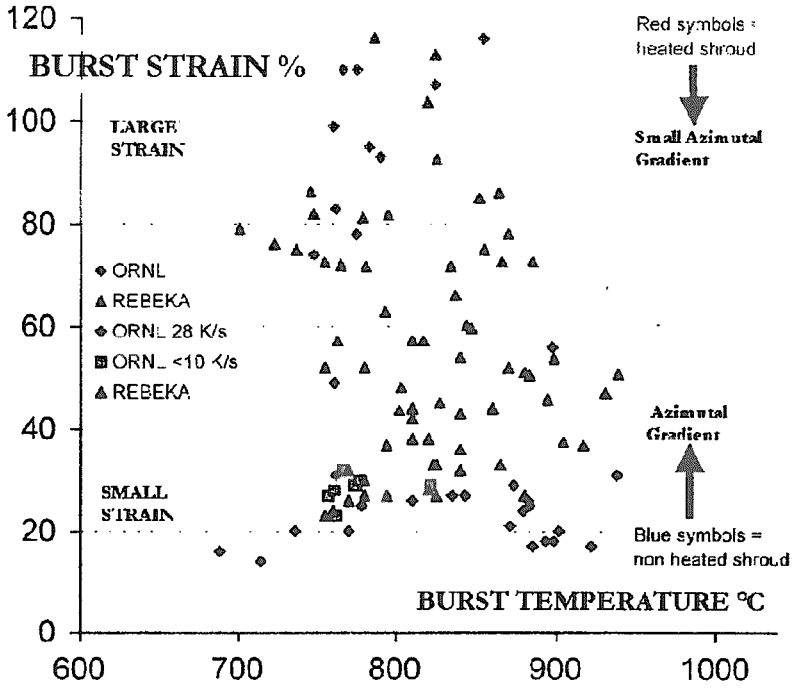


Figure 3

Additional reason for a bundle are the radial interactions between adjacent fuel rods that need to be taken into account because they modify the size and shape of the balloons.

Such kind of balloon interactions are clearly illustrated with the side picture (figure 4) from PHEBUS LOCA test 215. Having in mind that the amount of relocated fuel is associated with the size and the shape of the balloon, the picture demonstrates that realistic data will require a bundle geometry.

This bundle geometry requirement to ensure representative mechanical interactions with neighbour rods was stated in early 80ies – several years ago- in consideration of ORNL MRBT B5/B3 experiments [10]

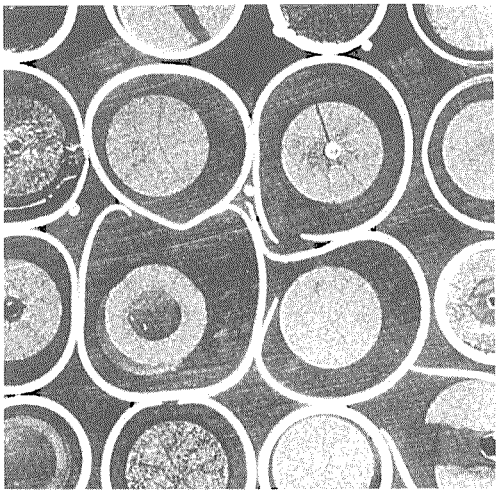


Figure 4

During core reflooding, a bundle is an obvious requirement for reproducing, on one hand, the correct flow blockage induced by the ballooning of the rods and their radial interactions and, on the other hand, the excess of heat generation at the blockage location due to the fuel fragments relocated in the balloons.

Finally, such a bundle geometry is also necessary to represent the axial and radial stresses induced by the grids and the adjacent rods which might restrain the rod contraction during quenching.

EXPERIMENTAL CONFIGURATIONS

Since it is hardly conceivable to carry out one type of experiments that will address all pending questions with any chance to provide some usable results, it appears more

appropriate to perform two kinds of in-pile experiments, namely separate effects tests and integral tests.

SEPARATE EFFECTS TESTS

The objectives of these tests are to address phenomenological aspects, in order to confirm or correct and extent the previous results relative to :

- rod deformation,
- fuel relocation,
- the resulting resistance to thermal shock loads, with or without effect of clad axial constraining.

These tests should be realised with one irradiated rod within a ring of 8 fresh fuel rods which will provide a representative thermal environment in order to ensure representative strains and subsequent phenomena. In addition, these in-pile separate effects tests should include a blowdown phase. As mentioned before, this phase will provide representative conditions for the temperature transient inside the fuel to study the consequences in terms of thermomechanical pre-fragmentation during blowdown.

INTEGRAL TESTS.

This kind of tests will address the aspects of :

- impact of blowdown phase
- flow blockage
- quenching behaviour and coolability.

These tests should allow to check the absence of unexpected phenomena or unexpected coupling between foreseen processes, and finally provide data for the validation of reactor computational tools.
These tests should be realised with 9 high burn up rods with a ring of 12 or 16 fresh fuel rods which will provide a representative thermal environment in order to ensure representative strains and subsequent phenomena. A blowdown phase will be simulated depending on its importance as observed in the previous studies. Finally, additional axial stress during quenching due to rod blockage in the assembly should be simulated during these tests.

SEVERE ACCIDENTS

A severe accident is an accidental sequence in a LWR reactor, during which the core undergoes a partial or a total loss of its initial geometry. During this sequence, fuel assemblies suffer from a dramatic degradation, and release a significant part of their components in a airborne or particles form.
The main concerns for reactor safety in case of severe accident sequences are core coolability and characteristics of the Source Term, as determined by fission product and containment behaviour. Since the TMI2 accident, in March 79, intensive efforts, both in terms of experiments and model developments, were made for acquiring knowledge on severe accident phenomenology. Today, the progress of research has made it possible to estimate the potential consequences of a rather large spectrum of severe accidents

sequences, and to judge about the efficiency or the necessity of certain mitigating equipments or measures to limit their consequences.

CURRENT STATUS AND PENDING ISSUES

Nevertheless, both national and international experts [16, 17] agree that there are still uncertainties about containment integrity and fission product behaviour issues which remain un-addressed and may impact the reliability of the previous estimates or judgements.

Regarding the containment, the main points are the input conditions from which estimates of the containment integrity will be calculated. One needed input is the amount and the properties of the corium which can be involved in phenomena such as interaction with water, interaction with concrete, direct containment heating. A second one is the quantity and the rate of hydrogen produced during core degradation and core quenching, which can be involved in case of burning or explosions. Some information exist for these points but large uncertainties subsist concerning the effect of MOX fuel or high burnup fuel on the degradation processes and the amount of corium produced. Furthermore, for the hydrogen and steam productions during core quenching, there is only few or no information available for conditions representative of a severe accident.

Regarding Fission Products, the main question is the amount, the nature and the chronology of fission products and actinides released from the fuel or re-entrained from previously deposited materials. Here, the uncertainties are obviously related to the release rates from the fuel which depend of its characteristics - MOX, UO_2 - and of its burnup level. Possibly, the release rates can also be affected by an unmodelled degradation process, like the so-called fuel foaming which might take place especially with high burn-up fuel. Furthermore, again regarding the quenching phase, there is no information available about additional new releases induced by temperature escalation or fuel fragmentation, possible re-entrainment of previously deposited materials in and above the core by large steam/hydrogen flow, and soluble species partition between steam and water.

The pending questions can be divided into four sub-programmes, each of them being devoted to a specific issue.

High burn-up UO_2 fuel

The need is to validate and to extend the results of various programmes for high burn-up UO_2 fuel. The pending issues are the degradation processes and fission product releases.
In fact, the computer codes which are used for core degradation and source term estimates were developed and validated with data bases which include very few information for burn-up above 33 GWd/tU. Unfortunately, changes in fuel and clad take place for burn-up ranging between 50 and 60 GWd/tU which induce uncertainties. For example, regarding the core degradation processes and the associated fission product releases, we do not know if foaming of the fuel, which is known for being enhanced by high burn-up, could lead to fuel degradation and fission product releases and if its contribution is important. In such a case, the present models for core degradation would have to be revisited.

MOX fuel

The needs are also conceived as an extension of the existing results to MOX fuel. The objective is to appreciate how the data bases available for UO_2 can be affected by the heterogeneity of the plutonium oxide distribution in the pellet, the PuO_2 chemical response to steam or hydrogen atmospheres, its interactions with zirconium (for which phase diagrams and reaction kinetics present large uncertainties), the larger actinide inventory. Some preliminary information [18] indicates that MOX and UO_2 might behave differently.. Therefore, tests are foreseen in specific programmes aiming at building a data base for MOX fuel degradation, low volatile fission products and actinides releases for bundle, debris bed and molten material geometries.

Air Ingress

There is a need for investigating the impact of air ingress on fuel degradation and fission product release. The phenomenology is relevant to both shutdown accidents and to circumstances where containment air enters the reactor vessel following lower head penetration and encounters the remnants of the degraded core. Spent fuel pool uncovery accident is also one of the possible circumstances.

Quenching

This forth research field is dedicated to quenching issues in terms of core degradation, hydrogen and steam productions, additional Source Term releases from fuel and from re-entrainment of deposited materials. Despite several research efforts [19, 20, 21], there are still large uncertainties regarding the previous issues during reflooding when the core is degraded beyond the LOCA-DBA conditions. The investigated core configurations should be bundle geometry at higher temperature than during a LOCA-DBA, debris bed and molten materials.

SEVERE ACCIDENTS FUTURE EXPERIMENTAL NEEDS

To reduce these uncertainties which affect the reliability of severe accident management, it is necessary to upgrade the codes and to develop realistic models for the previously mentioned processes. As a large part of the knowledge required for code developments does not exist, experimental programmes are necessary to build it. A first fraction of the needed information still exists or can be obtained from separate effects experiments. But, keeping in mind that the uncertainties are mainly associated with the specific responses of high burn up UO_2 or MOX fuels, their chemical transformations and degradation processes at high temperature or during quenching, the strong coupling existing between degradation and releases, it can be understood that separate effect experiments will not provide the largest part of the data requested for code developments and validation. The main part of the information will be obtained from experiments which will have to reproduce with enough correctness the physical mechanisms implied in the degradation and release processes. Three points are essential to obtain such a correctness and valuable data :

- ✓ Firstly, actual irradiated fuel, with appropriate burn-up, is necessary.
- ✓ Secondly, the heat source to the fuel has to be maintained despite its movements and its metallurgical transformations.
- ✓ Finally, release rates and degradation mechanisms being so strongly related, they cannot be tackled separately.

Therefore, a straightforward solution to these requests is an in-pile test programme which will provide the necessary representativeness of the data. An additional advantage of an in-pile experimental programme with realistic materials and representative conditions is to provide some garanties that no important phenomena are missing, and by this way some certitude about the completeness of the data bases which are used for code validations. Three examples, among several others, of such a role of in-pile programmes are provided by the Phébus-FP results. They reveal the importance of the fuel burn-up on the extent of its interaction with molten zircaloy and control rod material and, therefore, the effect of burn-up on core degradation. They also show that rod material release rates were largely unpredicted by the codes, especially for silver which arrives in the containment where it modifies the iodine chemistry and the source term estimates. A third example is the observation of gaseous iodine in the hot leg, which is thought to be associated with non equilibrium FP chemistry, while computer codes are unable to predict it.

These analyses lead IRSN to promote a new project, Phébus-2K [26], to be conducted in its Phébus facility after completion of the present Phébus-FP programme.

EXPERIMENTAL EQUIPMENT

The Phébus facility appears to be the only reactor in the world still capable of carrying out integral safety experiments with the associated requirements in terms of equipment, in terms of non-conventional measurements like γ-tomography of an entire in-pile test train, and in terms of fission products and active aerosols know-how of the staff. This reactor has already been used to perform the LOCA (1974-1984) and CSD (Severe Fuel Damage, 1978-1989) programmes[22,23,24,25]. The international Phébus Fission Products programme is presently underway in the facility.

Basically, the facility consists in two main parts, the in-pile equipment and a 350 m^3 leaktight housing called the 'caisson'.

The Phébus facility, in a first building, includes a pool type reactor, which can operate for several days.

The reactor consists of a driver core and a central cavity contained in an open-tank reactor vessel, see figure (5).

The core comprises PWR type fuel rods of 800 mm fissile length and is cooled by water forced convection. Its maximum power is 40 MW (limited to 23 MW for the FP programme).

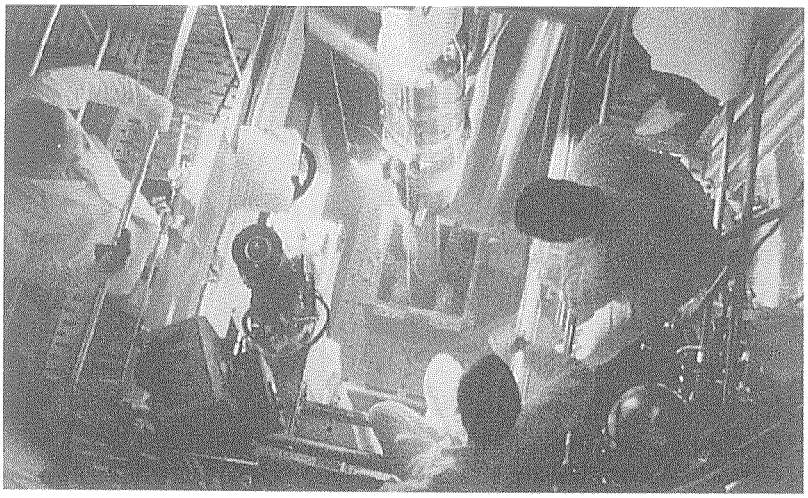


figure 5 : Looking at the driver core

The central cavity contains the test train assembly externally cooled by a pressurised water loop. Steam, hydrogen or helium are supplied to the test train through three injection lines. The caisson, a 350 m^3 leaktight housing, is installed in a second building adjacent to the reactor one, see figure (6). In this caisson a mock-up of the main elements of a nuclear power plant reactor is installed for the Phébus-FP programme : the reactor coolant system including a steam generator model, and a tank simulating the containment of the reactor building. For the Phébus-2K programme this caisson will receive the "Measurement Compartment", see figures (8,9). A complex instrumentation combining conventional detectors (thermocouples, flowmeters, pressure sensors), gamma spectrometry and sampling devices will allow the different physical parameters to be measured and the various fission product concentrations in the experimental circuits to be determined.

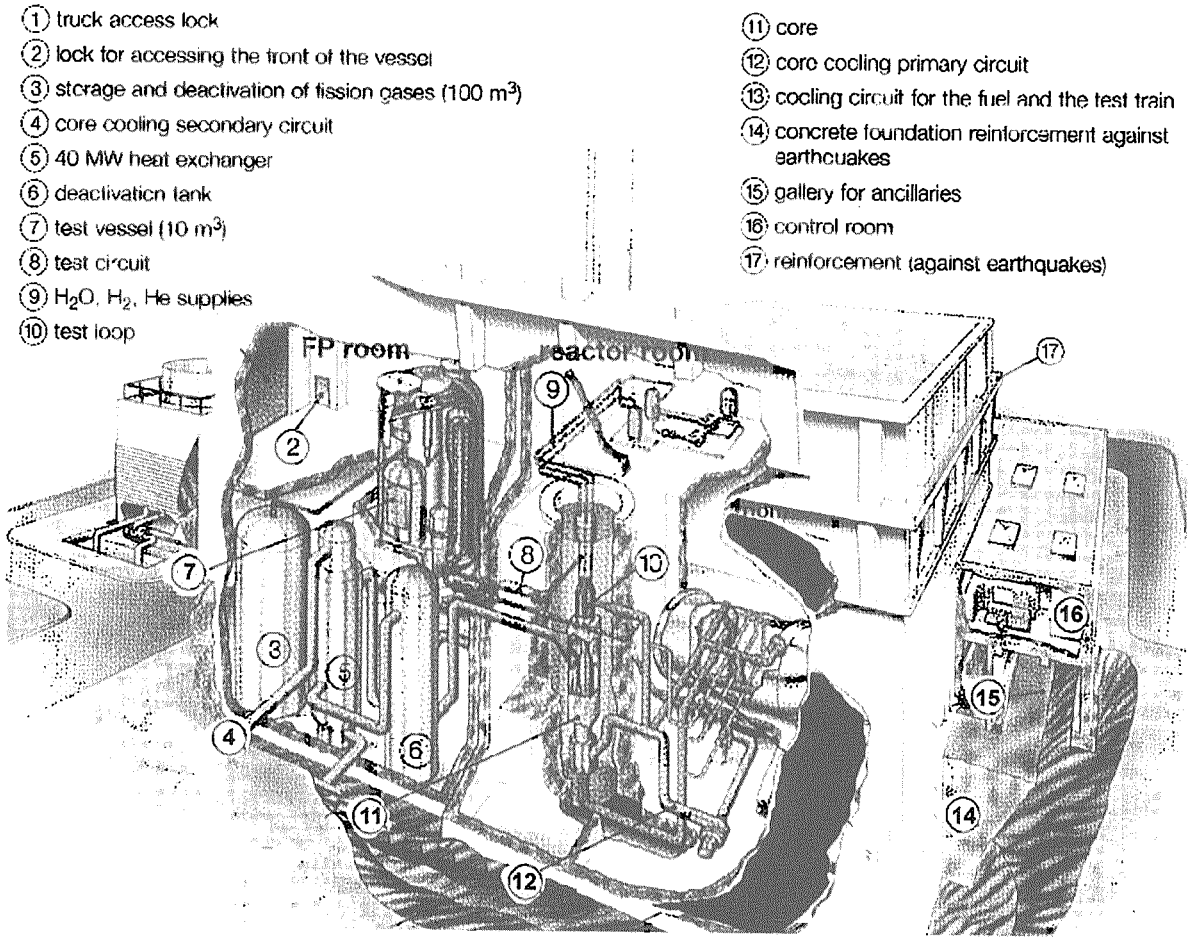
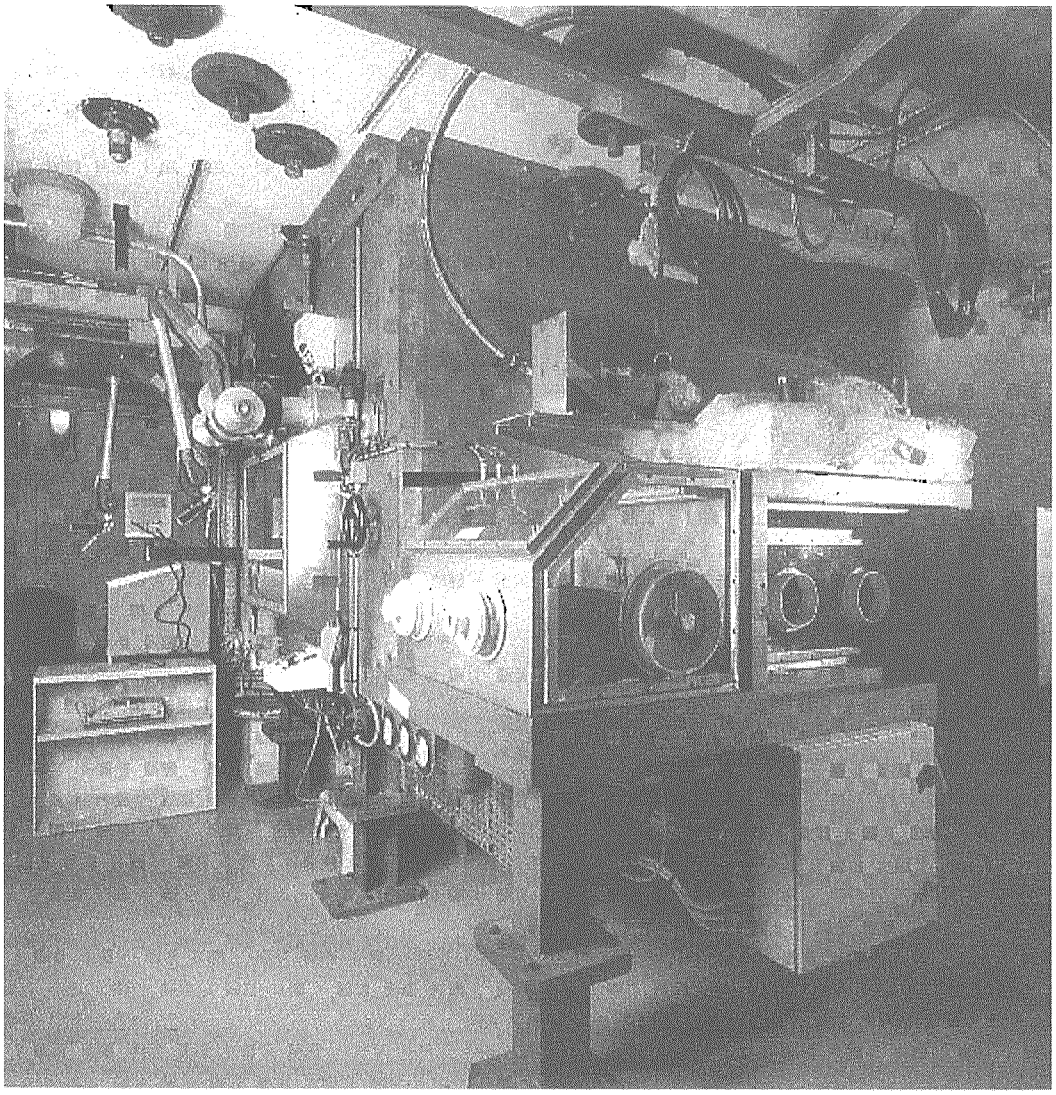


figure 6 : Inside the Phébus Facility

The facility also includes equipments which, after a test, permits handling of the experimental device and the sampling instruments, as well as their examination. For example, the test train is transferred to the "PEC" (Poste d'Examen et de Contrôle) for a gamma scanning in order to identify the fuel axial profiles, the fission products and structure materials distribution.



Fgure 7 : CECILE hot cell equipment

Besides, radiography and both absorption and emission tomographies provide a rapid overview of the extent of bundle degradation. A linear accelerator and an electronic camera specifically developed for the Phébus-FP programme allow accurate images of the fuel bundle damage as well as quantitative determination of mass distribution. The facility possesses also a hot cell, the so-called CECILE cell, figure (7), where the measurement devices extracted from the caisson are transferred.

There, quantitative gamma scanning of filters, impactors, etc., are performed. In addition, the samples are prepared before shipment to external laboratories

Taking account the Phébus FP project experience, the main guide line for preparing this Phébus-2K programmes and their associated equipments is to avoid any heavy decontamination operations which are time consuming and costly. Such a constraint can be accommodated because the previously described objectives of these Phébus-2K programmes do not require to investigate particular phenomena in the primary circuit (except the FP resuspension from core upper plenum) nor in the containment, the present Phébus-FP programme being supposed to provide all the necessary data for this latest aspect. Therefore, the experimental equipment and instruments, by comparison with the Phébus- FP ones, can be reduced, simplified and designed in an integrated way.

Basically, the Phébus-2K programme device will consist in a vertical test train incorporating the tested fuel and the connections to fluid supply lines.

The test train will be installed in the Phébus driver core and followed by a release line (see figure 8)..This line aims at transferring the vapour and aerosol materials released by the bundle to a high efficiency filtering compartment, integrating equipments whereas the gases will be directed to a condensing and storage unit

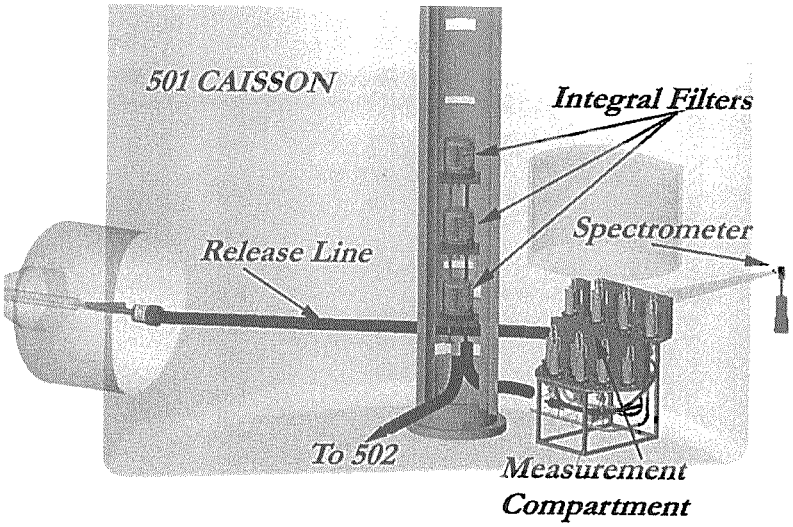


Figure 8 : PH-2K Caisson Equipment

Some specific instruments, like impactors for aerosol particle sizing, will also be installed in the measurement compartment (9). The basic technique will be γ-spectrometry, both on-line and on the samples after their transfer to the CECILE hot cell. In addition, for non-γ emitters, chemical analyses will be performed to complete the experimental data base.

It should be noted that the facility modifications needed for the Phébus-2K programme would allow to perform tests in the Phébus – FP configuration, if required.

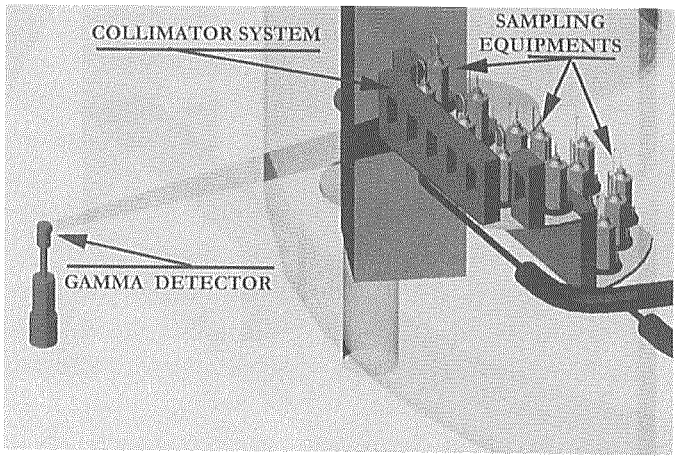


Figure 9 The measurement Compartment

Therefore, the Phébus-2K tests, unlike most of the Phébus-FP tests, will not require to dismantle and to replace consumable dedicated circuits and containment internal equipment from test to test. Only the test train and the measurement compartment will be replaced. This will greatly simplify the operations to be performed, allowing both cost decreases and shorter duration between two consecutive tests as compared to the current Phébus–FP programme.

The following elements provide some highlights on the measurement strategy which should be applied for the Phébus-2K tests. The measurement of fuel degradation will be basically the same as for the Phébus-FP programme, including a number of on-line sensors such as thermocouples and using sophisticated in-situ non destructive techniques (γ-spectrometry, absorption and emission computed tomography). Detailed destructive examinations will also be performed. A special attention will be paid to measure transient hydrogen and steam

productions during core reflooding. The upper part of the test train, above the fuel, will be equipped with instruments like thermal gradient tubes aiming at the determination of fission products deposition and re-entrainment in case of reflooding. Fission products and other released materials will be transferred through a "low retention" release line to a "Measurement Compartment".
The overall deposits in the release line can be measured by γ-scans after the test. The Measurement Compartment will include a number of sequentially operated filters in order to measure both the transient and overall releases.

CONCLUSIONS

In many countries, the production and distribution of electric power has experienced a dual evolution over the last decade. Firstly, the construction and commissioning of nuclear power plants virtually came to a complete stop. Secondly, the liberalisation and deregulation of the sector introduced a harsh competition. In order to improve effectiveness, operators are considering a variety of means to enhance plant performance and reduce costs, introducing measures such as burn-up extension, power up-rates and plant life extension
As a consequence of this evolution, there is a permanent need to reassess the reactor safety studies, in order to ensure that this progress takes place without détriment to safety. This implies improving the associated knowledge and upgrading the corresponding calculation tools.
According to this context, IRSN is preparing new experimental programmes in the CABRI and PHEBUS facilities. A companion paper (see : The CABRI International Program for Research and Development Studies) is devoted to the IRSN researches on the Reactivity Initiated Accidents The present paper provides an overview of the IRSN future programmes in the PHEBUS facility which consist in a two aspects Loss Of Coolant Accident (LOCA) and Severe Accidents.
Regarding LOCA, studies performed in IRSN and elsewhere pointed out that high burnup may induce specific effects under LOCA conditions, especially those related with fuel relocation. Uncertainties exist regarding how much these effects might affect the late evolution of the accident transient and the associated safety issues. IRSN estimates that a better knowledge of specific phenomena is required in order to resolve the pending uncertainties related to LOCA criteria and is preparing an High Burnup Fuel LOCA experimental programme. One of the important aspect of this programme is in-Pile experiments involving bundle geometries .
Regarding severe accidents, the Phébus-2000 programme has been built starting from the needs expressed by several experts concerning containment integrity and source term. Its aim is to provide new information about the impact of high burn-up and MOX fuels and of reflooding of a degraded core on core additional degradation, potential threat to containment and Source Term. A feasibility study is ongoing. Although not completed, it already shows that major simplifications of the experimental equipment can be made, as compared to the present Phébus-FP programme.

REFERENCES

1. C. Grandjean, R. Cauvin, C. Lebuffe, N. Waeckel, French Investigations of High Burnup Effect on LOCA Thermomechanical Behavior. Part Two : Oxidation and Quenching Experiments under Simulated LOCA conditions with High Burnup Clad Material. 24th Water Reactor Safety Information Meeting, Bethesda, Md, USA, October 21-23, 1996.
2. C. Grandjean, R. Cauvin, P. Jacques, Oxidation and Quenching Experiments with High Burnup Cladding under LOCA conditions. Revision of previous data and main trends of recent tests. 26th Water Reactor Safety Information Meeting, Bethesda, Md, USA, October 26-28, 1998
3. H. Uetsuka, T. Furuta, S. Kawasaki, Failure-Bearing Capability of Oxidized Zircaloy-4 Cladding under Simulated Loss-of-Coolant Condition. J. Nucl. Sc. and Tech., 20 (11), pp 941-950, Nov. 1983.
4. J.M. Broughton et al., PBF LOCA Tests Series. Tests LOC3 and LOC5 Fuel Behavior Report. NUREG/CR 2073, June 1981.
5. J.M. Broughton et al., PBF LOCA Test LOC6 Fuel Behavior Report. NUREG/CR 3184, April 1983.
6. E.H. Karb et al., LWR Fuel Rod Behavior in the FR2 in-pile Tests Simulating the Heat-up Phase of a LOCA. KFK 3346, March 1983
7. M. Bruet et al., High Burnup Fuel Behavior during a LOCA Type Accident : The FLASH5 Experiment. IAEA Technical Committee Meeting Behavior of Core Material and F.P. Release in Accident Conditions in LWRs, Cadarache, France, March 16-20,1992.
8. M.C. Billone et al., Test Plan for the Investigation of High Burnup LWR Cladding under LOCA and other Transient Conditions. IPS-263-Rev. 2, ANL Program Review Meeting, Bethesda, Md, October 29, 1998.
9. H. Uetsuka, Experimental Program on High Burnup Fuel Cladding Behavior under LOCA and other Transient Conditions at JAERI. 22nd NSRR Technical Review Meeting, Tokyo, November 9-10,1998.
10. R. H. Chapman et al. Effect of Bundle Size on Cladding Deformation in Loca Simulation Tests. 6th Int. Symp. Zirc. In the Nucl. Ind. ASM STP824, 1984, pp693-708.
11. J. Duco, M. Réocreux, A. Tattegrain, Ph. Berna, B. Legrand, M. Trotabas, In-pile investigations at the Phebus facility of the behavior of PWR-type fuel bundles in typical L.B. LOCA transients extended to and beyond the limits of ECCS criteria, 5th International meeting on Thermal Reactor Safety, Karlsruhe, Sept. 10-13, 1984.
12. E.F. Scott de Martinville, M.R. Pignard, International Standard Problem No. 19: Behaviour of a fuel rod bundle during a large break LOCA transient with a two peak temperature history, CSNI Report No. 133, (1987).
13. E.F. Scott de Martinville, C.R. Gonnier, Thermomechanics of a nuclear fuel bundle submitted to an L.B. LOCA evaluation transient: lessons drawn from the Phebus LOCA program, 9th SMIRT Conference, Lausanne, August 1987.
14. C. Gonnier, S. Fabréga, E. Scott, G. Geoffroy "In pile investigations at the Phebus facility on the behaviour of PWR-type fuel bundles in severe accident conditions beyond the design criteria" SFEN - NUCSAFE 88 Avignon 2, 7 October 1988.
15. A. Mailliat, C. Grandjean, B. Clément. "Research Needs to Resolve Pending LOCA Issues " EUROSAFE 2001, November 5-6, 2001, PARIS, France
16. Agence pour l'énergie Nucléaire, "Sûreté nucléaire, Recherches dans les pays de l'OCDE. Domaines d'accord, travaux futurs, besoins de collaboration accrus". OCDE 1996. Paris
17. B. Clément, J. Brisbois, "Use of the Phebus FP Test Results for Safety Evaluation of Severe Accidents, View of an Ad-hoc Group of Experts". CSARP Meeting, Albuquerque, May 99,NM,USA
18. G. Ducros and al, "Fission Product Release and Fuel Behaviour under Severe Accident Conditions. Synthesis of the Vercors 1 to 6 Experimental Program", Light Water Reactor Fuel Performance Conference, Apr 10-13, 2000, Park City, Utah, USA

19. Firnhaber M et al, "International Standard Problem 31 : CORA 13 Experiment on Severe Fuel Damage-Final Comparison Report", OECD/NEA/CSNI/R(93)17, GRS-106, KFK 5287, July 1993

20. P. Hofmann et al, "Hydrogen Source Term during Flooding of a Degraded Core : The QUENCH Program at FZK", 4th International Quench Workshop, Karlsruhe, Germany, Oct 6-8, 1998

21. R.R. Hobbins and G.D. McPherson, "A Summary of Results from the LOFT LP-FP-2 Test and Their Relationship to Other Studies at the Power Burst Facility and of the Three Mile Island Unit 2 Accident," Proc. Open Forum on the OECD/LOFT Project, Achievements and Significant Results, Madrid, Spain, May 9-11, 1990, Organization of Economic Cooperation and Development (1991).

22. Von der Hardt, P., Jones, A.V., Lecomte, C., Tattegrain, A., "Nuclear Safety Research. The Phebus FP Severe Accident Experimental Programme", Nuclear Safety, Vol. 35(2), July-December; 1994, pp. 187-205

23. Schwarz, M., Von der Hardt, P. "The Severe Accident Research Programme PHEBUS F.P. : First Results and Future Tests", Proc. of the 23rd Water Reactor Safety Information Meeting, Vol. 2 p 239-261 - Bethesda, Maryland - October 23-25, 1995

24. Jacquemain, D. Hanniet, N., Hueber, C., Poletiko, C. Chuaqui, C.A., Powers, D., Dickinson, S., Drossinos, Y., Funke, F., Herrero, B. "An overview of the iodine behaviour in PHEBUS FPT 0", 5th International Conference on Nuclear Engineering - ICONE 5 - Nice, France, May 26-30, 1997

25. M. Schwarz, B. Clément, A.V. Jones, "Applicability of Phebus-FP Results to Severe Accident Safety Evaluations and Management Measures", FISA-99, EC-Luxembourg, 29Nov-1Dec 1999

26. A. Mailliat, B. Clément, "The Phebus 2K Project on Severe Accidents", EUROSAFE 2000, 6-7 November 2000, Köln, Germany.

FUEL SAFETY RESEARCH
SPECIALISTS' MEETING
IN JAPAN

IPSN FUTURE PROGRAMES IN THE PHEBUS FACILITY

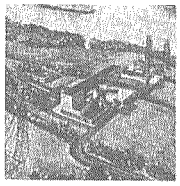
A. MAILLIAT



CONTENT

- The Safety Context
- Current Status and Future Needs
  - LOCA
  - Severe Accidents
- Rationale for Future Researches
- Conclusions

THE SAFETY CONTEXT



Evolution of the Market

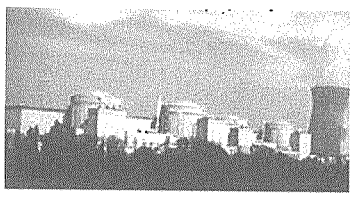
The production and distribution of electric power experience a dual evolution

✓ Constructions and commissioning of nuclear power plants come to very low levels.
✓ Liberalisation and deregulation induce competition between operators on domestic and international markets.

The answer : utilities enhance the effectiveness of their facilities.

Evolution of the Reactors

✓Increase in reactor power: from 900 MWe to 1,400 MWe
✓Increase in fuel burn-up: from 33 GWday/tU to 60 GWday/tU
✓Introduction of new types of fuel - from UO2 to MOX
✓Introduction of new cladding and control rods



IPSN

THE SAFETY CONTEXT

Formerly : Wide Margins

✓Nuclear safety models were designed with wide margins in order to allow for uncertainties between theory and reality

✓Conservative scenarios were taken as a basis for regulation and standard setting.

How much these margins are used by operators : The answer is not yet available

Now : a Permanent Adjustment

A permanent need to reassess reactor safety studies

✓Are the criteria always appropriate ?

✓Are the accident estimates always correct ?

The SAFETY Needs

Upgrading the calculation tools through knowledge improvements

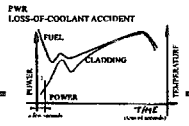
Needs small-scale or semi-integral , out-of-pile or in-pile experiments providing the additional data bases for code developments and their preliminary assessments.

Quantifying the calculation tool uncertainties through reactor realistic data bases

Needs integral in-pile experiments. Results allow code assessments in terms of reactor applicability and simulation completeness.

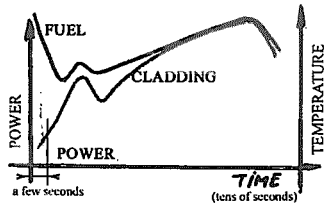
IPSN

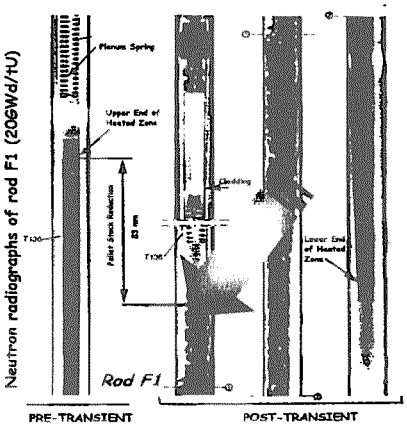
PENDING ISSUES LOCA



Pending Questions :

PWR
LOSS-OF-COOLANT ACCIDENT



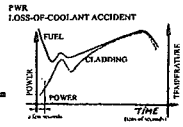


Pre-selection

- ✓ **Instant of fuel movement at high burnup ?**
- ✓ **Are they any delay due to fuel-clad bonding ?**
- ✓ **Filling ratio of clad balloon at high burnup, with fragmentation of UO2 rim or MOX clusters ?**
- ✓ **Fragment sizes, corresponding conductivity ?**

IPSN

PENDING ISSUES LOCA



Pending Questions :

P.C.T

E.C.R

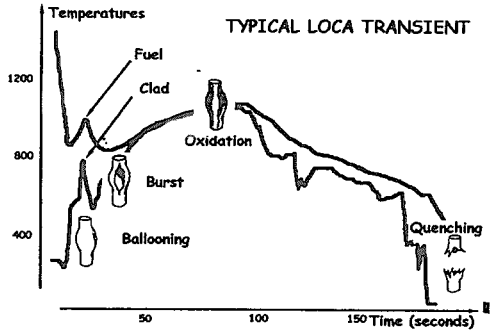
Effect on

- ✓ peak clad temperature
- ✓ final oxidation ratio and consequences for quenching
- ✓ hydrogen uptake and consequences for quenching

due to

- ✓ the increase of power
- ✓ the decrease in fuel-clad gap resulting from fuel accumulation

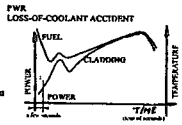
❒ Note that this question is particularly important for end-of-life MOX fuel where power generation is not reduced, unlike for UO2 fuel.



Fuel Safety Research Specialists' Meeting in Japan, March 4-5, 2002, ;

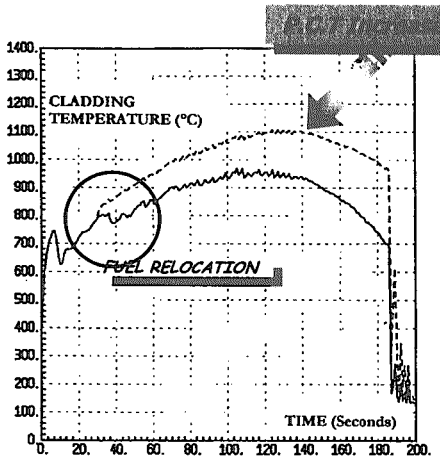
IPSN

PENDING ISSUES LOCA

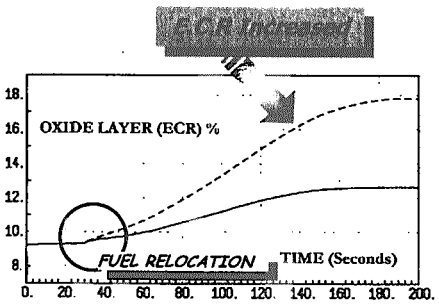


Fuel relocation impact from IPSN calculations

P.C.T increased



E.C.R increased



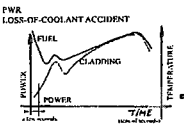
see :C. GRANDJEAN, G. HACHE, C. RONGIER, High Burnup UO2 Fuel Loca Calculations to Evaluate the Possible Impact of Fuel Relocation after Burst,Topical Meeting on LOCA Fuel Safety Criteria, Aix en Provence, 22-23 March,2001, France

Fuel Safety Research Specialists' Meeting in Japan, March 4-5, 2002, TOKAI *A. MAILLIAT*

6

IPSN

PENDING ISSUES LOCA

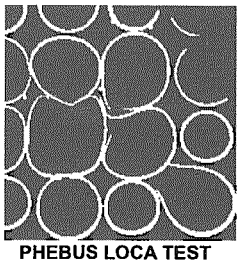


Pending Questions :

FLOW BLOCKAGE

What is the maximum flow blockage ratio that leaves coolable an irradiated rods bundle ?

The 90% value derived from results of flooding experiments (FEBA, SEFLEX et al) on unirradiated rods arrays is questionable since these experiments ***did not take account of any fuel relocation and associated effects (lineic and surfacic power increase, gap reduction)***



PHEBUS LOCA TEST

QUENCHING

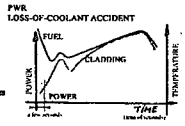
Which is the impact on failure during quenching if the fuel rod cannot totally accommodate the stresses due to rod blockage in the assembly ?

Long Term Cooling

Which is the residual ductility of the cladding after quenching ?

IPSN

FUTURE NEEDS LOCA



Such uncertainties have led IPSN to initiate new studies on the behaviour of irradiated rods and assemblies under LOCA conditions to investigate the combined behaviour of fuel and cladding under representative conditions.

APRP-Irradic programme under project will include :

- ✓ **Existing and future out-of-pile separate effects tests,**
  TAGCIR (F) ANL (US) JAERI (J)
- ✓ **In-pile specific experiments.**
  Single Rod test (OECD-Halden)
  Bundle tests (IPSN)
- ✓ **Code developments**

MAIN ASPECTS

The nature of fuel (UO2, MOX, Burnup),

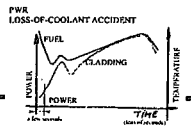
The fuel-clad thermomechanical coupling (i.e. fuel relocation)

Thermal azimutal gradients (main factor affecting cladding strain and blockage ratio)

Thermohydraulic aspects (i.e. quenching, coolability of blocked arrays)

IPSN

FUTURE NEEDS LOCA



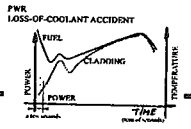
Investigate the combined behaviour of fuel and cladding with conditions representative of the reactor ones during LOCA

IN-PILE experiments are necessary requirement to fulfil the above representativity objectives :

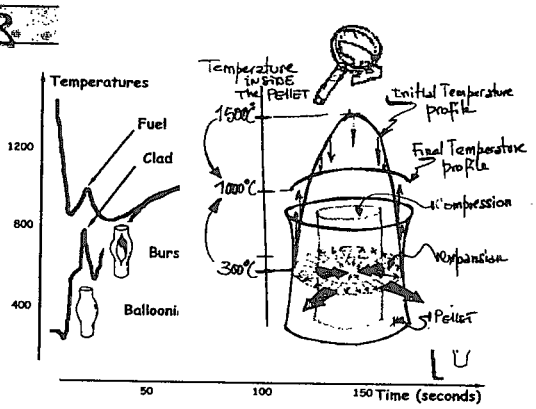
- **In-pile tests provide the unique way to maintain the heat generation in the fuel fragments whatever are the fuel movements induced by the relocation at burst.**
- **Heat generation correctness is one of the conditions for having representative estimates of the relocation consequences for ECR and PCT and cladding hydrogen uptake**
- **Heat generation is maintained during reflooding and provides representative results for quenching progress and consequences**

IPSN

FUTURE NEEDS LOCA



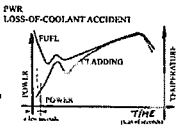
IN-PILE experiments are necessary requirement to fulfil the above representativity objectives :



During the early stage of blowdown phase, the release of the stored energy induces a temperature transient inside the fuel pellet.
There is no information regarding how much the induced thermal stresses may product additional rim and pellet fragmentation, may suppress clad-fuel bonding

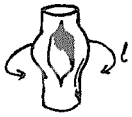
- **In pile tests with a blowdown phase provide the way to get the correct fuel temperature profile transient which induce pellet radial stresses and possible effects on the amount and the characteristics of the relocated fuel**

FUTURE NEEDS LOCA

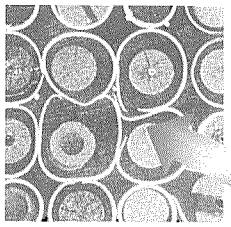


BUNDLE experiments are necessary to fulfil representativity objectives :

- **To get correct azimuthal temperature field around the tested fuel**



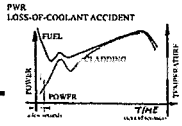
- **Temperature field correctness is crucial to produce realistic balloon size**



PHEBUS LOCA TEST 215
Year 1983

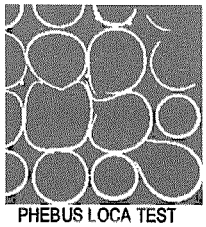
- **Radial interactions between adjacent fuel rods impact the balloon size and shape)**
- **Balloon size and shape impact the amount of relocated material**

FUTURE NEEDS LOCA



BUNDLE experiments are necessary to fulfil representativity objectives :

- **To represent the axial stresses induced by the grids which may restrain rod contraction during quenching**

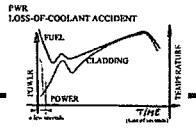


PHEBUS LOCA TEST

- **To get a realistic value of the flow blockage and the associated heat generation induced by fuel relocation**
- **To get the realistic complex flow behaviour and quench front progression during reflooding**

IPSN

FUTURE NEEDS LOCA



Two kind of tests

Studies devoted to fuel relocation characteristics and fuel relocation consequences :

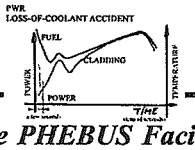
- **1 high burnup rod with a ring of 8 fresh fuel rods**
- **A blowdown phase which will include representative conditions for the residual power transient during a LOCA sequence.**

Studies devoted to Flow blockage, Quenching behaviour and Coolability :

- **9 High burn up rods with a ring of 16 fresh fuel rods**
- **Additional axial stress during quenching due to rod blockage in the assembly**

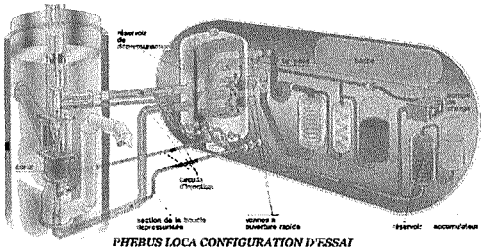
IPSN

FUTURE NEEDS LOCA

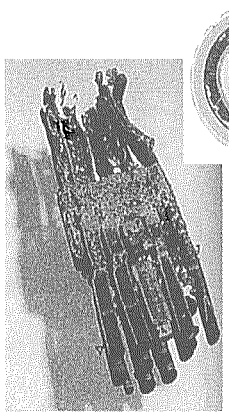


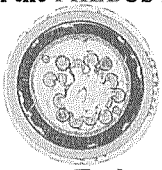
Such a programme should take place in the PHEBUS Facility. By this way IPSN will take advantage of the know-how accumulated when the previous LOCA programme with fresh fuel was run

Between Years 76 and 83 20 LOCA bundle tests were run in the PHEBUS Facility



PHEBUS LOCA CONFIGURATION D'ESSAI





To day we can measure the 3D location and determine the nature of a material fragment less than 100 microns in a bundle through tomography scanning.

Enhancement of the existing technique will provide several points inside the clad with an oxide/metal discrimination. Such a tomography measurement associated to post test examination in hot lab will provide the requested information about relocation.

PENDING ISSUES Severe Accidents

Pending Questions : CONTAINMENT INTEGRITY

How much corium will be involved in the interaction with water ?
which are the reacting corium properties ?
How much steam and hydrogen are produced during the degradation process and especially during the core quenching ?
Are there any risk of a late pressurisation of the primary circuit ?
are there any risk of a steam explosion endangering the containment ?

UO2 and MOX

Some information exist for these points but large uncertainties subsist concerning the effect of MOX fuel or high burnup fuel on the degradation processes

QUENCHING

For the steam and hydrogen productions during core quenching, there is not much information (PBF-ST, LOFT-FP2, PHEBUS-SFD-B9R) available for representative conditions of a severe accident, even if some material is available from separate effect tests or electrically powered tests (programmes CORA, QUENCH).

PENDING ISSUES Severe Accidents

Pending Questions : *SOURCE TERM*

the amount, the nature and the chronology of fission product and actinide releases from the fuel or re-entrainment from previously deposited materials.

UO2 and MOX

Uncertainties are related with
✓Release rates fuel MOX, High Burnup UO2
✓Possibly a different degradation process like the so called fuel foaming which might take place especially with high burnup fuel.

QUENCHING

None or very few information is available about
✓ Re-entrainment of previously deposited materials in and above the core by large steam flow
✓ Additionnal releases from fuel induced by temperature escalation or fuel fragmentation (LOFT-FP2),

IPSN

FUTURE NEEDS — Severe Accidents

High BU UO2 and MOX Fuels degradations and FP Releases
QUENCHING Consequences

To build valuable data bases, results are needed from experiments which will have to reproduce the physical mechanisms implied in the degradation and release processes with enough correctness.

Three points are essential to obtain such a correctness.

- **Firstly, actual irradiated fuel (UO2 and MOx), with the appropriate burnup, is necessary.**
- **Secondly, for degradation correctness, the heat source to fuel has to be maintained despite its movements, melting and its metallurgical transformations.**
- **Finally, release rates and degradation mechanisms being so strongly related, they cannot be tackled separately.**

IPSN

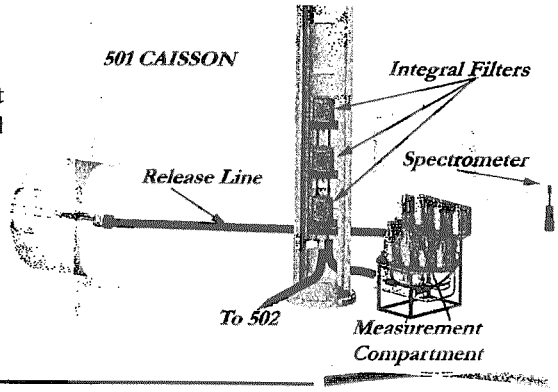
FUTURE NEEDS — Severe Accidents

Taking account the Phébus FP project experience, the main guide line for preparing this Phébus-2K programmes and their associated equipment is to avoid any heavy decontamination operations which are time consuming and costly.

Such a constraint can be accommodated because the previously described objectives of the Phébus-2K programmes do not require to investigate particular phenomena in the primary circuit (except the FP resuspension from core upper plenum) nor in the containment.

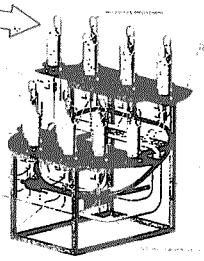
Therefore, the experimental equipment instruments, by comparison with the PI FP ones, can be

- ❑ **reduced,**
- ❑ **simplified,**
- ❑ **designed in an integrated way.**



IPSN

FUTURE NEEDS *Severe Accidents*



MEASUREMENT COMPARTMENT

ON LINE	GAMMA SPECTROMETRY
SEQUENTIAL	RELEASE RATE RESUSPENTION RATE
POST TEST	GAMMA SPECTROMETRY DESTRUCTIVE EXAMINATIONS CHEMICAL ANALYSES



BUNDLE AND UPPER PLENUM

CONVENTIONAL	PRESSURE TEMPERATURES MASS FLOW RATES POWER HYDROGEN, STEAM CONTENTS
SEQUENTIAL	RELEASE RATE DEPOSIT RATE RESUSPENSION RATE
POST TEST	GAMMA Spec, TOMOGRAPHY DESTRUCTIVE EXAMINATIONS CHEMICAL ANALYSES

IPSN

RATIONALE FOR SAFETY RESEARCHES AT IPSN

Answer the future safety requests

Taking advantage of existing information
By continuation of available tools
With a minimum of new studies

- Updating and upgrading by continuation of the models
  - Fuel behaviour, cladding properties, etc..
- A minimum of small-scale or semi-integral , out-of-pile or in-pile experiments
  - Providing the additional data bases for model updating
- A few integral in-pile experiments
  - Quantifying the calculation tool uncertainties and margins to criteria

SUMMARY

IPSN is preparing future LOCA and Severe Accident programmes in the PHEBUS Facility to ensure code assessments in terms of :

- **Reactor applicability**
- **Simulation Completeness**

in a coherent way with the international efforts devoted to code developments and separate effects experimental programmes.

According to the permanent need to reassess reactor safety studies within the next decades a methodology is proposed which should contribute to minimize the cost of such reassessments

Discussion:

Session No. 1-1 (Presenter: H. Uetsuka)

Q: (C. Otto)

You talked "55GWd/t" max. burnup. You mean average burnup?

A: "55GWd/t" is the average discharge burnup of assembly.

Session No. 1-2 (Presenter: W. Wiesenack)

Q: (D. Baron)

Is power level accuracy to be accounted for experiment analysis?

In "Lift off" experiment of high burnup fuel, there is no re-opening of the gap due to chemical binding between fuel and cladding. If there is re-opening, it is due to fuel pellet internal cracks, and this means that mechanical behavior is more complex to be accounted for. Re-opening depends on fuel behavior.

A: The accuracy depends on the type of experiment and the test rig design, and it is influenced by the ratio of power operated by the fuel and the amount of gamma-heating.

The latter can be minimized by design, e.g. in IFA-610 (rod over-pressure clad lift-off test) the test rod is inserted into an insulated channel which very much decreases the amount of water and structural components in which gamma heating is effective.

Also, in most experiments related to fission gas release, the fuel temperature is measured which eliminates the uncertainty in this very influential parameters (temperature) and obviates the need to calculate this quantity from power.

Comment (M. Kinoshita)

Threshold of steady state FGR, 900℃ at 55MWd/kgU is too low temperature for thermal activation based release. This is true at rim-structure, too. Therefore, the mechanism of this FGR threshold is "mechanical," such as fracturing and cracking. This mechanical fission gas release could be different at different fuel materials..

Session No. 1-3 (Presenter: J.C. Melis)

Q: (I. Sato) In order to clarify swelling mechanism of high burnup fuel during RIA, the role of separate effect tests is important. There is an on-going activity in JAERI with out-of-pile facility. In France, are you going to perform some separate effect tests?

A: We have a planning with the SILENE reactor focusing on fission gas release

behavior. As an out-of-pile study, we have the PROMETRA program which is related to the mechanical characteristic of cladding.

Q: (C. Otto) For what reason are you performing the same tests in the CABRI sodium and water loop?

A: To reconcile the Rep-Na database with the Water loop database, we need reference tests with same rods listed in Na and water environment. These tests (2x2) will concern with advanced claddings (ZIRLO and M5).

Q: (D.Bottomley) Cladding radial diameter will be measured. Will the cladding elongation be measured as in the Halden project experiments?

A: Yes, the cladding measurement system was developed by the Halden project.

Q: (G. Ledergerber) Are there any tests for BWR planned?

A: The CIP 5 series is devoted to open tests. Use of BWR tests in this series is not excluded, provided that a majority of participants express an interest.

Session No. 1-4 (Presenter: J.Conde)

Q: (W.Wiesenack) What is the link between correct behavior under normal operating condition and the safety research at CABRI/NSRR?

A: As a regulator. I'm concerned with safety research. However, a well characterized fuel which showed correct and predictable behavior under normal operation conditions is a solid base to attempt safety research.

Q: (J.C.Melis) Within the CABRI program, there is an agreement between industry (EDF) and IRSN. In Spain, I have the impression that the agreement is more between CSN and fuel vendor (ENUSA). What is the reason why?

A: You are right in what refers to the CABRI WLP, because in that case the CSN didn't get any support from the industry to participate in the project. However, a coordinated research program is established with the industry, in which research projects of common interest are included and financed through equal contributions. Most of the research projects in which the CSN is involved are included in this program with the industry.

Session No. 1-5 (Presenter: A. Mailliat)

Q: (G Ledergerber) How is the Halden-Test influencing the test planned for PHEBUS LOCA-High Burnup? The Halden-Test will be performed within the next 2 years.

A: The Halden PWR LOCA tests are complementary of the PHEBUS High Burnup LOCA tests. The reasons are the following. The Halden tests should provide the characteristics of the relocated fuel (filling up ratio, fragment size, etc....) if the instrumentation is convenient. The PHEBUS High Burnup LOCA tests objectives are to provide the information related to fuel relocation also but mainly the consequences of fuel relocation. Such an latter objective requires test conditions representative of the reactor conditions: bundle geometry for: correct thermal field around the test rods; correct flow blockage for having a representative quenching behavior.

Q: (M.Kissane) What is the basis for code development for LOCA issues (e.g. fuel relocation)?

A: IPSN has not yet finalized the detail of the models to be developed, exchange of views are taking place with various partners. It is clear that new model development are required specially those related with fuel relocation process, heat transfer between the balloon with relocated material and its surrounding, heat transfer for reflooding, etc.. Specifications for the new models should be released in a next future.

Q: (R.S.Dickson) Will the size distribution of the re-suspended material in the PHEBUS 2K tests be measured?

A: One of the important outcomes of the PH2K are the FP characteristics both for emission and re-entrainment phases. Therefore sampling of the releases during the tests will be performed immediately above the bundle in the test train and in the measurement compartment where impactors could be installed. The analyses of the sampling and impactor loadings will provide the aerosol sizes distributions.

Q: (P.Bottomley)
Will the Phebus 2k program and the Phebus LOCA programme be carried out?

A: The two programmes are prepared simultaneously. Our intention is to run both programme tests alternatively to optimize costs.

2. Session 2a : RIA Experimental Research on High Burnup Fuel

Session 2a-1

NSRR RIA Tests on PWR, BWR and MOX Fuels

Takehiko NAKAMURA, Hideo SASAJIMA,
Makio YOSHINAGA and Kazuyuki KUSAGAYA
JAERI

ABSTRACT

In order to quantify influence of fuel burnups on fuel behavior under reactivity initiated accident (RIA) conditions, series of pulse irradiation tests have been conducted in the Nuclear Safety Research Reactor (NSRR) of Japan Atomic Energy Research Institute (JAERI). Fuel failure behavior and consequences of the failure have been investigated under simulated RIA conditions using PWR fuels at burnups up to 50GWd/tU, BWR fuels at burnups up to 61GWd/tU, and mixed oxide (MOX) fuel at a burnup of 20GWd/HM irradiated in the Advanced Thermal Reactor (ATR).

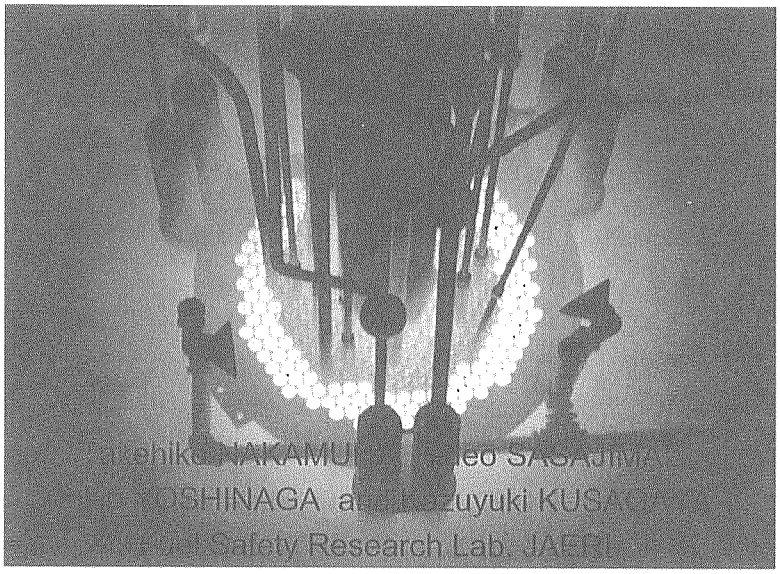
Characteristic failure of high burnup PWR and BWR fuel rods occurred at low fuel enthalpies in a manner different from those of fresh or low burnup fuels. The fuel failed early during the transient irradiation in brittle manners, before the cladding temperature rose up. Post test examination of the cladding suggested that hydrides accumulated in the cladding during base irradiation due to waterside corrosion played important roles for the incipient clack generation and its propagation. In the resent high burnup BWR fuel tests, it was found that the crack propagation and hydride distribution in the BWR cladding was different from those in the PWR cladding. From transient and post test measurement of the cladding deformation in comparison with code calculation, it was concluded that thermal expansion of the fuel pellets caused the deformation, which resulted in the failure.

When the high burnup PWR and BWR fuels failed in the NSRR tests, considerable amount of fission gases and fuel itself were released from the crack opening of the cladding. These behaviors are also studied to clarify the consequences and influence of the fuel failure. Not only that they are important in terms of source terms in RIAs, the abrupt releases of the gases and fuel caused pressure pulse and mechanical energy generation, which might threat integrity of the core system. The fission gas accumulated in the pellets during base irradiation caused significant cladding deformation in the pulse irradiation tests, when the cladding temperature escalated to close to or above a thousand K. Heterogeneity of Pu concentration in the MOX fuel seems to enhance the gas release in the transient heating conditions.

Outlines of these behavior, highlighting on resent PWR and BWR fuel test results, and future test plan are presented.

JAERI

NSRR RIA Tests on PWR, BWR and MOX Fuels



Prepared for FSRSM
on Mar. 4-5, 2002 at Tokai, Japan

1

JAERI

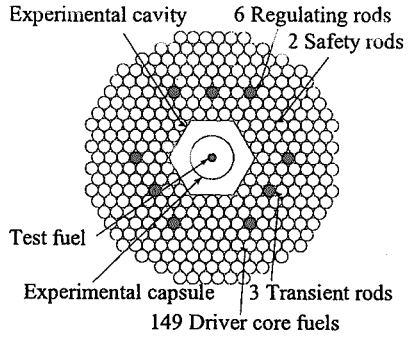
Contents

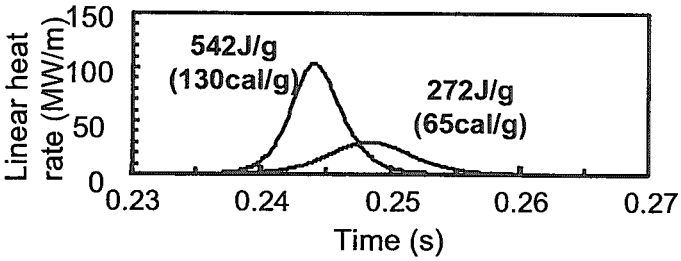
- Outline of NSRR tests
- Test matrix
- Key observations (from PWR, BWR and MOX fuel tests)
  - (1) Hydride-assisted PCMI failure at low enthalpies
  - (2) Fuel fragmentation and mechanical energy generation
  - (3) Large rod expansion and fission gas release
  - (4) Possible MOX effects (Roles of plutonium agglomerates)
- Recent test results
  - PCMI Deformation Measurement (FK-10, TK-10)
  - Fission Gas Release
    - Influence of Rod Internal Pressure (TK-3, 9)
    - Plenum Gas Temperature Measurement (TK-10)
- Summary

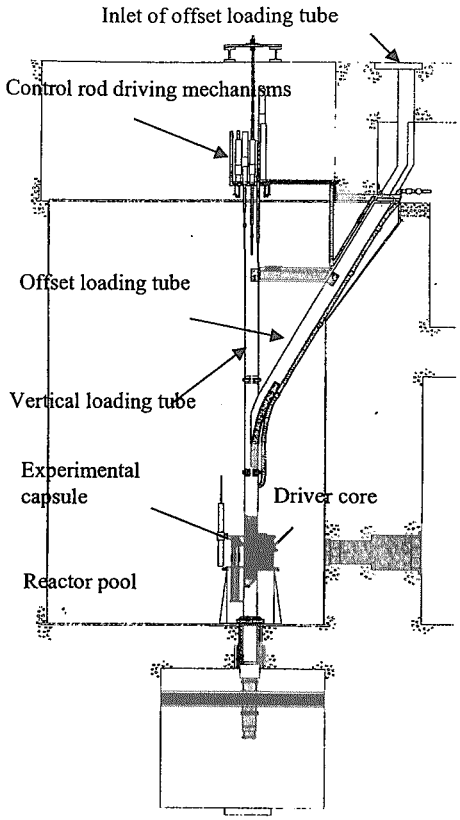
2

JAERI

NSRR (Nuclear Safety Research Reactor)



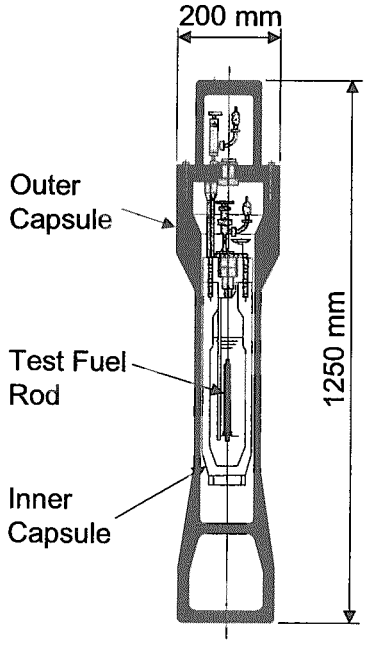




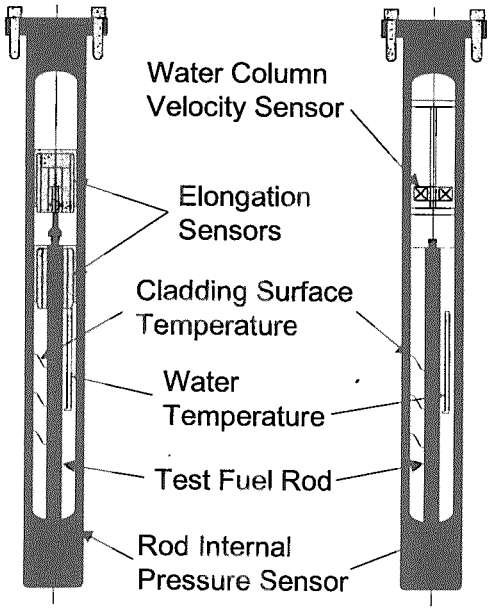
3

JAERI

Irradiation Capsule and Instrumentation



Test Capsule



Instrumentation

4

JAERI

Test Matrix

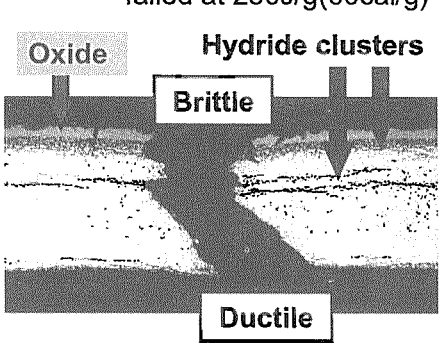
Fuel type	Burnup (GWd/t) 10 20 30 40 50 60	Number of tests Remarks	Progress in 2001-2002 (Objectives) [burnup]
PWR		24, failure >250J/g(60cal/g) at 50GWd/t	2 tests [50GWd/t] (Pre-pressurization) (Plenum gas temp/strain meas)
BWR		16, failure >259J/g(62cal/g) at 61GWd/t	2 tests (Strain measurement)[61GWd/t] (Power oscillation) [56GWd/t]
ATR/MOX		5, no failure < 584J/g (140cal/g) at 20GWd/t	*Preparation for tests with fuel at 30-40GWd/t
High enriched Irradiated in JMTR		22, failure >667J/g(160cal/g) at 38GWd/t	1 test at 25GWd/t (Power oscillation)

5

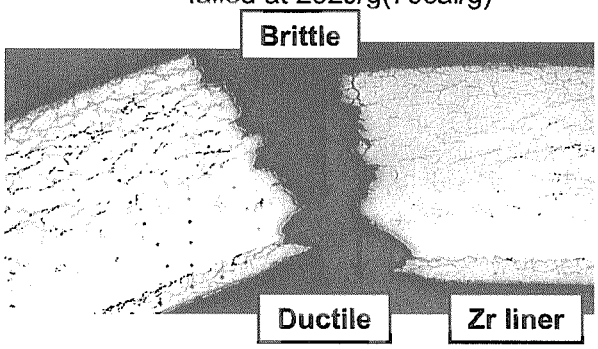
JAERI

Key Observations

PWR 50GWd/t failed at 250J/g(60cal/g)



BWR 61GWd/t failed at 292J/g(70cal/g)



KEY OBSERVATIONS in NSRR Experiments

(1) Hydride-assisted PCMI failure at low enthalpies

(2) Fuel fragmentation and mechanical energy generation

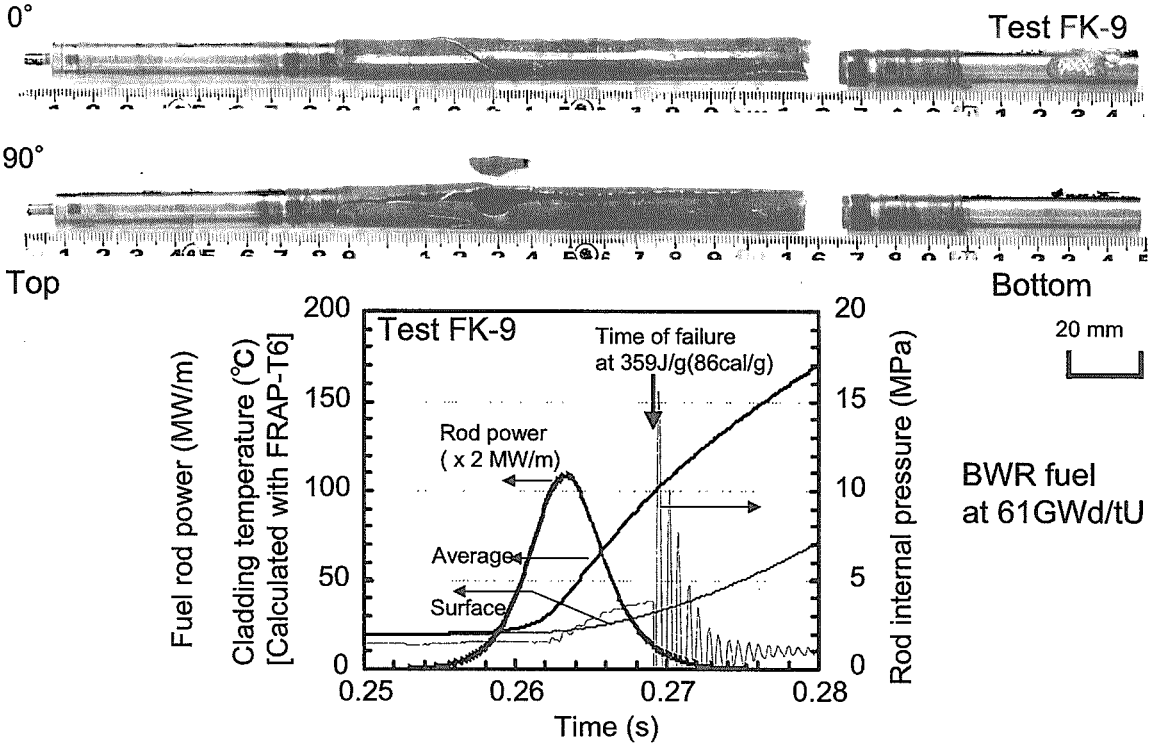
(3) Large rod expansion and fission gas release

(4) Possible MOX effect (Role of Plutonium agglomerates)

6

JAERI

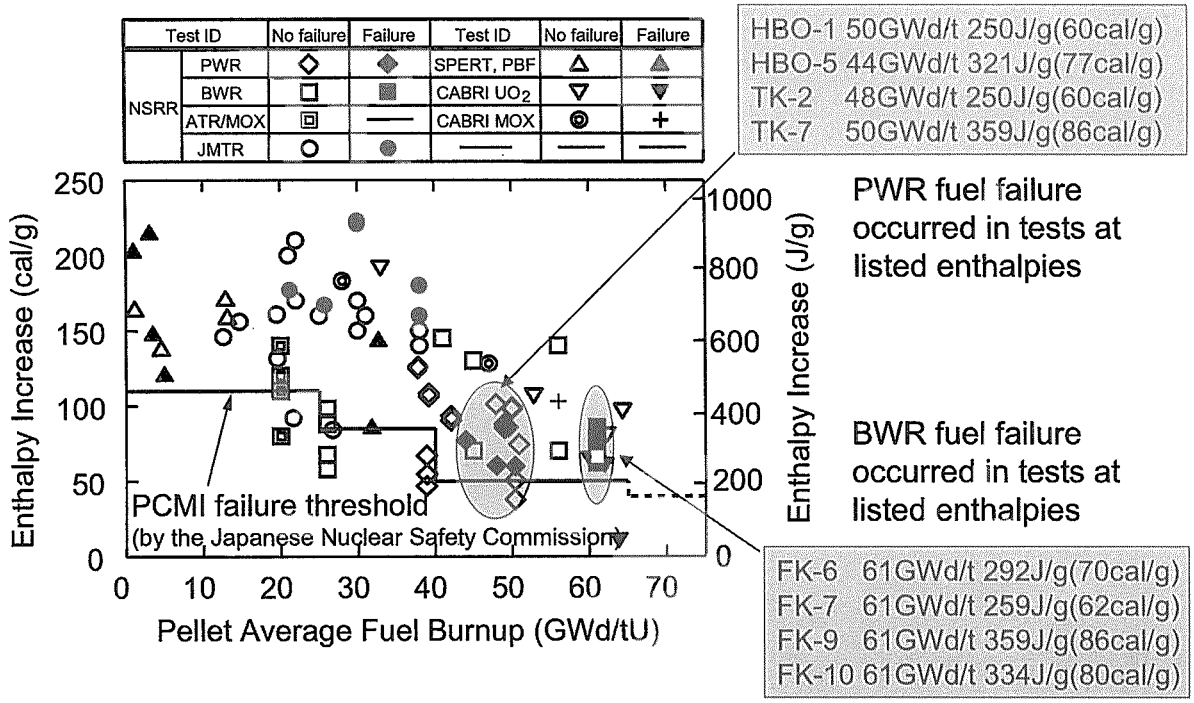
(1) Hydride-assisted PCMI failure at low enthalpies



7

JAERI

PCMI Failure Thresholds

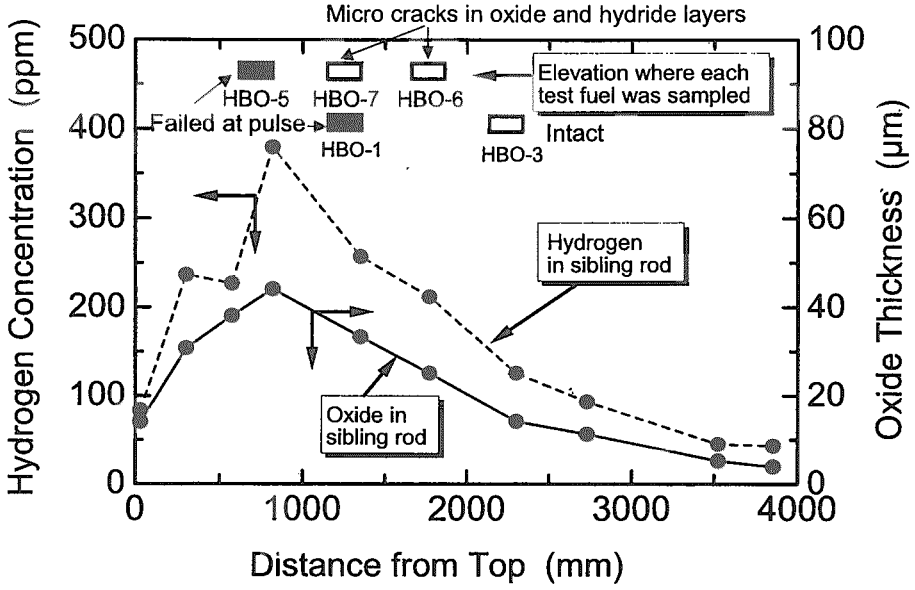


8

JAERI

Failure in segments at higher elevation

Thicker oxide and higher hydrogen content correlated well to failure in PWR fuel tests

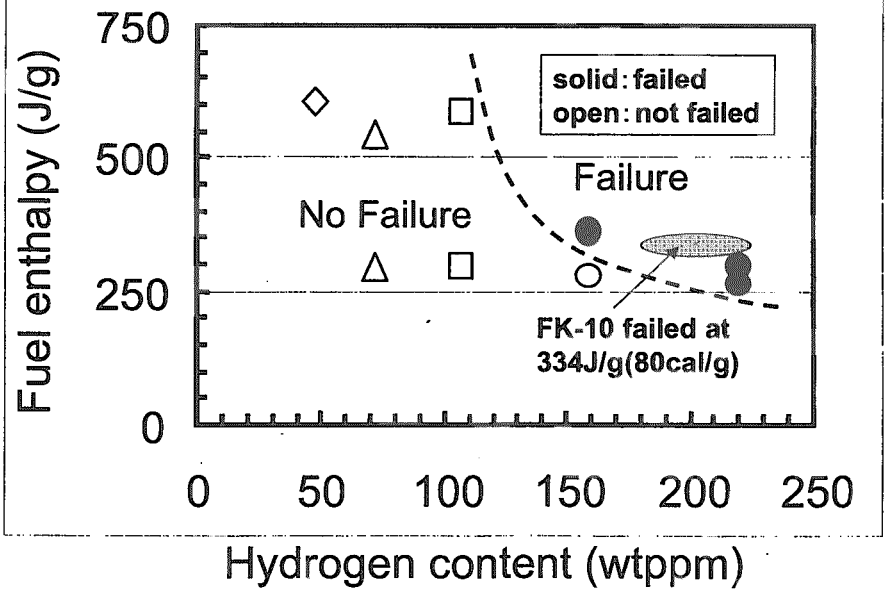


9

JAERI

Failure Map in Terms of Hydrogen Content and Fuel Enthalpy for BWR Fuel

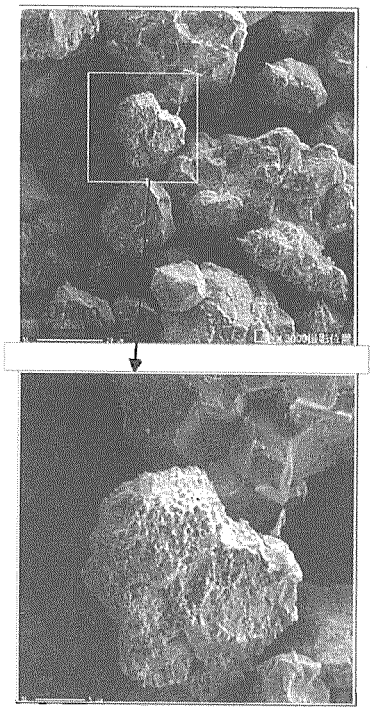
Fuel failure correlates well to hydrogen content in cladding in BWR fuel tests.



10

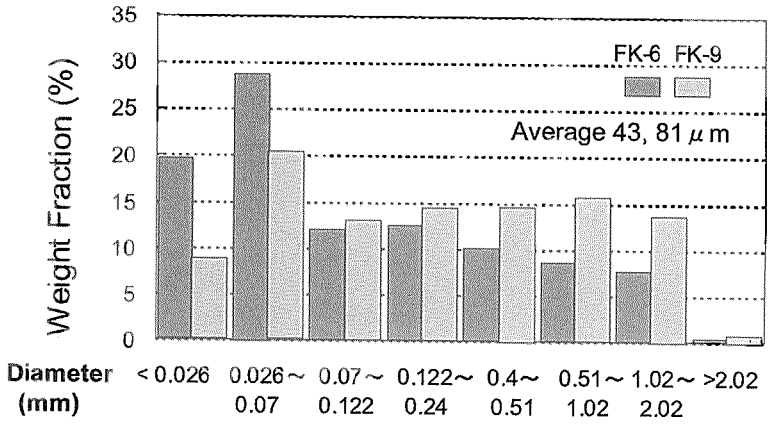
JAERI

Test FK-9



(2) Fuel Fragmentaion and Mechanical Energy Generation

- Thermal interaction of released fuel fragments and water could cause violent steam generation to convert thermal energy to mechanical.
- Coolability of fragments would depend on their size.



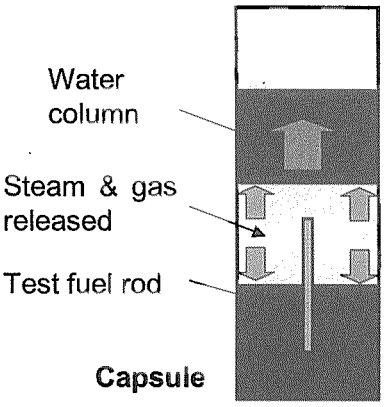
11

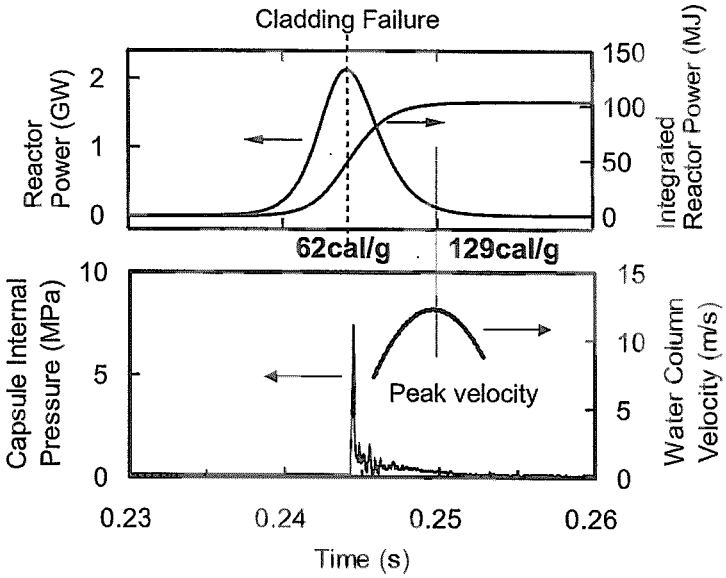
JAERI

Mechanical Energy Generation

- Pressure pulse
- Water hammer generation were observed

⇨ Data to assess impact of fuel failure for integrity of reactor components



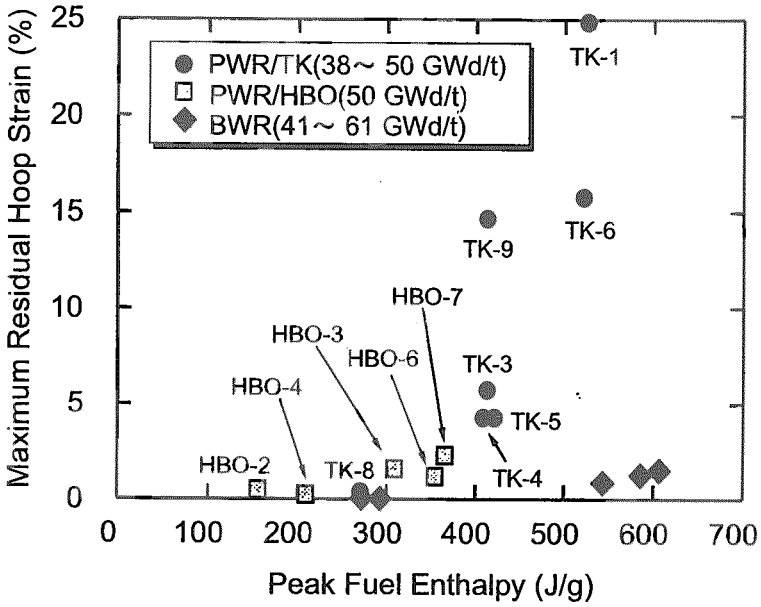


12

JAERI

(3) Large Rod Expansion and Fission Gas Release

Quite large fuel rod swelling occurred when cladding temperature escalated to about 1,000K or higher.

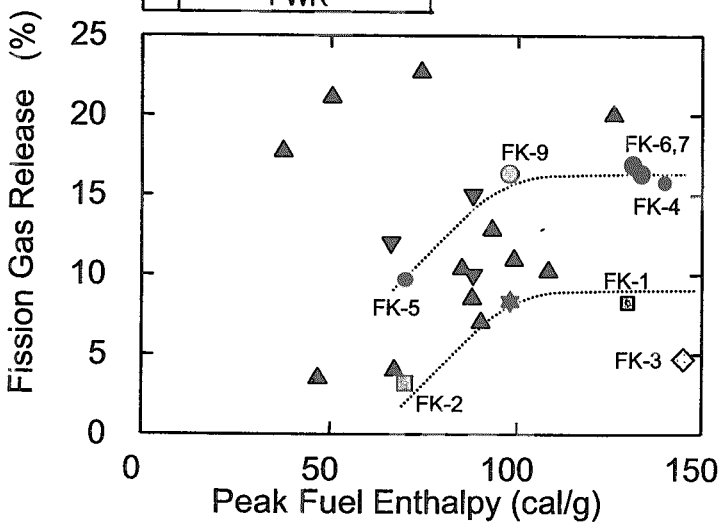


13

JAERI

Fission Gas Releases in PWR and BWR Fuel Tests

	Fuel Burnup (GWd/t)		FGR during base-irradiation
◎	FK-8,9	61	12
●	FK-6,7	61	14.2
◇	FK-3	41	0.35
▣	FK-1,2	45	1.5
●	FK-4,5	56	12.5
▼	TS	26	19.7
▲	PWR		



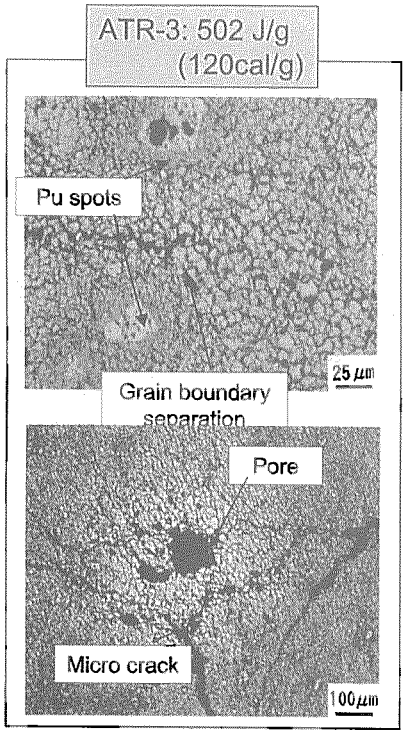
Fission gas releases of up to about 20% occurred during the simulated RIA transients additional to those released during base irradiation

Data to assess impact of fuel failure for source term evaluation

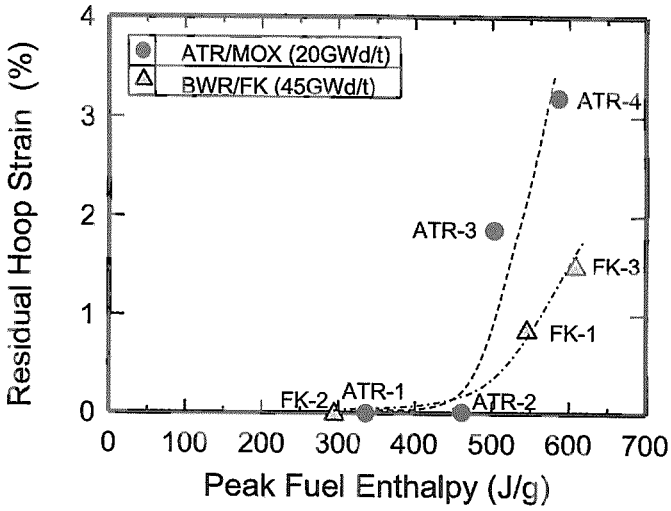
14

JAERI

(4) Possible MOX Effect (Role of Plutonium Agglomerates)



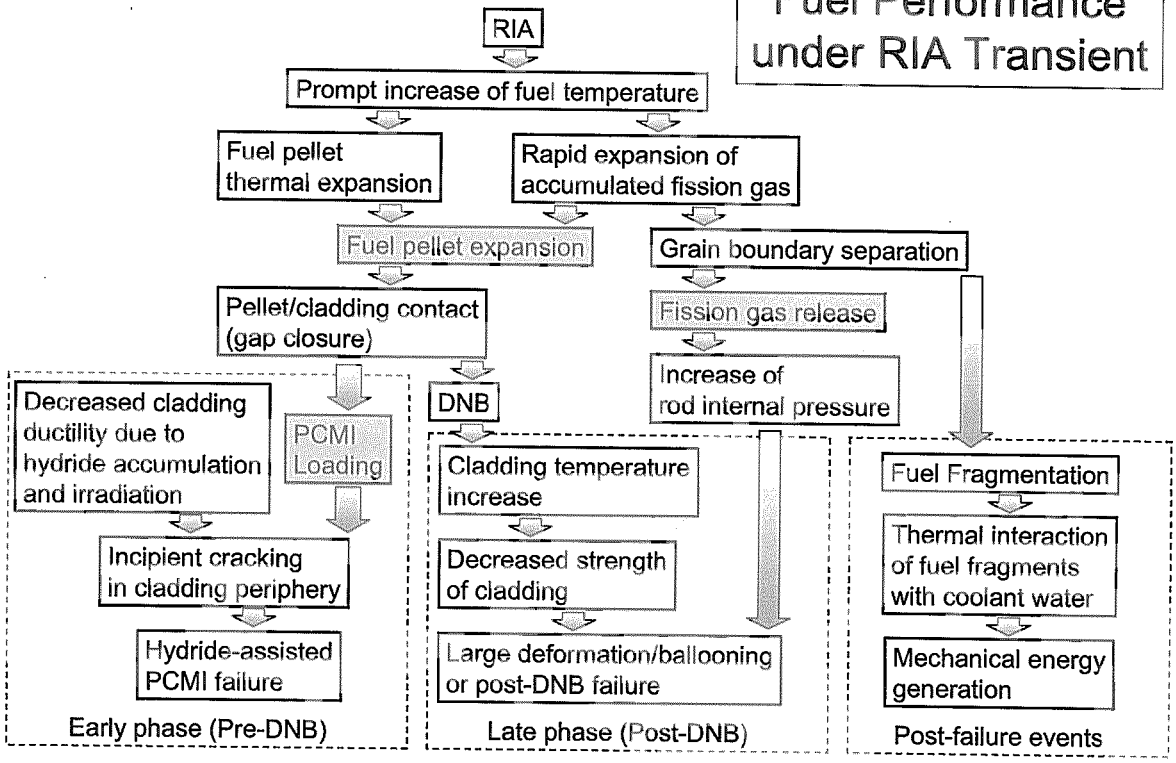
Relatively large rod swelling and fission gas released, which could be resulted from higher burnup and enthalpy at Pu agglomerates.



15

JAERI

Fuel Performance under RIA Transient



16

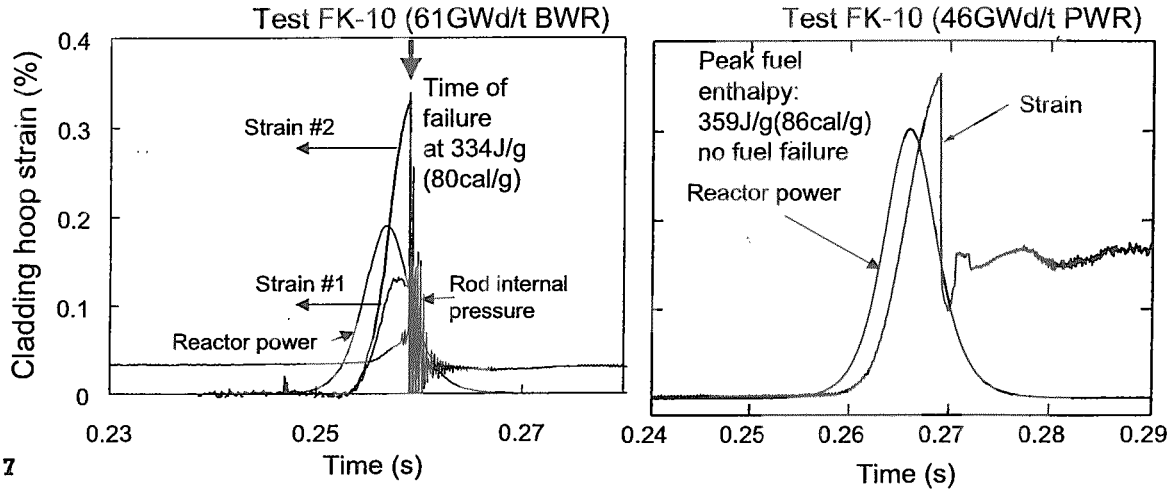
JAERI

Recent Test Results

First measurement of transient cladding hoop deformation by PCMI in Tests FK-10 &TK-10

Small hoop deformation (of about 0.4%) was measured at fuel enthalpy of about 80cal/g, suggesting that deformation could be explained only with thermal expansion of pellets.

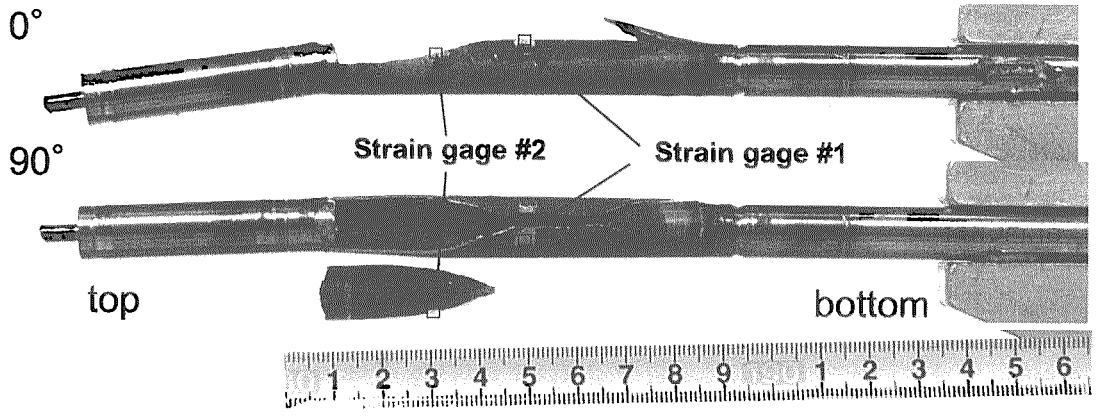
For quantification, improvement of reliability on attaching techniques of strain gages and data accumulation would be needed.



JAERI

Appearance of FK-10 Fuel Rod after Pulse Irradiation Test

Failed at 334J/g(80cal/g)

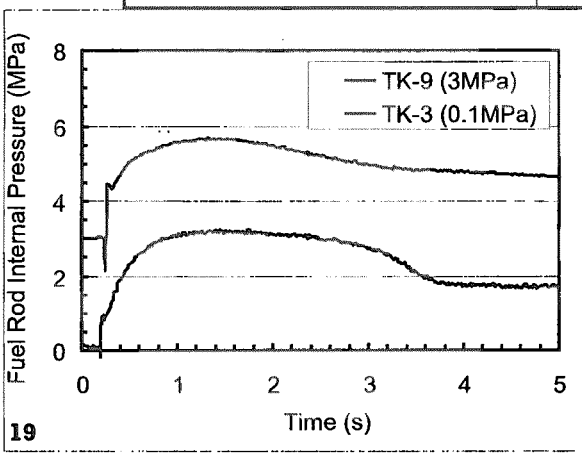


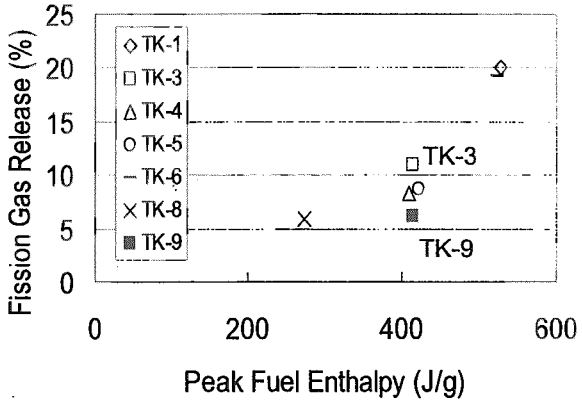
JAERI

Fission Gas Release

Influence of Rod Internal Pressure

Test No.	TK-3	TK-9
Initial Pressure (MPa)	0.1	3
Peak Fuel Enthalpy (cal/g)	99	99
Residual hoop strain (%)	6	14.6
Transient FGR (%)	10.9	6.2



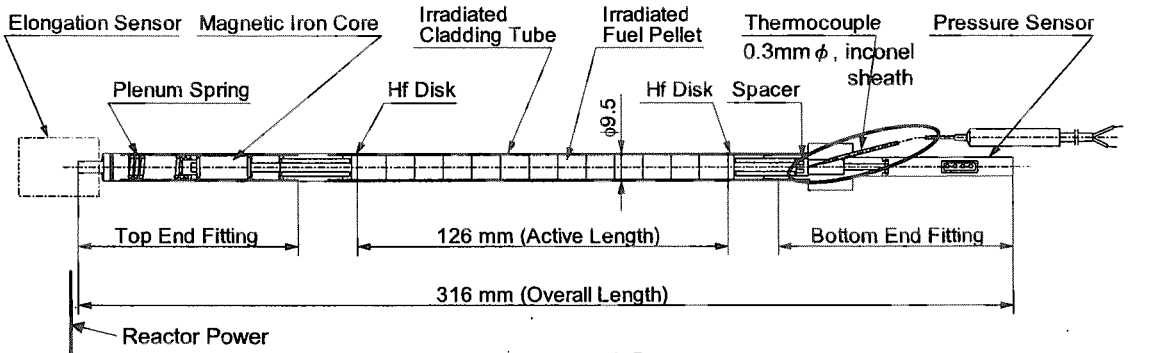


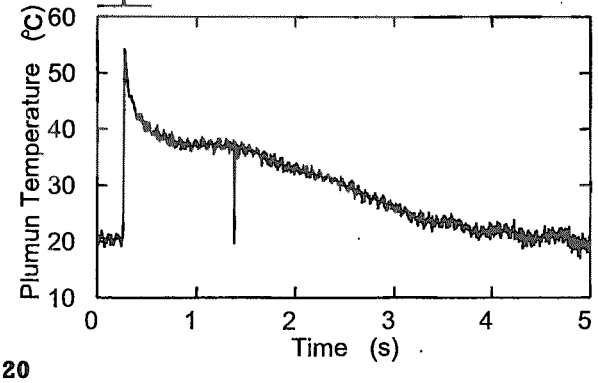
19

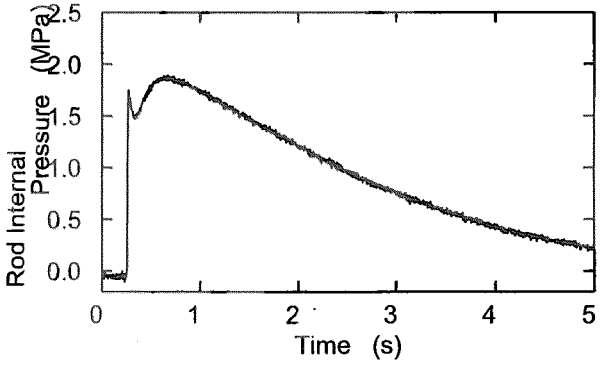
JAERI

Fission Gas Release

Plenum gas temperature measurement





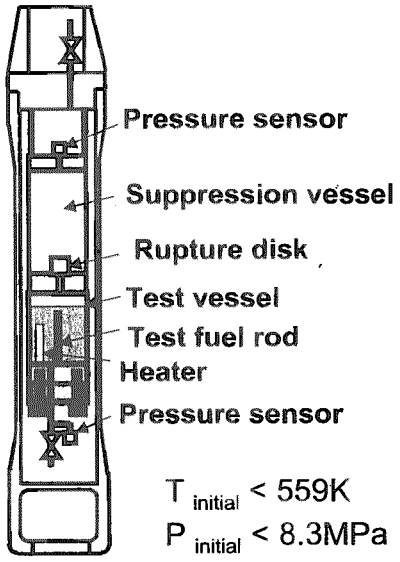


20

JAERI

Future plan of NSRR Tests

- ALPS program
- Domestic high burnup fuel tests
  PWR : ～60GWd/t with Zirlo/MDA/NDA
  BWR : ～65GWd/t, 9x9
  ATR/MOX : 30-45GWd/t .
- High temperature high pressure capsule tests
- Improvement of accuracy/reliability of new measurement, e.g. cladding hoop strain, plenum gas temperature
- Cladding mechanical testing
  (burst, ring tensile, fracture toughness)
- Test under power oscillation conditions



Schematic configuration of
high temperature high pressure capsule

21

JAERI

Summary of NSRR RIA Tests

- Outlines of NSRR RIA tests and key observations through them on high burnup PWR, BWR and MOX fuels are presented. The keys are,
  (1) Hydride-assisted PCMI failure of high burnup PWR and BWR fuels at low enthalpies,
  (2) Fuel fragmentation and mechanical energy generation,
  (3) Large rod expansion and fission gas release, and
  (4) Possible MOX effects.
- In the recent tests, measurement of transient cladding hoop deformation has been initiated using strain gages, in order to quantify the PCMI loading and its mechanism.
- The fission gas release was smaller in pressurized fuel rod than in those at atmospheric pressure. Plenum gas temperature measured in test TK-10, indicated limited temperature increase by about 30K for a few seconds.

22

Discussion:

Q: (D. Schrire)
Is slide No.1, dose the calculated Tclad with FRAP-T include direct gamma-heating of the clad?

A: Yes.

Q: (M. Billone)
In your slide No.6, you showed a much more brittle failure for the BWR cladding than the PWR cladding even though the hydrogen content is probably higher for the PWR Zry-4. Is it possible that some of the hydrides for BWR Zry-2 are radial and is it possible that the BWR Zry-2 has more radiation-induced embrittlement because it operates at a lower in-reactor temperature (. 290°C vs. . 340°C)?

A: Yes, we found some hydrides were oriented radially. The crack seemed to propagate along the hydrides. Hydrogen content in the BWR cladding was lower than that in the PWR cladding. Irradiation embrittlement in the matrix is one possible reason for the difference.

Q: (I. Sato / JNC)
There are two assumptions concerning impact of cladding failure. One is nominal failure where certain number of pins fails. The other is statistic failure assumption. In this assumption, only few pins will fail. But failure-propagation possibility in this statistic failure will be important.
How do you think about this possibility and do you feel that some evaluation is necessary in the future?

A: With the real bundle condition, the assembly wall is very strong and no significant impact of the pressure event is expected. Even with a consideration for possible fuel particle ejection from the failure rim, failure propagation seems very unlikely, so that I feel no need for evaluation for it.

Q: (BH. Lee)
Your test matrix includes the MOX test from ATR. I am wondering you have any testing plan for MOX fuel from LWR?

A: We will test MOX fuels from Europe in our ALPS program. Detail will be discussed on March 5.

Q: (H. Hayashi)
You compared cladding strains in ATR(MOX) fuels with those of BWR(UO_2). However, you should take account of the difference in fuel designs. Pellet diameter is larger and cladding tube of the ATR(MOX) fuel than in the BWR fuel.

A: We compared the results of ATR(MOX) fuel tests with those of BWR(UO_2) fuels, because they have similar fuel designs. However, as you mentioned, there are some differences in those designs. For the stress controlling deformation, e.g. ballooning, we should take account of the difference in stress due to the various cladding thickness.

Session 2a-2

NSRR Test Results under Simulated Power Oscillation Conditions of BWRs

Jinichi Nakamura, Makio Yoshinaga, Kazuyuki Kusagaya, Takehiko Nakamura,
Ryuji Hosoyamada, Motoe Suzuki and Hiroshi Uetsuka
JAERI

ABSTRACT

The power oscillation can occur in BWRs due to the void fraction fluctuation at low flow and high power conditions. The probability of this event is much higher than that of RIA. Therefore, it is recognized to be important to clarify the fuel behavior under power oscillation conditions. However, the period of the oscillation is about 2 seconds, and it was difficult to perform fuel irradiation tests in test reactors under such conditions. JAERI has developed new operational methods of the NSRR to execute tests under simulated power oscillation conditions of BWRs. The reactor control system in the NSRR was modified to achieve high power transients, which is named the Shaped Pulse (SP) operation. For the power oscillation test, a high accuracy simulator was developed for the best use of the capability of the NSRR. These modifications enable the NSRR to perform tests under simulate power oscillation condition of BWRs.

Three types of fuel were tested under simulated power oscillation conditions in the NSRR. One is high burnup BWR fuel (56GWd/t) test, with 4 power oscillation cycles, to clarify the behavior of high burnup fuel. The second one is high enriched fuel (20%) test, with 7 power cycles, to perform the test under smaller subcooling conditions. The third one is un-irradiated fuel test with fuel center thermocouple, to clarify the thermal behavior and cooling conditions during power oscillation.

The fuel behavior data, such as cladding elongation, fuel stack elongation, cladding temperature, etc. were obtained in these tests. The DNB did not occur in these tests. The PCMI was observed through cladding elongation and fuel stack elongation during power oscillation, but the residual strain of cladding was very small. In the high burnup fuel tets, cladding elongation was less than 0.05% and showed similar behavior with fuel stack elongation. FEMAXI-6 calculation suggested that the bonding will significantly suppress the pellet stack elongation during power oscillation. It is suggested that the PCMI during power oscillation remained relatively mild as long as the DNB does not occur.

JAERI

NSRR Test Results under Simulated Power Oscillation Conditions of BWRs

J.Nakamura, M.Yoshinaga, K.Kusagaya, T.Nakamura,
R.Hosoyamada, M.Suzuki and H.Uetsuka
JAERI

Fuel Safety Research Specialist's Meeting
March 4-5, 2002 at Tokai, Japan

1

JAERI

Contents

- Background and objective
- How to perform power oscillation tests in the NSRR

- Test results
  - High burnup BWR fuel(56MWd/kgU) : FK-11 test
  - JMTR pre-irradiated high enriched (20%) fuel (25MWd/kgU) : JMH-6 test

2

JAERI

Background

- Power oscillation can occur in BWRs due to the void fraction fluctuation at low flow and high power conditions.(e.g.Lasall-2,1988)
- The probability of this event is much higher than that of RIA. It is important to clarify the fuel behavior under power oscillation conditions especially at high burnup.

3

JAERI

Objective

- To perform fuel irradiation tests in the NSRR under simulated power oscillation conditions of BWRs
- To clarify the fuel behavior during power oscillation of BWRs

4

JAERI

How to perform power oscillation tests in the NSRR

- Reactor control system modification to achieve high power transient(1985)
- Development of high accuracy simulator for the best use of the capability of the NSRR safely

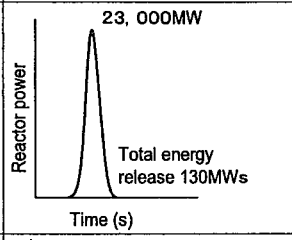
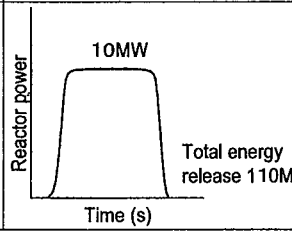
⇩

- These developments enable the NSRR to perform fuel irradiation tests under simulated power oscillation conditions of BWRs.

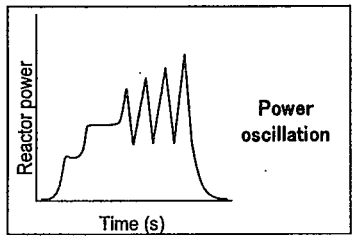
5

JAERI

NSRR operation modes and reactor power shapes

Operation mode	Typical reactor power shape
Natural pulse operation	 Reactivity initiated accident at zero power
Shaped pulse operation	 Abnormal power transient

Withdrawal of transient rod



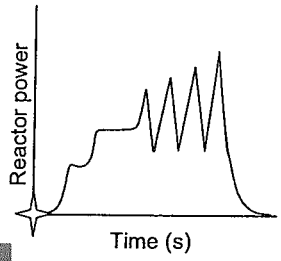
Rapid withdrawal and insertion of regulating rods

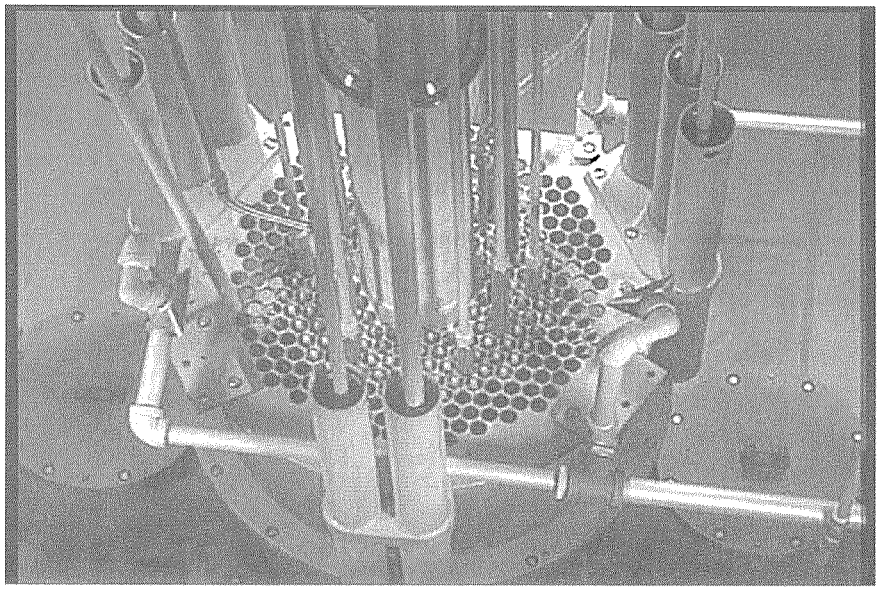
Development of high accuracy simulator for the best use of the capability of the NSRR safely

6

JAERI

Video of power oscillation operation





7

JAERI

Test matrix for power oscillation tests

	Test conditions		Coolant conditions	Instrumentation
	Number of power oscillation	MAX LHR (kW/m)		
High burnup BWR fuel(56GWd/t) (FK-11)	4	48	Room temperature	CE FE CT
JMTR preirradiated high enriched (20%) fuel (25GWd/t) (JMH-6)	7	95	Smaller subcooling conditions with heater Reduced amount of available coolant with channel tube	CE CT
Un-irradiated fuel with center thermocouples (563-1,563-2test)	4 or Two step ramp	61	Room temperature	FT CE FE CT

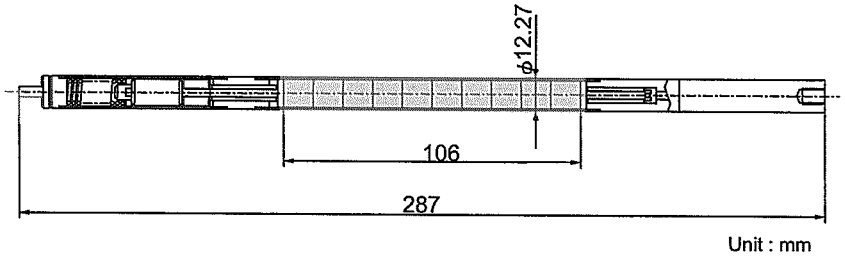
CE:cladding elongation, FE:fuel stuck elongation,

CT:cladding temp., FT:fuel center temp.

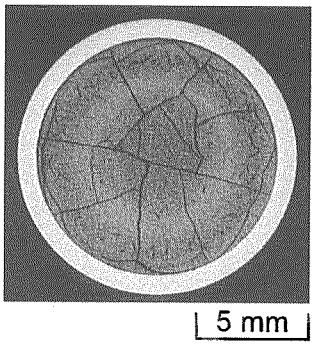
8

JAERI

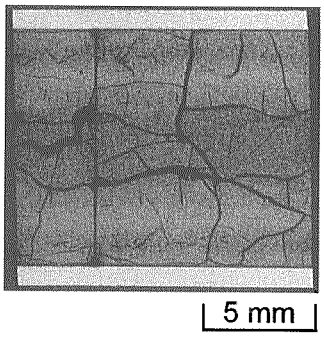
Fuel rod for FK-11 test

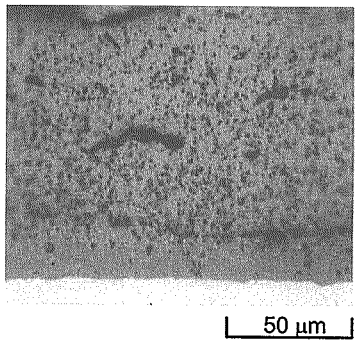


BWR 8x8 type rod, Burnup:56 GWd/t,



Sibling rod (4 cycle irradiation)



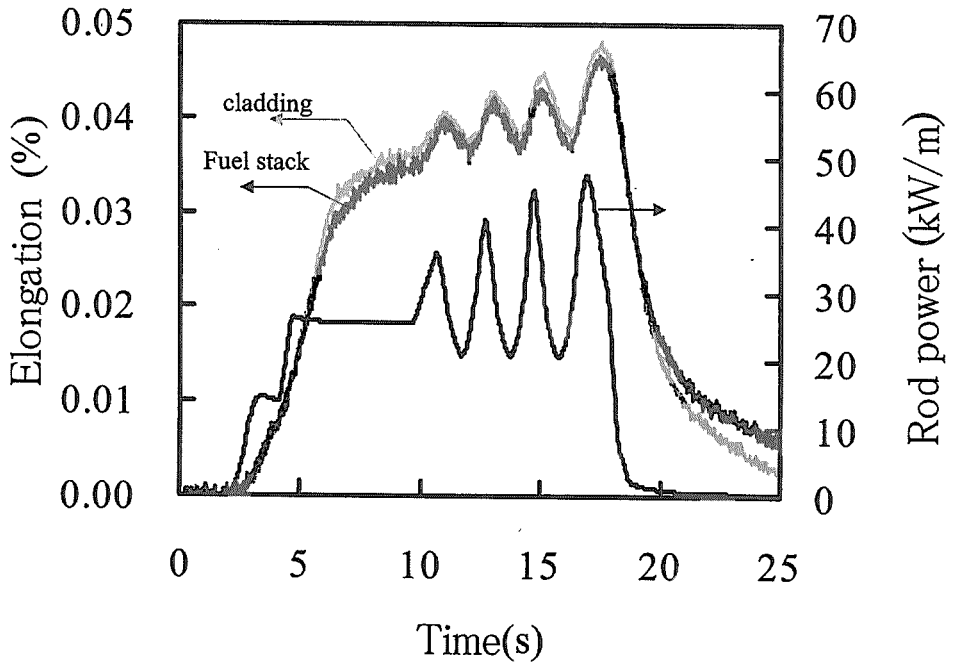


Bonding at pellet cladding gap

9

JAERI

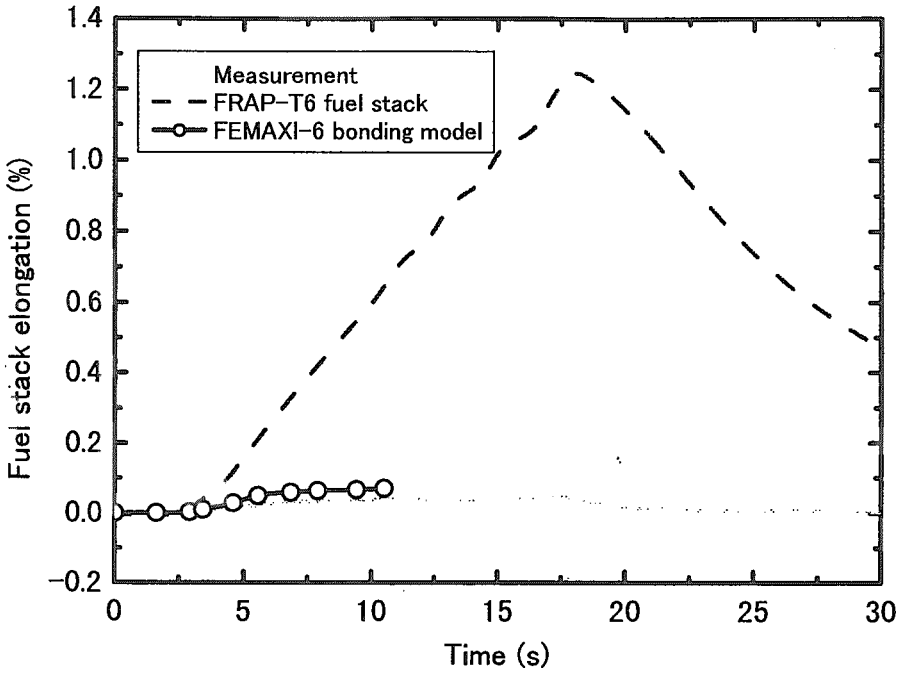
Rod power and elongation of High burnup BWR fuel(FK-11)



10

JAERI

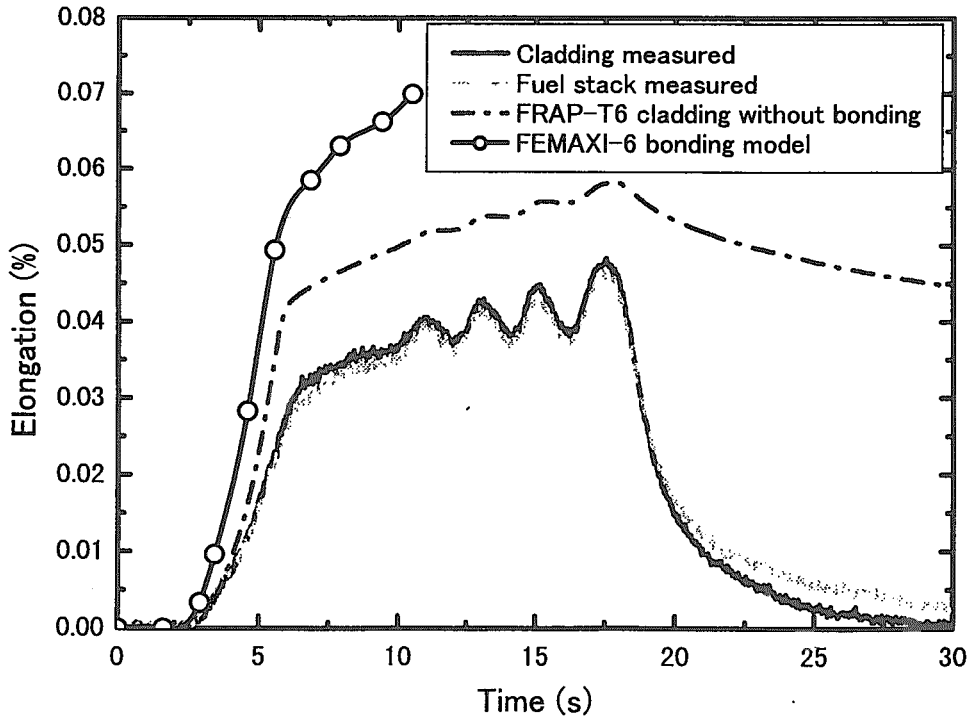
Fuel stack elongation of FK-11
Comparison of measurement and calculation



11

JAERI

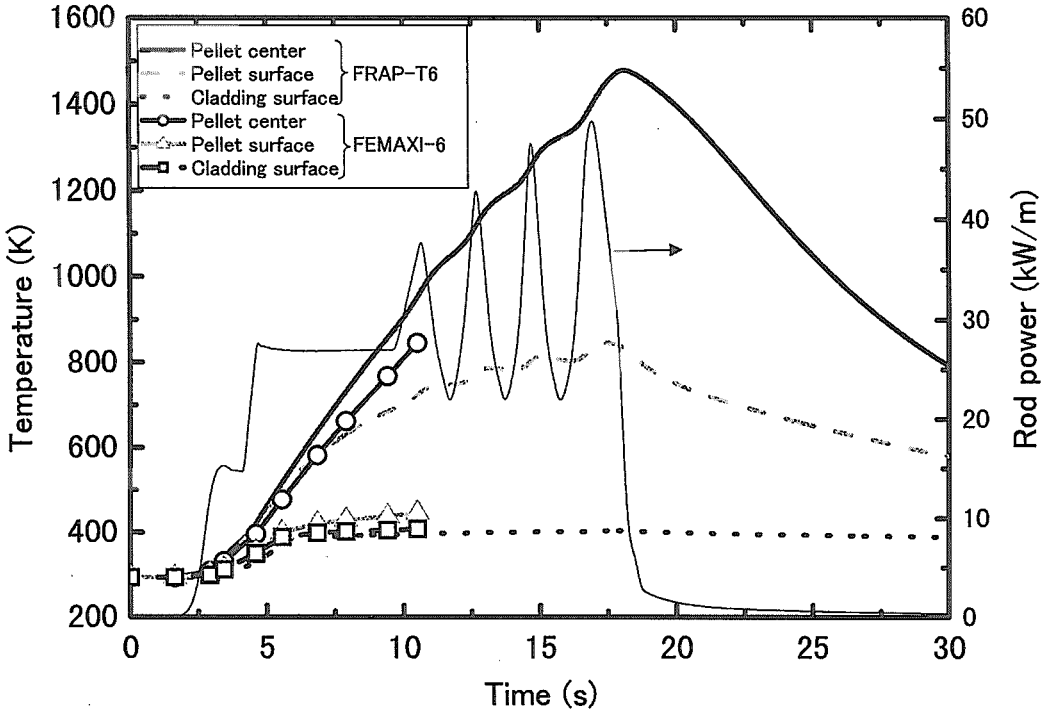
Cladding elongation and fuel stack elongation of FK-11
Comparison of measurement and calculation



12

JAERI

Calculation of fuel temperature FEMAXI-6 with bonding model and FRAP-T6



13

JAERI

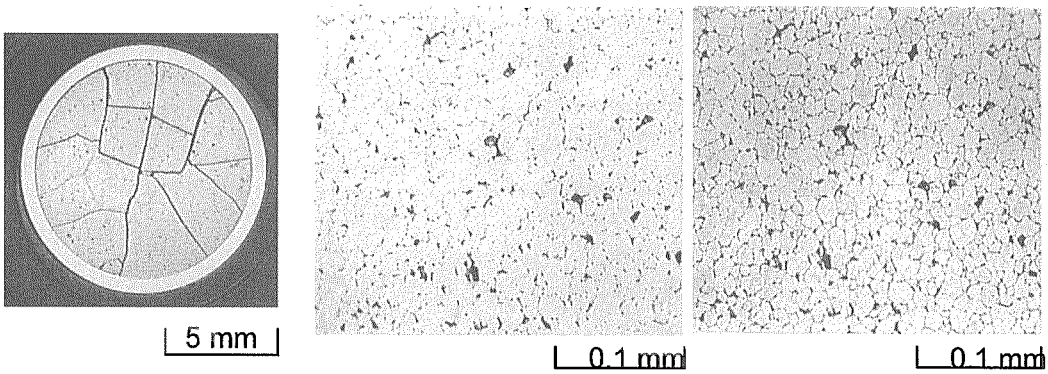
Fuel rod for JMH-6 test

To investigate fuel behavior under high power and smaller subcooling conditions

14x14 type PWR fuel rod with 20% enrichment

Pre-irradiated in JMTR up to 25GWd/t at about 30kW/m

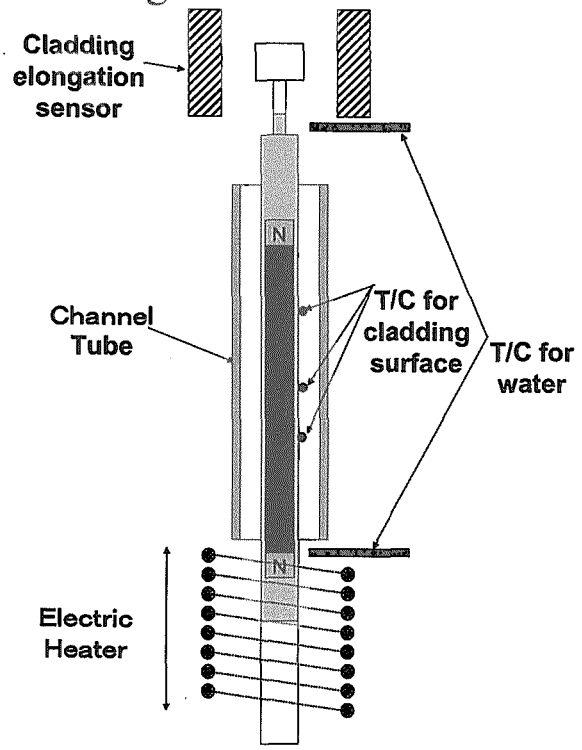
Initial gap :190μm, gap remains after pre-irradiation in JMTR



Sibling rod　　Polished(Center)　　Etched (Center)　14

JAERI

Configuration around fuel rod (JMH-6)

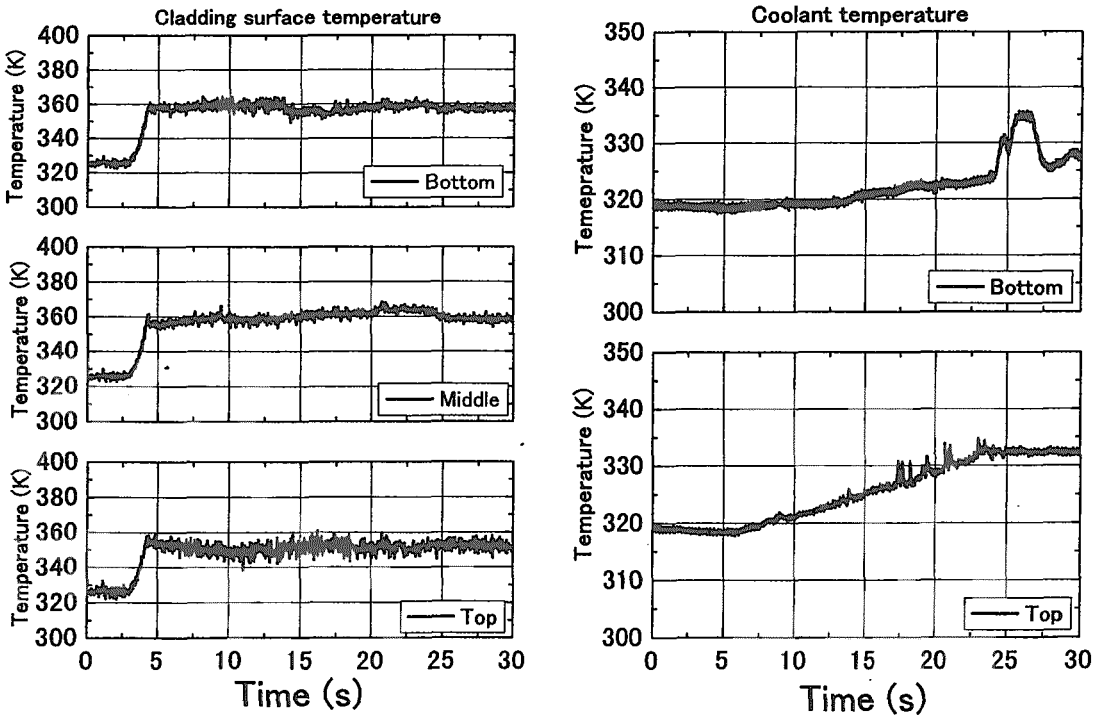


- Smaller subcooling with electric heater
- Reduced amount of available coolant with channel tube

15

JAERI

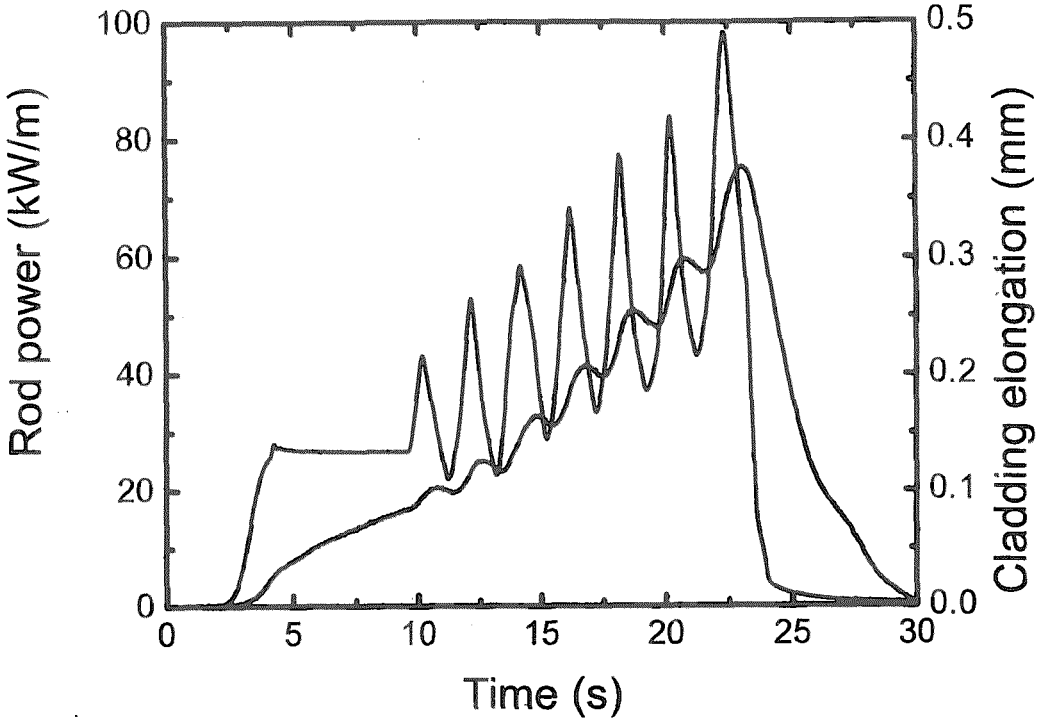
Cladding temperature and coolant temperature of JMH-6 test



16

JAERI

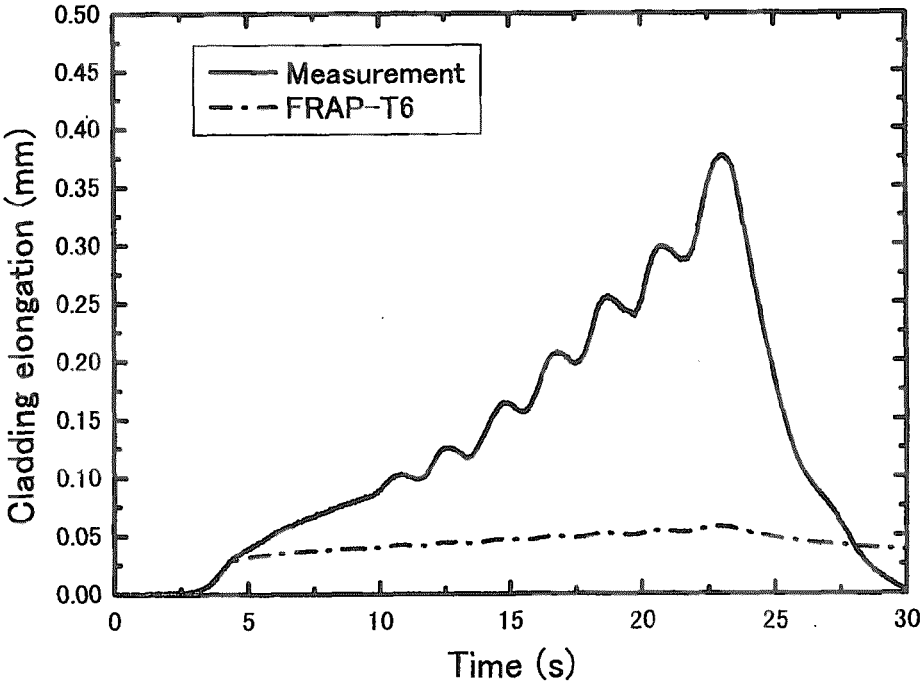
Rod power and cladding elongation of JMH-6 test



17

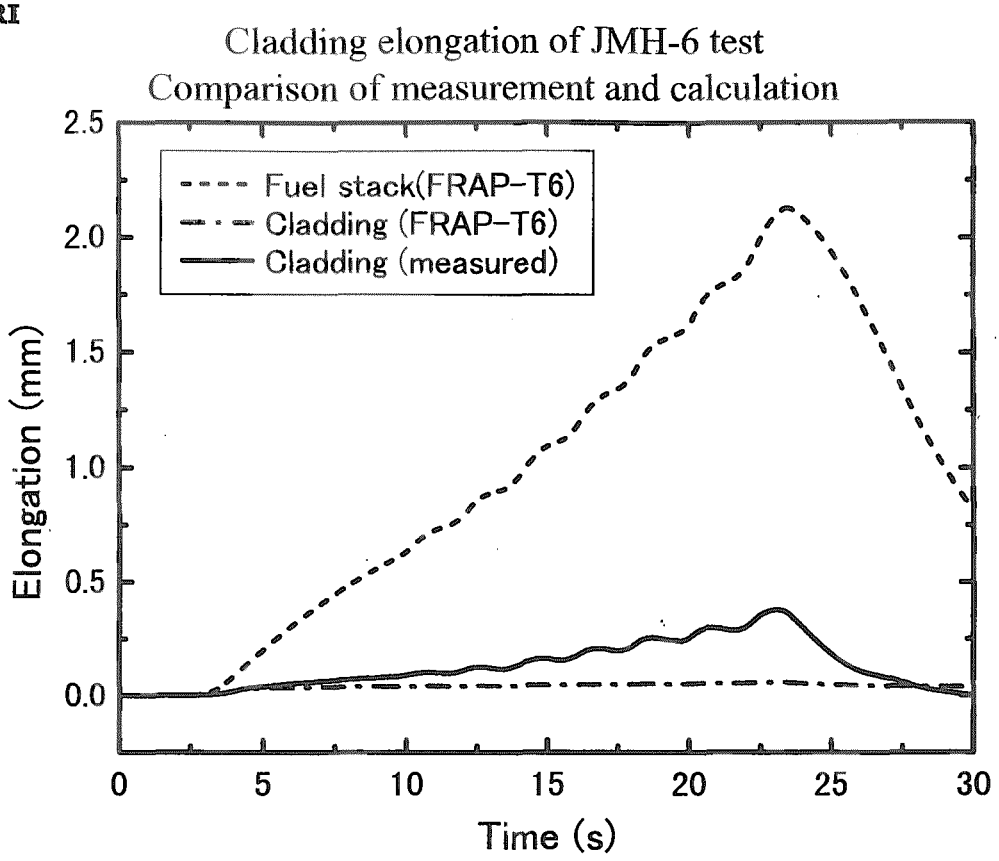
JAERI

Cladding elongation of JMH-6 test
Comparison of measurement and calculation



18

JAERI



19

JAERI

Future plan

- PIE work
  fission gas analysis, profilometry
  ceramography, SEM/XMA,
  density measurement, etc.

- Test to investigate fuel behavior under DNB conditions
  high power test with smaller subcooling condition

20

JAERI

Summary

- Irradiation tests under simulated power oscillation conditions of BWRs were performed in the NSRR with about 0.5 Hz oscillation frequency with the maximum power of 48-95 kW/m.
- PCMI was observed through cladding elongation and fuel stack elongation, but the residual strain of the cladding was very small.
- FEMAXI-6 calculation suggests that the bonding will significantly suppress the pellet stack elongation during power oscillation.
- It is suggested that the PCMI during power oscillation remained relatively mild and does not affect significantly the integrity of fuel rod as long as DNB does not occur.

21

Discussion:

Q: (D. Schrire)

Figure No.10. Response of cladding and fuel elongation to rod power oscillation. Did you evaluate from the time lag on effective time constant . to describe the response of cladding and fuel?

This would help to generalize the response (e.g. 'damping factor' = amplitude of EL_{clad} / amplitude of LHR) for various types of oscillations.

A: No, I have not yet evaluated the time constant from the lag of response.

Session 2a-3

Temperature Effect on BWR Cladding Failure under Mechanically Simulated RIA Conditions

V. Grigoriev, R. Jakobsson and D. Schrire
Studsvik Nuclear AB, SE-611 82, Nyköping, Sweden

Abstract

Samples of Zircaloy-2 cladding with different manufacturing processes from two BWR fuel rods with a burnup of 40-42 MWd/kgU have been mechanically tested at 25, 100, 130 and 300°C under RIA conditions simulated by means of the "Expansion-Due to-Compression" (EDC) testing technique developed at Studsvik. The hoop strain of the specimen at failure was determined and the Critical Strain Energy Density (CSED) for the cladding material was calculated according to earlier presented procedure [1].

Hydrogen extraction measurements were performed for each specimen and show wall-average concentrations between 60 and 900 ppm. The local oxide thickness and hydride morphology were examined metallographically in the area close to the fracture position in the specimen.

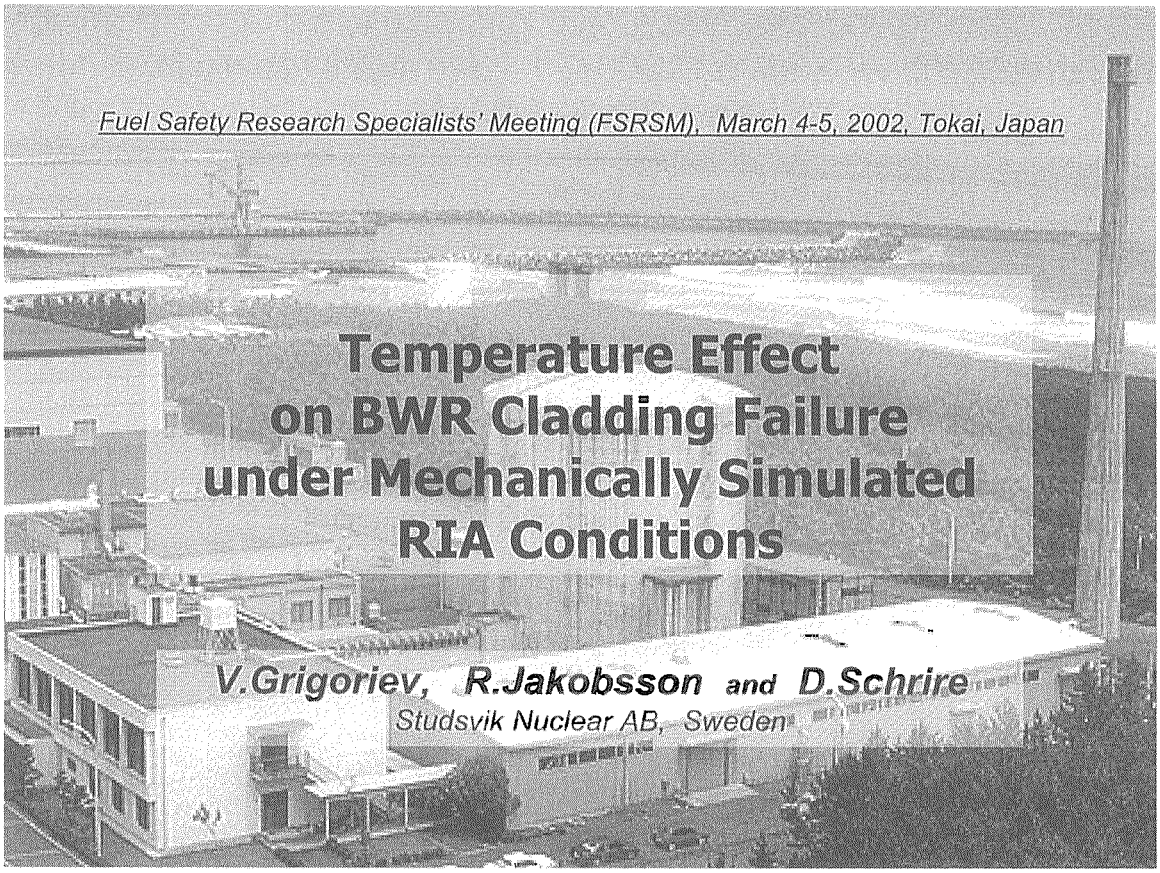
The information obtained allows analysis of the dependence of experimental CSED values on the hydrogen concentration and Oxide/Cladding Thickness (O/CT) ratio for the test temperatures below 150°C and above 280°C. The trends observed are compared to the published data on CSED values derived from mechanical property tests as well as from the in-reactor CABRI REP-Na tests and NSRR tests performed in the same temperature intervals [2, 3].

The CSED values obtained from the laboratory EDC test agree reasonably well with the published values. Test temperature and hydrogen concentration appear to be the controlling factors for cladding failure. The O/CT ratio alone cannot properly describe the variation of the CSED values for hydrogen concentrations below 200-300 ppm. An abrupt increase of the CSED values appears to occur at temperatures about 100°C (at least, for the investigated hydrogen concentrations of 60-130 ppm). The strain rate ("pulse width") did not appear to have a significant effect on the failure strain and CSED when the samples were tested at "pulse widths" of 25-100 ms. Only one sample has been tested at 300°C and at lower loading rate corresponding to the "pulse width" of ~1000 ms. That sample failed at lower hoop strain (lower CSED), that could mean a noticeable strain rate effect at 300°C. More data are needed to verify this observation.

The information obtained confirms the suitability of the EDC test method for evaluation of the parameters related to cladding failure under simulated RIA conditions.

References

1. Grigoriev, V., Jakobsson, R. and Schrire, D., (2001), 'Experimental Evaluation of Critical Strain Energy Density for Irradiated Cladding under Simulated RIA Conditions', *Proceedings of ENS Topfuel 2001*, Stockholm, Sweden.
2. Montgomery, R.O., Rashid, Y.R., Ozer, O., and Yang, R.L., (1997), 'Review and Analysis of RIA-Simulation Experiments on Intermediate and High Burnup Test Rods', *Proceedings of the ANS International Topical Meeting on LWR Fuel Performance*, Portland, USA, March 1997.
3. Rashid, Y.R., Montgomery, R.O., Lyon, W.F., and Yang, R.L., (2000), 'A Cladding Failure Model for Fuel Rods Subjected to Operational and Accident Transients', *IAEA Technical Committee Meeting on Nuclear Fuel Behaviour Modelling at High Burnup and its Experimental Support* (Windermere, UK). IAEA TECDOC-1233, 2000.



Fuel Safety Research Specialists' Meeting (FSRSM), March 4-5, 2002, Tokai, Japan

BWR cladding: Materials for Investigation

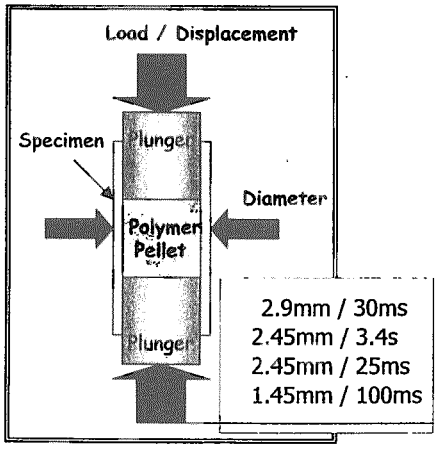
BWR Cladding Material	Elevation 1	Elevation 2
Zircaloy-2 (42.4 MWD/kgU)		
Local oxide thickness (μm)	10-15	40
Average through-wall hydrogen (ppm)	270-370	500-900
Zircaloy-2 (39.9 MWD/kgU)		
Local oxide thickness (μm)	10	15
Average through-wall hydrogen (ppm)	60-100	100-200

BWR cladding: Test program

- EDC tests (14 specimens, mechanical simulation of RIA)
- Macro-photo before and after test
- Hydrogen extraction (14 specimens)
- Metallography (6 specimens)
- Fractography (3 specimens)
- Ring tension test (6 specimens)

EDC Test Data: Derivation of CSED Values

To get the Critical Strain Energy Density (*CSED*) :

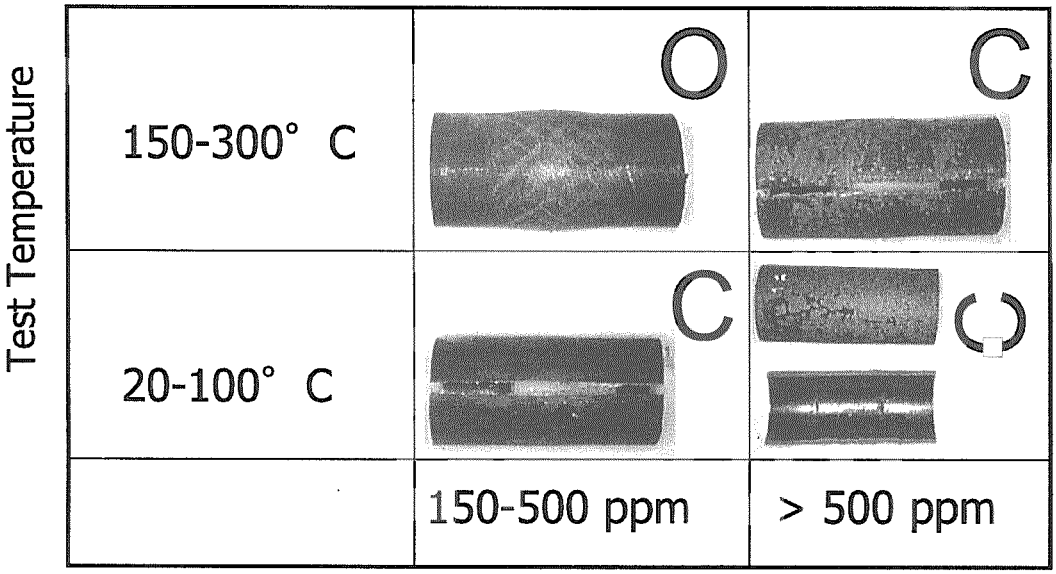


- Load-Displacement Curve (*LDC*) is corrected for machine compliance and for Polymer Pellet contraction
- Area under corrected *LDC* gives an energy (W_{abs}) absorbed by specimen
- W_{abs} determines an average Strain Energy Density (SED_{aver}) within the specimen volume (V_{spec})
- Local *SED* is proportional to a local hoop strain of the specimen
- *CSED* is derived as a local SED in the specimen cross-section with maximum hoop strain at failure

$$W_{abs} / V_{spec} \rightarrow SED_{aver} \rightarrow CSED$$

Fuel Safety Research Specialists' Meeting (FSRSM), March 4-5, 2002, Tokai, Japan

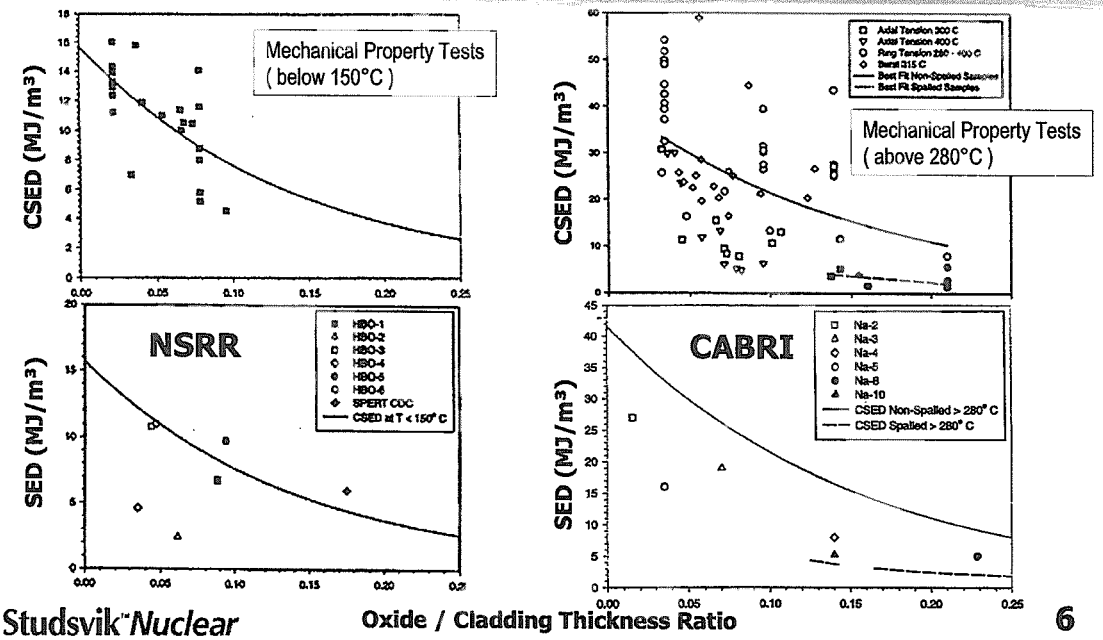
EDC test: Specimen failures



Studsvik Nuclear 5

Fuel Safety Research Specialists' Meeting (FSRSM), March 4-5, 2002, Tokai, Japan

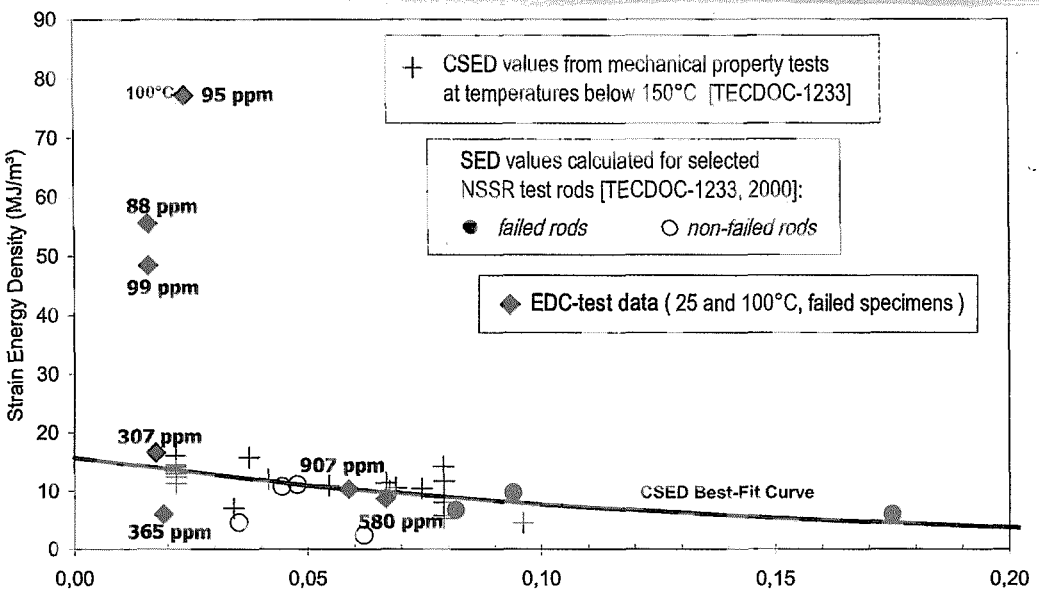
CSED Data: *J. Rashid et.al.*, IAEA TECDOC-1233, 2000



Studsvik Nuclear 6

Fuel Safety Research Specialists' Meeting (FSRSM), March 4-5, 2002, Tokai, Japan

EDC Test Data & TECDOC-1233 (< 150°C)

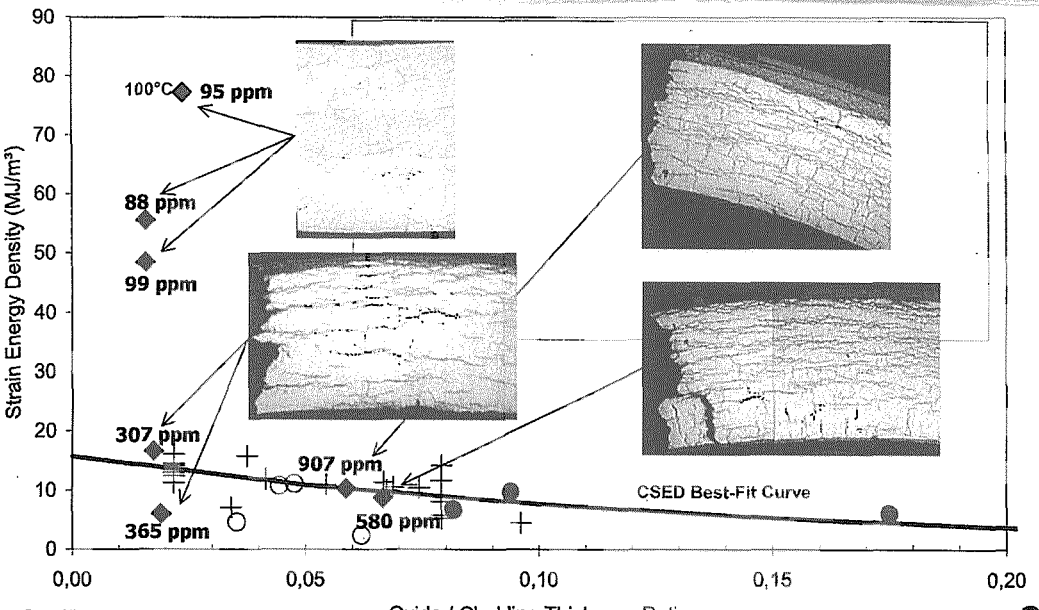


Studsvik Nuclear

7

Fuel Safety Research Specialists' Meeting (FSRSM), March 4-5, 2002, Tokai, Japan

EDC Test Data: Hydride Morphology

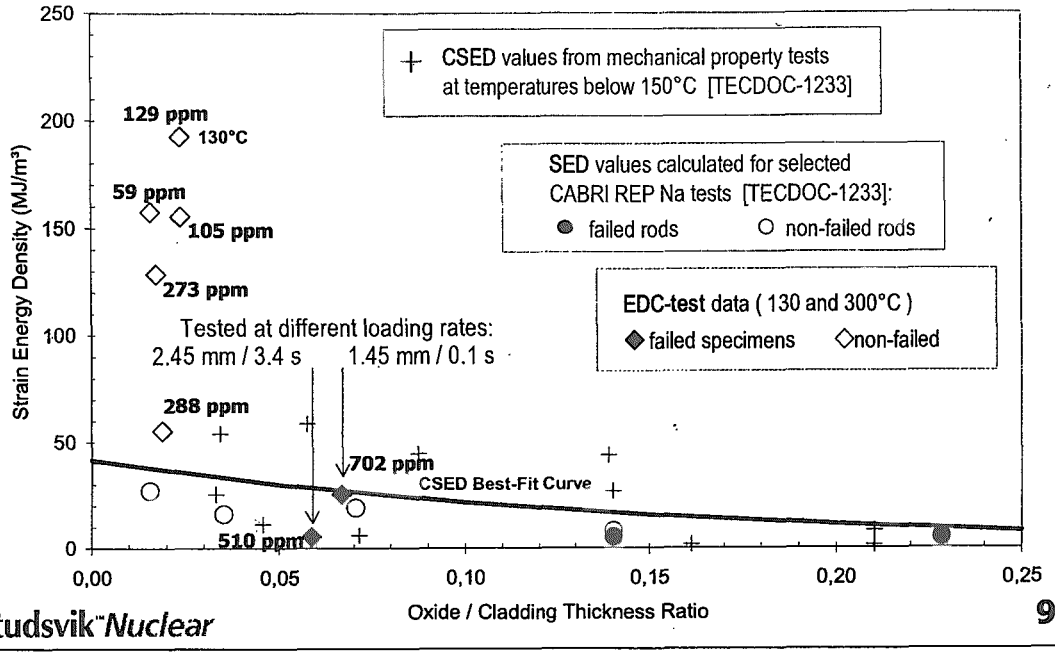


Studsvik Nuclear

8

Fuel Safety Research Specialists' Meeting (FSRSM), March 4-5, 2002, Tokai, Japan

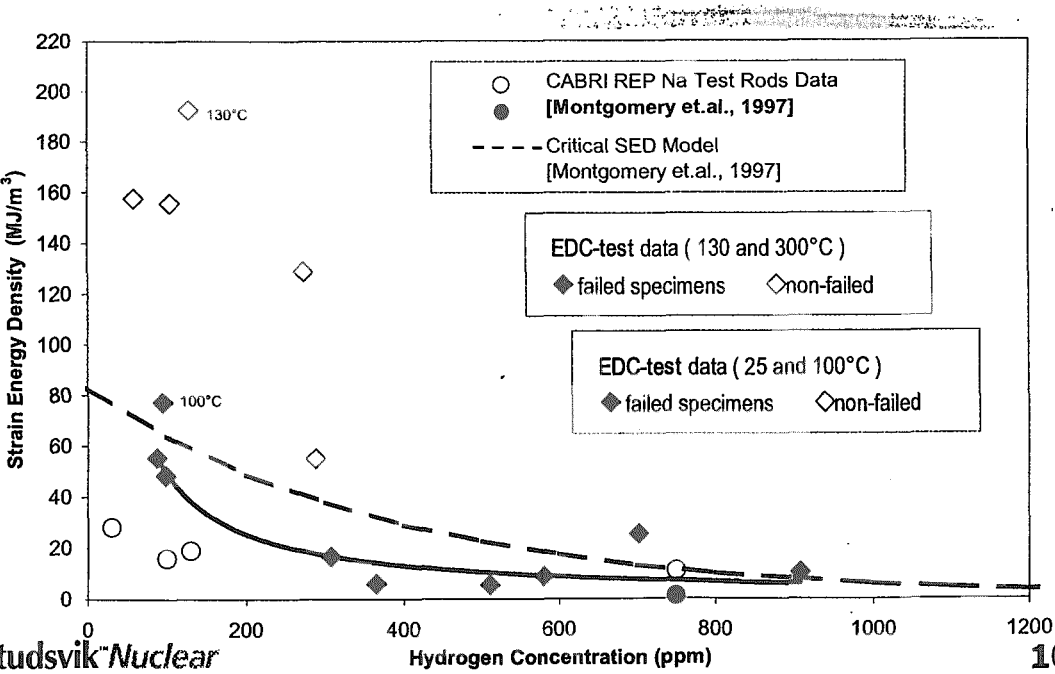
EDC Test Data & TECDOC-1233 (> 280°C)



Studsvik Nuclear 9

Fuel Safety Research Specialists' Meeting (FSRSM), March 4-5, 2002, Tokai, Japan

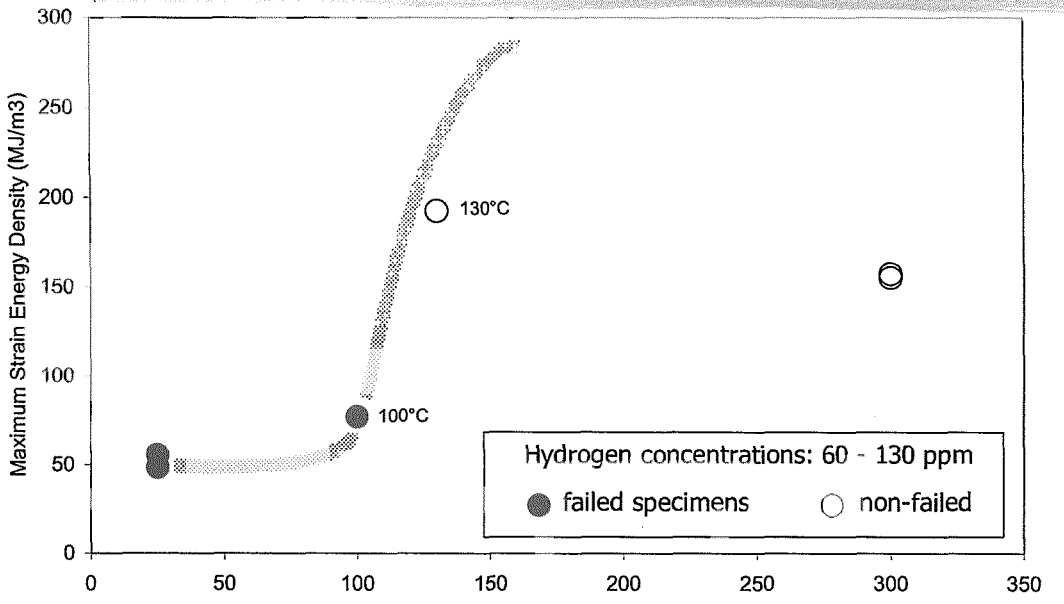
EDC-test Data: Hydrogen Effect



Studsvik Nuclear 10

Fuel Safety Research Specialists' Meeting (FSRSM), March 4-5, 2002, Tokai, Japan

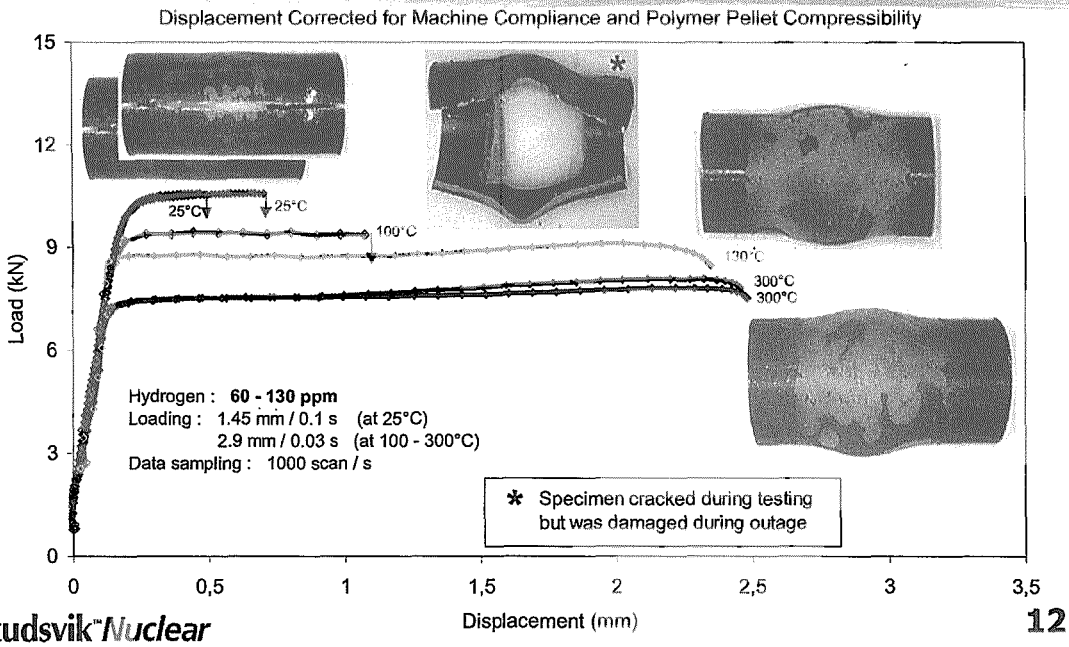
EDC-test Data: Temperature Effect



Studsvik Nuclear 11

Fuel Safety Research Specialists' Meeting (FSRSM), March 4-5, 2002, Tokai, Japan

EDC Test Data: Temperature Effect (2)



Studsvik Nuclear 12

Conclusions

- The EDC-technique has been applied to BWR irradiated cladding with burnup of ~40 MWd/kgU. The Critical Strain Energy Density (CSED) values obtained from the EDC-test agree reasonably well with the published CSED data.
- Test temperature and hydrogen concentration appear to be the controlling parameters for cladding failure. The oxide/cladding thickness ratio alone cannot properly describe the variation of the CSED values for hydrogen concentrations below 200-300 ppm.
- An abrupt increase of the CSED values appears to occur at temperatures about 100°C (at least, for investigated hydrogen concentrations of 60-130 ppm).

Planned Continuation

- To establish the temperature dependence at intermediate temperatures using BWR cladding from high burnup KKL rods (~ 66 MWd/kgU). Behaviour at intermediate temperatures may be important for real BWR RIA scenarios.

Acknowledgements

Many people from Studsvik as well as from other organisations have contributed to the results of this work. Without their efforts, which are gratefully acknowledged, the present work would not be possible. The investigations were jointly sponsored by Vattenfall Fuel, OKG, Barsebäck Kraft, Westinghouse Atom AB and Studsvik AB.

Discussion:

Comment (R. Montgomery)

Two points should be made about the data used from Rashid et al (TECDOC-1233).

First, the oxide to thickness ratio was developed for use with samples tasted from PWR cladding. For this condition, the hydrogen uptake ratio is relatively constant as a function of oxide thickness and between different Zry-4 cladding materials. It may not be appropriate to utilize the same approach for Zry-2 BWR material which has a different hydrogen pickup fraction. Certainly, it might be more appropriate to use the actual hydrogen measured for the sample. For the data report in Rashid et al hydrogen contents were not available for all the samples.

Second, the CSED date and correlations report in Rashid et al (TECDOC-1233) were developed for biaxial loading conditions. This was accomplished by applying a biaxiality correction factor to the total elongation values from the uniaxial tests. This factor will influence the date with high ductility/CSED.

Q: (D. Bottomley)

Was fractography performed on the failed cladding samples? Was a variation with temperature observed?

A: Fractography of the EDC specimens failed at room temperature and at 300°C has been performed. The character of fracture surfaces is different depending on test temperature.

Q: (P. Yvon)

What is the maximum temperature reached with this technique? Is there any lubrication between polymer pellet and clad? If there is no friction between polymer and clad, do you think this test is representative of what happens in a fuel rod with a fuel pellet?

A: The upper temperature limit for this technique is 340°C and is related to the properties of polymer pellets. There is no lubrication between clad specimen and polymer pellet. It is believed that this is relevant to the case of high burnup fuel where the rim layer is present in the fuel.

Session 2a-4 (p1, p2)

RIA-related studies at JAERI: Studies on fracture behavior and mechanical properties of cladding

Toru TAKEDA, Sadayuki UCHIKAWA
Department of Reactor Safety Research, JAERI

ABSTRACT

To obtain the fundamental data for evaluating behavior of the high burn-up fuel rod under accident conditions as well as normal operation conditions, (1) influence of radial hydride on fracture behavior of Zry-2 cladding tubes and (2) mechanical properties of hydrided Zry-4 cladding tubes in hoop direction have been examined recently.

Influence of radial hydride on fracture behavior of Zry-2 fuel cladding tube

Burst tests of hydrided Zry-2 fuel claddings (200-650wtppm), which were heat-treated for hydride re-orientation in radial direction, were performed. The objective of the present tests is to obtain basic data for evaluating the influence of radial hydride on the failure behavior of high burnup BWR fuel rods during pulse irradiation at the NSRR.

As a result of the burst test at RT to 373K, long axial cracking, which was observed in the high burn-up BWR fuel rods failed during pulse irradiation at the NSRR, could be simulated. At RT to373K, residual strain decreased as hydrogen concentration increased, but both burst pressure and residual strain was not influenced by radial hydride. As temperature increased, burst pressure decreased and residual strain increased. At 553K, effects of hydrogen absorption vanished, and remarkable axial crack propagation was not observed. The present test results indicate that brittle fracture with small residual strain, as observed in the high burnup BWR fuel rods failed during pulse irradiation, cannot be caused only by the effect of hydrogen absorption. It is considered that such brittle fracture would be caused not only by hydriding but also by irradiation.

Mechanical properties of hydrided cladding in hoop direction (Modified ring tensile test)

Modified methods in ring tensile test with a specimen with gauge section have been developed to measure mechanical propertied in hoop direction of cladding tubes quantitatively. We optimized tensile method and specimen geometry through FEM analysis on specimen deformation and tensile test on specimens with various gauge section geometries to obtain uniform and uni-axial hoop strain in the gauge section.

In recent studies, the modified ring tensile tests have been performed on artificially hydrided PWR 17x17 type cladding tubes in order to evaluate influence of the hydrogen concentration (10 to 1600wtppm) and test temperature (RT to 573K) on mechanical properties in hoop direction. As a result of the tests, yield stress, tensile stress, uniform elongation and fracture strain could be successfully measured as functions of hydrogen concentration and test temperature.

JAERI－Conf 2002－009

Fuel Safety Research Specialists' Meeting, March 4-5, 2002 in JAERI, Japan

RIA-related studies at JAERI:

Studies on fracture behavior and mechanical properties of cladding

T. TAKEDA and S. UCHIKAWA

1

JAERI

Recent results of mechanical tests with hydrided cladding at JAERI

To investigate the fracture behavior and mechanical properties of high burn-up fuel cladding, the following items are examined at JAERI.

Part 1: Influence of radial hydride on fracture behavior of Zry-2 fuel cladding tube
T.Takeda

Part 2: Mechanical properties in hoop direction of hydrided cladding
S.Uchikawa

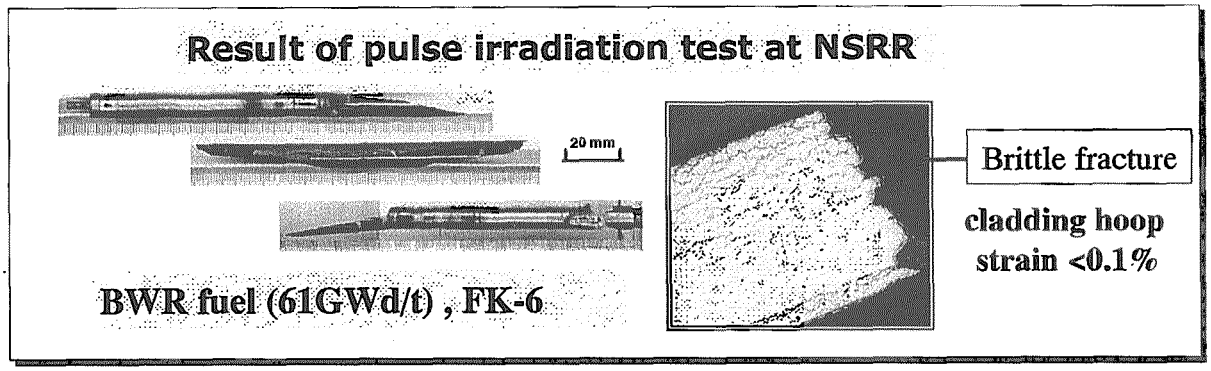
2

JAERI

Background

At NSRR, BWR fuels(61 GWd/t) were pulse irradiated under RIA conditions, and failures were observed for the first time in BWR fuels. (FK-6, FK-7, FK-9)

Failed BWR fuels showed small residual strain
→ influenced by hydrogen absorption?



JAERI

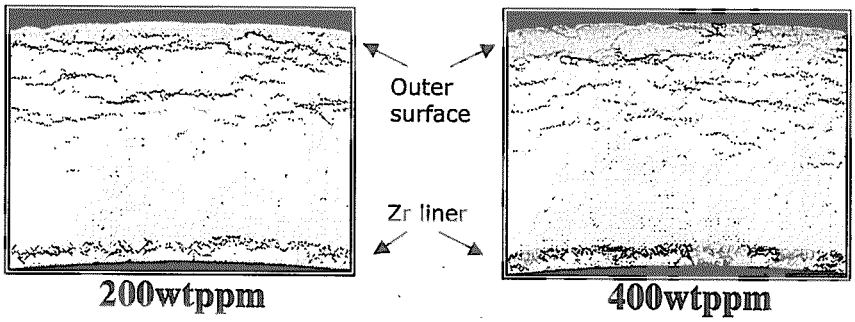
Objective

- **To evaluate the effect of hydrogen absorption on burst behavior**
  - **Hydrogen concentration**
    → ・5wtppm (non-hydrided)
    ・200～650wtppm (hydrided)
  - **Orientation of hydride**
    → ・circumferential direction
    ・random distribution

JAERI

Sample

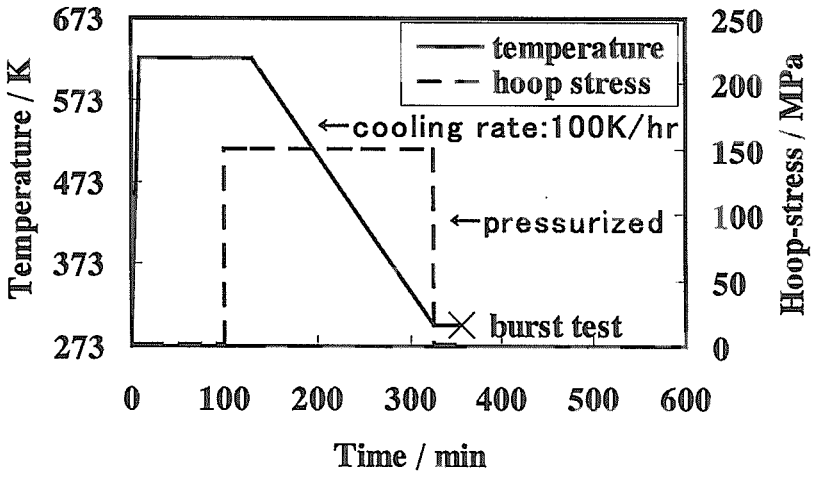
- **Materials**
  - Zry-2 cladding tube with Zr-liner (BWR 9 × 9 type)
- **Hydrogen absorption treatment**
  - by gaseous hydrogen charging method at 673K



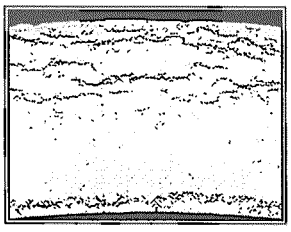
5

JAERI

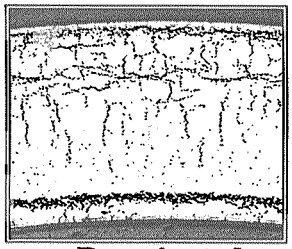
Heat treatment for hydride re-orientation



Typical diagram of heat treatment for hydride re-orientation



Hydrided, 200wtppm

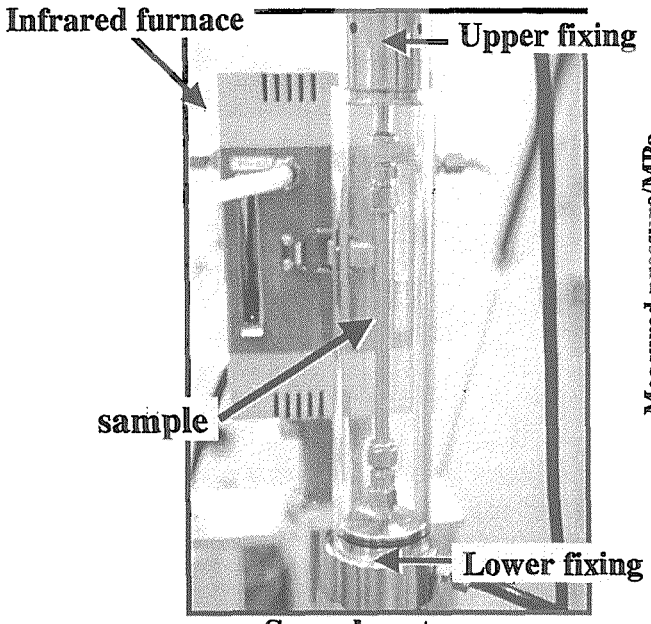


Re-oriented, 200wtppm

6

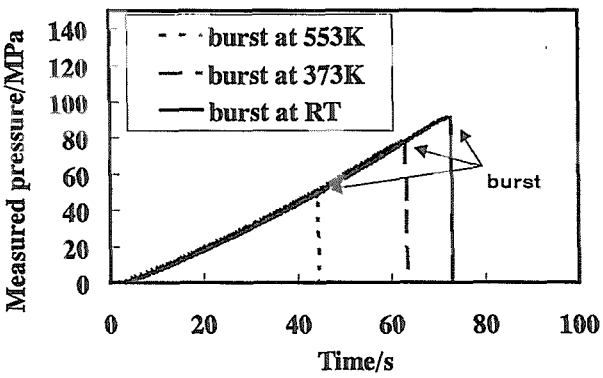
JAERI

Experimental procedure



Sample setup

Pressure change on burst test

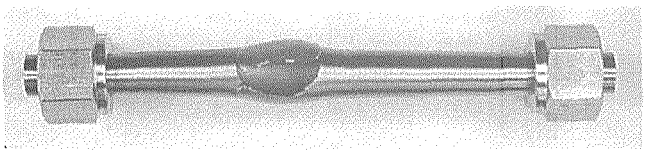


Pressurization rate:2MPa/s

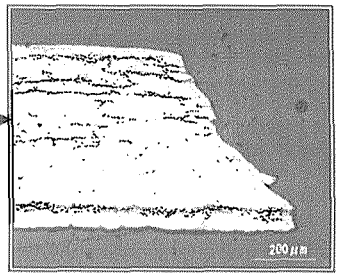
7

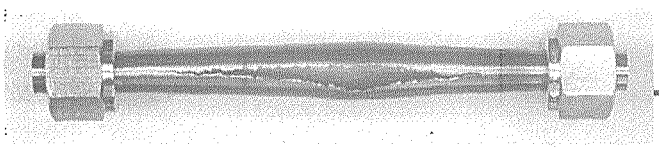
JAERI

Result (1) — fracture morphology (*burst at RT*)

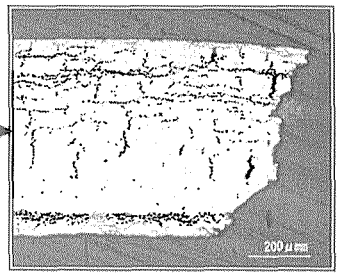


Burst at RT, 215ppm, Non-heat-treated





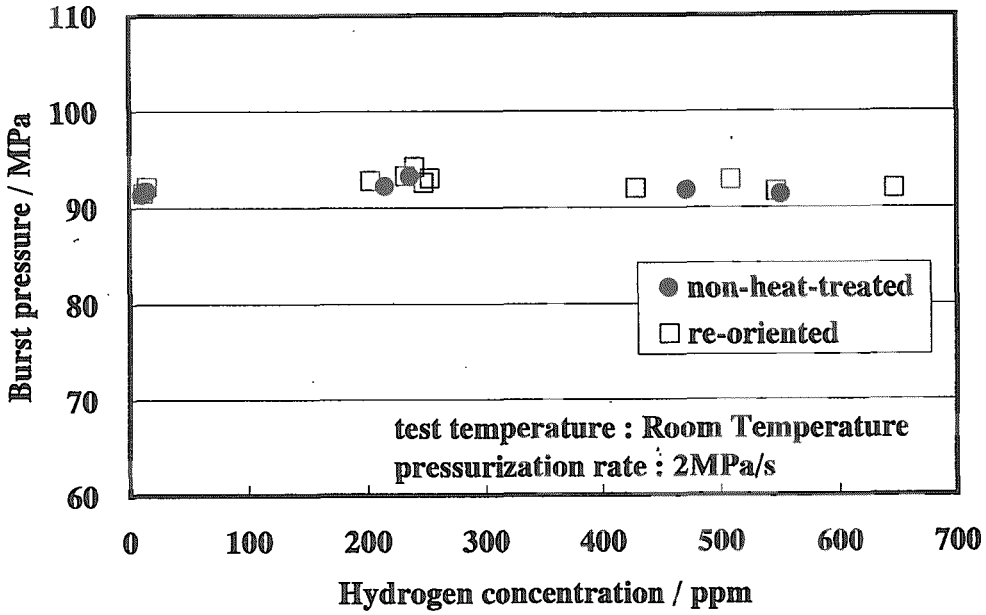
Burst at RT, 248ppm, re-oriented(150MPa)



8

JAERI

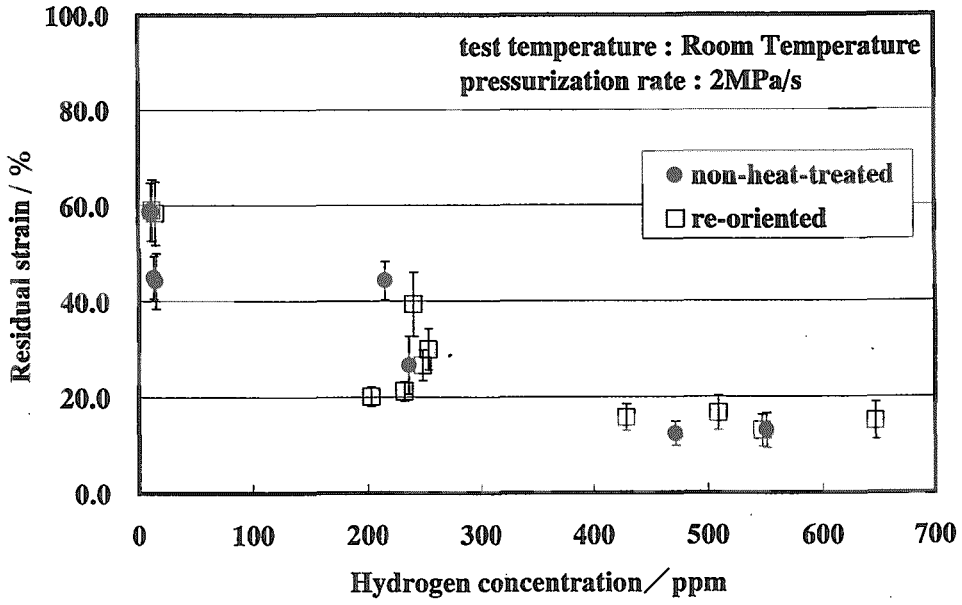
Result (2) — burst pressure (*burst at RT*)



9

JAERI

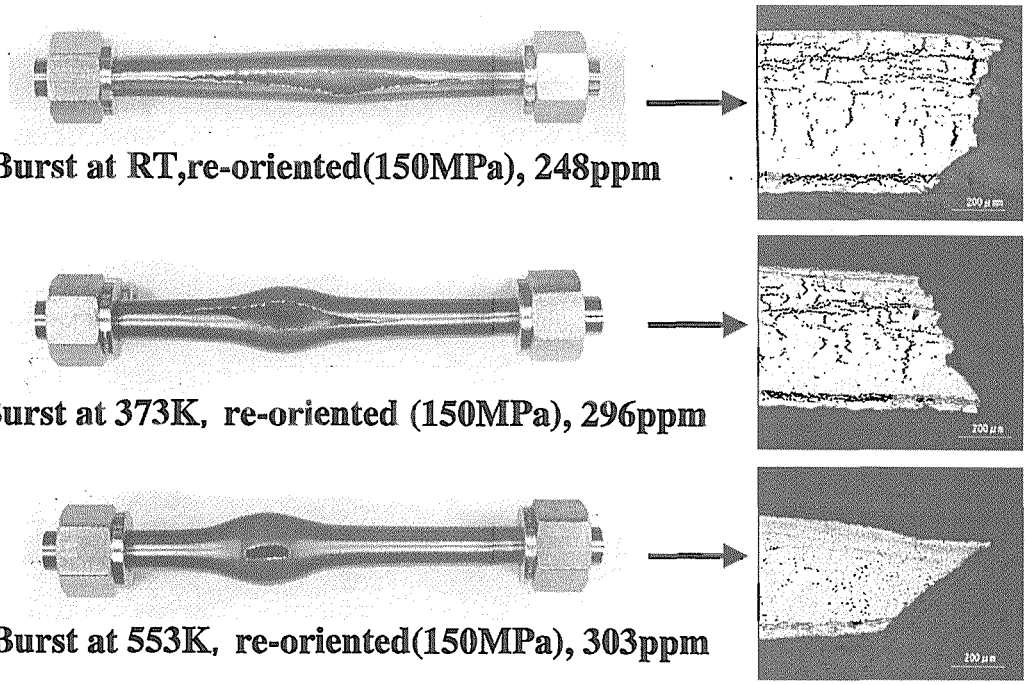
Result (3) — residual strain (*burst at RT*)



10

JAERI

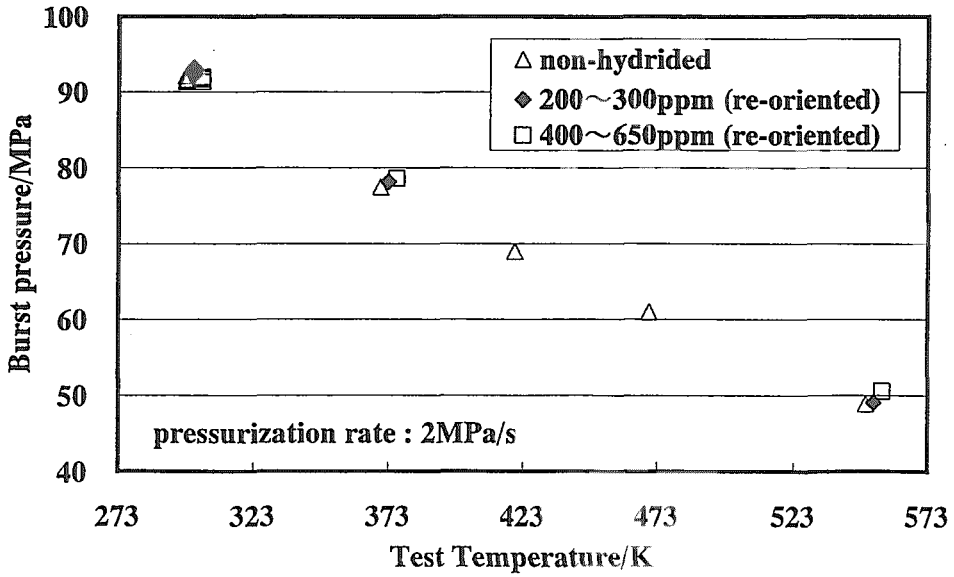
Result (4) － fracture morphology effect of temperature (373K, 553K)



11

JAERI

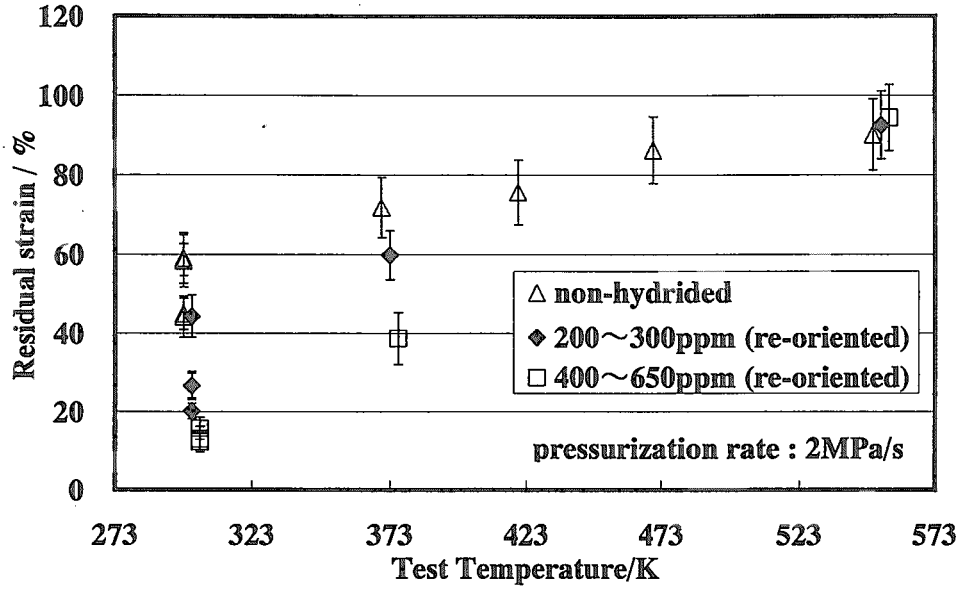
Result (5) － burst pressure effect of temperature (RT～553K)



12

JAERI

Result (6)－ residual strain (*RT～553K*)



13

JAERI

Test summary

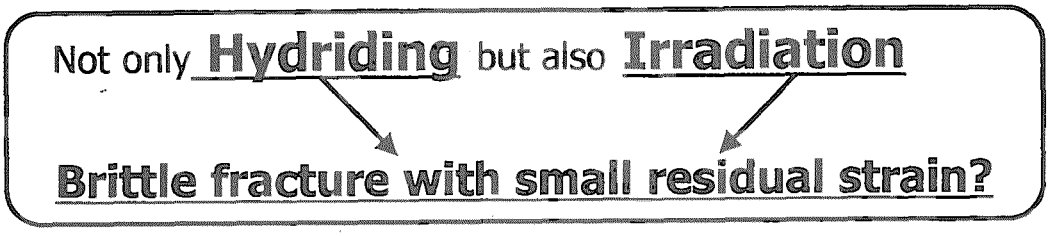
- Long axial crack propagation which observed in FK-tests could be simulated by this test method.
- Hydrogen absorption had no effect on the burst pressure, but residual strain decreased as hydrogen concentration increased.
- Radial hydride developed the long axial crack but did not influenced on both burst pressure and residual strain.
- Effects of hydrogen absorption to the fracture behavior vanished at 553K.

14

JAERI

Discussion and future plan

- **Brittle fracture with small residual strain (e.g. 0.1%) could not be simulated only by the effect of hydrogen absorption in un-irradiated fuel.**



→ **Future plan**
- ✓ **fracture behavior of irradiated fuel**
- ✓ **mechanical properties of irradiated fuel (modified ring tensile test, fracture toughness)**

15

Mechanical properties in hoop direction of hydrided cladding (Modified Ring Tensile Test)

Sadayuki UCHIKAWA

Fuel Safety Research Laboratory
Department of Reactor Safety Research
JAERI

March 4-5, 2002
Prepared for FSRSM, JAERI-Tokai,Ibaraki, Japan

16

Background

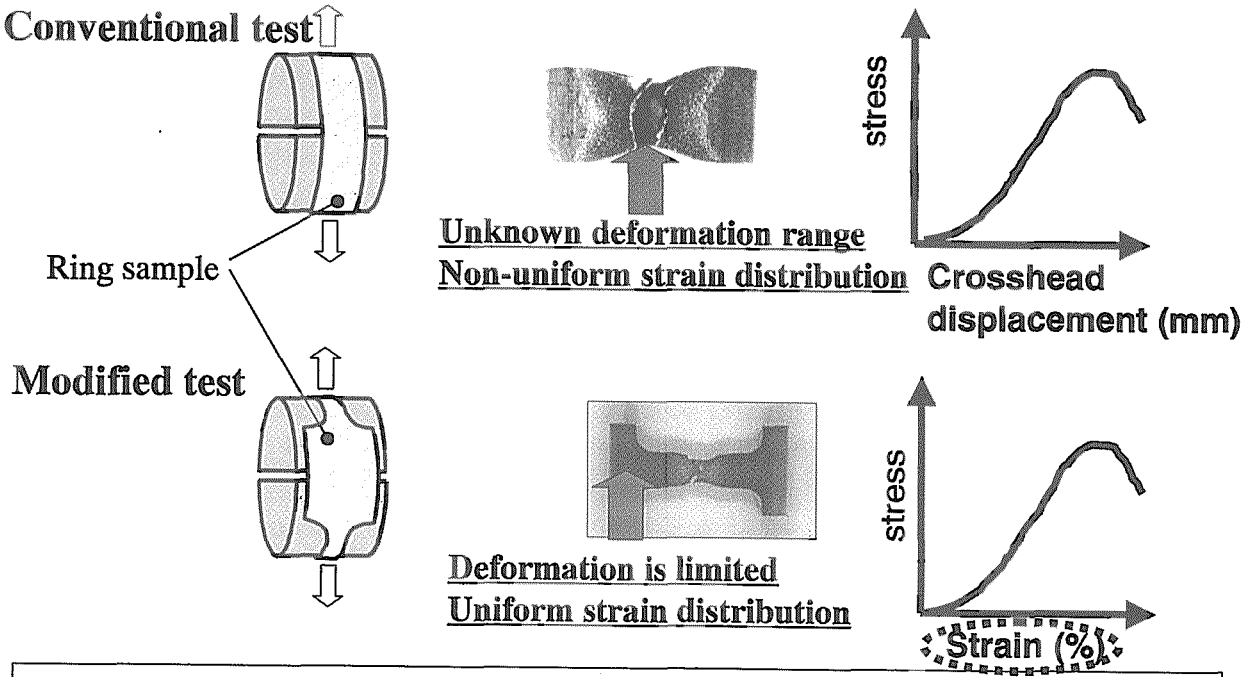
JAERI

It is important to evaluate mechanical properties of high burn-up fuel cladding.

Modified ring tensile test has been developed to measure mechanical properties in hoop direction.

17

Advantage of modified ring tensile test



It is possible to evaluate cladding ductility in hoop direction.

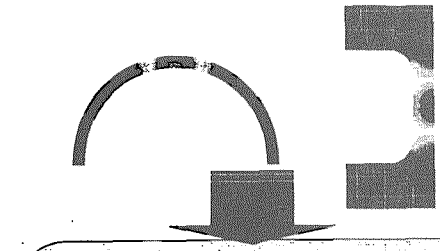
18

Optimization of test method

JAERI

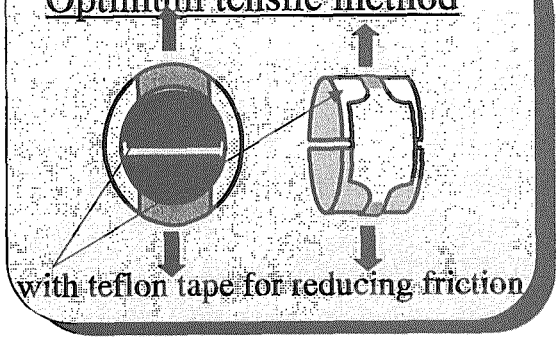
FEM analysis

Experiment

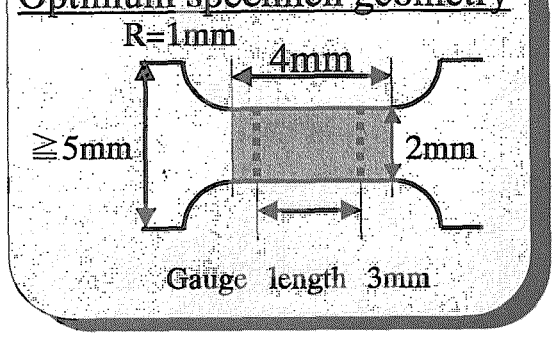


Tensile test on specimens with various gauge section geometries

Optimum tensile method



Optimum specimen geometry



Uniform and uni-axial hoop strain

19

JAERI

Recent study

Influence of

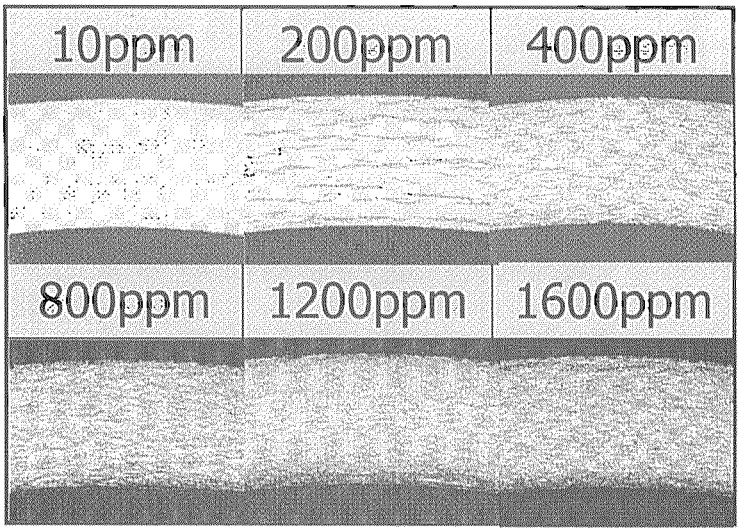
- Hydrogen concentration
- Temperature

20

Test condition

JAERI

- **Zircaloy-4 cladding (Non-irradiated)**
- **Hydrogen concentration: 10～1600wtppm**



- **Test temperature: RT(300K),373K,473K,573K**

21

Derivation of Stress-Strain data

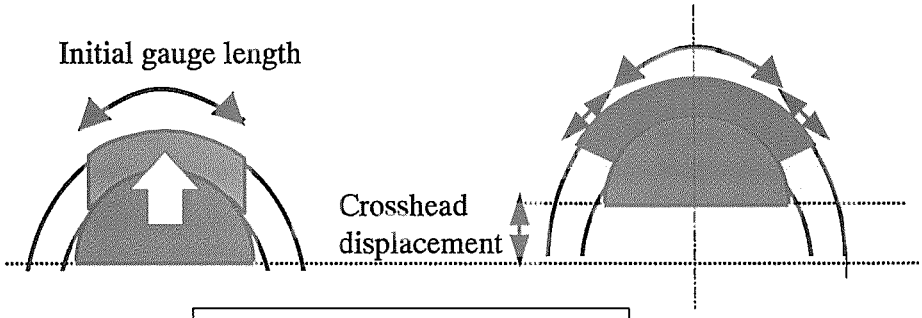
JAERI

Engineering stress =measured load /2(W・t)

W, t = Width and thickness of gauge section

$$\text{Strain} = \frac{\text{crosshead displacement} \times 2}{\text{GL}}$$

GL=gauge length

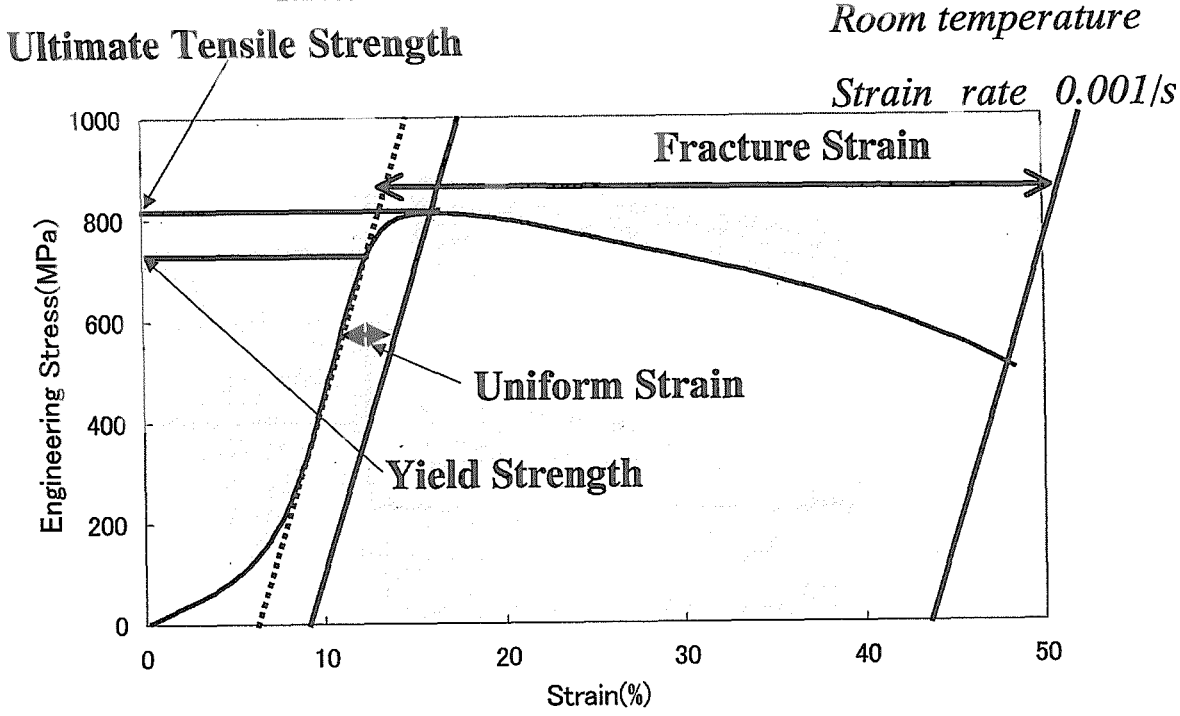


Gauge length elongation = Crosshead displacement × 2

22

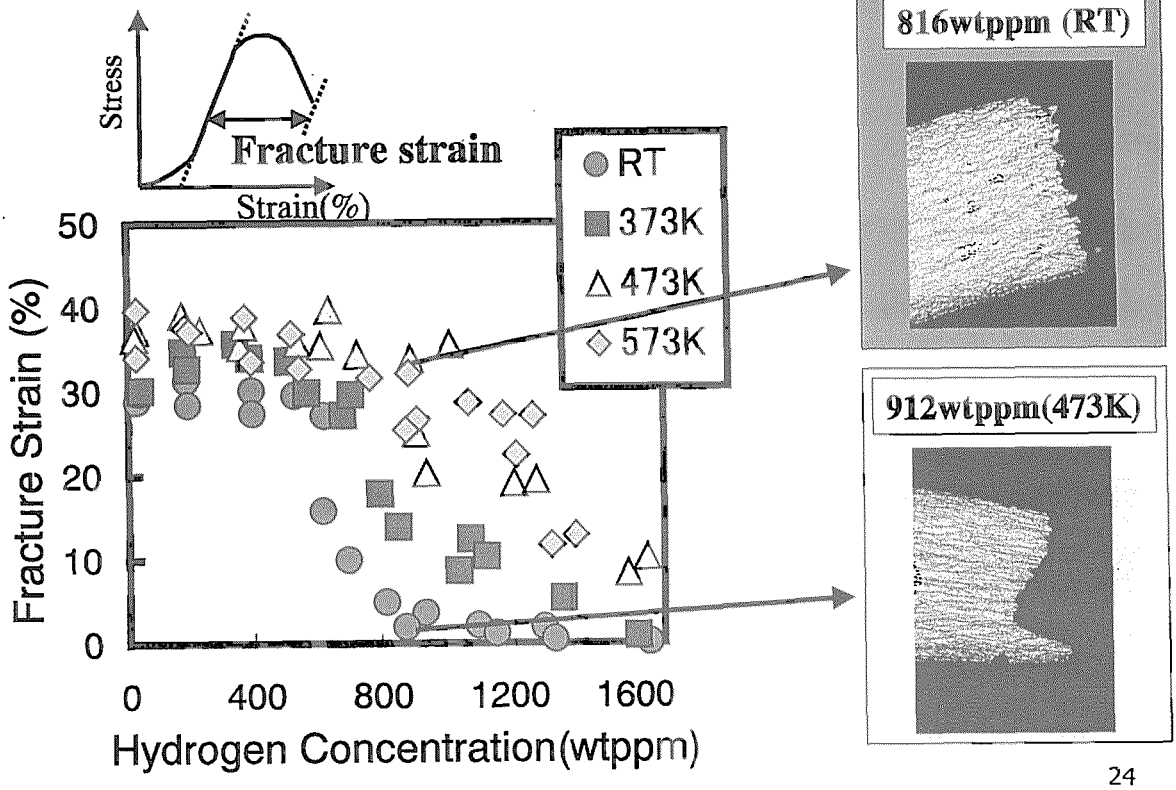
JAERI

Stress-Strain Curve



23

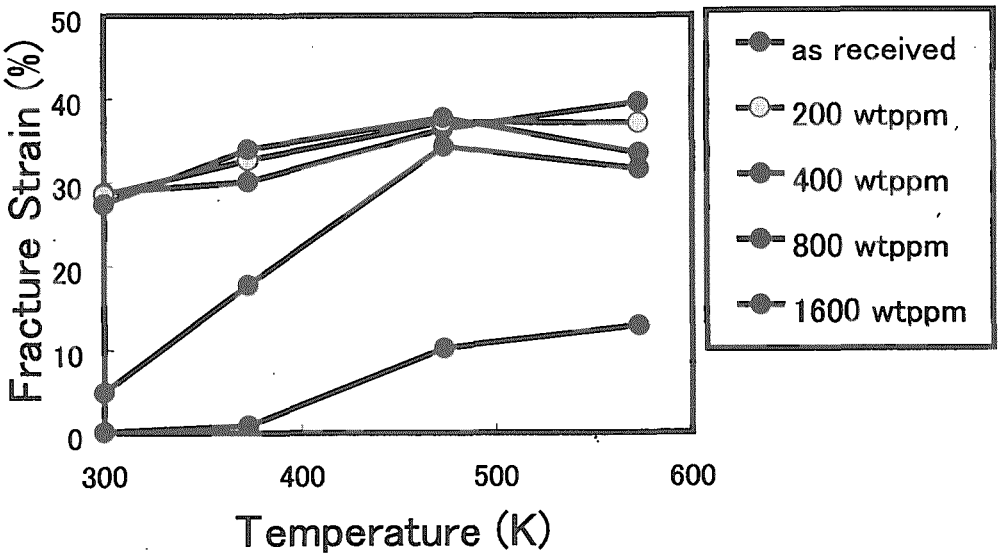
Influence of hydrogen concentration



24

JAERI

Results(2／2)



25

JAERI

Summary

- **Mechanical properties in hoop direction of hydrided cladding tubes were evaluated as functions of hydrogen concentration and temperature by using modified ring tensile test.**

26

Discussion:

Q: (P. Yvon)
Which type of technique are you going to use to perform fracture toughness test (Pin loading testing, Internal conical mandrel, Valleciros embedded charpy, ...).

A: I am going to use a modified pin load testing method. We are developing the test method, now.

Q: (R.S. Dickson)
Could the oxide layer on the irradiated material be affecting the amount of strain at time of failure?

A: Since coherency of oxide layer to Zircaloy metal is low at the tested temperatures, we think that the influence of oxide layer is small.

Session 2a-5

Influence of Hydrogen on the Integrity of Zircaloy Cladding under Accidental conditions

S. Yamanaka, M. Kuroda and D. Setoyama
Department of Nuclear Engineering, Graduate School of Engineering, Osaka University,
Yamadaoka 2-1, Suita, Osaka 565-0871, Japan
F. Nagase and H. Uetsuka
Department of Reactor Safety Research, Japan Atomic Energy Research Institute,
Tokai-mura, Ibaraki-ken 319-1195, Japan

ABSTRACT

Integral thermal shock tests for simulated high burnup fuel cladding have been carried out by JAERI to evaluate the influence of burnup extension on fuel behavior under LOCA conditions. Hydrogen pick up was found to affect the burst and failure of the cladding under LOCA conditions. The burst temperature decreased with increasing hydrogen content of cladding. The pre-hydriding decreased the failure threshold value under restraint conditions. The influence of pre-hydriding was observed for the microstructure of prior-beta phase region.

The elastic properties of zirconium-hydrogen solid solution at high temperature were examined in the present study to clarify the influence of hydrogen on the mechanical properties of zirconium. Dissolved hydrogen markedly decreased the elastic moduli of zirconium such as Youngs' and shear moduli. The hydrogen (solid solution type) appears to increase the ductility of the cladding. Since the failure threshold appears to be closely related to the mechanical properties of prior-beta phase of the cladding, the Zr-O-H ternary system was examined to elucidate the hydrogen effect on the mechanical properties of prior-beta phase. The phase diagram was calculated by the CALPHAD method. The calculated isothermal section of the Zr-O-H ternary system at 700 C well agreed with the experimental one. From the calculated phase diagram, it was found that hydrogen strongly affect the phase relationship in the Zr-O system and the oxygen content of alpha-Zr in equilibrium with alpha+beta-Zr increased by hydrogen addition. Hydrogen appears to increase the oxygen content of initially precipitated alpha-phase from prior-beta. This may cause the embrittlement of the prior-beta phase region of the cladding oxidized at high temperatures.

In NSRR of JAERI, pulse irradiation tests have been extensively carried out for high burnup fuel rod. Burst tests have been also made for hydrided cladding in JAERI to clarify the influence of hydride on the cladding failure.

The analysis based on the fracture mechanics has been performed at room temperature to elucidate the influence of irradiation damage and hydride on the fracture behavior of the cladding tube. It was found from the FAD that hydrogenation dominated the failure strength depending on the distribution and orientation of hydride precipitates, rather than irradiation damage.

Influence of Hydrogen on the Integrity of Zircaloy Cladding under Accidental Conditions

Department of Nuclear Engineering,
Osaka University

Fuel Safety Research Specialist's Meeting 2002/3/4-5

Osaka University: **S. YAMANAKA, M. KURODA, D. SETOYAMA**
JAERI: **F. NAGASE** and **H. UETSUKA**

Contents of Presentation

- ◇ Introduction
- ◇ Influence of hydrogen on the cladding integrity under LOCA conditions
- ◇ Influence of hydrogen on the cladding integrity under RIA conditions
- ◇ Summary

Address: yamadaoka 2-1, Suita, Osaka 565, Japan
Tel: 06-6879-7904, Fax: 06-6879-7889, E-mail: yamanaka@nucl.eng.osaka-u.ac.jp

1

Influence of Hydrogen on the Integrity of Zircaloy Cladding under Accidental Conditions

Department of Nuclear Engineering,
Osaka University

Purpose

To elucidate the influence of hydrogen on the integrity of high burn up fuel cladding under normal and accidental conditions

Outline of Our Studies

- ◇Thermochemical properties of the Zr-H system
- ◇Thermophysical properties of the Zr-H system
- ◇Fracture mechanism of hydrided cladding tube

2

Cladding Integrity under LOCA conditions

Department of Nuclear Engineering,
Osaka University

BACKGROUND

◆ Integral thermal shock test for simulated high burnup fuel cladding

Burst and failure behavior of the cladding has been clarified by JAERI

Hydrogen affects the burst and failure of the cladding under LOCA conditions

PURPOSE

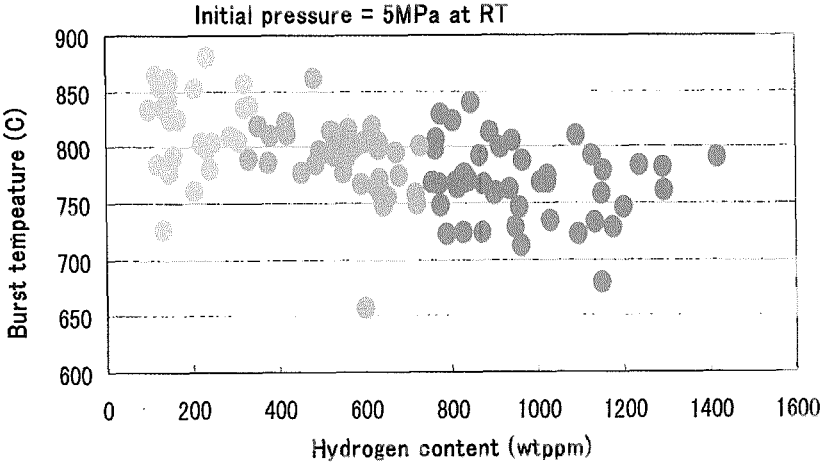
To obtain the fundamental data required for estimation of the influence of hydrogen on the mechanical properties of the cladding under LOCA conditions.

3

Mechanical Properties of Z-H Solid Solution

Department of Nuclear Engineering,
Osaka University

Change in the burst temperature with hydrogen content



4

Mechanical Properties of Zr-H solid solution

Department of Nuclear Engineering,
Osaka University

BACKGROUND

◆ The burst temepature of cladding was reduced by hydrogen addition

Burst temperature appears to be closely related to the influence of hydrogen on the mechanical properties of zirconium

Hydrogen induces ductility or embrittlement of the cladding?

PURPOSE

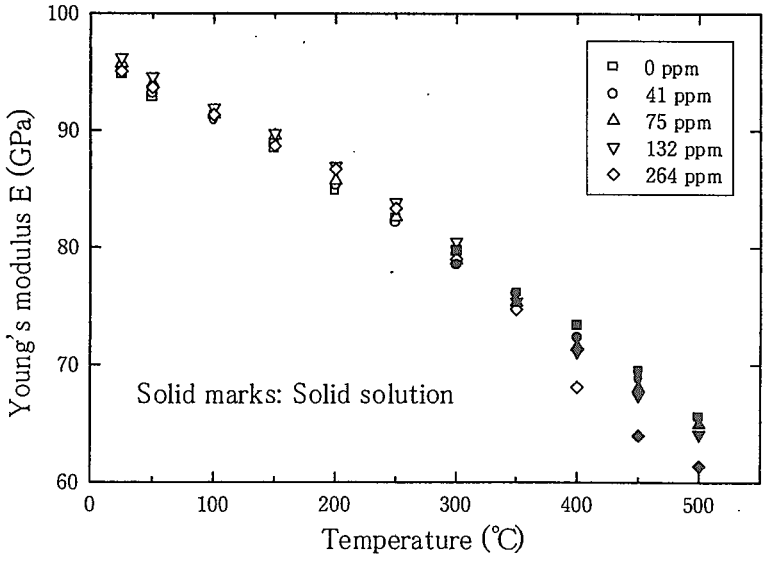
To obtain the elastic properties of Zr-H solid solution at high temperatures.

5

Mechanical Properties of Z-H Solid Solution

Department of Nuclear Engineering,
Osaka University

Change in the Young's modulus with temperature

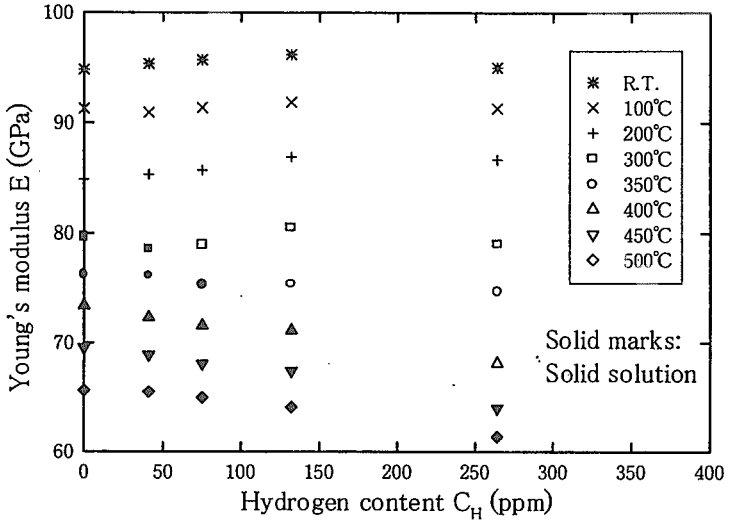


6

Mechanical Properties of Z-H Solid Solution

Department of Nuclear Engineering,
Osaka University

Change in the elastic modulus with hydrogen content

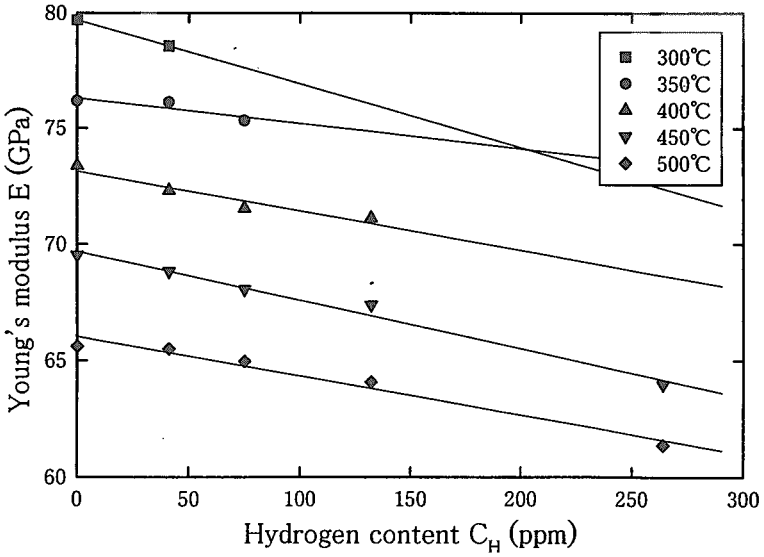


7

Mechanical Properties of Z-H Solid Solution

Department of Nuclear Engineering,
Osaka University

Change in the Young's modulus with hydrogen content



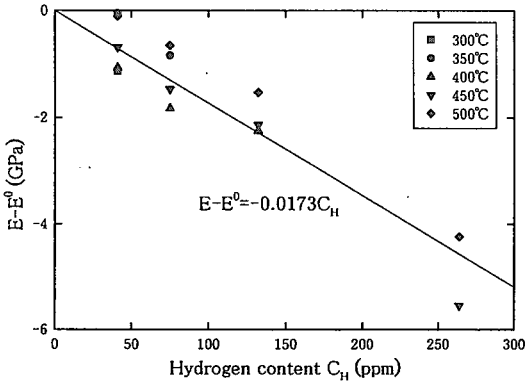
8

Mechanical Properties of Z-H Solid Solution

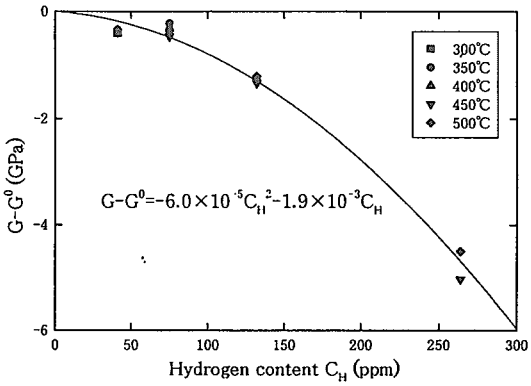
Department of Nuclear Engineering,
Osaka University

Change in the elastic modulus with hydrogen content

Young's modulus



Shear modulus



E⁰, G⁰ : Young's modulus and shear modulus for 0 ppm hydrogen content

9

Mechanical Properties of Zr-H Solid Solution

Department of Nuclear Engineering,
Osaka University

Conclusions

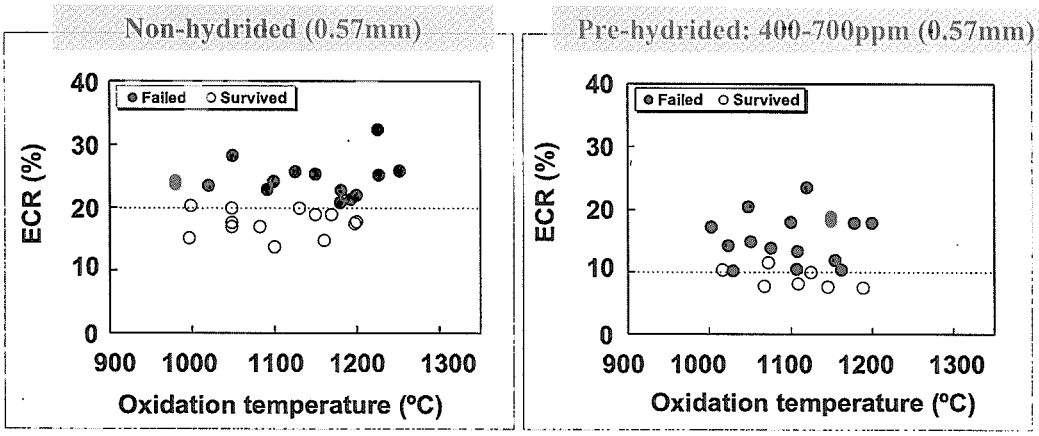
- **The hydrogen markedly decreased the elastic moduli of α Zr-H solid solution such as Youngs' and shear moduli.**
- **The hydrogen (solid solution type) appears to increase the ductility of the cladding.**

10

Phase Diagram of the Z-O-H Ternary System

Department of Nuclear Engineering,
Osaka University

Failure map (Full restraint condition)



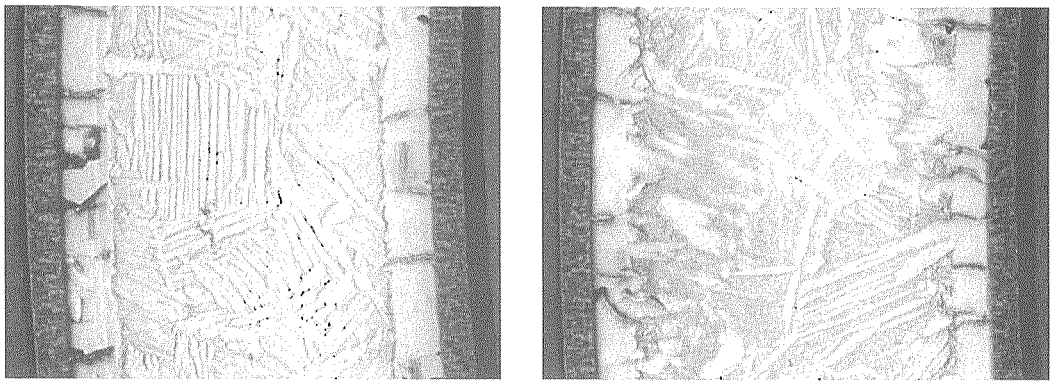
The influence of pre-hydriding was observed for the failure threshold value under restraint conditions.

11

Phase Diagram of the Z-O-H Ternary System

Department of Nuclear Engineering,
Osaka University

Microstructure of the cladding after oxidation(1473K,300s)



Non-hydrided(10wtppm H)　　Pre-hydrided(1600wtppm H)

The influence of pre-hydriding was observed for the microstructure of prior-β phase region.

12

Phase Diagram of the Z-O-H Ternary System

Department of Nuclear Engineering,
Osaka University

BACKGROUND

◆ The hydrogen strongly influenced the failure threshold

The failure threshold appears to be closely related to the mechanical properties of prior-β phase of the cladding

Hydrogen affects the microstructure of prior-β phase?

PURPOSE

To obtain the fundamental data of the Zr-O-H system for the estimation of hydrogen effect on the mechanical properties of prior β phase

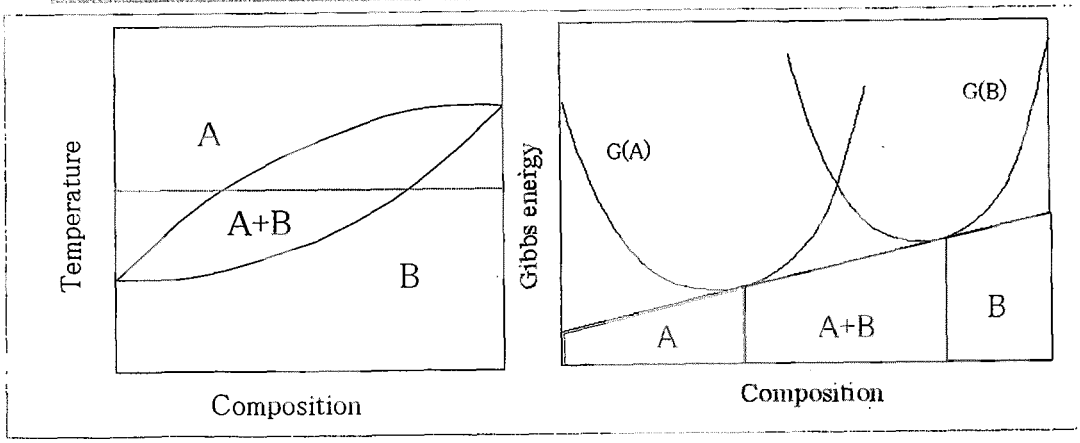
13

Phase diagram of the Zr-O-H Ternary System

Department of Nuclear Engineering,
Osaka University

Calphad method: Calculation of Phase Diagram

Minimization of total Gibbs energy of the system gives the equilibrium conditions

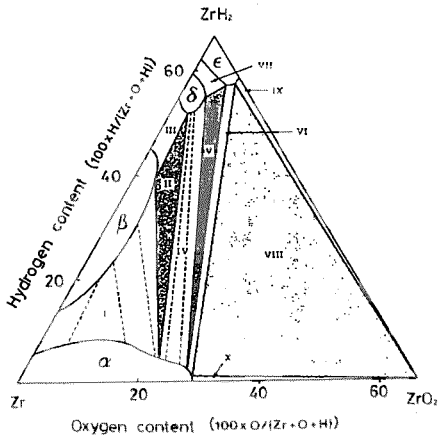


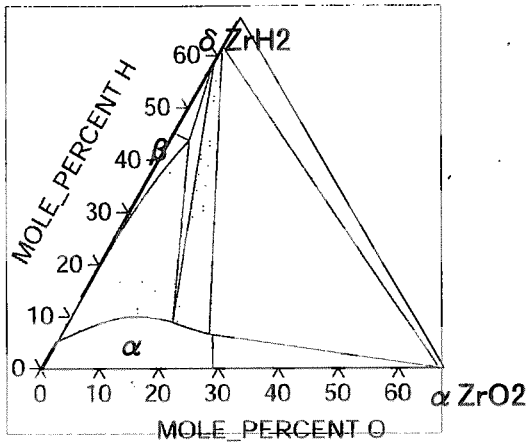
14

Phase Diagram of the Zr-O-H Ternary System

Department of Nuclear Engineering,
Osaka University

Isothermal sections of Zr-O-H system





Experiment　　Calculation

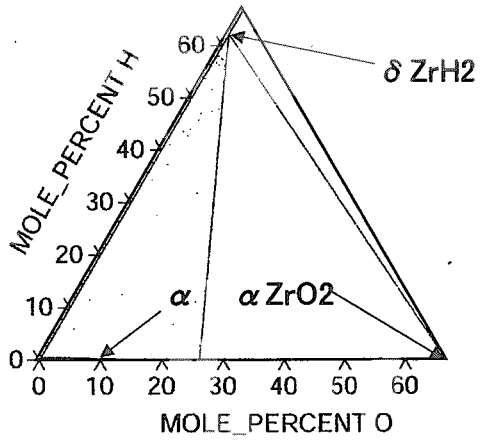
Isothermal section at 700 ℃

15

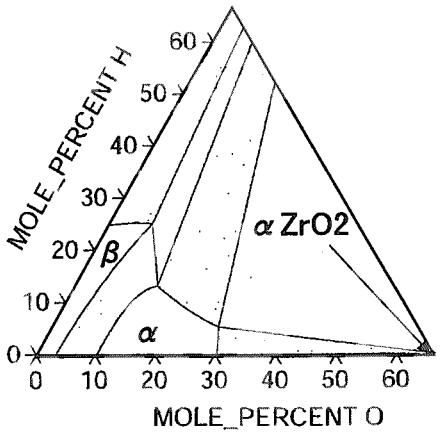
Phase Diagram of the Zr-O-H Ternary System

Department of Nuclear Engineering,
Osaka University

Calculated isothermal sections of the Zr-O-H system



300 ℃



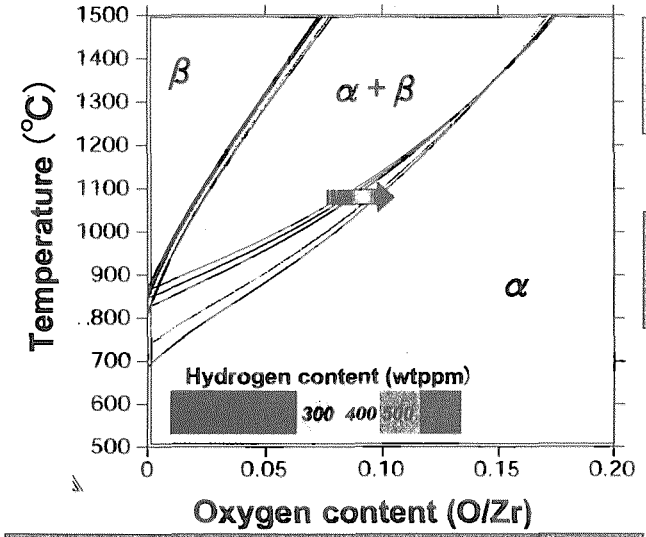
1200 ℃

16

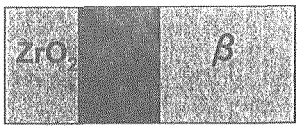
Phase Diagram of the Zr-O-H Ternary System

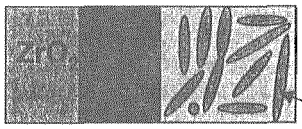
Department of Nuclear Engineering,
Osaka University

Hydrogen effect on the Zr-O system



With hydrogen addition the α+β region expands to higher oxygen content





◆ The oxygen content of initially precipited α' increases with H addition.
◆ The precipited α' with higher oxygen content embrittles the cladding

17

Phase Diagram of the Zr-O-H Ternary System

Department of Nuclear Engineering,
Osaka University

Conclusions

◆ The hydrogen was found from the calculated phase diagram to strongly affect the Zr-O system. The oxygen content of αZr in equilibrium with α+β was found to be increased by hydrogen addition.

◆ The hydrogen appears to increase the oxygen content of initially precipited α' phase and produce the embrittlement of the prior-β layer.

18

Cladding Integrity under RIA conditions

Department of Nuclear Engineering,
Osaka University

BACKGROUND

- Pulse irradiation test for high burnup fuel rod
- High-pressurization-rate burst test for hydrided cladding

Fracture behavior of the hydrided cladding has been clarified by JAERI

Analysis of the experimental results

PURPOSE

To interpret the experimental results of the pulse irradiation and burst tests by fracture mechanics

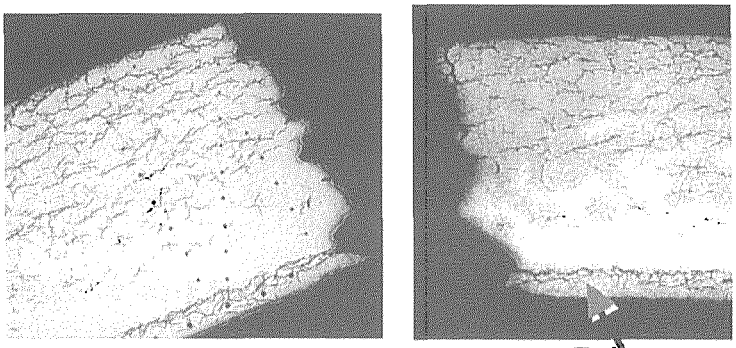
19

Failure Behavior of BWR Fuel Cladding

Department of Nuclear Engineering,
Osaka University

NSSR pulse irradiation test for BWR fuel rod

BWR fuel cladding (61GWd/tU) (Hydrogen content: about 200ppm)

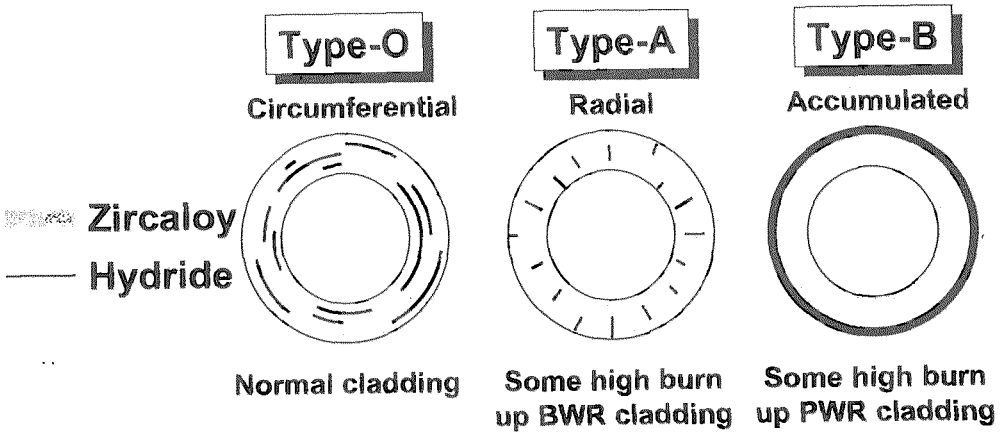


FK-6, 70 cal/g

20

Typical Distribution of Hydride

Department of Nuclear Engineering,
Osaka University



Type-O Irradiation damage is the dominant factor (Huang)

Type-A Hydrogenation is a dominant factor for the
Type-B cladding strength degradation rather than irradiation?

21

Cladding Integrity under RIA conditions

Department of Nuclear Engineering,
Osaka University

PURPOSE

◆ The failure stress of the irradiated / hydrogenated Type-A and Type-B fuel claddings at room temperature is estimated by constructing the failure assessment diagram (FAD) using fracture mechanics

◆ Which of the effect, irradiation or hydrogenation, dominates the cladding strength primarily is discussed in terms of the FAD

22

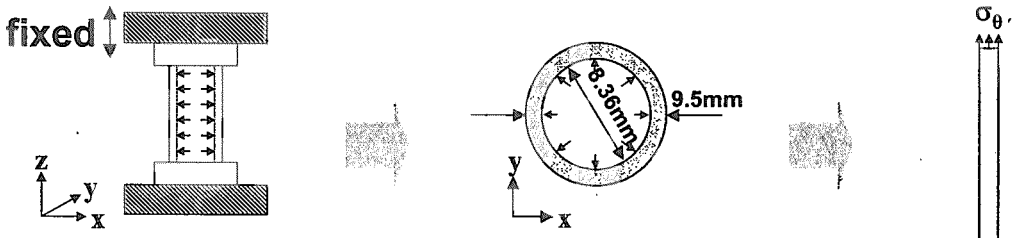
Modeling

Department of Nuclear Engineering,
Osaka University

Modeling of the pulse irradiation test

Pulse irradiation test for cladding tube

Tension test for panel



Plane strain
$\varepsilon_z=0$

Thin-walled cylinder
$\sigma_r=0$

23

Type-A Model

Department of Nuclear Engineering,
Osaka University

Phase: Matrix Zircaloy-2

Hydride distribution

Zircaloy

Hydride

Axial direction

Edge hydride **Center hydride**



✓Failure stress of hydride is extremely low
✓Hydride platelet is modeled as micro-crack (Chans' concept)

Crack distribution

Zircaloy

Crack

Axial direction

Edge crack **Center crack**



4

Type-B Model

Department of Nuclear Engineering,
Osaka University

Phase: Matrix Zircaloy-4, Hydride δ $ZrH_{1.73}$

Hydrogen content : 1000ppm ⇒ Volume ratio of hydride: 6%

Hydride distribution

Zircaloy

Hydride

Axial direction

Accumulated hydride

✓Failure stress of hydride is extremely low
✓In accordance with our formerly proposed modeling

Crack distribution

Zircaloy

Crack

Axial direction

Edge crack

W

a

25

Failure Assessment Diagram

Department of Nuclear Engineering,
Osaka University

Concept

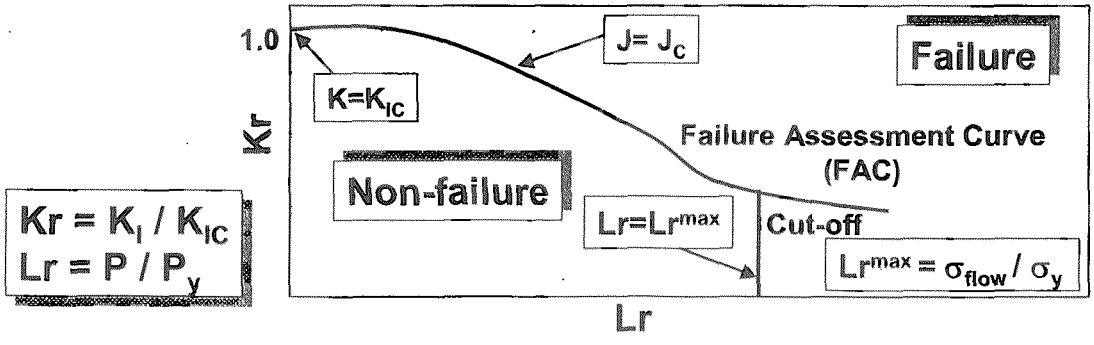
Scale of yielding

K-based fracture criterion	$K_I=K_{IC}$
J-based fracture criterion	$J=J_C$
Plastic collapse criterion	$Lr=Lr^{max}$

Unification of the criteria

FAD

Schematic diagram of FAD

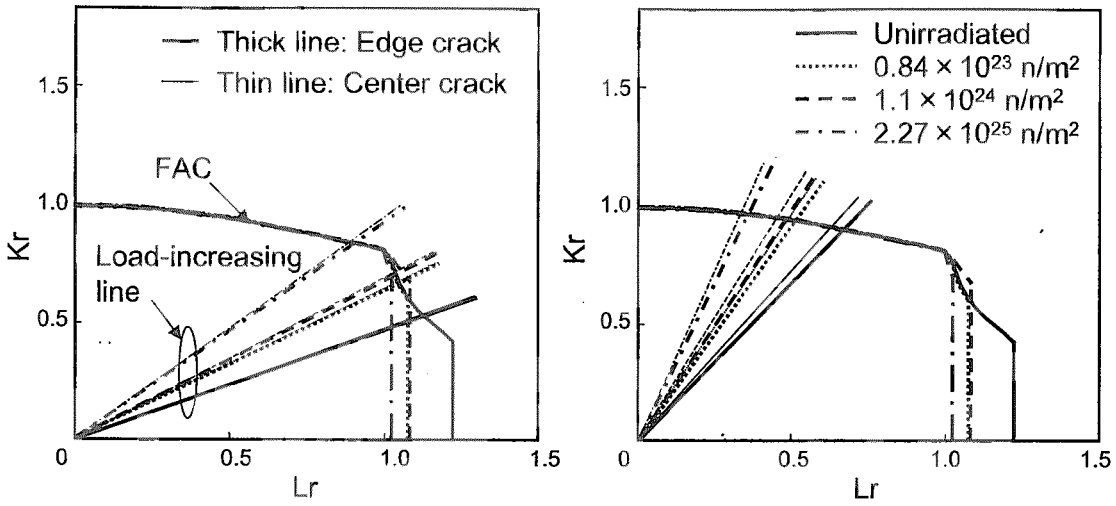


Kr = K_I / K_{IC}
Lr = P / P_y

26

FAD for Type-A model

Department of Nuclear Engineering,
Osaka University



Crack length ratio: 0.015 **Crack length ratio: 0.2**

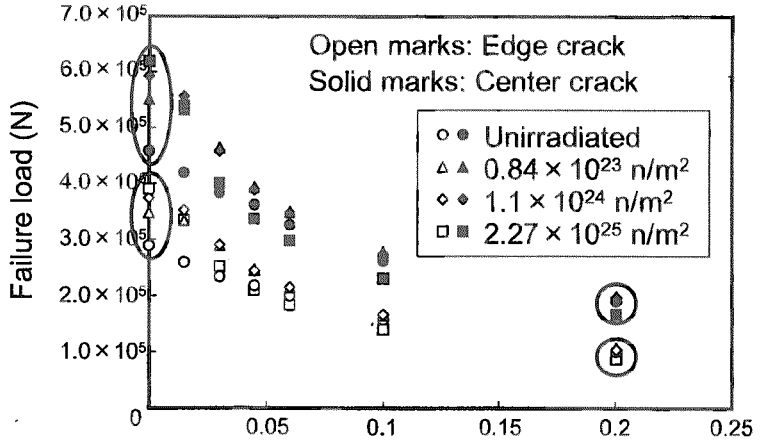
- **The slope of the load-increasing line increases with the fluence and the crack length ratio**

27

Failure Load for Type-A model

Department of Nuclear Engineering,
Osaka University

Failure load calculated from FAD



- **Failure load decreases drastically with crack length ratio**
- **Fluence greatly affects the failure load (no crack length)**
- **Fluence little affects the failure load (some crack length)**

28

Dominant Factors for Type-A model

Department of Nuclear Engineering,
Osaka University

Modeling (formerly mentioned)

Hydride is modeled as crack



- **Failure strength is dominated by irradiation (no hydride precipitation)**
- **Failure strength is dominated by hydrogenation rather than irradiation (hydride precipitation)**

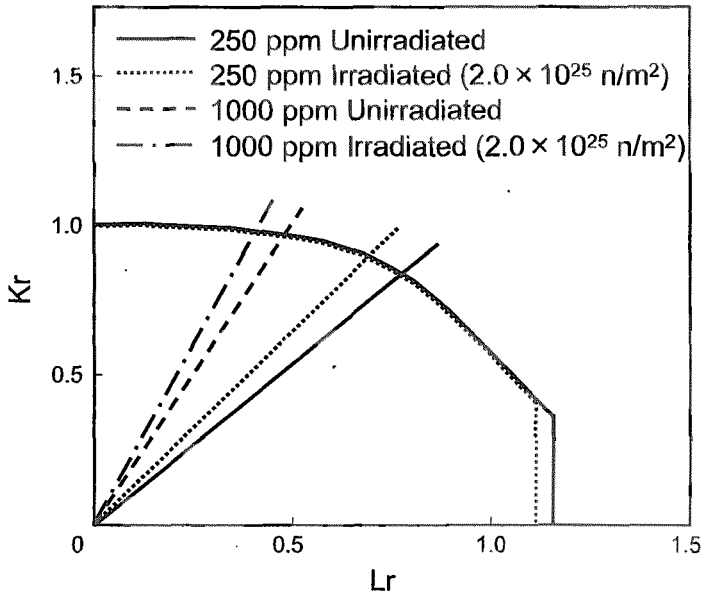
Conclusion

Hydrogenation is the dominant factor for the failure strength degradation of Type-A cladding rather than irradiation

29

FAD for Type-B model

Department of Nuclear Engineering,
Osaka University



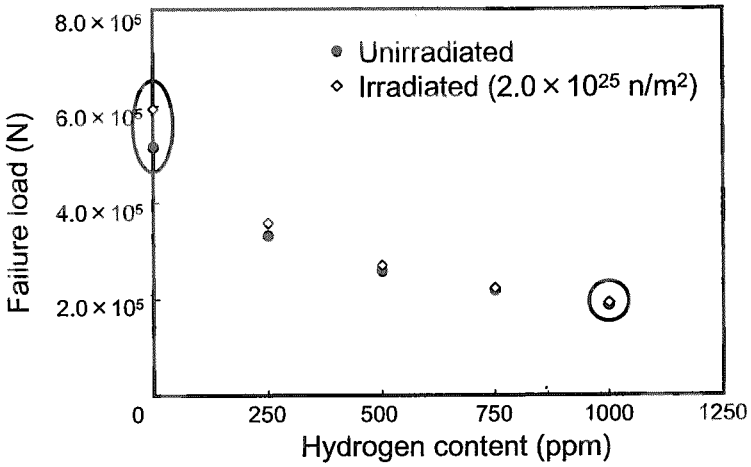
- **The slope of the load-increasing line increases with the neutron fluence and the hydrogen content**

30

Failure Load for Type-B model

Department of Nuclear Engineering,
Osaka University

Failure load calculated from FAD



- Failure load decreases drastically with hydrogen content
- Fluence greatly affects the failure load (no hydride)
- Fluence little affects the failure load (with hydrogen content)

31

Dominant Factors for Type-B model

Department of Nuclear Engineering,
Osaka University

- Failure strength is dominated by irradiation (no hydride precipitation)
- Failure strength is dominated by hydrogenation (hydride precipitation)

Conclusion

For the failure strength degradation of Type-B cladding

Hydrogenation is the dominant factor

Irradiation effect is the secondary factor

- These are identical with the results of Type-A model

32

Fracture Behavior of Cladding Tube

Department of Nuclear Engineering,
Osaka University

Conclusions

◆ It is concluded from the results of Type-A and Type-B models that not irradiation but hydrogenation can dominate the failure strength depending on the distribution and orientation states of the hydride precipitates

33

Summary

Department of Nuclear Engineering,
Osaka University

◆ The elastic moduli of the Zr-H solid solution decreased with increasing hydrogen content.
◆ The thermodynamic calculation for the Zr-O-H ternary system showed that hydrogen influenced the phase boundary of $\alpha+\beta/\alpha$ in the Zr-O system.
◆ The FADs at RT were constructed. The influence of hydride distribution in the cladding on the fracture lode and mode was found to be more important than neutron irradiation effect.

34

List of Publications

Department of Nuclear Engineering,
Osaka University

Thermophysical properties of zirconium hydride

(1) Thermal and mechanical properties of zirconium hydride
S. Yamanaka, K. Yoshioka, M. Uno, M. Katsura, H. Anada, T. Matsuda and S. Kobayashi, J. Alloys and Compounds, 293-295(1999)23-29
(2) Isotope effects on the physicochemical properties of zirconium hydride
S. Yamanaka, K. Yoshioka, M. Uno, M. Katsura, H. Anada, T. Matsuda and S. Kobayashi, J. Alloys and Compounds, 293-295(1999)908-914
(3) Thermal properties of zirconium hydride
S. Yamanaka, K. Yamada, K. Kurosaki, M. Uno, K. Takeda, H. Anada, T. Matsuda and S. Kobayashi, J. Nucl. Mater., 294(2001)99-103
(4) Characteristics of zirconium hydride and deuteride
S. Yamanaka, K. Yamada, K. Kurosaki, M. Uno, K. Takeda, H. Anada, T. Matsuda and S. Kobayashi, J. Alloys and Compounds, 330-332(2202)307-312
(5) Electronic states of zirconium hydride
S. Yamanaka, K. Yamada, K. Kurosaki, M. Uno, K. Takeda, H. Anada, T. Matsuda and S. Kobayashi, J. Alloys and Compounds, 330-332(2002)313-317

35

List of Publications

Department of Nuclear Engineering,
Osaka University

Thermochemical properties of zirconium-hydrogen system

(1) Effect of oxygen on hydrogen solubility in zirconium
S. Yamanaka, T. Tanaka and M. Miyake, J. Nucl. Mater., 167(1989)231-237
(2) Influence of interstitial impurity on hydrogen solubility in zirconium
S. Yamanaka, Y. Sato, H. Ogawa and M. Miyake, J. Nucl. Sci. Technol., 28(1991)135-143
(3) Influence of interstitial elements on hydrogen solubility in the group IV metals
S. Yamanaka and M. Miyake, J. Nucl. Mater., 201(1993)134-141
(4) Hydrogen solubility in zirconium alloys
S. Yamanaka, H. Higuchi and M. Miyake, J. Alloys and Compounds, 231(1995)503-507
(5) Study on the hydrogen solubility in zirconium alloys
S. Yamanaka, M. Miyake and M. Katsura, J. Nucl. Mater., 247(1997)315-321
(6) On the zirconium-oxygen-hydrogen ternary system
M. Miyake, M. Uno and S. Yamanaka, J. Nucl. Mater., 270(1999)233-241
(7) Hydrogen dissolution into zirconium oxide
S. Yamanaka, T. Nishizaki, M. Uno and M. Katsura, J. Alloys and Compounds, 293-295(1999)38-41
(8) Influence of interstitial oxygen on hydrogen solubility in metals
S. Yamanaka, Y. Fujita, M. Uno and M. Katsura, J. Alloys and Compounds, 293-295(1999)42-51

36

List of Publications

Department of Nuclear Engineering,

Osaka University

Fracture behavior of hydrided cladding

(1) Influence of precipitated hydride on the fracture behavior of Zircaloy fuel cladding tube
M. Kuroda, K. Yoshioka, S. Yamanaka, H. Anada, F. Nagase and H. Uetsuka, J. Nucl. Sci. Technol., 37 (2000) 670–675.
(2) Analysis of the fracture behavior of hydrided fuel cladding by fracture mechanics
M. Kuroda, S. Yamanaka, F. Nagase and H. Uetsuka, Nucl. Eng. Des., (2000)in press.
(3) Tensile test of hydrided Zircaloy
M. Kuroda, S. Yamanaka, D. Setoyama, M. Uno, K. Takeda, H. Anada, F. Nagase and H. Uetsuka, J. Alloys Comp., 330–332(2002)404–407
(4) Analysis on the fracture behavior of hydrided cladding tube at elevated temperatures by fracture mechanics
S. Yamanaka, M. Kuroda, D. Setoyama, M. Uno, K. Takeda, H. Anada, F. Nagase and H. Uetsuka, J. Alloys Comp., 330–332(2002)400–403
(5) Assessment of the Combined Effects of Irradiation and Hydrogenation on the Fracture Behavior of Zircaloy Fuel Claddings by Fracture Mechanics
M. Kuroda and S. Yamanaka, J. Nucl. Sci. Technol., 39(2002), In press.

JP0250415

3. Session 2b : RIA Analytical Code and Modeling

Session 2b-1

Numerical Simulation of the Expansion-Due-to-Compression Test

O. Dufourneaud[3], A.G. Varias[1], V. Grigoriev[2], R. Jakobsson[2] and D. Schrire[2]

[1]Materials Science, Technology and Society, Malmö University, SE-205 06, Malmö, Sweden
[2]Studsvik Nuclear AB, SE-611 82, Nyköping, Sweden
[3]Ecole Polytechnique, F-91128 Palaiseau Cedex, France

Abstract

The Expansion-Due-to-Compression (EDC) test has been developed, by Studsvik Nuclear (e.g. [1]), for the study of irradiated cladding failure, under hoop strain rates as high as 1 to 10 s^{-1}. During this test, which is proposed for the mechanical simulation of a reactivity initiated accident or in-pile test (e.g. [2]-[4]), a piece of cladding tube is circumferentially loaded in tension due to the expansion of a polymer pellet, axially compressed inside the tube.

A finite element simulation of the EDC-test is discussed [5]. The objective of the study is: (i) to understand the deformation of the cladding, during the experiment, including the effect of cladding material properties, and (ii) to provide information, necessary for the development of failure criteria.

The material properties for both zirconium alloy cladding and polymer pellet correspond to room temperature. Three different values of cladding material yield stress were considered as well as both hardening and non-hardening behavior. Thus the effect of irradiation on cladding material properties is implicitly taken into account.

The distributions of important field quantities, with respect to the damage of the cladding, as well as the evolution of their maximum values, during loading, are studied. It is shown that, before cladding yielding as well as after substantial plastic deformation, the radial displacement, on the external surface, and the total energy per unit volume, when appropriately normalized, vary along the cladding axis according to specific distributions, which do not depend on the level of loading [5].

The calculated profile of the cladding, after deformation, is in agreement with experimental measurements [1]. Also the calculated axial distribution of total energy per unit volume supports the assumptions made for the development of a cladding failure criterion [1].

References

1. Grigoriev, V., Jakobsson, R. and Schrire, D., (2001), 'Experimental Evaluation of Critical Strain Energy Density for Irradiated Cladding under Simulated RIA Conditions', *Proceedings of ENS Topfuel 2001*, Stockholm, Sweden.
2. Fuketa, T., Sasajima, H., Mori, Y. and Ishijima, K., (1997), 'Fuel Failure and Fission Gas Release in High Burnup PWR Fuels under RIA Conditions', *Journal of Nuclear Materials*, Vol. 248, pp. 249-256.
3. F. Lemoine, (1997), 'High burnup fuel behavior related to fission gas effects under reactivity initiated accidents (RIA) conditions', *Journal of Nuclear Materials*, Vol. 248, pp. 238-248.
4. Bibilashvili, Yu. et al, (2000), 'Experimental Study of VVER High Burnup Fuel Rods at the BIGR Reactor under Narrow Pulse Conditions', *Proceedings of the ANS International Topical Meeting on LWR Fuel Performance*, Park City, USA, April 2000.
5. Dufourneaud, O. and Varias, A.G., (2001), 'Elastic-Plastic Deformation of a Nuclear Fuel Cladding Specimen under the Internal Pressure of a Polymer Pellet', *Report PA-03-06-01*, Malmö Univeristy, Malmö, Sweden.

NUMERICAL SIMULATION OF THE EXPANSION-DUE-TO-COMPRESSION TEST

O. Dufourneaud[3], A.G. Varias[1], V. Grigoriev[2], R. Jakobsson[2] and D. Schrire[2]

[1]Materials Science, Technology and Society, Malmö University, SE-205 06, Malmö, Sweden
[2]Studsvik Nuclear AB, SE-611 82, Nyköping, Sweden
[3]Ecole Polytechnique, F-91128 Palaiseau Cedex, France

Abstract

The Expansion-Due-to-Compression (EDC) test has been developed, by Studsvik Nuclear, for the study of irradiated cladding failure, under hoop strain rates as high as 1 to 10 s^{-1}. During this test, which is proposed for the mechanical simulation of a reactivity initiated accident or in-pile test, a piece of cladding tube is circumferentially loaded in tension due to the expansion of a polymer pellet, axially compressed inside the tube.

A finite element simulation of the EDC-test is discussed. The objective of the study is: (i) to understand the deformation of the cladding, during the experiment, including the effect of cladding material properties, and (ii) to provide information, necessary for the development of failure criteria.

The material properties for both zirconium alloy cladding and polymer pellet correspond to room temperature. Three different values of cladding material yield stress were considered as well as both hardening and non-hardening behavior. Thus the effect of irradiation on cladding material properties is implicitly taken into account.

The distributions of important field quantities, with respect to the damage of the cladding, as well as the evolution of their maximum values, during loading, are studied. It is shown that, before cladding yielding as well as after substantial plastic deformation, the radial displacement, on the external surface, and the total energy per unit volume, when appropriately normalized, vary along the cladding axis according to specific distributions, which do not depend on the level of loading.

The calculated profile of the cladding, after deformation, is in agreement with experimental measurements.

1. Introduction

Stimulated by the prudent utilization of natural resources, associated also with financial advantages, and encouraged by experience concerning fuel behavior under normal operating conditions, the energy industry has increased fuel discharge burnup of commercial power-producing light water reactors. In order to support the trend towards higher burnup and longer operating cycles, studies have been initiated on the behavior of high burnup fuel, during off-normal and accident conditions (e.g. Fuketa et al., 1997; Schmitz and Papin, 1999; Bibilashvili, et al., 2000). Reactivity initiated accident (RIA) conditions are of particular interest and could lead to a transient increase of the nuclear power in a group of fuel assemblies. Abrupt fuel overheating could produce pellet cladding mechanical interaction, due to both pellet thermal

expansion and the expansion of fission gases (Xe, Kr) in the fuel pellet (e.g. Lemoine, 1997), and cause cladding failure.

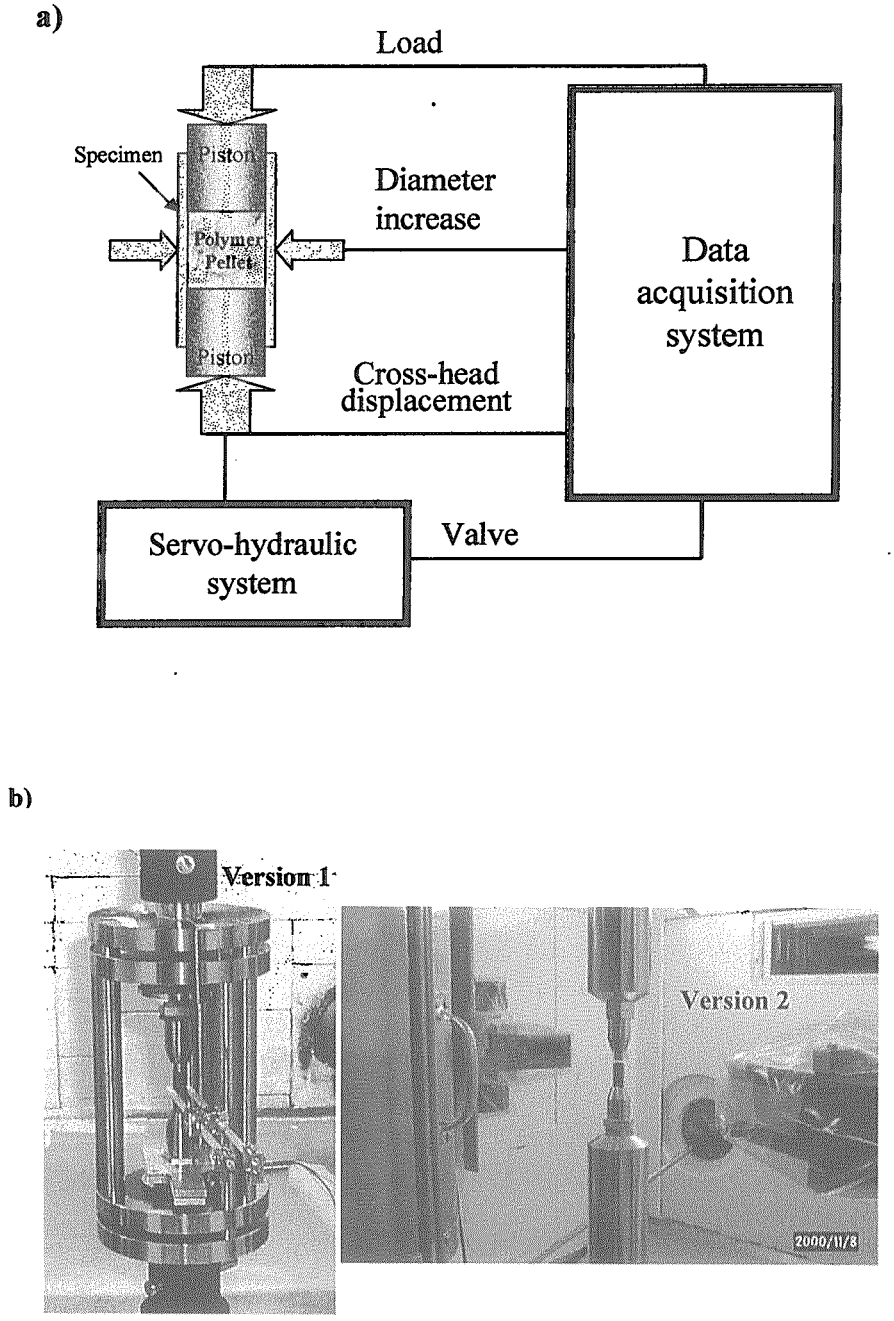


Figure 1. Experimental device of the Expansion Due to Compression (EDC) test. **a)** Schematic of the test set-up. **b)** Two versions of the experimental device. Version 2 has smaller compliance, during load application. (Courtesy of Studsvik Nuclear AB.)

During reactor operation, cladding corrosion results into the development of an oxide layer, on the external surface, and the introduction of hydrogen into the metal ($Zr+2H_2O \rightarrow ZrO_2+2H_2$). Initially hydrogen is in solid solution and diffuses

towards regions of low concentration, high hydrostatic stress and low temperature. However, with increasing time of reactor operation, the hydrogen concentration may exceed its terminal solid solubility and brittle zirconium hydrides may precipitate (e.g. Northwood and Kosasih, 1983). Indeed hydrides are present in high burnup fuel cladding, which is therefore more susceptible to failure, depending on hydride volume fraction and existing defects on the oxide layer (e.g. Varias and Massih, 2001, 2000).

The embrittlement of zirconium alloy, caused by the precipitation of hydrides, drives the effort for better understanding of high burnup fuel behavior, under RIA-like conditions. Besides the in-reactor experiments, effort has been put into the development of mechanical tests, which reproduce the high strain rates, expected under RIA conditions. For example, Kuroda et al. (2000) developed a high-pressurization-rate burst test, in order to mechanically simulate the expansion of fuel cladding during a reactivity initiated accident. The expansion due to compression (EDC) test is such a purely mechanical testing technique (Grigoriev, Jakobsson and Schrire, 2001), which produces pellet cladding mechanical interaction, under high strain rate. During the experiment, a pair of pistons compresses a polymer pellet, which is placed inside a fuel cladding tube (Fig.1). The diameter of the pellet increases, leading to development of contact pressure on the internal surface of the tube. The part of the tube, which is in contact with the pellet, suffers relatively high tensile hoop stress. Due to the small size of the specimen, the test allows the study of cladding performance at locations of relatively high hydride content and the efficient utilization of limited amounts of irradiated cladding material available for testing.

A finite element simulation of the EDC-test is discussed in the present paper. The objective of the study is to understand the deformation of the cladding, during the experiment, and the effect of cladding material properties as well as to provide information, necessary for the development of failure criteria. The structure of the paper is as follows. In section 2, the boundary value problem as well as the pellet and cladding material properties are discussed. In section 3, numerical results on the distribution of important field quantities with respect to the damage of the cladding, such as the maximum principal stress and energy densities, are presented. Finally, concluding remarks are given in section 4.

2. Boundary Value Problem and Material Properties

In the present analysis, the polymer pellet has length equal to 10mm and radius equal to 4.175mm. The zirconium alloy cladding tube is twice as long and has external radius, R_0, equal to 4.825mm and wall thickness t_0=0.65mm. Therefore, it is assumed that there is no initial gap between the cladding and the pellet. Note that, according to the experiments, performed at Studsvik (Grigoriev, Jakobsson and Schrire, 2001), the effect of initial gap, on the deformation of the cladding and the total injected energy up to failure, is negligible. Such a condition is also in agreement with PWR operation, where fuel/cladding gap closure occurs due to cladding creep, within a period of about 1.5 years (e.g. Schmitz and Papin, 1999). The polymer pellet is assumed to be in the middle of the cladding during the application of the loading by the pistons. Such an assumption may not be rigorously satisfied in the actual experiment, because only one of the pistons is moving, during loading. However, this deviation from symmetry is not expected to affect the deformation of the cladding in the region of contact with the pellet. There, local symmetry is expected to be valid

with respect to the mid-plane of the pellet. The deformation of the cladding and the pellet are also symmetric with respect to their common axis.

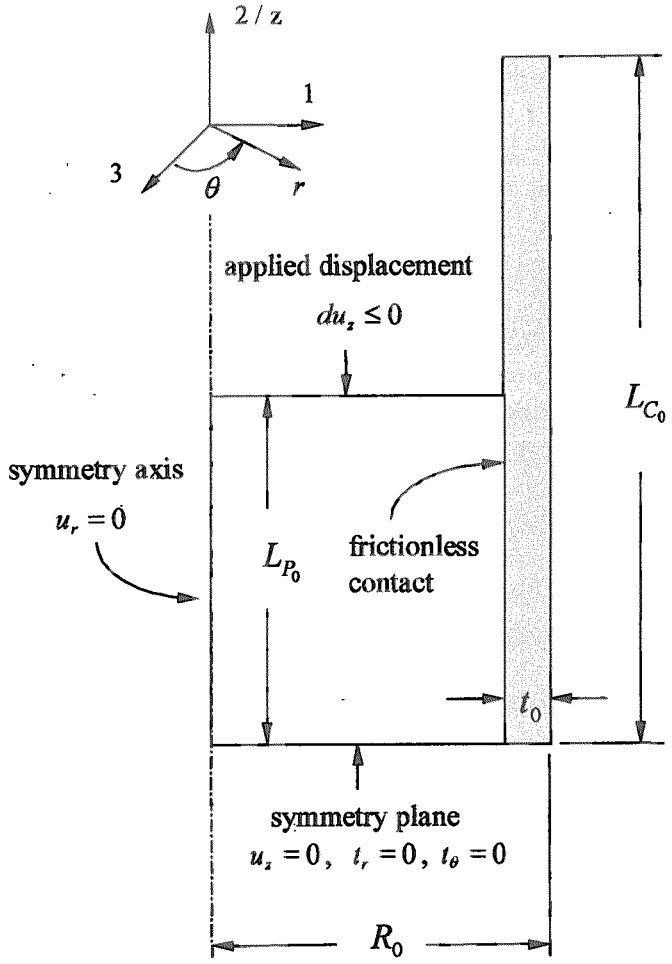


Figure 2. Geometry and boundary conditions for the finite element simulation of the pellet cladding mechanical interaction, produced by the EDC-test. Note that the origin of the coordinate systems is on the pellet/cladding mid-plane (i.e. the symmetry plane).

The geometry, used in the finite element simulation, is shown in Fig. 2 together with the boundary conditions. The symmetries with respect to the pellet/cladding axis and the mid-plane require the consideration of only one quarter of the axial section of the pellet and the cladding. Therefore L_{P0} and L_{C0} are the half-lengths of the pellet and the cladding, respectively. Cartesian, (x_1, x_2, x_3), and cylindrical, (r, θ, z), coordinates are considered. x_2/z is the symmetry axis and (x_1 x_3) is the symmetry plane, i.e. the pellet/cladding mid-plane. Note that, although not shown in Fig. 2, the origin of the coordinate system is on the symmetry plane.

The loading is applied by displacements along the symmetry axis, prescribed on the top pellet boundary. These displacements result into the reduction of the length of the pellet and the development of compressive stresses in the pellet. Due to axial symmetry and material cohesion, the radial displacement, u_r, is equal to zero along the symmetry axis. On the symmetry plane at z=0, (i) the axial displacements are zero,

u_2=0, and (ii) the tangential traction is zero, t_1=t_3=0. Between the pellet and the cladding, frictionless contact is considered.

The simulations were performed, by considering the material properties at room temperature. The zirconium alloy cladding was assumed to be elastic-plastic. Young's modulus, E, and Poisson's ratio, ν, were taken equal to 97000 MPa and 0.4 respectively. The plastic behavior of the zirconium alloy was modeled by considering J_2-flow theory and isotropic hardening:

$$\bar{\sigma} = H\left(\bar{\varepsilon}^p\right) = \sigma_0\left(1+\frac{\bar{\varepsilon}^p}{\varepsilon_0}\right)^{1/n}, \qquad (1)$$

where $\bar{\sigma}$ and $\bar{\varepsilon}^p$ are Mises effective stress and the accumulated effective plastic strain, respectively. Also σ_0 is the initial yield stress in tension, ε_0 is a reference strain, equal to the elastic strain at yielding initiation in simple tension, and n is the hardening exponent. Calculations have been performed for hardening material with σ_0 equal to 600MPa and n equal to 7.76 as well as for non-hardening material, ($1/n$=0), with σ_0 equal to 400, 600 and 800MPa. Note that the hardening exponent was derived from an ultimate tensile stress, in a simple tension test, equal to 780MPa. Thus the effect of irradiation on cladding deformation can be taken into account implicitly, by varying yield stress and hardening. Hardening is also affected by hydride precipitation (Arsène and Bai, 1998). However, in nuclear fuel cladding, hydrides precipitate mainly next to the oxide layer, on the water-side of the cladding. Therefore an appropriate simulation should take into account the non-homogenous hydride distribution.

The properties of the pellet polymer were calculated, by analyzing pellet compression tests, which were performed at Studsvik Nuclear. The pellet material was assumed to be elastic-plastic. Young's modulus, E_P, and Poisson's ratio, ν_P, were derived to be equal to 594 MPa and 0.474, respectively. Plastic behavior was again simulated, by using J_2-flow theory and isotropic hardening. It was found that a combination of Johnson-Cook and linear hardening laws provide the best fitting to the experimental data:

$$\bar{\sigma} = H\left(\bar{\varepsilon}^p\right) = \sigma_{P0} + K\left(\bar{\varepsilon}^p\right)^N, \qquad \bar{\varepsilon}^p \le 0.05, \qquad (2a)$$

$$\bar{\sigma} = H\left(\bar{\varepsilon}^p\right) = \sigma_{P0} + K(0.05)^N + KN(0.05)^{N-1}\left(\bar{\varepsilon}^p - 0.05\right), \quad \bar{\varepsilon}^p \ge 0.05. \qquad (2b)$$

The coefficient K and the hardening exponent N provide the best fit, when being equal to 19MPa and 0.22, respectively. The yield stress in compression, σ_{P0}, was derived to be equal to 6.4MPa.

No rate effects of the pellet material were considered. Indeed, the duration of the EDC-test is a fraction of a second (e.g. 0.05 to 0.2 s). Therefore, the relaxation of the material is negligible. The test, for a certain loading rate, could be adequately simulated, by considering the stress-strain curve of the polymer, for the loading rate under consideration. In order to estimate the effect of polymer yield stress variation, due to different loading rates, an additional calculation was performed with polymer yield stress by 20% smaller than that used in all other calculations. No variation on the hardening function was assumed. The normalized distribution of cladding radius

change and total energy density, along the symmetry axis, were identical for both yield stress values of the polymer. Therefore, the results on the deformation of the cladding do not depend on the rate-effects of the polymer, for the temperature and the rates under consideration.

The numerical simulation was performed, by using the commercial finite-element code ABAQUS/Standard (version 6.1).

According to the options of ABAQUS program, the 'hard' contact model was considered. Then, no pressure was applied while surfaces were not in contact, and any level of pressure could be applied without penetration, once contact was established. For more details, one is referred to ABAQUS/Standard User's Manual. The numerical simulation of contact required special care, when meshing the different parts. In order to prevent numerical penetration of pellet inside the cladding, the element size in the pellet mesh should be no more than twice that of the cladding. As the behavior of the cladding is the object of our study, this is the part one needs to refine, but pellet refinement has to be kept adequate.

CAX4R elements without twist were selected, which are 4-node bilinear axisymmetric solid elements. 100x85 elements of equal size were used in the pellet and 400x26 equal-size elements were used in the cladding.

3. Discussion of Results

The deformation of the cladding depends on zirconium alloy elastic-plastic properties, cladding geometry and distribution and level of applied loading. The area over which contact pressure is applied and consequently the distribution of applied loading depend on the initial pellet length, L_{P0}. A measure of loading is the ratio of the length of the deformed pellet over its initial value, L_P/L_{P0}. Note that, given the pellet properties, including hardening, L_P/L_{P0} has a one-to-one relation with the traction, applied by the pistons. However, L_P/L_{P0} depends on pellet's properties and consequently it generally provides a different cladding deformation status for different pellet material. An alternative loading measure, is the ratio of the change of the cladding external radius over its initial value at the mid-plane, $\Delta R/R_0$. Note that $\Delta R/R_0$ provides the engineering hoop-strain on the external surface of the cylinder at the mid-plane and it can be measured during the performance of the experiment. Therefore cladding deformation depends mainly on the following dimensionless parameters:

(a) material parameters: zirconium alloy yield stress over Young's modulus, Poisson's ratio and the hardening exponent, (σ_0/E, ν, n),

(b) characteristic lengths: cladding thickness over radius, cladding length over radius and pellet length over radius (t_0/R_0, L_{C0}/R_0, L_{P0}/R_0), and

(c) loading parameters: deformed pellet length over initial pellet length, L_P/L_{P0}, or equivalently, engineering hoop-strain on the external surface of the cylinder at the mid-plane, $\Delta R/R_0$.

If the pellet is made of a nearly incompressible material with low yield stress, the deformation of the cladding is nearly independent of pellet material properties. Note that, variation of polymer's yield stress by 20% did not alter the normalized distributions of radius increase and total energy density, along the axis of the

cladding. In the following discussion, $\Delta R/R_0$ has been chosen to specify the level of applied loading. Detailed calculations on the elastic-plastic deformation of the cladding are given by Dufourneaud and Varias (2001).

3.1 Distribution of Major Field Quantities – Effect of Cladding Yield Stress and Hardening

Emphasis is placed in the distribution of the maximum principal stress, the dissipated energy density (i.e. the plastic work per unit volume) and the total energy density in the cladding. Maximum principal stress may trigger the fracture of brittle hydrides in the cladding, especially in the external layer of the cladding, where hydride-rich areas are formed in high burnup fuel rods. All of the field distributions, within the cladding, are for the case of hardening zirconium alloy with yield stress equal to 600MPa. On the other hand, the evolution of the maximum values of the critical field quantities, with applied loading, are given for all material cases, under consideration.

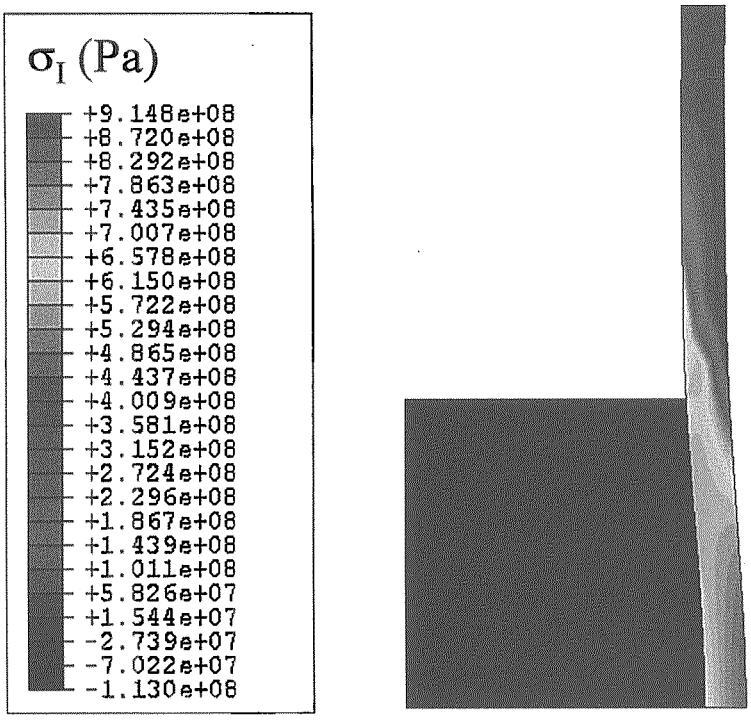


Figure 3. Distribution of maximum principal stress, σ_I, for a hardening zirconium alloy with σ_0 = 600MPa, at $\Delta R/R_0$ =6.0%.

Figure 3 shows the distribution of the maximum principal stress, at $\Delta R/R_0 = 6.0\%$. Note that the position of the maximum value moves from the internal layer to the external layer of the cladding, when yielding occurs. This is a consequence of the larger permanent stretching, along the circumference, of the inner layer of the cladding with respect to the plastic stretching of the outer layer of the cladding. Consequently, after yielding, the maximum principal stress takes larger values in the area, where the brittle hydride layer is expected to form.

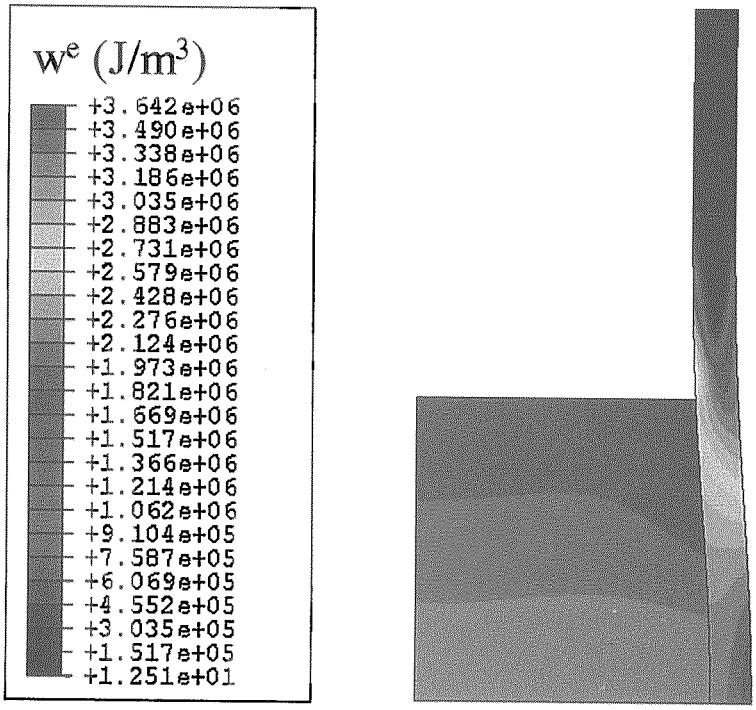


Figure 4. Distribution of the elastic strain energy density, w^e, for a hardening zirconium alloy with σ_0 = 600MPa, at $\Delta R/R_0$ =6.0%.

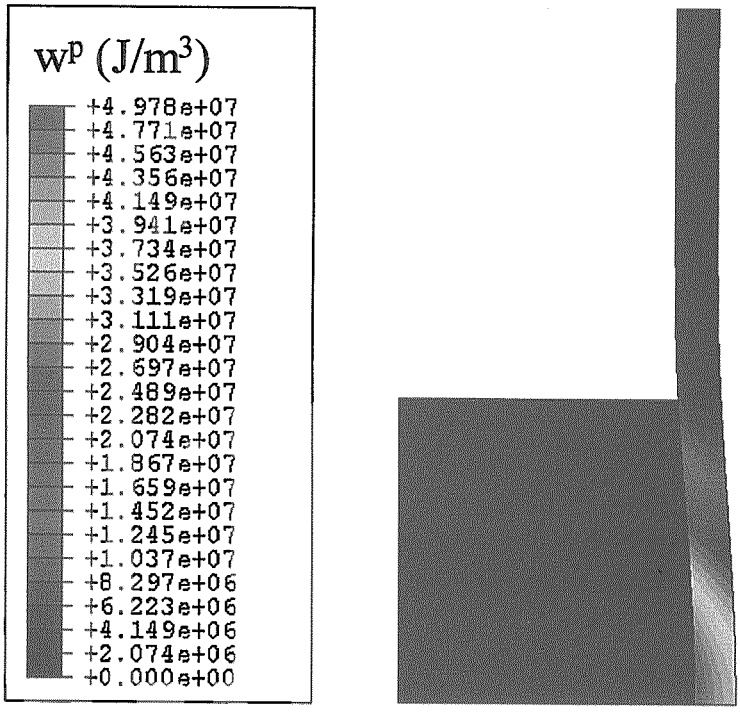


Figure 5. Distribution of the dissipated energy density (i.e. the plastic work per unit volume), w^p, for a hardening zirconium alloy with σ_0 = 600MPa, at $\Delta R/R_0$ =6.0%.

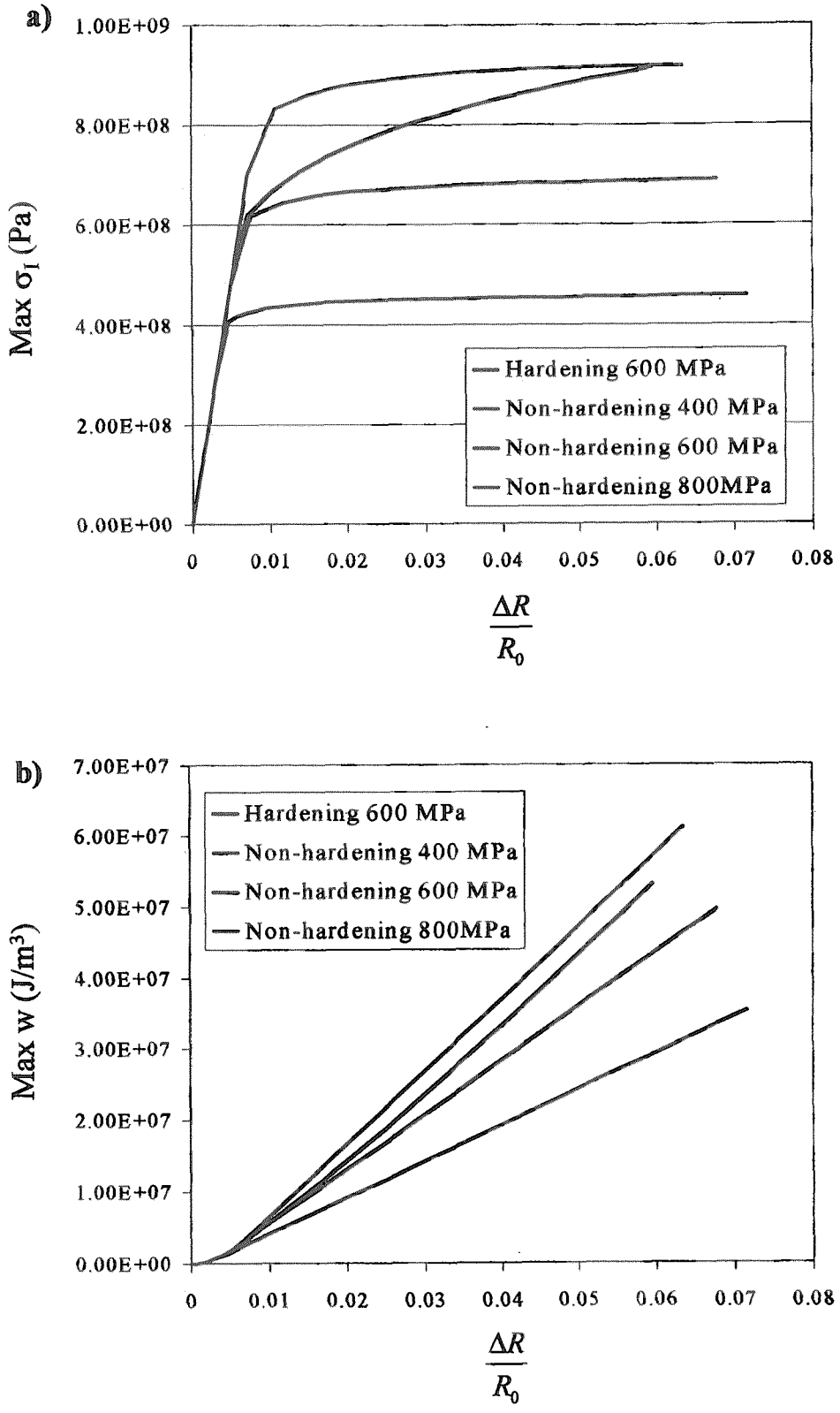


Figure 6. Variation of the maximum value of a) the principal stress σ_1, at the symmetry plane, and b) the total energy per unit volume, w, with cladding straining, given by $\Delta R/R_0$.

Figure 4 shows the distribution of the elastic strain energy density, w^e, in the cladding at $\Delta R/R_0 = 6.0\%$. As in the case of σ_I, the local maximum value of w^e is initially at the internal cladding surface, before yielding, and subsequently moves to the external cladding surface. However, the elastic strain energy density is an order of magnitude smaller than the density of the dissipated plastic work, w^P (see Fig. 5). Therefore it is not expected to have a strong contribution to the failure of the cladding, after significant plastic deformation. On the other hand, either the accumulated effective plastic strain or the dissipated plastic work is an appropriate quantity for the development of a cladding ductile failure criterion. The total energy density, w, which includes both elastic and dissipated energy densities, is also a relevant quantity for the development of a ductile failure criterion.

The effects of cladding hardening and yield stress on the evolution of the maximum values of σ_I and w with $\Delta R/R_0$ are presented in Figs. 6a and 6b. Note that the maximum of w is reached at the internal cladding surface, due to the contribution from plastic dissipation. For a given value of $\Delta R/R_0$, the reduction of hardening and yield stress leads to the reduction of the maximum values of σ_I and w.

3.2 Injected Energy

During the performance of the EDC-test, the engineering hoop strain, at the mid-plane of the specimen, as well as the energy, which is injected in the loading device and the specimen, are measured (Grigoriev, Jakobsson, and Schrire, 2001). The injected energy is subsequently corrected in order to remove the elastic strain energy, which is stored in the loading device. Some other corrections are also made in order to remove a part of the energy, which is dissipated or stored in the pellet. For this purpose, the displacement of the pellet, when compressed in a rigid cylinder, is subtracted from the total cross-head displacement. By this correction, a significant part of the total injected energy is subtracted. The subtracted energy can be about 1/3 (or even larger) of the total energy, which is injected in the cladding and the pellet; the actual proportion depends on cladding straining. In the present section it is verified that the energy, which is dissipated or stored in the pellet, is indeed a significant part of the total injected energy.

Figure 7 shows the injected energy, W, in the cladding and the pellet as well as in the cladding alone. The curves correspond to hardening and non-hardening cladding with yield stress $\sigma_0 = 600\text{MPa}$. Note that the energy, which is dissipated or stored in the pellet, is an appreciable part of the total injected energy. For example, at $\Delta R/R_0 = 6.0\%$, the total injected energy is 6.9J, when the cladding hardens. In this case, the energy injected in the pellet is equal to 2.2J, i.e. one third of the total injected energy. In the case of non-hardening cladding, at $\Delta R/R_0 = 6.8\%$, the total injected energy and that of the pellet are equal to 5.9J and 1.8J, respectively; the energy, which is dissipated/stored in the pellet, is again about 1/3 of the total injected energy. At smaller cladding strains, the fraction of the energy, dissipated/stored in the pellet, is even larger. For example, at $\Delta R/R_0 = 2\%$, in the case of hardening cladding, the total energy is about equal to 2.6J and the pellet part is about equal to 1.1J. The respective figures for non-hardening cladding, at $\Delta R/R_0 = 2\%$, are 2.1J and 0.9J.

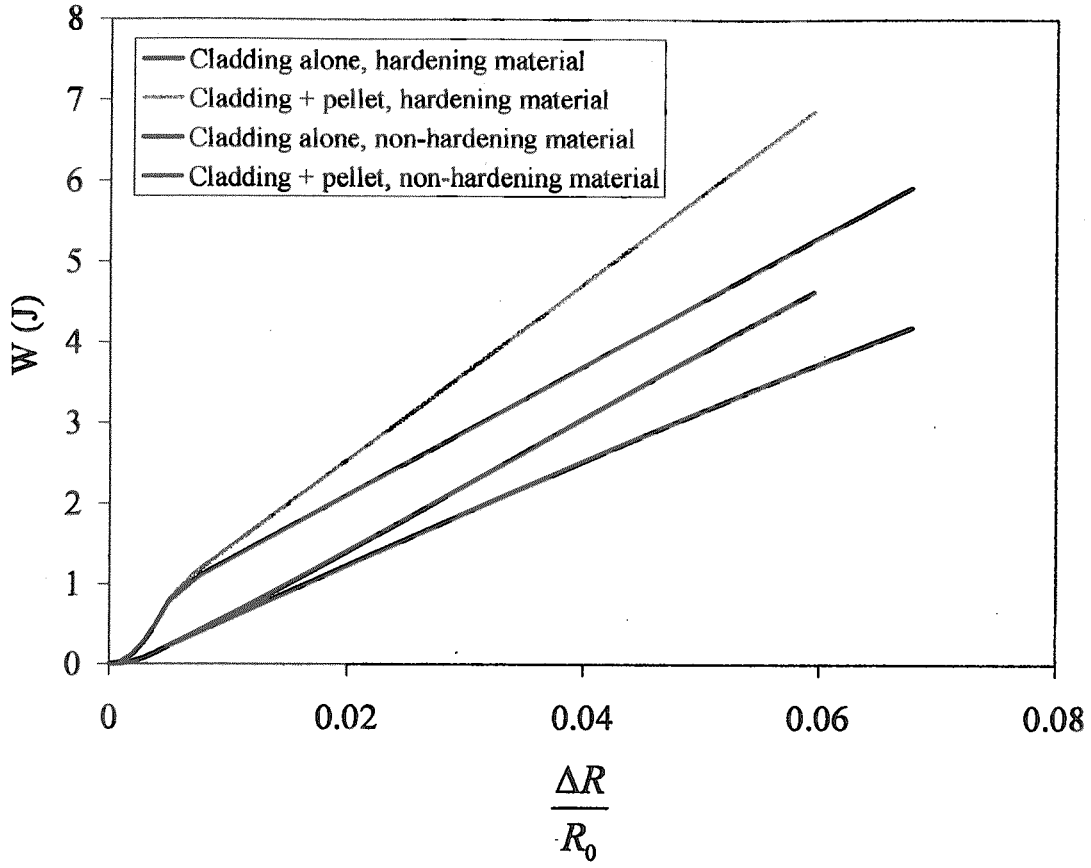


Figure 7. Variation of injected energy in pellet/cladding and cladding alone with cladding straining, given by $\Delta R/R_0$. The cladding yield stress is 600MPa.

The present numerical estimates of the energy injected in the cladding are comparable with the experimental values given by Grigoriev, Jakobsson, and Schrire (2001), (see Fig. 4b of their paper). However, it should be mentioned, that the yield stress and hardening of the cladding material, in the above experiments, may not be the same as those used in the present simulations.

3.3 Axial Distributions of Cladding Radius Change and Total Energy Density

Cladding external radius is a quantity, which is measured easily. Its distribution along the symmetry axis provides information on the elastic-plastic deformation of the cladding. It can also be associated with the development of stresses, during the deformation of the cladding. Therefore, it could facilitate the development of cladding failure criteria. Indeed, Grigoriev, Jakobsson and Schrire (2001) have measured the distribution of the permanent change of cladding external diameter along its symmetry axis, in the unloaded condition after the performance of experiments, which did not result into the fracture of the cladding. Subsequently, they assumed a linear relation between total energy density and external radius change or equivalently the respective engineering hoop strain. Based on this assumption, they provided estimates on the critical total energy density for the cases of cladding failure. The objectives of section 3.3 are the following:

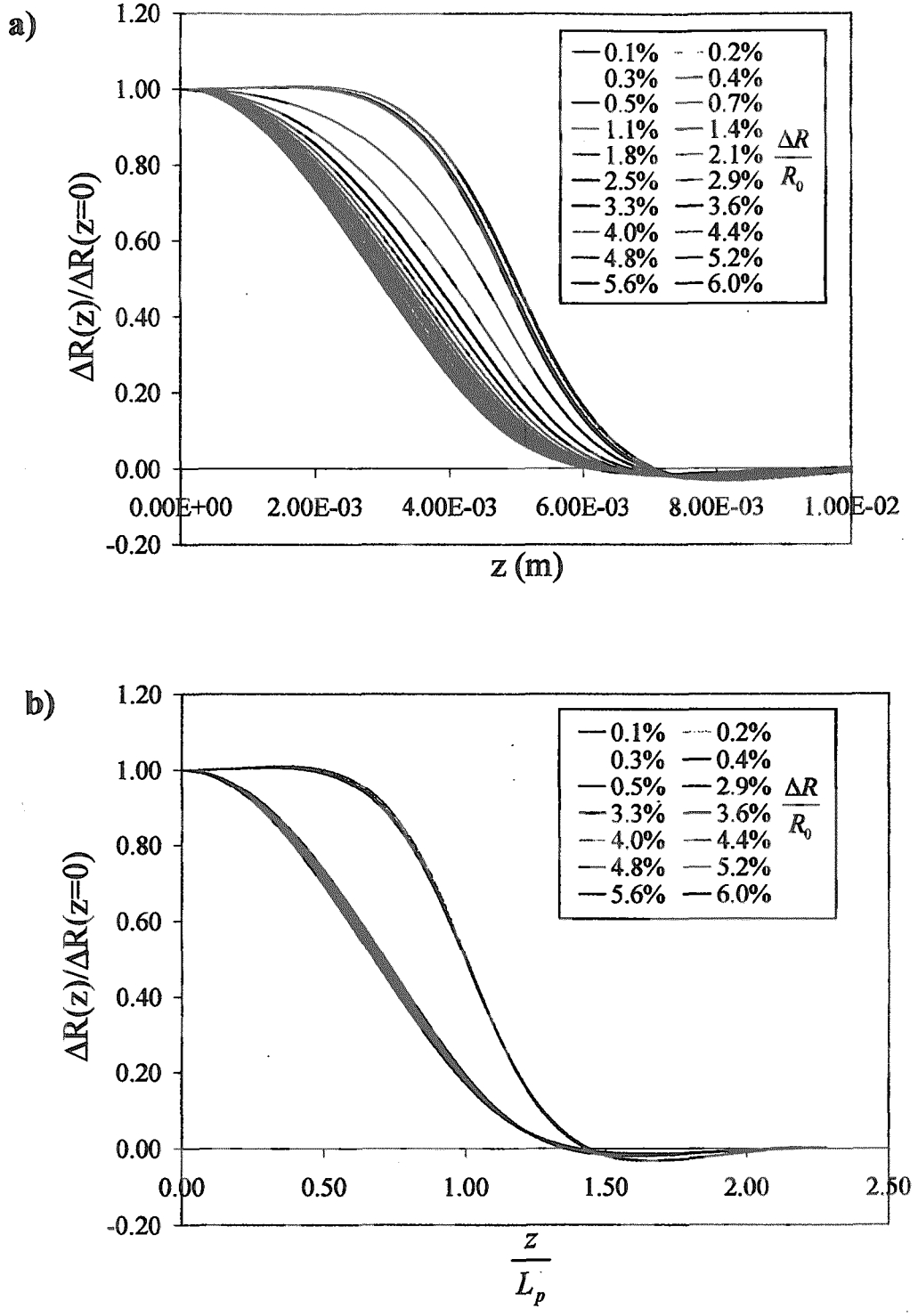
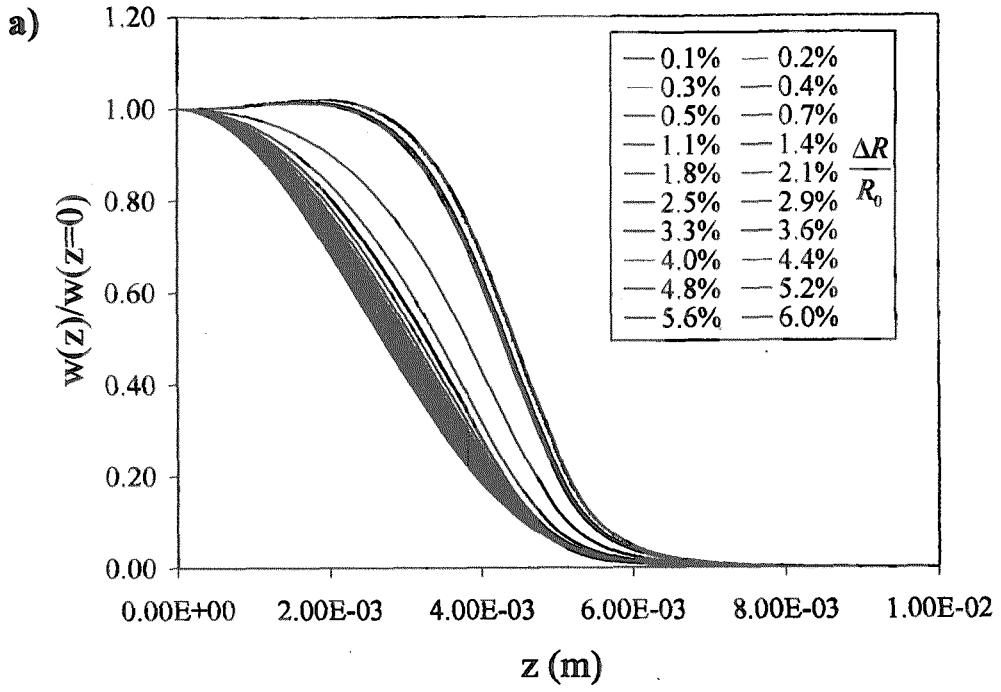


Figure 8. Axial distribution of the increase of the cladding external radius, $\Delta R(z)$, normalized by its value on the symmetry plane, $\Delta R(0)$, vs. a) z-position in the deformed state and b) z/L_P . Hardening cladding material with yield stress equal to 600MPa.



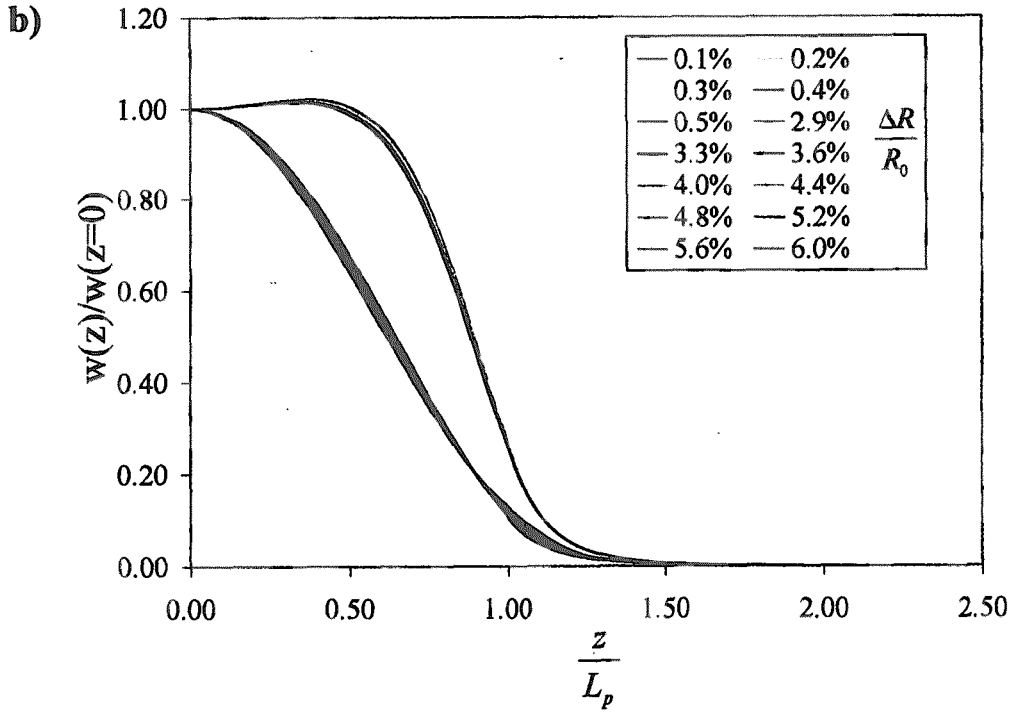


Figure 9. Axial distribution of total energy density in the cladding, $w(z)$, normalized by its value on the symmetry plane, $w(0)$, vs. a) z-position in the deformed state and b) z/L_p . Hardening cladding material with yield stress equal to 600MPa.

(a) to calculate the axial distributions of external radius change and total energy density in the cladding,
(b) to investigate the dependence of these distributions on applied loading and
(c) to investigate if cladding external radius change and total energy density are linearly related.

Figure 8a shows the axial distribution of cladding radius change for various levels of applied loading, expressed by $\Delta R/R_0$. The distributions correspond to the case of hardening cladding. The radius change has been normalized by its value at the symmetry plane. Note that the distributions before cladding yielding, i.e. at $\Delta R/R_0 \le 0.5\%$, differ only slightly. Also the distributions seem to converge at relatively high plastic deformation, i.e. $\Delta R/R_0 \ge 3\%$. On the other hand, the respective distributions at the initial stage of plastic deformation vary significantly with loading. The axial distribution of any field quantity is expected to depend on the size of the contact surface, where internal pressure is applied on the cladding. It is therefore expected that the axial distributions of field quantities depend on the current pellet length, L_P. For this reason $\Delta R(z)/\Delta R(0)$ has been plotted again as a function of z/L_P (Fig. 8b). Note that the distributions of this dimensionless quantity collapse, with a negligible error, onto two lines, one for $\Delta R/R_0 \le 0.5\%$ and another for $\Delta R/R_0 \ge 3\%$. Therefore the axial distribution of $\Delta R(z)/\Delta R(0)$ vs. z/L_P does not depend on the level of applied loading for $\Delta R/R_0 \le 0.5\%$ and $\Delta R/R_0 \ge 3\%$, in the case of hardening cladding with yield stress equal to 600 MPa. The same conclusion has been derived for the case of total energy density (see Figs. 9a and 9b). The effect of cladding hardening on the existence of load-independent axial distributions has been checked by considering the case of non-hardening cladding with yield stress equal to 600MPa. Figures 10a and 10b show the respective axial distributions of the normalized quantities $\Delta R(z)/\Delta R(0)$ and $w(z)/w(0)$. Note that load independent distributions are indeed valid for $\Delta R/R_0 \le 0.5\%$ and $\Delta R/R_0 \ge 3.5\%$. In the case of total energy density, there is a deviation from the load independent distribution in the neighborhood of $z = L_P$. However, the energy density is relatively small in this region and no failure initiation is expected. Therefore there is no consequence on the development of failure criteria.

Based on the existence of the load-independent distributions of $\Delta R(z)/\Delta R(0)$ and $w(z)/w(0)$ vs. z/L_P, one may derive a critical total energy density from experimental measurements. Indeed, the following procedure could be adopted:

(1) experimental measurement of the total injected energy, up to cladding failure, minus the elastic strain energy stored in the loading device,
(2) subtraction of the energy dissipated/stored in the pellet, by numerically deriving a diagram similar to that in Fig. 7, and estimation of the average injected energy density in the cladding, w^{ave},
(3) numerical derivation of the load-independent $w(z)/w(0)$ vs. z/L_P curve as well as of the average value of $w(z)/w(0)$ over the whole range of z/L_P, $(w(z)/w(0))^{ave}$,
(4) calculation of the critical total energy density in the cladding, w^{cr} $(= w^{ave}/(w(z)/w(0))^{ave})$.

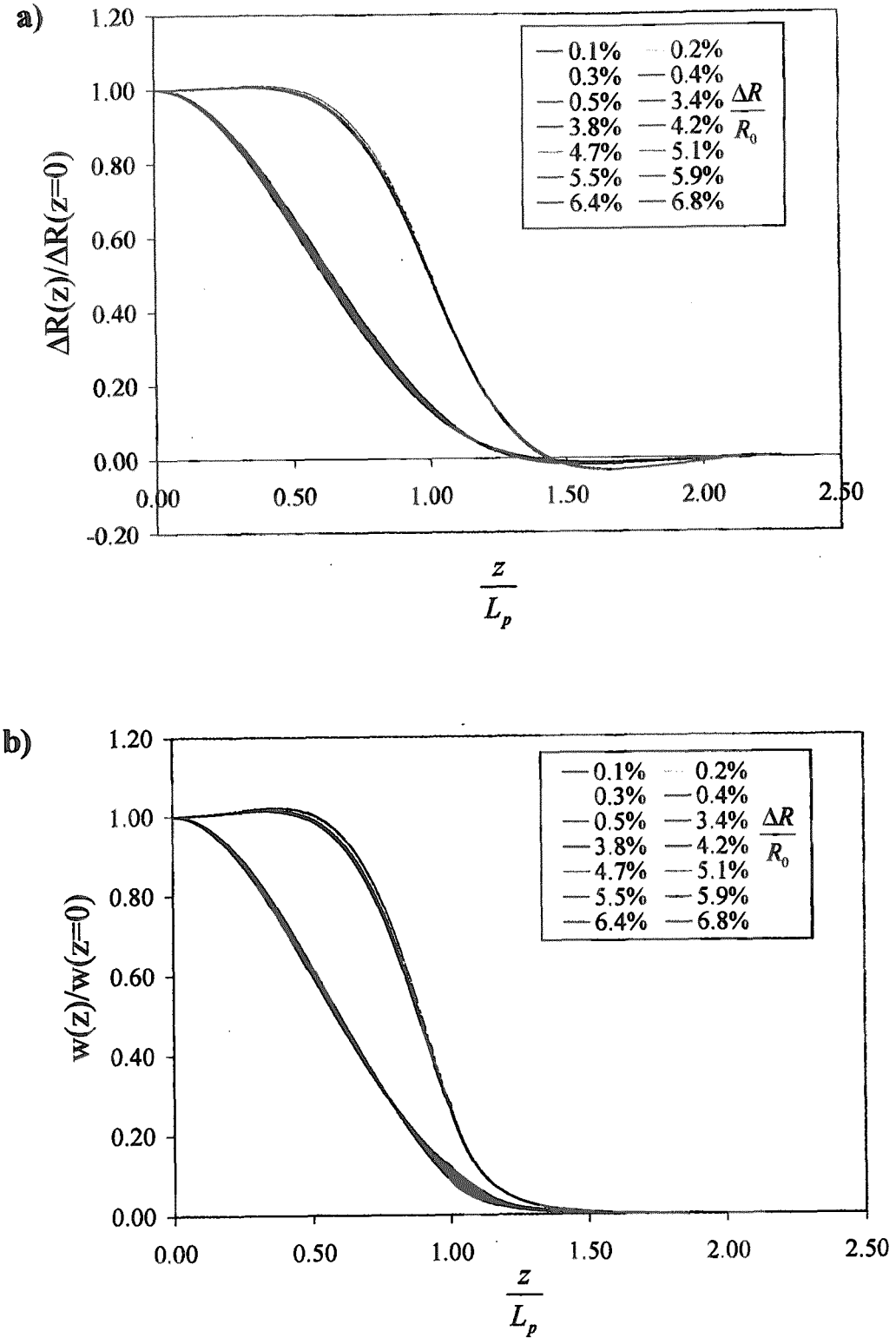


Figure 10. Axial distribution of a) the increase of the cladding external radius, $\Delta R(z)$, normalized by its value on the symmetry plane, $\Delta R(0)$, and b) the total energy density in the cladding, $w(z)$, normalized by its value on the symmetry plane, $w(0)$, vs. z/L_P . Non-hardening cladding material with yield stress equal to 600MPa.

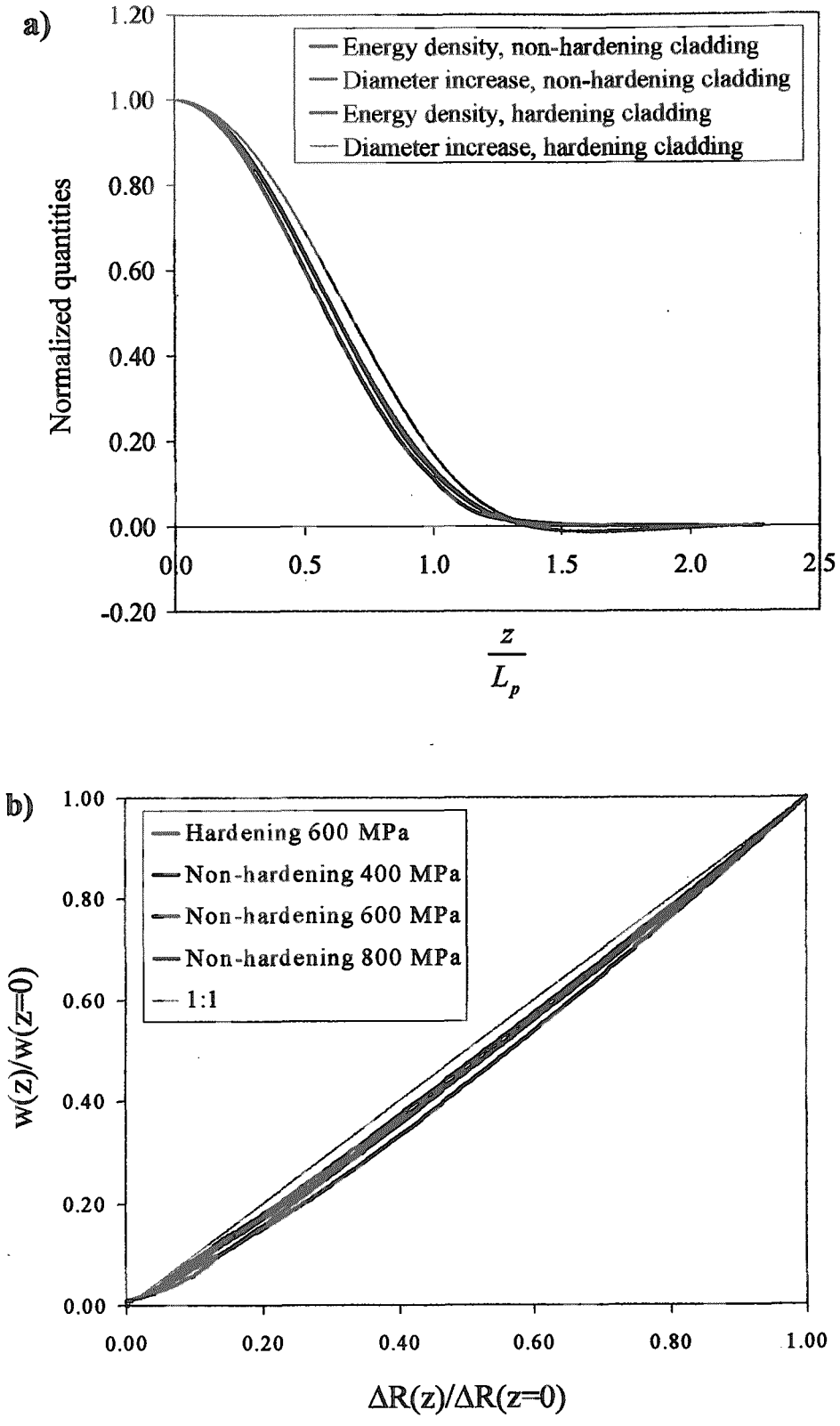


Figure 11. Investigation of existence of linearity between total energy density and external radius increase in the cladding. a) Normalized quantities vs. z/L_P, (σ_0 = 600 MPa). b) Total energy density vs. external radius increase.

However, the detailed numerical calculations could be avoided, at least in deriving preliminary estimates, if the linearity assumption, made by Grigoriev, Jakobsson and Schrire (2001), is true within an acceptable error. Figure 11a shows the load-independent profiles of radius change and total energy density for hardening and non-hardening cladding with yield stress equal to 600MPa. The profiles deviate only slightly. Note that if the linearity assumption was satisfied exactly the total energy density and radius change profiles should collapse for a given cladding material. The level of deviation of $\Delta R(z)/\Delta R(0)$ and $w(z)/w(0)$ from a linear relation is clearly shown in Figure 11b. The 1:1 line corresponds to the exact satisfaction of the linearity assumption. Note that the 1:1 line is approached when hardening and yield stress decrease. The maximum deviation varies between 2.9% for $\sigma_0 = 400\text{MPa}$ (non-hardening material) and 6.9% for $\sigma_0 = 600\text{MPa}$ (hardening material). The error is below 5% for all non-hardening cases, considered in the present study. If the linearity assumption is used, then the critical total energy density could be calculated by considering the equality (Grigoriev, Jakobsson and Schrire, 2001):

$$w^{cr} = w^{ave} \cdot \frac{\Delta R^{cr}}{\Delta R^{ave}}, \tag{3}$$

where ΔR^{cr} is the external radius increase at the mid-plain, when failure occurs, and ΔR^{ave} is the average external radius change. Note that ΔR^{ave} can be estimated experimentally. However, the numerical derivation of ΔR^{ave} is expected to be less expensive, in which case the procedure (1) to (4) could instead be applied.

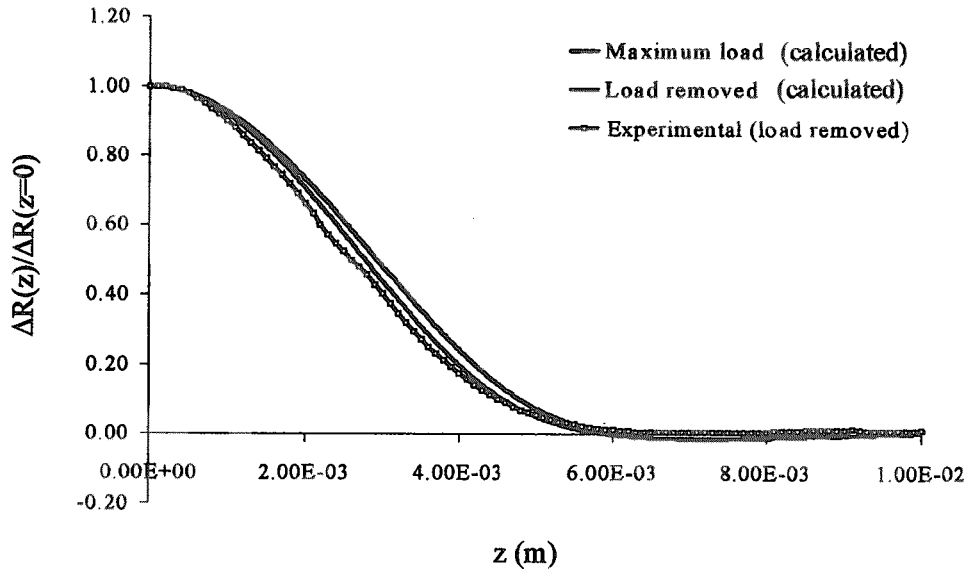


Figure 12. Axial distribution of the increase of the cladding external radius, $\Delta R(z)$, normalized by its value on the symmetry plane, $\Delta R(0)$, in the deformed state at maximum load and after removal of loading for hardening cladding material. The maximum load corresponds to $\Delta R/R_0 = 6.0\%$. After load removal, $\Delta R/R_0 = 5.2\%$. The experimentally derived distribution is also included.

The above discussion is valid for the distributions at applied loading. Note that these are the distributions of interest, since the prediction of cladding failure is the objective of the theoretical and the experimental studies. The cladding diameter increase, at the mid-plane, is indeed measured during the application of the loading. However, as mentioned previously, its axial distribution has been measured after the removal of loading and the creep of the polymer pellet. For this reason, the effect of load and pellet removal on the axial profile of cladding radius change has been considered. The pellet was removed, during the numerical calculation, in order to take into account the effect of polymer creep. Figure 12 shows the respective distributions in the case of hardening cladding. The profile changes with the removal of loading, but very little with the removal of the pellet. In the same figure the experimentally derived profile is also presented. Note the good agreement between the calculated and the experimentally derived profile. The yield stress and hardening of the cladding material in the above experiment may not be the same as those used in the present simulations. However, according to Fig. 11, the effect of these properties on cladding normalized profile is weak.

4. Concluding Remarks

A finite element simulation of the EDC-test has been performed. Both pellet and cladding were considered to be elastic-plastic. Their plastic deformation was simulated by J_2-flow theory. The calculations included, three different values of cladding material yield stress as well as both hardening and non-hardening behavior. Thus the effect of irradiation on cladding material properties is implicitly taken into account.

It is shown that, before cladding yielding as well as after substantial plastic deformation, the radial displacement, on the external surface, and the total energy per unit volume, when appropriately normalized, vary along the cladding axis according to specific distributions, which do not depend on the level of loading.

The calculated profile of the cladding, after deformation, is in agreement with experimental measurements.

A procedure is proposed for the estimation of the critical total energy density at cladding failure, which is based on the load-independent axial distribution of the total energy density. The procedure is described in section 3.3.

Acknowledgment

The present study is part of the project on 'Hydrogen Embrittlement and Fracture in Hydride Forming Metals', which is financed by the Foundation for Knowledge and Competence Development (Project Grant Hög 2000, KK-Stiftelsen, Sweden). The project is performed with the cooperation of Studsvik Nuclear AB and Barsebäck Kraft AB.

References

1. ABAQUS/Standard, Version 6.1, User's Manual, Hibbitt Karlsson & Sorensen Inc, Pawtucket, RI, USA.
2. Arsène, S. and Bai J., (1998), 'Effect of Hydriding and Irradiation on the Mechanical Properties of Zircaloy Cladding', Report, Ecole Centrale Paris, France.
3. Bibilashvili, Yu., Sokolov, N., Nechaeva, O., Salatov, A., Sokolov, F., Asmolov, V., Yegorova, L., Kaplar, E., Trutnev, Yu., Smirnov, I., Ustinenko, V., Sazhnov, V., Smirnov, V. and Goryachev, A., (2000), 'Experimental Study of VVER High Burnup Fuel Rods at the BIGR Reactor under Narrow Pulse Conditions', *Proceedings of the ANS International Topical Meeting on LWR Fuel Performance*, Park City, USA, April 2000.
4. Dufourneaud, O. and Varias, A.G., (2001), 'Elastic-Plastic Deformation of a Nuclear Fuel Cladding Specimen under the Internal Pressure of a Polymer Pellet', *Report PA-03-06-01*, Malmö Univeristy, Malmö, Sweden.
5. Fuketa, T., Sasajima, H., Mori, Y. and Ishijima, K., (1997), 'Fuel Failure and Fission Gas Release in High Burnup PWR Fuels under RIA Conditions', *Journal of Nuclear Materials*, Vol. 248, pp. 249-256.
6. Grigoriev, V., Jakobsson, R. and Schrire, D., (2001), 'Experimental Evaluation of Critical Strain Energy Density for Irradiated Cladding under Simulated RIA Conditions', *Proceedings of ENS Topfuel 2001*, Stockholm, Sweden
7. Kuroda, M., Yoshioka, K., Yamanaka, S., Anada, H., Nagase, F. and Uetsuka, H., (2000), 'Influence of Precipitated Hydride on the Fracture Behaviour of Zircaloy Fuel Cladding Tube', *Journal of Nuclear Science and Technology*, Vol. 37, pp. 670-675.
8. Lemoine, F., (1997), 'High Burnup Fuel Behavior related to Fission Gas Effects under Reactivity Initiated Accidents (RIA) Conditions', *Journal of Nuclear Materials*, Vol. 248, pp. 238-248.
9. Northwood, D.O. and Kosasih, U., (1983), 'Hydrides and Delayed Hydrogen Cracking in Zirconium and its Alloys', *International Metals Reviews*, Vol. 28, pp. 92-121.
10. Schmitz, F. and Papin, J., (1999), 'High Burnup Effects on Fuel Behaviour under Accident Conditions: the Tests CABRI REP-Na', *Journal of Nuclear Materials*, Vol. 270, pp. 55-64.
11. Varias, A.G. and Massih, A.R., (2001), 'Material Degradation and Fracture in Zirconium Alloys', *Transactions of the 16th International Conference on Structural Mechanics in Reactor Technology*, Washington, DC, USA.
12. Varias, A.G. and Massih, A.R., (2000), 'Simulation of Hydrogen Embrittlement in Zirconium Alloys under Stress and Temperature Gradients', *Journal of Nuclear Materials*, Vol. 279, pp. 273-285.

Discussion:

Q: (M. Billone)

Analysis was done for room temperature properties of polymer pellet. How would the results change vs. temperature? In specific, how would the energy ratio (plug-to-total) change?

Have you benchmarked analysis by directly measuring hoop strain of Zircaloy ring vs. piston load?

A: Under the conditions of relatively small pellet material yield stress and near incompressibility, the effect of temperature, on load-independent axial distributions for radius change and total energy density of the cladding, is expected to be weak.

The energy which is stored/ dissipated in the pellet is removed from the total injected energy in pellet + cladding and therefore it does not have any effect on derivation of cladding failure criteria.

The actual level of the energy fraction in the pellet depends on the pellet material used at high temperatures.

A preliminary comparison between experiment and theory is given in Fig.12 of the paper. Detailed comparison will follow.

Session 2b-2

Three Dimensional Analysis of RIA in PWR and BWR with High Burnup Fuel

T. Nakajima, I. Komatsu, R. Yoshiki

Nuclear Power Engineering Corporation (NUPEC), 17-1, 3-Chome, Toranomon, Minato-ku, Tokyo 105-0001, Japan Tel:+81(3)4512-2777, Fax:+81(3)4512-2799, e-mail:nakajima@nupec.or.jp

ABSTRACT

The results of recent reactivity insertion accident (RIA) experiments with high burnup fuel performed in France (CABRI) and in Japan (NSRR) indicated that some fuel failed at the lower deposited energy in the fuel than was previously assumed. Taking it seriously, Japanese Nuclear Safety Commission (NSC) had reviewed the current licensing criteria for RIA, and the failure threshold for high burnup fuel was revised based on the new experimental data. The new failure threshold related to PCMI is defined as function of fuel burnup and it decreases stepwise with increasing fuel burnup. This change would directly affect the safety assessment of RIA.

Historically, the point kinetics model or one dimensional kinetics model using core wide coefficients having a significant conservatism has been employed for the safety assessment of RIA. This approach is insufficient to evaluate the distribution of fuel enthalpy in the core considering the variation of fuel burnup. In order to investigate the influences of fuel burnup and decreased threshold on the safety assessment of RIA, the realistic analysis by using detailed three dimensional method is necessary.

The three dimensional analysis of RIA in typical PWR and BWR with high burnup fuel was performed using the EUREKA-JINS/S code to understand the realistic fuel behavior during the transient and to evaluate the safety margin accurately. The fraction of fuel failure was evaluated applying the newly revised failure threshold. For the analysis of RIA in BWR, the void reactivity feedback was considered to understand how it affects on the fuel behavior under the RIA.

The results of three dimensional analysis of control rod ejection accident for a typical 4-loop PWR showed that none of fuel failure occurs under this event. The results of three dimensional analysis of control rod drop accident for a typical BWR considering the void reactivity feedback indicated that the void reactivity feedback significantly influenced to decrease the maximum fuel enthalpy and the fraction of fuel failure.

This paper presents the outline of three dimensional neutronic transient code "EUREKA-JINS/S" and calculated results of the RIA in typical PWR and BWR.

This study was performed under the sponsorship of the Ministry of Economy, Trade and Industry (METI).

Ins./Nupec

Fuel Safety Research Specialist' Meeting(FSRSM)

Three Dimensional Analysis of RIA in PWR and BWR with High Burnup Fuel

T.Nakajima/INS/NUPEC

March 4-5, 2002
Tokai, JAPAN

This study was performed under the sponsorship of the Nuclear and Industrial Safety Agency of the METI

Ins./Nupec

Background

- Currently, the regular adoption of high burnup fuel aiming up to 55 GWd/t was started in BWRs and is scheduled in PWRs in Japan.
- Japanese Nuclear Safety Commission(NSC) has reviewed the current licensing criteria for RIA, and PCMI failure threshold for high burnup fuel was revised in 1998 based on the new data from CABRI and NSRR experiments.
- In order to investigate the influences of fuel burnup and lower failure threshold on the safety assessment of RIA, the realistic analysis by using three dimensional method was performed.

Ins/Nupec 1

Outline of Presentation

- Outline of RIA
- Safety Assessment of RIA
- RIA Criteria in Japan
- EUREKA-JINS/S Code
- 3D Analysis of RIA in PWR
- 3D Analysis of RIA in BWR
- Sensitivity Analysis
- Summary

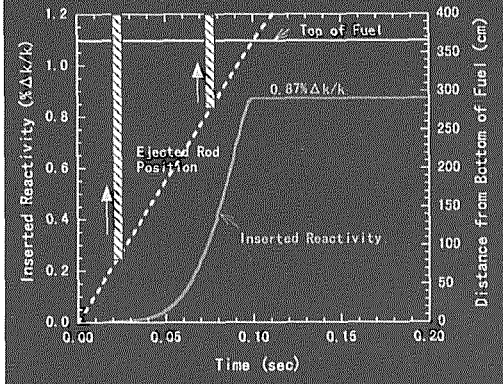
Ins/Nupec 2

Outline of RIA in PWR

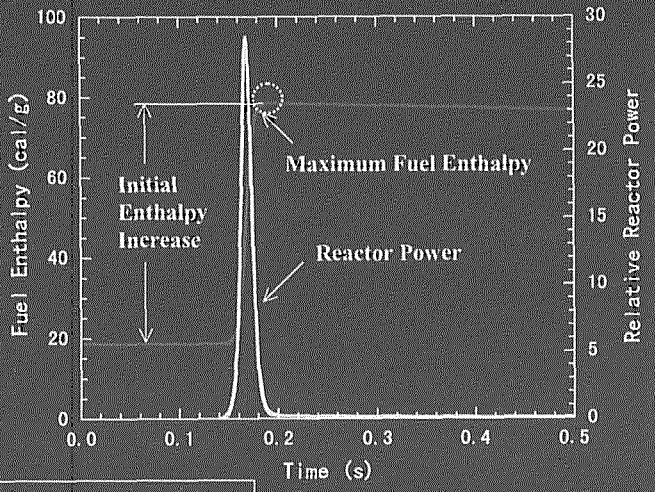
Control Rod Ejection

- Rod Ejection Time : 0.1 sec

Inserted Reactivity



Reactor Power and Fuel Enthalpy



- PCMI Failure occurs in early phase of RIA, so it is evaluated by initial enthalpy increase.
- Fuel failure related to DNB is evaluated by maximum fuel enthalpy.

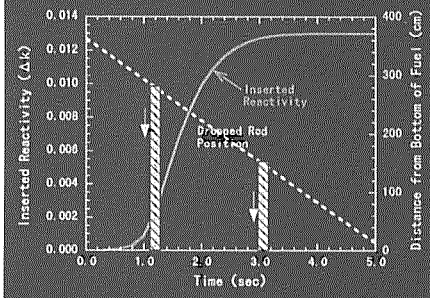
3

Outline of RIA in BWR

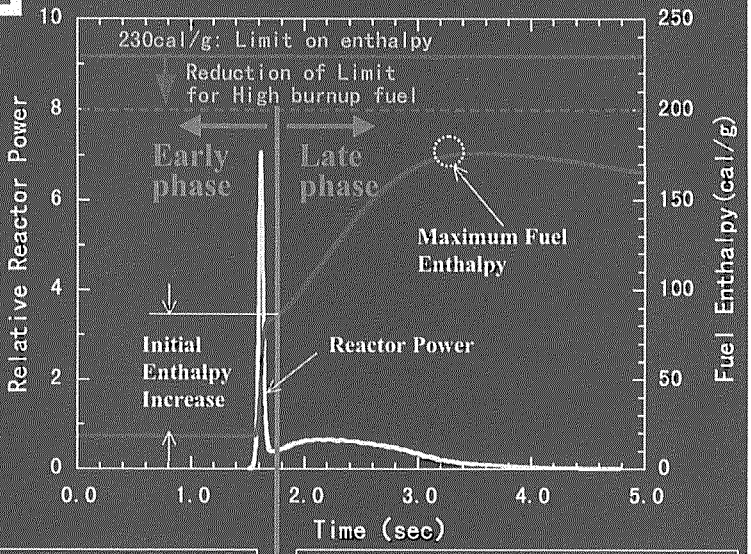
Control Rod Drop

- Rod Drop Time : about 5 sec

Inserted Reactivity



Reactor Power and Fuel Enthalpy



■ PCMI Failure occurs in early phase of RIA, so it is evaluated by initial enthalpy increase.

■ High-Temperature Rupture occurs in late phase of RIA, so it is evaluated by maximum fuel enthalpy.

4

Safety Assessment of RIA

RIA Event	Items to be Assessed	Criteria
Control Rod Ejection(PWR) / Control Rod Drop(BWR)	Maximum Fuel Enthalpy	1. Peak fuel enthalpy must not exceed the prescribed limit.
	Reactor Pressure	2. Maximum pressure to the pressure boundary must be lower than 1.2 times of the design pressure.
	Fuel Failure Fraction for Dose Calculation • PCMI failure • High temperature rupture • Fuel failure related to DNB	3. Undue radiation exposure to the neighboring public must be avoided.
	Mechanical Energy generated by • PCMI failure • waterlogged fuel rupture • Coolant pressure pulse • Water Hammer	Additional Criteria for RIA 4. The reactor vessel must not be damaged due to the mechanical energy generated by PCMI failure and waterlogged fuel rupture.*

*Note :
Assessment of item 4 is escaped for the cases that satisfy the provided conditions.

5

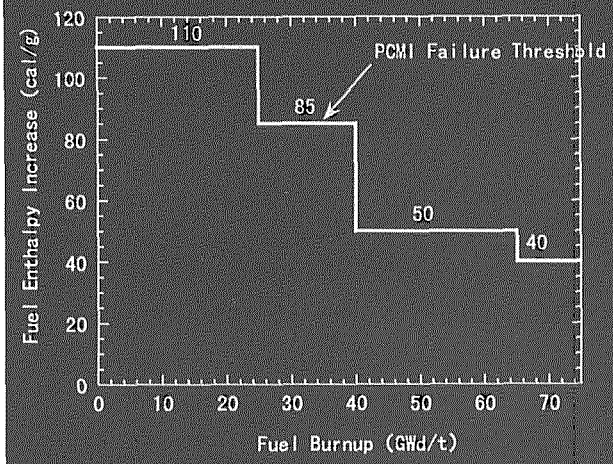
Limit on Peak Fuel Enthalpy

- To avoid the generation of coolant pressure pulses due to fuel melting, peak fuel enthalpy must not exceed the prescribed limit 230cal/g.
- The corresponding amount of enthalpy equivalent to the decrease of fuel melting point due to burnup increase, addition of gadolinium, plutonium etc. must be subtracted from 230cal/g.
- In the analysis of RIA for LWRs concerned, the reduced enthalpy limit was used for high burnup fuels concerned:
  - — for PWR UO_2 fuel ; 230 cal/g ➡ 189 cal/g
  - — for BWR UO_2 fuel ; 230 cal/g ➡ 200 cal/g

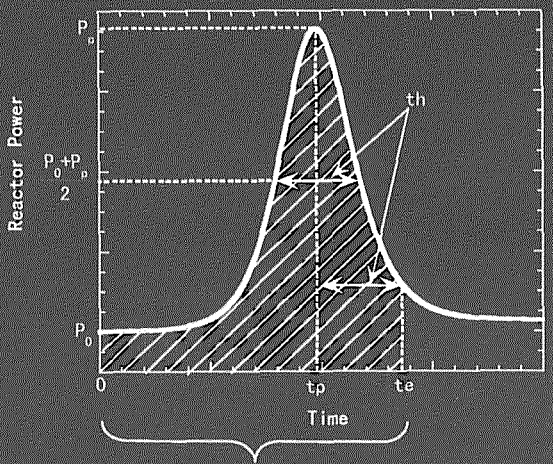
6

PCMI Failure Threshold

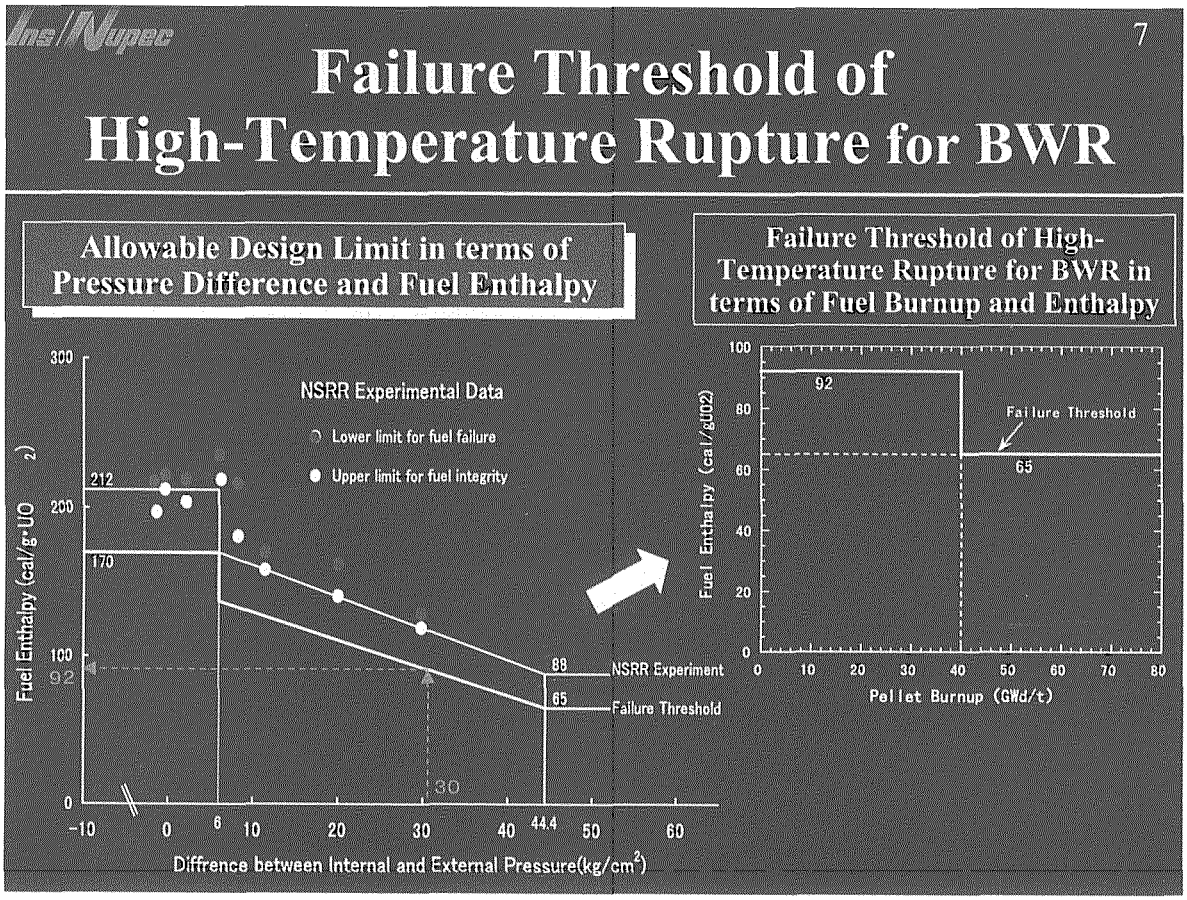
PCMI Failure Threshold in terms of Fuel Burnup and Enthalpy Increase

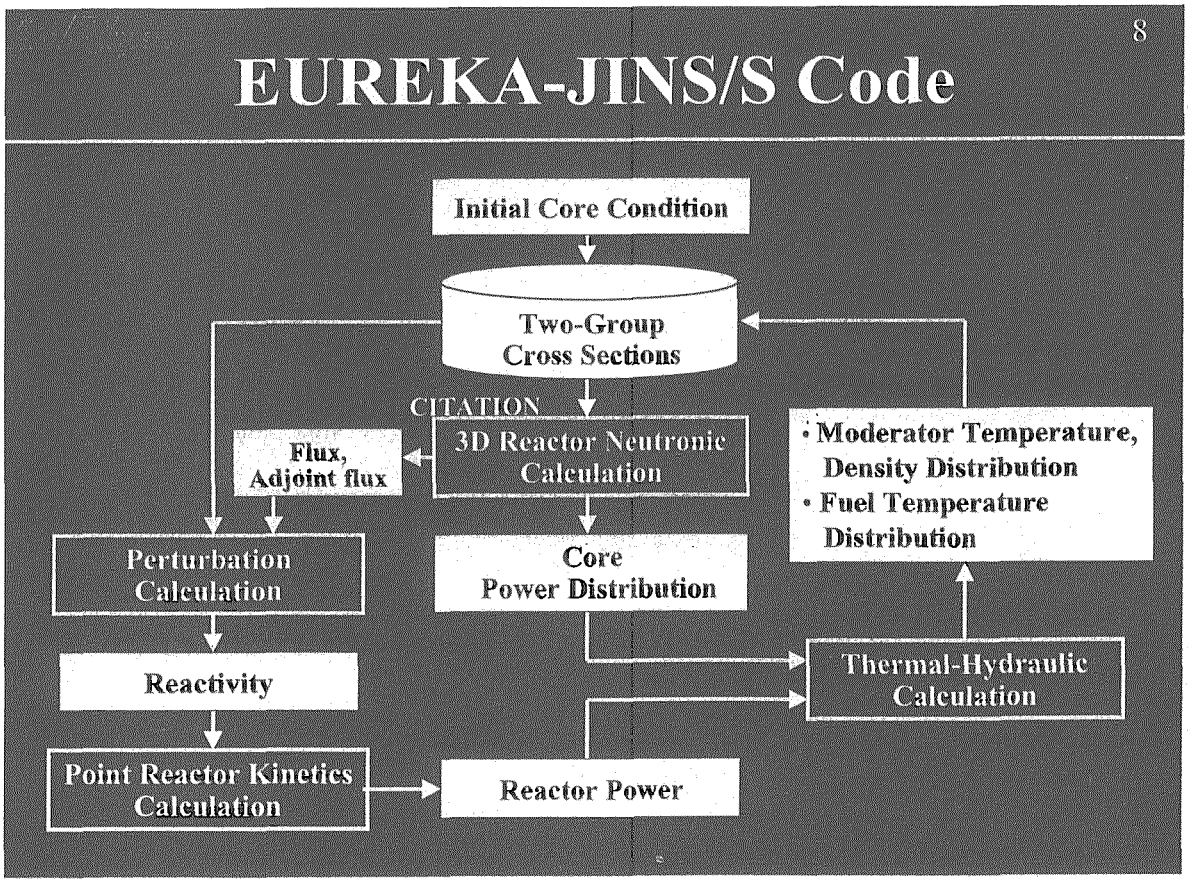


Definition of Initial Enthalpy



- PCMI Failure is evaluated by initial energy deposition defined by the shaded area.


Ins/Nupec
7
Failure Threshold of High-Temperature Rupture for BWR
Allowable Design Limit in terms of Pressure Difference and Fuel Enthalpy
NSRR Experimental Data
Lower limit for fuel failure
Upper limit for fuel integrity
Fuel Enthalpy (cal/g•UO2)
212
170
92
88
65
NSRR Experiment
Failure Threshold
30
44.4
Diffrence between Internal and External Pressure(kg/cm2)
Failure Threshold of High-Temperature Rupture for BWR in terms of Fuel Burnup and Enthalpy
Fuel Enthalpy (cal/gUO2)
92
65
Failure Threshold
Pellet Burnup (GWd/t)


8
EUREKA-JINS/S Code
Initial Core Condition
Two-Group Cross Sections
CITATION
3D Reactor Neutronic Calculation
Flux, Adjoint flux
Perturbation Calculation
Reactivity
Point Reactor Kinetics Calculation
Core Power Distribution
Reactor Power
• Moderator Temperature, Density Distribution
• Fuel Temperature Distribution
Thermal-Hydraulic Calculation

3D Analysis of RIA in PWR
— Control Rod Ejection Accident —

9

PWR Core Model	
Plant type	A typical 4-loop PWR
Core condition	End of Cycle(EOC) and Hot Zero Power(HZP)
Fuel assemblies	17 × 17 fuel configuration
Assembly maximum burnup	55 GWd/t
Ejected rod worth (% Δ k/k)	0.87 Conservatively, increased by 45%.
Radial mesh in the neutronic model	2 × 2 mesh／assembly
Axial planes in the fuel region	30
Thermal-hydraulic channels	120

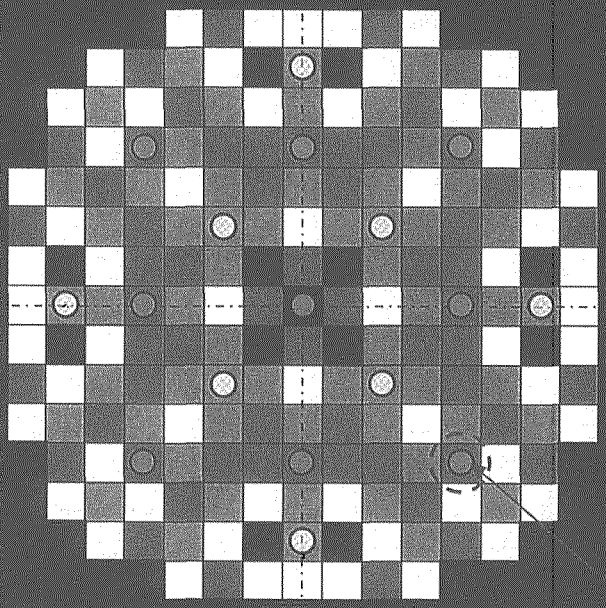
Core Conditions and Assumptions

10

Parameters	Values/Assumptions
Initial Power Level(MW)	3.411×10^{-9}
Coolant Inlet Pressure(kg/cm^{2}A)	158.2
Coolant Inlet Temperature(℃)	288.3
Coolant Flow	45% of nominal
Ejected Rod Worth(% Δ k/k)	0.87 Conservatively, increased by 45%.
Rod Ejection Time(sec)	0.1
Delayed Neutron Fraction(%)	0.47 Conservatively, decreased by 20%.
Prompt Neutron Lifetime(μ s)	7.0 Conservatively, decreased by 20%.
Doppler Reactivity Feedback	Conservatively, decreased by 20%.
Moderator Density Reactivity Feedback	Conservatively, decreased by 20%.
Ratio of Direct Moderator Heating	0.026

Fuel Loading Pattern and Control Rod Pattern

11



Fresh Fuel Assembly

2nd Cycle Fuel Assembly

3rd Cycle Fuel Assembly

4th Cycle Fuel Assembly

D Bank Rod(100% inserted)

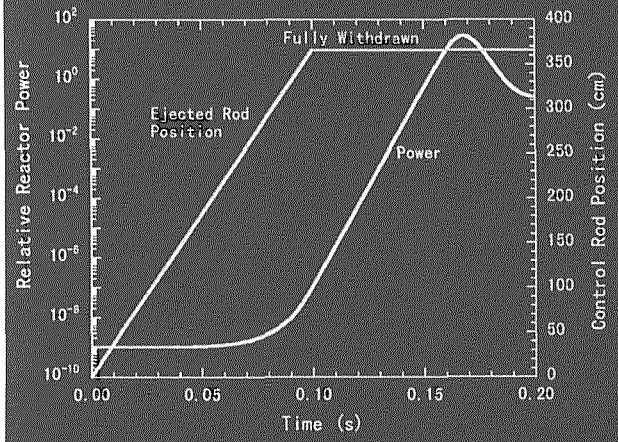
C Bank Rod(60% inserted)

Ejected Control Rod

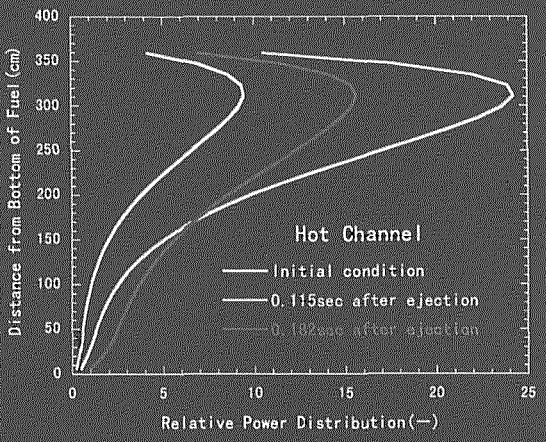
Control Rod Ejection Analysis — EOC, HZP —

12

Reactor Power and Ejected Rod Position

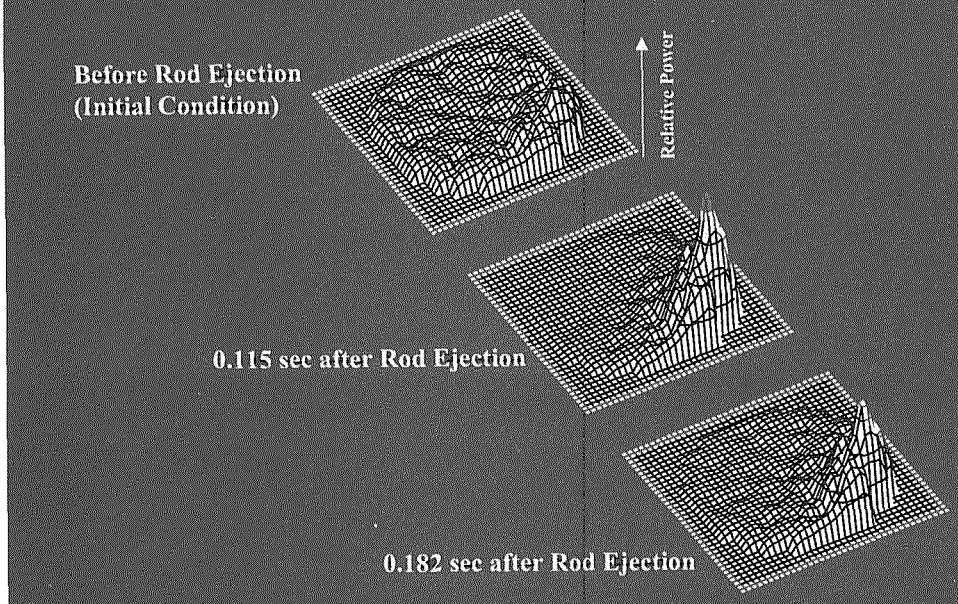


Axial Power Distribution



13

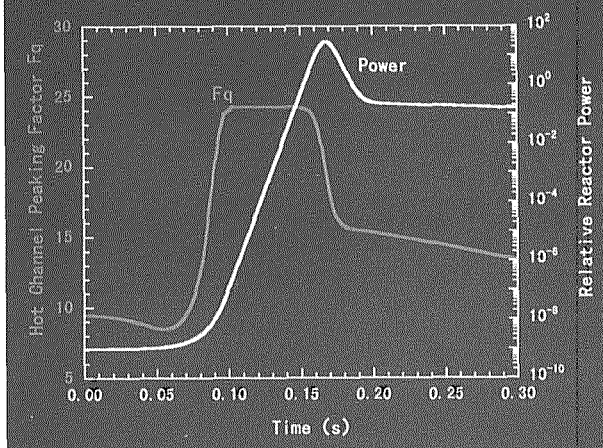
Core Power Distributions during RIA
－ EOC, HZP －



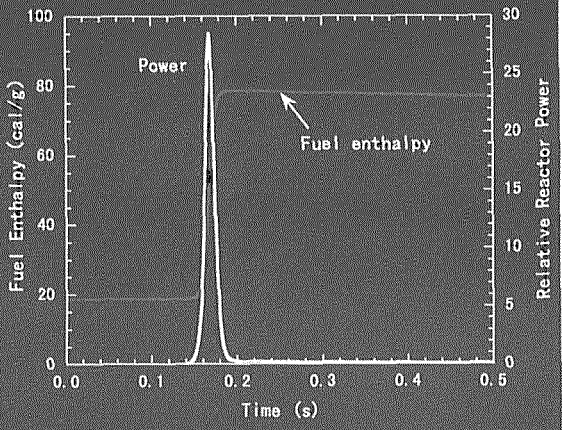
14

Control Rod Ejection Analysis
－ EOC, HZP －

Reactor Power and Fq



Fuel Enthalpy and Power



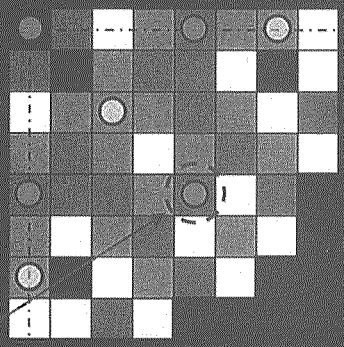
15

Distribution of Peak Fuel Enthalpy in Each Assembly
－ EOC, HZP －

			20	20	20	20	21	21	21				
		20	20	20	20	20	20	20	22	21	22	22	
	20	20	20	20	20	21	20	21	21	22	22	22	23
	20	20	20	20	20	20	20	21	22	22	21	24	24
20	20	20	20	21	20	21	21	22	22	23	23	24	24	25
20	20	20	20	20	20	21	22	21	21	24	25	24	26	25
20	20	21	21	21	21	21	22	22	24	26	26	27	24	27
20	20	20	20	21	22	22	21	25	27	27	26	27	25	29
21	21	22	22	22	21	22	25	24	27	33	36	39	33	35
21	22	21	22	22	21	24	28	27	30	40	44	42	46	41
21	22	22	22	24	24	26	27	34	41	53	49	54	47	43
	22	23	22	23	25	26	27	38	46	53	64	65	55	
	22	22	24	25	25	28	28	41	45	61	78	57	55	
		23	24	25	27	25	25	35	51	53	64	61		
				25	26	28	30	37	45	47				

Unit : cal/g

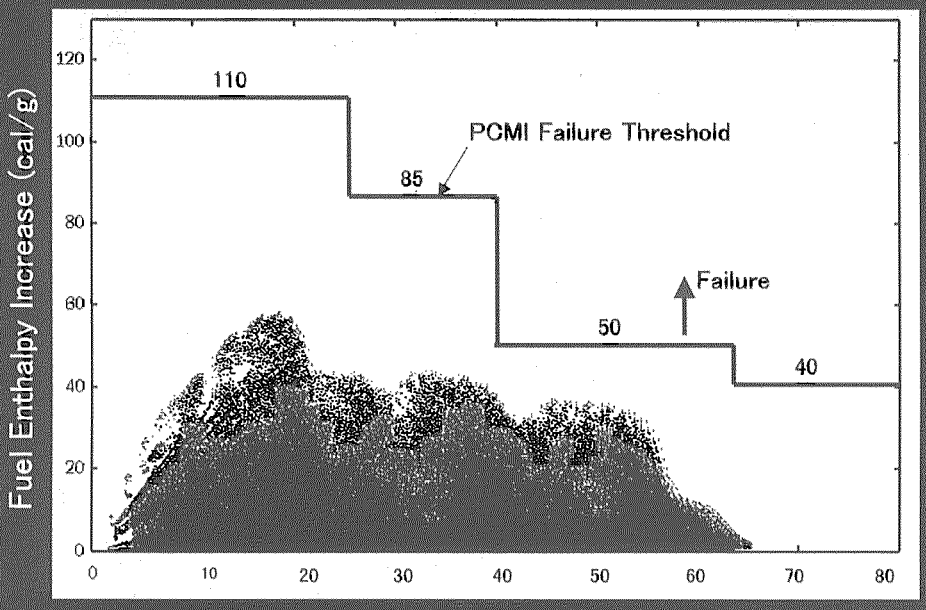
Fresh Fuel Assembly
2nd Cycle Fuel Assembly
3rd Cycle Fuel Assembly
4th Cycle Fuel Assembly



Ejected Rod Position

16

Fuel Enthalpy Increase during RIA
versus Pellet-average Burnup



17

Summary of Results
— Control Rod Ejection Analysis at EOC, HZP —

Item	Results
Maximum reactor power (ratio to nominal)	28.5
Maximum fuel enthalpy (cal/g)	78
Maximum initial fuel enthalpy increase (cal/g)	59
Maximum hot channel peaking factor Fq	24.3
Number of fuel failures due to PCMI	0

18

3D Analysis of RIA in BWR
— Control Rod Drop Accident —

BWR Core Model		
Plant type	A typical BWR-5	
Core condition	End of Cycle(EOC) and Cold Zero Power(CZP)	End of Cycle(EOC) and Hot Zero Power(HZP)
Fuel assembly	STEPⅢ 9×9 (type-A) fuel assembly	
Assembly maximum burnup	55 GWd/t	
Dropped rod worth (%Δk/k)	1.3 Conservatively increased	
Radial mesh in the neutronic model	2×2 mesh／assembly	
Axial planes in the fuel region	48	
Thermal-hydraulic channels	100	112

19

Core Conditions and Assumptions

Parameters	Values/Assumptions	
	Cold Zero Power(CZP)	Hot Zero Power(HZP)
Initial power level (MW)	3.293×10^{-5} (10^{-8} rated)	3.293×10^{-3} (10^{-6} rated)
Coolant inlet pressure (kg/cm^{2}A)	1.58	72.3
Coolant inlet temperature (℃)	20	286
Coolant flow	20 % of nominal	
Dropped rod worth (%Δk/k)	1.3	
Control rod drop speed (m/s)	0.95	
Delayed neutron fraction (%)	0.58	0.56
Prompt neutron lifetime (μs)	48	41
Void reactivity feedback	Applied and calculated by using the current models	
Ratio of direct moderator heating	0.02	

20

Treatment of Void Reactivity Feedback in BWR RIA Analysis

Current Safety Analysis → Without Void Reactivity Feedback

This Study → With Void Reactivity Feedback

Assumptions

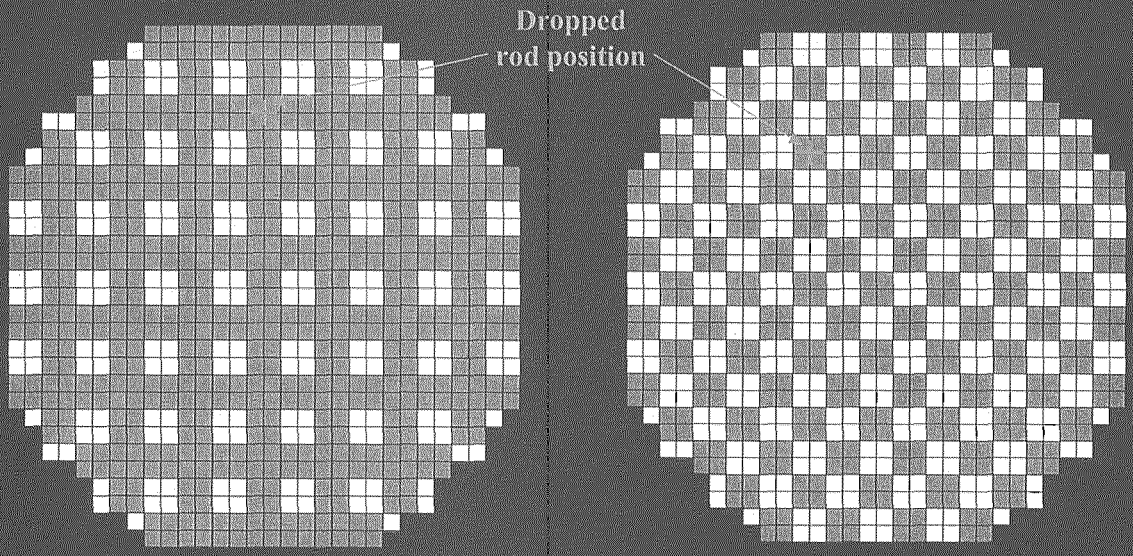
1. The current void generation models are based on the experiments under steady-state conditions.
2. These models are not verified against the prompt heating condition found during RIA.
3. The void reactivity feedback calculated by the current models was applied in the analysis of BWR RIA to understand the realistic fuel behavior during RIA.

21

Initial Control Rod Pattern

Cold Zero Power(CZP)

Hot Zero Power(HZP)



: Control rod withdrawn cells

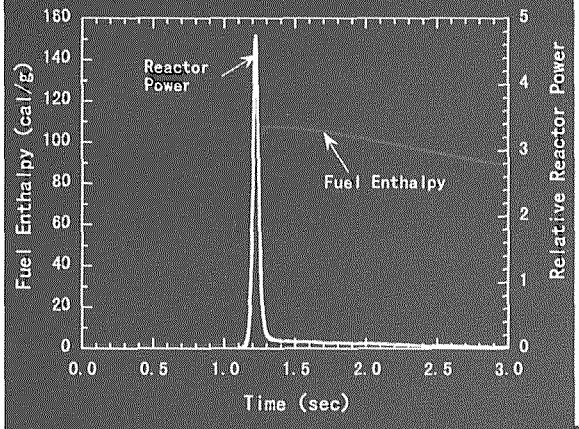
: Control rod inserted cells

22

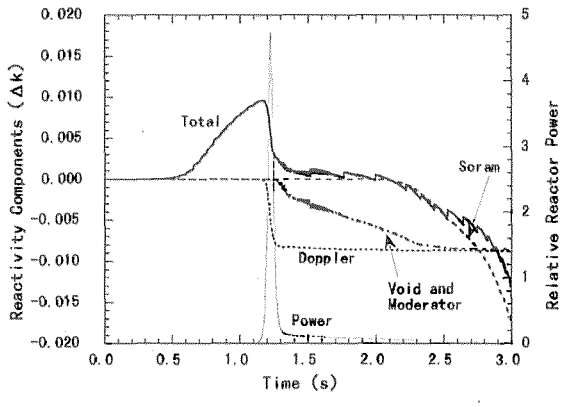
Control Rod Drop Analysis

— EOC, CZP —

Fuel Enthalpy and Power



Reactivity Components



Ins/Nupec 23

Distribution of Max. Fuel Enthalpy in Each Assembly

－ Control Rod Drop Analysis / EOC, CZP －

Control Rod Inserted Cells　　Dropped Rod Position

Unit : cal/g

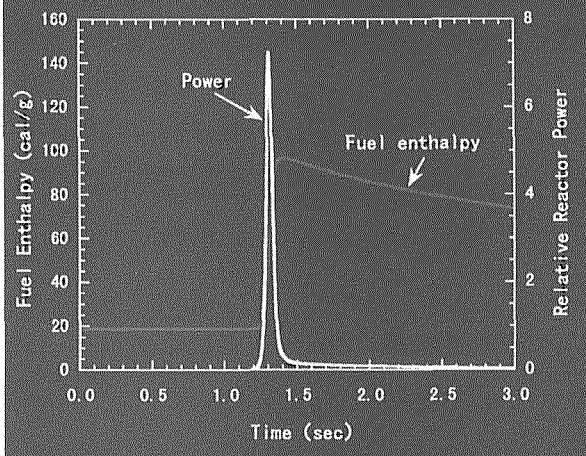
						3	3	3	3	3	3	3	3	3	3	3	3	3						
					3	4	4	19	25	36	32	34	35	31	33	24	18	4	4	3				
				3	3	4	6	31	22	38	64	84	47	50	81	58	36	21	31	6	4	3	3	
				3	4	4	6	6	25	31	70	67	77	66	66	65	30	24	6	6	4	4	3	
			3	4	4	4	3	4	18	34	40	71	92	88	70	39	33	18	4	3	4	4	4	3
		3	3	4	3	3	3	4	3	17	19	37	44	87	108	45	37	20	17	3	4	4	3	4	4	3
		3	4	6	5	3	3	6	9	15	26	38	64	36	35	67	38	27	15	9	6	3	3	5	6	4
	3	4	4	9	6	3	3	6	6	13	15	33	27	18	19	27	34	15	13	6	6	3	3	6	9	4
3	4	3	4	3	4	3	4	4	4	8	14	16	19	10	12	19	16	14	8	4	4	4	3	4	3	4
3	4	4	3	4	3	4	3	4	3	7	6	10	8	11	9	8	9	6	6	3	4	3	4	3	4	3
3	5	3	4	6	6	3	4	6	6	3	3	6	9	3	3	9	6	3	3	6	6	4	3	6	6	4
3	6	4	3	9	6	4	3	9	6	3	3	6	6	4	4	6	6	3	3	6	9	3	4	6	9	3
3	3	4	4	3	4	3	4	4	4	3	4	4	3	3	3	3	4	4	3	4	4	4	3	4	3	4
3	3	3	3	4	3	3	3	4	3	4	3	3	3	3	4	3	3	3	4	3	4	3	3	3	4	3
3	5	4	4	6	5	3	3	6	6	3	4	6	6	3	3	5	6	4	3	5	6	3	3	6	6	4

Ins/Nupec 24

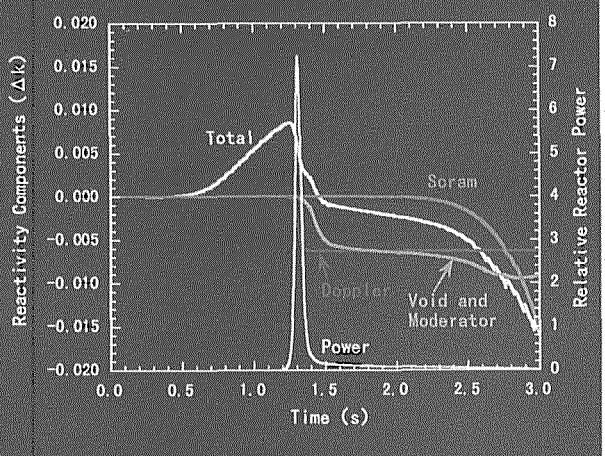
Control Rod Drop Analysis

－ EOC, HZP －

Fuel Enthalpy and Power



Reactivity Components



25

Distribution of Max. Fuel Enthalpy in Each Assembly
－ Control Rod Drop Analysis / EOC, HZP －

Control Rod Inserted Cells　　Dropped Rod Position

Unit : cal/g

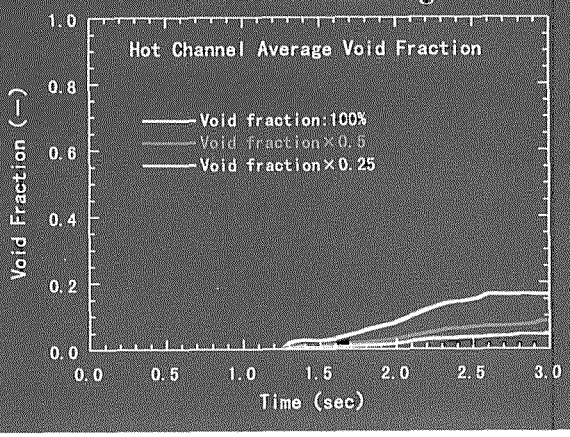
					20	20	20	20	20	20	20	20	20	20	20	20		
				20	31	31	39	34	35	31	35	38	22	24	24	25	22	22	20	
			20	20	31	38	46	36	42	46	51	34	33	39	34	32	22	25	24	22	20	20
			20	32	36	47	45	44	41	54	44	40	37	34	34	22	22	24	24	22	22	20
		20	31	43	53	41	51	57	71	45	48	44	42	32	31	34	24	23	22	25	24	22	20
	20	20	31	31	51	46	46	46	76	63	54	41	51	48	31	31	24	24	22	22	24	25	22	22	20
	20	22	34	39	33	36	52	83	79	97	67	67	35	31	39	34	32	22	25	24	22	22	25	24	22
20	22	22	34	34	32	35	56	59	85	75	72	47	32	29	34	34	22	22	24	24	22	22	24	25	22
20	22	24	34	31	31	37	44	41	56	65	83	50	46	35	33	32	22	34	24	23	22	24	24	22	22	24
20	22	34	34	32	22	43	36	42	37	55	47	42	33	42	36	22	22	24	24	22	23	24	25	22	23	24
20	25	22	22	34	34	30	33	37	41	33	32	37	43	30	27	34	24	22	22	24	24	22	22	24	24	22
20	24	23	22	34	24	31	28	39	31	27	28	35	31	29	28	24	24	22	22	24	25	22	23	24	25	22
20	24	24	24	22	22	24	34	22	22	34	34	22	24	24	24	24	22	24	24	22	22	24	24	22	22	24
20	22	25	24	23	22	39	24	23	22	34	24	24	22	25	24	22	24	24	25	22	23	24	25	22	23	24
20	25	22	23	24	25	22	22	24	24	22	23	24	24	22	22	25	24	23	22	25	24	22	22	24	24	23

26

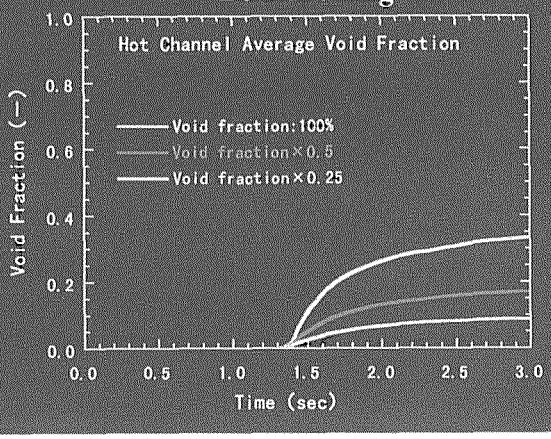
Sensitivity Analysis of Void Reactivity Feedback Effect

- Calculated void fraction was reduced by 50%, 25% and zero to evaluate the effect of void reactivity feedback on the reactor power and peak fuel enthalpy.

Void Fraction (CZP) －Subcooled Boiling－



Void Fraction (HZP) －Bulk Boiling－

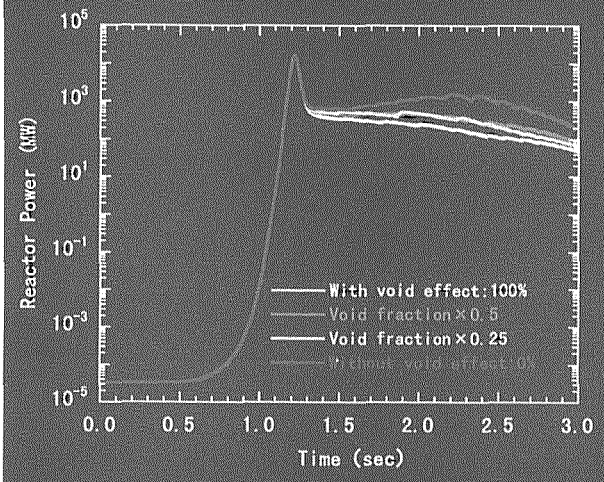


27

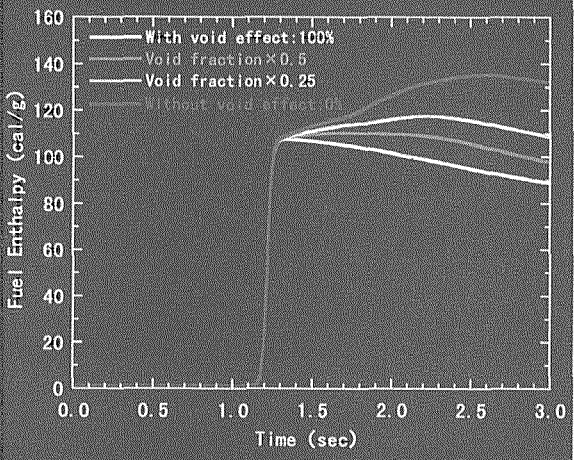
Sensitivity Analysis of Void Reactivity Feedback Effect

— EOC, CZP —

Reactor Power



Fuel Enthalpy

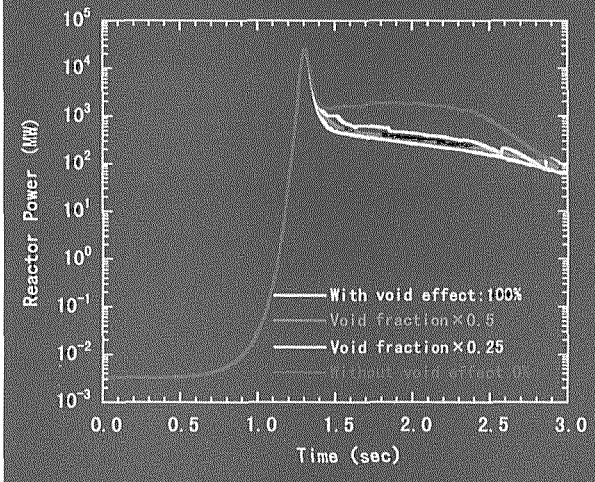


28

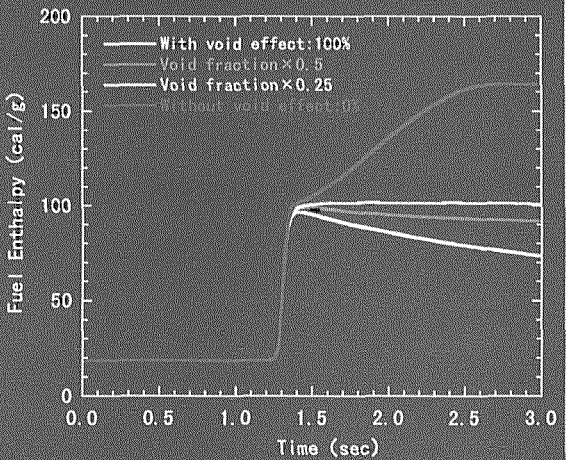
Sensitivity Analysis of Void Reactivity Feedback Effect

— EOC, HZP —

Reactor Power



Fuel Enthalpy



29

Summary of Results
— Control Rod Drop Analysis at EOC, CZP —

Item	Results	
	With Void Reactivity Feedback	Without Void Reactivity Feedback
Maximum reactor power (ratio to nominal)	4.7	4.8
Maximum fuel enthalpy (cal/g)	108	135
Maximum initial fuel enthalpy increase (cal/g)	106	108
Number of fuel failures due to PCMI	110	127
Number of fuel failures due to high-temperature rupture	36	329

30

Summary of Results
— Control Rod Drop Analysis at EOC, HZP —

Item	Results	
	With Void Reactivity Feedback	Without Void Reactivity Feedback
Maximum reactor power (ratio to nominal)	7.2	7.5
Maximum fuel enthalpy (cal/g)	97	164
Maximum initial fuel enthalpy increase (cal/g)	77	81
Number of fuel failures due to PCMI	26	49
Number of fuel failures due to high-temperature rupture	57	576

Summary(1)

- 3D analysis of RIA for a typical PWR and BWR with high burnup fuel were performed using the EUREKA-JINS/S code to understand the realistic fuel behavior during the transient.
- The fraction of fuel failure was evaluated by applying the newly revised failure threshold.
- The results of 3D analysis of control rod ejection accident for a typical PWR showed that the fuel safety criteria is adequately satisfied and none of fuel failure occurs under this event even though the significant conservatism is employed in the key parameters.

Summary(2)

- The results of 3D analysis of control rod drop accident for a typical BWR showed that the fuel safety criteria is adequately satisfied and fuel failures are quite small under this event, even though the significant conservatism is employed in the dropped rod worth.
- As part of the analysis, the influence of void reactivity feedback was studied to understand how it affects on the fuel behavior under the RIA in BWR.
- The results indicated that the void reactivity feedback greatly reduces the maximum fuel enthalpy and fuel failure for this event.

Discussion:

Q: (W. Wiesenack)

The PWR and BWR cases assume the same burn up (55 MWd/kg). In the PWR case, you reduce the delayed neutron fraction by 20% while it is retained at its nominal value in the BWR case. What is the reason for making these different assumptions?

The uncertainty due to burn up (Pu-content) should be the same in both cases.

A: This is the difference of licensing approach between PWR and BWR utilities. Each utility uses different approach for the assumptions of key parameters in licensing calculation. We just followed their approaches in the analysis. It depends on the design concept of each utility.

Q: (D. Schrire)

How is the void fraction calculated? Is it based on steady-state correlation? In that case, the void fraction is probably overestimated due to inertia effects during rapid heating of water.

A: The void fraction was calculated using the steady-state models. Yes, the void fraction is probably overestimated, if the steady-state models are used. Therefore, the sensitivity analysis is conducted by reducing void fractions. To apply void effect on the RIA analysis, the void models in the rapid heating, condition must be proposed and be verified through the transient void experiments.

JP0250416

Session 2b-3

RIA modeling - a comparison between TRANSURANUS and FREY

Ch. Hellwig[1], H. Wallin[1], K. Lassmann[2],

[1]Paul Scherrer Institut, CH-5232 Villigen PSI, Switzerland

[2]European Commission, Directorate General JRC, Institute for Transuranium Elements (ITU), D-76125 Karlsruhe, Germany

Abstract

At PSI, modeling the behavior of fuel and cladding under RIA conditions (Reactivity Initiated Accident) can be performed with the codes FREY[1] (from EPRI) and TRANSURANUS [2,3] (from ITU). A comparison of the codes was done by calculating the behavior of a UO_2 fuel rod during a 1.75 $ RIA with both codes. RIA was assumed in a PWR at hot zero power with an average rod burnup of 47.7 GWd/tU. The TRANSURANUS results of the base irradiation were used as initial values for the TRANSURANUS calculation as well as for the FREY calculation. Coolant flow channel models were excluded from the code comparison.

The resulting peak enthalpy rise in this moderately loaded rod was ΔH_{max} = 51 cal/g (H_{max} = 70 cal/g). The fuel center temperatures calculated with FREY were 40-50°C higher than those given by TRANSURANUS. Differences were also found in the calculated fuel axial elongation, fuel radial expansion, and stresses in the cladding.

Neither FREY nor TRANSURANUS calculated melting of fuel or clad failure. Finally, the capability of the present versions of FREY and TRANSURANUS to deal with high burnup issues is discussed and possible improvements for modeling high burnup rods are listed.

Both code-versions used are neither extended nor validated for accidents at high burnup and for accidents with a significant influence of gaseous swelling.

It should be noted that this applies also to the performed calculations due to the elevated burnup in the selected RIA case (max. cross-sectional average 55 GWd/tU). Therefore, the presented results must be seen merely as a comparison of two codes and not as validated results for a RIA.

[1] "FREY-01: Fuel Rod Evaluation System", EPRI NP-3277a, Volumes 1-4, Revision 3, EPRI, August 1994.

[2] K. Lassmann, "TRANSURANUS: a fuel rod analysis code ready for use", J. Nucl.Mater. 188 (1992) 295-302.

[3] K. Lassmann, A. Schubert, J. van de Laar, C.W.H.M. Vennix, "Recent Developments of the TRANSURANUS Code with Emphasis on High Burnup Phenomena", IAEA TCM on Nuclear Fuel Behaviour Modelling at High Burnup, Lake Windermere, UK, June 2000.

RIA modeling - a comparison between TRANSURANUS and FREY

Ch. Hellwig[1], H. Wallin[1], K. Lassmann[2],

[1]Paul Scherrer Institut, CH-5232 Villigen PSI, Switzerland
[2]European Commission, Directorate General JRC, Institute for Transuranium Elements (ITU), D-76125 Karlsruhe, Germany

Abstract

At PSI, modeling the behavior of fuel and cladding under RIA conditions (Reactivity Initiated Accident) can be performed with the codes FREY [1] (from EPRI) and TRANSURANUS [2,3] (from ITU). A comparison of the codes was done by calculating the behavior of a UO_2 fuel rod during a 1.75 $ RIA with both codes. RIA was assumed in a PWR at hot zero power with an average rod burnup of 47.7 GWd/tU. The TRANSURANUS results of the base irradiation were used as initial values for the TRANSURANUS calculation as well as for the FREY calculation. Coolant flow channel models were excluded from the code comparison.

The resulting peak enthalpy rise in this moderately loaded rod was $\Delta H_{max} = 51$ cal/g ($H_{max} = 70$ cal/g). The fuel center temperatures calculated with FREY were 40-50°C higher than those given by TRANSURANUS. Differences were also found in the calculated fuel axial elongation, fuel radial expansion, and stresses in the cladding. Neither FREY nor TRANSURANUS calculated melting of fuel or clad failure.

Finally, the capability of the present versions of FREY and TRANSURANUS to deal with high burnup issues is discussed and possible improvements for modeling high burnup rods are listed. Both code-versions used are neither extended nor validated for accidents at high burnup and for accidents with a significant influence of gaseous swelling. It should be noted that this applies also to the performed calculations due to the elevated burnup in the selected RIA case (max. cross-sectional average 55 GWd/tU). Therefore, the presented results must be seen merely as a comparison of two codes and not as validated results for a RIA.

Introduction

Modeling the fuel rod behavior under normal conditions is used world wide to increase the safety and efficiency of the fuel management. Modeling the fuel rod behavior under accident conditions (i.e. RIA and LOCA) gains increasing importance due to more powerful computers available and the very restricted base of experimental data. As the focus of interest shifts towards high burnup issues, computer codes with the capability of modeling the behavior of high burnup fuel rods under accident conditions are needed. At PSI, modeling the behavior of fuel and cladding under RIA conditions (Reactivity Initiated Accident) can be performed with the codes FREY [1] (from EPRI) and TRANSURANUS [2,3] (from ITU). The code TRANSURANUS has been used at PSI to calculate the behavior of pellet pins under normal conditions. Despite this code not been developed explicitly for modeling of accident conditions, it can be used for RIA and LOCA calculations in cases where its limitations are insignificant. TRANSURANUS is a "1.5 dimensional code", i.e. a superposition of a one-dimensional radial and a one-dimensional axial mechanical analysis. A generalized plane strain condition in axial direction is assumed and therefore real two-dimensional geometries like the hour-glass effect cannot be simulated. Additionally, PSI purchased the code FREY (Fuel Rod Evaluation

System), which is especially developed for transient and accident conditions. FREY works fully on a 2-dimensional approach using the finite element method (FEM).

A comparison between TRANSURANUS and FREY was performed in order to evaluate the advantages and disadvantages of the present code versions. The behavior of a moderately loaded UO_2 fuel rod during the RIA was calculated with both TRANSURANUS and FREY. For the FREY calculation, the base irradiation was modeled with TRANSURANUS and the output data was used as an input for FREY, since FREY is not intended for steady state calculations and since it is recommended to model base irradiation with a fuel performance code.

In general, the fuel, cladding and reactor data are comparable to a typical PWR with the standard fuel assembly and to RIA calculations for that plant. Nevertheless, the chosen model case was especially defined for the benchmark calculation FREY-TRANSURANUS and might in some aspects be less realistic.

The aim of the report is to compare the results of TRANSURANUS and FREY, to discuss the modeled processes during a RIA and the applicability of the used code versions to high burnup rods.

Outlines of the code comparison

The codes TRANSURANUS and FREY were compared by calculating a RIA in a PWR at hot zero power. The present RIA case corresponds to a typical 1.75 $ rod ejection case calculated with 3-dimensional kinetics. The peaking factor of the chosen fuel rod was smaller than for the peak rod. It was equally divided in 20 axial slices for the FREY and for the TRANSURANUS calculations. The radial node scheme was different for the FREY and the TRANSURANUS calculations and will be discussed below.

The average rod burnup was 47.7 MWd/kgU. The highest cross-sectional average burnup was 54.5 MWd/kgU in axial slice 7, which had a local burnup of 48 MWd/kgU in the fuel center and 119 MWd/kgU in the rim. As the formation of the High Burnup Structure (HBS or "Rim"-structure) starts when the local burnup reaches the threshold of 60 - 75 GWd/tM [4-6], HBS has started to form in the rim in all axial slices except in the lowest and highest slice (slices 1 and 20). The lower thermal conductivity of the HBS is taken into account in TRANSURANUS but not in the used FREY version. Neither TRANSURANUS nor FREY have transient swelling models for the HBS as very little data exist on this topic [7,8]. Therefore the code results should be seen more as a comparison of two codes and not as an attempt for realistic RIA modeling.

Both FREY and TRANSURANUS have a flow channel model, which calculates thermal boundary conditions for fuel pin analysis (rod-to-coolant heat transfer coefficients and coolant temperatures). The flow channel model of TRANSURANUS cannot handle extreme accident conditions and was not adjusted to model departure from nucleate boiling (DNB) in the present version. The flow channel model of FREY has also its limitations. The thermal boundary conditions (heat transfer coefficients from cladding to coolant) should be provided by a separate thermal-hydraulics code for licensing analysis as recommended in the manual. Therefore, the flow channel models were excluded from the code comparison. The clad outer temperatures during the RIA were calculated with FREY and these values were used as a boundary condition for the TRANSURANUS calculation. Consequently, clad outer temperatures are identical in both TRANSURANUS and FREY calculations. The comparison focused on temperature calculations, stresses in the cladding, and radial power distribution.

The base irradiation (modeled with TRANSURANUS)

The pin, fuel and cladding data are listed in ***Table 1***.

Table 1: *Pin, fuel and cladding data in the base irradiation.*

Pin Data		
Fuel column length	mm	3'023.0
Upper plenum length	mm	145.8
Free upper plenum volume	mm^3	9067.7
Free lower plenum volume	mm^3	-
Fillgas		He
Fillgas composition	vol. fraction	1
Fillgas pressure at fabrication	MPa	2.3
Fillgas temperature at fabrication	°C	25
Fuel Data (UO_2)		
Inner pellet radius	mm	-
Outer pellet radius	mm	4.6455
Dish volume/Pellet volume	vol. fraction	0.0223
Enrichment (U^{235})	wt%	4.3
Stoichiometry (O/M)		2
Grain diameter (as fabricated)	mm	0.01
Fabrication porosity	vol. fraction	0.05
Open porosity	vol. fraction	0.00
Porosity at the end of sintering (from sinter test)	vol. fraction	0.035
"End-of-sintering" burnup	MWd/tU	4500
Surface roughness	mm	0.001
Cladding Data		
Cladding material		Zircaloy
Inner cladding radius	mm	4.743
Outer cladding radius	mm	5.360
Texture factor for irrad. growth, radial		0.5740
Texture factor for irrad. growth, tangential		0.3370
Texture factor for irrad. growth, axial		0.0890
Cold work; fraction of cross-sectional area reduction		0.20
Surface roughness	mm	0.001

A typical power profile was applied on the 20 axial slices. The same profile was used for the fast neutron flux. The coolant temperature during the base irradiation was prescribed according to normal reactor operation experience.

The input reactor data used for the base irradiation is listed in ***Table 2***. The temperature history during the base irradiation is shown in ***Figure 1*** together with various results of the base irradiation. Some integral results at end of base irradiation are listed in ***Table 3***.

Table 2: Reactor data for the base irradiation

Reactor		PWR
Number of cycles		5
linear rod power (pin average) $1^{st}/2^{nd}/3^{rd}/4^{th}/5^{th}$ cycle	kW/m	14/15.5/23/22/20
Time per cycle at max. linear rod power (steady state) $1^{st}/2^{nd}/3^{rd}/4^{th}/5^{th}$ cycle	h	7500/7500/7500/ 7499/7200
at the beginning of cycle, the duration of increase to full power	h	1
at the end of cycle, the duration of decrease to zero power	h	1
Coolant pressure	MPa	15.75
Coolant temperature	°C	286 - 315
Fast neutron flux (E_n > 1 MeV, pin average) / linear heat rate	[n/cm^{2}s] / [kW/m]	$3.2*10^{12}$
Coolant flow rate	g/h	$8.08463*10^5$
Outer hydraulic diameter	mm	14.1224
Gamma heating of cladding / coolant / structure	%	0.3 / 3.7 / 0.0

Table 3: Integral results at end of base irradiation, cold condition.

Fission gas production	(cm^3)	2817.15
Fission gas release	(cm^3)	8.84
Fission gas release	(%)	0.31
Fuel axial elongation	(mm)	25.88 = 0.86 (%)
Clad axial elongation	(mm)	13.80 = 0.44 (%)
Average burn-up	(MWd/kgU)	47.654
Upper plenum pressure	(MPa)	2.99

The RIA calculation

The used RIA power history is shown in ***Figure 2***. The fuel enthalpy, shown in ***Figure 3*** (TRANSURANUS calculation), never exceeds 295 J/g (70 cal/g). The pulse width at half maximum is 14.2 milliseconds.

The concept of the TRANURANUS code is a consistent treatment of normal operation and off-normal or accidental situation. Therefore, with TRANSURANUS, the RIA on the irradiated fuel was modeled following the base irradiation calculation and no transfer of data was necessary. The coolant temperature during the RIA was prescribed following the FREY calculation as mentioned above. The corrosion model in TRANSURANUS had to be turned off for the RIA calculation, because it was not developed for temperature peaks and would deliver unreasonable high corrosion rates at temperatures above the temperature range of normal operation. The models for fuel and cladding creep were also not developed for a RIA temperature peak and were restricted to a linear heat rate of some

1000 W/cm to avoid unreasonable "softening" of the fuel during the short power and temperature peak. As the mentioned processes are diffusion controlled and RIA is an extremely short event, the incorporation of better high temperature properties and models may not alter the results significantly.

For the FREY calculation, a new grid was constructed to model the rod geometry instead of using a standard finite element grid (part of the FREY model library). The structure of the used finite element grid and the numbering of the elements are shown in ***Figure 4***. In FREY, the largest allowed number of fuel elements is 75. Therefore, the finite element grid construction is a trade-off between the number of axial slices and the number of radial elements. The used model with 20 axial slices has the maximum possible number of radial elements, giving 7 radial fuel nodes and 3 cladding nodes. This can be compared with the 66 radial nodes in the TRANSURANUS calculations presented in this paper (with the highest density in the rim region). However, the methods for calculating temperature and stress in TRANSRANUS differ from the finite element method (FEM) used in FREY. In FEM, variables are approximated over the element with linear combinations of shape functions. Direct comparison of the available radial nodes gives thus a wrong picture of FREY's capabilities. However, modeling the rim zone, where the material properties and the power are changing in a very narrow area, might need a denser node scheme.

To compare the RIA calculation of FREY with the TRANSURANUS calculation, both codes used identical input data where it was possible. However, problems arose when the results of the TRANSURANUS base irradiation calculation were transferred to the input of FREY. Both codes have a slightly "different way of thinking" in the sense that they use different models and parameters having slightly different definitions. Therefore the data transfer was not straightforward but required considerable work in the form of hand calculations and iterations. A lot of effort was put into the development of a procedure to correctly transfer the fuel and clad deformations, gas pressure and different gas volumes after base irradiation and, at the same time, not influence other parameters.

As an example, the fission gas concentrations after the base-irradiation and their distribution over different locations (fuel matrix, bubbles, grain boundaries, etc.) were calculated with TRANSURANUS. The total amount of fission gas that was created during the base irradiation was 0.126 mol, corresponding 2817.2 cm^3 at STP[1]. The released gas after the base irradiation was 0.000394 mol, corresponding 8.84 cm^3 at STP. Besides these values, FREY required the input of the concentration of intra-granular and inter-granular fission gas after base irradiation to calculate the fission gas burst release during a RIA. The data for each mesh point was given by TRANSURANUS, but in the present version of FREY the data for only one axial position was accepted as input. In the end, the maximum concentration was used to approximate the behavior. However, in the postulated RIA case, the fuel temperatures were low and no extensive fission gas burst release occurred.

Most of the material properties and calculation models used in FREY are presented in MATPRO [9]. The models for fuel thermal conductivity, its porosity correction and degradation of conductivity with increasing burnup were changed to the same models as used in TRANSURANUS by adding them into the FREY source code in a separate subroutine (the standard Harding & Martin correlation for thermal conductivity [10]). This was done to focus the code comparison on the basic calculation strategies of the codes and to exclude model differences.

Results of the code comparison

[1] For comparison, the fuel volume in the rod was 207 cm^3, i.e. the fission gas created during the base irradiation has 14 times larger volume at STP than the fuel.

As expected neither FREY nor TRANSURANUS calculated failing of the cladding for this medium loaded rod.

The most important peak values and integral data are listed in ***Table 4*** for comparison.

Table 4: *Important parameters for the RIA on irradiated fuel.*

Parameter	TRANSURANUS results:			FREY results:		
	Max. value	At time	In ax.slice	Max. value	At time	In ax.slice
fuel centre temperature	1130 °C	2.87 s	7	1174 °C	2.56 s	7
fuel rim temperature *	724 °C	0.234 s	7	779 °C	0.232	7
fuel enthalpy	293 J/g	1.152 s	7	not given in output		
clad inner temperature	681 °C	0.70 s	8	668 °C	0.700	10
Pin inner pressure	8.75 MPa	1.74 s	-	7.27	1.00	-
avg. equiv. stress in clad	196 MPa	0.238 s	5	not given in output		
clad hoop stress	178 MPa	0.238 s	4	287 MPa	0.232	5
Fission gas burst release	not calculated			0.053%		

* Refers only to the most outer fuel region. Temperature is notably higher slightly towards the fuel centre.

Comparison of temperatures

Clad outer temperatures were the same in TRANSURANUS and FREY calculations because TRANSURANUS used the clad outer temperatures calculated by FREY as a boundary condition. Clad inner temperatures and fuel outer temperatures calculated with TRANSURANUS and FREY are therefore nearly identical.

The comparison of fuel centre temperatures calculated with TRANSURANUS and FREY is shown in ***Figure 5***. FREY gives 40-50°C higher centre temperatures than TRANSURANUS. This is in spite of the same Harding & Martin correlation for fuel thermal conductivity (including the same corrections for local porosity and local burnup). The specific heat of the fuel is calculated with different correlation in both codes, leading to a maximal difference of 3%. The somewhat higher value used in TRANSURANUS might help to slightly lower the fuel centre temperatures but it is not large enough to explain the mentioned differences of 40-50°C. A possible explanation is the difference in the radial power profile, which in FREY is flatter than in TRANSURANUS due to the different models (see ***Figure 6***), and due to the sparser radial noding in FREY. Consequently, at the same linear heat rate, FREY calculates less heat production in the fuel rim area, where potential for gaseous swelling in RIA is highest (either in HBS or in the restructured fuel).

Comparison of stresses in cladding

Average tangential hoop stresses in cladding are compared in ***Figure 7***. While the qualitative appearance of the plots is similar, the stresses calculated with FREY were smaller than those given by TRANSURANUS during most of the calculation period. However, during the initial phase of RIA, FREY gives higher stresses than TRANSURANUS (due to a higher fuel radial expansion in FREY) and during the rest of the calculation period, lower hoop stresses.

In ***Figure 7***, both codes show a peak in stresses at the end of the calculation period (see also ***Figure 8*** and ***Figure 9***). The peaks in the figures coincide with the slow temperature decrease some seconds after the power peak which is caused by the end of DNB phase. At the end of DNB, clad cools down more than fuel. As clad contracts against the fuel, stresses in cladding increase.

Fuel rod failure mechanisms in RIA and their importance for high burnup

With increasing burnup, the cladding material is known to harden and loose ductility below 1 % uniform strain due to the formation of hydrides (source of hydrogen being the cladding waterside oxidation) and to irradiation damage caused by fast neutron fluence.

Due to extensive increase in fuel volume during the RIA, the fuel-clad gap closes (if the gap exists prior to the RIA), and the clad is forced outwards by the expanding fuel. The increase in fuel volume is due to thermal expansion of the fuel and to gaseous fuel swelling. The gaseous swelling is due to several different processes and the total depends highly on the amount and localization of the fission gas (in the fuel matrix, in larger pores or very small bubbles and on grain boundaries). In the HBS, the localization and thus the gaseous swelling behavior is different than in unrestructured fuel. Depending on the cladding alloy and burnup, brittle or ductile cladding failure can occur in the early phase of the RIA due to the pellet-cladding-mechanical-interaction (PCMI) caused by radially and axially expanding fuel. Additionally, the rod inner gas pressure might increase over the failure limit of the cladding if the fuel temperatures stay high for a longer period of time, and significant fission gas release (diffusional release and burst release) takes place. Presupposition for this failure type is considerably high burnup.

In conclusion, the mechanical behavior of the cladding (hardness and ductility), the transient fuel swelling behavior and the fission gas burst release are phenomena to be addressed in future RIA modeling efforts on high burnup rods.

Both investigated code versions offer the possibility to use defined cladding correlations for specific calculations. This is of importance as the codes have only very limited models for cladding behavior, limited with regard to burnup and to alloy composition. For a valid RIA analysis, using the implemented standard correlations might deliver only a rough estimation of the envisaged fuel rod behavior.

Neither of the codes is able to model transient fuel swelling. Especially for the HBS it is not clear if the transient swelling behavior might contribute significantly to the cladding hoop strain. Therefore, a more mechanistic model for the calculation of the fission gas behavior and hence the transient swelling in the unrestructured fuel and in the HBS would be a necessary step towards the development of a RIA code for high burnup fuel.

TRANSURANUS has no model for the fission gas burst release, while FREY calculates it with a simple, non-mechanistic correlation [11], which was neither developed nor validated for high burnups and especially for the HBS. The correlation depends only on fuel temperature; i.e., it does not take into account the fission gas distribution in fuel determined by the operation history prior to the RIA. As the location of the retained fission gas in the fuel is also completely different from unrestructured fuel compared to the HBS, a strong dependence of the burst release behavior from the fuel structure must be expected. If a mechanistic fission gas model is implemented in a code to calculate the transient fuel swelling, the burst release could be combined with this model.

Discussion and conclusions

The coolant flow channel had to be excluded from the code comparison by using common thermal boundary conditions. The differences between the code calculations were small. Clad inner temperatures and rim temperatures were nearly identical due to boundary conditions. A possible explanation for the 40-50°C higher centre temperatures in FREY calculation could be the flatter radial power profile in FREY than in TRANSURANUS. The Harding & Martin correlation for fuel thermal conductivity (with porosity and burnup corrections) was installed into FREY, which is the same correlation used in TRANSURANUS. The differences in the specific heat are too small to explain the temperature differences. However, a temperature difference of 40-50°C is negligible in fuel modelling calculations.

The increase in fuel radius calculated using FREY was larger than calculated by TRANSURANUS. Neither FREY nor TRANSURANUS calculated melting of fuel or cladding failure for this moderately loaded rod. Nevertheless, differences were found in the calculated fuel temperatures, fuel axial elongation, fuel radial expansion, and stresses in the cladding. Possible explanations were given. RIA calculations on peak rods must be performed in the future to evaluate the significance of the differences.

The applicability of the codes to high burnup is limited due to the limited cladding correlations (if no user-defined correlations are used) and to the missing models for transient swelling for unrestructured fuel and HBS. Furthermore, no correlation for fission gas burst release in the HBS is implemented in the codes.

References

[1] "FREY-01: Fuel Rod Evaluation System", EPRI NP-3277a, Volumes 1-4, Revision 3, Electric Power Research Institute (EPRI), August 1994.

[2] K. Lassmann, "TRANSURANUS: a fuel rod analysis code ready for use", J. Nucl. Mater. 188 (1992) 295-302.

[3] K. Lassmann, A. Schubert, J. van de Laar, C.W.H.M. Vennix, „Recent Developments of the TRANSURANUS Code with Emphasis on High Burnup Phenomena", IAEA Technical Committee Meeting on Nuclear Fuel Behaviour Modelling at High Burnup, Lake Windermere, UK, June 2000.

[4] C.T. Walker, "Assessment of the radial extent and completion of recrystallisation in high burn-up UO_2 nuclear fuel by EPMA", J. Nucl. Mater., 275 (1999), 56-62.

[5] K. Lassmann, C.T. Walker, J. van der Laar, F. Lindström, "Modelling the high burnup UO_2 structure in LWR fuel", J. Nucl. Mater ., 226 (1995), 1-8.

[6] K. Une, M. Hirai, K. Nogita, T. Hosokawa, Y. Suzaa, S. Shimizu, Y. Etoh, "Rim structure formation and high burnup fuel behaviour of large-grained UO_2 fuels", J. Nucl. Mater., 278 (2000), 54-63.

[7] F. Lemoine, "High burnup fuel behaviour related to fission gas effects under reactivity initiated accidents (RIA) conditions", J. Nucl. Mater ., 248 (1997), 238-248.

[8] T. Fuketa, H. Sasajima, Y. Mori, K. Ishijima, "Fuel failure and fission gas release in high burnup PWR fuels under RIA conditions", J. Nucl. Mater ., 248 (1997), 249-256.

[9] MATPRO-Vers. 11, "A handbook of material properties for use in the analysis of lightwater reactor fuel rod behaviour", NUREC/CR 0497 TREE 1280, EG&G Idaho, Inc. (1979), Idaho Falls, Idaho 83415, USA.

[10] J.H. Harding and D.G. Martin, "A Recommendation for the Thermal Conductivity of UO_2", J. Nucl. Mat. 166 (1989) 223-226.

[11] Gehl S.M., et al., "Fission gas release from irradiated PWR fuel during simulated PCM-type accidents", Progress report, NUREG/CR-0088, ANL-77-80, May 1978.

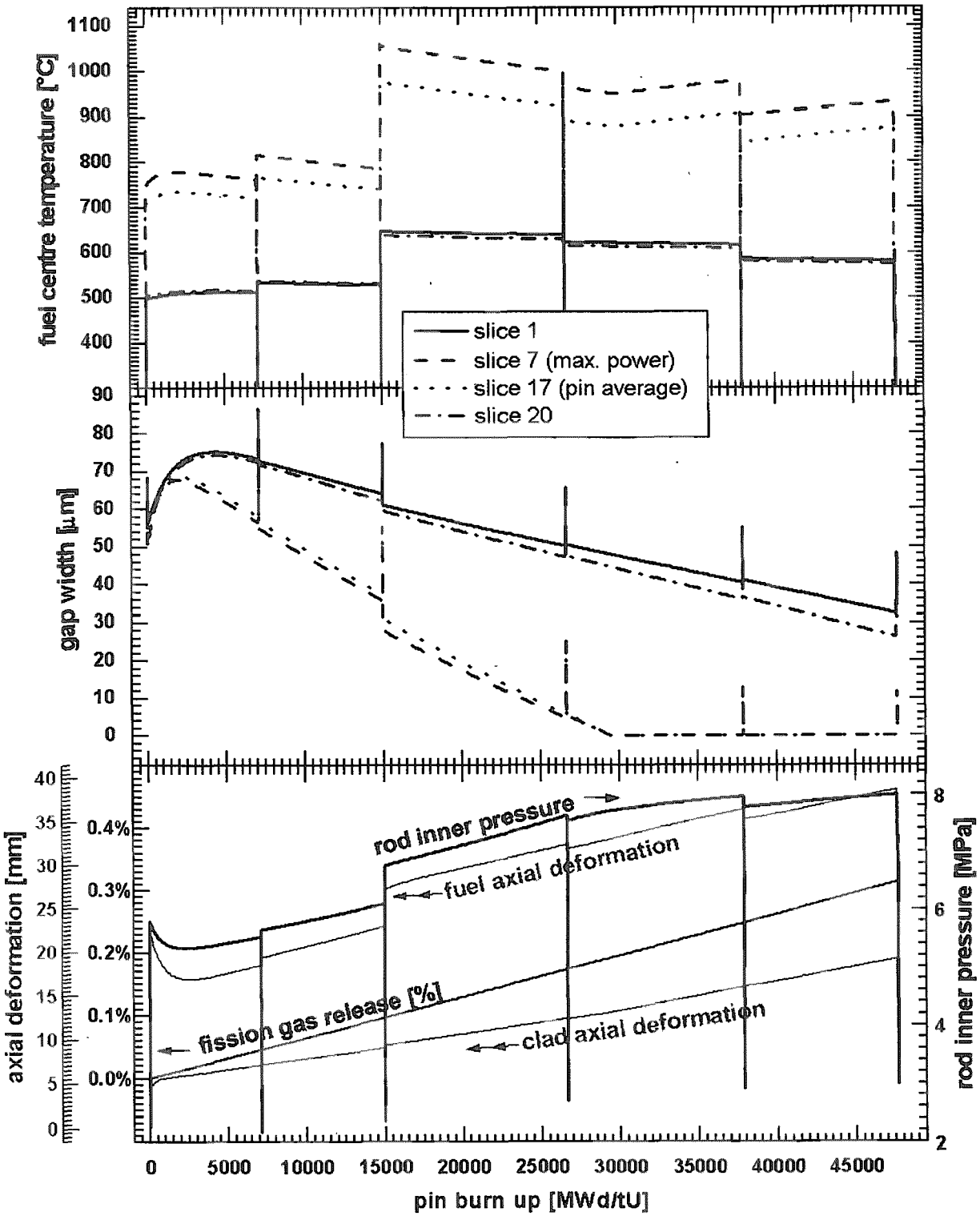


Figure 1: Base irradiation: temperature history and selected results of the TRANSURANUS-calculation.

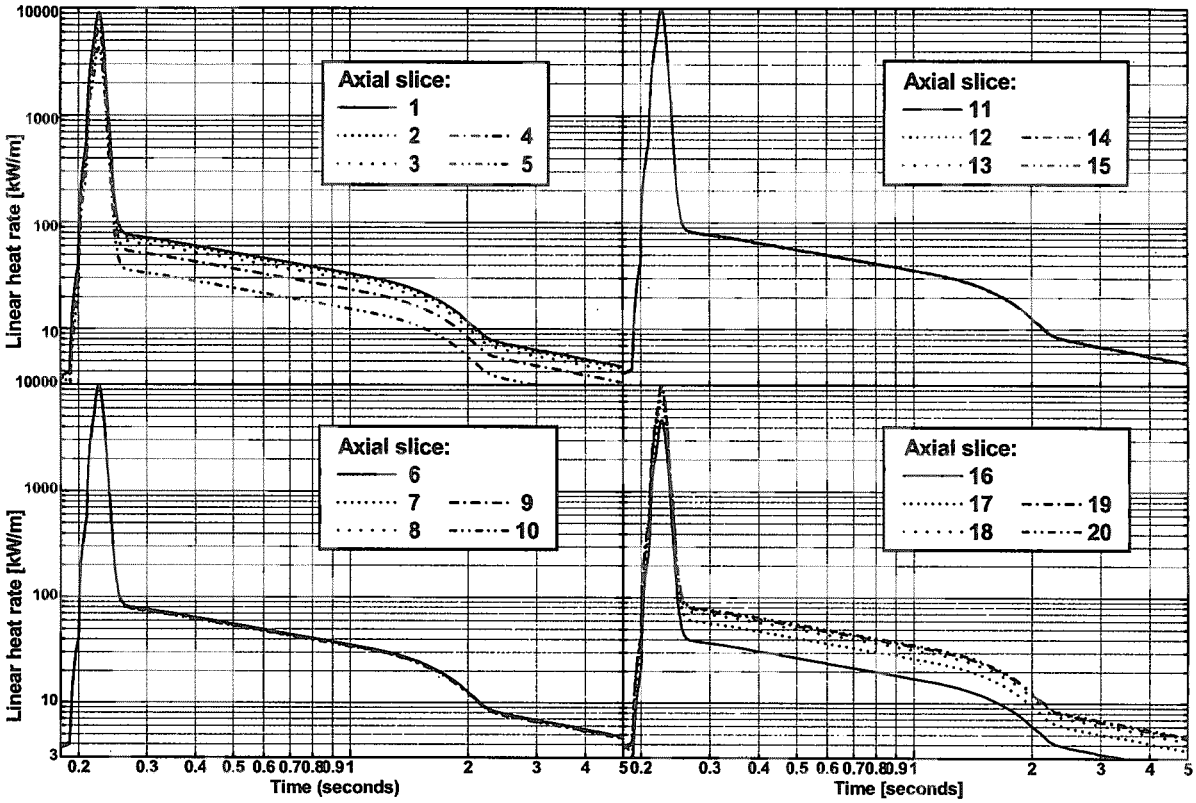


Figure 2: Linear heat rate in RIA in all slices. Note the still considerable power (~25 kW/m) after 1 s.

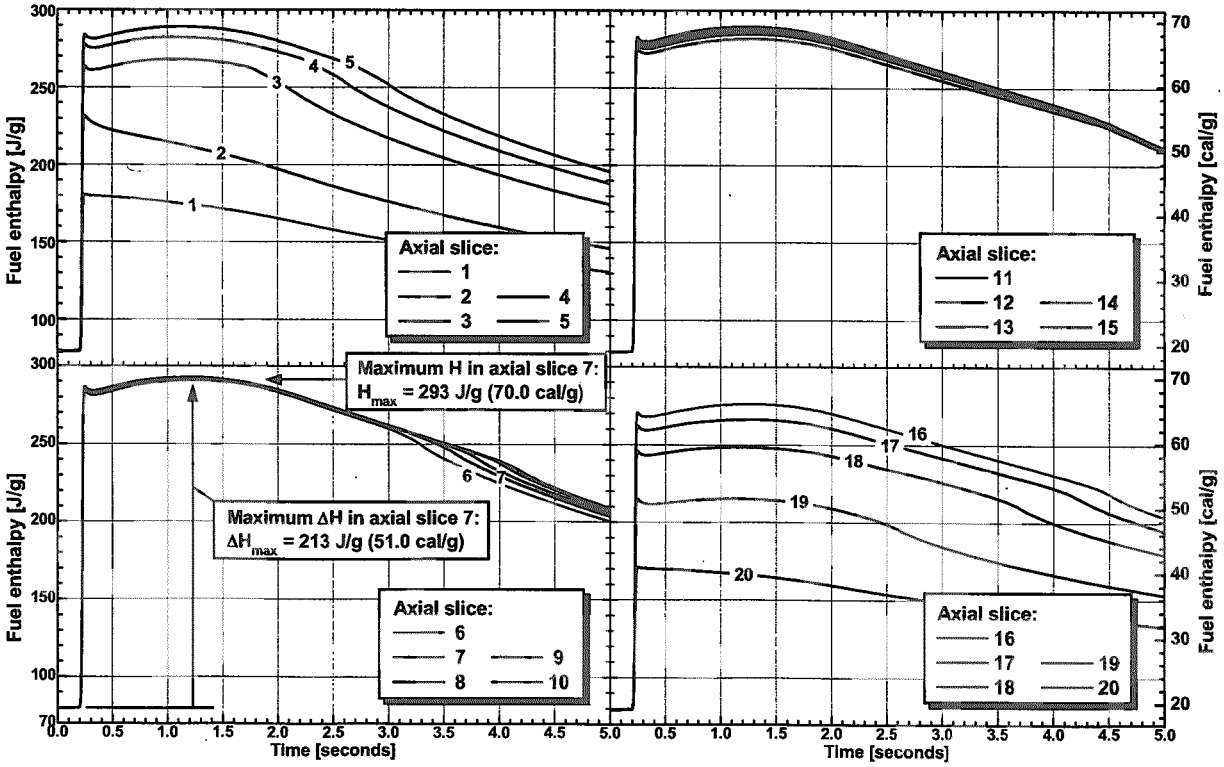


Figure 3: RIA irradiation: Fuel enthalpy versus time in all axial slices.

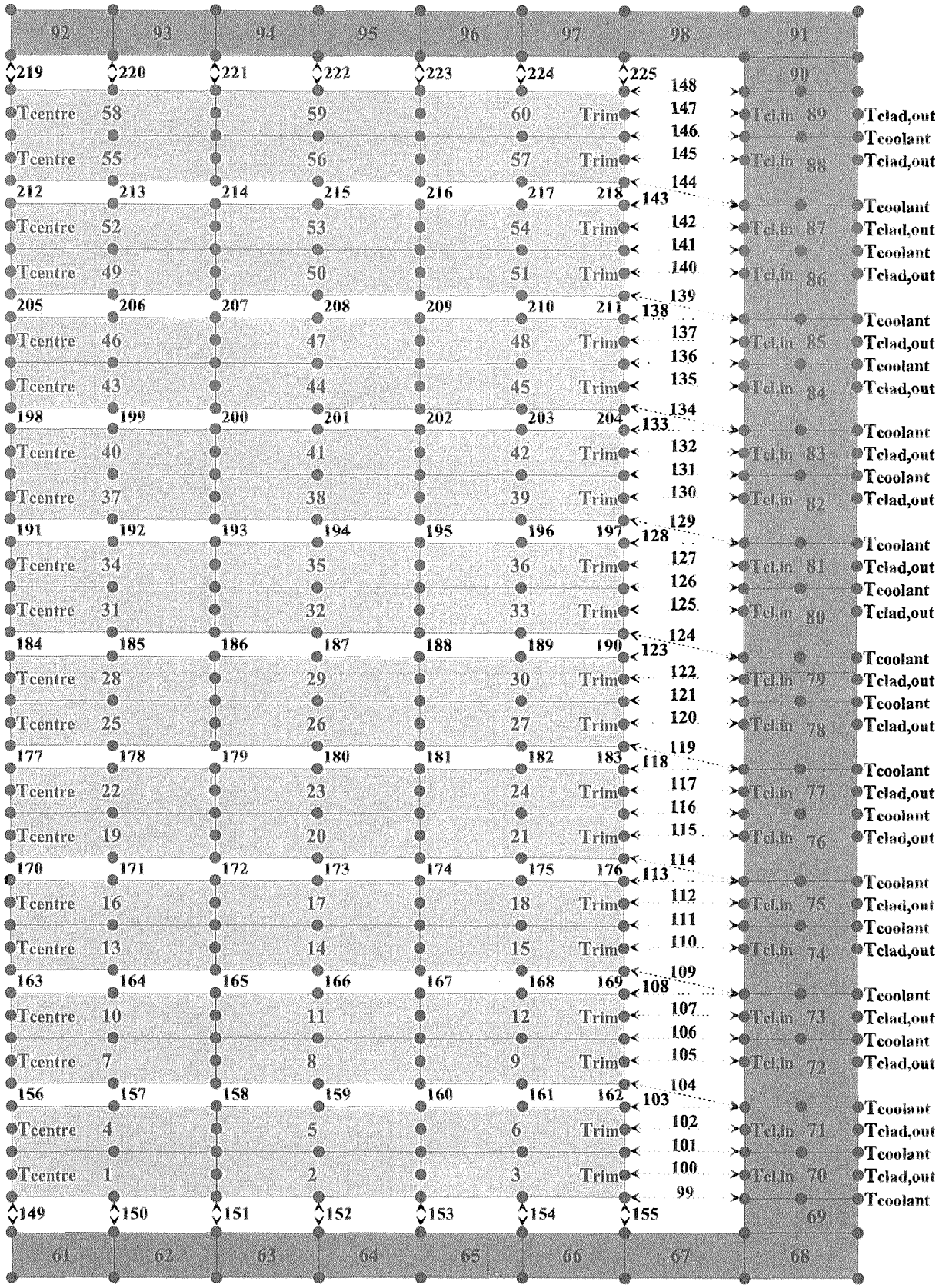


Figure 4: *The finite element grid created for RIA calculations with FREY. Temperatures are calculated in the nodes:* T_{Centre}, T_{Rim}, $T_{Cl,In}$, $T_{Clad,Out}$, $T_{Coolant}$. *Hoop stress is calculated as average over each clad element.*

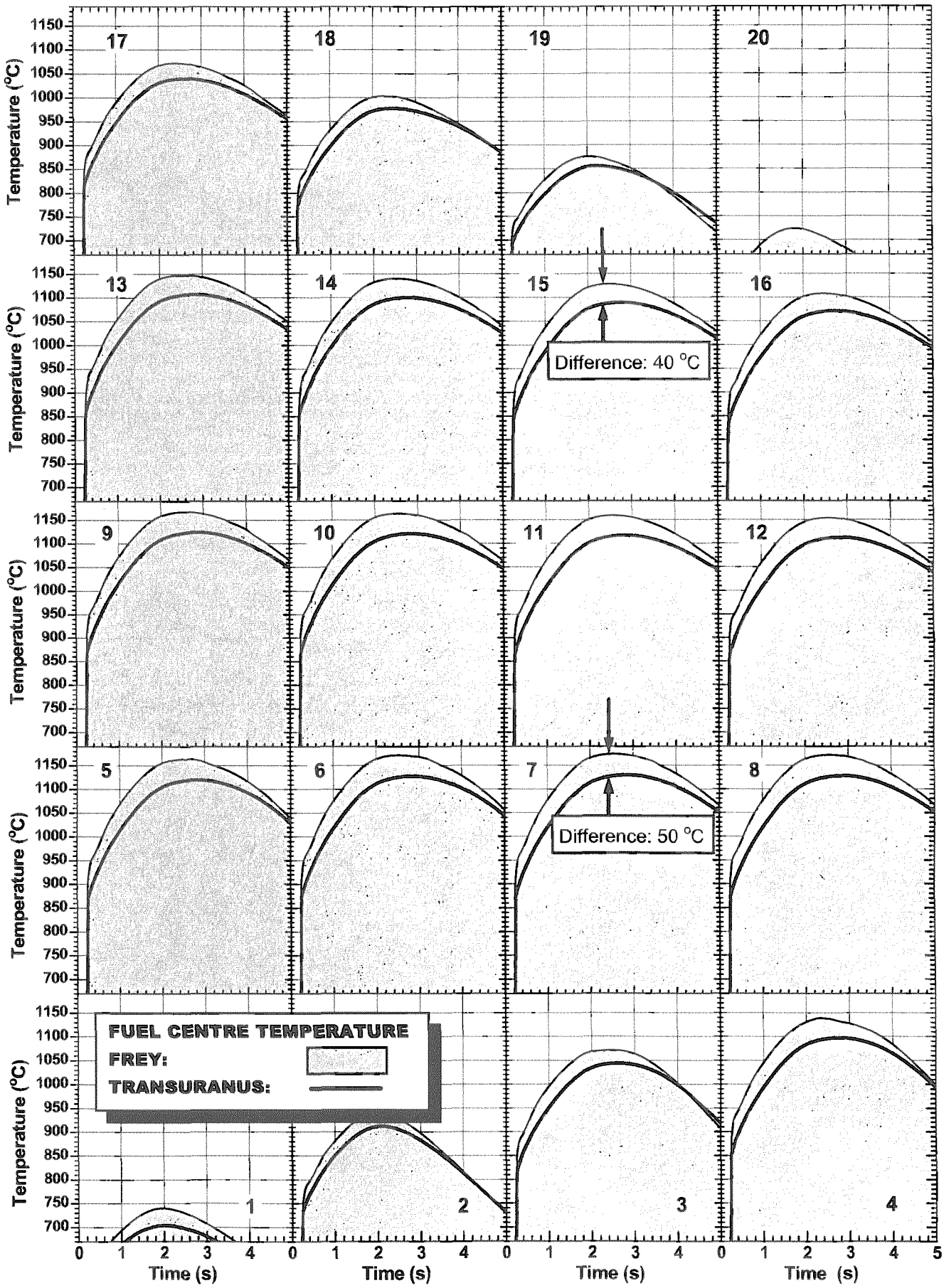


Figure 5: Fuel centre temperature, FREY and TRANSURANUS compared (1 plot per slice).

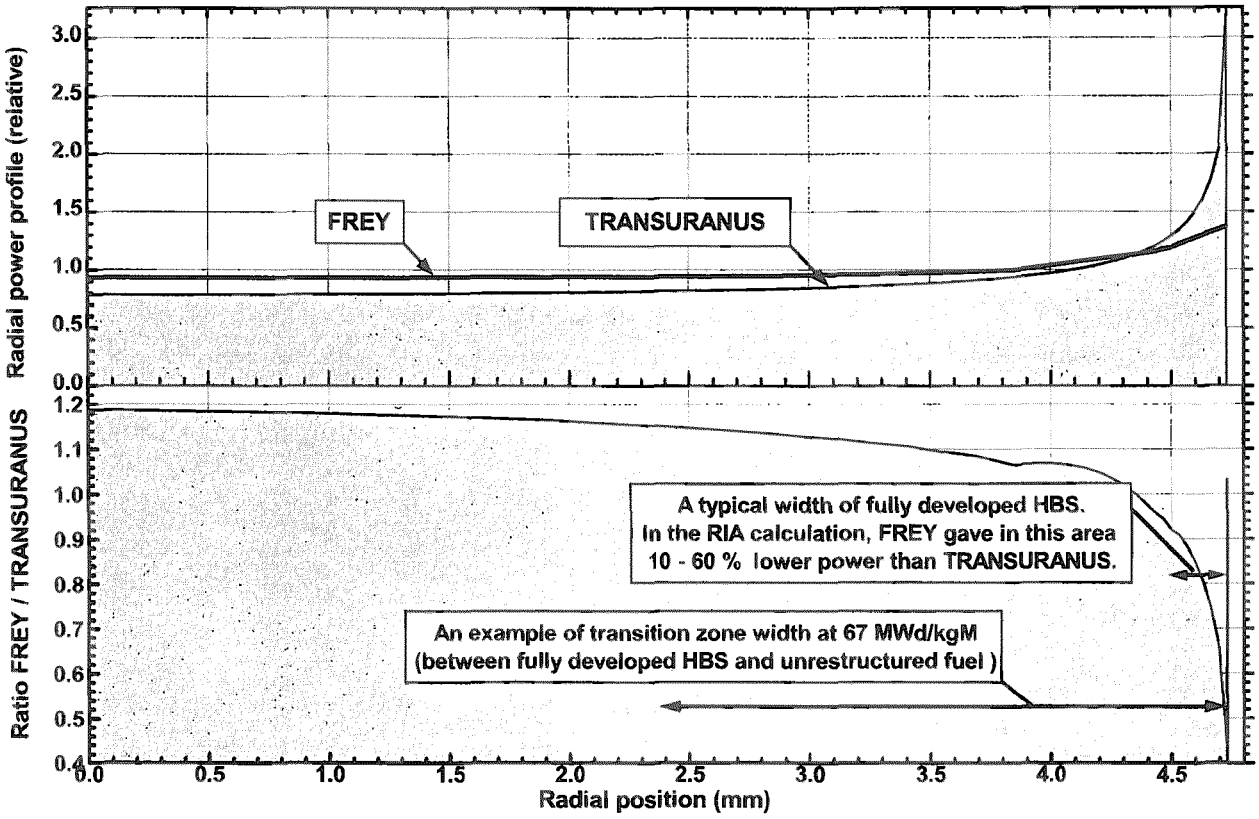


Figure 6: Comparison of radial power profiles in TRANSURANUS and FREY. FREY uses the RADAR model for calculating the radial distribution of fissile isotopes and power production while TRANSURANUS uses the well-validated TUBRNP model. The RADAR model could also be chosen in TRANSURANUS (only a newer version than the one implemented in FREY).

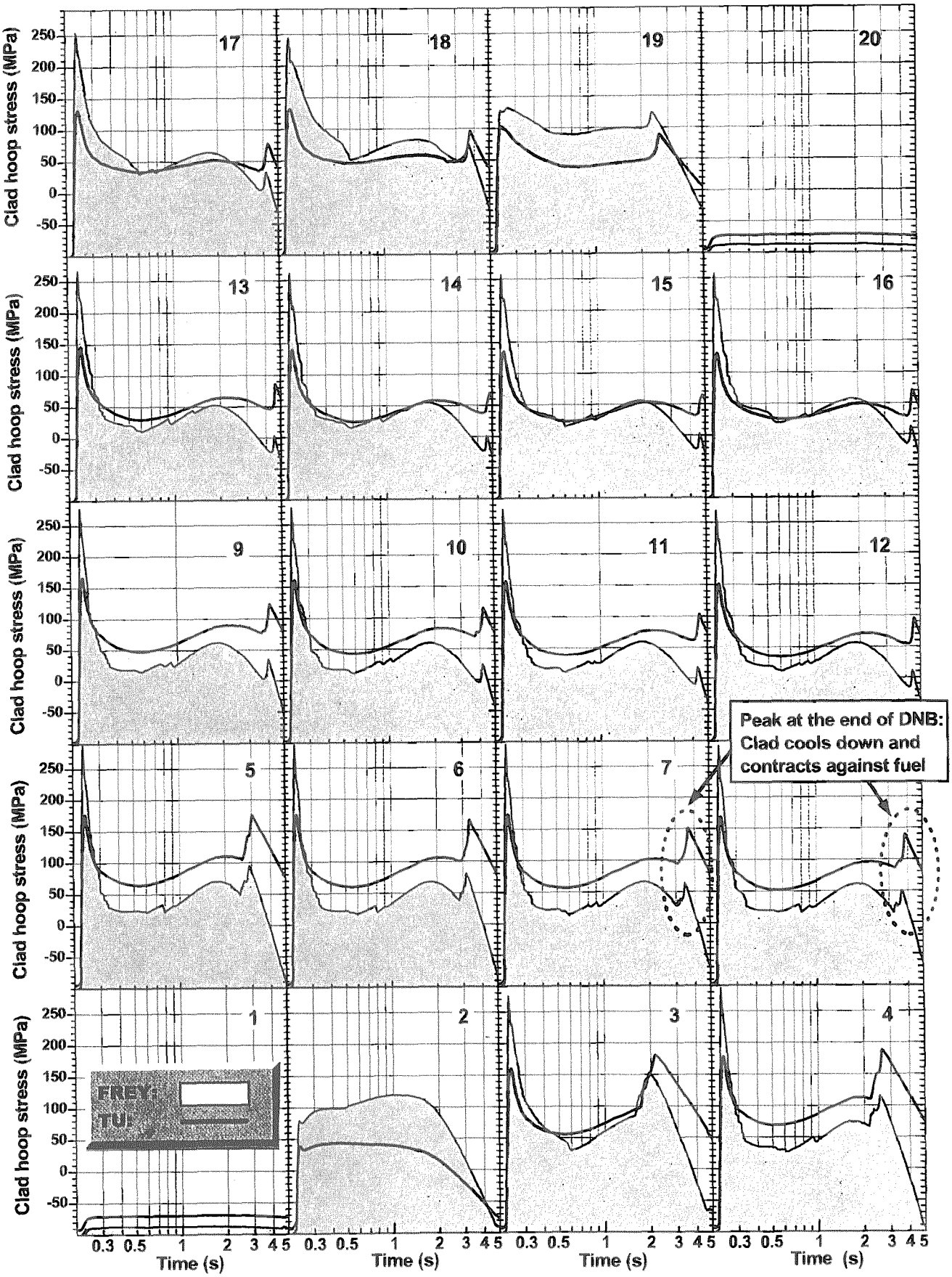


Figure 7: *Clad tangential hoop stress (FREY and TRANSURANUS compared). Hoop stress is calculated as average over each clad element. Negative value = compressive stress, positive value = tensile stress.*

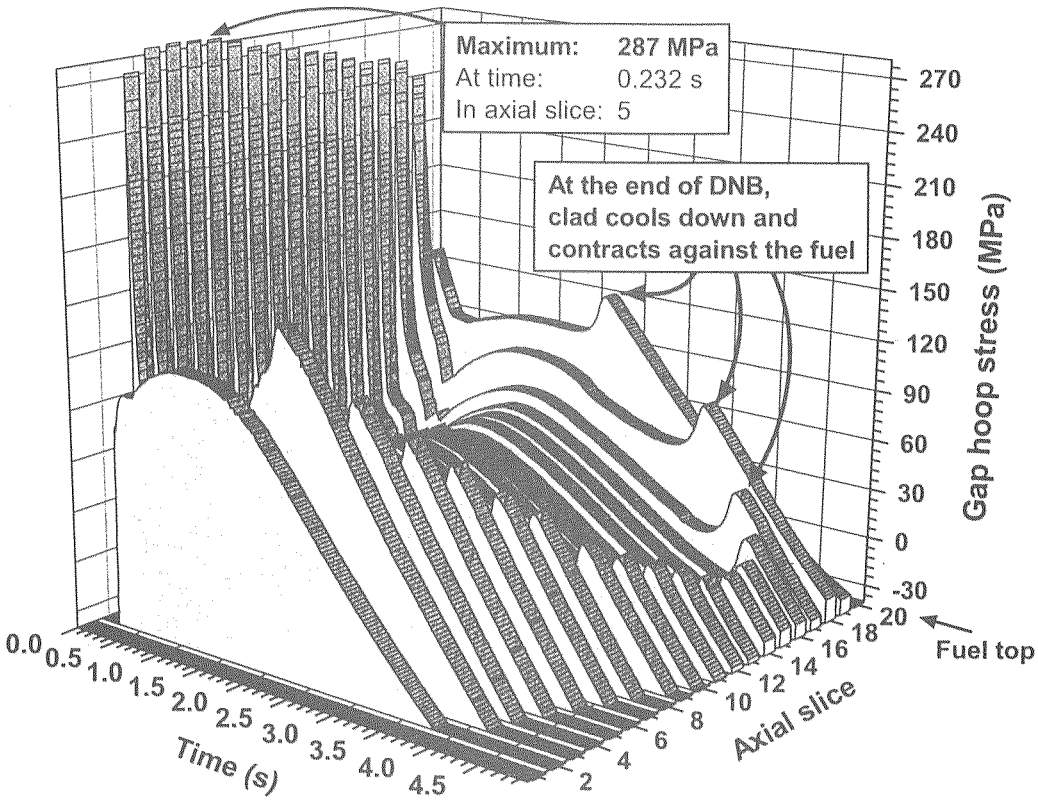


Figure 8: *Tangential hoop stress in clad (FREY calculation).*

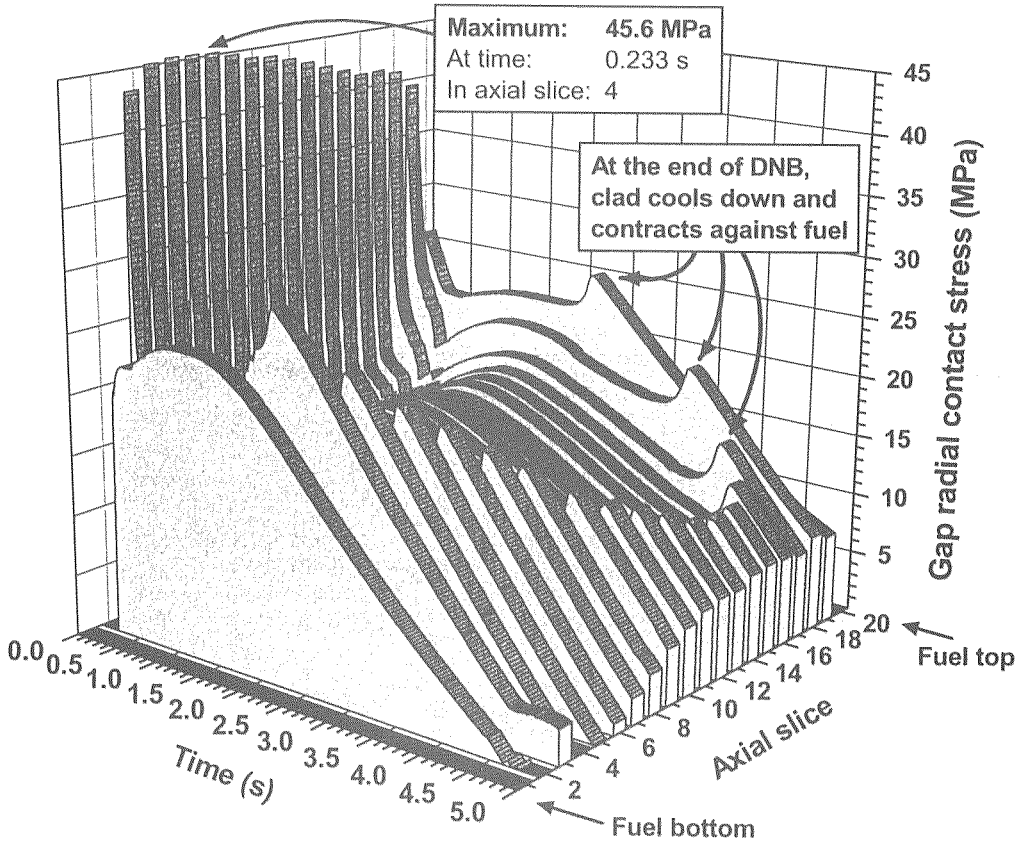


Figure 9: Radial contact stress in fuel-clad gap (FREY calculation).
Contact stress is calculated in the same nodes as $T_{rim}/T_{cl,in}$ (see fig. 4).

Discussion:

Q: (J. Papin)
Proper description of transient behavior of fission gases is important. It is shown by NSRR and CABRI experiments. What do you foresee to describe the coolant channel which is of importance to simulate the rod behavior after onset of boiling crisis? (Effect on clad temperature increase is significant.)

A: At PSI, RIA and LOCA phenomena are investigated in the frame of a project combining the expertise of different groups. The focus of the FREY/TRANSURANUS calculations is the rod behavior, the boundary being the clad outer-surface. The clad outer-surface therefore focus the interface to the thermal-hydraulic calculations performed and investigated in another group with dedicated thermal-hydraulic codes.

Q: (C.Ott)
Which one is the best? TRANSURANUS or FREY? Do you continue to use FREY and FALCON in the future?

A: In the present, neither TRANSURANUS nor FREY can be recommended for RIA modeling at high burnup. PSI will continue to work on TRANSURANUS and will evaluate FALCON and eventually purchase it. Further comparison investigations would then follow.

Q: (M.Kinoshita)
Could you implement models of gas release based on separate tests of the rim structure(HBS), especially focused on impulse pressure development? (including pressure wave after fuel failure)

A: Model of driving force due to fission gas will be done step by step, firstly develop a model before the HBS formation and compare results with available separate effect tests. Afterwards the model might be expanded to the HBS.

Q: (D. Baron)
To conclusion you must add "an improvement is needed in the assessment of the real fuel mechanical properties at high burnup". An extensive work is undergoing since 6 years to develop acoustic methods and micro-indentation techniques to assess to elastic and viscous properties. (Collaboration ITU/EDF/CEA/Montpellier University) A paper will be prepared for the next meeting presenting the first results.

A: The mechanical properties of high burnup fuel is surely of high importance. We are looking forward to your presentation next meeting. TRANSURANUS takes it account the modified mechanical properties in a simplified manner by correcting the properties for the enhanced porosities.

JP0250417

4. Session 3 : LOCA-related Research on High Burnup Fuel

Session 3-1

THERMOMECHANICAL BEHAVIOUR OF IRRADIATED ZR-1%NB ALLOYS CLADDINGS IN LOCA SIMULATING CONDITIONS

N.B. Sokolov[1], L.N. Andreeva-Andrievskaya[1], V.Yu. Tonkov[1], A.V. Salatov[1], A.M. Morosov[2], V.P. Smirnov[3]

[1] A.A. Bochvar VNIINM, P.O.Box369 123060, Moscow, Russia
[2] VTI, Avtozavodskaya St. 14/23, 109280 Moscow, Russia
[3] RIAR, Dimitrovgrad, Russia

ABSTRACT

The research of Zr1%Nb fuel rod claddings of VVER type reactor behaviour and characteristics in loading conditions simulating accidents with loss of the coolant and active zone quenching experimental data are presented.

The experimental data on the deformation and oxidation behaviour of Zr-1%Nb fuel rod claddings in LOCA simulating conditions are illustrated.
The thermal shock experiments under loading conditions simulating accidents with loss of the coolant (temperature, environment, deforming, limitation of the claddings axial deforming, quenching rate, irradiation) data are presented.

The experimental data allow to estimate type and numerical value of the embrittlement criteria parameters (ECR) taking into consideration Zr1%Nb fuel rod claddings resistance during quenching and further fuel rod claddings assemblies removing and transportation.

It is shown, that the mechanical characteristics of the oxidized unirradiated and irradiated claddings material (Zr1%Nb) after thermal shock (residual ductility) are sufficient to withstand quenching and further removing and transportation.

THERMOMECHANICAL PROPERTIES OF IRRADIATED ZR1%NB ALLOY CLADDINGS IN LOCA SIMULATING CONDITIONS

N.B. Sokolov[1], L.N. Andreeva-Andrievskaya[1], V.Yu. Tonkov[1], A.V. Salatov[1], A.M. Morosov[2], V.P. Smirnov[3]

[1] Federal State Unitary Enterprise A.A. Bochvar All-Russia Research Institute of Inorganic Materials, VNIINM, Moscow, Russia
[2] All-Russia Heat Engineering Institute, VTI, Moscow, Russia
[3] State Scientific Center Research Institute of Atomic Reactors, RIAR, Dimitrovgrad, Russia

Abstract

The research of Zr1%Nb fuel rod claddings of VVER type reactor behaviour and characteristics in loading conditions simulating accidents with loss of coolant and active zone quenching experimental data are presented.

The experimental data on the deformation and oxidation behaviour of Zr1%Nb fuel rod claddings in LOCA simulating conditions are illustrated.

The thermal shock experiments under loading conditions simulating accidents with loss of coolant (temperature, environment, deforming, limitation of the claddings axial deforming, quenching rate, irradiation) data are presented.

The experimental data base is sufficient to assess character and numerical value of the embrittlement criterion parameters (PCT, ECR) ensuring the cladding ability to withstand thermal-force loading upon quenching and to keep the mechanical strength after LOCA sufficient for subsequent manipulations with the FA (unloading, transportation).

It is shown, that the mechanical characteristics of the oxidized unirradiated and irradiated claddings material (Zr1%Nb) after thermal shock (residual ductility) are sufficient to withstand quenching and further removing and transportation.

1. INTRODUCTION

The first stage of the fuel rod cladding behaviour research, fuel safety substantiation for all designed operating regimes for zircaloy type alloys and for Russian Zr1%Nb alloy was completed in the beginning of the 80th. At the same time the embrittlement criterion was justified.

The second stage is carried out now. One of the reasons for rise of interest to works in this field is increase of fuel burnup up to 60-70 MWd/kgU. On the first stage of the substantiation fuel burnup didn't exceed 40 MWd/kgU.

Dangerous consequences of irradiation for the claddings stability under loss-of-coolant-accident (LOCA) conditions are as follows:
- changes (degradation) of the claddings mechanical properties;
- changes in the fuel (FP release and accumulation, change of the material structure on the inner cladding surface fuel-cladding gap overlapping, etc.).

Moreover, we should mention, that a range of factors that influence the cladding thermal resistance such as cladding deforming, presence of the axial mechanical loading on the cladding, hydrogen content, have been either unsufficiently investigated or not taken into account.

The second reason is appearance of new materials - Zr-based alloys ZIRLO, MDA, M5, E635 in Russia.

The work in this field has been carried out since the 70th. The methods have been developed. They are improved according to the increase of understanding of the problem and new requirements to the fuel.

Now under VNIINM (designer-technologist of VVER-type fuel rods) leadership the Programm of cladding behaviour under LOCA conditions experimental research is been realized. It includes:

1) safety criteria substantiation for high burnup fuel (Zr1%Nb alloy). Revision of the existing data base with the purpose of detection and investigation of unsufficiently explored characteristics of unirradiated Zr1%Nb claddings;
2) investigation of E635 alloy properties in initial and oxidized states (mechanical, thermo-physical);
3) safety criteria substantiation for E635 alloy;
4) integral experiments with the purpose of investigation of fuel assembly (FA) elements (claddings, spacer grids (SG)) deforming and rupture (depressurization), oxidation and thermal resistance (fragmentation).
   19-element (TEFSAI-19 rig - VNIINM) and 37-element (PARAMETER rig - SRI RPA "Lutch") FA's with unirradiated claddings and 19-element (PVP-2 - RIAR) FA's with irradiated claddings are tested.

2. DEFORMATION BEHAVIOUR

The research of the irradiated fuel rod claddings deformation behaviour were carried out with 160 mm simulators, fuel was not removed from the cladding. Simulators with fuel burnup ~ 50 MWd/kgU were tested.

The indirect heating regime was non-isothermal (Fig.1). The tests were carried out in Ar-steam media under atmospheric pressure (constant argon inflow), fuel rod simulators internal environment – argon. The loading scheme is presented in Fig.1. The claddings were slowly heated up to 600°C at the rate of 1 grad/sec and after that underwent 600sec exposure at 600°C. After isothermal exposure at 600°C the simulator pressure was increased to the required level. The claddings were heated at the rate of (2-4) grad/sec up to the temperature of the second isothermal exposure and the cladding rupture. Heating stopped after the cladding rupture.

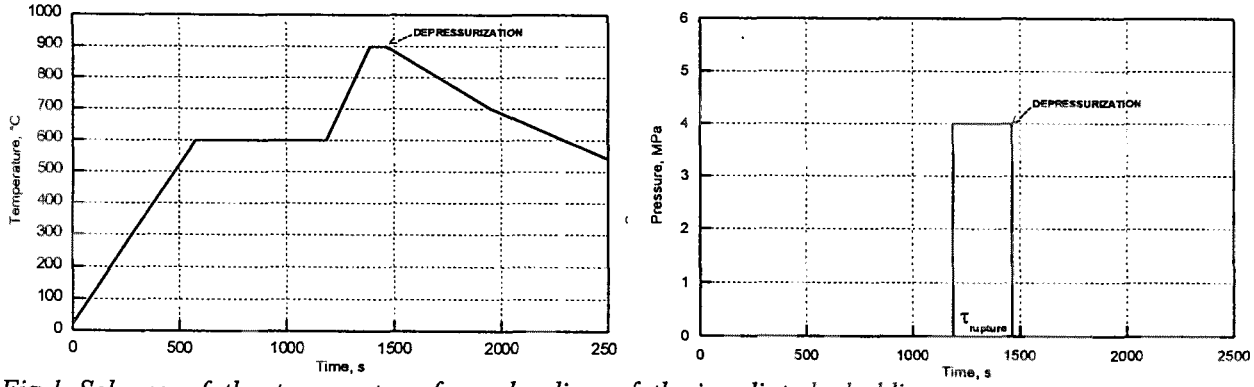
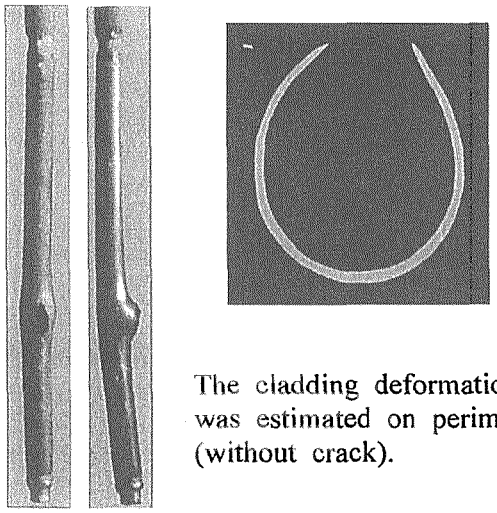


Fig.1. Scheme of the temperature-force loading of the irradiated claddings.

The following post-test research were carried out:
visual examination;
photographing of the simulators post-test appearance and claddings place of rupture;
measurement of the claddings outer diameter in various cladding height cross-sections;
determination of the relative cladding hoop strain.

Fig.2 illustrates fuel rod simulator post-test appearance and cross section of the deformed cladding.

The results of the deformation (and rupture) tests with irradiated claddings are shown in Fig.3. It also contains the experimental data obtained in tests with unirradiated single fuel rods and 19-element assemblies. Comparison of data on unirradiated and irradiated claddings shows no noticeable difference in rupture parameters (temperature, pressure , time, hoop strain).



The cladding deformation was estimated on perimeter median (without crack).

Fig.2. Fuel rod simulator post-test appearance and cross section of the deformed cladding.

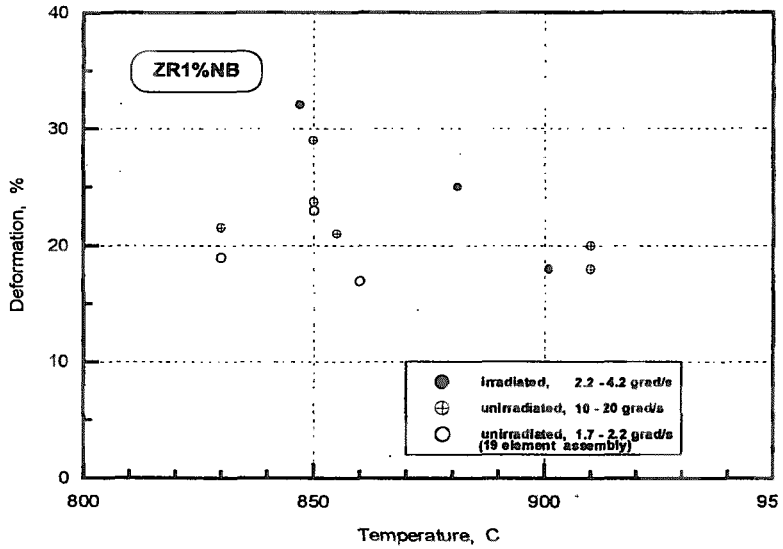


Fig.3. LOCA 2^{d} stage simulating conditions. Cladding hoop strain vs temperature.

3. HIGH TEMPERATURE OXIDATION

The first stage of the fuel rod cladding oxidation behaviour research was completed in the beginning of the 80th. The main results of the studies have been reported in papers and articles; the basic results and dependences are dealt with in [2].

Since 1996 VNIINM and RIAR have been studying Zr1%Nb irradiated claddings oxidation kinetics. Works with E635 alloy claddings start this year.

The requirements to the oxidation experimental procedure are the following:
- indirect method of the specimens heating in accurately temperature-controlled working zone;
- accurately controlled temperature field uniform along height and over radius of the specimens heating zone;
- possibility of ensuring of isothermal regimes at specified pressure and steam flow rate;
- quality and composition of steam (or other oxygen containing environment) must not change during the experiment;
- vertical arrangement of the specimen within the facility work zone;
- careful degreasing of the simulators surfaces that will be oxidized;

- high accuracy of specimen temperature measurements, despite formation of substantially thick oxide films and possible deformation of the specimen;
- use of experimentally defined simulators weight gain as oxidation reaction measure (continuous weighting during the experiment).

3.1. Oxidation degree estimation

The degree of Zr1%Nb claddings oxidation is estimated via weight gain (Δm), or local depth of oxidation (ECR) value.

The local depth of the cladding oxidation (ECR) is understood as the total equivalent Zr-layer thickness (that would react with steam assuming that all locally absorbed oxygen goes on formation of stoichiometrical zirconium dioxide ZrO_2) related to the initial cladding thickness. If the fuel rod cladding is *depressurized, oxidation of both outer and inner surfaces of the cladding is taken into account.*

The weight gain can be defined simultaneously with oxidation (the experimental weight gain), or by calculation using the dependence, derived on experimentally obtained data base (calculated weight gain).
The weight gain Δm and the local depth of oxidation ECR are related by the ratio [2]

$$ECR = N \times (\delta_e / \delta_o) \times 100, \ \%$$

where
N the coefficient taking into account two side oxidation of the cladding, $N = 2$;
δ_o initial thickness of the specimen, cm;
δ_e thickness of the equivalent layer (calculated Zr thickness, which goes on ZrO_2 formation), cm.

It is to be pointed out that the specific weight gain of the cladding is found by dividing the weight gain by the area of the initial cladding surface. This gives a conservative estimation of the specific weight gain. Real oxidation area can be larger due to possible cladding deforming.
Relation for the ECR definition has a kind

$$ECR = N \times 4{,}355 \times 10^{-2} \times \Delta m / \delta_o, \ \% \qquad (1)$$

In the temperature range (900-1200)°C and the oxidation time up to 900 sec the parabolic rate equation is recommended as a conservative one for assessment of the degree of Zr1%Nb claddings oxidation [2]

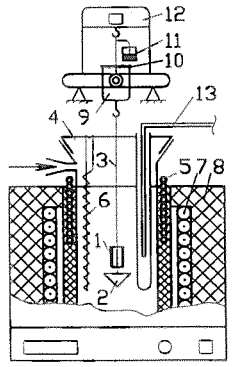
$$\Delta m = 920 \times \exp(-10410/T) \times \sqrt{\tau} \qquad (2)$$

where
Δm specific weight gain, mg/cm^2;
T temperature, K;
τ time, s.

The experimental results have shown, that in the indicated temperature-time range the dependence (2) defines Zr1%Nb claddings weight gain with the safety margin for the cases: availability of hydrogen addition in steam; excessed steam pressure; fuel rod claddings deformation, irradiation and steam-drop cooling.

3.2. Experimental procedure, results

A large experimental data array was obtained using UNOPRO facility (Fig.4) with continuously recorded weight gain of the specimen during the Zr-steam reaction [2].



1	specimen
2	Pt bowl for ZrO_2 collecting
3	Pt suspender
4	working zone
5	Pt heater
6, 7	compensating heater
8	furnace shaft
9	frame
10	balance pan
11	liquid damper
12	scale-beam
13	Pt- Pt/Rh thermocouple

Fig.4. Scheme of UNOPRO facility heating modulus.

Fig.5 illustrates smoothed "weight gain – time" curves obtained when studying the kinetics of Zr1%Nb alloy oxidation on facility continuously recording the specimen weight gain. The experimental data given in Fig.5 represent the average values of weight gains.

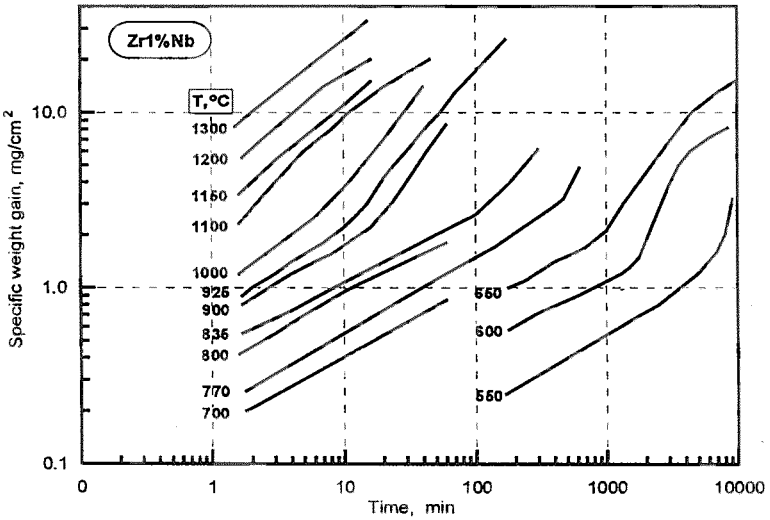


Fig.5. Weight gain of VVER fuel claddings of Zr1%Nb alloy effected by steam oxidation at atmospheric pressure.

Fig. 6 demonstrates the experimentally obtained values of the oxidation reaction rate constant, dependence (2) for Zr1%Nb alloy, as well as Zry-4 oxidation rate [17] and Baker - Just dependence, obtained for zirconium.

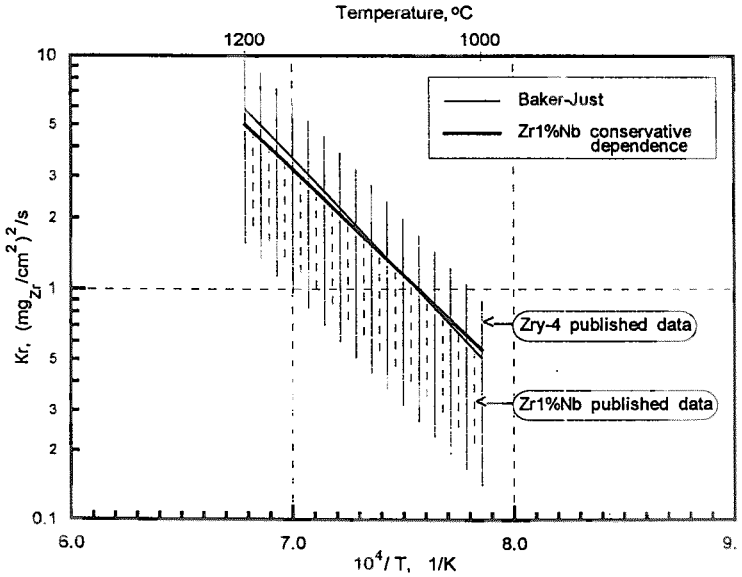
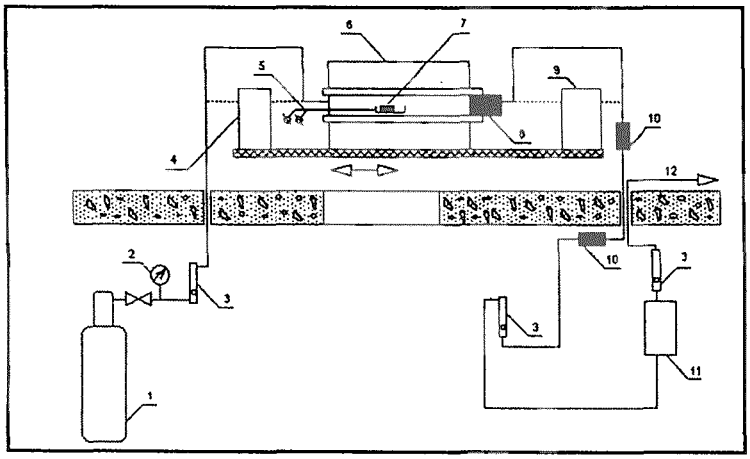


Fig.6. Temperature dependence of reaction rate constant for Zr1%Nb and Zry-4.

The scheme of the rig used in tests aimed to study oxidation of irradiated Zr1%Nb fuel rod claddings is presented in Fig.7. Fuel rod fragments (burnup of ~ 50 MWd/kgU) were used as samples for these tests. Fuel was removed from the samples.
The following studies were conducted before further manipulations:

gamma-scanning;
vortex-current defectoscopy;
profilometry.



1 argon cylinder
2 rotameter
3 manometer
4 steam generator
5 thermocouple
6 heating modulus on a movable plate
7 sample in the capsule (crucible)
8 main filter
9 condenser
10 supplementary filter
11 gas-analyzer
12 discharge

Fig.7. Scheme of the rig for corrosion tests.

The isothermal exposure temperatures were (800 – 1200)°C. Sample weight gain and oxidation degree (ECR) were defined before and after the tests.
Results of the experiments at the temperature of 1200°C are presented in Fig.8. Data on unirradiated claddings weight gain obtained by VNIINM are shown in the figure. Heating in these tests was isothermal. Fig.8. also shows calculated conservative dependence (2).
Analysis of the experimental data on fuel rod claddings oxidation has revealed that weight gain values of irradiated and unirradiated claddings are virtually identical. Only during first several minutes irradiated claddings oxidation rate is slightly higher compared to unirradiated claddings.
It is reasonable to describe irradiated Zr1%Nb fuel rod claddings oxidation using dependence (2).

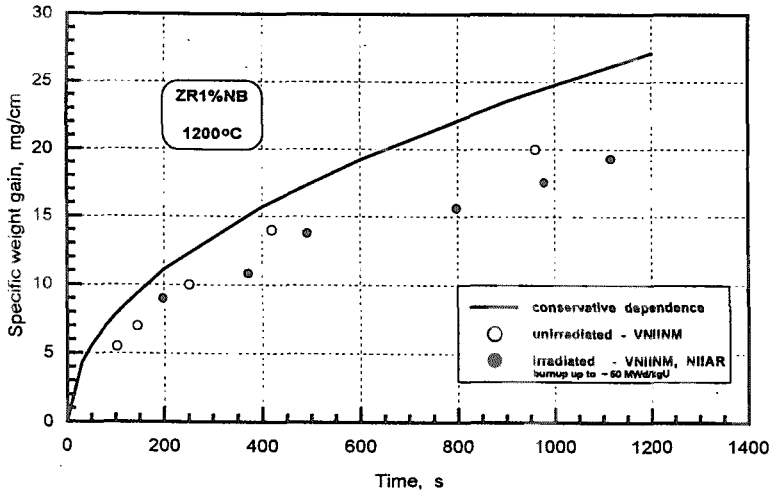


Fig.8. Specific weight gain of the Zr1%Nb claddings vs time of oxidation.

4. EMBRITTLEMENT CRITERION

The experimental research to justify the Zr1%Nb fuel rod cladding of VVER-type embrittlement criterion have been under way in Russia since the 70th.

Several last years much attention is paid to substantiation of the embrittlement criterion for high burnup fuel rod claddings and to study of E635 alloy oxidized claddings thermo-mechanical properties and the embrittlement criterion substantiation.

Under LOCA conditions, there may be a short period of time before the fuel rods are recovered with cooling water. During this period, the decay heat causes the fuel rods to undergo a temperature excursion, and Zr1%Nb fuel rod claddings may reach temperatures of about 1200°C. Under such conditions they are intensively oxidized by steam. The degree of the claddings oxidation is governed by the level of temperature, pressure, time of oxidation, deformation and other factors.

Owing to the cladding material embrittlement the initial thermo-phisical and mechanical properties of Zr1%Nb alloy, characteristics of ductility change. Thickness of the claddings non-oxidized metal decreases.

At the stage of core flooding with cool water of emergency cooling system oxidized claddings are likely to fail under the action of thermal stresses.

The main design requirements to the fuel rod in LOCA are the feasibility of cooling down a fuel rod having a distorted cladding as well as core disassembly (removal) availability after the accident.

The former requirement limits the degree of cladding ballooning (plastic deforming and rupture). The second one restricts cladding fragmentation (brittle fracture).
The degree of the cladding material (Zr1%Nb alloy) - coolant interaction is stipulated by the maximal design limit of fuel rod damage in the Russian document of norms [1].

The cladding embrittlement criterion limits the local oxidation depth (equivalent cladding reacted (ECR)) and maximal temperature of cladding (peak cladding temperature (PCT)):
1) maximum temperature of cladding must not exceed 1200^{0}C;
2) maximum local depth of cladding oxidation is not to be higher than 18% of its original thickness.

The conservative dependence (2) [2] is recommended to be used for estimation of the claddings oxidation degree (oxygen weight gain).

The adherence to the criterion values ensures preservation of the fuel rod geometry. The cladding has to withstand thermal shock as well as dynamic loads caused by the fuel assembly (fuel rod) removal from the core, placing to a storage and subsequent transportation.

4.1. Experimental research of Zr1%Nb claddings thermal resistance

The experimental research comprises two stages.

First - the research of Zr1%Nb alloy oxidation in steam with the purpose of defining the dependences conservatively describing the kinetics of Zr1%Nb alloy oxidation in a wide temperature range. The rate of "Zr1%Nb - steam" reaction was studied under the influence of several factors. They are: cladding deforming under the action of heightened internal or external pressure; presence of hydrogen, air, nitrogen additives in steam; the heightened steam pressure, steam-drop conditions of cooling, irradiation.

The second part of the research involved the experiments to asses the thermal resistance of oxidized claddings.

The heat resistance is assumed to be the cladding ability to withstand thermal-force loading under LOCA conditions and after that to preserve sufficient mechanical strength for subsequent manipulations with the FA (removal, transportation).

The objective of the thermal resistance experiments is ascertainment of minimum time of claddings oxidation and the corresponding degree of oxidation (ECR), resulting in the claddings failure: on quenching, during removal from the experimental facility, during disassembly, during handling.

4.2. Thermal resistance of oxidized claddings

Two types of experiments were employed.

1) Research of oxidized fuel rod claddings ability to withstand cold water quenching (thermal shock tests);
   The results of this research directly confirm whether the embrittelment criterion was fulfilled (not fulfilled) at the flooding stage in LOCA.
2) Estimation of the physico-mechanical state of the oxidized claddings after thermal shock (cold water bottom flooding or quick (1-2sec) moving into the vessel, filled with distilled water of room temperature) : estimation of impact elasticity, residual ductility, estimation of hydrogen content, metallographic examinations of oxidized claddings after the thermal shock (measurements of "Zr-alloy - steam" interaction layers thickness and microhardness of these layers).
   The residual ductility, the availability of which is corroborated by the results of mechanical tests ensures fulfilment of the embrittlement criterion after LOCA (FA removal and transportation).

4.2.1. Thermal shock testing

The requirements to the experimental procedure used for thermal shock tests comprise the following:
- indirect method of the simulators heating in accurately temperature-controlled working zone;
- accurately controlled temperature field uniform along height and over radius of the specimens heating zone;
- isothermal exposure, time and temperature are fixed;
- quick (1-2sec) moving of the simulator into the vessel, filled with distilled water of room temperature (or cold water bottom flooding);
- analysis of the tested simulator state;
- formation of the simulators failure chart.

The experiments were carried out with short fuel rod simulators. Main loading factors present in LOCA were taken into account in the experiments.
1) Temperature stresses in the cladding upon quenching provided with presence of UO_2 or sintering Al_2O_3 pellets in the simulator.
2) Cladding deforming (ballooning).
3) Axial mechanical load on the cladding (simulation of jamming in SG).

The thermal shock experiments with unirradiated claddings are carried out on two rigs: with heating of the simulator cladding by a heater located in the central hole of UO_2 pellets (TEFSAI) and with continuous recorded weight gain of the specimen during oxidation (UNOPRO).

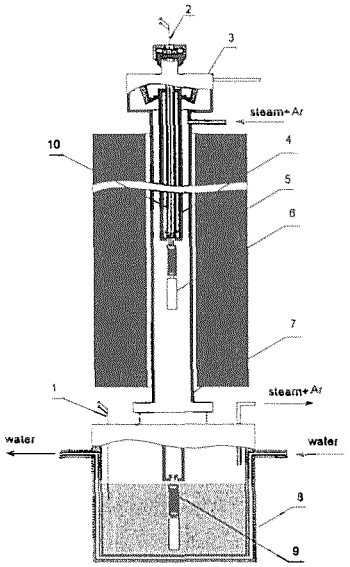
Thermal shock tests were carried out in a wide temperature range (900 - 1300)°C. The degree of claddings oxidation was various (up to 60 % ECR).

The thermal resistance data for the VVER type Zr1%Nb fuel rod claddings irradiated up to burnup of 46,2; 48,3; 49,5; 49,8 $MW \cdot d/kg_U$ were obtained.

The experiments with irradiated claddings were carried out on the universal rig designed to investigate the behaviour of core materials overheated above the operating temperatures in inert gas, air and steam-gas environments (UVS). The main element of the rig is the heating modulus (Fig.9).

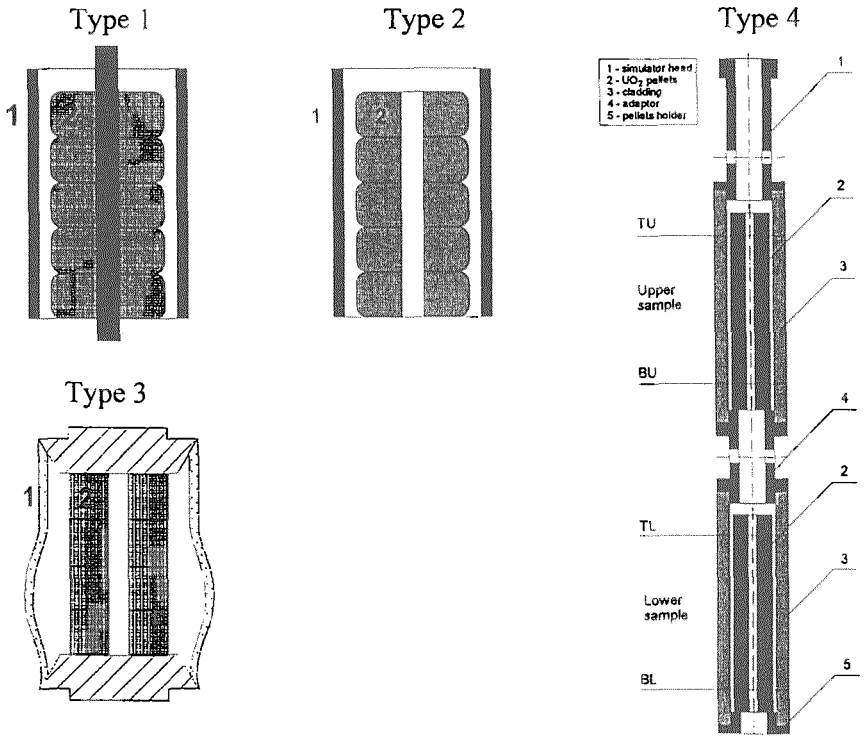
The schemes of the simulators with unirradiated (type 1, 2, 3) and irradiated undeformed claddings (type 4) used for thermal shock tests are given in Fig.10.

The flooding rate values (or moving into the water) were chosen in view of the maximal conservatism of the received results (in terms of cladding ability to withstand thermal shock). It was shown in works [3, 4], that quick cooling causes larger stresses in the cladding during the thermal shock (in case of large oxidation degree especially).
The parameters of the thermal shock tests are listed in Table I.



1, 2	thermocouple
3	specimen withdrawal mechanism
4	cylinder
5	heating module
6	specimen
7	channel
8	water containing tank
9	specimen position after withdrawal
10	channel for the thermocouple

Fig.9. General-purpose rig. Scheme of the heating modulus.



1 - cladding
2 - pellet (Al_2O_3 - type 1, 3, UO_2 - type 2)
3 - tungsten heater
4 - plug
5 - brace
6 - stopper

Fig.10. Schemes of simulators.

Table I. Parameters of the thermal shock tests

Parameter		Facility		
		UNOPRO	TEFSAI	UVS
Simulator cladding temperature,	°C	(900 - 1200)	(900 - 1300)	(1000 - 1200)
Simulator heating rate,	grad/s	var	10 - 20	1÷3 (from 800°C)
Steam pressure,	MPa	0,1	0,1	0,1
Specific steam flow rate,	$mg/cm^2/s$	7	50	2 g/min
Gas flow rate (argon),	cm^3/min	-	-	140 ± 6
Flooding water temperature (immersion),	°C	20	20	25÷35
Flooding rate	m/s		0,2	
(lowering in),	s	0,2		0,5 - 0,8
Cooling rate,	grad/s	~ 100	~ 100	~ 100

The ability of the Zr1%Nb cladding to withstand thermal shock (by bottom flooding with water or fast removing into the cold water) is shown in a chart - the *failure chart*. The thermal shock tests results are shown in the chart in coordinates «time of oxidation» – «temperature of oxidation».

The cladding allowable state range is shown in the chart. Borders of the allowable state range are:

PCT	"Maximal allowable temperature"	vertical line
ECR	"The maximal allowable degree of oxidation" (ECR - dependence (1), weight gain – dependence (2))	inclined line

The results of the thermal shock tests (failure charts) are shown in Fig. 11 – 14 (Zr1%Nb).

The results of the above mentioned tests unambiguously confirm that Zr1%Nb claddings of VVER type fuel rods both unirradiated and irradiated to high burnup (~ 50 $MW \cdot d/kg_U$) adhere to the embrittlement criterion "1200°C - 18% ECR" at the stage of core flooding in LOCA.

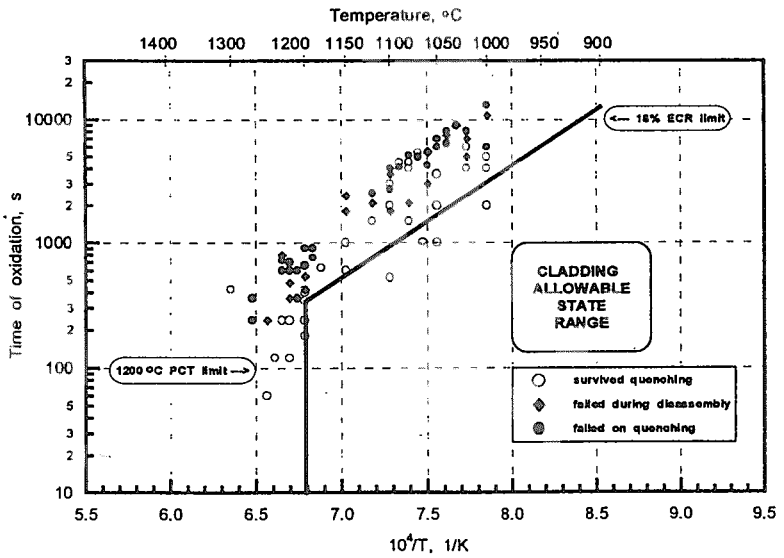


Fig.11. Failure chart. Simulator of type 1.

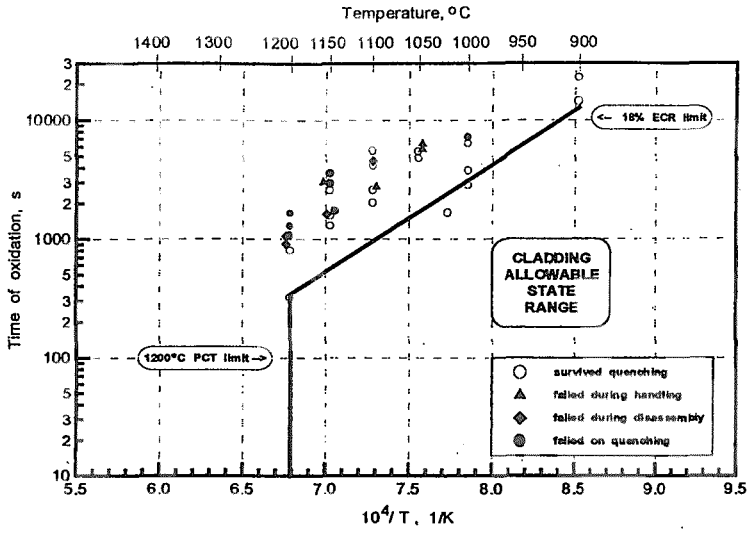


Fig.12. Failure chart. Simulator of type 2.

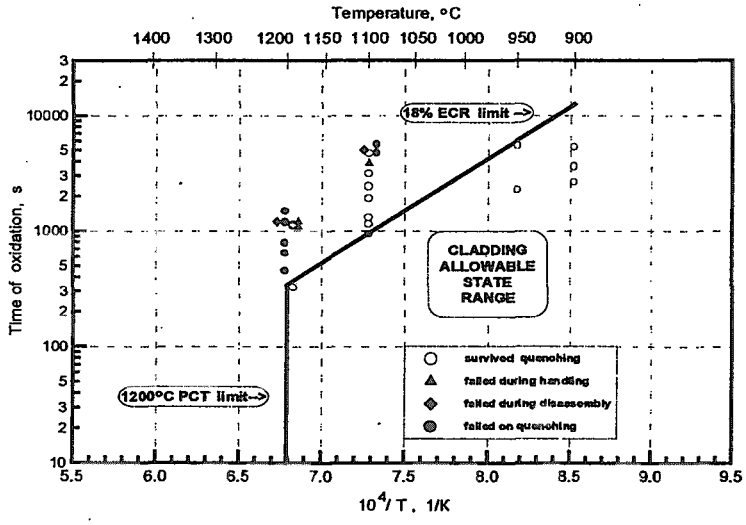
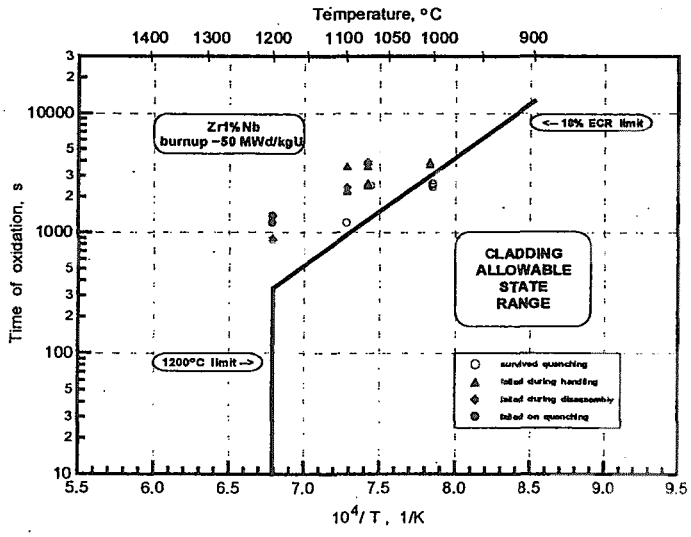


Fig.13. Failure chart. Simulator of type 3.



burnup 49,5 MW·d/kg$_U$

a simulator № 1 τ = 40 min

b simulator № 2 τ = 40 min

c simulator № 3 τ = 40 min

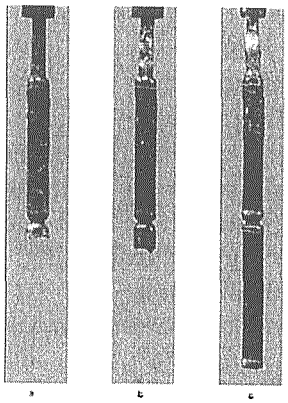
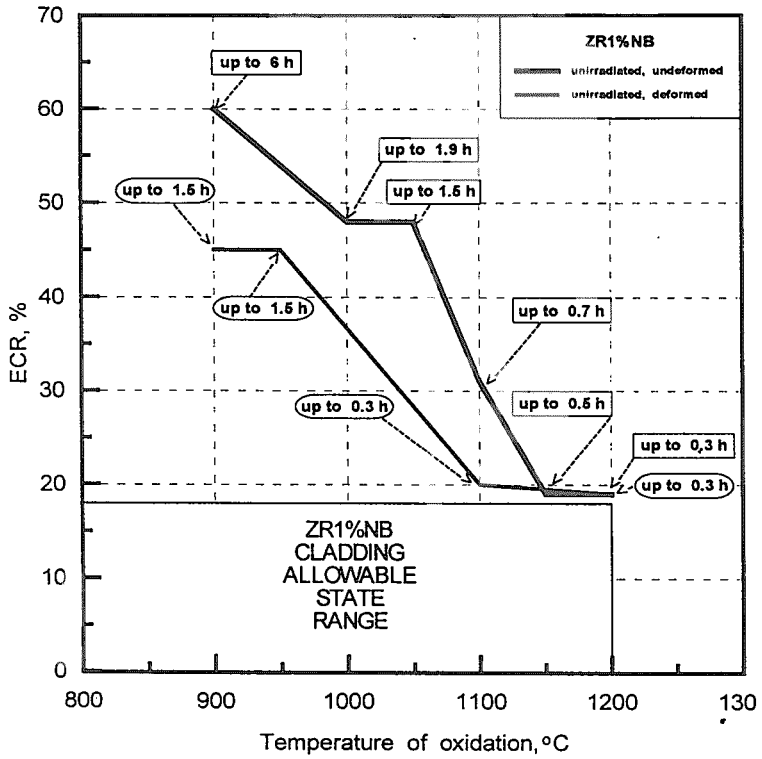


Fig.14. Post-test appearance and failure chart. Simulator of type 4.



The generalized data of the thermal shock tests analysis - the critical parameters of the Zr1%Nb fuel rod claddings fracture are represented in Fig. 15. The figure illustrates the critical parameters (oxidation temperature, ECR, time) at which Zr1%Nb fuel rod claddings did not fracture upon quenching, disassembly, subsequent handling.

One of the important parameters of cladding "viability" is the time during which it assuredly will not fragment under thermal shock. The critical time is larger for Zr1%Nb alloy than for Zircaloy (two side oxidation).

Fig.15. The fracture critical parameters. Simulators of type 1－4.

Compare: during 340 s at 1200°C Zr1%Nb cladding oxidizes to 18% ECR (weight gain calculated from dependence (1)), while zircaloy cladding reaches 17% ECR during ~200 s at 1204°C (as calculated from Baker-Just relation).

Apparently, when dealing with the margin of criterion values one has not to miss from consideration an important factor such as *time* of cladding "viability".

4.2.2. Estimation of the oxidized claddings physico-mechanical state after the thermal shock

The physico-mechanical state of the claddings after the thermal-shock tests is estimated basing on impact, compression, bending tests results. Metallographical research is carried out, and the hydrogen content is defined. The report contains compression tests results.

Compression tests

Mechanical compression tests are carried out using specimens of various lengths, specifically, annular ones. Ring specimen testings (both compression and tensile) fail to give exact quantitative results.
A substantial scatter in the results of compression tests (grip displacement, strain, fracture load) may be explained by:

- different lengths of specimen;
- method used to prepare the specimens;
- initial state of oxidized specimens (one side/two side oxidation);
- morphology of oxide film;
- method of testing;
- method of processing mechanical test diagram, etc.

Some of the afore mentioned parameters were identified before in [3] where it is also pointed out that the results of the tests are not quite correct since circumferential loads on cladding in LOCA are not known.

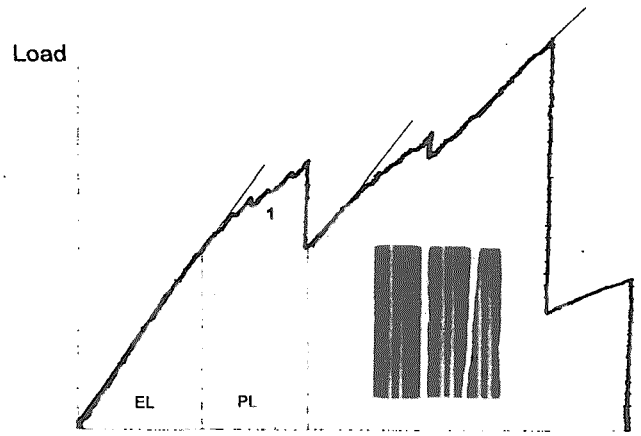
Comparison of compression tests results may be made if tested specimens have close geometrical dimensions and oxidation conditions; procedures of mechanical testing and interpreting results are similar.

The previously oxidized pieces of 30 mm length without fuel were used as specimens. The specimens were cut out from the thermal shock tested unirradiated and irradiated claddings which have kept the integrity. Record of the diagram "load" - "grip displacement" was made during each test. The fracture deformation ε_D was accepted as the ratio of the grip displacement, corresponding to the first load peak, to the initial diameter of the specimen (in percentage). The fracture deformation ε_D included the elastic and plastic components of the deformation.

The results of the compression tests are divided into three groups (Table II).
Table II.

Type of fracture	Deformation (1st load peak), %
Brittle	does not exceed 0,1%
Low ductility	does not exceed 4,0%
Partial ductility (ductility is present)	more than 4,0%

However the critical values bounding the deformation margins for the "partial ductility" and "low ductility " are assigned neither in Russia, nor abroad.



EL - elastic component of deformation
PL - plastic component of deformation

Fig.16. Compression tests at T=20°C on Zr1%Nb claddings. Deformation diagram.

The results of compression tests of oxidized unirradiated (type 2) and irradiated (type 4) Zr1%Nb fuel rod claddings are presented in Fig.17.

The technique of the deformation estimation in cases of unirradiated and irradiated claddings was the same. The comparison of the results revealed absence of distinction in residual ductility values of the irradiated and unirradiated Zr1%Nb claddings.

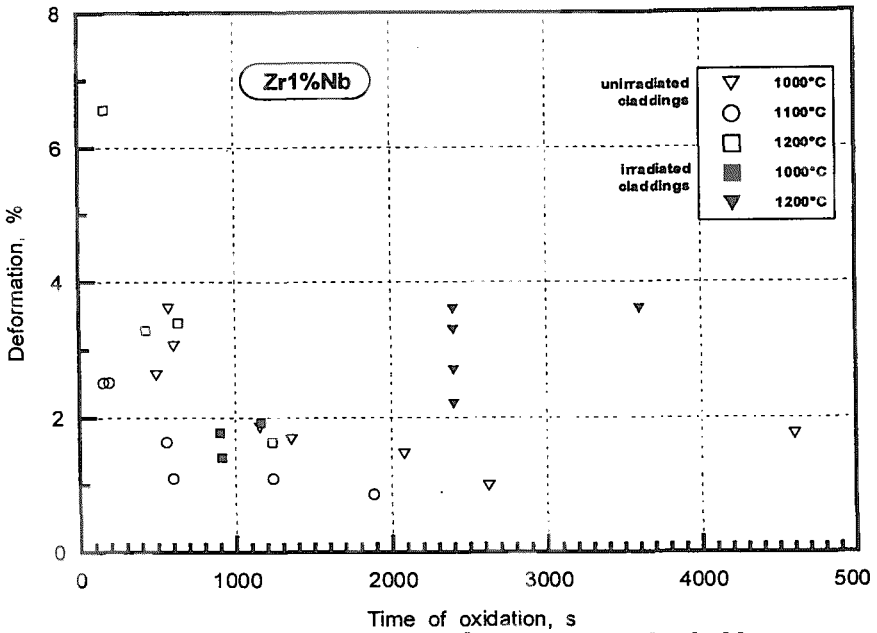


Fig.17. Compression tests at T=20°C on Zr1%Nb claddings. Deformation vs time of oxidation.

The following figures (Fig. 18, 19) illustrate Zry-4 claddings properties [7, 8].

The data of Hobson [7] represented in axes "time of oxidation" – "inverse temperature" show brittle rupture of claddings, oxidized at 1950, 2000F (1065, 1093°C) up to ECR < 17% (calculations using Baker-Just relation).

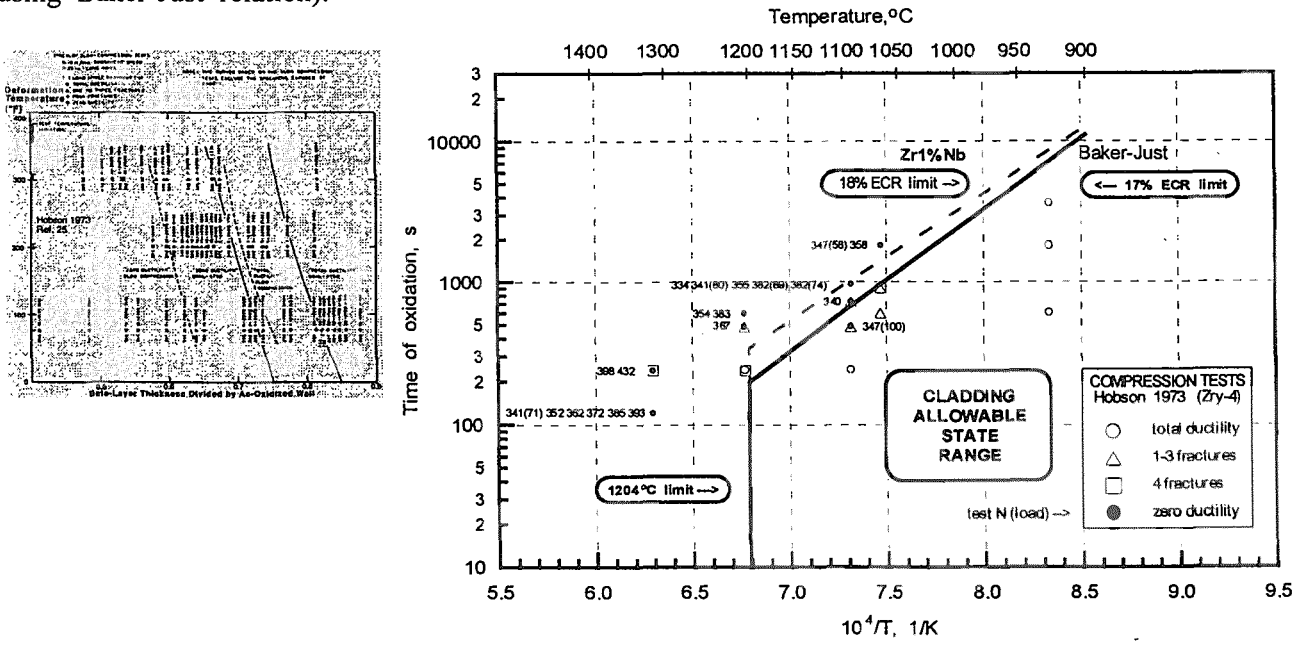


Fig.18. Data of compression tests carried out on Zry-4 by Hobson [7].

The data of Uetsuka [8] (Fig. 19) also reveal rather low characteristics of Zry-4 claddings oxidized at 900°C in flowing steam and for all temperatures in stagnant steam.

It's important to mention, that for correct comparative analyses of the materials properties, especially in case of oxidized claddings, full knowledge of the methods of the corrosion tests and the results handling (ECR evaluation, compression diagram processing, etc.) are required.

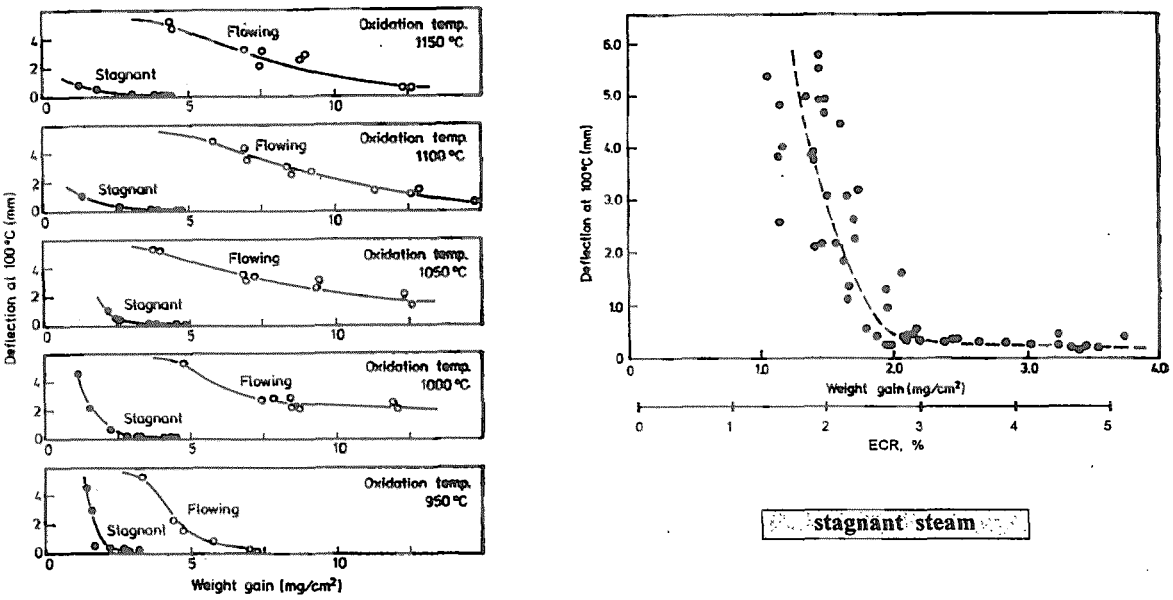


Fig.19. Grip displacement vs specific weight gain of Zry-4 claddings [8].

4.3. Absorbed hydrogen content

The analysis on the absorbed hydrogen content in oxidized Zr1%Nb claddings after thermal shock tests was carried out on the RH-2 device of the Leco firm by high-temperature vacuum extraction from melt in flow of gas-carrier.

Zr1%Nb alloy possesses great ability for hydrogen absorption at 1000°C. This fact is explained by formation of the flaking oxide films on the cladding surface. Probably dense oxide film is a good barrier for hydrogen penetration into the cladding.

Comparison between the data on Zr1%Nb and Zry-4 indicates that the hydrogen content is governed by the oxidation temperature and the oxide film morphology.

For the large degrees of oxidation (15, 18 % ECR) the hydrogen content in oxidized at 1000°C Zr1%Nb specimens is higher, and after oxidation at the temperature 800°C is lower.

The dependence of the hydrogen content in zircaloy based claddings on the oxidation time is submitted in Fig.20.

The results of thermal shock and compression tests with unirradiated and irradiated oxidized claddings demonstrate their similar behaviour and properties as well as availability of a margin in the embrittlement criterion parameters. This is likely to be explained by the comparable content of hydrogen in unirradiated and irradiated oxidized Zr1%Nb claddings. It is known that the initial hydrogen quantity in irradiated Zr1%Nb claddings is low (30－80 ppm) [14].

However, the initial content of hydrogen in irradiated Zry claddings is higher, up to 800 ppm [15]. The low ductility properties of Zry claddings of high hydrogen content are evidenced by the data of [8] (Fig.21) and [16] (Fig.22).

Aside from this, the procedure used to determine the hydrogen content of high oxidized claddings needs an accurate interpretation. To a significant extent this refers to claddings oxidized at 1000°C. This temperature gives rise to flaking oxide films formation on the Zr1%Nb claddings. The quantity of ZrO_2 that remains on a sample used to determine hydrogen content is different. This may be one of the reasons for incorrect determined hydrogen content in high-oxidized samples.

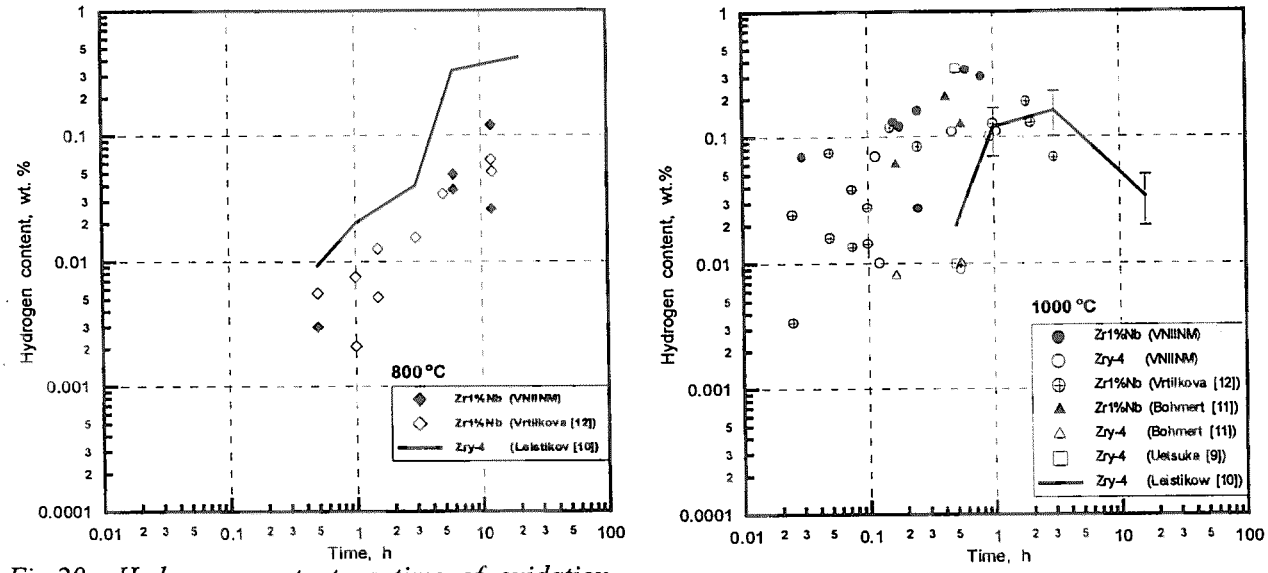


Fig.20. Hydrogen content vs time of oxidation.

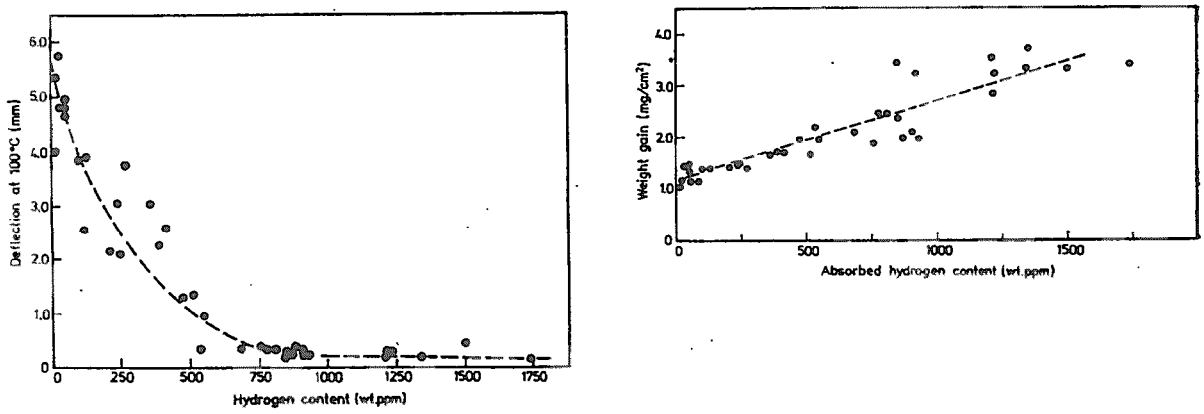


Fig.21. Compression tests at $T_{compression}$=100°C [8].
Grip displacement and Zry-4 claddings weight gain vs hydrogen content.

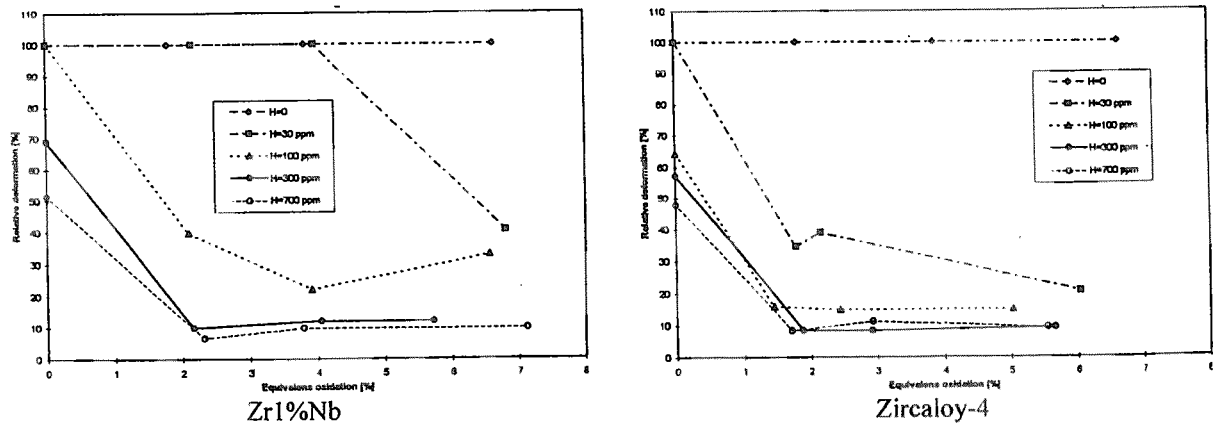


Fig.22. Compression tests at $T_{compression}$=20°C.
Relative deformation (Zr1%Nb and Zry-4 [16] claddings oxidized at 900°C) vs ECR.

5. CONCLUSIONS

Behaviour and properties of Zr1%Nb claddings for VVER type fuels were investigated under loading conditions simulating LOCA.

① The deformation behaviour of irradiated and unirradiated Zr1%Nb claddings under 2^{d} LOCA stage simulating conditions shows no difference.

② Weight gain values of irradiated Zr1%Nb claddings virtually do not differ from data on unirradiared claddings, obtained using various facilities. At several temperatures only during first several minutes of irradiated claddings oxidation the oxidation rate is slightly higher compared to unirradiated claddings.
It is reasonable to describe irradiated Zr1%Nb fuel rod claddings oxidation using dependence (2).

③ The experimental data base is sufficient to assess character and numerical value of the embrittlement criterion parameters ensuring the cladding ability to withstand thermal-force loading upon quenching and to keep the mechanical strength after LOCA sufficient for subsequent manipulations with the FA (unloading, transportation).

The numerical values "1200^{o}C - 18 % ECR" for Zr1%Nb claddings have been justified by the data experimentally obtained in studies of the Zr-steam reaction kinetics and by thermal resistance tests data.

The results of thermal shock tests corroborate directly the fulfilment of the embrittlement criterion by unirradiated and irradiated (burnup of 50 MW·d/kgU) Zr1%Nb claddings at the flooding stage in LOCA.

The partial ductility the availability of which is confirmed by the mechanical tests ensures fulfilment of the embrittlement criterion after LOCA, viz., upon FA's unloading and transportation.

REFERENCES

[1] Nuclear safety rules for NPP reactor facilities. Effective since 01.09.90.

[2] *Yu.K. Bibilashvily, N.B. Sokolov, L.N. Andreeva-Andrievskaya, A.V. Salatov, A.M. Morozov* High-temperature Interaction of Fuel Rod Cladding Material (Zr1%Nb alloy) with Oxygen-containing Media. Proceedings of IAEA Technical Committee on Behaviour of LWR Core Materials under Accident Conditions, held in Dimitrovgrad, Russia, 9-13 October 1995. IAEA-TECDOC-921, Vienna, 996, pp.117-128.

[3] *Williford R.E.* Safety margins in zircaloy oxidation and embrittlement criteria for emergency core cooling system acceptance. // Nuclear Technology, 1986, v. 74, pp. 333-346.

[4] *Chang H.M., Garde A.M., Kassner T.F.* Development of oxygen embrittlement criterion for zircaloy cladding applicable to loss-of-coolant accident conditions in light-water reactors. In: Zirconium in the Nuclear Industry (Fourth Conference), ASTM STP 681, ASTM, 1979, pp. 600-627.

[5] *Yu.K. Bibilashvily, N.B. Sokolov, A.V. Salatov, L.N. Andreeva-Andrievskaya, O.A. Nechaeva, F.Yu. Vlasov.* RAPTA-5 Code: Modelling of Behaviour of Fuel Elements of VVER Type in Design Accidents. Verification Calculations. Proceedings of IAEA Technical Committee on Behaviour of LWR Core Materials under Accident Conditions, held in Dimitrovgrad, Russia, on 9-13 October 1995. IAEA-TECDOC-921, Vienna, 1996, pp. 139-152.

[6] *Kawasaki, S.* A review of studies on behaviour of fuel cladding under LOCA^s. Proc. of Japan-USSR seminar on LWR Fuels, held in Tokyo, Japan, 29-31 October, 1990.

[7] *Hobson, D.O.*, Ductile-brittle behavior of Zircaloy fuel cladding, Proc. ANS Topical Meeting on Water Reactor Safety, Salt Lake City, 26 March, 1973.

[8] *Uetsuka H., Furuta T., Kawasaki S.* Embrittlement of Zircaloy-4 due to Oxidation in Environment of Stagnant Steam // Journal of Nuclear Science and Technology, 1982, v.19, N 2, pp. 70-77.

[9] *Uetsuka H., Furuta T., Kawasaki S.* Failure-bearing capability of oxidized zircaloy-4 cladding under simulated loss-of-coolant condition // Journal of Nuclear Science and Technology , 1983, v.20, N 11, pp. 941-950.

[10] *S.Leistikow, G. Schanz* Oxidation kinetics and related phenomena of Zircaloy-4 fuel cladding exposed to high temperature steam and hydrogen-steam mixtures under PWR accident conditions // Nuclear Engineering and Design, 1987, v.103, N 1, pp. 65-84.

[11] *Bohmert, J. et al.* High-temperature corrosion of ZrNb1 and Zircaloy-4 // Nuclear Engineering and Design, 1993, v.147, pp.53-62.

[12] *Vrtilkova V., Valach M., Molin L.*. Oxiding and hydriding properties of Zr1%Nb cladding material in comparison with zircaloys. Technical committee meeting on influence of water chemistry on fuel cladding behaviour. Rez, Czech Republic, 4-8 October 1993.

[13] Justifications of the M5^{TM} behavior in LOCA. Paper presented at LOCA topical OECD meeting. 22-23 March, 2001.

[14] *A.Smirnov, V. Smirnov, B.Kanashov et al.* Behaviour of WWER-440 and WWER-1000 Fuel in a Burnup Range of 20-48 MW·d/kgU/ Proceedings of the Second International Seminar on WWER Reactor Fuel Performance, Modelling and Experimental Support, 21-25 April 1997, Sandanski, Bulgaria, p. 40-46.

[15] *Romary H., Deydier D.* Corrosion behaviour of zircaloy-4 fuel rod cladding in EDF plants. Ibid [12], pp. 55-71.

[16] *L. Maroti* Ring compression tests with Zr alloys - the effect of H and O content. 5th International QUENCH Workshop, Forschungszentrum Karlsruhe, October 19-21, 1999.

[17] *Erbacher F.J., Leistikow S.* Zircaloy fuel cladding behaviour in a LOCA, Proc. 7th Int. ASTM-Conf. On Zirconium in the Nuclear Industry, Strasburg, France, 24-27 June, 1985.

Discussion:

Q: (D. Schrire)

For the irradiation, E110 cladding, what was the oxide thickness before the simulated LOCA tests?

A: The oxide thickness at external surface was 6 to 10. m for cladding irradiated up to 50MWd/kgU.

Session 3-2

STATUS OF LOCA RESEARCH IN THE HIGH BURNUP CLADDING PERFORMANCE PROGRAM

M. C. Billone, R. V. Strain and Y. Yan
Argonne National Laboratory (ANL)
Argonne, IL USA

ABSTRACT

The High Burnup Cladding Performance program is being conducted at ANL to provide data in support of Loss-of-Coolant Accident (LOCA) and Reactivity-Initiated Accident (RIA) licensing criteria assessments for fuels at high burnup, as well as licensing criteria assessment for spent nuclear fuels under dry storage conditions. The USNRC Office of Nuclear Regulatory Research and the Electric Power Research Institute (EPRI) sponsor the program. Seven Limerick (GE-11 design) BWR fuel rods (≈57 GWd/MTU), ten H. B. Robinson (15x15 design) PWR fuel rods (≈67 GWd/MTU) and two TMI-1 (15x15 design) PWR fuel rods (≈49 GWd/MTU) have been provided to ANL for testing purposes.

The current LOCA acceptance criteria (10 CFR50.46) limit peak cladding temperature to 2200°F (1204°C) and maximum Equivalent Cladding Reacted (ECR) to 17% during high temperature steam oxidation to ensure adequate ductility during the Emergency Core Cooling System (ECCS) quench and during possible post-LOCA seismic events. In addition, NRC Information Notice 98-29 specifies that the ECR should be based on the total oxidation, including oxide layers formed during normal reactor operation. For high burnup PWR cladding, this would leave very little margin for the LOCA transient oxidation. The primary high burnup phenomena that may affect cladding response during ballooning and burst, steam oxidation, quench and post-quench events are: loss of base metal thickness due to oxidation, hydrogen pickup and formation of an inner-surface oxide layer, all during normal operation; the effective thickness and chemistry (i.e., H_2 and O_2 content) of the prior-beta phase layer following steam oxidation and quench; decreased fuel permeability to gas flow from the plenum; and the tightness of the fuel-cladding bond. The LOCA Integral Tests will be conducted with high burnup fueled cladding segments (300-mm long) in order to include all the phenomena highlighted. The oxidation kinetics results at ≈1200°C are being used to plan the LOCA Integral Test experimental times that correspond to ECR values equal to 17% and above and below 17%.

The first LOCA Integral Tests will be conducted using fueled Zircaloy-2 (Zry-2) samples from a Limerick BWR rod. Progress made to date includes: determination of the oxidation kinetics of archival and irradiated Limerick Zry-2 (1000-1200°C); construction/testing of an out-of-cell, "hands-on" LOCA mockup apparatus; detailed design for the remotely-operated in-cell LOCA apparatus based on the mockup experience; construction of, and out-of-cell testing in, the LOCA Integral Test apparatus; and construction of devices to partially remove fuel from the sample top/bottom and to weld end-caps and thermocouples to the sample, as well as to perform overall test train assembly. The BWR LOCA tests will be conducted with pre-stabilization at 300°C, 5 °C/s temperature ramp, hold time at 1204°C based on desired ECR, slow (≈3°C/s) furnace cooling to 800°C, and water quenching initiated at 800°C. For the first test, "plenum" volume, sample internal pressure and test time have been set at 10 cm^3, 8.7 MPa and 10 minutes, respectively. Based on the oxidation kinetics tests, Cathcart-Pawel model predictions agree quite well with weight-gain and oxide-layer-growth data for unirradiated and irradiated Zry-2. However, for irradiated Zry-2, enhanced (≈46%) alpha-layer growth during oxidation and formation of oxygen-stabilized alpha "islands" within the prior beta layer during cooling lead to a smaller effective ductile layer, which may have a negative impact on the quench and post-quench ECR failure thresholds.

STATUS OF LOCA RESEARCH IN THE HIGH BURNUP CLADDING PERFORMANCE PROGRAM

M. C. Billone, R. V. Strain and Y. Yan
Argonne National Laboratory, USA

Fuel Safety Research Specialists' Meeting
Session 3: LOCA-related Research on High Burnup Fuel
JAERI Advance Science-Research Center
Tokai, Japan March 4-5, 2002

ANL LOCA-RELEVANT TESTS FOR HIGH BURNUP FUEL CLADDING

- **Steam Oxidation Kinetics Studies**
  - 900-1300°C, emphasis on 1204°C for 5-20 minutes
  - Emphasis on kinetics of weight gain, (oxide + α) layer growth rate, effective β layer thickness vs. ECR
- **LOCA Integral Tests**
  - Test adequacy of 10CFR50.46 ECCS licensing criteria (ECR $\leq$ 17%, T $\leq$ 1204°C) for high burnup fuel
  - Determine high burnup fuel failure threshold for thermal quench fragmentation
- **Post-Quench Ductility Tests (e.g., Ring Compression)**

HIGH BURNUP LOCA ISSUES

- **BWR Fuel Rods (Limerick at ≈57 GWd/MTU, ≈10 μm OD Oxide)**
  - Effect of tight fuel-cladding bond and restricted gas flow on ballooning, burst, inner-surface-oxidation/hydrogen-pickup, etc.
  - Effect of irradiation on high temperature oxidation in steam
  - Effect of fuel-cladding mechanical interaction on fragmentation resistance during water quench; post-quench ductility
- **PWR Fuel Rods (HBR at ≈67 GWd/MTU, ≤ 100 [m OD Oxide)**
  - Similar fuel-cladding issues as for BWR
  - Effect of in-reactor oxide layer on oxidation kinetics and ECR.
  - Effect of hydrogen pickup on oxidation kinetics, fragmentation-resistance during water quench and post-quench ductility.
- **ECCS Acceptance Criteria**
  - Are ECR ≤ 17% and PCT ≤ 2200°F (1204°C) conservative?
  - Margins to quench fragmentation and post-quench embrittlement?
  - Include pre-transient oxidation in ECR calculation?

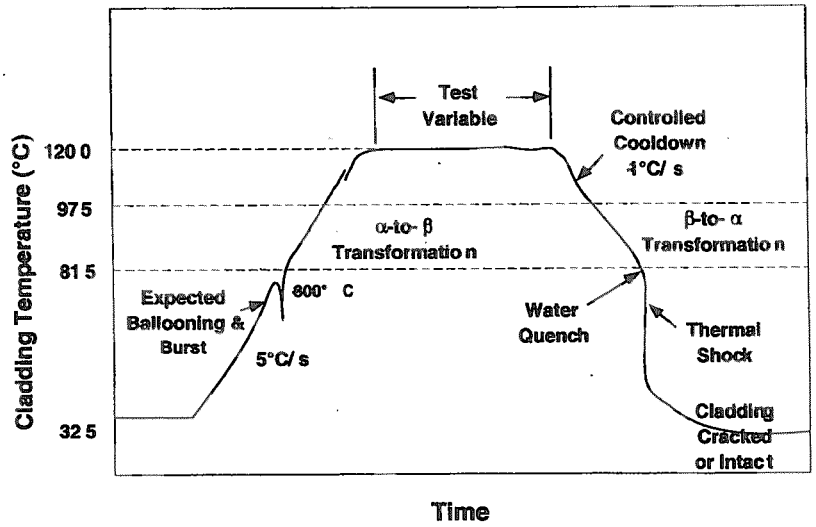
LOCA INTEGRAL TESTING SCOPE

- **Parameters Common to BWR and PWR Tests**
  - Fuel-cladding samples = 305-mm long; fueled region = 270 mm
  - PCT = 1204±20°C, temperature ramps relevant to SB-LB LOCA
  - Internal pressure P_i <1.3×system pressure, plenum V = 5 to 10 cc
  - Best-estimate 17% ≤ ECR < ≈30% → oxidation time ≈2-20 min.
- **High Burnup BWR Rods (Limerick)**
  - Temperature ramp rate = 5° C/s (2.5-7° C/s for SB-to-LB LOCA)
  - Cladding $\Delta P = P_i - P_s \leq 8.6$ MPa [6.7 MPa (SB)- 8.6 MPa (LB)]
- **High Burnup PWR Rods (H. B. Robinson)**
  - Temperature ramp rate = 5° C/s (1-2° C/s for SB, 7-10° C/s for LB)
  - Cladding $\Delta P = P_i - P_s < 20$ MPa [P_s = 3.4 → 0.2 MPa (SB → LB)]

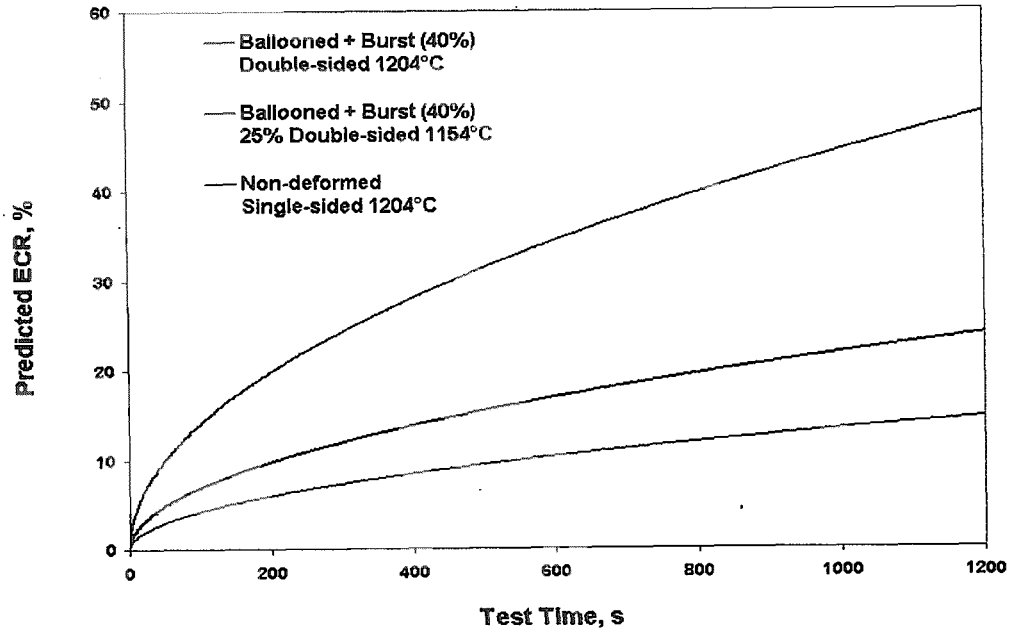
LOCA INTEGRAL TESTING SCOPE

- **Steam and Quench Water Flow-rates/Volumes**
  - Steam flow = 5-10 g/minute
  - Cool-down rate = 3°C/s from 1204°C to 800°C (1-8°C/s for BWR)
  - Quench water velocity = 5 mm/s (initiated at 800°C)
- **First BWR Test Time = 10 min. → ?? Measured ECR**
  - Ignore in-reactor-formed oxygen pickup (10 [m) in ECR
  - Wall thickness before transient ≈0.7 mm (0.71 mm as-fabricated)
  - Use Cathcart-Pawel (CP) best-estimate oxidation model
  - Assume double-sided oxidation around 25% of circumference
  - Assume wall-thickness reduction ≤ 40% in burst region
  - ECR = 10% for 1-sided oxidation, non-ballooned region at 1204°C

CLADDING PEAK TEMPERATURE RAMPS BASED ON PWR LOCA (PUMP-DISCHARGE LEG BREAK)



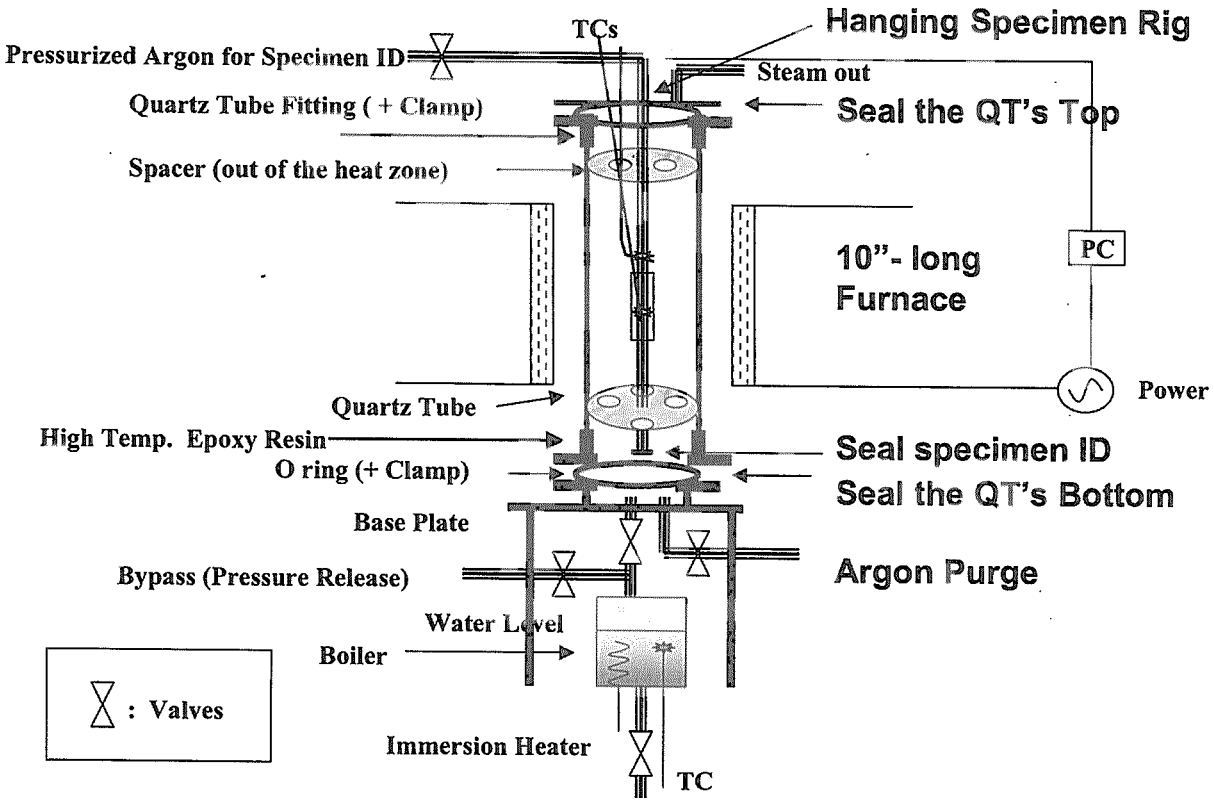
Calculated ECR Values for 1st BWR LOCA Test



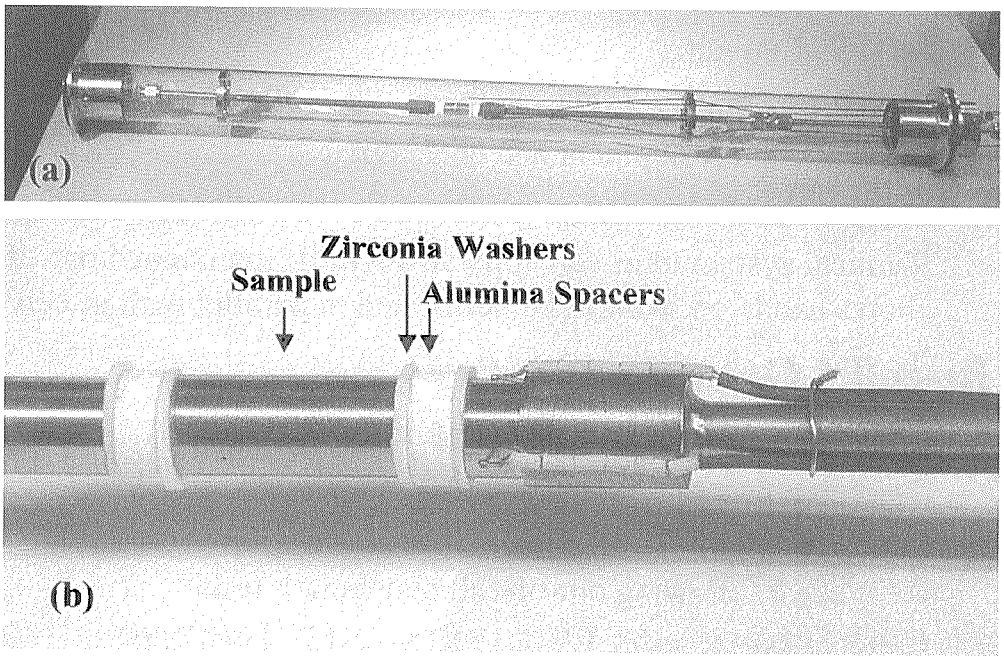
LOCA INTEGRAL TEST APPARATUS

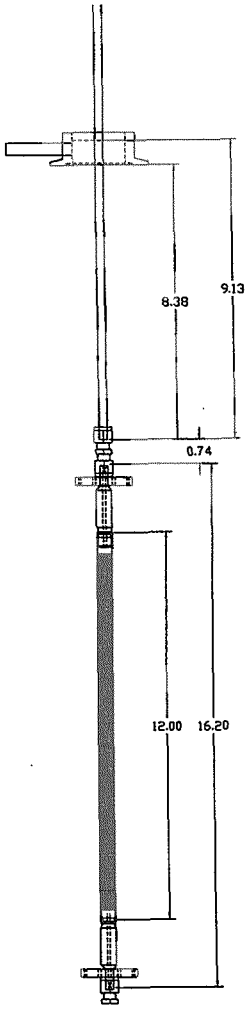
- **Out-of-Cell LOCA Apparatus**
  - LOCA Mock-up
    Samples: Zircaloy-2 tubes with zirconia pellets
    Component development and checkout
    Experience used to design/construct final in-cell apparatus
  - Identical system to in-cell apparatus will be maintained out-of-cell; allows hands-on work to be performed in parallel with in-cell tests
- **In-cell LOCA Apparatus**
  - Capable of doing both oxidation and LOCA tests
  - Oxidation part of LOCA apparatus is operable in-cell
  - In-cell installation of the internal pressurization , quench, etc. will commence following out-of-cell benchmark tests
  - Conduct 1st Limerick BWR LOCA Test in April 2002

Schematic illustration of the new oxidation system



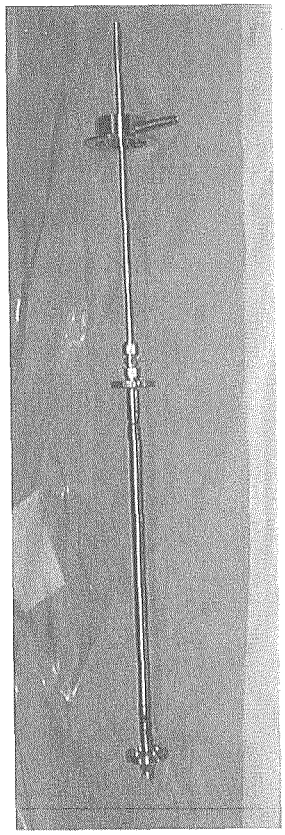
Test Rig for Improved Oxidation Apparatus



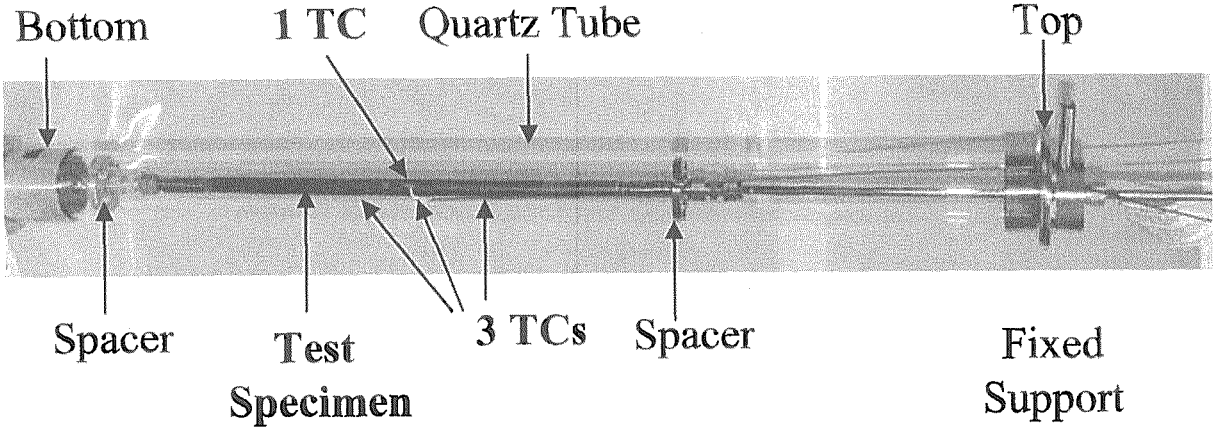


LOCA Hanging Test Train

(Units in inches)



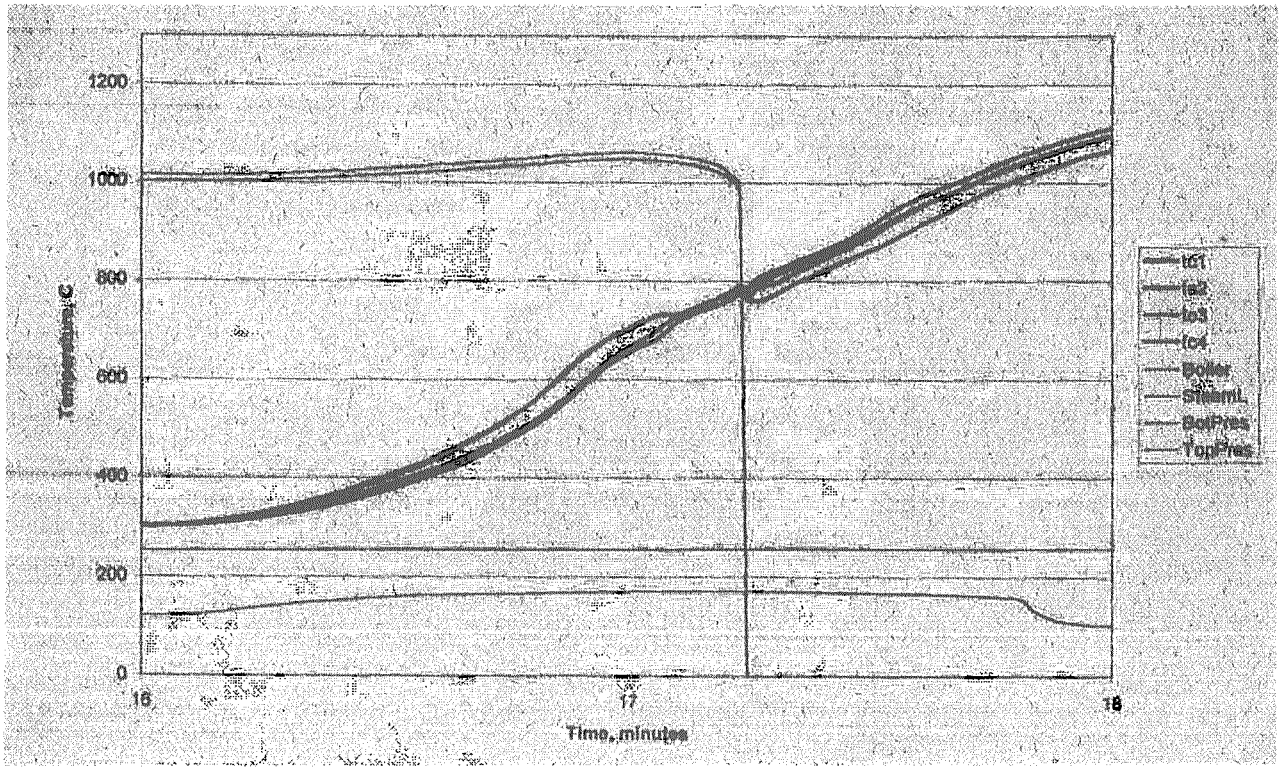
LOCA TEST TRAIN ASSEMBLY



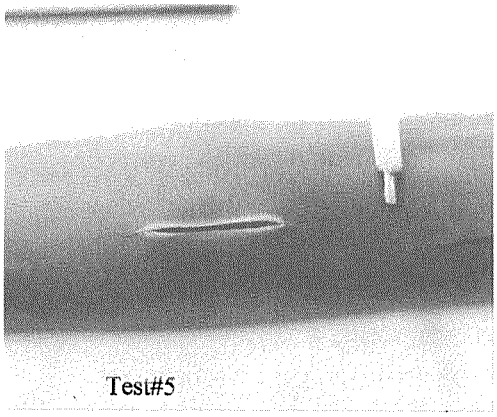
SUMMARY OF LOCA MOCK-UP TESTS

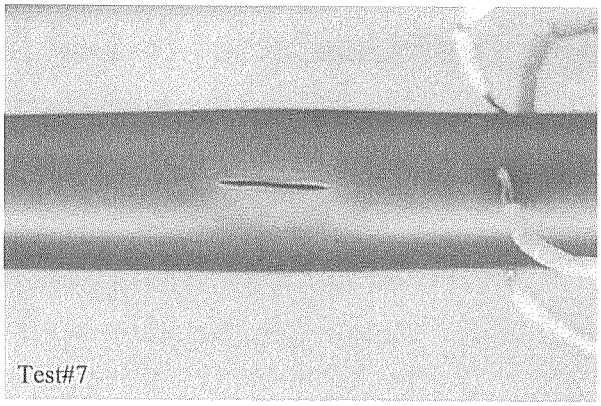
- **Tests Conducted with GE-10 Zry-2 Cladding (0.81-mm wall) with Zirconia Pellets and void (gas) volume of only 3.6 cm^3**
- **Unpressurized Test (#6) to Benchmark Temperature Distribution (T_Θ) at Specimen Midplane and Oxidation Kinetics**
  - T_θ = 1211 ±15°C (based on 4 TCs 90° apart)
  - Weight gains and oxide layer thickness determined from metallography and oxygen measurements agree with Cathcart-Pawel model predictions
- **Pressurized Tests (#5, #7, #8, #9) with water quench**
  - Internal pressure set at ≈7 MPa, remains relatively constant during ramp
  - T_θ = 1208± 15°C for Test #8 (based on 4 TCs 90° apart)
  - Characterization of ballooned/burst region:
    - ΔD/Do ≈40%
    - Burst at ≈760-800°C, small burst openings ≈10-mm by ≈1-mm
    - Oxidation of <25% of inner surface

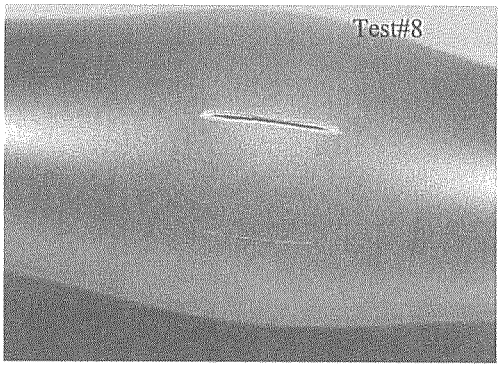
CONDITIONS AT CLAD BURST - TEST #8

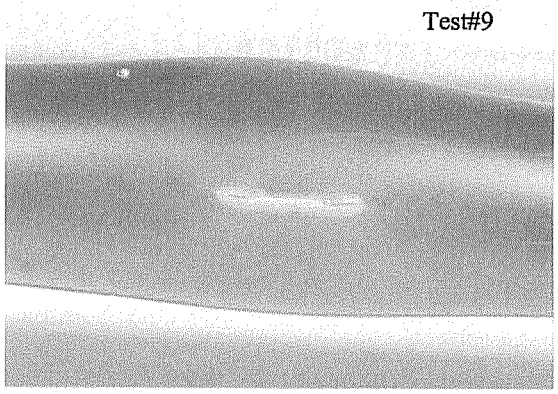


PHOTOS OF BREACH SITES

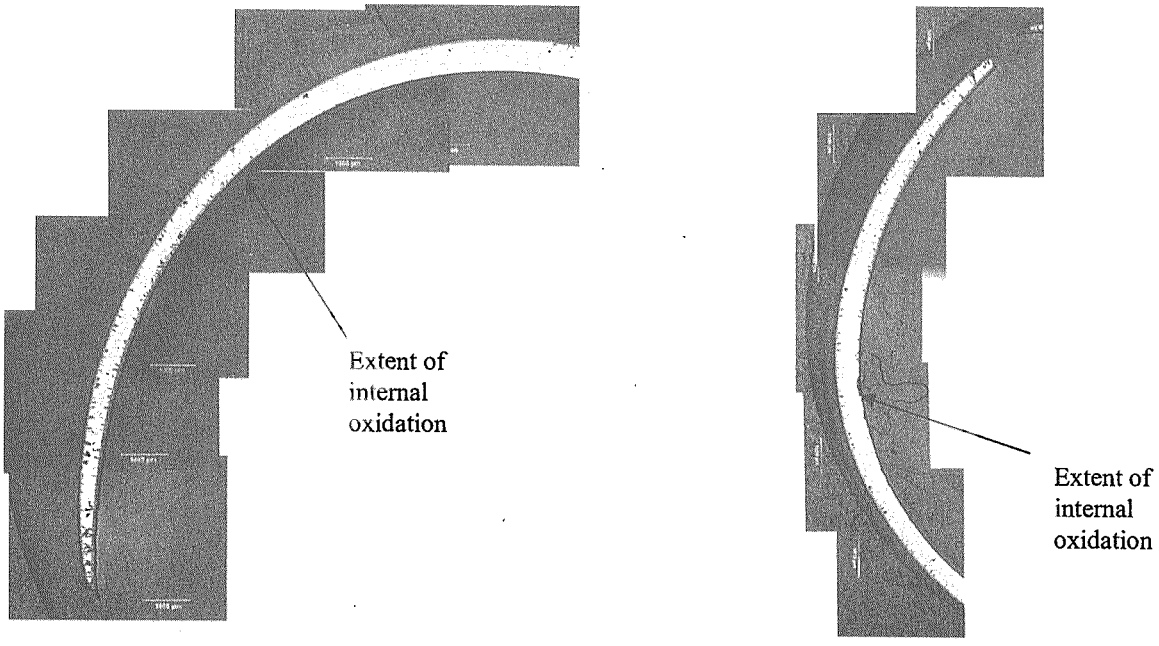








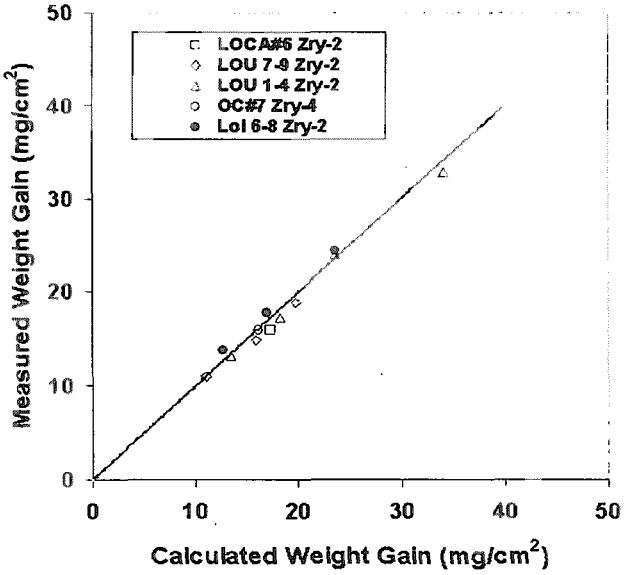
Breach Site, Test #8 Transverse Section



OXIDATION KINETICS RESULTS (Ø1200° C)

- **Tests Conducted In-Cell for 5, 10 and 20 Minutes**
  - Unirradiated (archival) Limerick Zircaloy-2 (Zry-2)
  - High burnup Limerick Zry-2 (≈10-μm OD oxide, ≈70 wppm H)
  - PWR Zry-4 (≈49 GWd/MTU, ≈30-μm OD oxide, ≈150 wppm H)
- **Results to Date (Detailed MET Analysis in Progress)**
  - Weight gain based on MET analysis of oxide, α and β layers most reliable (vs. direct sample weight and oxygen increases)
  - Weight gain kinetics data agree (within 6%) with Cathcart-Pawel (CP) best-estimate model predictions
  - Enhanced growth of oxygen-stabilized α layer observed
  - Highly irregular α-β interface observed for irradiated cladding

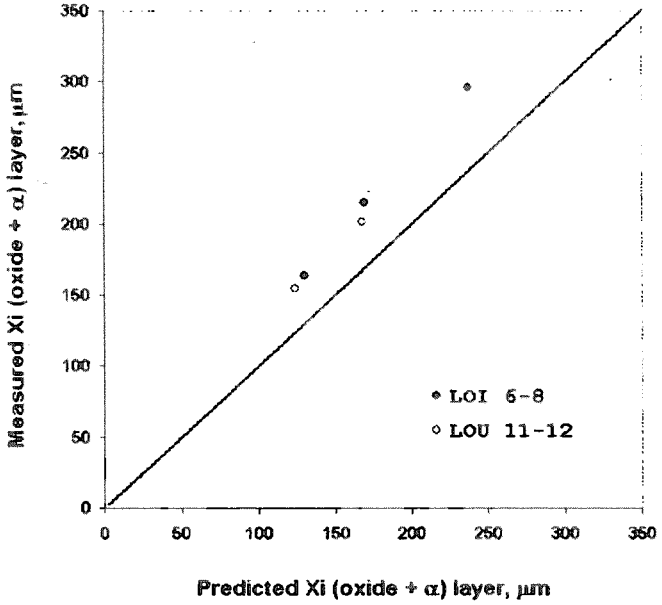
WEIGHT GAIN FOR UNIRRADIATED AND IRRADIATED (LOI 6-8) LIMERICK ZRY-2



OXIDE, α AND β LAYER CHARACTERISTICS
(Unirradiated Zry-2 in Steam at 1204°C for 10 Minutes)

OXIDE, α AND β LAYER CHARACTERISTICS
(Irradiated Zry-2 in Steam at 1204°C for 10 Minutes)
Prior β
α
Oxide
250 μm

OXYGEN KINETICS DATA AT ≈1200° C FOR OXIDE + ALPHA (Xi) LAYER THICKNESS



SUMMARY

- **Steam Oxidation Kinetics Studies: BWR Zircaloy-2**
  - Weight gain data at ≈1200° C for unirradiated/irradiated Zry-2 agrees quite well (±6%) with Cathcart-Pawel (CP) model
  - Xi (oxide+ α) thickness data larger (20-30%) than CP model
    Irradiated cladding has highly irregular α - β interface
- **LOCA Integral Tests**
  - 1st high burnup BWR test scheduled for April 2002
    Aggressive test with 10-minute hold time at PCT = 1204° C
    2-5 additional BWR tests with varying test-times/ECRs
  - PWR LOCA tests will follow with 6-12 samples taken from GS#2 (50-μm OD oxide) and GS#4 (100-μm OD oxide)

Discussion:

Q: (K. Hon'ma)
Do you have a detailed figure of test apparatus for the LOCA integral test? Do you plan to test the LOCA integral test under no restraint condition?

A: Yes, here is a "cartoon" schematic. However, we have changed from bottom-supported test train to top-supported, hanging test train to minimize specimen bowing. The test specimen will have a small tensile stress due to dead-weight loading. However, we do not plan to add axial restraint. We will rely on post-quench ductility tests to come the unknown additional axial loads during a real LOCA.

Q: (J. Alonso)
What are the plans for completing the PWR LOCA tests with a new test series with modern PWR cladding material (e.g., ZIRLO, M5...) since LOCA behavior is very material dependent?

A: NRC has just signed a Memorandum of Understanding (MOU) with Framatome for ANL to obtain unirradiated M5 to perform post-quench ductility tests vs. hydrogen content. This opens the door for ANL to receive high burnup M5 fuel rods in the future for LOCA Integral Testing. NRC also plans to sign an MOU with Westinghouse to obtain unirradiated ZIRLO (short-term) and irradiated ZIRLO rods (long-term).

Q: (M. Valach)
Why did you use Cathcart-Pawel correlation, please? What was the main reason?

A: Cathcart-Pawel model is one of several "best-estimate" models. As the ECR and Oxide/Alpha/Beta codes at ANL are based on Cathcart-Pawel rate constants, there is a very strong historical reason for comparing our oxidation kinetics data to this model. Also, Cathcart et al. determined weight gain by means of detailed metallographic analysis. We agree with this approach and have adopted it for our own work.

Q: (S. Vaidyanathan)
Why does the Cathcart-Pawel model underpredict the alpha layer growth measured in your experiments?

A: Cathacrt et al. developed their models based on rapid (e.g. 100°C/s) heating and cooling rates. The rapid cooling rate "freezes" the oxygen-stabilized alpha layer to what exists at high temperature. Our cooling rate is 4-5°C/s from 1200°C to 800°C.

This gives time for oxygen to diffuse from "alpha" to "beta" to form thicker alpha layers and irregular alpha incursions. The CP model, as observed by Cathcart et al., does a poor job of predicting this transient phase transformation, particularly the non-uniform . /. boundary due to incursions.

Q: (A. Mailliat)

You do not mention any tests with MOX fuel. Does it mean you are thinking that the information provided by UO_2 tests will be applicable to MOX fuel behavior during LOCA?

Could you say a few words about the measurements which will be performed after the tests for getting the information related with fuel relocation (filling up ratio, fragment size, etc.)?

A: No. Currently, our sponsor (USNRC), is not interested in immediate LOCA-relevant data on MOX fuel. USNRC has mentioned in press release ("Inside NRC") possible MOX testing at ANL. Our priorities are (in order of importance): thermal shock fragmentation threshold; post-quench embrittlement failure threshold; axial fuel relocation. Our current plans for assessing fuel relocation are to use HORIZONTAL gamma scanning. This approach may not be adequate.

Session 3-3

Results from JAERI research program on high burnup fuel behavior under LOCA conditions

Fumihisa NAGASE, Takashi OTOMO and Masataka TANIMOTO
JAERI

ABSTRACT

Burnup extension causes significant corrosion, hydrogen uptake and ductility reduction in the Zircaloy fuel cladding. Effects of the burnup extension on the fuel behavior under loss of coolant accident (LOCA) conditions have been great concern, and research on the high burnup fuel behavior under LOCA conditions is one of the most important subjects in the fuel safety research. The Japan Atomic Energy Research Institute (JAERI) performs the systematic research that covers a wide range of testing conditions, with a view to evaluating the effect of burnup extension on fuel behavior under LOCA conditions and to acquiring basic data necessary for the regulation. In this study, various fundamental experiments are planned for evaluating oxidation rate, mechanical property changes after β-quench, ballooning and burst behavior, and failure bearing capability on the quench of cladding tubes which are pre-oxidized, pre-hydrogenated, and/or irradiated at a research reactor (JRR-3) as well as those sampled from spent fuel rods.

Hydrogen uptake is expected to have the biggest impact on the fuel behavior under LOCA conditions. The experiments have been performed so far with non-irradiated Zircaloy cladding tubes with various hydrogen contents, prior to those for irradiated cladding tubes. Obtained results are summarized as shown below.

- The influence of absorbed hydrogen on the Zircaloy oxidation rate varied depending on the temperature and hydrogen concentration. The influence was not significant within the conditions of postulated LOCA and hydrogen concentration in high burnup fuel cladding.
- The mechanical property of pre-hydrided or irradiated Zircaloy-4 cladding tube was degraded after short time annealing at temperatures above α to α+β phase transformation temperature of Zircaloy.
- The integral thermal shock test with pre-hydrided cladding tube has indicated almost no influence of absorbed hydrogen on the threshold value defined by oxidation condition, ECR, for cladding failure by quenching under no restraint condition. On the other hand the threshold ECR is obviously reduced by absorbed hydrogen for severe loading conditions.

1

Results from JAERI research program on high burnup fuel behavior under LOCA conditions

F. Nagase
JAERI

Fuel Safety Research Specialists' Meeting
March 4 – 5, 2002
JAERI Tokai, Japan

This study was partly performed as the collaboration program between JAERI and Japanese PWR utilities.

JAERI

2

Contents

- Background
- Outline of research program
- Experimental results

  Hydrogen effects on

  - *Burst behavior*
  - *Failure-bearing capability on quenching*
  - *Mechanical property after temperature transient*
  - *High temperature oxidation*
- Summary

JAERI

3

Background

- Extensive investigations on fuel behavior under LOCA conditions in '70 and '80
  - Basis of current criteria
  - Most experiments performed with non-irradiated materials
- Extension of fuel burnup
- Changes in pellet and cladding
  - Significant corrosion, hydrogen pickup and increase in fast neutron dose
    - ▶Degradation of cladding ductility
    - ▶Possible reduction of safety margin under LOCA conditions

JAERI

4

Outline of research program

- ***Objective***
  - To evaluate the influence of burnup extension on fuel behavior under LOCA conditions
- ***Research items***
  - Failure-bearing capability of highly oxidized cladding on quench (by Integral thermal shock test)
  - Oxidation rate
  - Mechanical property change after temperature transient, etc.

JAERI

5

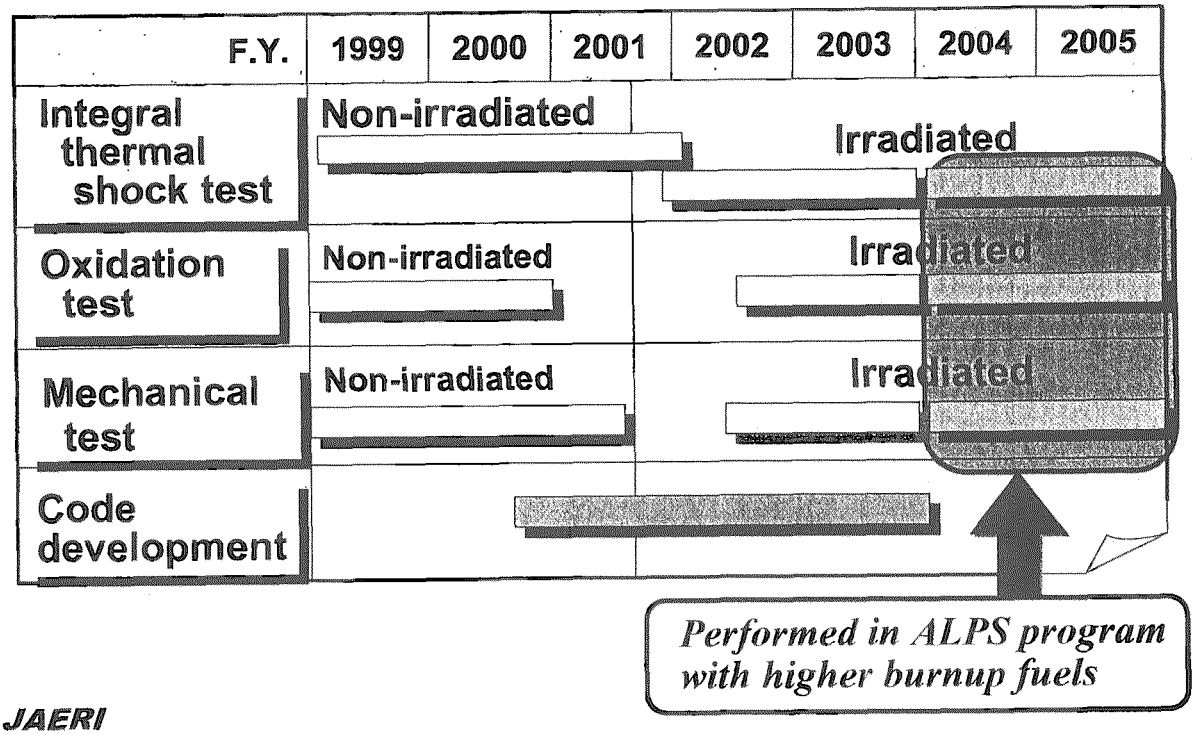
Test samples

- 'Simulated high burnup fuel cladding'
  pre-oxidized, pre-hydrided, and/or
  irradiated at a research reactor
  ⇨ *Separate effect, Wide range of data base*
- High burnup fuel cladding from commercial reactors

JAERI

6

Schedule of research program



JAERI

7

Hydrogen effects on

- Burst behavior
- Failure-bearing-capability on quenching

JAERI

8

LOCA criteria for fuel safety

- **Safety limits**
  - Peak cladding temperature <1200°C (U.S., 2200F)
  - Total oxidation of the cladding < 15%ECR (17%ECR)

- **Basis of current criteria**
  - -U.S.
    - ✓**Zero ductility limit** to avoid excessive embrittlement and fragmentation of oxidized cladding during quenching
  - -Japan
    - ✓**Threshold ECR condition of rod failure** determined by integral thermal shock tests under fully and consevatively simulated LOCA conditions

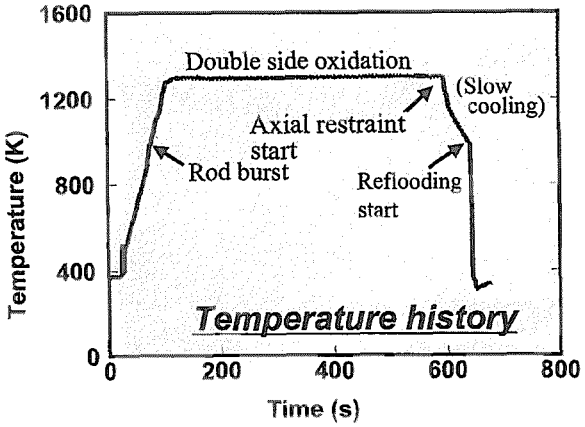


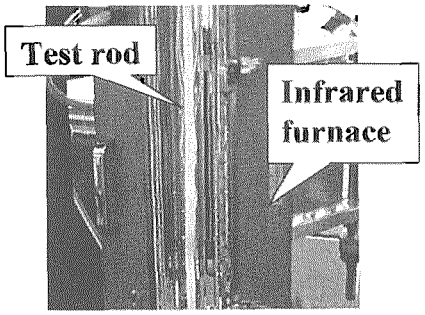
- Ballooning/Burst (Wall thinning)
- Double-sided oxidation (Cladding embrittlement)
- Local hydrogen absorption due to inner surface oxidation
- Thermal shock & Mechanical loading due to axial constraint

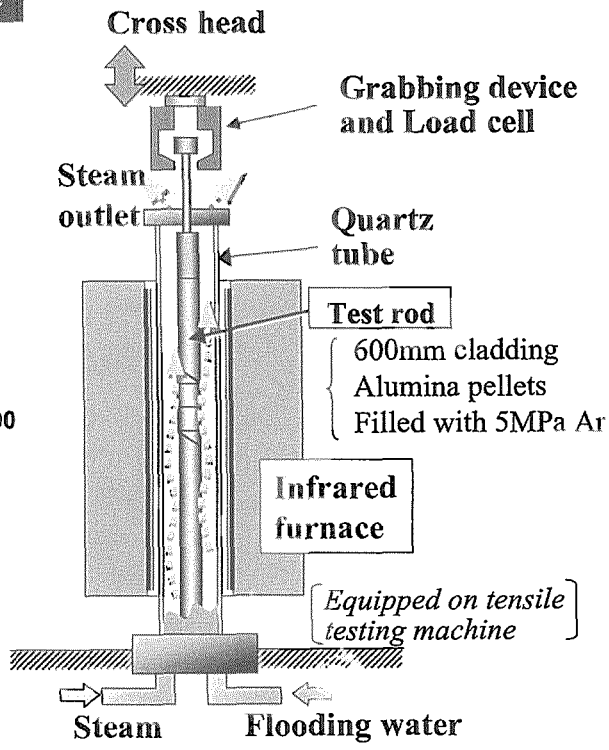
JAERI

9

Integral thermal shock test







Schematic drawing of test apparatus

JAERI

10

Test conditions

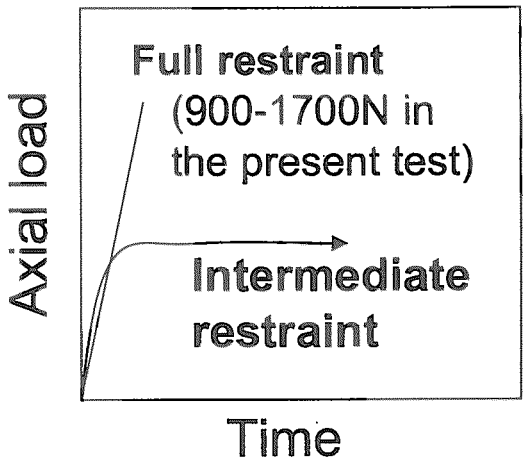
- ***Sample***
  - Cladding tube type:
    Zircaloy-4 PWR cladding (Non-irradiated)
  - Hydrogen concentration :
    100 - 1200wtppm
  - Wall thickness :
    0.57mm
    0.513mm (simulating wall thinning of 10% by water-side corrosion)

- ***Isothermal oxidation***
  - Temperature: 1223 – 1523 K
  - Time: 30 - 5500s

JAERI

11

- *Axial restraint condition during quench*
  - Full restraint condition
  - Intermediate restraint condition
    Limited to 735N (75kgf), 540N (55kgf), 390N (40kgf)
  - No restraint condition

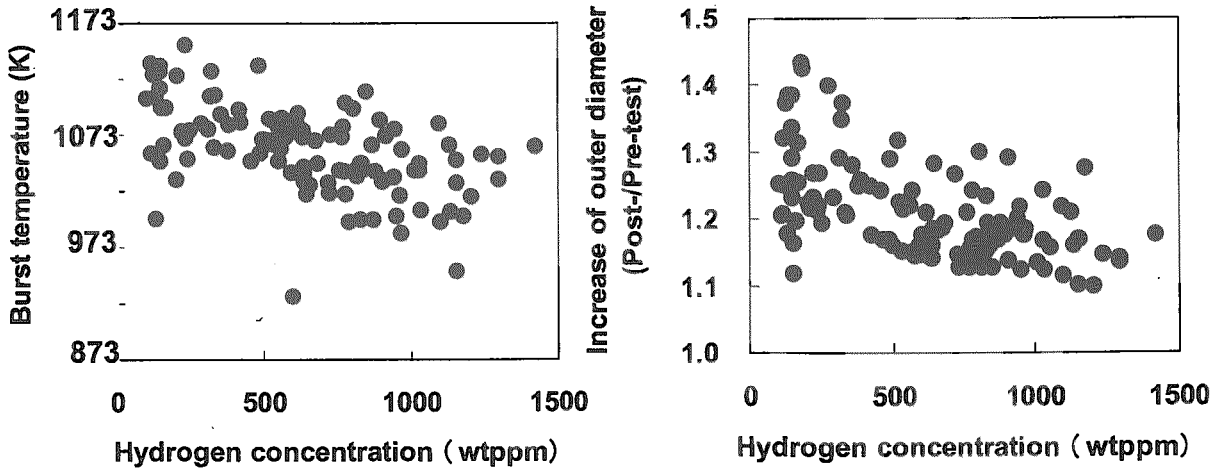


JAERI

12

Influence of hydrogen absorption on burst temperature and ballooning

Initial pressure : 5MPa (Ar)
Heat up rate : 10 K/s



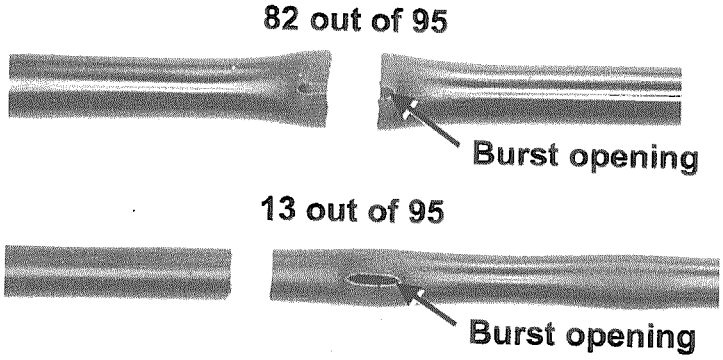
JAERI

This study was performed as the collaboration program between JAERI and Japanese PWR utilities.

13

Failure morphology

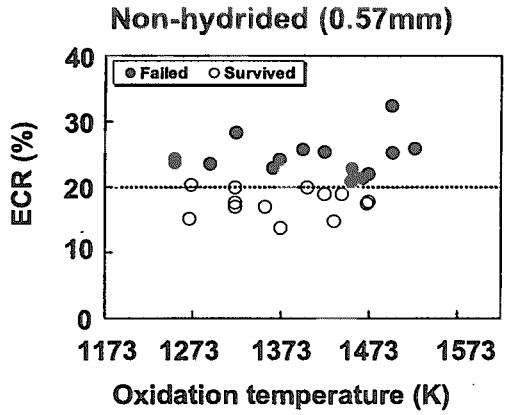
- Dominant failure morphology :
  Split failure with circumferential cracking
- Fragmentation :
  only at very high ECR
- Failure position

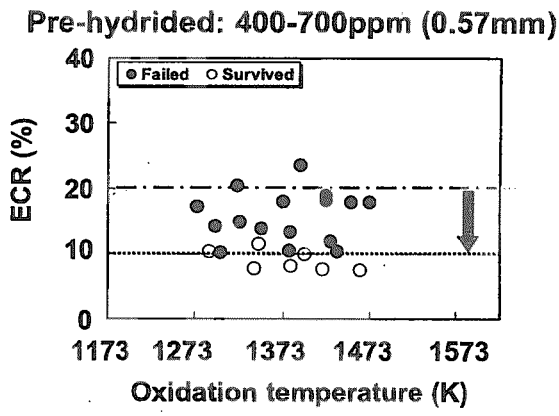


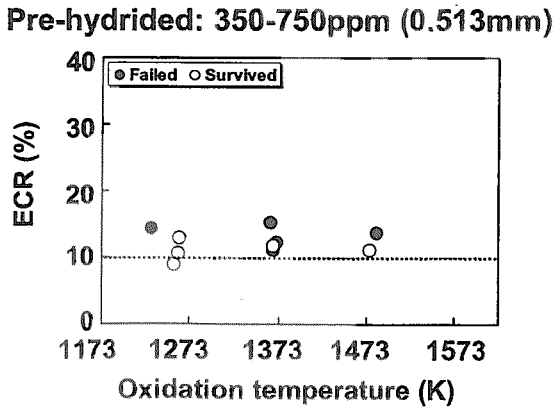
JAERI

14

Failure map (Full restraint condition)





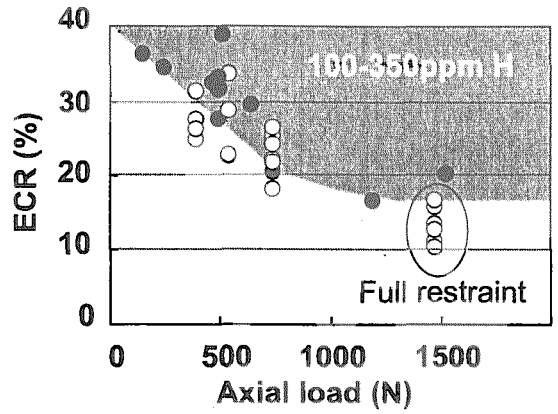


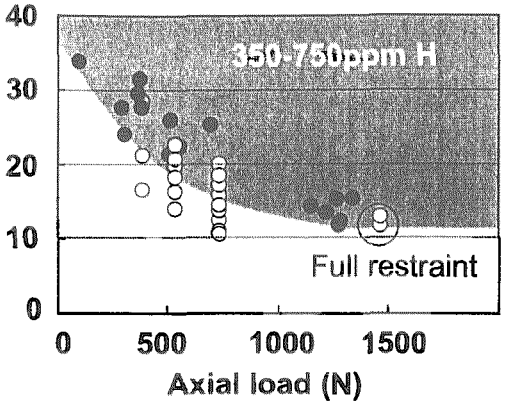
ECR was calculated with the Baker-Just equation taking account of double sided oxidation after rupture and increase of circumference by ballooning.

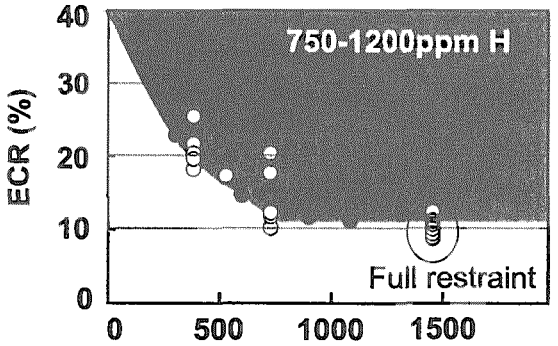
JAERI

15

Failure map as a function of axial load







This study was performed as the collaboration program between JAERI and Japanese PWR utilities.

JAERI

16

An attempt for evaluating restraint force on fuel cladding

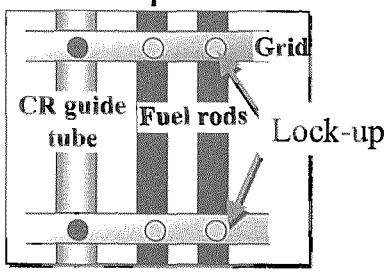
JAERI

A possible mechanism and assumptions for evaluation

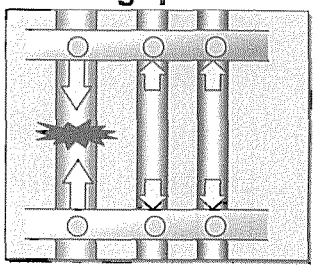
17

- **Assumption for conditions before quenching**
  - Complete lock-up at fuel rod/grid and guide tube/grid contact positions
  - Guide tube temperature
    << fuel rod temperature
    on locking up
- **Load direction during quench**
  - Fuel rod : Tensile
  - Guide tube : Compressive
- The number ratio of guide tube/fuel rod is very small. → **Maximum tensile load in fuel rod may be limited by resistance of guide tube to compressive load**

Before quench



During quench



JAERI

Compression tests of control-rod guide tube

18

Test condition

- Sample
  - OD : 12.2mm, t : 0.41mm, L : 600mm
  - Fresh, Pre-oxidized and quenched
- Pre-oxidation
  - Temperature : 1273 – 1473 K
  - Time : 150 - 1800 s
  - Proportion of oxide layer thickness : 13 - 24%
- Compression test
  - Room temperature
  - Displacement rate : 10 mm/min

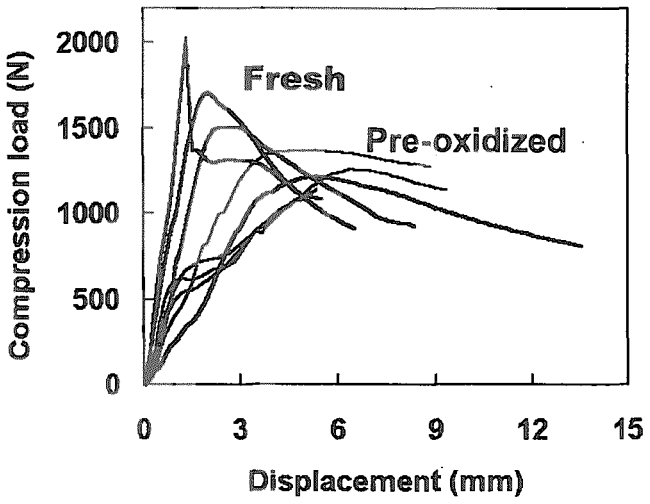


Post-test appearances of pre-oxidized samples

JAERI

19

Estimation of tensile load on fuel rod from resistance of guide tube to compressive load



Load-displacement curves obtained from compression tests of fresh and pre-oxidized guide tube

Measured maximum load
< 2000N for fresh tubes
< 1400N for oxidized tubes

⇩

Number ration of
Guide tube/Fuel rod
= 1/11
(PWR 17x17 bundle)

⇩

Estimated maximum tensile load on a fuel rod :
< 190N

JAERI

20

Hydrogen and irradiation effects on

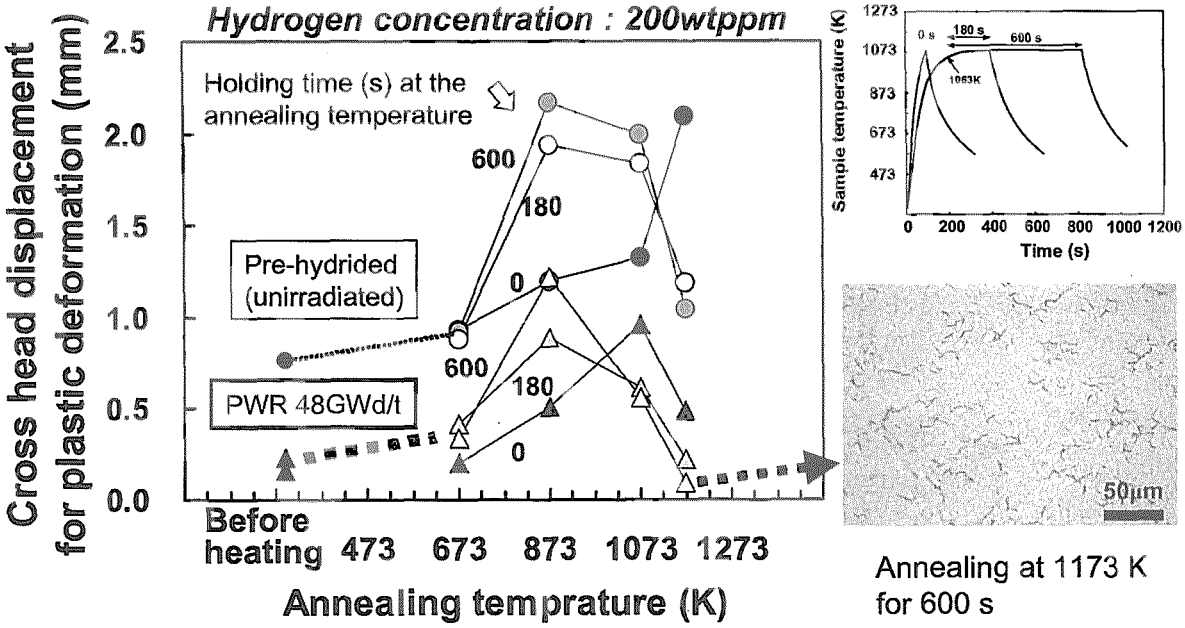
- Mechanical property change after temperature transient

JAERI

21

Mechanical property change after temperature transient
- Comparison between irradiated and non-irradiated cladding tubes -





22

Summary (1/2)

1. Various experiments have been performed with non-irradiated Zircaloy cladding tubes with various hydrogen contents, in the research program on high burnup fuel behavior under LOCA conditions at JAERI.
2. Variations of the failure threshold were evaluated as functions of hydrogen concentration and restraint condition during quenching.
   - The failure threshold generally decreased with the increases in axial tensile load.
   - The influence of pre-hydriding was obviously seen on the failure threshold value under restraint conditions.

JAERI

Summary (2/2)

3. The mechanical property of pre-hydrided or irradiated Zircaloy-4 cladding tube was degraded after short time annealing at temperatures above α to α+β phase transformation temperature of Zircaloy.

5. Session 4 : FP Release from Fuel under Severe Accident

Session 4-1

Overview of VEGA Program on Radio-nuclide Release from Fuel under Severe Accident Conditions and Effect of Pressure on Release Behavior

Akihide HIDAKA, Tamotsu KUDO, Takehiko NAKAMURA, Toru KANAZAWA and Hiroshi UETSUKA

Fuel Safety Research Laboratory, Japan Atomic Energy Research Institute

ABSTRACT

To clarify the mechanisms of radionuclides release from irradiated fuel under severe accident conditions, the VEGA (Verification Experiments of radionuclides Gas/Aerosol release) program is being performed at JAERI. Up to now, four tests under inert helium (He) atmosphere including the highest pressure or temperature condition among previous studies and one test under oxidizing condition were conducted. In the first two tests, the effect of system pressure on radionuclides release from PWR fuel of 47GWd/tU was investigated by heating up to 2,773K in He under the same conditions except for the pressures at 0.1 and 1.0MPa.

The release rate of cesium (Cs) at 1.0MPa was suppressed by about 30% for temperatures between 1,600 and 2,773K compared with that at 0.1MPa. If it is assumed that the release behavior be determined only by the diffusion process inside UO_2 grain as in the Booth model, the diffusion coefficients of Cs obtained from the tests at 0.1 and 1.0MPa mostly followed the Arrhenius form while those at 1.0MPa were mostly equal to one fourth of those at 0.1MPa. The elevated pressure causes the increase of gas density in the open pores of the fuel pellet and the decrease of gaseous diffusion velocity. These result in the increase of Cs concentration in a small volume of the pores and at the grain surface although the diffusion velocity in the grain is much slower that that in the pores. The increase of concentration at the grain surface could suppress the Cs release from the grain because it decreases the concentration gradient in the grain that is a driving force of diffusion. The current VICTORIA2.0 could not reproduce the observed pressure effect because the Booth model used in the code assumes the concentration at the grain surface equal to zero. However, a similar framework model could predict the pressure effect by numerical solution of the diffusion equation in the grain considering the increase of concentration at the grain surface.

The behavior of short-life or low-volatile nuclides and actinides released from high burnup UO_2 or MOX fuel with re-irradiation at JAERI's research reactor will be systematically investigated under various kinds of atmospheres such as air, steam or hydrogen.

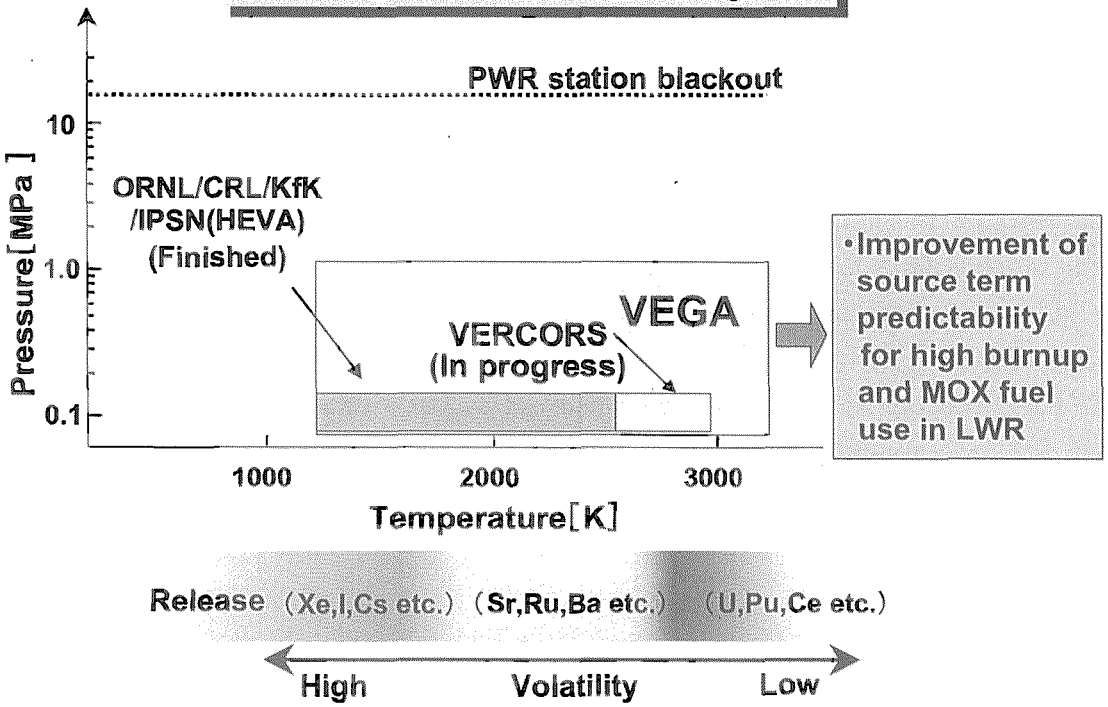
Overview of VEGA Program on Radionuclide Release from Fuel under Severe Accident Conditions and Effect of Pressure on Release Behavior

A. Hidaka

Japan Atomic Energy Research Institute

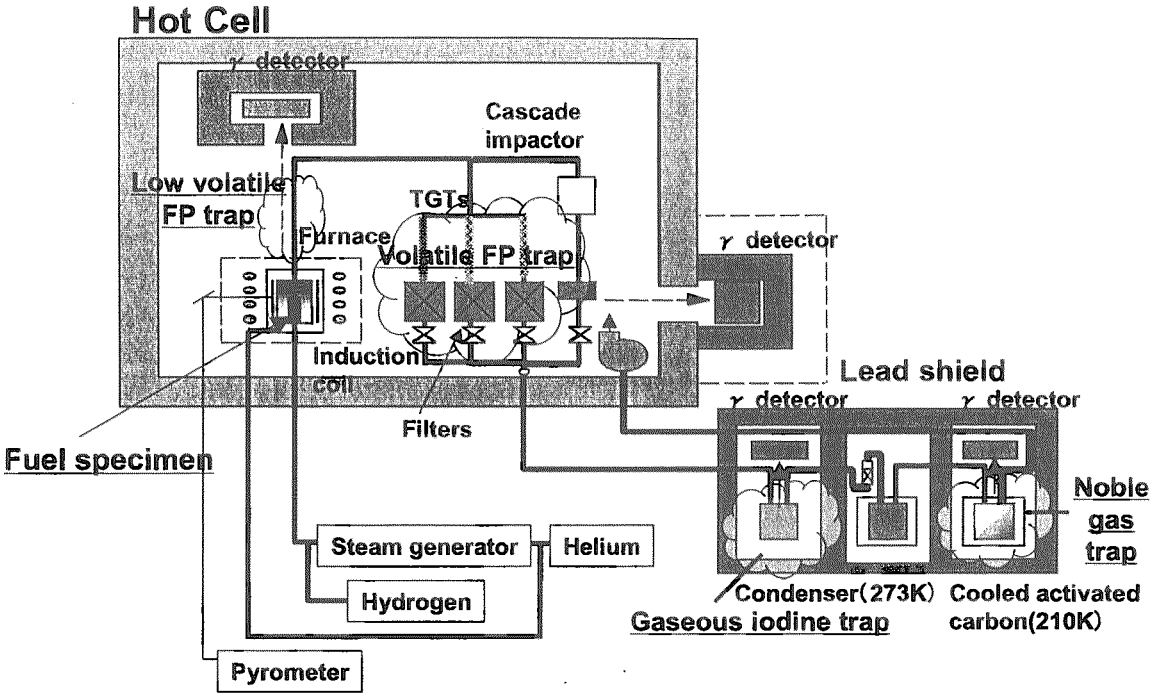
Presented at Fuel Safety Research Specialists' Meeting
March 5, 2002, Tokai-mura, Japan

Scope and Target



VEGA (Verification Experiments of Radionuclides Gas/Aerosol Release)

Schematic of VEGA Facility



2

Test Schedule (2 Tests/yr)

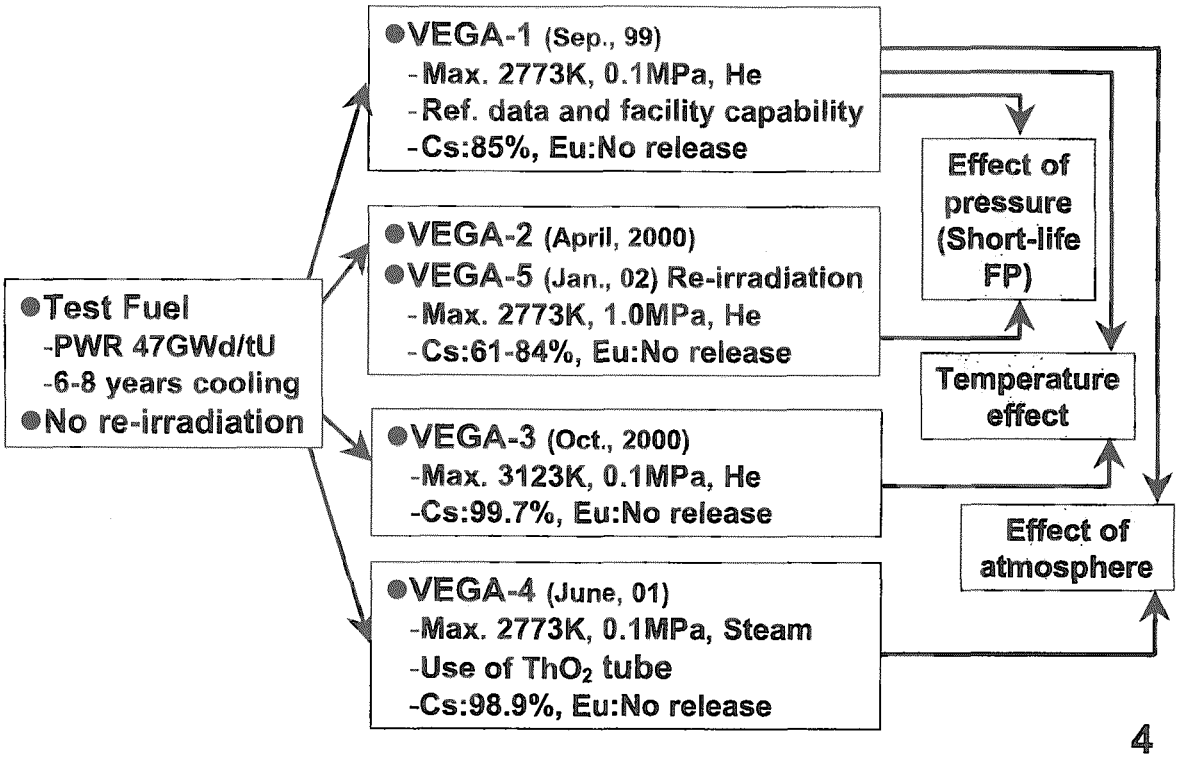
	1996		1998		2000		2002		2004	
Construction of facility	→			Unoxidizing condition				Oxidizing condition		
Experiments				UO2 fuel				UO2 or MOX fuel		
Analyses				Test analyses and model development					Incorporation into THALES-2	
							Verification		Application	

Experimental Conditions

- Max. temperature ; 3,100K, pressure ; 0.1~1.0MPa
- Ambient gas species ; He, H_2, Air and Steam (5N ℓ /min)
- 2cm long, about 10g (with/without cladding)
- Fuel specimen
  - BWR & PWR fuel ; 26~61 GWd/tU, MOX fuel ; 20~40 GWd/tHM
- Re-irradiation of test fuel to accumulate short-life radionuclides

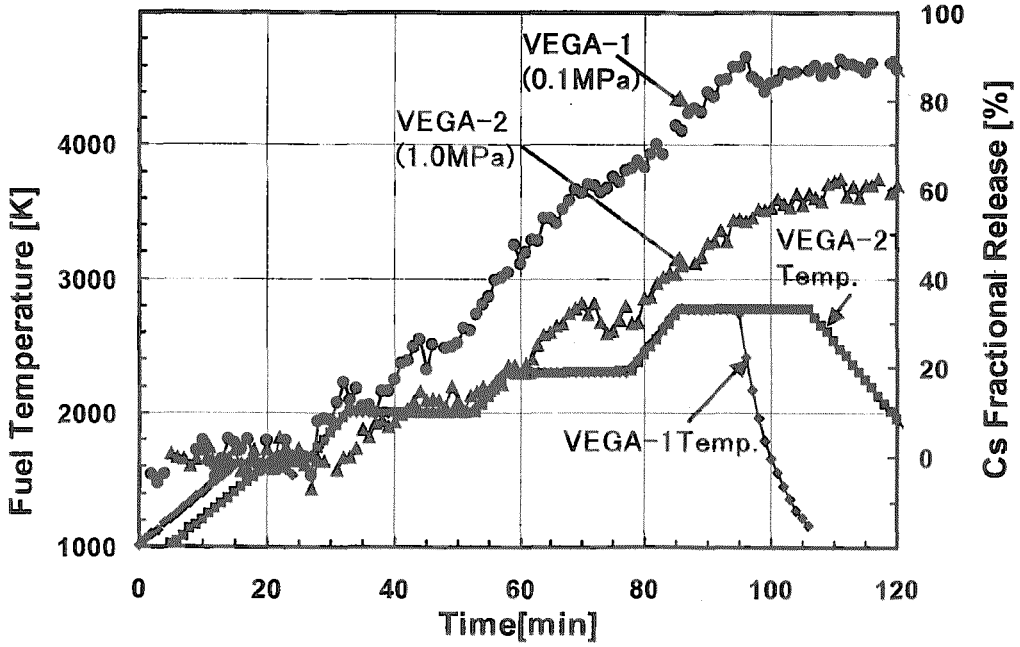
3

Overview of Previous VEGA Tests



4

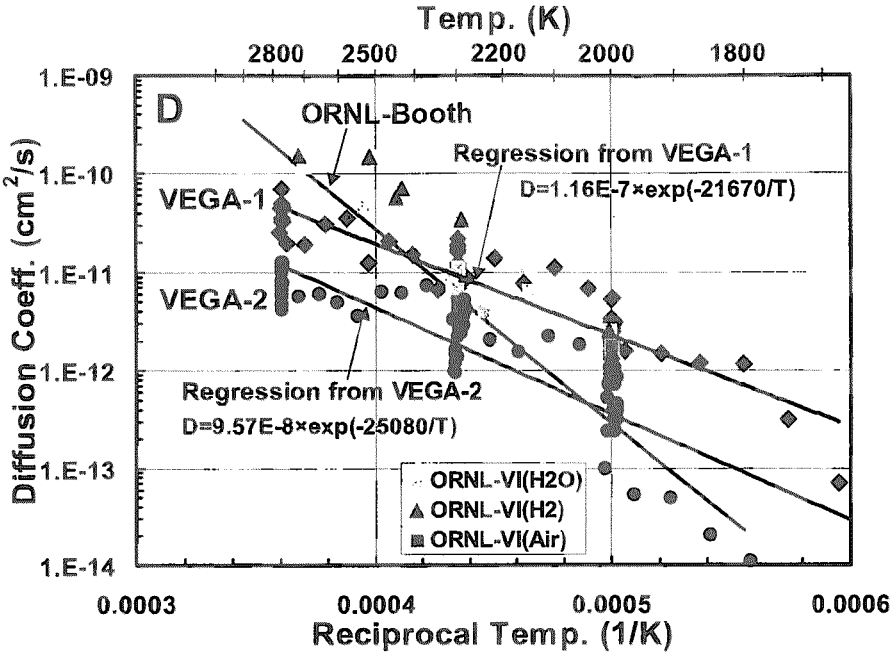
Effect of Pressure on Release Rate



➡ Cs release rate at 1.0MPa decreased by 30% compared with that at 0.1MPa for temperatures between 1600 and 2773K.

5

Diffusion Coefficients on Assumption of Rate-Determining Step inside UO_2 Grain



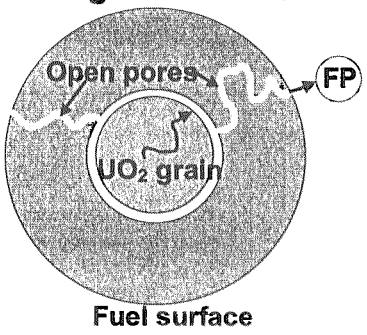
D of VEGA-1 & 2 mostly agree with Arrhenius form. D of VEGA-2 ≒ 1/4 × D of VEGA-1
ORNL exp. with cladding→Eutectic reaction above 2500K→Enhanced release

6

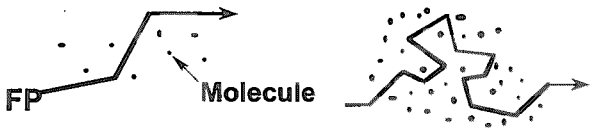
Consideration on Mechanism of Pressure Effect on Cs Release

➡ $D_{VEGA1} > D_{VEGA2}$

VICTORIA2.0 model
(2 stage diffusion)



1) Diffusion in solid UO_2 grain
   $D \propto \exp(-1/T)$
2) Gaseous diffusion in open pores
   $Dg \propto T^{1.5}/P$ ⬅



Increase of gaseous density at elevated pressure →Decrease of distance between molecules →Increase of collision frequency →Decrease of diffusion velocity

⇩

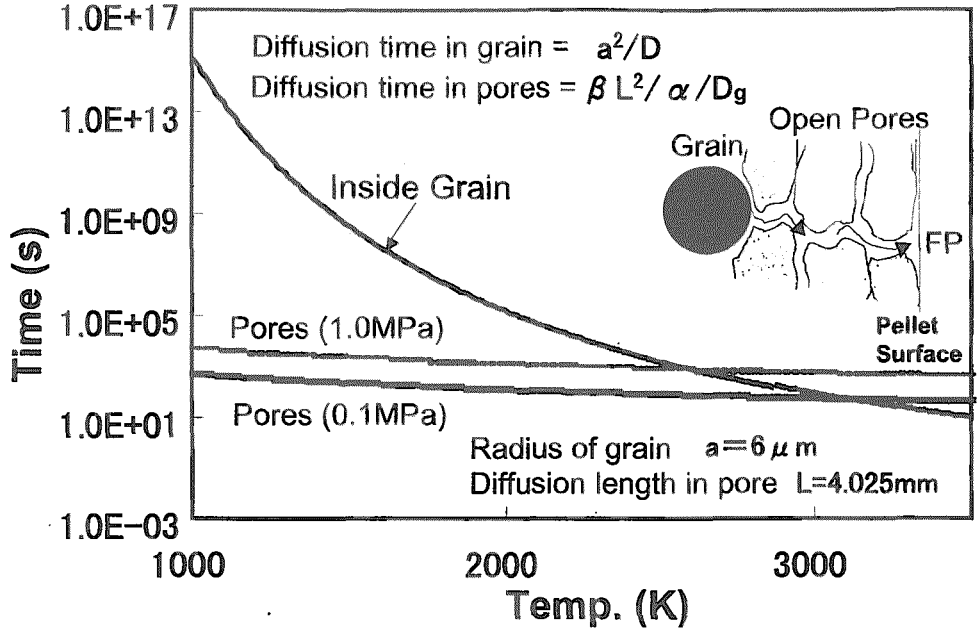
Rate-determining step may change from inside grain to pores due to small gaseous diffusion velocity at elevated pressure ?

⇩

Possible explanation for pressure effect

7

Diffusion Time in UO_2 Grain and Pores



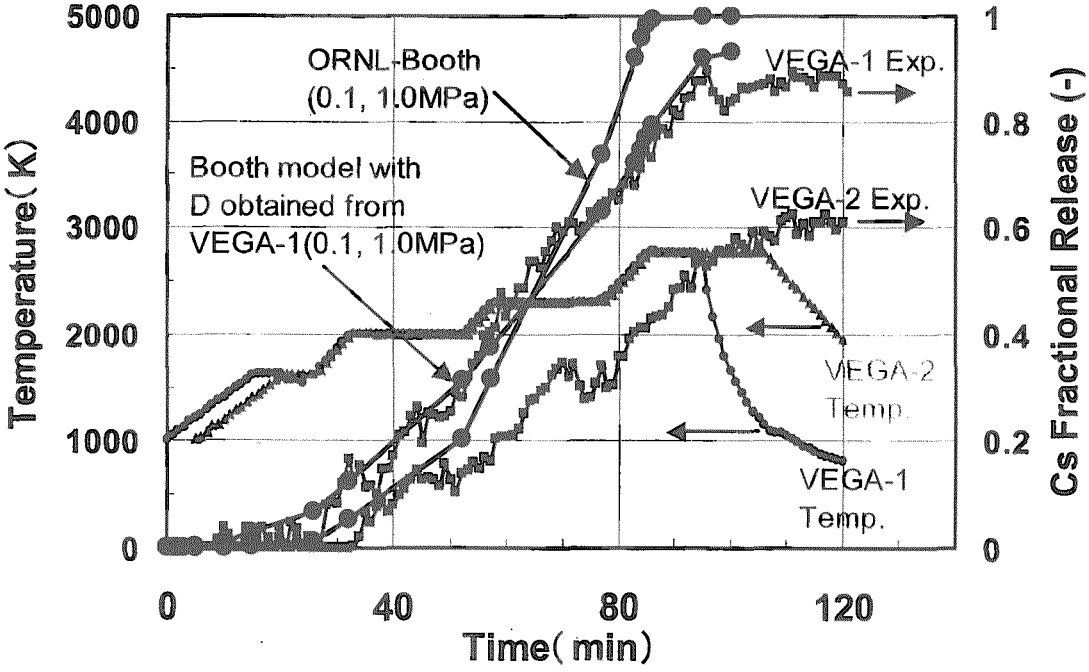
Total porosity of fuel α = 0.05, Interconnected porosity of fuel β = 0.0001

The slowest diffusion process located inside grain both at 0.1 and 1.0MPa

➡ Pressure effect cannot be explained only by increase of diffusion time in pores.

8

Comparison between VICTORIA2.0 and VEGA Tests



Pressure effect cannot be reproduced by current VICTORIA2.0 (Booth model + gaseous diffusion in pores).

9

FP Release Model of VICTORIA2.0

(Two-stage diffusion models)

● Inside UO_2

$$\frac{\partial}{\partial t}C(i)=\frac{1}{r^2}\frac{\partial}{\partial r}\left[r^2 D_G(i)\frac{\partial}{\partial r}C(i)\right]$$

※Booth model assumes concentration of grain surface =0.

$$f(t,i)=6\left[\frac{\tau(i)}{\pi^3}\right]^{1/2}-3\frac{\tau(i)}{\pi^2}\qquad(\tau(i)<1)\qquad\tau(i)=\frac{\pi^2 D_G(i)(t-t_0)}{a^2}$$

$$f(t,i)=1-6\frac{\exp[-\tau(i)]}{\pi^2}\qquad(\tau(i)\geq 1)$$

● Open pores in

$$\alpha\frac{\partial}{\alpha t}C(i)=\frac{1}{r}\frac{\partial}{\partial r}\left[\underbrace{r\beta D(i)\frac{\partial}{\partial r}C(i)}_{\text{Diffusion}}-\underbrace{rC(i)u}_{\text{Advection}}\right]+\underbrace{Sp(i)}_{\text{Inflow rate from grain to pores}}$$

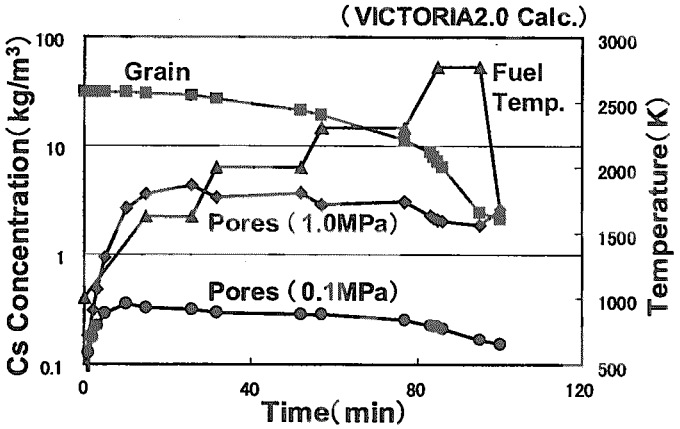
α : Total porosity of fuel=0.05、β : Interconnected porosity of fuel～

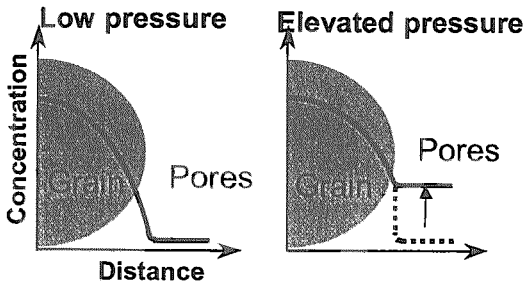
$\frac{\beta}{\alpha}D(i)$: Apparent diffusion coefficient

$\frac{Sp(i)}{\alpha}$: **Increase of apparent Sp due to small porosity** ⟹ **Easy to increase FP concentration in pores**

10

Mechanism of Pressure Effect on FP Release





Under elevated pressure, increase of gas density and decrease of diffusion velocity

⇓

Increase of conc. in pores due to its small volume irrespective of slow diffusion in grain

⇓

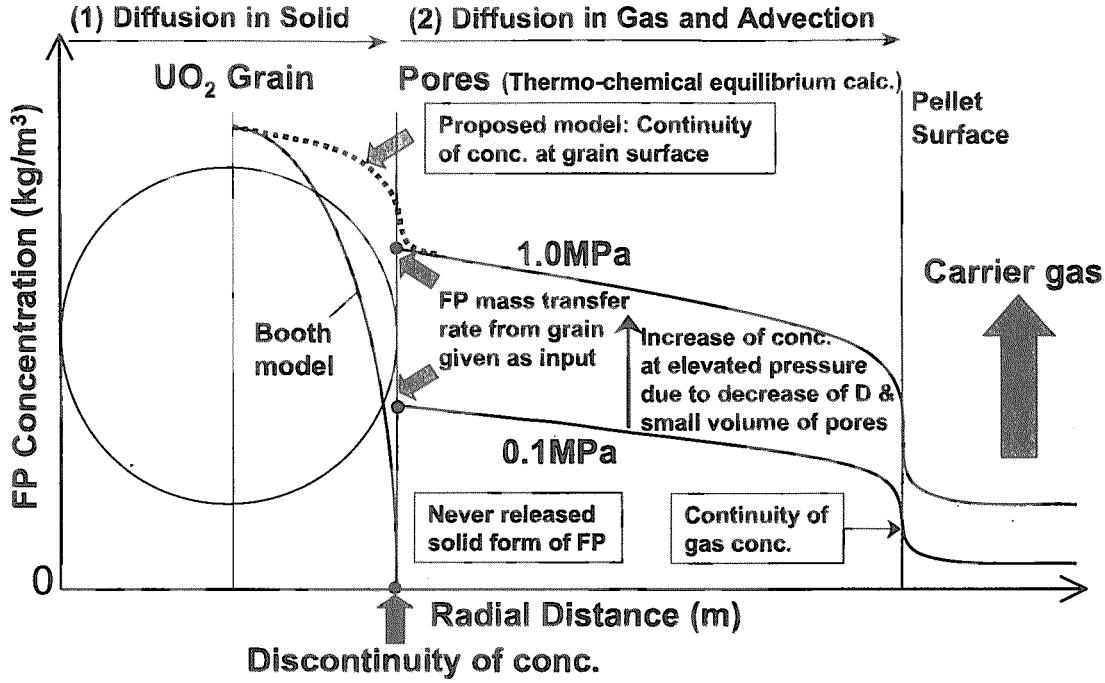
Decrease of driving force for grain diffusion due to gentle conc. gradient

⇓

Decrease of FP release from grain and eventually from fuel

11

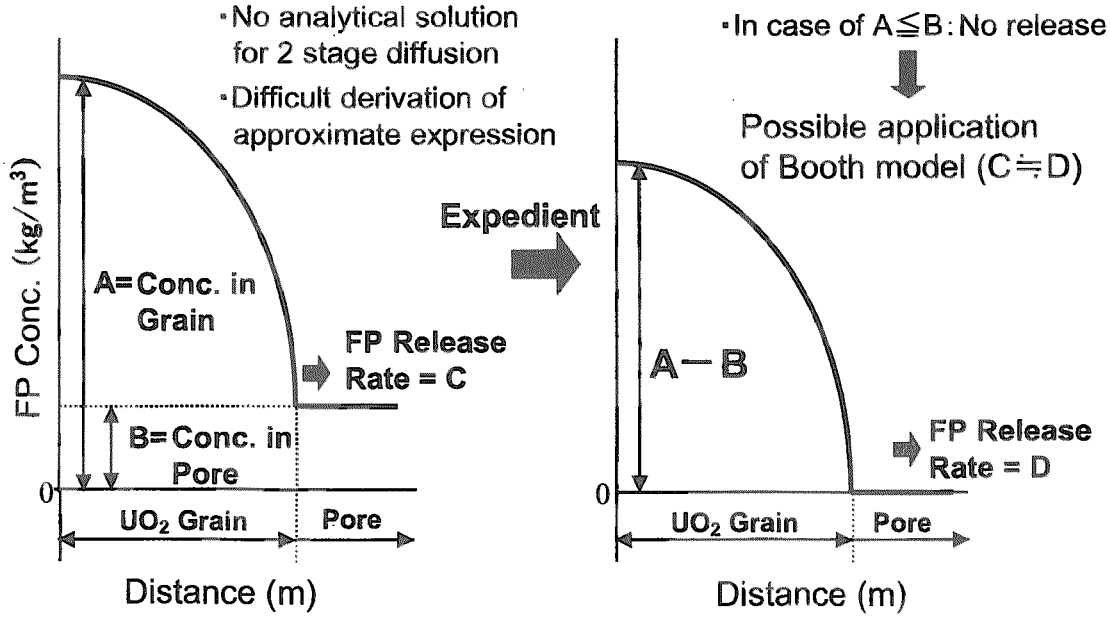
FP Conc. In Fuel Calculated by VICTORIA2.0



※ Present model solves two diffusion equations independently.
Low pressure ⇒ OK, Elevated pressure ⇒ Overestimation of FP release

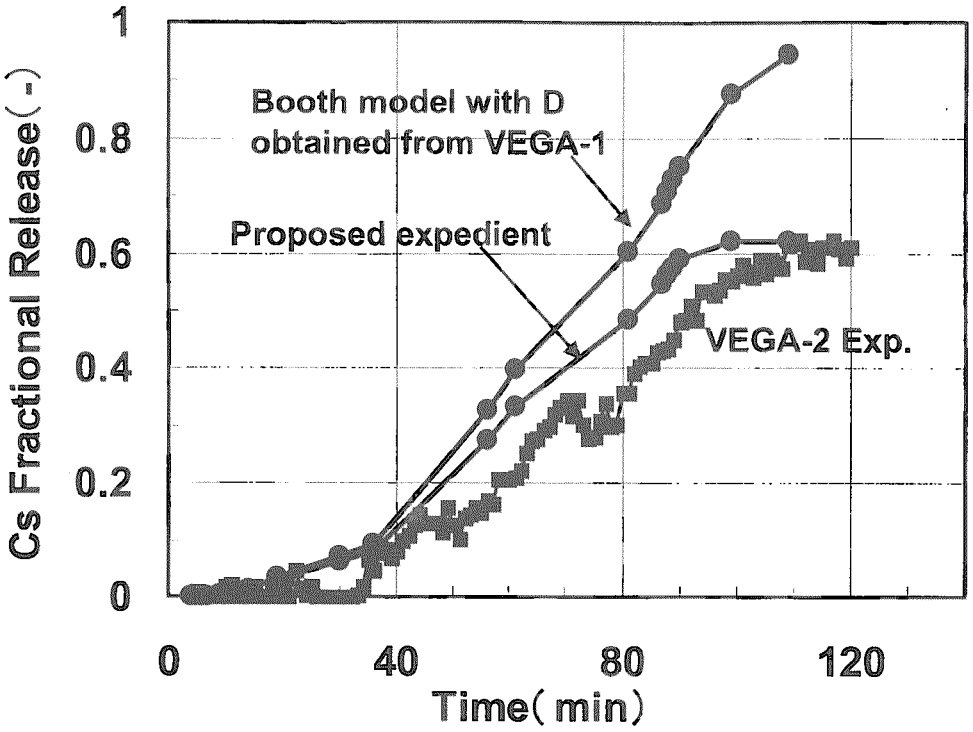
12

Expedient for Release Rate Calculation In Case of Conc. at UO_2 Grain Surface≠0



13

Release Calculation for VEGA-2 at 1.0MPa



14

Summary

- Four tests under inert helium including the highest pressure or temperature among previous studies and one test under oxidizing condition were performed in VEGA program so far.
- VEGA-2 test at 1.0MPa showed first in the world that Cs release could be suppressed by about 30% compared with that at 0.1MPa. The effect was also confirmed by VEGA-5.
- Diffusion coefficients of Cs obtained from VEGA-1 & -2 mostly follow the Arrhenius form while those in VEGA-2 were mostly equal to one fourth of those in VEGA-1.
- Elevated pressure causes increase of gas density in open pores and decrease of gaseous diffusion velocity. These result in increase of FP concentration in pores and at grain surface although the diffusion velocity in grain is much slower than that in pores. Concentration increase at grain surface may suppress FP release from grain because it decreases concentration gradient in grain that is a driving force of diffusion.
- Release of low-volatile or short-life FP and actinides from high burn-up UO_2 and MOX fuel will be systematically investigated using various atmospheres.

15

VEGA Test Matrix (2 Tests/yr～2005)

Test name	VEGA-1	VEGA-2	VEGA-3	VEGA-4	VEGA-5	VEGA-6	VEGA-7	VEGA-8	VEGA-9
Date of test	1999 Sep.	2000 Apr.	2000 Oct.	2001 Jun.	2002 Jan.	2002 Jun.	2002 Dec.	2003 Jun.	2003 Dec.
Fuel specimen	UO_2 PWR	UO_2 PWR	UO_2 PWR	UO_2 PWR	UO_2 PWR	UO_2 BWR	MOX ATR	UO_2 BWR	MOX ATR
Burnup (GWd/tU)	47	47	47	47	47	56	40	61	40
Re-irradiation	No	No	No	No	NSRR	JRR-3	JRR-3	JRR-3	JRR-3
Max Temp. (K)	2773	2773	3123	2773	2773	3123	2773	3123	3123
Carrier gas	He	He	He	Steam	He	Steam	He	Steam	Steam
Pessure (MPa)	0.1	1.0	0.1	0.1	1.0	0.1	0.1	1.0	0.1
Remarks	Ref. test	High press.	High temp.	Steam ref.	Re-irradiation	Short-life / High temp.	MOX Ref.	High temp. / High press.	MOX Steam

16

● How to calculate Release Rate Coefficient k

$k = k_0 \exp(-Q/RT)$, $f(\Delta t) = F_P \cdot (1-\exp(-k \cdot \Delta t))$

$f(\Delta t)$; Amount of release during Δt, F_P; Inventory at start of each Δt,
T; Temperature, Q; Activation energy, A, B, K_0; Coefficients

$$k = -\ln(1-(F_2-F_1)/(1-F_1))/(t_2-t_1)$$

F_1; Fraction of original inventory released at start of time period(－)
F_2; Fraction of original inventory released at end of time period(－)
t_1; Time corresponding to F_1(s), t_2; Time corresponding to F_2(s)

● How to calculate Diffusion Coefficient D

$D = D_0 \exp[-\theta/T]$ θ ; Activation temperature

$$F(t) = 6\tau^{0.5}/\pi^{1.5} - 3\tau/\pi^2 \quad (\tau < 1)$$

$$F(t) = 1 - 6\exp(-\tau)/\pi^2 \quad (\tau \geqq 1)$$

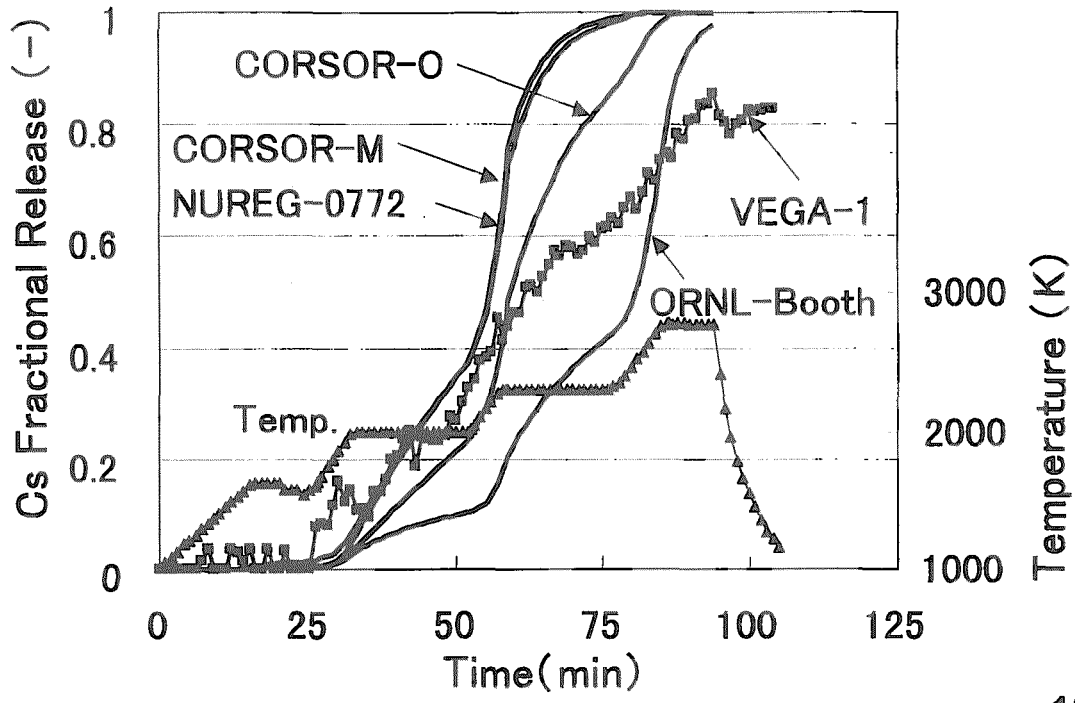
$\tau = \pi^2 \cdot D \cdot (t-t_0)/a^2$ (a; Grain radius, t_0; Release initiation time)
F(t); Fraction of original inventory released at time t(－)

$$D = a^2/(t_2-t_1) \times \{-(F_2-F_1)/3 - 2[(1/\pi^2 - F_2/3/\pi)^{0.5} - (1/\pi^2 - F_1/3/\pi)^{0.5}]\} \quad (F_2 < 0.85)$$

$$D = a^2/(t_2-t_1) \times \{-1/\pi^2 \times [\ln(\pi^2(1-F_2)/6) - \ln(\pi^2(1-F_1)/6)]\} \quad (F_1 \geqq 0.85)$$

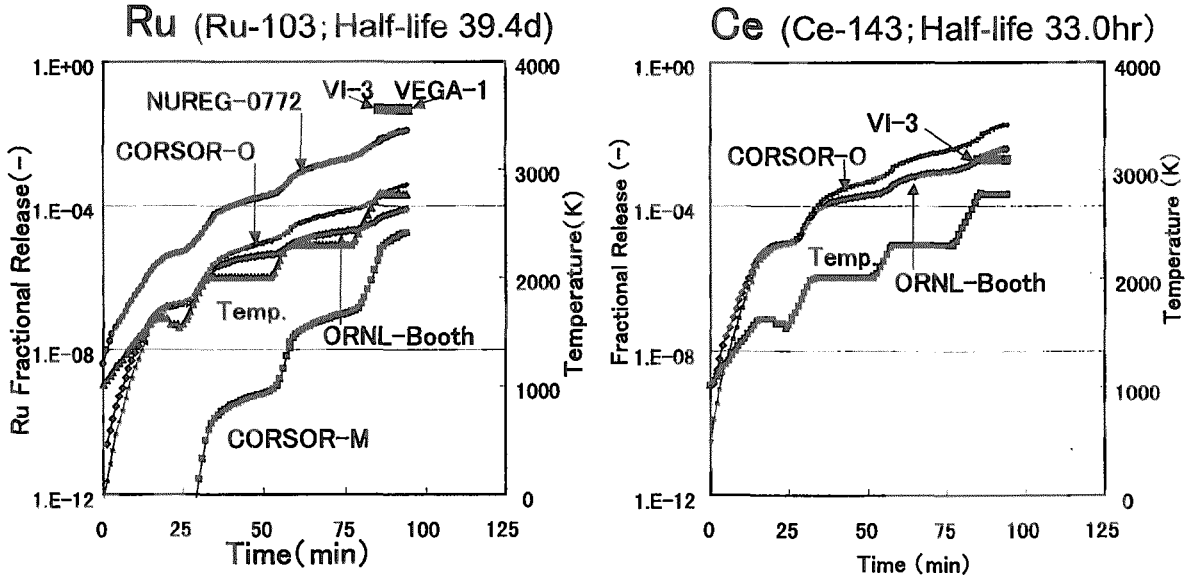
17

Comparison of Cs Release of VEGA-1 between Measurement and Calculation



18

Comparison of Ru and Ce Release of VEGA-1 between Measurement and Calculation



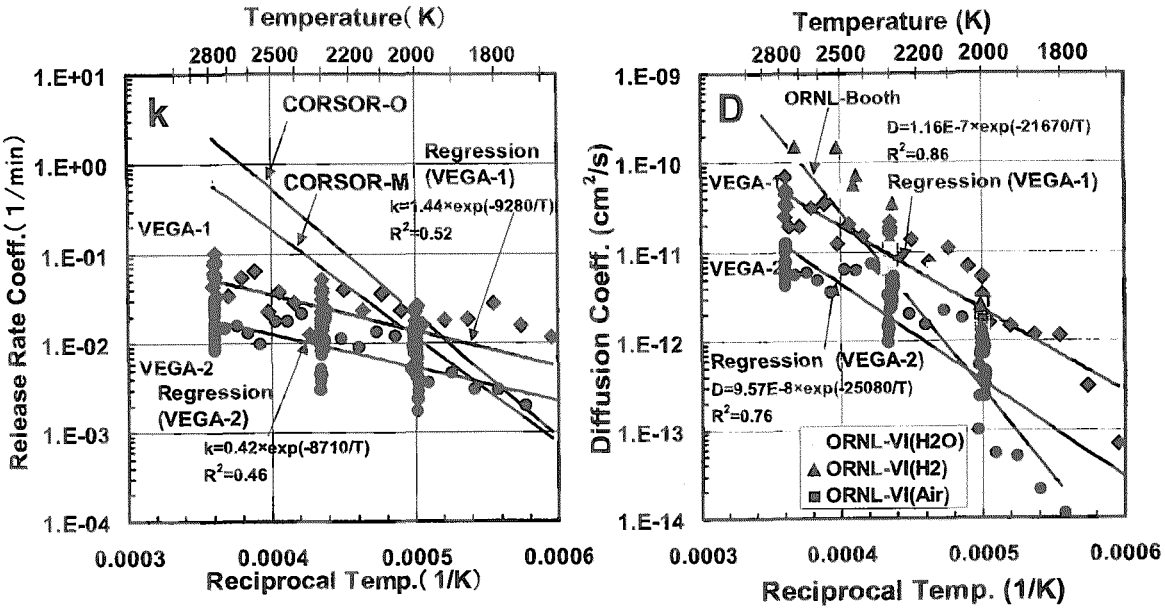
● Insufficient release data

● VEGA-1 results evaluated by insufficient γ intensity → Ignored error

⇨ Reevaluation using short-life nuclides generated by re-irradiation

19

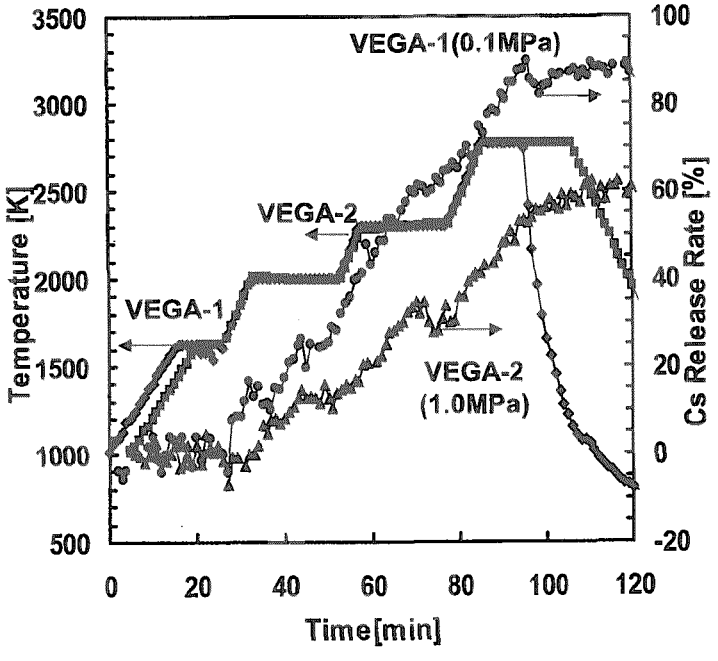
Release Rate and Diffusion Coefficients for Cs Release in VEGA-1 and -2 Tests



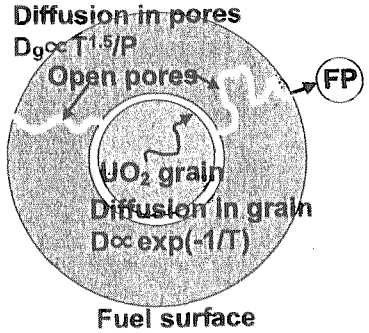
Multiple correlation coefficient ($0 \leqq R^2 \leqq 1$) expresses degree of agreement.
D agrees with Arrhenius form better than k. Rate-determining step at diffusion in grain
ORNL exp. with cladding→Eutectic reaction above 2500K→Enhanced release

20

Effect of Pressure on Release Rate

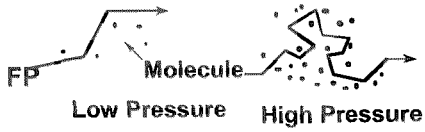


VICTORIA2.0（2 stage diffusion）



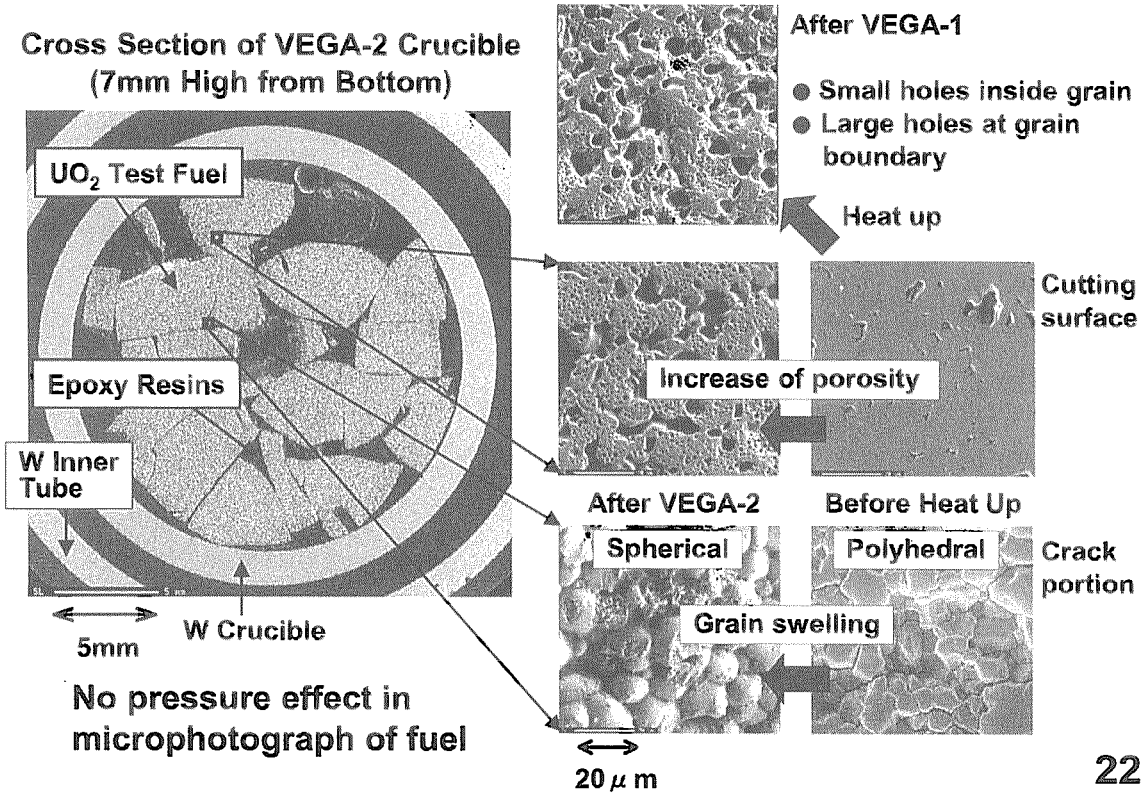
Decrease of D_g and increase of gas density at elevated pressure

Possible explanation for pressure effect



21

Microphotograph of VEGA Test Fuel



22

Fractional Release Estimated from Intensity Changes of γ Peaks

(Assuming no release of Eu-154)

Nuclides		Cs-134		Cs-137	Sb-125	Ba-140	Ru-106
Half-life		2.06y		30.0y	2.77y	12.8d	368d
Energy (keV)		605	796	662	428	537	622
Test, Condition	Re-irradiation	Released (%)					
VEGA-1 He, 2773K, 0.1MPa	×	85	85	86	-	-	4.7
VEGA-2 He, 2773K, 1.0MPa	×	62	61	61	-	-	0
VEGA-3 He, 3123K, 0.1MPa	×	99.5	99.9	99.5	-	-	0
VEGA-4 H_2O, 2773K, 0.1MPa	×	98.9	99.3	93.4	-	-	52
VEGA-5 He, 2773K, 1.0MPa	○	82	85	84	67	7	0
VI-3 H_2O, 2700K, 0.1MPa	×	-	99.87	-	99.2	26.8	5.01

Preliminary data for VEGA-5

23

Current Status of VEGA Post-Test Analyses

Test	Thermo -hydraulics & release trends	FP distribution	Nitric acid leaching	SEM/ EPMA	Analyses
VEGA-1	○	○	○	○	○
VEGA-2	○	○	○	○	△
VEGA-3	○	○	○	○	×
VEGA-4	○	×	×	×	△
VEGA-5	○	×	×	×	×

Presented at previous NSRR meetings

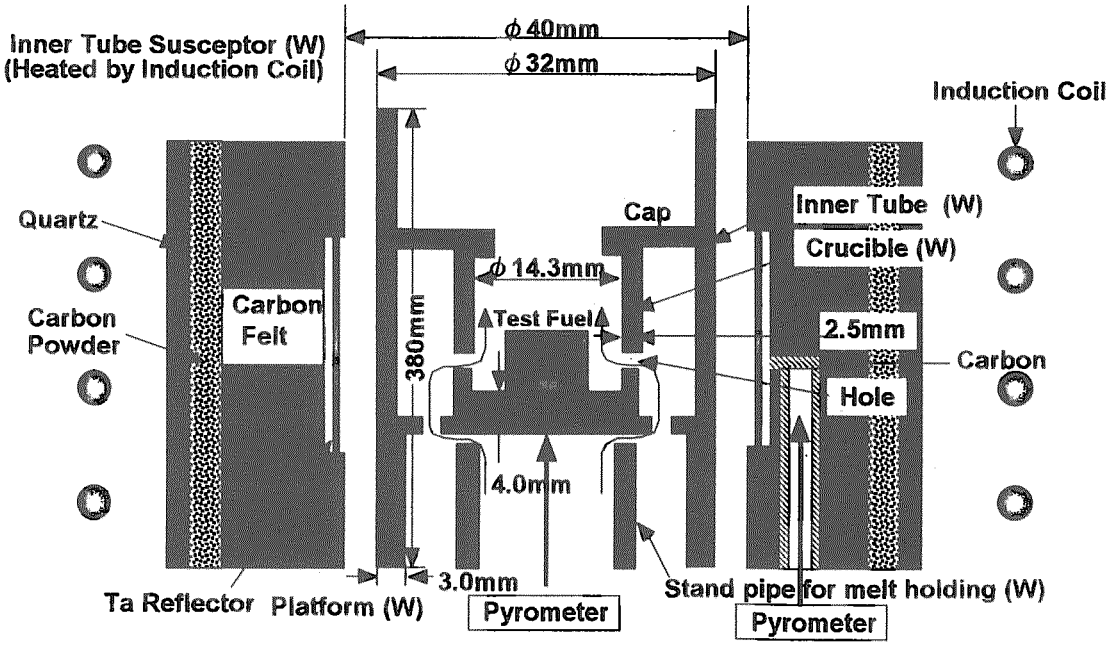
Presented by T. Kudo

Presented by A. Hidaka

○; Finished, △; Under way, ×; Not yet started

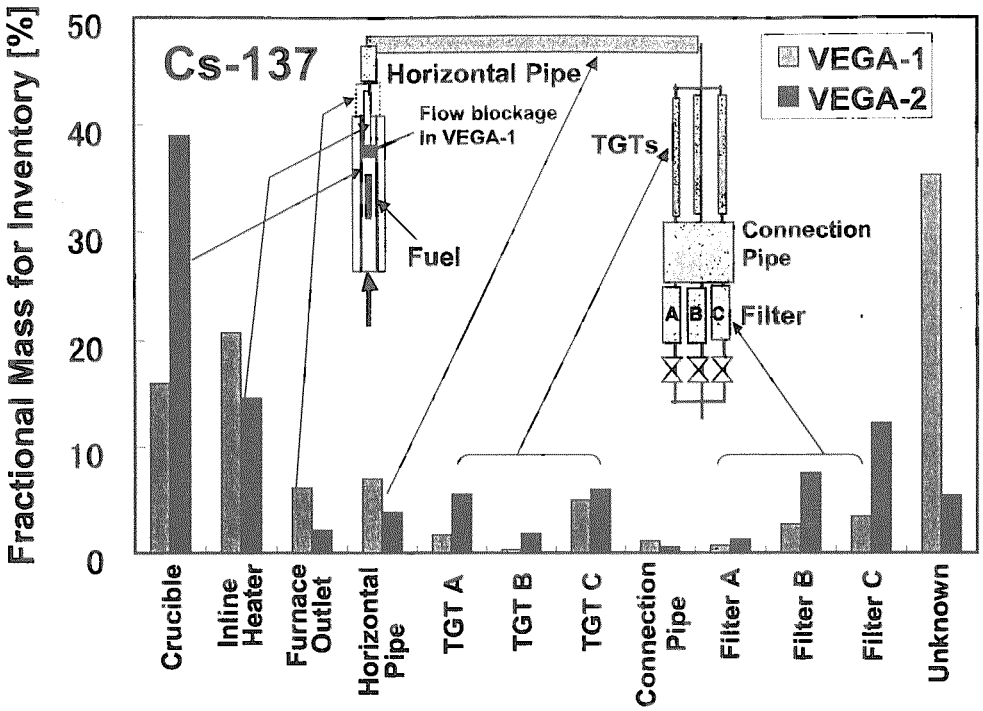
24

VEGA Furnace for Inert Condition



25

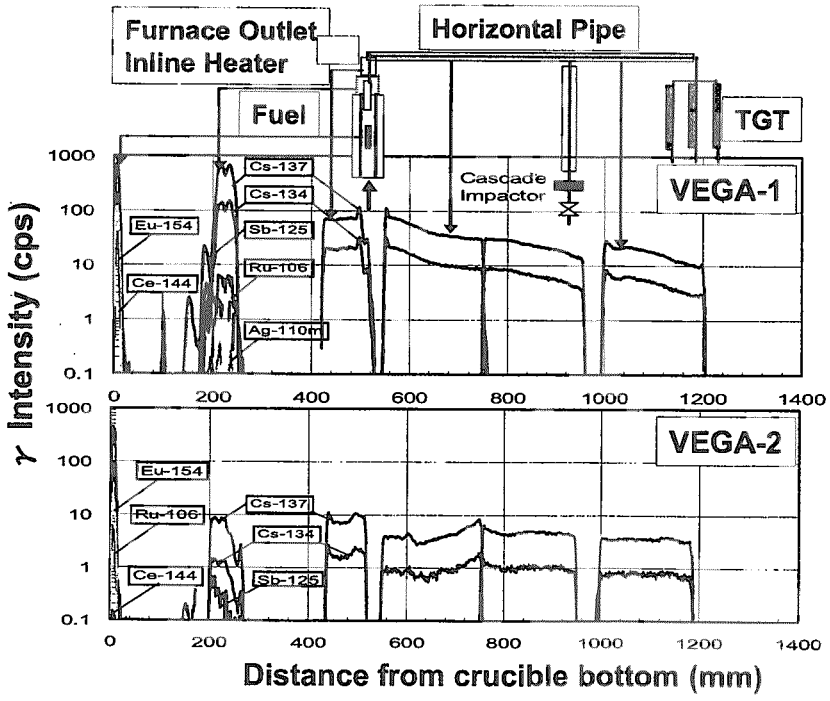
Mass Balance of Cs in Test Facility



- Large fraction of unknown mass in VEGA-1 due to flow blockage
- Better collection rate in VEGA-2 without flow blockage

26

Distribution of γ Intensity in Test Facility



- Widely distribution of volatile Cs from crucible to downstream
- Low volatile Eu and Ce found only at crucible
- Small amount of Cs deposition in VEGA-2 due to large gas flow rate

27

Discussion:

Q: (H. Ohashi)
Some induction period is observed in your VEGA-2 experimental results of Cs fractional release. Did you consider the fact in your proposed expedient ? I think the agreement between the proposed expedient and the experimental data become better if you consider the induction period in the initial stage of the experiment.

A: As you pointed out, consideration of the induction period will certainly lead to better agreement between proposed expedient and measurements. However, I did not consider it in the proposed expedient because Cs release at low temperature actually occurred in VEGA-1 and the release had to be considered in the expedient for VEGA-2.

Q: (D. Schrire)
Did the difference in retained Cs in VEGA-1 vs. VEGA-2 depend on the amount retained in closed pores (bubbles) ?

A: The difference may partly come from the amount retained in closed pores. However, it is considered that most of the difference comes from the difference in the amount retained in the grain between VEGA-1 and -2 tests if the proposed mechanism is assumed to be correct.

Session 4-2

Effect of temperature and atmosphere on release of nuclides including short-life FPs -- Results of recent VEGA-3 through –5 tests --

Tamotsu KUDO, Akihide HIDAKA, Takehiko NAKAMURA, Tsutomu NAKAMURA,
Toru KANAZAWA and Hiroshi UETSUKA
JAERI

ABSTRACT

In order to investigate the radionuclides release mechanisms from fuels of light water reactor, VEGA program was initiated at Japan Atomic Energy Research Institute (JAERI). In this program, release behavior of volatile/low volatile fission products (FPs) has been investigated under high temperature condition covering melting temperature of the fuels, and at elevated pressure condition up to 1.0 MPa. This article describes the results of VEGA-3 (temperature up to about 3100K, other VEGA tests; 2750K), VEGA-4 (mixture of steam and helium, others; helium only) and VEGA–5 (elevated pressure with re-irradiated fuel, others; without re-irradiation) tests.

In VEGA-3 test with maximum temperature of about 3100K, the release rate of cesium around 3100K was increased due to fuel melting in comparison with that below about 3000K. The fuel melting was confirmed by SEM observation.

VEGA-4 test was performed under mixture of steam and helium atmosphere condition. The release rate of cesium in VEGA-4 became larger than that in VEGA-1 under helium atmosphere probably due to increase of the uranium vacancy concentration by fuel oxidation and fuel liquefaction by eutectic reaction of UO_2 with ZrO_2. The fractional release of ruthenium increased due to formation of volatile ruthenium oxide in comparison with other VEGA tests under inert helium gas condition.

In VEGA-5 test, the fuel was re-irradiated in advance at linear heat rate of 1.1kW/m in NSRR for 8 hours. The test was performed at system pressure of 1.0MPa. The fractional releases of short-life Ba-140 and Ru-103, which had not yet been observed in the previous VEGA tests without re-irradiation, could be estimated. The cesium release started from low temperature (above about 1000K) probably due to the release from grain boundary. It was observed in VEGA-2 that the elevated pressure at 1.0MPa could result in decrease of the release rate by about 30%. The VEGA-5 results showed that the pressure effect was smaller than VEGA-2 but Cs release at temperature above about 2200K was obviously suppressed compared with the atmospheric pressure tests.

Effect of temperature and atmosphere on release of nuclides including short-life FPs -- Results of Recent VEGA-3 through -5 Tests --

KUDO Tamotsu

Japan Atomic Energy Research Institute

Presented at Fuel Safety Research Specialists' Meeting
March 5, 2002, JAERI, Tokai-mura

Contents

- Test conditions
- Temperature Effect : VEGA-3
- Atmosphere Effect : VEGA-4
- Quick look of VEGA-5
- Summary

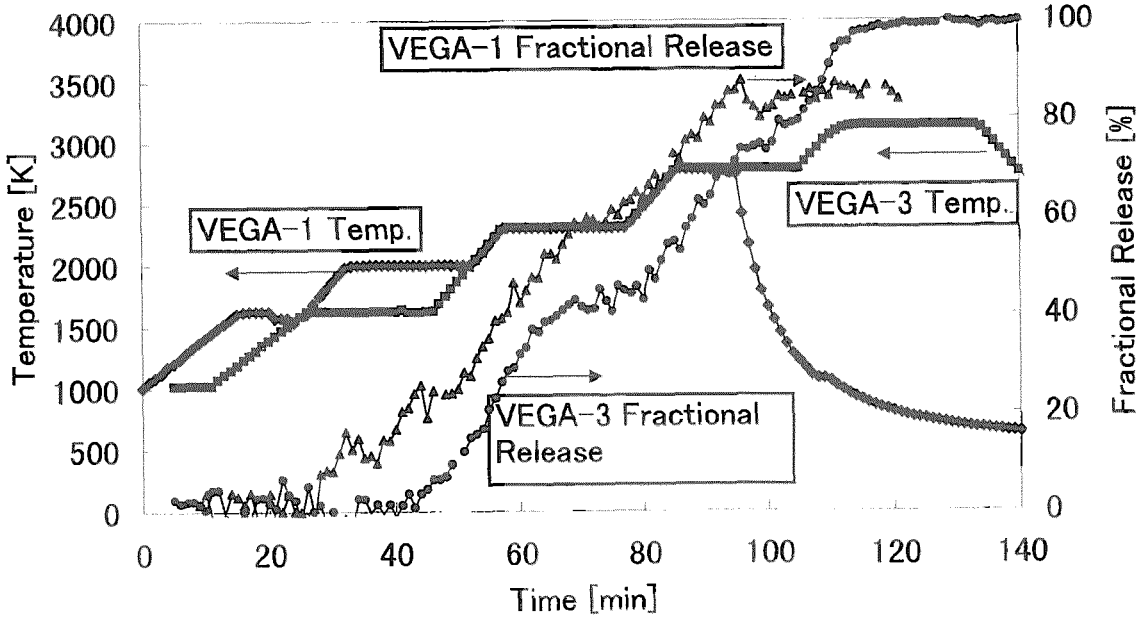
Test Conditions

	VEGA-1	VEGA-3	VEGA-4	VEGA-5
Fuel	PWR, 47GWd/tU, 2 pellets			
Cladding	No	No	Yes	No
Pressure [MPa]	0.1	0.1	0.1	1.0
Max. Temp. [K]	2773	3123	2773	2773
Atmosphere	He	He	Steam+He	He
Re-irradiation	No	No	No	Yes
Furnace Material	W	W	ThO_2	W

1

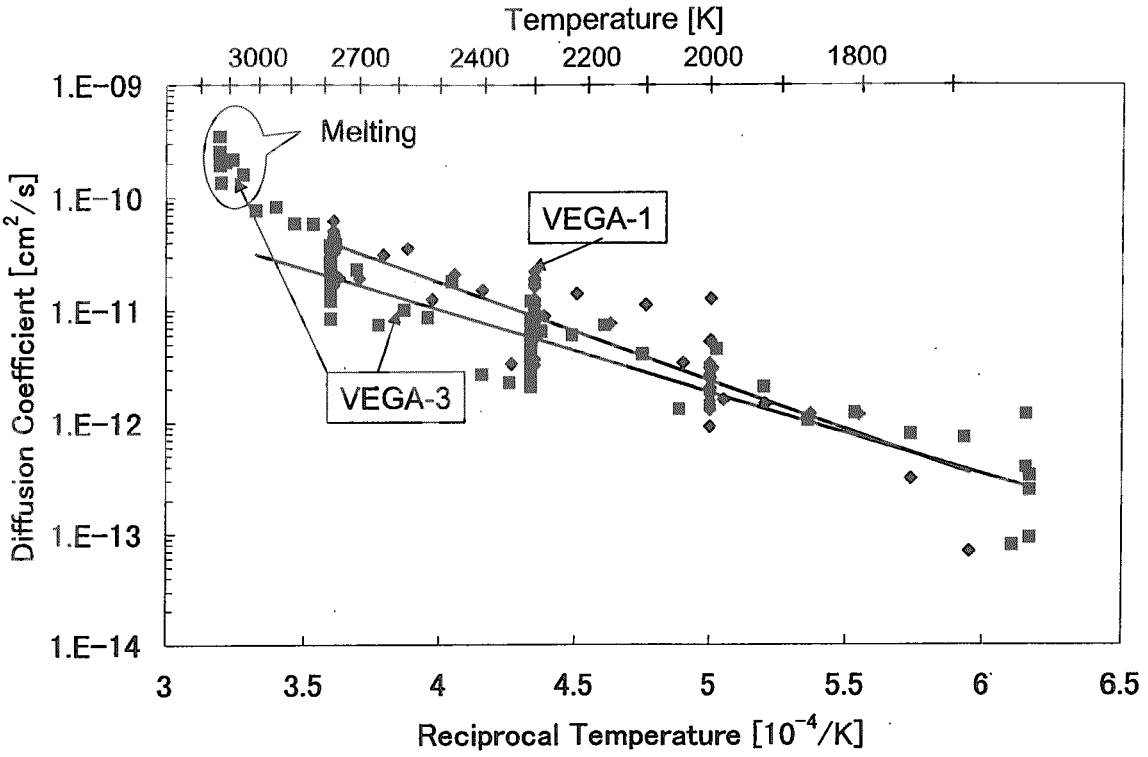
Temperature Effect : VEGA-3

Comparison of Fractional Release Histories of Cs between VEGA-1 and -3



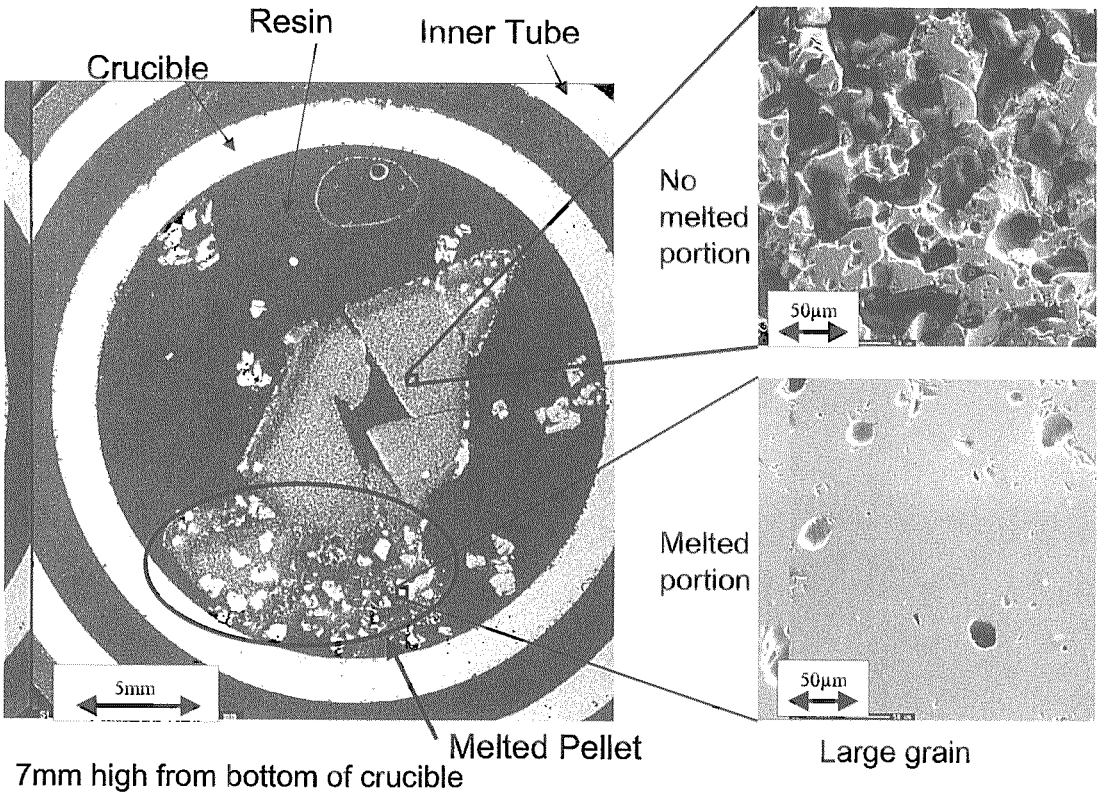
2

Comparison of Diffusion Coefficients between VEGA-1 and -3



3

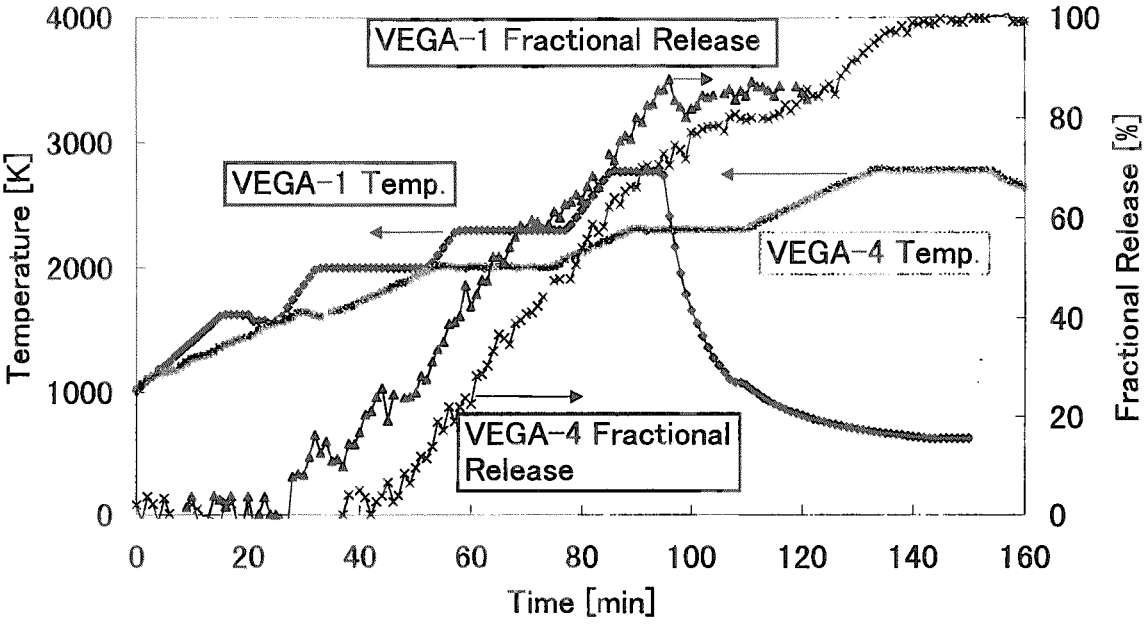
SEM Observation of VEGA-3



4

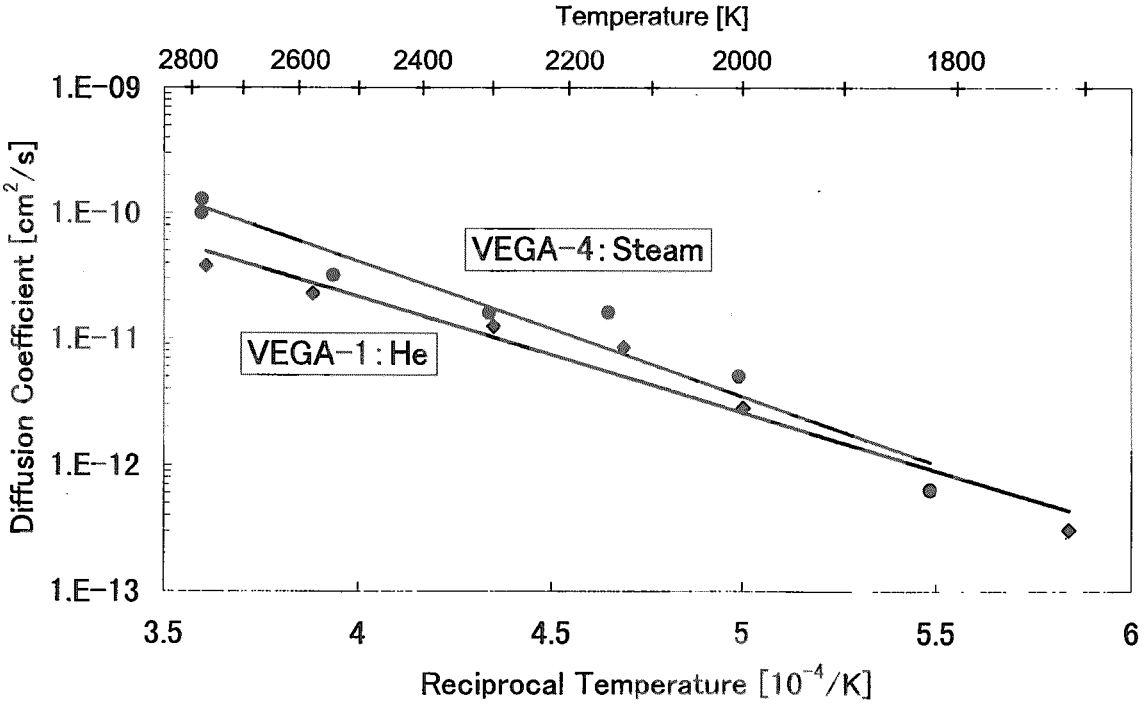
Atmosphere Effect : VEGA-4

Comparison of Fractional Release Histories of Cs between VEGA-1 and -4



5

Comparison of Diffusion Coefficients between VEGA-1 and -4



6

Possible Effect of Steam Atmosphere and cladding on Cs Release

☆ Under oxidizing condition, increase of oxygen interstitial concentration

⇩

Increase of uranium vacancy concentration

⇩

Increase of Cs mobility in grain

☆ Eutectic of urania with zirconia

⇩

Liquefaction of fuel

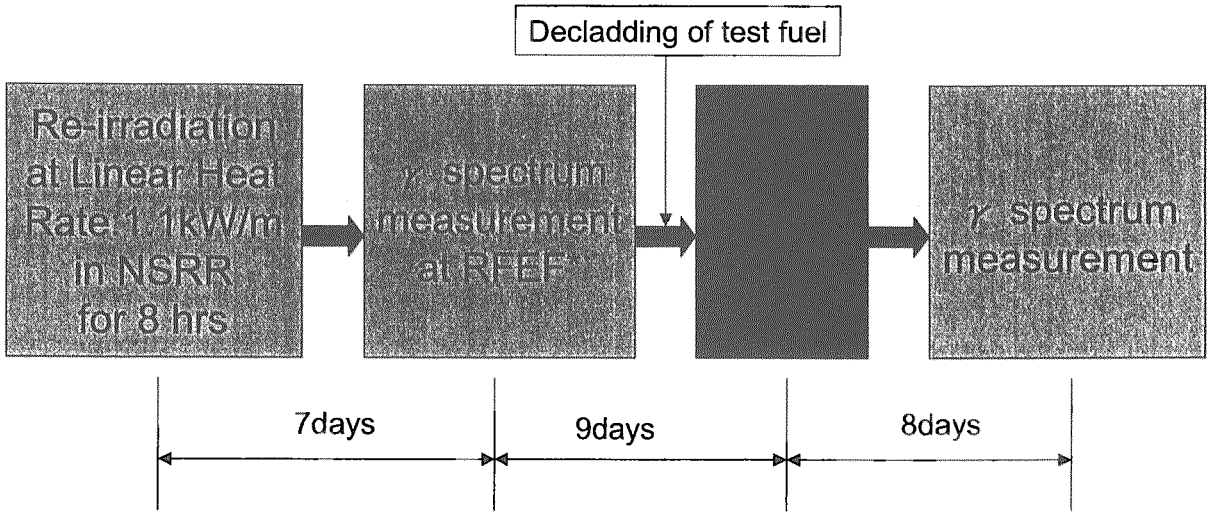
⇩

Enhancement of Cs release

7

Quick Look of VEGA-5

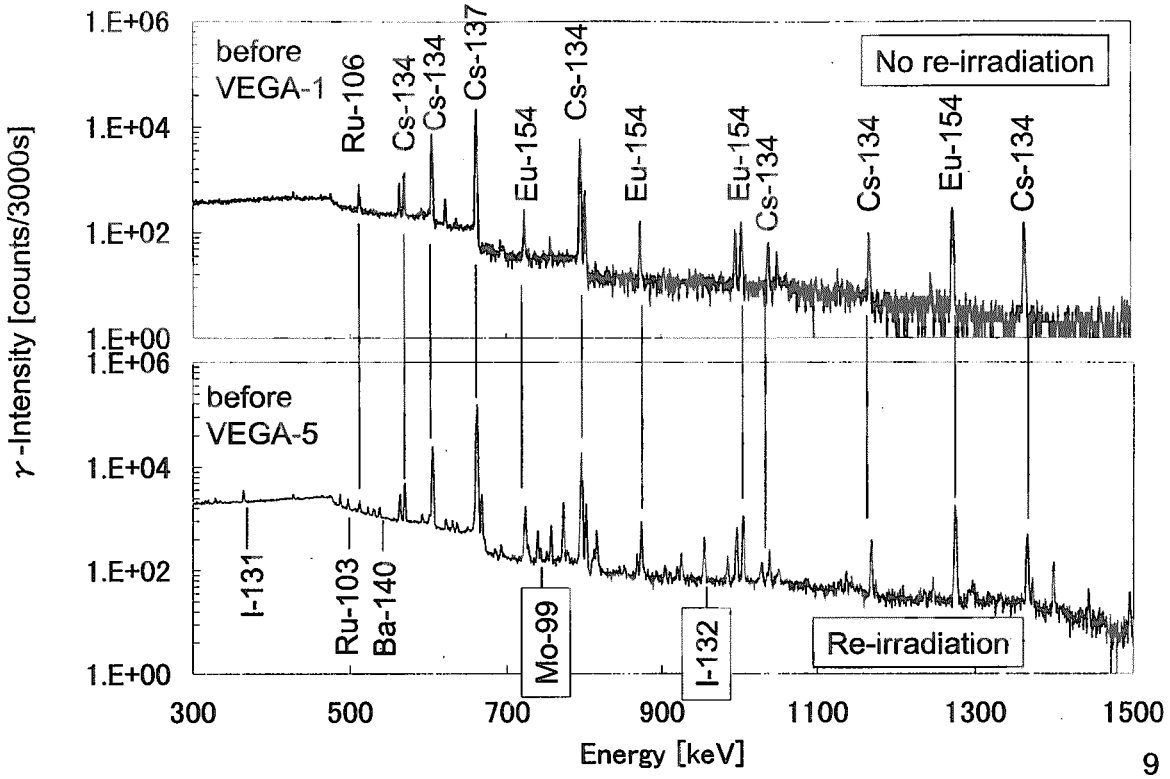
Test Schedule



*RFEF : Reactor Fuel Examination Facility

8

Comparison of γ spectra of fuel before heat up test between without and with re-irradiation



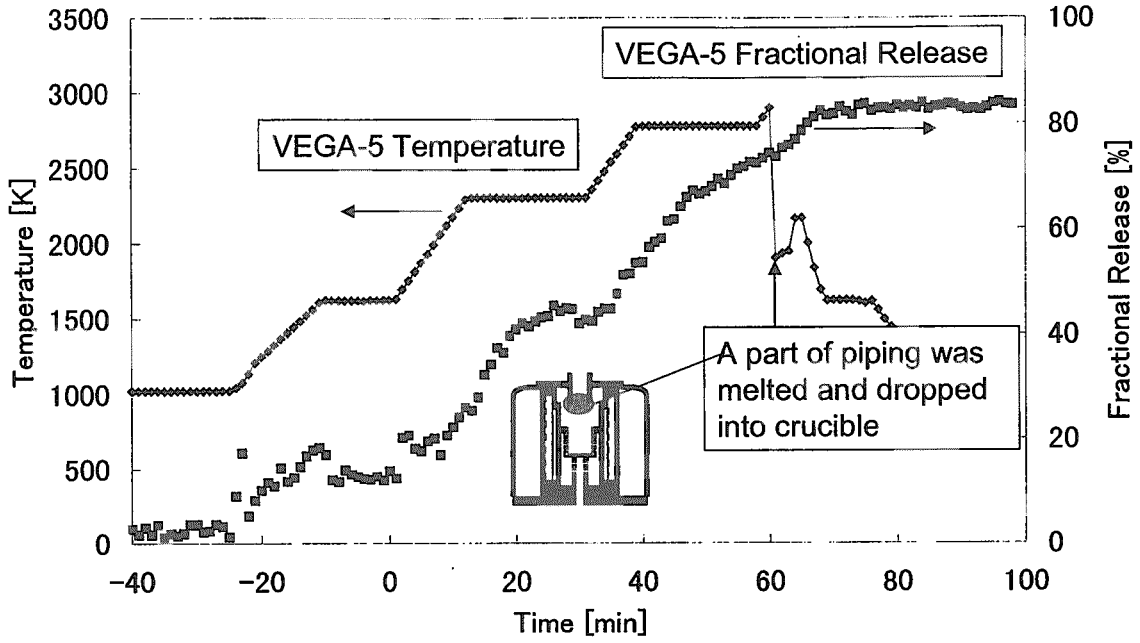
9

Fractional Releases Estimated from Change of γ-Intensities

Assuming no Eu release

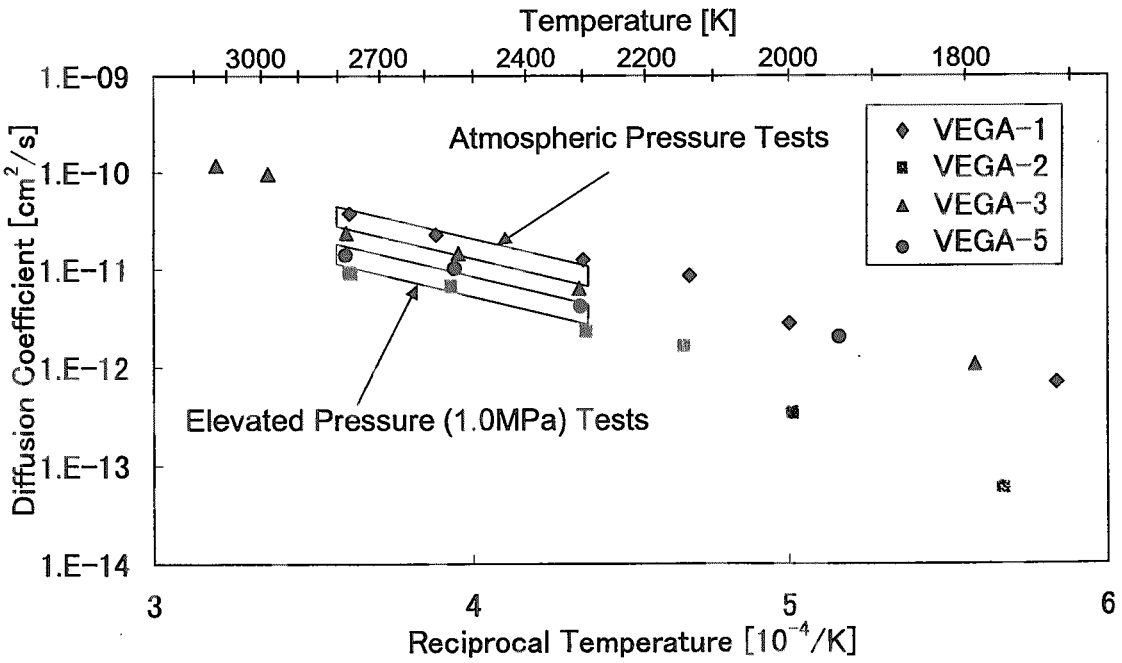
Radio-nuclides	Half-life [days]	γ-Energy [keV]	VEGA-3 He,3123K 0.1MPa		VEGA-4 Steam,2773K 0.1MPa		VEGA-5 He,2773K 1.0MPa	
			Release [%]	Error [%]	Release [%]	Error [%]	Release [%]	Error [%]
Cs-134	753	605	99.5	0.1	98.9	0.4	82	0.4
		796	99.9	0.1	99.3	0.2	85	0.2
Cs-137	10950	662	99.5	0.1	93.4	0.1	84	0.1
Sb-125	1011	428	－		－		67	11.1
Ba-140	12.75	537	－		－		7	13.8
Ru-103	39.35	497	－		－		0	8.9
Ru-106	368	622	0	19.0	52	18.7	0	9.4

Fractional Release History of Cs in VEGA-5



11

Comparison of Diffusion Coefficients among VEGA-1~3 and -5



Diffusion coefficient of VEGA-5 below 2000K did not follow the Arrhenius form under influence of release from grain boundary. However, difference of diffusion coefficients above 2200K between atmospheric and elevated pressure was re-confirmed. 12

Summary

- In VEGA-3 test at maximum temperature of about 3100K, Cs release rate around 3100K increased due to fuel melting.
- VEGA-4 test under steam-He mixture condition showed that Cs release rate enhanced in comparison with VEGA-1 probably due to increase of uranium vacancy concentration by fuel oxidation and fuel liquefaction by eutectic reaction of UO_2 with ZrO_2. Fractional release of Ru enhanced due to formation of volatile ruthenium oxide.
- In VEGA-5 test using re-irradiated fuel under elevated pressure condition,
  - －fractional releases of short life Ba-140 and Ru-103 could be estimated,
  - －Cs release started from low temperature (above about 1000K),
  - －pressure effect observed in VEGA-5 was not so larger than VEGA-2, but VEGA-5 indicated that Cs release above about 2200K was obviously suppressed compared with the atmospheric pressure tests.

13

Discussion:

Q: (G. Ducros)
The irradiation time in VEGA-5 seems too short to create short-life FPs at the same activity level as long-life FPs. In addition, decrease time between irradiation time and VEGA-5 test was long. Therefore, short-life FPs such as Mo-99, Te-137, Ce-143 could not have been measured.

A: We wanted to re-irradiate the fuel for more than one week but it was impossible due to the limitation of NSRR operation. In future, we plan to re-irradiate for 2 or 3 weeks using JRR-3. The duration between re-irradiation and VEGA-5 test was the minimum according to the procedures allowed inside JAERI

Q: (G. Ducros)
I am surprised by the high level of Ru-106 release in VEGA-4. In VERCORS-5 conducted in similar conditions, we have only measured 6% release of this element. I suggest that your Ru-106 measurement at 622 keV before the test could have been interfered by I-132 live at the same energy.

A: Since the 6 years cooling fuel was used in VEGA-4 test, the gamma intensity of Ru-106 was so small and the experimental error could not be ignored. The re-evaluation of Ru release will be performed based on Ru-103 which is generated by re-irradiation in future VEGA tests.

Q: (I. Sato)
In the radial cut of VEGA-3, you have mentioned that the part was molten. But if it was molten, draining will result in different shape. It seems possible to have direct transfer from solid fuel to vapor and reverse at this high temperature condition. Uncertainty of temperature measurement could lead to another interpretation.

A: Possible draining will be checked by cutting in the future. Uncertainty of the temperature measurement is quite good, so that we are sure of reaching the melting point.

JP0250418

JAERI−Conf 2002−009

Session 4-3

Fission-Product Releases from CANDU Fuel at 1650°C: The HCE4 Experiment

L.W. Dickson and R.S. Dickson
Fuel Safety Branch, Atomic Energy of Canada Limited
Chalk River Laboratories, Chalk River, Ontario, Canada K0J 1J0

ABSTRACT

The HCE4 (Hot-Cell Experiment 4) experiment was performed to study fission-product releases (FPR) from CANDU fuel at 1650°C. Three sets of tests were conducted to assess the effects of fuel element length, atmosphere, and heating rate on fission-product release. The fuel samples were from the Darlington reactor (burnup of ~8.8MWd/kgU, maximum linear power of 42 kW/m) and an irradiation in the NRU reactor (burnup of 6.3MWd/kgU, maximum linear power of 64 kW/m).

The first set of tests was performed to assess the effect of fuel element length on fission-product release from clad samples of CANDU fuel at 1650°C in a 76mol% steam and 0.5mol%H_2 (balance Ar) environment. For most fission products released under the test conditions (Xe, Kr, Cs and I), no significant differences were found between the releases from clad fuel samples of different lengths (20 and 100 mm). The fractional Te-129m release seems to have been higher from one of the shorter fuel samples, but the uncertainty in this result is large due to poor counting statistics. The difference in the Te-129m releases may arise from its affinity for unoxidized Zircaloy and local differences in the extent of clad oxidation. These results indicate that it may not be necessary to account specifically for any effect of fuel element length on releases of volatile fission products from the fuel in CANDU safety analysis. The possible exceptions to this conclusion are those species that are known to have a specific chemical interaction with the cladding that may be affected by steam ingress into the fuel element, e.g., Te and Sb.

The second set of tests was performed to assess the effect of environment (inert, steam and air) on fission-product release from clad samples of CANDU fuel at 1650°C. The releases of the volatile fission products (Kr, Xe, Cs and I) from the clad fuel samples were low (<10%) in the Ar/2%H_2 environment, and high (75-100%) in the steam and air environments. The Te-129m release in the inert atmosphere test was negligible. The Te-129m releases in the oxidizing atmospheres varied significantly (30-80%) and did not appear to depend on the nature of the oxidant (steam or air). Some Ru release (~15%) was observed beginning about 3600 s after the onset of rapid Cs release in the air environment. No Ru release was observed in the inert or steam atmosphere tests. No statistically significant releases of Ba, Eu, La, Nb, Nd, Pr, Y and Zr were observed in these tests.

The third set of tests was performed to assess the effect of heating rate on fission-product release from full-pellet-cross-section fuel fragment samples in an inert (Ar/2%H_2) environment. Good results were obtained on releases of volatile fission products (Cs, I) in these tests, but the noble gas (Kr, Xe) release data are not as reliable because of experimental difficulties. There appeared to be little effect of heating rates between 0.2 and 6°C/s on FPR from fuel samples heated to ~1650°C in an inert (Ar/2%H_2) atmosphere. Heating rate effects are thought to be more significant for fission products located on grain boundaries and the fuel used in the HCE4 experiment had a relatively small grain-boundary inventory.

The full paper will present the results of the HCE4 experiment on the effect of sample length, atmosphere and heating rate on FPR from CANDU fuel at temperatures up to 1650°C. The data from the HCE4 fission-product release experiment appear to be suitable for use in the validation of the SOURCE fission-product release code. The CANDU Owners Group (COG) Safety and Licensing R&D program under the joint sponsorship of Ontario Power Generation, Hydro Québec, New Brunswick Power and AECL supported this work.

FISSION-PRODUCT RELEASES FROM CANDU FUEL AT 1650°C: THE HCE4 EXPERIMENT

L.W. DICKSON AND R.S. DICKSON

Fuel Safety Branch
AECL, Chalk River Laboratories
Chalk River, Ontario, Canada K0J 1J0

ABSTRACT

The HCE4 (Hot-Cell Experiment 4) experiment was performed to study fission-product releases from CANDU fuel at 1650°C. Three sets of tests were conducted to assess the effects of fuel element length, gaseous environment, and heating rate on fission-product release. No significant effect of fuel element length was observed for most fission products released under the test conditions. Consistent with previous observations, oxidizing atmospheres increased the releases of most fission products. There was no significant effect of heating rate on fission-product releases from full-cross-section fuel fragment samples for the particular fuel and the range of heating rates studied.

INTRODUCTION

This paper describes the results of an experiment that was performed to assess the effects of fuel element length, gaseous environment and heating rate on fission-product releases (FPR) from CANDU fuel at 1650°C. The experiment, designated HCE4 (Hot-Cell Experiment 4), was part of a research program to determine fission-product release, deposition and transport from fuel under accident conditions [1-3]. In the HCE4 experiment, sheathed and unsheathed samples of CANDU fuel were heated to peak temperatures of 1600-1650°C under controlled conditions. The tests were conducted in flowing atmospheres of air, steam and/or argon. Fission-product release data were collected using γ-spectrometers to view the fuel directly, and to view the effluent gases.

EXPERIMENTAL APPARATUS AND FUEL SAMPLES

A general schematic of the experimental apparatus is shown in Figure 1. A SATEC Systems model FH-080-RA-33-3x12 split horizontal tube furnace with Super Kanthal 33 molybdenum disilicide heating elements was used for the HCE4 experiment. The furnace was mounted on a travelling track, and achieved temperature ramps of up to 8 $K \cdot s^{-1}$ by moving the pre-heated furnace over the fuel sample. While the furnace was moved, the fuel sample (located inside an alumina furnace tube) was held stationary in the field of view of a γ-spectrometer by means of a magnetic pushrod assembly. The hot zone of the furnace could be moved over the fuel sample

with no loss of carrier gas or system pressure. The gas flows were controlled using Cole-Parmer type N112-02 valved rotameters and measured using Matheson model 8175 mass flow meters. The gas supply flows (Ar/2%H_2 or air) were 297 ± 14 $\mu mol \cdot s^{-1}$. A steam generator added steam to the flowing carrier gas for the tests that used steam (water supply flow 930 ± 50 $\mu mol \cdot s^{-1}$). Oxygen sensors were located upstream and downstream of the fuel sample to monitor kinetics of fuel and sheath oxidation [4]. The fuel sample temperature was monitored using a type R thermocouple (measurement uncertainty ± 10°C at 1600°C). One Aptec γ-spectrometer with an AP series high-purity germanium detector viewed the sample directly through a collimated port in the hot-cell wall, to monitor the fractional retention of fission products in the fuel sample on-line during a test. A second high-purity germanium γ-spectrometer was used to monitor the noble-gas activity in the gas stream downstream of a steam condenser. Deposition coupons and aerosol collectors located downstream of the fuel sample in some tests were γ-scanned after the experiment. The deposition and aerosol results will be reported elsewhere.

The fuel samples used in most of the tests in the HCE4 experiment were from an outer element (#16) of bundle Q53150C irradiated in channel K17 in the Darlington Unit 2 reactor at a maximum linear power of 42 $kW \cdot m^{-1}$ to a burnup of ~210 $MW \cdot h \cdot (kg\ U)^{-1}$. The HCE4 experiment was conducted one to two months after the irradiation in the Darlington reactor. Fuel samples for the J07 and J08 tests were taken from a fuel element from the FDO-717 experiment (with the same diameter and sheathing as the CANDU 37-element bundle design) irradiated in the E-12 (Blowdown Test Facility) test section of the U-1 loop in the NRU (National Research Universal) reactor at a maximum linear power of 64 $kW \cdot m^{-1}$ to a burnup of 150 $MW \cdot h \cdot (kg\ U)^{-1}$. A fuel element from the same irradiation was used for the BTF-105B experiment [5]. The fuel samples for the J07 and J08 tests were cooled for about 15 months prior to the HCE4 experiment.

TEST CONDITIONS

Three sets of tests were conducted in the HCE4 experiment (see Table 1). The first set of tests (J01, J02, J03 and J04) was performed to assess the effect of the gaseous environment (inert, steam and air) on fission-product release from clad samples of CANDU fuel at 1650°C. In all of these tests, the fuel samples were heated to the test temperature in an effectively "inert" atmosphere (Ar/2%H_2), prior to being exposed to the test atmosphere. The second set of tests (J07 and J08), together with the J03 and J04 tests from the first set, was performed to assess the effect of fuel element length (20 or 100 mm) on fission-product release from sheathed samples of CANDU fuel at 1650°C, in a gas supply mixture containing 76 mol% steam and 0.5 mol% H_2 (balance Ar). The fuel samples used in the J07 and J08 tests were heated to the test temperature in the test atmosphere. The third set of tests (J05, J06, J09 and J10) was performed to assess the effect of heating rate on fission-product release from full-pellet-cross-section fuel fragment samples in an inert (Ar/2%H_2) environment.

DATA ANALYSIS

In this experiment, the direct-viewing γ-spectrometer (Figure 1) detected Y-91, Zr-95, Nb-95, Ru-103, Ru-106, Te-129m, I-131, Cs-134, Cs-137, Ba-140, La-140, Pr-144 and Eu-156. Release

percentages were normalized, using selected γ-ray peaks of La-140, Zr-95 and Pr-144, to correct for attenuation and sample geometry changes [1]. The release percentages for Te-129m were calculated from the count rate changes of the 696 keV peak, which contained contributions from Te-129 and Pr-144. The γ-ray peaks of some fission-product elements of considerable interest (e.g., I and Cs) had poor counting statistics. For the calculation of integral releases, the combined spectra obtained before the sample was inserted into the furnace were compared with those obtained after the test in order to improve the counting statistics. Table 1 shows the normalized integral fission-product releases and their statistical uncertainties (1σ) for the 10 tests in the HCE4 experiment. The data processing procedure gave negative (but not statistically significant) values of fractional release for some isotopes. These non-physical negative values of fractional release were re-assigned a value of zero. The release percentage of selected isotopes as a function of time for selected tests are plotted in Figures 2-6.

The gas-monitoring γ-spectrometer detected peaks from Kr-85, Xe-131m, Xe-133m and Xe-133. The initial calculated percentage releases of the noble-gas isotopes varied widely, and were not very similar to the Cs-137 percentage release, probably due to systematic errors in γ-spectrometer efficiency calibration. Since noble gases and cesium showed similar release behaviour and have shown similar release percentages in previous experiments [1,6,7], the noble-gas releases in each test were scaled to give the same final cumulative percentage release as Cs-137.

RESULTS AND DISCUSSION

The fuel samples were cut, polished and etched after the tests to assess the changes in the fuel and sheath microstructure. Post-test micrographs of the fuel sample from test J03 are shown in Figure 7. There was no statistically significant change in fuel grain size due to the post-irradiation temperature transient. There was some evidence of UO_2-Zircaloy interaction in the tests performed using sheathed fuel samples. The macrographs in Figure 7 show UO_2-Zircaloy alloy formation where Zircaloy came into contact with the fuel, and also show limited intrusion of molten material into some cracks. The macrographs indicate that less than 5% of the UO_2 fuel interacted with the Zircaloy in these tests. Solid/solid interaction between UO_2 and Zircaloy occurs locally in regions of good contact at temperatures above 1500°C, in the absence of an external overpressure [8]. Zircaloy reduces UO_2 to metallic uranium, and the metallic uranium reacts with zirconium to form a (U,Zr) alloy which is molten at temperatures above ~1150°C. Gaseous fission products form bubbles in the molten (U,Zr) alloy. The microstructure in the interaction zone (shown in the lower left frame of Figure 7), with its large voids and lack of apparent grain structure, is typical of previously molten (U,Zr) alloys. About 1500 s after the J03 and J04 fuel samples reached 1600°C, they were exposed to steam, which oxidized the Zircaloy, UO_2 and material from the (U,Zr) interaction. The absence of layers in the sheath microstructure located away from the UO_2-Zircaloy interaction zones indicates that the sheath was fully oxidized, and that the oxidation occurred only from the outside in test J03.

The first set of tests (J01, J02, J03 and J04) was performed to assess the effect of environment (inert, steam and air) on fission-product release from clad samples of CANDU fuel at 1650°C. The releases of the volatile fission products (Kr, Xe, Cs and I) from the clad fuel samples were

low (<10%) in the Ar/2%H_2 environment, and were high (75-100%) in the steam and air environments. Rapid release of Kr and Xe began several hundred seconds after exposure to steam, consistent with the time required to fully oxidize the fuel sheath [1,7]. The Te-129m release in the inert atmosphere test was negligible. The Te-129m releases in the oxidizing gaseous environments varied significantly (30-80%), and did not appear to depend on the nature of the oxidant (steam or air). Some Ru release (~15%) was observed, beginning about 3600 s after the onset of rapid Cs release in the air environment. No Ru release was observed in the inert or steam atmosphere tests. No statistically significant releases of Ba, Eu, La, Nb, Nd, Pr, Y and Zr were observed in these tests.

The second set of tests (J03, J04, J07 and J08) was performed to assess the effect of fuel element length on fission-product release from sheathed samples of CANDU fuel at 1650°C in a gas-supply mixture containing 76 mol% steam and 0.5 mol% H_2 (balance Ar). For most fission products released under the test conditions (Xe, Kr, Cs and I), no significant differences were found between the releases from clad fuel samples of different lengths (20 and 100 mm). The fractional Te-129m release seems to have been higher from one of the shorter fuel samples, but the uncertainty in this result is large. No firm conclusions can be drawn due to the large uncertainties, but the difference in the Te-129m releases may arise from its affinity for unoxidized Zircaloy and local differences in the extent of oxidation of the cladding. These results indicate that in CANDU safety analysis it may not be necessary to account specifically for any effect of fuel element length on releases of volatile fission products from the fuel. The possible exceptions to this conclusion are for those species that are known to have a specific chemical interaction with the cladding, and that may be affected by steam ingress into the fuel element, e.g., Te and Sb.

The third set of tests (J05, J06, J09 and J10) was performed to assess the effect of heating rate on fission-product release from full-pellet-cross-section fuel fragment samples in an inert (Ar/2%H_2) environment. The heating rates in tests J05, J09 and J10 were 0.2, 1-2 and 6 $K \cdot s^{-1}$, respectively. In test J06, the fuel sample was subjected to two temperature ramps to ~1626°C (the first at a heating rate of 1-2 $K \cdot s^{-1}$ and the second at ~4.7 $K \cdot s^{-1}$). Good results were obtained on releases of volatile fission products (Cs, I) in these tests, but the noble gas (Kr, Xe) release data are not as reliable because of experimental difficulties. There appeared to be little effect of heating rates between 0.2 and 6 $K \cdot s^{-1}$ on FPR from fuel samples heated to ~1650°C in an inert (Ar/2%H_2) atmosphere. Heating rate effects are thought to be most significant for fission products located on grain boundaries. The fuel used in the HCE4 experiment had a relatively small grain-boundary inventory [3].

CONCLUSIONS

The HCE4 (Hot-Cell Experiment 4) experiment was performed to study fission-product releases from CANDU fuel at 1650°C. Three sets of tests were conducted to assess the effects of fuel element length, gaseous environment, and heating rate on fission-product release. No significant effect of fuel element length was observed for most fission products released under the test conditions. Consistent with previous observations, oxidizing gaseous environments increased the releases of most fission products. There was no significant effect of heating rate on

fission-product releases from full-cross-section fuel fragment samples for the particular fuel and the range of heating rates studied. The data from the HCE4 fission-product release experiment are suitable for use in the validation of the SOURCE fission-product release code [9].

ACKNOWLEDGEMENTS

The authors would like to thank R.D. Barrand, R.F. O'Connor and D.D. Semeniuk for technical assistance in the HCE4 experiment. This work was partially supported by the CANDU Owners Group (COG) Safety and Licensing R&D program under the joint sponsorship of Ontario Power Generation, Hydro Québec, New Brunswick Power and AECL.

REFERENCES

1. BARRAND, R.D., DICKSON, R.S., LIU, Z. AND SEMENIUK, D.D., "Release of Fission Products from CANDU Fuel in Air, Steam and Argon Atmospheres at 1500-1900°C: The HCE3 Experiment", Proc. 6th Int. Conf. CANDU Fuel, Niagara Falls, Canada, 1, 271-280, Canadian Nucl. Soc., Toronto, ISBN 0-919784-64-X (1999).
2. LIU, Z., DICKSON, R.S., DICKSON, L.W., BILANOVIC, Z. AND COX, D.S., "Fission-Product Release During Transient Heating of Irradiated CANDU Fuel", Nucl. Technol., 131, 22-35, July (2000).
3. DICKSON, R.S., O'CONNOR, R.F. AND SEMENIUK, D.D., "Grain Boundary Inventories of Krypton in CANDU Fuel", Proc. IAEA Seminar on Fission Gas Behaviour in Water Reactor Fuels, Cadarache, France, 337-346, ISBN 92-64-19715-X (2000).
4. COX, D.S., O'CONNOR, R.F. AND SMELTZER, W.W., "Measurement of Oxidation/Reduction Kinetics to 2100°C Using Non-Contact Solid-State Electrolytes", Solid State Ionics, 53-56, 238-254 (1992).
5. IRISH, J.D., CRAIG, S.T., BOURQUE, L.R., JONCKHEERE, M.G., KYLE, G., VALLIANT, P.J., DICKSON, L.W. AND PEPLINSKIE, R.T., "Preliminary Results of the BTF-105B Experiment: An In-Reactor Test of Fuel Behaviour and Fission-Product Release and Transport Under LOCA/LOECC Conditions", Proc. 19th Annual Canadian Nucl. Soc. Conf., Toronto, Vol. 2, Paper C-2, Canadian Nucl. Soc., Toronto, ISSN 0227-1907 (1998).
6. IGLESIAS, F.C., BRITO, A.C., LIU, Y., PETRILLI, M.A., HU, R., RICHARDS, M.J., ELDER, P., COX, D.S. AND LEWIS, B.J., "Fission Product Release Mechanisms and Groupings" Proc. 4th Int. Conf. CANDU Fuel, Pembroke, Canada, 2, 5B-23 – 5B-44, Canadian Nucl. Soc., Toronto, ISBN 0-919784-53-4 (1995).
7. IGLESIAS, F.C., LEWIS, B.J., REID, P.J AND ELDER, P.H., "Fission Product Release Mechanisms During Reactor Accident Conditions", J. Nucl. Mater. 270, 21-38 (1999).
8. DIENST, W., HOFMANN, P. AND KERWIN-PECK, D.K., "Chemical Interactions Between UO_2 and Zircaloy-4 from 1000 to 2000°C", Nucl. Technol. 65, 109-124 (1984).
9. BARBER, D.H., IGLESIAS, F.C., HOANG, Y., DICKSON, L.W., DICKSON, R.S., RICHARDS, M.J. AND GIBB, R.A., "SOURCE IST 2.0: Development and Beta Testing", Proc. 6th Int. Conf. CANDU Fuel, Niagara Falls, Canada, 1, 393-402, Canadian Nucl. Soc., Toronto, ISBN 0-919784-64-X (1999).

TABLE 1: NORMALIZED INTEGRAL FISSION-PRODUCT RELEASES (%) [1] FROM FUEL SAMPLES HEATED TO ~1650°C

Test	J01	J02	J03	J04	J05	J06	J07	J08	J09	J10
Fuel Length /mm	20	20	20	100	5	5	107	20	5	5
Sheathed	Yes	Yes	Yes	Yes	No	No	Yes	Yes	No	No
Environment	Ar/H_2	Air	H_2O/H_2	H_2O/H_2	Ar/H_2	Ar/H_2	H_2O/H_2	H_2O/H_2	Ar/H_2	Ar/H_2
Heating Rate /$K{\cdot}s^{-1}$	-	-	-	-	0.2	1-2 / 5	-	-	1-2	~6
Max. Temp. /°C	1620	1645	1640	1650	1629	1626	1628	1631	1627	1612
Time at Temp. /s	5733	6712	6360	6462	4840	5780	3737	4052	4240	1960
Ba-140	1 ± 3	0 ± 4	0 ± 3	0 ± 4	1 ± 2	0 ± 4			0 ± 5	2 ± 2
Cs-134	2 ± 5	75 ± 1	84 ± 1	82 ± 2	24 ± 2	19 ± 2	59 ± 1	100 –9	24 ± 2	16 ± 2
Cs-137	0 ± 6	74 ± 2	86 ± 1	84 ± 2	24 ± 3	18 ± 3	68 ± 1	70 ± 2	18 ± 4	13 ± 4
Eu-156	6 ± 4	5 ± 5	4 ± 6	7 ± 5	10 ± 6	3 ± 9			10 ± 13	0 ± 6
I-131	11 ± 4	100 –10	79 ± 3	100 –10	16 ± 3	13 ± 5			6 ± 9	7 ± 4
Kr-85	8 ± 1	100 –11	74 ± 10	73 ± 8	4 ± 1	13 ± 2	58 ± 8	57 ± 7	15 ± 2	10 ± 2
La-140	1 ± 4	1 ± 4	2 ± 4	0 ± 3	1 ± 2	3 ± 3			0 ± 6	0 ± 4
Nb-95	0 ± 6	0 ± 5	4 ± 5	0 ± 4	2 ± 3	0 ± 3	0 ± 2	0 ± 2	1 ± 2	0 ± 2
Nd-147	9 ± 8	0 ± 11	15 ± 8	12 ± 11	3 ± 9	0 ± 17			ND [4]	8 ± 10
Pr-144	0 ± 5	0 ± 5	2 ± 5	1 ± 5	0 ± 5	0 ± 5	0 ± 3	0 ± 2	0 ± 5	0 ± 4
Ru-106 [2]	0 ± 4	13 ± 3	1 ± 3	0 ± 3	0 ± 3	0 ± 3	2 ± 2	0 ± 2	0 ± 4	4 ± 2
Ru-103	0 ± 4	19 ± 3	0 ± 4	0 ± 3	0 ± 3	2 ± 3	0 ± 16	1 ± 12	0 ± 3	0 ± 2
Te-129m [3]	2 ± 17[3]	37 ± 14[3]	86 ± 12[3]	34 ± 12[3]	7 ± 8[3]	26 ± 11[3]			18 ± 15[3]	0 ± 7[3]
Xe-131m	5 ± 1	100 –7	84 ± 7	90 ± 6	5 ± 1	11 ± 1			22 ± 2	15 ± 2
Y-91	4 ± 5	0 ± 10	17 ± 4[d]	0 ± 5	4 ± 3	0 ± 12			1 ± 16	6 ± 4
Zr-95	0 ± 6	0 ± 5	7 ± 5	0 ± 3	2 ± 3	0 ± 3	0 ± 1	0 ± 1	2 ± 2	0 ± 2

[1] Statistical uncertainty values are ± 1σ. Non-physical negative release percentages that were not statistically significant were reassigned a value of zero. Release percentages of 100% were assigned negative uncertainties only.

[2] Detected as Rh-106.

[3] Non-physical Te-129m release percentages (>100%) were obtained in some tests due to Pr-144 interference with the 696 keV peak, and a large uncertainty in the relative fission and gamma yields of Pr-144 and Te-129m. The Te-129m releases quoted in this table were scaled to the Cs-137 releases in test J03.

[4] The Nd-147 gamma-ray at 531 keV was not detected in this test.

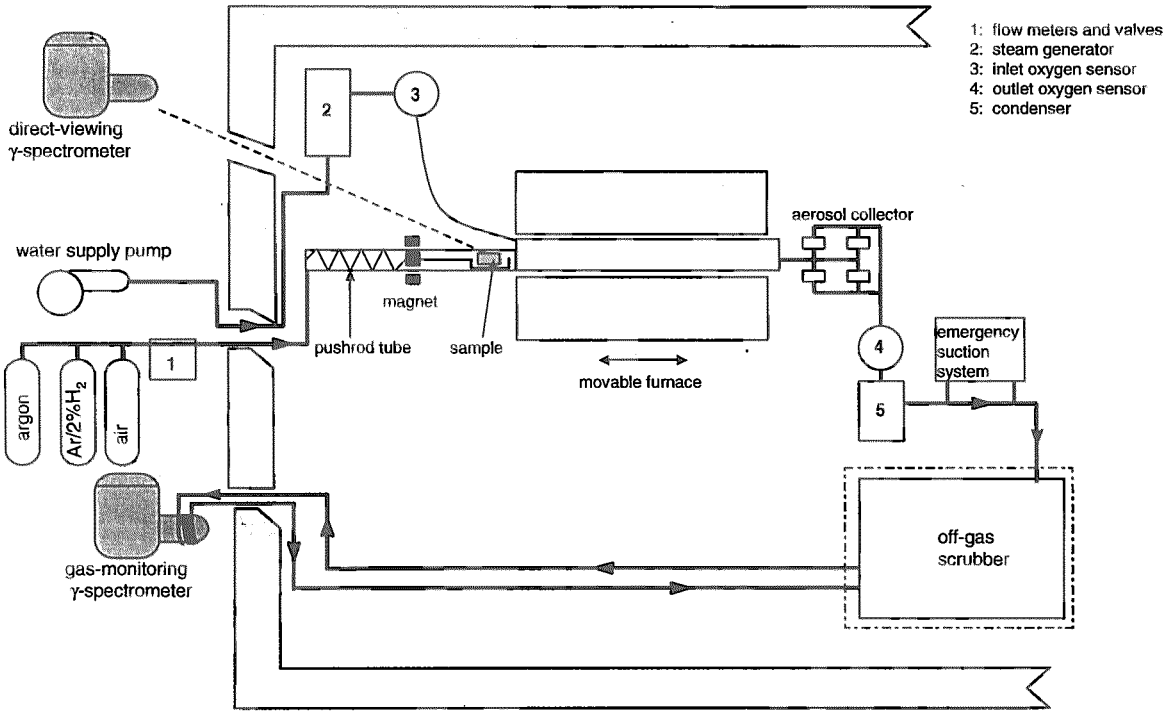


FIGURE 1: SCHEMATIC OF HCE4 HOT-CELL APPARATUS

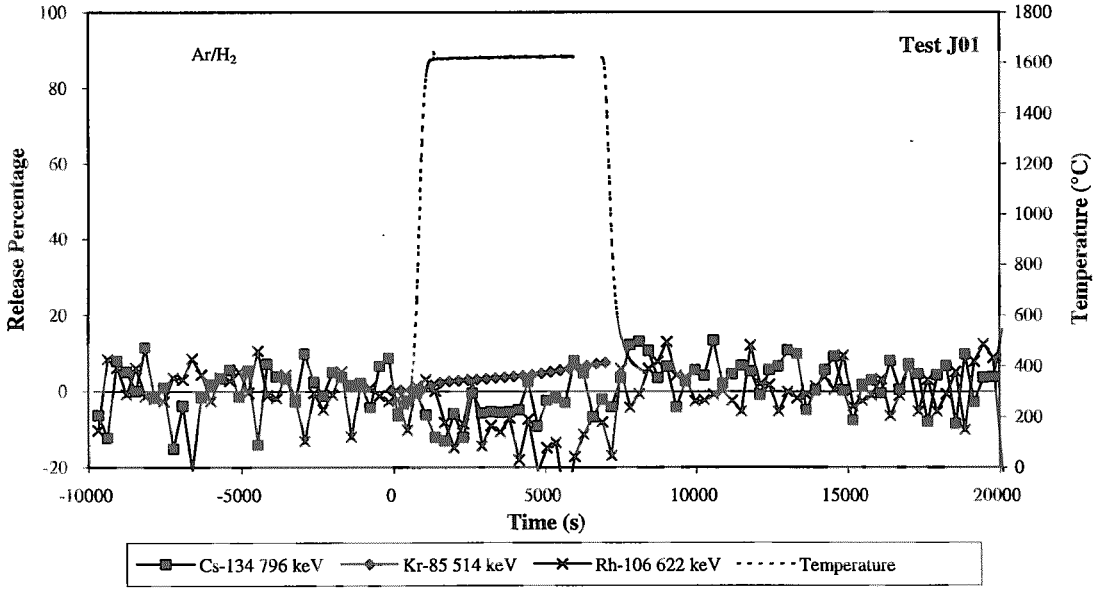


FIGURE 2: CESIUM, KRYPTON AND RUTHENIUM (AS Rh-106) RELEASE (%) AS A FUNCTION OF TIME FOR HCE4 TEST J01 (20-mm-LONG SHEATHED DARLINGTON FUEL, Ar/H_2, 1620°C).

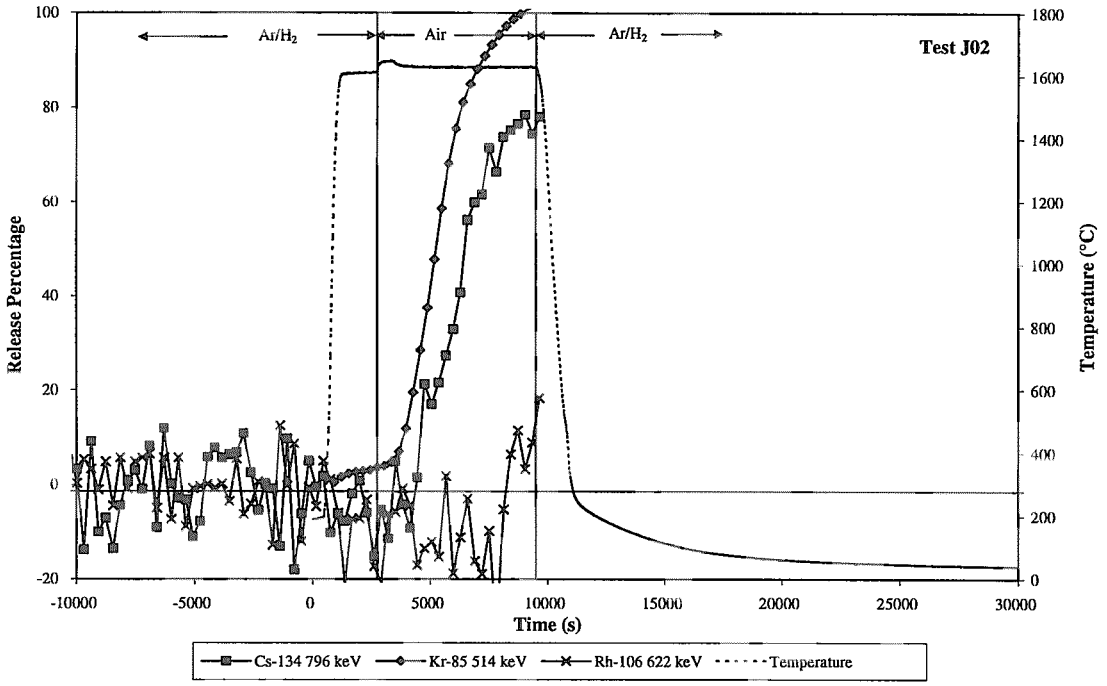


FIGURE 3: CESIUM, KRYPTON AND RUTHENIUM (AS Rh-106) RELEASE (%) AS A FUNCTION OF TIME FOR HCE4 TEST J02 (20-mm-LONG SHEATHED DARLINGTON FUEL, AIR AND Ar/H_2, 1645°C).

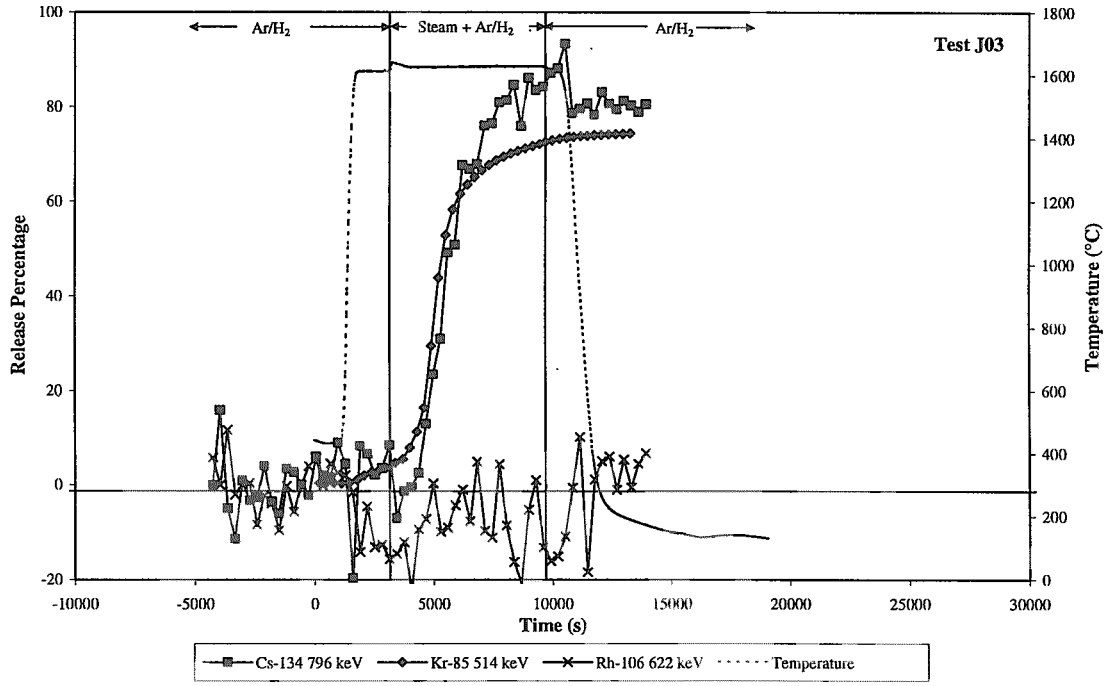


FIGURE 4: CESIUM, KRYPTON AND RUTHENIUM (AS Rh-106) RELEASE (%) AS A FUNCTION OF TIME FOR HCE4 TEST J03 (20-mm-LONG SHEATHED DARLINGTON FUEL, STEAM + Ar/H_2, 1640°C).

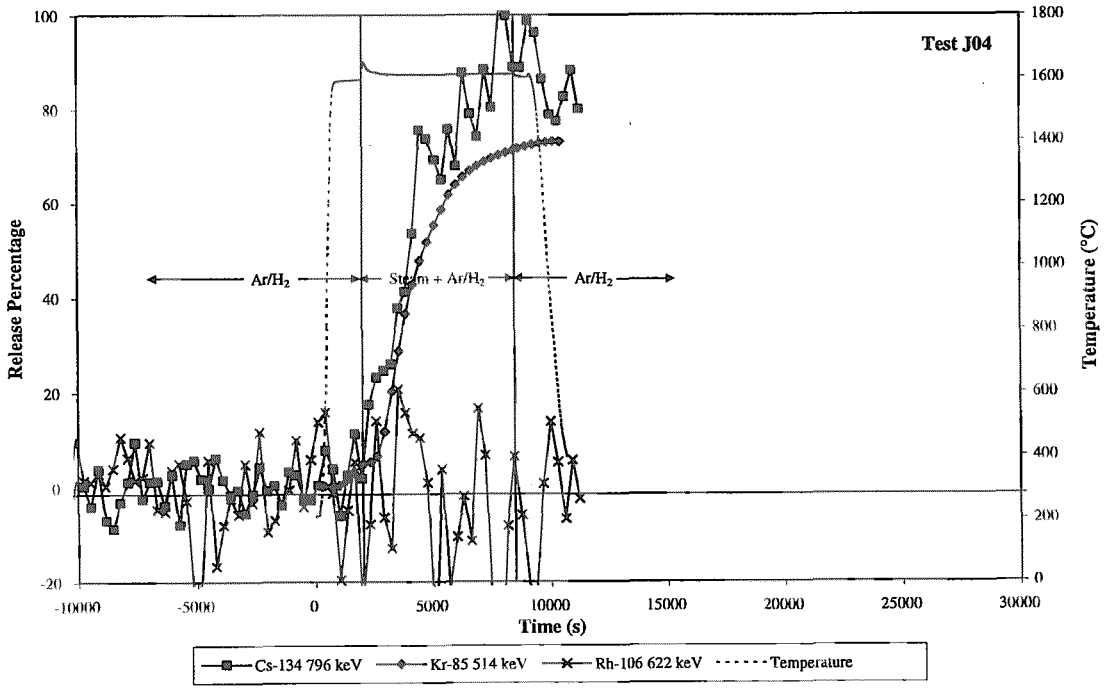


FIGURE 5: CESIUM, KRYPTON AND RUTHENIUM (AS Rh-106) RELEASE (%) AS A FUNCTION OF TIME FOR HCE4 TEST J04 (100-mm-LONG SHEATHED DARLINGTON FUEL, STEAM + Ar/H_2, 1650°C).

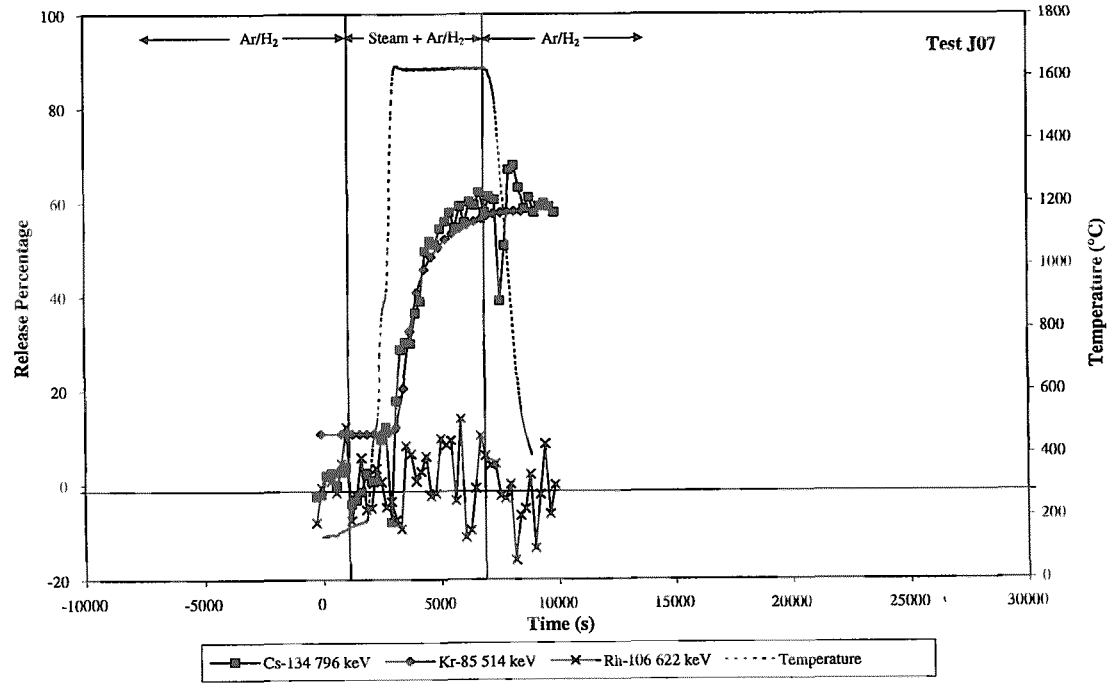


FIGURE 6: CESIUM, KRYPTON AND RUTHENIUM (AS Rh-106) RELEASE (%) AS A FUNCTION OF TIME FOR HCE4 TEST J07 (107-mm-LONG SHEATHED FDO-717 FUEL, STEAM + Ar/H_2, 1628°C).

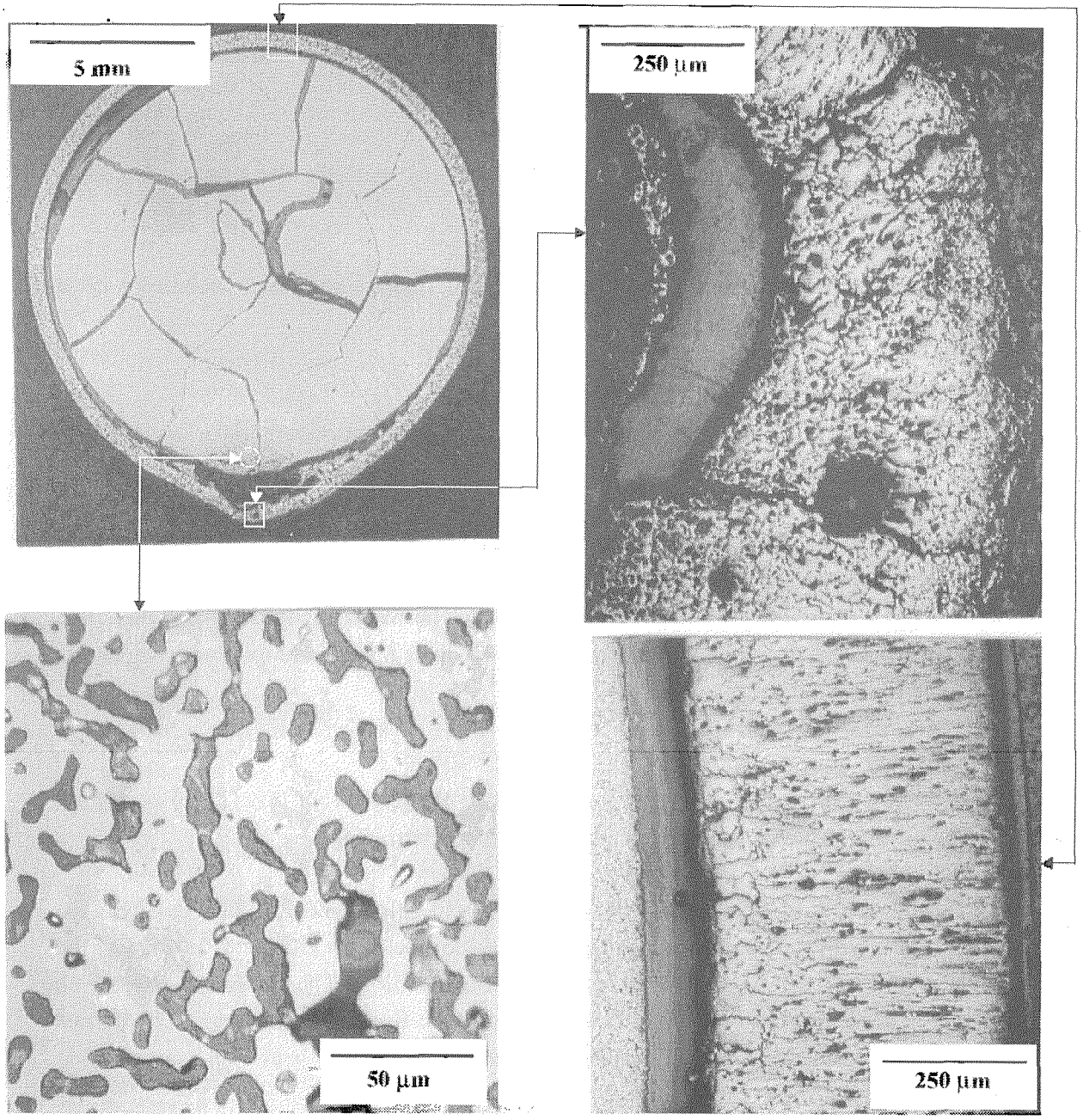


FIGURE 7: POST-TEST CERAMOGRAPHS OF THE J03 FUEL SAMPLE (1640°C, STEAM PLUS Ar/2%H_2). UPPER LEFT: MACROGRAPH OF FUEL. UPPER RIGHT: MICROGRAPH OF SHEATH AT DEFORMATION, AS POLISHED. LOWER RIGHT: MICROGRAPH OF FULLY OXIDIZED SHEATH REMOTE FROM DEFORMATION, AS POLISHED. LOWER LEFT: MICROGRAPH OF FUEL PERIPHERY NEAR DEFORMED PORTION OF THE SHEATH. THIS SHOWS MICROSTRUCTURE TYPICAL OF UO_2-ZIRCALOY INTERACTION.

Discussion:

Q: (P. Tempest)

Was it possible from your data on oxidized fuel to quantify the increased release kinetics in terms of a diffusion / oxidation model ?

A: These tests are being used for validation of a computer code that includes such a model.

Q: (P.D.W. Bottomley)

I noticed a slight increase in temperature increase upon introducing air or steam to the sample. Is this due to heat of Zircaloy oxidation?

A: The temperature increase is due in part to improved heat transfer within the furnace, because temperature increases at the start of steam flow even if no sample is present. However, part of the temperature increase is due to the heat of Zircaloy oxidation. The greatest excursion was found in test JO4, which had a large sample with a greater Zircaloy area.

Q: (G. Ducros)

How do you explain the relatively low release of Ru in your air test (13%) compared to similar tests you have performed in air on fragment bare UO_2 ?

A: The JO2 test was terminated just after rapid Ru release began. The delay in Ru release after the start of air flow is due to competition between UO_2 and Ru for O_2; the UO_2 is oxidized to UO_{2+x} and the Ru is oxidized to $RuO_4(g)$. The UO_2 must usually be oxidized to nearly its equilibrium stoichiometry before Ru release can begin. If the test had continued for another short time, the Ru release would have been more comparable to releases from UO_2 fragments.

Session 4-4

Fission-product release and transport analysis in severe accident conditions: strategy and illustrations

M.P. Kissane[1], N. Davidovich[2], R. Dubourg[1], C. Fiche[1], P.K. Mason[3] and W. Plumecocq[1]
[1]Institut de Protection et de Sûreté Nucléaire (IPSN), Département de Recherches en Sécurité, CEA Cadarache, 13108 St Paul lez Durance, France
[2]Ente per le Nuove Tecnologie l'Energia e l'Ambiente (ENEA), Dipartimento Energia, ENEA/Casaccia, SP 301 00100 Rome, Italy (under contract to IPSN)
[3]AEA Technology Engineering Services Inc., 241 Curry Hollow Rd., Pittsburgh, PA 15236, USA (under contract to IPSN)

Abstract

The work performed by IPSN on analysis of fission-product (FP) release and transport aims to identify and model the principal phenomena governing radionuclide behaviour. This has led to development of the MFPR release code[1] for a thorough physical understanding of mechanisms governing release of volatile and semi-volatile FPs from solid fuel. In parallel, reliable modelling of FP behaviour must be produced for analysis of nuclear plant, i.e. for the ASTEC integral code developed by IPSN and GRS. This has led to development of the ELSA release code for relatively fast indication of all core releases and the transport code SOPHAEROS for behaviour in the reactor coolant system (RCS).

The objective with MFPR is to model fully solid-fuel phenomenology with the possibility of treating conditions up to pre-foaming following liquefaction. Phenomena modelled include: FP production during irradiation; atomic diffusion in the UO_2 lattice; bubble nucleation, migration and re-solution; grain growth; oxidation and volatilization of UO_2 for arbitrary steam-air mixtures. While treating the UO_2 as a solid solution containing dissolved fission products (as well as bubbles), the code allows for three other condensed phases: caesium iodide; a grey phase comprising ternary compounds such as uranates of alkali and alkali-earth elements; and a metallic phase comprising *Ru*, *Mo* and *Sb*. The recent validation of this code presented here comprises examination of post-irradiation distribution of volatile FPs (based on data from AECL's GBI tests[2]) and FP release during temperature transients (VERCORS[3] tests 4 and 5). These comparisons along with other analyses not shown here indicate that MFPR is now a robust and instructive tool for exploring FP behaviour within UO_2 fuel.

With simplified modelling, the ELSA code covers all the principal core configurations involving significant releases: intact fuel rods, rod liquefaction and candling, control-rod release, solid-fuel debris and molten pools. The approach is semi-empirical where limiting phenomena have been assigned to the above configurations with appropriate models defined and tuned on experimental data. We focus here on description of the newest modelling addition, that of release from a molten pool based on chemical equilibrium within the pool and evaporation at the surface. The SOPHAEROS code is used to analyze FP behaviour outside the fuel rod. Vapour phenomena (chemistry, homogeneous nucleation, etc.) and aerosol phenomena (agglomeration and deposition mechanisms as well as mechanical resuspension) are modelled. In the context of reactor analyses, it is important to take account of transport aspects immediately after emission from the fuel rod since retention within the core can be high for FPs such as *Mo*, *Ba* and *Ru*. Light is being shed on this near-point-of-release retention by results from Phebus FP and VERCORS experiments. Some results of SOPHAEROS analysis of deposits in the vicinity of the fuel in the VERCORS HT1 test are shown here where good agreement is seen for *Mo* while that for *Ba* is less satisfactory.

In conclusion, the strategy of developing complementary modelling approaches for analysis of FP release is seen to be effective: MFPR allows detailed understanding of complex solid-fuel processes helping, in particular, to identify key phenomena; ASTEC, via the ELSA code, is fast-running for plant analyses with full coverage of all releases from intact and degraded states. Finally, plant analyses must take account of transport aspects within the core if release to the RCS is to be calculated correctly. In addition, certain of the FPs concerned by this in-core retention are significant emitters of decay heat and their retention may influence core degradation.

[1] MFPR is co-developed with IBRAE (Nuclear Safety Institute, Russian Academy of Science, Moscow).
[2] The Grain-Boundary Inventory experiments were performed by AECL at Chalk River Laboratories for the CANDU Owners' Group.
[3] VERCORS tests are carried out by CEA/DEN for IPSN in association with Electricité de France.

Fuel Safety Research Specialists' Meeting,
JAERI/Tokai Research Establishment,
4-5 March 2002

FISSION-PRODUCT RELEASE AND TRANSPORT IN SEVERE-ACCIDENT CONDITIONS: STRATEGY AND ILLUSTRATIONS

M.P. Kissane[1], N. Davidovich[2], R. Dubourg[1], C. Fiche[1], P.K. Mason[3] and W. Plumecocq[1]

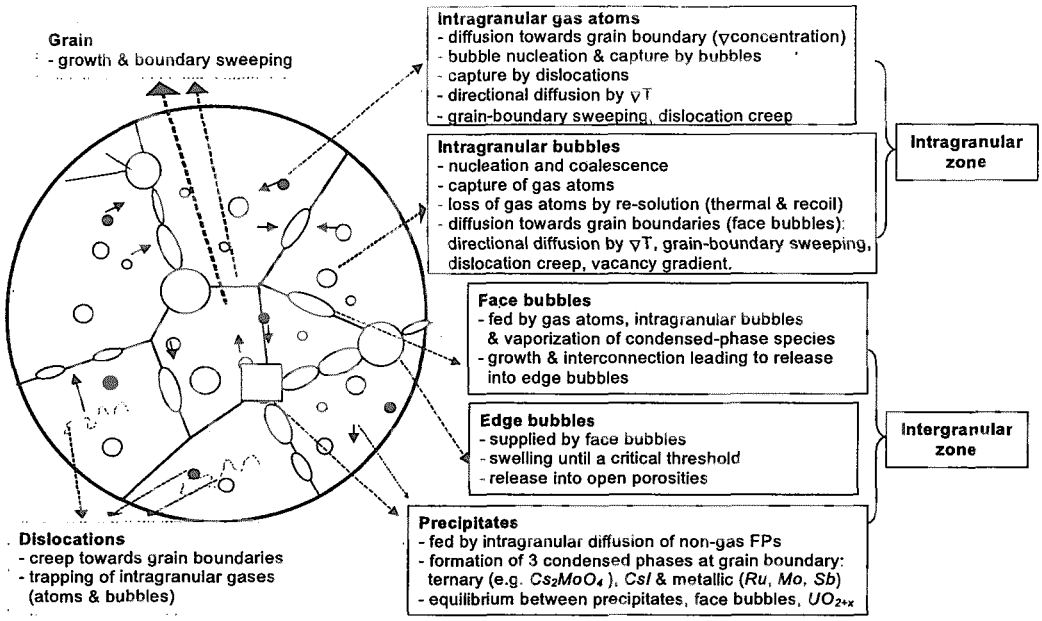
[1] *Institut de Protection et de Sûreté Nucléaire (IPSN), Département de Recherches en Sécurité, CEA Cadarache, 13108 St Paul lez Durance, France*
[2] *Ente per le Nuove Tecnologie l'Energia e l'Ambiente (ENEA), Dipartimento Energia, ENEA/Casaccia, SP 101 00100 Rome, Italy (under contract to IPSN)*
[3] *AEA Technology Engineering Services Inc., 241 Curry Hollow Rd., Pittsburgh, PA 15236, USA (under contract to IPSN)*

Approach

- **Release analyzed using a dual approach via two codes:**
  - *thorough understanding of solid-fuel processes including the objective of identifying dominant phenomena*
    ⇒ **MFPR** *(co-developed with IBRAE, Moscow)*
  - *relatively fast-running analysis for all core configurations*
    ⇒ **ELSA** *(a module of the IPSN-GRS integral code* ASTEC*)*
- **Transport analyzed using a dual approach via the same code:**
  - *full analysis (complete chemistry database, all models active)*
  - *simplified analysis (reduced database, optional models)*
    ⇒ **SOPHAEROS** *(a module of the IPSN-GRS integral code* ASTEC*)*
- **Extensive validation**

FP RELEASE AND TRANSPORT ANALYSIS IN SEVERE-ACCIDENT CONDITIONS: STRATEGY AND ILLUSTRATIONS

Detailed modelling MFPR v1.2: UO_{2+x} solid solution + precipitates



FP RELEASE AND TRANSPORT ANALYSIS IN SEVERE-ACCIDENT CONDITIONS: STRATEGY AND ILLUSTRATIONS

Simplified modelling full coverage of core configurations

ELSA v2.0: identify limiting phenomena, define model, adjust the model on analytical data (semi-empiricism), validate on other data.

- **solid fuel** (pellets and debris):

class	description	elements	model
Ia	volatile FPs	*Xe, Kr, I, Br, Cs, Rb, Cu, Ag*	atomic diffusion, including UO_{2+x}
Ib	volatile FPs	*Te, Se, Sb*	as above + trapping by Zrly
II	semi-volatile FPs	*Sr, Ba, Ru, Mo, La, Ce, Y, Eu*	simplified chemistry + evaporation
III	non-volatiles	*Rh, Pd, Tc,Nb,Zr,Np Pu Nd, Pm, Gd, Tb, Dy, Ho, Er, Tm, Yb, Pr, Am, Cm, Sm, U, Zn, As, Cd, Sn, Ga, Ge, In*	mass-transfer limited UO_2 volatilization

INSTITUT DE PROTECTION ET DE SURETE NUCLEAIRE
DEPARTEMENT DE RECHERCHES EN SECURITE
CENTRE D'ETUDES DE CADARACHE

FP RELEASE AND TRANSPORT ANALYSIS IN SEVERE-ACCIDENT CONDITIONS: STRATEGY AND ILLUSTRATIONS

Simplified modelling full coverage of core configurations

- **molten pool**:
  - thermodynamic equilibrium at free surface (Gibbs-energy minimization) for a general composition of

origin	elements
fuel and gases	*U, Pu, H, O*
cladding and control rods	*Zr, Sn, Ag, In, Cd, B, C*
steel/Inconel alloys	*Fe, Cr, Ni*
volatile/low-volatile FPs	*Cs,Rb,Te,Sb,Ba,Sr,Mo,Ru,Y*
lanthanides and actinides	*La, Ce, Eu, Nd, Pr, Np, Pu*
concretes (ex-vessel)	*Na, K, Al, Si, Ca, Mg, Ti*
non-prototypic elements (experiments)	*Hf, W, Re, He*

  $\Rightarrow$ >800 chemical species
  - mass transfer, $dm_i/dt = (Sh_i D_i/l).(\rho_{i,\,surface} - \rho_{i,\,bulk})$, Sh correlation
- **also models**: release during candling, release from control rods

FP RELEASE AND TRANSPORT ANALYSIS IN SEVERE-ACCIDENT CONDITIONS: STRATEGY AND ILLUSTRATIONS

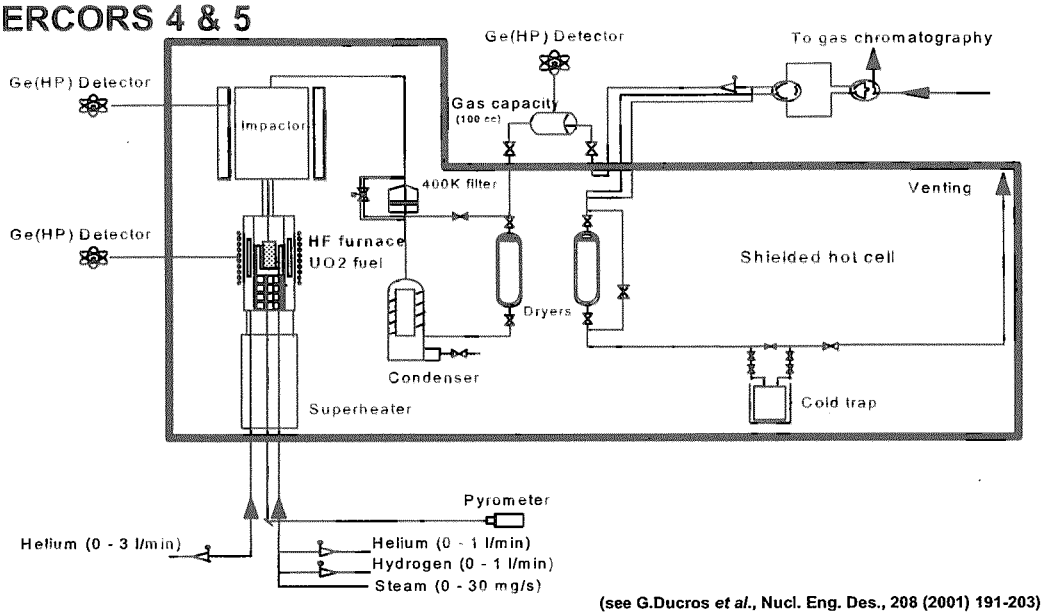
Detailed modelling volatile FP release rates

- **Why?**
  Release rates affect concentrations and hence chemical forms in the circuit, thus affecting retention.
- **How?**
  Data from VERCORS 4 and 5 are instructive;
  can be used to validate the MFPR code.

FP RELEASE AND TRANSPORT ANALYSIS IN SEVERE-ACCIDENT CONDITIONS: STRATEGY AND ILLUSTRATIONS

Detailed modelling volatile FP release rates

- VERCORS 4 & 5



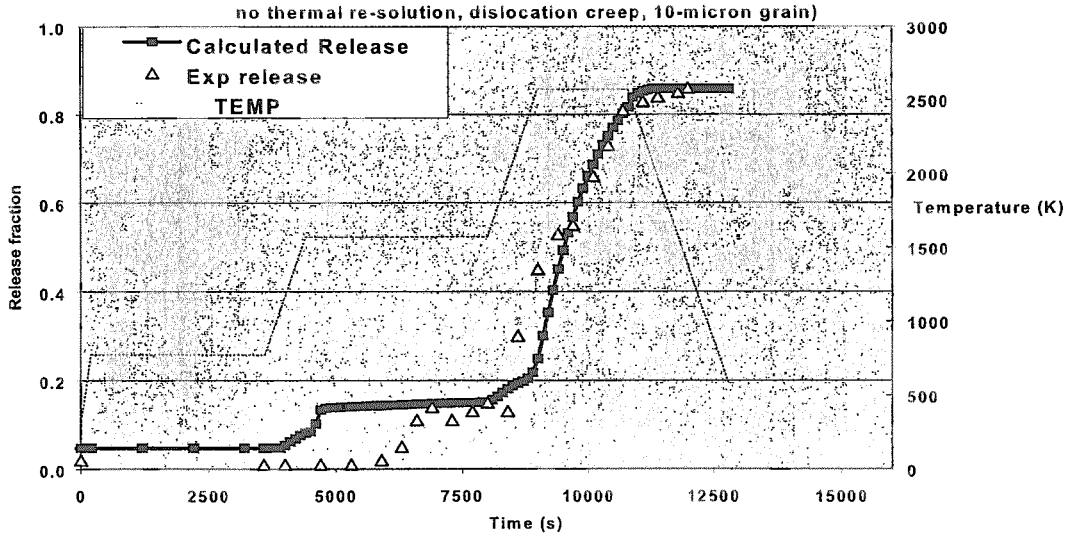
(see G.Ducros *et al.*, Nucl. Eng. Des., 208 (2001) 191-203)

FP RELEASE AND TRANSPORT ANALYSIS IN SEVERE-ACCIDENT CONDITIONS: STRATEGY AND ILLUSTRATIONS

Detailed modelling volatile FP release rates

- VERCORS 4 (38 GWd/tU, *He*/H_2 atm., T_{max}=2300C)

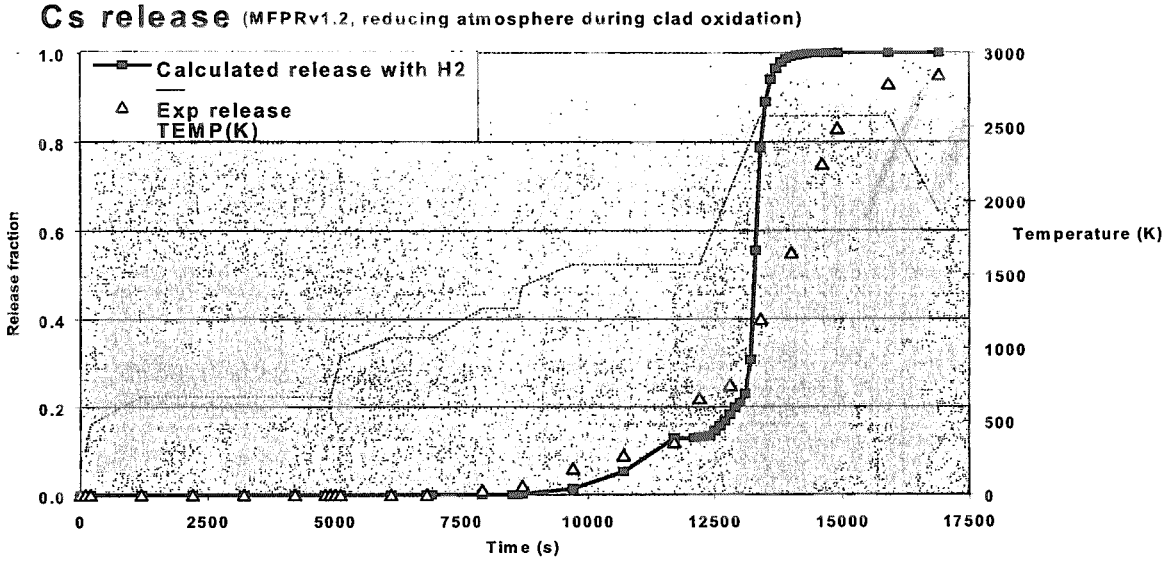
Xe release (MFPRv1.2 with grain boundary sweeping, Nelson model, no thermal re-solution, dislocation creep, 10-micron grain)



FP RELEASE AND TRANSPORT ANALYSIS IN SEVERE-ACCIDENT CONDITIONS: STRATEGY AND ILLUSTRATIONS

Detailed modelling volatile FP release rates

- VERCORS 5 (38 GWd/tU, H_2O atm., T_{max}=2300C)



FP RELEASE AND TRANSPORT ANALYSIS IN SEVERE-ACCIDENT CONDITIONS: STRATEGY AND ILLUSTRATIONS

Detailed modelling post-irradiation FP distribution

- **Why?**

  Influences release kinetics and swelling since, when the accident transient starts, a FP can be partly:
  - contained in intragranular bubbles (*Xe*, *Kr*);
  - dissolved in the fuel (*Xe*, *Kr*, *I*, *Cs*, *Te*, *Mo*, etc.);
  - contained in intergranular precipitates (*I*, *Cs*, *Ru*, *Mo*, etc.);
  - contained in intergranular bubbles (*Xe*, *Kr*).

- **How?**

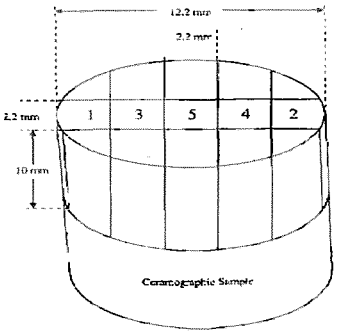
  AECL's Grain-Boundary Inventory tests are instructive providing data for fission gases, *Cs* and *I* ;

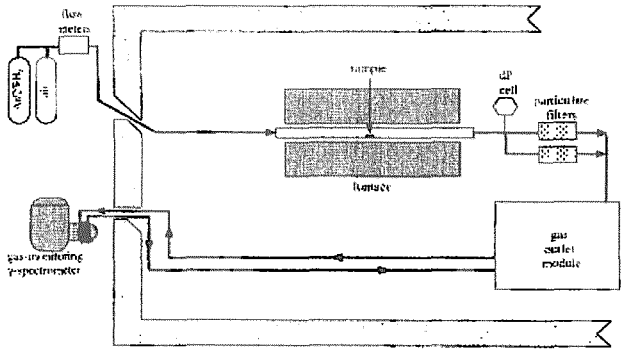
  used to validate the MFPR code.

FP RELEASE AND TRANSPORT ANALYSIS IN SEVERE-ACCIDENT CONDITIONS: STRATEGY AND ILLUSTRATIONS

Detailed modelling post-irradiation FP distribution

- **GBI experimental procedure:**
  - **reirradiate CANDU fuel**: create short-lived ^{133}Xe in grains so as to distinguish between intragranular gas & intergranular ^{85}Kr ;
  - **cut pellets radially**: 5 samples to study radial heterogeneity ;
  - **oxidize in air at 500C**: $UO_2 \rightarrow U_3O_8$ frees gas along grain boundaries.





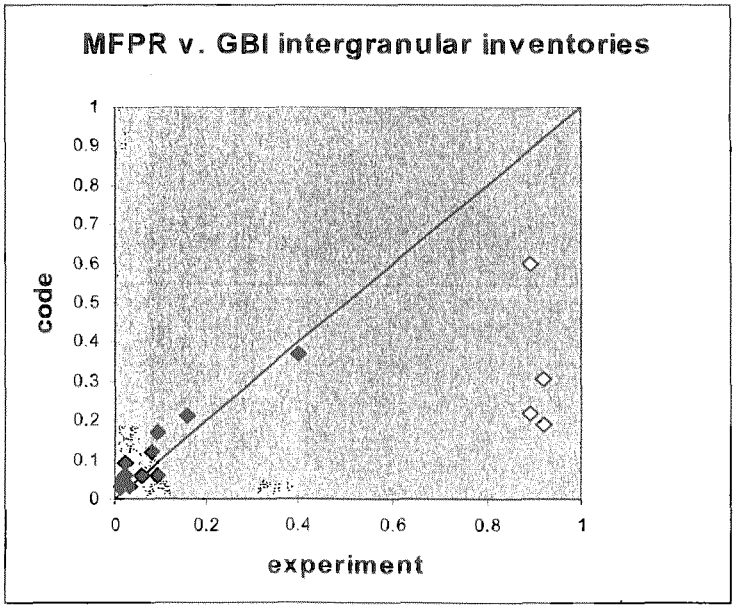
(see R.S.Dickson *et al.*, in 'Fission Gas Behaviour in Water Reactor Fuels', Seminar, Sept. 2000, Cadarache, Proceedings, pp337-346, OECD/NEA)

Schematic of Furnace Apparatus for GBI3, GBI5 and GBI6 Experiments

FP RELEASE AND TRANSPORT ANALYSIS IN SEVERE-ACCIDENT CONDITIONS: STRATEGY AND ILLUSTRATIONS

Detailed modelling post-irradiation FP distribution

- Pre-transient intergranular inventory can be very significant, ∝ irradiation T
- MFPR captures this trend with good reproduction of the intergranular gas fraction except for very high values (pellet centre with high irradiation T)



FP RELEASE AND TRANSPORT ANALYSIS IN SEVERE-ACCIDENT CONDITIONS: STRATEGY AND ILLUSTRATIONS

Detailed modelling near-point-of-release retention

- **Why?**

  Retention within the core of FPs such as
  - *I*, *Cs*, *Te*, *Sb*, etc. is not expected to be significant,
  - *Ce*, *Eu*, *La*, *Nb*, etc. is expected to be very high,
  - but what about "semi-volatile" FPs such as *Ba*, *Mo* and *Ru* ?

  Relocation of significant decay-heat emitters can affect degradation.

- **How?**

  Data from Phebus FP, VERCORS (and VEGA?) are instructive; used to validate the SOPHAEROS transport code which models
  - vapour-phase chemistry,
  - condensation (nucleation or on structures),
  - aerosol phenomena.

FP RELEASE AND TRANSPORT ANALYSIS IN SEVERE-ACCIDENT CONDITIONS: STRATEGY AND ILLUSTRATIONS

Detailed modelling near-point-of-release retention

- **VERCORS HT1**

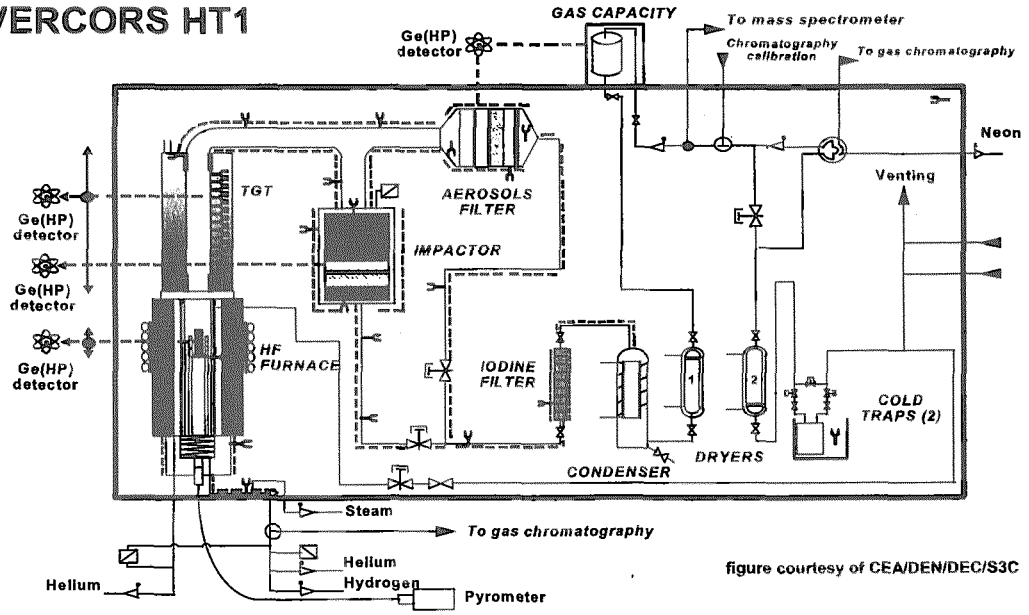


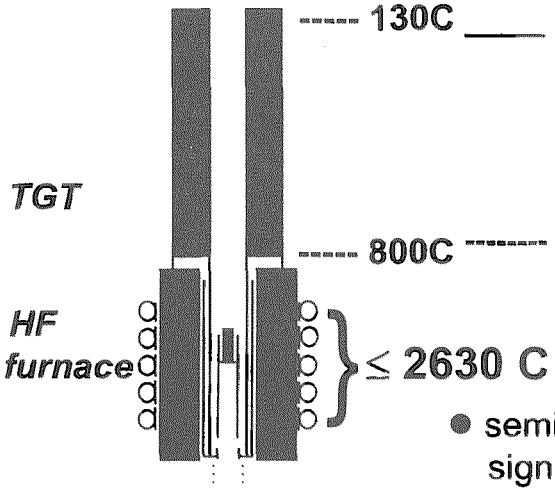
figure courtesy of CEA/DEN/DEC/S3C

INSTITUT DE PROTECTION ET DE SURETE NUCLEAIRE
DEPARTEMENT DE RECHERCHES EN SECURITE
CENTRE D'ETUDES DE CADARACHE

FP RELEASE AND TRANSPORT ANALYSIS IN SEVERE-ACCIDENT CONDITIONS: STRATEGY AND ILLUSTRATIONS

Detailed modelling near-point-of-release retention

- VERCORS HT1



retention / % of release			
Ba		*Mo*	
exp. data	code	exp. data	code
18	12	12	20
4	2	2	4
47	**4**	**53**	**35**

- semi-volatile FP deposition can be very significant near the point of release
- SOPHAEROS adequate for *Mo*, poor for *Ba*

FP RELEASE AND TRANSPORT ANALYSIS IN SEVERE-ACCIDENT CONDITIONS: STRATEGY AND ILLUSTRATIONS

Conclusions

- **Dual approach to FP release analysis is necessary and effective:**
  - in-depth understanding;
  - corroboration of simplifying modelling assumptions
  - relatively fast reactor analyses with improved confidence

- **Transport aspects within the core must not be neglected:**
  - in-core retention of FPs such as *Ce*, *Eu*, *La*, *Nb*, etc. is high;
  - in-core retention of semi-volatile FPs such as Ba, Mo, Ru, etc. can be significant dependent on ambient conditions;
  - comparable to FP relocation modifying both release to the RCS and decay-heat distribution in the core.

Discussion:

Q: (D. Schrire)

In Figure 3, detailed modeling of release. Do you have evidence (e.g. from EPMA) that specific mechanisms such as grain boundary sweeping vs diffusional release describe the release from grain to grain boundary ?

A: Evidence that these phenomena exist, yes, but not their relative importance, i.e. only qualitative evidence in general.

Q: (P.D.W. Bottomley)

In the molten pool model, Sn is treated as non-volatile but Sn in the cladding will volatise during Zircaloy oxidation. Would it better not be better to treat Sn as semi-volatile ?

A: There is no assumed volatility concerning Sn. Oxidation of the Zircaloy will release some of the, Sn, the remaining Sn will relocate, during degradation, to the molten pool as partially oxidized Zircaloy forms an eutectic with the UO_2. The key is proper coupling between release models and degradation modeling.

JP0250419

JAERI－Conf 2002－009

Session 4-5

Overview of fission product behaviour in the Phebus FP tests, including latest experimental results on the FPT2 test

M. Zabiégo[1], J.J. Cochaud[1], B. Cornu[1], Y. Garnier[1], J.M. Girard[1], G. Grégoire[1], D. Jacquemain[1], L. Pantera, E. Ragagli, P. Zavaleta[1], R. Zeyen[2]

[1]Institut de Protection et de Sûreté Nucléaire (IPSN), Département de Recherches en Sécurité (DRS)

[2]European Commission

CEA Cadarache, F-13108 Saint-Paul-lez-Durance, France

ABSTRACT

The *Phebus FP* program is a wide international effort to investigate *LWR* severe accident phenomena, through a series of in-pile integral experiments, dealing with fuel degradation, hydrogen production, fission product release and subsequent transport to the containment. Three tests simulating a low-pressure cold-leg break have already been successfully performed:

- *FPT0*, in December 1993, with trace-irradiated fuel and steam-rich atmosphere;
- *FPT1*, in July 1996, with re-irradiated fuel (*23-GWd/tU* fuel burn-up) and steam-rich atmosphere;
- *FPT2*, in October 2000, with re-irradiated fuel (*32-GWd/tU* fuel burn-up) and a significant reducing phase.

These tests provided experimental data of high interest, particularly regarding:

- Fuel degradation with prototypic bundle material;
- Fission product, fuel and structure material release from the test bundle;
- Transport and deposition in the model Reactor-Coolant-System (*RCS*, including a steam-generator model);
- Fission product behaviour in the model containment (including a sump model and reactor-representative painted surfaces), emphasising iodine source-term issues.

The data analysis of *FPT0* and *FPT1* is now terminated (and available in public domain literature), while that of *FPT2* is still under progress. The following observations can be made from these tests:

- All three tests resulted in the formation of a melted UO_2/ZrO_2 pool. The re-location temperature was significantly lower than expected in *FPT0* and *FPT1* (*< 2550 °K*).
- Main release/transport phases were found to correlate with specific bundle degradation events (zircaloy cladding oxidation and material re-locations).
- Volatile fission products (I, Cs, Te and Mo) and noble gases (Kr and Xe) were strongly released from the degraded fuel. Large fractions of these elements reached the containment vessel.
- Deposition in the *RCS* essentially occurred in the circuit hot-leg (in sections above the degraded fuel and at the entrance of the steam-generator), with larger deposits in *FPT2* (also characterised by significant deposits on the moderately-degraded upper-part of the fuel bundle) owing to the lower steam injection rate than in previous tests.
- Aerosols conveying fission products through the *RCS* were multi-component, with structure material dominant in mass.
- Gaseous iodine was transported in significant quantities to the containment vessel during zircaloy oxidation phases.
- Sump chemistry exhibited marked iodine trapping by silver (originating from the degradation of the Ag-In-Cd control rod), preventing the formation of volatile iodine by radiolysis and hydrolysis.
- On the long term, containment gaseous iodine species were dominated by organic iodides released from painted surfaces in *FPT0* and *FPT1*, and by molecular iodine in *FPT2*. These differences in gaseous iodine speciation may result from differences in release processes associated with trapping surfaces (painted condensers in *FPT1* versus stainless-steel vertical wall in *FPT2*).

The results of the *Phebus FP* programme are currently used by the different partners for validating and improving severe accident codes (ICARE/CATHARE, ATHLET-CD, SCDAP/RELAP5, ASTEC, MELCOR, ...). An example is given in the paper, regarding the interpretation of fission-products and control-rod-material release during the *FPT1* experiment, with code ELSA (with bundle degradation data from ICARE2).

Overview of fission product behaviour in the *Phebus-FP* tests, including latest experimental results on the *FPT2* test

M. Zabiégo, J.J. Cochaud, B. Cornu, Y. Garnier, J.M. Girard,
G. Grégoire, D. Jacquemain, L. Pantera, E. Ragagli, P. Zavaleta
Institut de Protection et de Sûreté Nucléaire (IPSN), Département de Recherches en Sécurité (DRS)
CEA Cadarache, F-13108 Saint-Paul-lez-Durance, France

Abstract

The *Phebus-FP* programme is a wide international effort to investigate *LWR* severe accident phenomena, through a series of in-pile integral experiments, dealing with fuel degradation, hydrogen production, fission product release and subsequent transport/deposition in the Reactor Coolant System down to the containment building. Three tests (*FPT0-2*) simulating a low-pressure cold-leg break have so far been successfully performed, which provide experimental data of high interest to characterise and improve *LWR* safety in the event of a severe accident. The data analysis of *FPT0* and *FPT1* is now terminated (and available in public domain literature for *FPT0*), while that of *FPT2* is still under progress[1]. The present paper gives a brief overview of the lessons learnt so far regarding fission product release, emphasising latest experimental results on the *FPT2* test.

1. Introduction

The *Phebus-FP* programme [1][2] is a wide international research programme, managed by the French *Institut de Protection et de Sûreté Nucléaire* (*IPSN*[2]), in collaboration with the *European Commission* and partner institutions: *EdF* (France), *USNRC* (United States of America), *COG* (Canada), *JAERI* and *NUPEC* (Japan), *HSK* and *PSI* (Switzerland), and *KAERI* (Korea). Its objective is to investigate, through a series of in-pile integral experiments, key phenomena involved in a Light Water Reactor (*LWR*) severe accident, in the frame of a low-pressure cold-leg break scenario. These include:

- Irradiated-fuel degradation, with prototypic material, under steam-rich or reducing conditions;
- Fission product (*FP*), fuel, control-rod and structure-material release from the test bundle;
- Released-material transport and deposition in the Reactor Coolant System (*RCS*);
- *FP* behaviour in the containment building, emphasising the iodine source-term issue.

As illustrated by the *Phebus-FP* test matrix shown in table 1, the experimental programme comprises six tests (*FPT0-FPT5*), four of which have already been successfully performed (*FPT0* [3], *FPT1* [4], *FPT2* [5] and *FPT4* [6]). Different partners currently use results obtained so far to:

- Validate accident codes (*ICARE/CATHARE, ATHLET-CD, SCDAP/RELAP5, ASTEC, MELCOR, ...*);
- Refine reference source-term evaluation;
- Evaluate accident management procedures;
- Assess the safety of next-generation power plants.

The experimental programme is conducted in the *Phebus-FP* facility[3], schematised in figure 1. Regarding the released *FP*s and their subsequent behaviour in the *RCS* and the containment building, the whole installation is scaled down by a factor *1:5000* relative to a *900-MWe* Pressurised Water Reactor (*PWR*).

Except for the *FPT4* test, which was performed with a fuel/cladding debris-bed, the test bundle, illustrated in figure 2, consists of twenty Zircaloy-cladded UO_2 fuel-rods[4], held in place[5] by two Zircaloy spacer-

[1] Owing to confidentiality constraints, *FPT2* results appear only qualitatively in this paper: access to quantitative data, to be distributed to partners of the programme by mid-2002 under the form of the *FPT2 preliminary report*, is temporarily restricted.
[2] Now *Institut de Radioprotection et de Sûreté Nucléaire* (*IRSN*).
[3] Operated by the *Commissariat à l'Energie Atomique*, at the *Cadarache* research centre, in France.
[4] Eighteen irradiated fuel rods and two fresh-fuel instrumented rods, with 1-metre-long fissile length. The irradiated fuel burn-up varies from one test to the other (see table 1).
[5] In a vertical position, following a 5×5 cornerless square lattice.

grids, with a stainless-steel-cladded control-rod[6] occupying the central position. Except for the *FPT3* test, which will be performed with Boron-Carbide (B_4C), the control-rod material is Silver-Indium-Cadmium (*SIC*). The fuel bundle is surrounded by an insulating ceramic shroud fitted into a pressure tube, cooled by an external pressurised water flow circulated through the experimental cell placed at the centre of the *40-MW Phebus* driver core, which provides nuclear power for the degradation of the test bundle. Some upward fluid flow is continuously sustained in between rods, during the bundle degradation, by some adjustable steam injection through a valve located at the bottom of the device. A fraction of the injected steam is converted to hydrogen (H_2) during partly-controlled oxidation phases[7].

The test bundle is connected, by its upper-plenum, to an experimental circuit that simulates the *RCS* of a *PWR*, including a Steam Generator (*SG*). The latter, which consists of one 4-metre-high inverted U-tube, insures temperature transition[8] between the circuit hot leg, regulated to *700 °C*, and the circuit cold leg, regulated to *150 °C*. Released material conveyed with the fluid flow through the fuel bundle and the experimental circuit, mostly under aerosol form, ends up in a *10 m^3* vessel simulating the containment building. This containment vessel is equipped with a water-filled sump and painted[9] surfaces, both properly scaled to analyse the Iodine containment behaviour under reactor-representative conditions.

The test bundle, the experimental circuit and the containment vessel are extensively instrumented, in order to collect the largest possible amount of data through the test. Data acquisition consists of both on-line measurements and sampling operations (for delayed analysis) performed at selected moments of the experimental sequence or on selected elements of the installation collected after the test:

- The bundle degradation kinetics is essentially characterised by thermocouple measurements, which detect heat-up phases, relocation events and the molten-pool progression with some fair spatial resolution.
- In addition to information provided by destructive physico-chemical analyses performed on a limited number of selected samples, the final state of the bundle is characterised by a large amount of post-test non-destructive examinations: radiographs, transmission tomograms, axial gamma scanning and gamma emission tomograms. The latter allow identifying the precise location of *FP*s left in the fuel zone, which contribute to the residual power.
- The *FP*-release kinetics[10] is characterised by both sampling data (circuit hot-leg and cold-leg) and on-line gamma-emission measurements obtained from gamma stations targeted at various positions along the experimental circuit and in the containment vessel. Measurements in the containment vessel are particularly important to refine the evaluation of the reference *environment* source-term. Iodine-specific measurements are performed by means of dedicated sampling devices, implementing selective filtering media that discriminate between chemical forms of iodine (molecular iodine versus organic iodides, for the gaseous fraction that subsists in the containment atmosphere on the long term).
- The concentration, the sizing and the chemical form of the aerosol populations present at different stages of the experimental sequence are documented by both post-test analyses of sampling data (impactors, filters and deposition coupons) and on-line photometric measurements (in the circuit hot-leg and the containment atmosphere).

The experimental sequence consists of several distinct phases:

- The short-lived *FP* inventory is first re-built during a ~9-day re-irradiation phase[11], followed by a transition phase aimed at preparing the installation for the actual experimental phase (bring down reactor Xenon poisoning, dry the bundle, establish desired boundary conditions: temperatures, pressures, steam flow, sump *pH*...).
- The ~5-hour degradation phase, illustrated in figure 3 for the *FPT1* and *FPT2* tests, proceeds through two main periods. After a thermal calibration period with gradual step-increase in the core power, the actual

[6] The control rod is held in a fixed fully-inserted position. It is not actually used as a control rod, but rather as source of prototypic material to allow reactor-representative material interactions to take place during and after the degradation process.
[7] Oxidation in the test bundle essentially involves the fuel-rods' Zircaloy cladding. The magnitude of the resulting hydrogen production is mostly controlled by adjusting the steam injection rate (relative to the power increase): pure reducing conditions are transiently achieved in *FPT2*, by lowering the steam injection rate to *0.5 g/s*, to compare with *2.2 g/s* in *FPT1*.
[8] The temperature regulation transition is located at the *SG* inlet. Regulation of circuit-wall temperature aims at characterising deposits in the *RCS*.
[9] Painted surfaces, of the *Ripolin Epoxy* type used by *EdF* in French power plants, play a key role regarding the *environment* source-term issue, as a source of gaseous organic iodides that appears to represent a major contribution to the potential radiological hazard in the event of an *FP* release beyond the plant limits.
[10] Regarding validation of *FP*-release-codes (such as ELSA), it must be noted that no direct measurement of the release kinetics at the fuel level is actually obtained from *Phebus-FP* tests. As a result, experimental measurements must be corrected of deposits in the experimental circuit before comparison to code calculations.
[11] The fuel bundle is cooled by some pressurised water flow through this phase.

bundle temperature escalation is initiated. The degradation starts[12] by an oxidation runaway[13], leading to the *SIC* control-rod rupture[14], followed by the first major *FP* release[15]. After the oxidation runaway, when steam-rich conditions have been restored in the bundle, a heat-up phase is conducted by applying a steady power ramp-up to the bundle until degradation objectives[16] are reached, concluding this phase by the reactor shutdown. Material relocation occurs through the heat-up phase, producing some oxidation in the lower part of the test bundle[17], and the formation/progression of a molten pool. *FP*s and structure material are significantly released during the relocation phase, unambiguously pointing to the relationship between degradation and release events.

- A few hours after the reactor shutdown, the so-called aerosol phase is initiated by isolating the containment vessel from the test bundle and the experimental circuit. The objective of this phase is to analyse the settling of aerosols in suspension in the containment atmosphere, in the absence of condensation[18].
- After 1.5-3 days, when most aerosols have been deposited on the containment bottom[19], a washing phase is performed by draining deposited aerosols to the sump by means of some sump-water spray applied to the containment floor during ~20 minutes.
- The draining of deposited aerosols to the sump aims at taking full benefit of potential radiolysis processes[20] on the long-term sump chemistry. This so-called chemistry phase, which lasts ~1.5-3 days, is particularly devoted to studying the iodine source-term issue, under the more realistic possible conditions. The influence of sump conditions on exchanges with the containment atmosphere and boundary surfaces (emphasising the role of painted surfaces on the gaseous iodine speciation) can be adjusted by varying the sump *pH* and/or temperature.

2. Fuel degradation

Considering that the objective of the present paper is to report on the *FP* behaviour, this section exclusively comments on the final state of the test bundle, as documented by post-test non-destructive examinations. Important results, obtained from the *Phebus-FP* tests performed so far, regarding degradation processes and their kinetics, are not detailed here: details can be found in a separate publication [7]. The most important finding, in this respect, is the observation of a fuel relocation temperature *~200-300 °C* lower than the UO_2/ZrO_2 melting point: in the *FPT0* (resp. *FPT1*) test, *~2200±100 °C* (resp. *2150±100 °C*) for the estimated fuel liquefaction temperature, versus *~2447±30 °C* (*2487±25 °C*) for the post-test measured corium melting point. Although this point is not completely clarified[21] yet, degradation codes (such as *ICARE2 [8]*) have been modified to account for the low relocation temperature observed in *Phebus-FP* tests. In *FPT2*, the estimated relocation temperature is higher than in *FPT0* and *FPT1*, but disagreements with *ICARE2* pre-calculations were observed

[12] Degradation actually starts during the thermal calibration phase, by the early fuel-clad failure, detected by both photometric measurements of some sparse aerosol population in the experimental circuit, and spectrometric measurements of a minor Xenon release in the containment atmosphere.

[13] The progression of the Zircaloy fuel-clad oxidation-front, away from the maximum-power-flux level, is followed by thermocouples and ultra-sonic-thermometers distributed axially in the bundle. While it only briefly peaked to *50 %* in *FPT1*, steam consumption was total, over a significant steam-starvation phase, in the *FPT2* test, thereby transiently providing pure reducing conditions in the upper part of the bundle and through the experimental circuit.

[14] This event is detected by photometric measurements, both in the experimental circuit and the containment atmosphere. In *FPT2*, the observation that aerosol photometric detection occurs earlier in the containment atmosphere than in the circuit hot-leg suggests that the initial aerosol release-burst consists of Cadmium (which cannot be detected in the circuit hot-leg where it exists under vapour form only).

[15] This event is detected by on-line gamma-stations, both in the circuit and in the containment atmosphere, and further quantified (in terms of the composition of the released material) by delayed analysis of samplings triggered through this phase.

[16] Degradation objectives are expressed in terms of some relocated material mass and/or some liquefied material mass, carefully estimated from bundle temperature measurements, on the basis of pre-calculations with the ICARE2 code. Alternatively, pre-defined safety-related criteria can lead to the reactor scram, but this situation was never encountered in the tests performed so far.

[17] This oxidation results from the local temperature increase induced by the relocation of hot material in the lower part of the bundle.

[18] During the degradation phase, the gravitational settling mechanism is in competition with diffusiophoresis (entrainment of aerosols by condensation on the containment condensers), and to a lesser degree with deposition on the vertical stainless-steel containment wall (by mechanisms yet to be clarified: wall heated-up to avoid condensation).

[19] Aerosols deposit both directly into the sump and on the containment bottom end, but the latter dominates owing to the associated 1/8 deposition-surface ratio between the sump/atmosphere interface and the containment floor.

[20] In this respect, the *FPT0* test, performed with fresh pre-irradiated fuel, is less representative than the *FPT1* and *FPT2* tests, owing to its lower *FP* inventory and resulting dose rate.

[21] The reasons for the low relocation temperature are at present uncertain, but are being investigated by separate-effects tests and modelling studies, which include looking at the dissolution of irradiated fuel by molten Zircaloy, and the effects of iron and chromium oxides on reducing the melting temperature of corium mixtures.

concerning the molten-pool progression. Regarding the comparison of *FP*-release kinetics, between *FPT2*, on the one hand, and *FPT0* & *FPT1*, on the other hand, it is worth noting that degradation was more progressive in *FPT2*: owing to the lower steam injection rate, the propagation of the Zircaloy oxidation front away from the maximum-power-flux level was slower in *FPT2*, as a result of the reduced steam availability in the upper part of the bundle.

Material relocation, throughout the degradation phase, is primarily documented by post-test non-destructive examinations of the bundle. Radiographs, illustrated in figure 4 for tests *FPT0-FPT2* (with same scale in the density colour-code), provide some clear picture of the bundle final state. These are complemented by transmission tomograms, which provide a 3-dimensional density map of the degraded bundle. Some transmission tomograms of the *FPT2* bundle are shown in figure 5, illustrating the material distribution at selected axial positions representative of various characteristic zones:

- The lower part of the bundle exhibits moderately degraded fuel rods, with some material accumulation in between rods. All twenty fuel rods can be identified (some of them with fragmented fuel pellets) in the second tomogram (level *30 mm/BFC*, *i.e.*, above the Bottom of the Fissile Column), while the *SIC* control-rod leaves an empty space at the centre of the column.
- Upwards in the bundle, a molten-pool can be identified, which is more extended in *FPT2* than in *FPT0* and *FPT1* (see figure 4). The bundle axial mass-distribution profile, illustrated in figure 7, indicates that relocated material primarily ends up in the molten pool. An overall post-test mass-excess is found in the bundle, which is essentially accounted for by molten-pool material and may be attributed to the Zircaloy fuel-clad oxidation[22], consistently with hydrogen production measurements. In figure 6, gamma scanning of ^{95}Zr (known to be a fair fuel tracer) and ^{110m}Ag (an activation product of Silver from the control-rod), indicate that fuel and control-rod material primarily relocate in and below the molten-pool, respectively. Further investigations confirm that the molten-pool consists of a UO_2/ZrO_2 mixture.
- Above the molten-pool, a cavity (where relocated material essentially originates from) is visible; clearly in *FPT0* and *FPT2* where it vertically extends over *~1/3* of the bundle, with no rod-remnant left over a significant extension; less in *FPT1* where degradation is more limited (although faster than in *FPT2*, as mentioned above), with deformed rods left in place at the bundle periphery all along the cavity.
- At the top of the bundle, rod remnants are left in place; in a moderately degraded state in *FPT2*, owing to the progressive character of the degradation, as opposed to *FPT0* and *FPT1*.

3. Fission product behaviour

FP release is measured both on-line (by gamma stations located at various locations along the *RCS* and in the containment) and through sampling devices (operated at selected times through the test, for delayed analysis). *FP* release from the fuel itself can be characterised by post-test analyses only, *i.e.*, with no direct information regarding kinetics. Table 2 summarises quantitative release results for representative elements (fuel, control-rod and structure material, in additions to *FP*s). Quantitative results for *FPT2* are presently restricted, but tendencies are in general agreement with those presented for *FPT0* and *FPT1*. Releases are documented under two forms, relative to the initial bundle inventory[23]: the fraction left in the fuel[24], which relates to the residual-power issue, and the fraction released to the containment[25], which relates to the *environment* source-term issue. The main comments regarding results shown in table 2 are the following:

- Noble gases (Xe & Kr) and volatile *FP*s (primarily I, Cs, Te) are almost entirely released from fuel. Regarding the residual-power issue, these generally have a low contribution. However, it is observed, that released volatile *FP*s can deposit in the upper fuel zone, where they then contribute to the residual power. As illustrated in figure 8 for ^{137}Cs, the volatile-*FP* inventory at the level of rod-remnants in the upper-part of the degraded bundle is typically doubled[26] in *FPT2*, while it is nearly entirely depleted[27] in *FPT1*. This observation is consistent with both the more extensive degradation and the higher fluid flow in *FPT1* relative

[22] $Zr + 2\ H_2O \rightarrow ZrO_2 + 2\ H_2$, leaves a *32 g* mass-excess in the bundle for each mole of oxidised Zirconium.
[23] As far as *FP*s and activation products are concerned, this initial bundle inventory is calculated by taking the whole irradiation history into account.
[24] This is either measured by post-test gamma scanning of the bundle (data expressed with an uncertainty), or deduced from cumulative measurements of the inventory transported through the circuit hot-leg (data expressed by an upper-bound).
[25] This cumulated release is deduced from on-line activity measurements in the containment atmosphere, by correcting the latter from radioactive decay and containment deposits.
[26] In figure 8, two extreme hypotheses are considered for the analysis of the *FPT2* gamma scanning: ^{137}Cs is distributed either in the fuel or on the shroud. Preliminary results from emission tomograms indicate that the distribution is roughly halfway between these two hypotheses, suggesting that releases that deposit in the upper-part of the bundle are mostly located on the shroud.
[27] Volatile-*FP* depletion in *FPT1* is due to the important degradation achieved in the upper-part of the bundle.

to *FPT2*. A released fraction of these elements in excess of *50 %*, relative to the initial inventory, reaches the containment vessel, where they are potentially available for release beyond the plant limit (the so-called *environment* source-term). Deposits in the experimental circuit, which appear to be significant for all species except for noble gases, can be estimated as the complement of the combined fuel and containment inventories to *100 %*.

- Low-volatile elements are identified, which almost entirely remain in the fuel zone, where they contribute to the residual power. These include fuel material (U, Np, Pu) and *FP*s (Ba, Sr, Ru, Zr, Nb, La, Ce, Nd, Sm). The finding that Barium is only weakly released from fuel (less than *1 %* of the initial inventory[28]) contrasts with observations made in the separate-effects experiments *HI/VI* [9] and *HeVa/Vercors* [10], which led to recommending some ~ *50 %* release for this element [11]. Some tentative interpretation of this discrepancy is discussed in reference [12].
- Intermediate between volatile and low-volatile elements, semi-volatile species are identified. These include *FP*s (Sb, Mo and Tc), control-rod material (Ag, In and Cd), structure material (Sn, Fe, Co) and the non-prototypic Re associated with bundle instrumentation.
- Material transported to the containment, mostly under a multi-component aerosol form, mainly consists of Ag (~ *30 w%*), Re (~ *30 w%*), Sn (~ *10 w%*), U (*5-10 w%*, although weakly released relative to the initial inventory), In (~ *5-10 w%*) and Cd (~ *5 w%*). Regarding *FP*s, present in significant quantities in the *FPT1* test only (pending *FPT2* data), Mo and Cs, which have the largest initial inventory, bring a significant contribution to the aerosol composition: ~ *5 w%* each. Modelling attempts indicate that Molybdenum could play a key role in the circuit chemistry through the formation of Cs_2MoO_4 (except during reducing phases when Mo release is inhibited). Indeed, this could have hindered the initially expected CsOH and CsI formation, thus subsequently affecting such issues as the Iodine release to the containment.

FPT2 results regarding *FP*-release kinetics are illustrated[29] in figure 9, together with on-line aerosol-concentration measurements in the containment atmosphere. The following comments can be made on this figure:

- Significant aerosol release to the containment is detected first, prior to the steam-starvation phase. This event, related to some control-rod failure signature on bundle thermocouples, is not detected by aerosol-concentration measurements in the circuit hot-leg, suggesting that the detected aerosol release consists of Cadmium from the control-rod.
- The first significant *FP* release is observed at about the beginning of the steam-starvation phase. Xenon exhibits a faster[30] initial release-kinetics than Iodine and Caesium, which are themselves released to the containment faster than Tellurium and Molybdenum.
- Molybdenum release is delayed to after the steam-starvation phase, consistently with the well known low-volatility of its metallic form (*i.e.*, the only existing form under the reducing conditions of the steam-starvation phase), as opposed to its oxide form (which is produced only after the steam-starvation phase).
- The case of Tellurium is very instructive. Tellurium is characterised by important circuit deposits in *FPT2*, as illustrated in figure 10, where kinetic differences between circuit deposits and containment accumulation of ^{132}Te are visible, mostly during the steam-starvation phase[31]. Figure 10 points to the difficulty of estimating the release-from-fuel kinetics (considered by codes such as *ELSA*) from the release-to-containment kinetics (which consists of the prime piece of data obtained from *Phebus-FP* tests to characterise *FP*-release kinetics), if no accurate measurements/modelling of transport phenomena are made available. Whether

[28] This upper-bound is validated for *FPT0* and *FPT1*, both performed with steam-rich conditions. Regarding *FPT2*, preliminary results seem to confirm this tendency, despite the occurrence of a significant pure-reducing phase, which was found to favour Barium release in *Heva/Vercors* tests [10]. The latter remark must be balanced with the fact that, in *Heva/Vercors* tests, Barium release was found to occur above some temperature threshold which might not be reached during the *FPT2* steam-starvation phase, or possibly reached only locally (owing to the important temperature gradient through the *Phebus-FP* bundle) and thus leading to subsequent deposits at colder locations above the release zone.

[29] Activities shown in figure 9 are normalised to their value at the time of the reactor shutdown. They correspond to on-line activity measurements in the containment atmosphere, corrected for both radioactive decay and deposition processes in order to obtain the cumulated activity injected into the containment through the degradation/release phase.

[30] Differences between noble-gas and volatile-*FP* release are not abnormal. On the one hand, noble gases do not interact with circuit material, contrary to volatile *FP*s, so that differences in noble-gas and volatile-*FP* release to the containment are possibly accounted for by differences in circuit deposits. On the other hand, fundamental release processes are different for noble gases (bubbling) and volatile *FP*s (grain diffusion).

[31] Temperature regulation systems transiently failed to maintain circuit hot-leg temperature at *700* °C during the steam-starvation phase, for reasons probably related to the high hydrogen concentration, but yet to be clarified. Important unplanned deposits certainly occurred in *cold* zones (inlet of circuit hot-leg and inlet of *SG*).

Tellurium circuit deposits can account for the slower initial release kinetics of this element relative to other volatile *FP*s is yet to be elucidated[32].

- *FP* release to the containment occurs at a fairly steady rate after the steam-starvation phase (except for Tellurium, as mentioned above), in agreement with the fact that bundle degradation is progressive in *FPT2*.
- Despite the continued temperature increase in the bundle until the reactor shutdown (more than *30* minutes later), *FP* release to the containment appears to significantly[33] slow-down through the phase identified by bundle thermocouple measurements as the molten-pool formation/progression.

4. Iodine-specific results

In the context of a severe *LWR* accident, iodine plays a key role regarding the *environment* source-term issue, given its large contribution to potential radiological hazards in the event of a short-term gaseous release to the environment by containment depressurisation or leakage. The *Phebus-FP* programme specifically aims at studying this issue[34], under reactor-representative conditions and with some important dedicated instrumentation (filtering media allowing discrimination between various forms of iodine). The following results have been obtained so far:

- Gaseous iodine is measured in significant quantities in the containment atmosphere during Zircaloy oxidation phases. Its concentration significantly decays after the reactor shutdown, when long-term equilibrium is controlled by exchanges between the atmosphere, the sump solution and boundary surfaces, which mostly emphasise to role of painted surfaces in producing organic iodides. The short-term kinetics are illustrated in figure 11, for the *FPT2* test. Owing to the sparseness of samplings available through the degradation phase, it is not possible to assess whether gaseous iodine is injected from the experimental circuit or produced in-situ. The long-term gaseous-iodine behaviour is illustrated in figure 12, providing a comparison between *FPT1* and *FPT2* results[35]. Gaseous iodine represents typically less than *0.1 %* of the total iodine containment inventory in the long term, as far as *FPT1* is concerned.
- The lower gaseous-iodine containment concentration after the reactor shutdown appears primarily related to the marked iodine trapping by Silver (AgI formation) originating from the *SIC* control-rod and deposited into the sump (as mentioned above, Ag represents a large fraction of the aerosol material released to the containment). This trapping effect appears very efficient under acidic sump conditions specific to *FPT0* and *FPT1* (*pH-5*). It tends to inhibit the formation of volatile gaseous iodine species by radiolysis[36], which is usually favoured by acidic sump conditions. The increase in gaseous-iodine concentration observed at the beginning of the chemistry phase in *FPT1*, results from the draining of aerosols (settled on the containment bottom during the aerosol phase) into the sump during the washing phase. This effect, which is correctly modelled by codes, was not observed in *FPT0*, owing to the higher Silver/Iodine concentration ratio and resulting trapping effect than in *FPT1* (burn-up differences). In the *FPT2* test, performed with basic sump conditions[37] (*pH-9*), some further decrease in gaseous iodine concentration is observed through the chemistry phase (see figure 12). This decrease, initiated after the washing phase, correlates with some increase in sump temperature[38], which is expected to strengthen the destruction of volatile iodine species by hydrolysis under *pH-9* sump conditions.
- Discrimination between chemical forms of gaseous iodine is investigated in *Phebus-FP* tests by implementing specific filtering media, with particular attention paid to molecular/organic speciation. Organic iodides are produced by interaction with reactor-representative painted surfaces (condensing surface

[32] Tellurium release is also known to be reduced by some Zircaloy-clad trapping effect if cladding oxidation is only partial [13]. Owing to the progressive character of the degradation in *FPT2* (slower propagation of the oxidation front, relative to *FPT0* and *FPT1*), delayed Te-release could partly result from this effect. This is particularly suggested by the transient sharp-increase in Te-release during the second oxidation peak, identified as the *first-fuel-relocation* in figure 9, based on bundle thermocouple measurements. The oxidation of a lower zone of the bundle through this phase could account for delayed Tellurium release from the previously weakly-oxidised Zircaloy-cladding there (while no such release is observed for Iodine and Caesium, which are not trapped by the Zircaloy-cladding, whatever its oxidation state, when they escape fuel by grain diffusion).

[33] Nonetheless, as illustrated in figure 9, ^{132}Te release appears only moderately slowed-down on circuit hot-leg measurements. Circuit measurements being only partly available at this stage of the analysis, this difference will have to be clarified.

[34] Acknowledged as of prime importance by a panel of international experts representing the industry, utilities, nuclear research organisations and regulatory institutions [14].

[35] Results are given in arbitrary units for *FPT2*, owing to temporary restricted use of quantitative data to partners of the programme.

[36] Dushman's reaction (*i.e.*, inverse hydrolysis) also contributes to gaseous iodine formation, but radiolysis dominates under *pH-5* sump conditions.

[37] Basic sump conditions somewhat inhibit AgI formation by hindering the intermediate step of Ag oxidation.

[38] Sump temperature increases from *90 °C* through the degradation and aerosol phases to *120 °C* through the chemistry phase.

exposed to the containment atmosphere, which collects released material deposited by diffusiophoresis, and immersed surface exposed to the sump solution). In both *FPT0* and *FPT1*, organic iodides were the dominant species through all the long-term phase: iodine release from painted condensers was observed early in the aerosol phase. On the contrary, preliminary results indicate that molecular iodine dominated[39] in *FPT2*. Owing to the lower steam injection rate, in *FPT2* relative to *FPT1*, diffusiophoresis was less important in *FPT2*. As a result, competing deposits on the stainless-steel containment-wall were found to be substantially larger in *FPT2* than in *FPT1*, thus reinforcing the molecular-iodine source[40] (desorption from stainless-steel containment-wall) at the expense of the organic-iodide source (desorption from painted condensers).

In all tests performed so far, volatile iodine formation is strongly limited. In *FPT0* and *FPT1*, performed with acidic (*pH-5*) *cold* (*90 °C*) sump conditions, this results from iodine trapping through AgI formation in the sump. In *FPT2*, performed with basic (*pH-9*) *warm* (*120 °C*, through the chemistry phase) sump conditions, this results from volatile iodine destruction by hydrolysis. The *FPT3* test, planned for end-2003, will be performed with no *SIC* control-rod (B_4C instead), and acidic (*pH-5*) *warm* (*120 °C*, through the chemistry phase) sump conditions, which should favour gaseous iodine formation.

5. Conclusion

The *Phebus-FP* programme is a wide international effort to investigate *LWR* severe accident phenomena, through a series of in-pile integral experiments, dealing with fuel degradation, hydrogen production, Fission Product (*FP*) release and subsequent transport/deposition in the Reactor Coolant System (*RCS*) down to the containment building. Three tests (*FPT0,1&2*) simulating a low-pressure cold-leg break have so far been successfully performed, which provide experimental data of high interest to characterise and improve *LWR* safety in the event of a severe accident, particularly regarding:

- Irradiated fuel degradation, with prototypic material, under steam-rich or steam-poor conditions;
- *FP*, fuel, control-rod and structure-material release from the test bundle;
- Released-material transport and deposition in the *RCS*;
- *FP* behaviour in the containment building, emphasising the iodine source-term issue.

The data analysis of *FPT0* and *FPT1* is now terminated (and available in public domain literature, as far as *FPT0* is concerned), while that of *FPT2* is still in progress[41]. The following observations can be made from these tests:

- All three tests resulted in the formation of a melted UO_2/ZrO_2 pool. In *FPT0* and *FPT1*, the relocation temperature was significantly lower than the UO_2/ZrO_2 melting point. Relocation temperature was somewhat higher in *FPT2*, but discrepancies were found between experimental results and *ICARE2* pre-calculation regarding the molten-pool progression.
- Main release/transport phases were found to correlate with specific bundle degradation events (Zircaloy cladding oxidation and material relocations).
- Volatile *FP*s (I, Cs, Te, Sb and Mo) and noble gases (Kr and Xe) were strongly released from the degraded fuel. Large fractions of these elements reached the containment vessel.
- Deposition in the *RCS* essentially occurred in the circuit hot-leg (in sections above the degraded fuel and at the entrance of the steam generator), with larger deposits in *FPT2* owing to the lower steam injection rate relative to previous tests. The *FPT2* test is also characterised by significant deposits on the moderately-degraded upper-part of the fuel bundle.
- Aerosols conveying *FP*s through the *RCS* were multi-component, with structure material dominant in mass.
- Gaseous iodine was transported in significant quantities to the containment vessel during Zircaloy oxidation phases.
- Sump chemistry exhibited marked iodine trapping by silver (originating from the degradation of the Ag-In-Cd control rod), preventing the formation of volatile iodine by radiolysis in *FPT0* and *FPT1*. In *FPT2*, gaseous iodine formation was further limited on the long term, owing to warm and basic sump conditions (*120 °C* and *pH-9*, versus *90 °C* and *pH-5* in *FPT0* and *FPT1*), which favoured gaseous iodine destruction by hydrolysis.

[39] This result must be balanced with the fact that no iodine speciation measurement was available through the late chemistry phase (owing to instrumentation difficulties), when organic iodide release from painted surfaces was eventually observed.
[40] In this respects, *FPT2* is not strictly reactor-representative regarding iodine speciation, since stainless-steel surfaces are not properly scaled with the *1:5000* factor relative to a *900 MWe PWR* applied to painted surfaces (the effective scale factor of stainless-steel surfaces is larger than *1:5000*, implying that molecular iodine production is over-estimated).
[41] Owing to confidentiality constraints, *FPT2* results appear only qualitatively in this paper: access to quantitative data, to be distributed to partners of the programme by mid-2002 under the form of the *FPT2 preliminary report*, is temporarily restricted.

- On the long term, containment gaseous iodine species were dominated by organic iodides released from painted surfaces in *FPT0* and *FPT1*, and by molecular iodine in *FPT2*. These differences in gaseous iodine speciation may result from differences in desorption processes associated with trapping surfaces (painted condensers in *FPT0* & *FPT1* versus stainless-steel vertical wall in *FPT2*).

The execution of the *FPT3* test, planned for end-2003, with a B_4C control-rod (hence different interactions), should provide interesting complementary results. On the longer term, these experimental efforts should be pursued by carrying out complementary programmes in the *Phebus* facility, emphasising such issues as high-burnup and MOX fuel behaviour under severe accident conditions, possibly including re-flooding and subsequent quenching of the degraded test bundle, as described in the companion paper [15].

Acknowledgements

B. Clément, T.J. Haste, G. Ducros and R. Dubourg are acknowledged for interesting discussions. A. Jones, E. Krausmann, K. Mueller, M. Schwarz and R. Zeyen are acknowledged for comments they made on the manuscript. The synthesis of *FPT0* and *FPT1* results is largely inspired of the report (in French): B. Clément and M. Schwarz, *Les enseignements tirés du programme Phébus-PF*, document Phébus PF IP/99/451 (October 1999) - Private communication.

References

[1] P. von der Hart, A.V. Jones, C. Leconte and A. Tattegrain, *Nuclear safety research - The Phebus-FP severe accident experimental programme*, Nuclear Safety **35** (1994) 187.

[2] M. Schwarz, B. Clément and A.V. Jones, *Applicability of Phebus FP results to severe accident safety evaluations and management measures*, Nuclear Engineering and Design **209** (2001) 173.

[3] N. Hanniet and G. Repetto, *FPT0 final report*, document Phébus PF IP/99/423 (February 1999) - Private communication.

[4] D. Jacquemain, S. Bourdon, A. de-Bremaecker and M. Barrachin, *FPT1 final report*, document Phébus PF IP/00/479 (September 2000) - Private communication.

[5] G. Ritter, M. Zabiégo et al., *FPT2 preliminary report*, to be delivered to partners of the *Phebus-FP* programme by mid 2002 - Private communication.

[6] M.C. Anselmet, F. Jeury S. Bourdon, S. Bayle, C. Cochaud, F. Arreghini, G. Grégoire and D. Jacquemain, *FPT4 preliminary report*, document Phébus PF IP/00/481 (November 2000) - Private communication.

[7] S. Bourdon et al., *Phebus FPT0 and FPT1 preliminary synthesis of the test analyses using the ICARE2 code*, report Phebus PF IP/98/409 (1998).

[8] R. Gonzalez, P. Chatelard and F. Jacq, *ICARE2 - A computer program for severe core damage analysis in LWRs*, report NT SEMAR 93/33 (1993).

[9] R. Lorenz and M. Osborne, *A summary of ORNL fission product release test with recommended release rates and diffusion coefficients*, report NUREG/CR-6261 (July 1995).

[10] J.P. Leveque, B. Andre, G. Ducros, G. Le Marois and G. Lhiaubet, *The HeVa experimental program*, Nuclear Technology **108** (1994) 33.
G. Ducros, P.P. Malgouyres, M. Kissane, D. Boulaud and M. Durin, *Fission product release under severe accidental conditions: general presentation of the program and synthesis of VERCORS 1-6 results*, Nuclear Engineering and Design **208** (2001) 191.

[11] G. Ducros, *Relâchement des produits de fission et actinides en situation d'accident grave de REP: synthèse expérimentale*, CR-DEC/SECC n°98.008A (1998) - in french.

[12] R. Dubourg and P. Taylor, *A qualitative comparison of Barium behaviour in the Phebus FPT0 test and analytical tests*, Journal of Nuclear Material **294** (2001) 32.

[13] F.C. Iglesias, B.J. Lewis, P.J. Reid and P. Elder, *Fission product release mechanisms during reactor accident conditions*, Journal of Nuclear Material **270** (1999) 21.

[14] B. Clément and J. Brisbois, *Use of Phebus-FP results for safety evaluation of severe accidents*, CSARP meeting (Albuquerque, May 1999); or report of the Ad-Hoc Group (Chairman: J. Brisbois - Technical secretary: B. Clément), *Impact of Phebus-FP test results on severe accident safety evaluation*, document Phébus PF IP/99/424 (March 1999).

[15] A. Maillat, *IPSN Future Programmes in the Phebus Facility*, this meeting.

Tables

Test	Type of fuel	Fuel bundle	Primary circuit	Containment vessel	Date
FPT-0	20 fresh fuel rods, 1 Ag-In-Cd (SIC) control rod, 9-day pre-irradiation	Melt progression & FP release in steam-rich conditions	FP chemistry & deposits	Aerosol deposition, Iodine radiochemistry with pH-5 / 90°C condensing sump	Dec. 2, 1993
FPT-1	BR3 fuel ~23GWd/tU, 1 SIC control rod, 9-day re-irradiation	As FPT-0 with irradiated fuel	As FPT-0	As FPT-0	July 26, 1996
FPT-2	BR3 fuel ~32GWd/tU, 1 SIC control rod, 9-day re-irradiation	As FPT-1with steam poor conditions & boric acid injection	As FPT-1 with steam-poor conditions & boric acid	pH-9 / 120°C evaporating sump	Oct. 12, 2000
FPT-3	As FPT-1, but with 1 B_4C control rod	As FPT-2 with B_4C products instead of boric acid	As FPT-2 with B_4C products instead of boric acid	pH-5 / 120°C evaporating sump, H_2 recombiner coupons	end 2003
FPT-4	EdF fuel ~38GWd/tU in fragments, No re-irradiation	Low volatile FP & actinide release from UO_2/ZrO_2 debris bed, up to melting	Integral filters in test device Post-test studies on samples		July 22, 1999
FPT-5	Fuel degradation, FP release/deposition/chemistry in air conditions, likely to be postponed to Phebus-2K programme				

Table 1
The *Phebus-FP* test matrix

Initial inventory (i.i.) Left in bundle Release to containment	FPT0 (fresh fuel +9-day re-irradiation)			FPT1 (23 GWd/tU + 9-day re-irradiation)		
	i.i. [g]	Fuel [%i.i.]	Containment [%i.i.]	i.i. [g]	Fuel [%i.i.]	Containment [%i.i.]
Noble gases						
Kr	-			2.55	16	84
Xe	-			29.6	22.6	77.4
Volatile FPs						
I	*0.036*	< 13.5	63	1.12	13 ± 4	64.1
Cs	*0.144*	< 40	51.2	15.9	16 ± 0.8	43.8
Te	*0.0473*	< 9	79	2.54	17 ± 1	52.5
Sb	*0.00114*	< 37	56	0.05	-	31.2
Mo	-			20.2	44 ± 4	23
Low-volatile FPs						
Ba (Sr & Ru)	*0.149*	< 99.17	0.6	10.1	< 98.96	0.65
Zr	*0.281*	< 99.965	0.0084	24.3	< 99.97	0.015
Control rod material						
Ag	477	< 87.2	10.5	477	85 ± 5	6.7
In	90	< 90.9	8.3	90	< 91	7.8
Cd	30	< 53	19	30	< 33.3	> 10.4
Fuel & structure material						
U	10500	< 99.87	0.065	9160	< 99.86	0.119
Sn	50.6	< 78.6	20	49.5	< 61.6	> 11.9

Table 2
Release summary table for *FPT0* and *FPT1*, including data for fission products, fuel, control-rod and structure material. For each test and considered element, the first column indicates the initial bundle inventory in grams, the second column indicates the fraction of the initial bundle inventory left into the bundle (related to the residual power issue), the third column indicates the fraction of the initial bundle inventory that reached the containment vessel (related to the *environment* source-term issue).

Figures

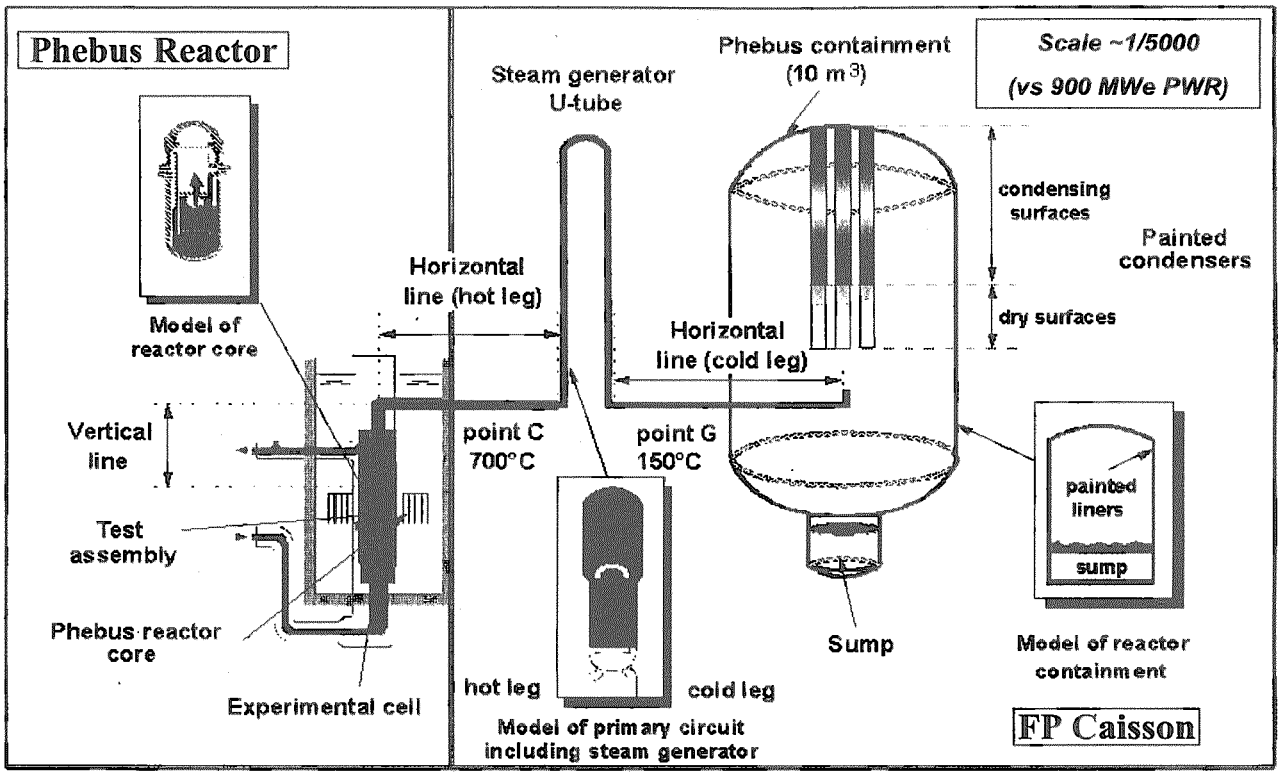


Figure 1
Schematic view of the *Phebus-FP* installation

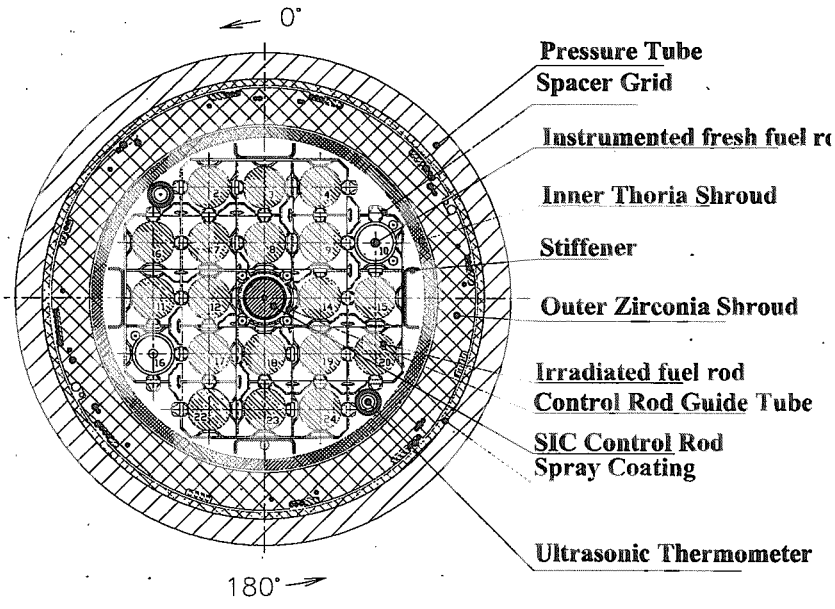


Figure 2
Radial section of the *Phebus-FP* test bundle

This is a blank page.

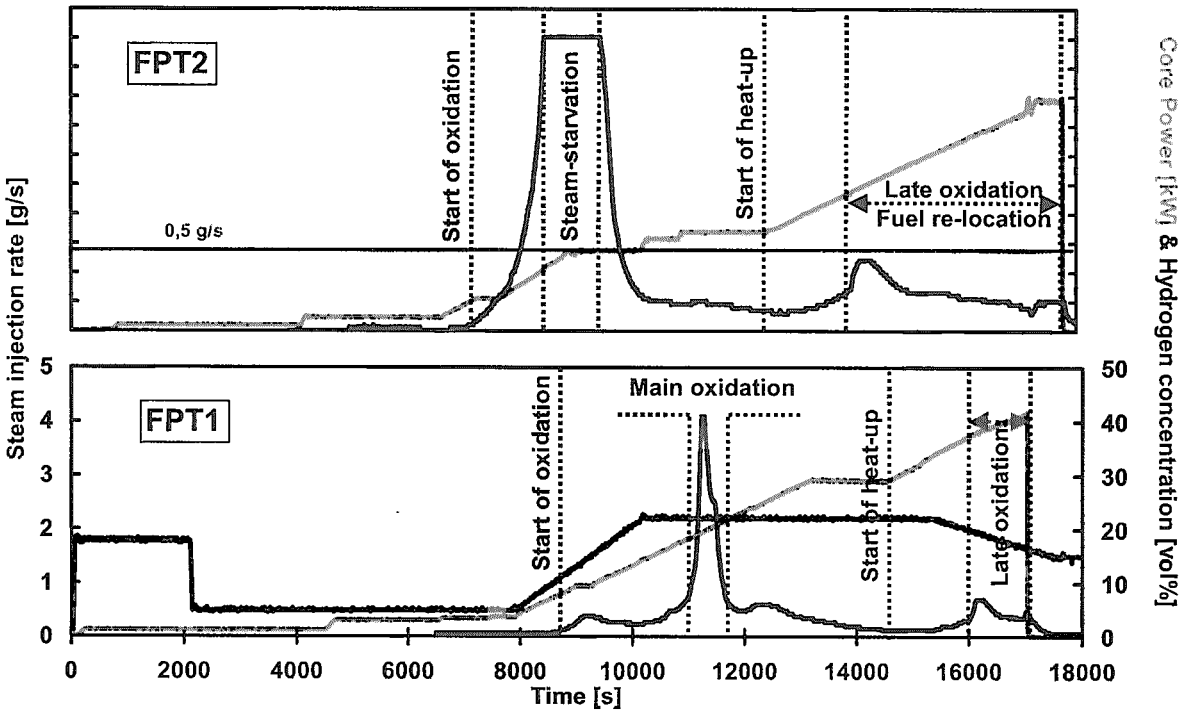


Figure 3

FPT1 and *FPT2* experimental sequence, showing the core power, the steam injection rate and the hydrogen concentration in the experimental circuit, highlighting important experimental phases

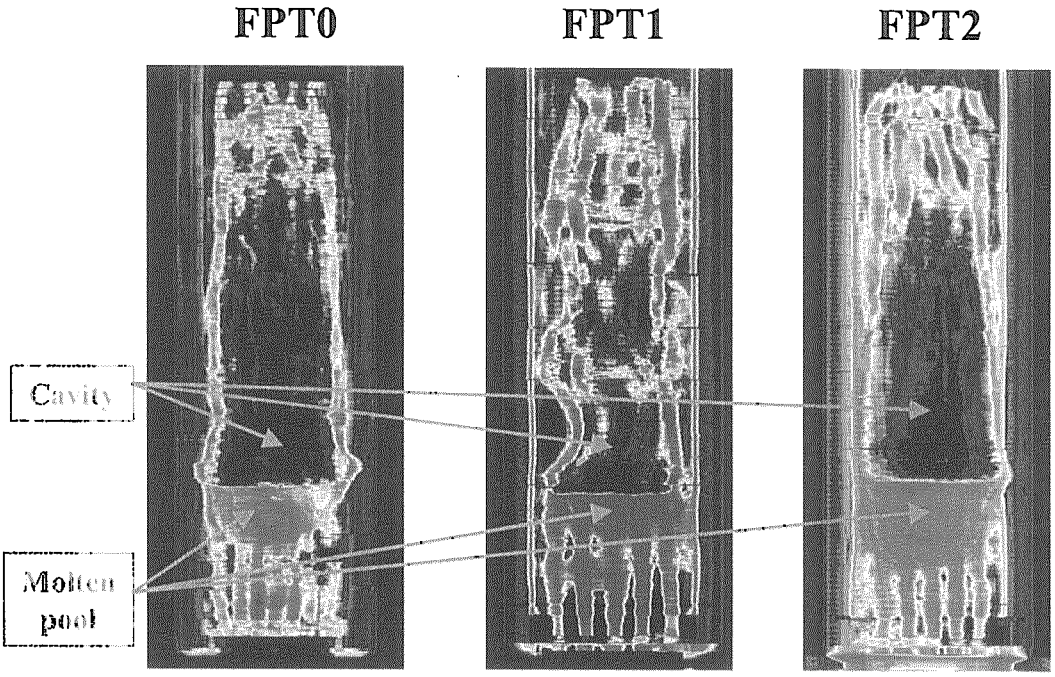


Figure 4

FPT0-2 post-test radiographs

(colour code: high-density material in red, low-density material in yellow, empty space in black)

This is a blank page.

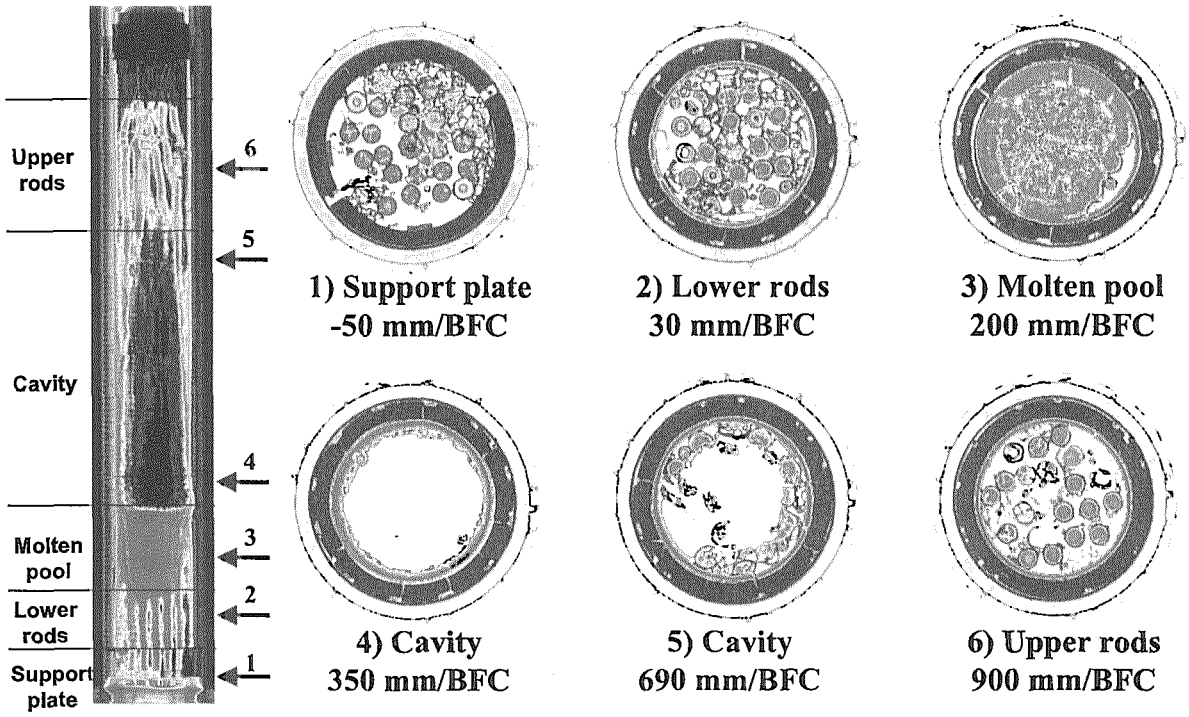


Figure 5

FPT2 post-test transmission tomograms at selected level of the degraded test bundle, showing: some melted-material accumulation on the support plate, moderately degraded fuel rods in the lower-part of the bundle, the extended molten-pool and cavity, and moderately degraded rods in the upper-part of the bundle.

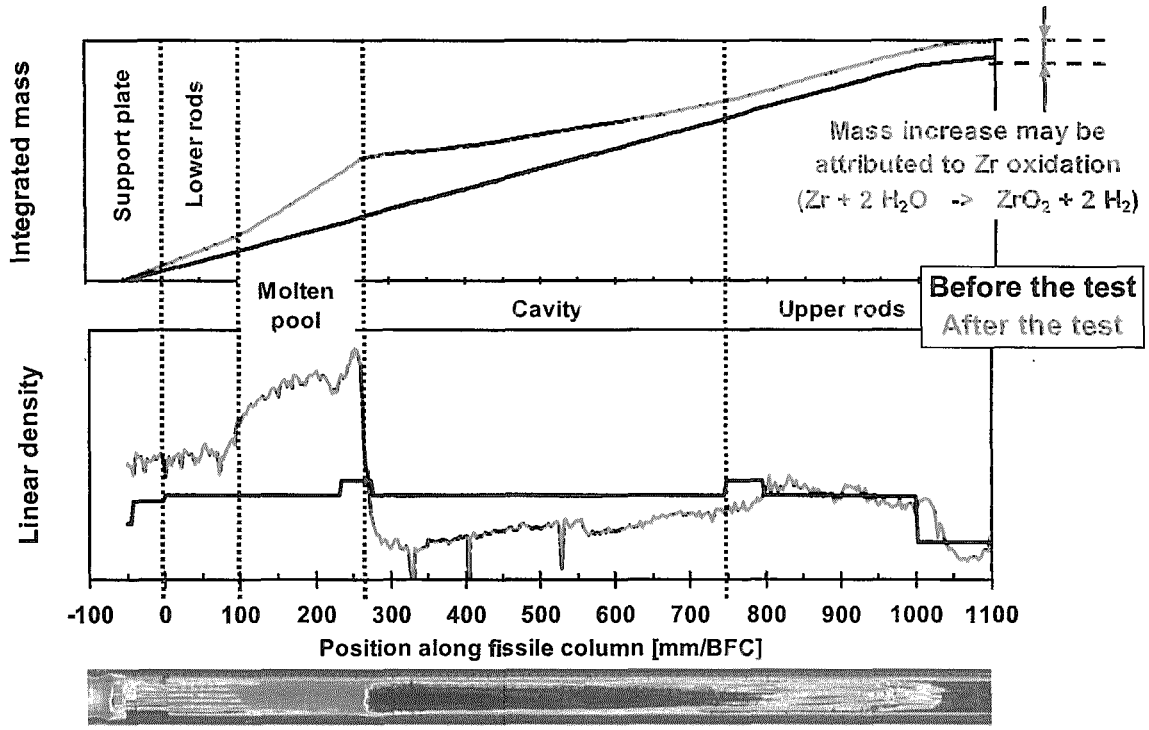


Figure6

FPT2 post-test mass distribution along the degraded bundle, showing the main material relocation at the molten-pool level, with some local mass increase attributed to Zircaloy-cladding oxidation.

This is a blank page.

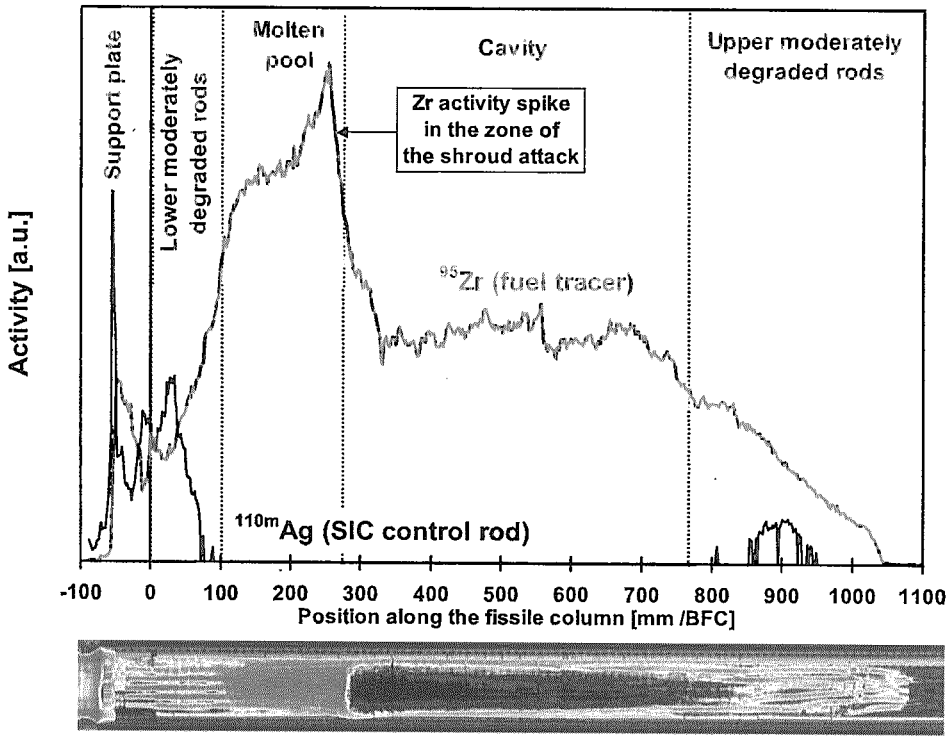


Figure 7

FPT2 post-test gamma scanning of the degraded bundle, for ^{95}Zr (fuel tracer) and ^{110m}Ag (activation product from control-rod). Fuel mostly relocates at the molten-pool level. Control-rod material essentially relocates in between rods below the molten-pool.

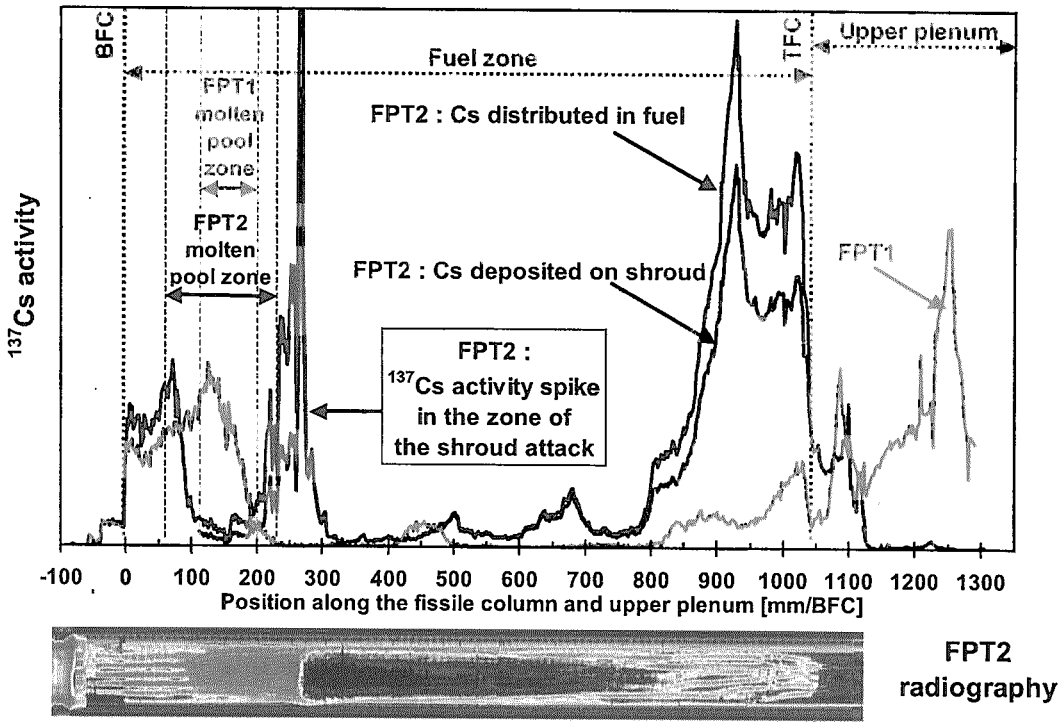


Figure 8

FPT1/2 post-test gamma scanning of the degraded bundle and upper plenum for ^{137}Cs. Pending data from emission tomograms, two hypotheses are considered for *FPT2*: Cs either distributed in fuel or deposited in shroud. Linear activity profiles indicate that volatile *FP*s are depleted from the molten pool and partly re-deposited in the upper-part of the device. Owing to the lower steam injection rate in *FPT2* than in *FPT1*, deposits primarily occured on the upper moderately-degraded rods for *FPT2*, as opposed to in the upper plenum for *FPT1*.

This is a blank page.

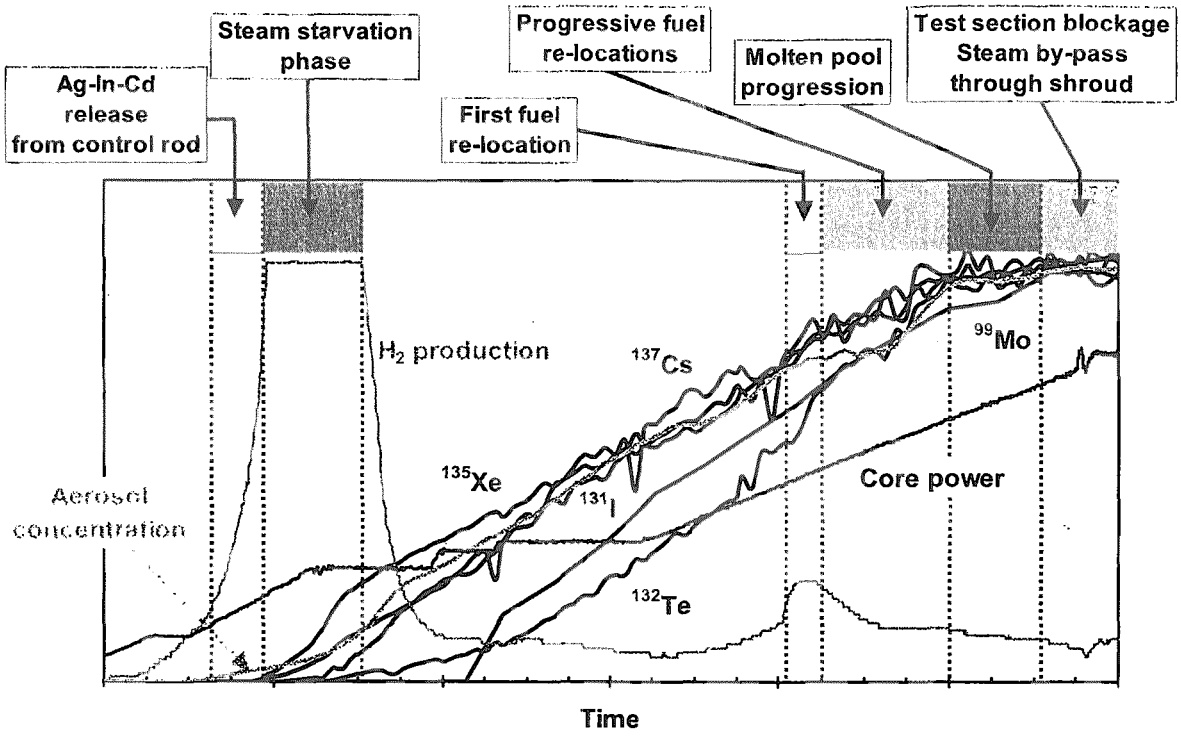


Figure 9

FPT2 aerosol and *FP* release to the containment through the degradation phase, highlighting the relationship between bundle degradation phases (steam-starvation, fuel relocation and molten-pool formation/progression) and release events.

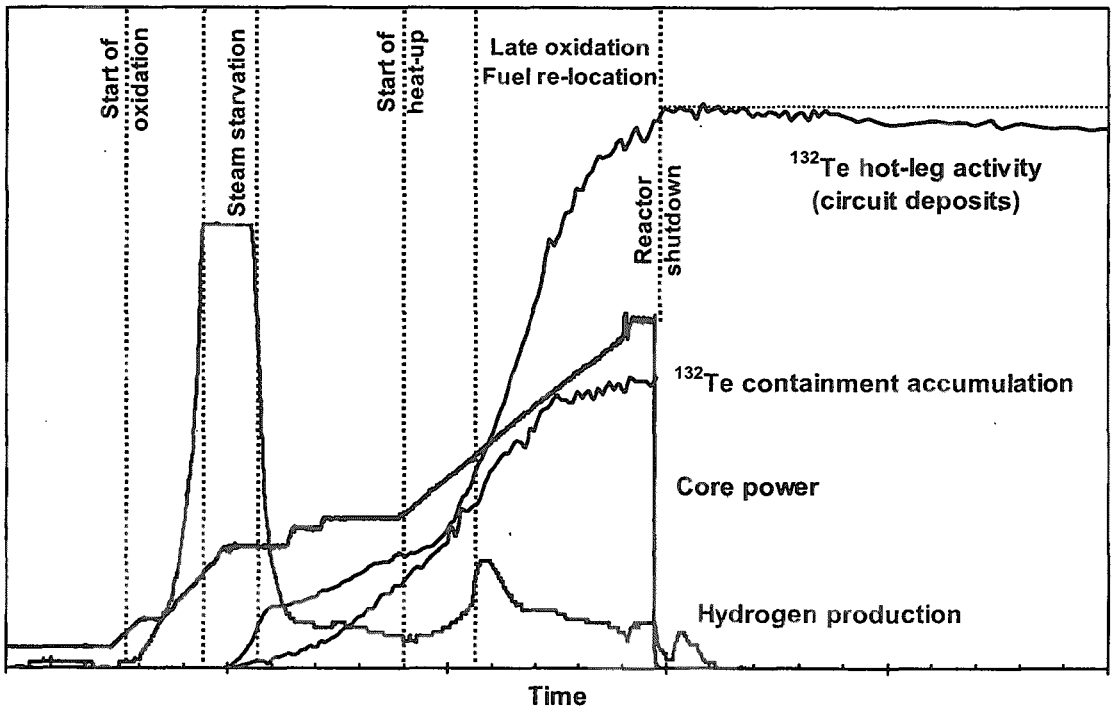


Figure 10

^{132}Te release in the *FPT2* test, illustrated by both circuit hot-leg deposits and containment accumulation. Differences between circuit and containment kinetics point to the difficulty of estimating release-from-fuel on the basis of the available measurements, owing to perturbations induced by deposits in between the fuel zone and the measurement location.

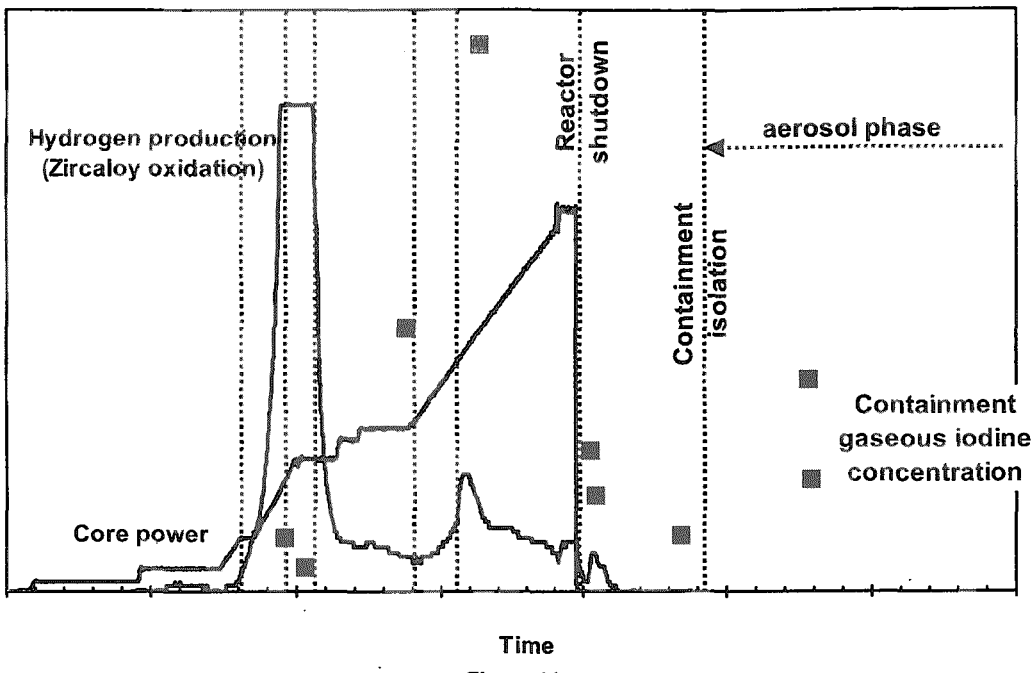


Figure 11

Short-term gaseous iodine concentration (logarithmic scale) in the containment in the *FPT2* test, showing that maximum concentration is achieved during oxidation phases, while some substantially lower concentration is measured after reactor shutdown, owing to efficient Iodine trapping (AgI formation) by Silver released from control-rod and deposited into the sump.

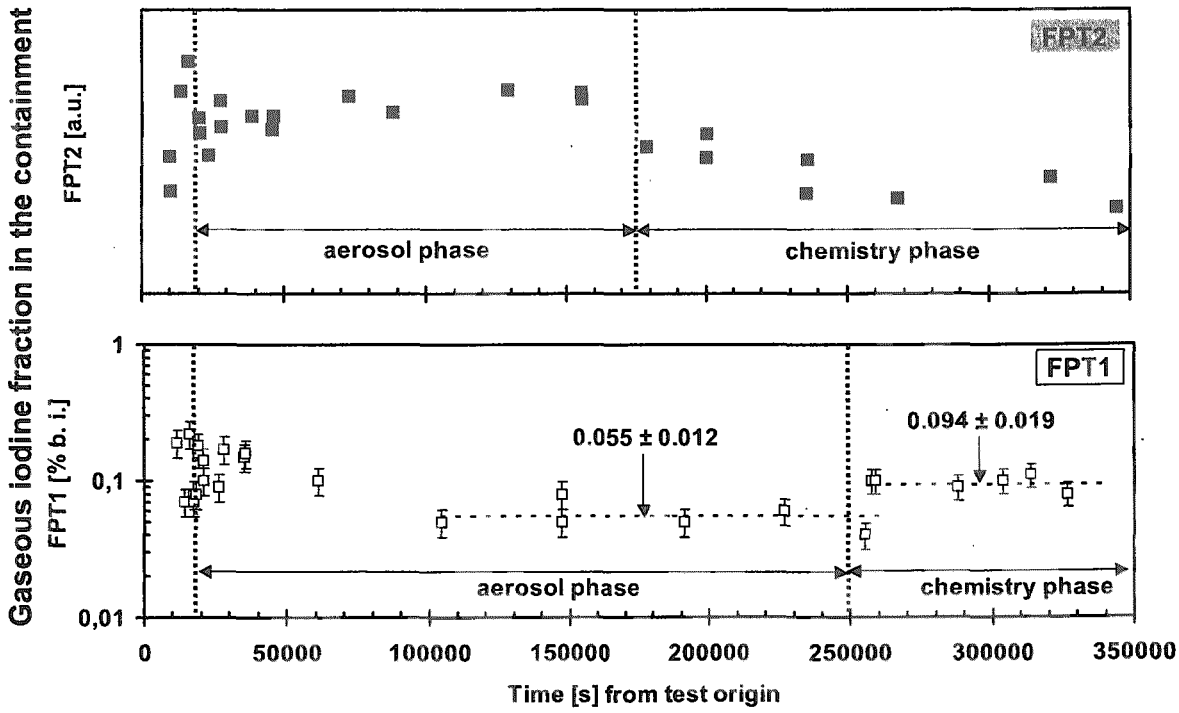


Figure 12

FPT1/2 gaseous iodine concentration (logarithmic scale, arbitrary units for *FPT2*) through the long-term phase. Gaseous iodine production is limited by iodine trapping through AgI formation in the sump (favoured in *FPT1* by acidic sump conditions: *pH-5*), and further reduced by hydrolysis destruction of volatile iodine species in *FPT2* (favoured by warm sump conditions: *120 °C*).

Discussion:

Q: (A.Hidaka)

In the PHEBUS/FP test, carrier gas flows outside of the shroud at the time of molten pool formation. In that case, the furnace could be isolated under stagnant flow condition. Are there any possibilities that the release rates of FPs are underestimated in the PHEBUS/FP test ?

A: The steam bypass through shroud occurred about 20 minutes after the molten pool formation when the molten pool extension was large. In addition, the bypass channel is initiated close to the top level of the molten pool, where the chimney gets totally clogged. Finally, FP release in FPT-2 appears to come to an end at about the end time of the molten pool formation, that is well before the steam blockage occurs. As a result, it is unlikely that the FP release is underestimated in FPT-2 (note that steam blockage is specific to FPT-2): as shown by the Cs-137 gamma scanning, volatile FPs are completely depleted from the molten-pool.

Q: (G.Ducros)

Concerning transparency 11 (FPT-2, Cs distribution in fuel and on shroud), do you have similar distribution for Ba-140 for instance ?

A: The 3-dimensional distribution of gamma-emitting species in the test bundle is available from emission tomograms. These are not presented in this talk because their analysis is still in progress. Emission tomograms, as the present preliminary stage of their analysis, confirm that the cesium inventory in the upper-part of the bundle is half-located in fuel and half-deposited on the shroud. As far as Barium is concerned, the distribution appears related to the fuel.

JP0250420

JAERI－Conf 2002－009

Session 4-6

Analysis of Phebus FPT1 samples carried out at ITU, Karlsruhe

D. Bottomley, C.T. Walker, J-P. Glatz
European Commission
Institute for Transuranium Elements,
Postfach 2340
D-76125 Karlsruhe, Germany

ABSTRACT

The Phebus FP (fission Product) project is an international reactor safety project led by IPSN Cadarache and with European Commission as partner along with other EU national institutes as well as 5 other non-EU countries.

The project simulates severe reactor accidents using a 20-rod bundle of medium burn-up fuel rods, and monitors the degradation of the bundles as well as the release of fission products and structural materials along the simulated primary circuit and into the containment.

ITU Karlsruhe was involved in the macroscopic and microscopic examination of the degraded FPT1 bundle and the molten pool of corium, and the examination of deposits from various filters positioned along the primary circuit mainly the hotter (upstream) points. An examination of the vertical line deposits directly above the overheating bundle were also carried out. These were examined as part of a supplementary shared cost action project (Phebus Revaporisation Project) examining the potential for volatilisation of deposits at later stages of a reactor accident.

Selected results will be given to illustrate the main features of the reactor accident and comparison with the initial, base-line test (FPT0-using only trace-irradiated fuel) indicates the degradation mechanisms. That is, how fuel rods deform, and liquid phases (corium) collects to form a pool, as well as how the fission products are released and deposited along the primary circuits and that these distributions may change in the course of the accident.

Fuel Safety Research Specialists Meeting
JAERI, Japan 4-5 March 2002

Analysis of Phebus FPT1 Samples carried out at ITU Karlsruhe

D. Bottomley , C.T. Walker, J.-P. Glatz, M. Sheindlin, D. Papaioannou

European Commission, Institute for Transuranium Elements
Postfach 2340,Hermann-von-Helmholtz Pl. 1
76125 Karlsruhe - Germany

Abstract

The Phebus FP (fission Product) project is an international reactor safety project led by IPSN[1] Cadarache and with European Commission as partner along with other EU national institutes as well as 5 other non-EU countries.
The project simulates severe reactor accidents using a 20-rod bundle of medium burn-up fuel rods, and monitors the degradation of the bundles as well as the release of fission products and structural materials along the simulated primary circuit and into the containment.
ITU Karlsruhe was involved in the macroscopic and microscopic examination of the degraded FPT1 bundle and the molten pool of corium, and the examination of deposits from various filters positioned along the primary circuit mainly the hotter (upstream) points. An examination of the vertical line deposits directly above the overheating bundle were also carried out. These were examined as part of a supplementary shared cost action project (Phebus Revaporisation Project) examining the potential for volatilisation of deposits at later stages of a reactor accident.
Selected results will be given to illustrate the main features of the reactor accident and comparison with the initial, base-line test (FPT0-using only trace-irradiated fuel) indicates the degradation mechanisms. That is, how fuel rods deform, and liquid phases (corium) collect to form a pool, as well as how the fission products are released and deposited along the primary circuits and that these distributions may change in the course of the accident.

1 Introduction

The Phebus pf project is an international project on severe accidents lead by IPSN[1] Cadarache and the European Commission and supported by other national institutes and other non-EU countries: Japan, Korea, Canada, USA, Switzerland [1]. A bundle composed of 20 1m rods was heated with increasing power by the surrounding driver core of the Phébus reactor and then the bundle's separate steam supply was gradually reduced. This caused severe overheating and degradation and resulted in fission product release into a simulated primary circuit. The fission product release was monitored along the instrumented primary circuit and into a simulated containment (with sump) by coupons, impactors and γ-spectroscopy. The behaviour of the fission product aerosols in the containment could also be monitored during settling and washing phases so that a complete range of behaviours during a reactor accident could be simulated.
The first test FPT0 used trace-irradiated fuel (9 days in the Phénix reactor to recreate the short-lived isotopes) and acted as a baseline test for the series [1-3]. The second test (FPT1) used 18 BR3 rods of moderate burn-up (23 GWd/tU mean-burn-up) – along with 2 non-irradiated but

[1] known since March 2002 as IRSN (Institut de radioprotection et surêté nucleaire)

instrumented fuel rods [2,3]. The bundle underwent degradation in a steam atmosphere in which the effect of irradiation on bundle behaviour during degradation could be seen by comparison with FPT0 and, more locally, radiation effects on fuel could be observed with the comparison between the instrumented and the non-instrumented rods. The FPT1 bundle was embedded in resin to hold the structure firmly in position and examined non-destructively by X-ray tomography at Cadarache using software developed by IRSN specifically for this purpose, to ascertain its structure. Then it was transported to ITU Karlsruhe where the bundle was cut up to confirm its structure. Subsequently locations in the sections were selected for microscopic examination and analysis. In addition to the bundle ITU also received the vertical line and filters from the simulated primary circuit for analysis.

2 Macroscopic and Microscopic Examination of the bundle and corium

2.1 Macroscopic Examination: Tomography

The tomography of both the FPT1 and the FPT0 bundles is shown in Fig. 1 with the density of the material indicated from the tomography by a colour coding in which black is a void and the increasing density from 0 to 10g.cm^{-3} is represented by the sequence violet, blue, green, yellow, orange and red. Red usually represents the UO_2 rods or the ThO_2 liner on the ZrO_2 thermal shielding, whereas green would be typical for steels (~7g.cm^{-3}).

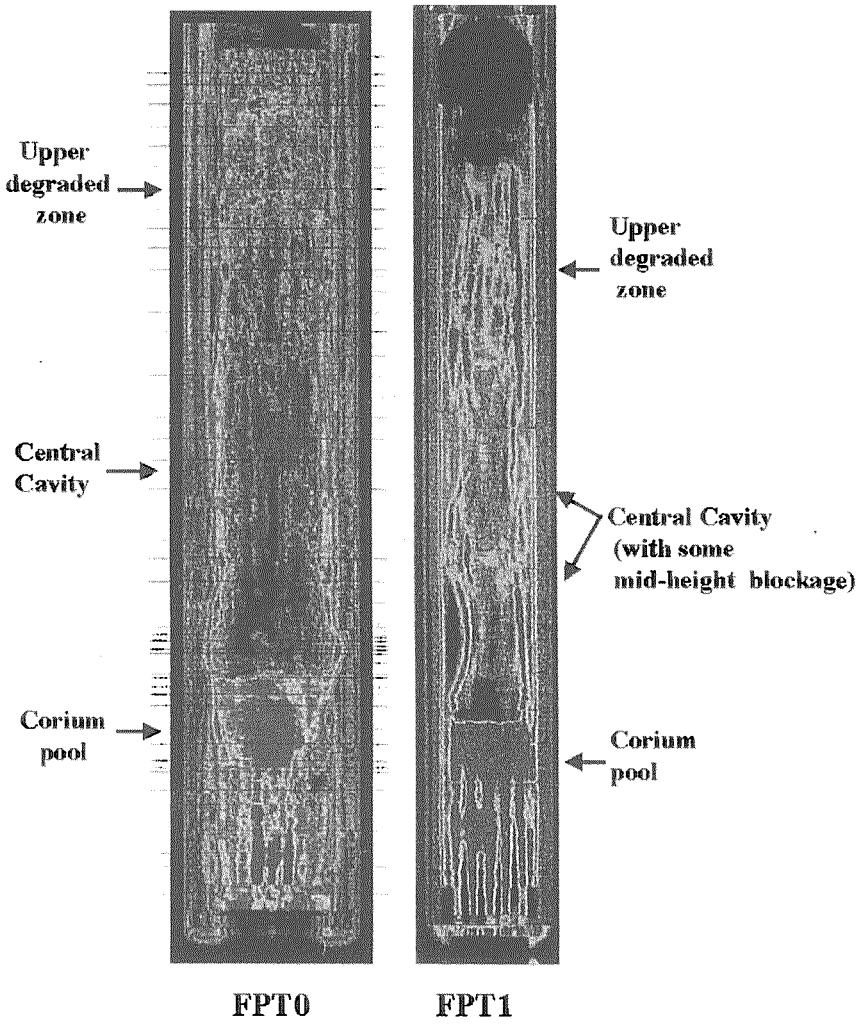


Fig.1 The tomography of FPT1 bundle showing the colour density scale (red-most dense - violet -least dense) showing the melting of fuel to collect in a pool, and leave a cavity above (courtsey IRSN Cadarache).

The bundles both display similar features: a pool of fully melted and uniform material (or corium) at approximately one-quarter height of the bundle, then a central cavity, then an upper region of degraded and distorted rods (with some blockage on upper spacer assembly for the FPT0 bundle) [2-4]. It is seen that the upper fuel rods have a reduced density especially for FPT1, and are mostly orange in colour (excepting the non-irradiated rods). The similarity in structure implies that the degradation behaviour is generic. It is nevertheless seen that the attack of the inner shroud is greater and the central cavity is larger for FPT0 than for FPT1. This was because FPT0 continued for a slightly longer time than for FPT1.

2.1.1 Macroscopic Examination

Bundle was sectioned at 20 heights over the entire section from the candled zone below the corium pool to the upper rods ends to determine the cross-sectional structure and compare with that determined by non-destructive tomography. Below three sections (Fig. 2) cut from the corium pool, the central cavity and the upper degraded zone are shown alongside the tomographies for the same height. Very good agreement with tomography sections is evident. Thus for the corium pool the outer solid crust (density ~10g.cm^{-3}) around a more porous central area is displayed. The yellow in the central area implies a less dense material but in the macrography it is seen to be a uniform material and that the lower density is probably as result of the fine porosity, since the large pores are evident in the tomography.

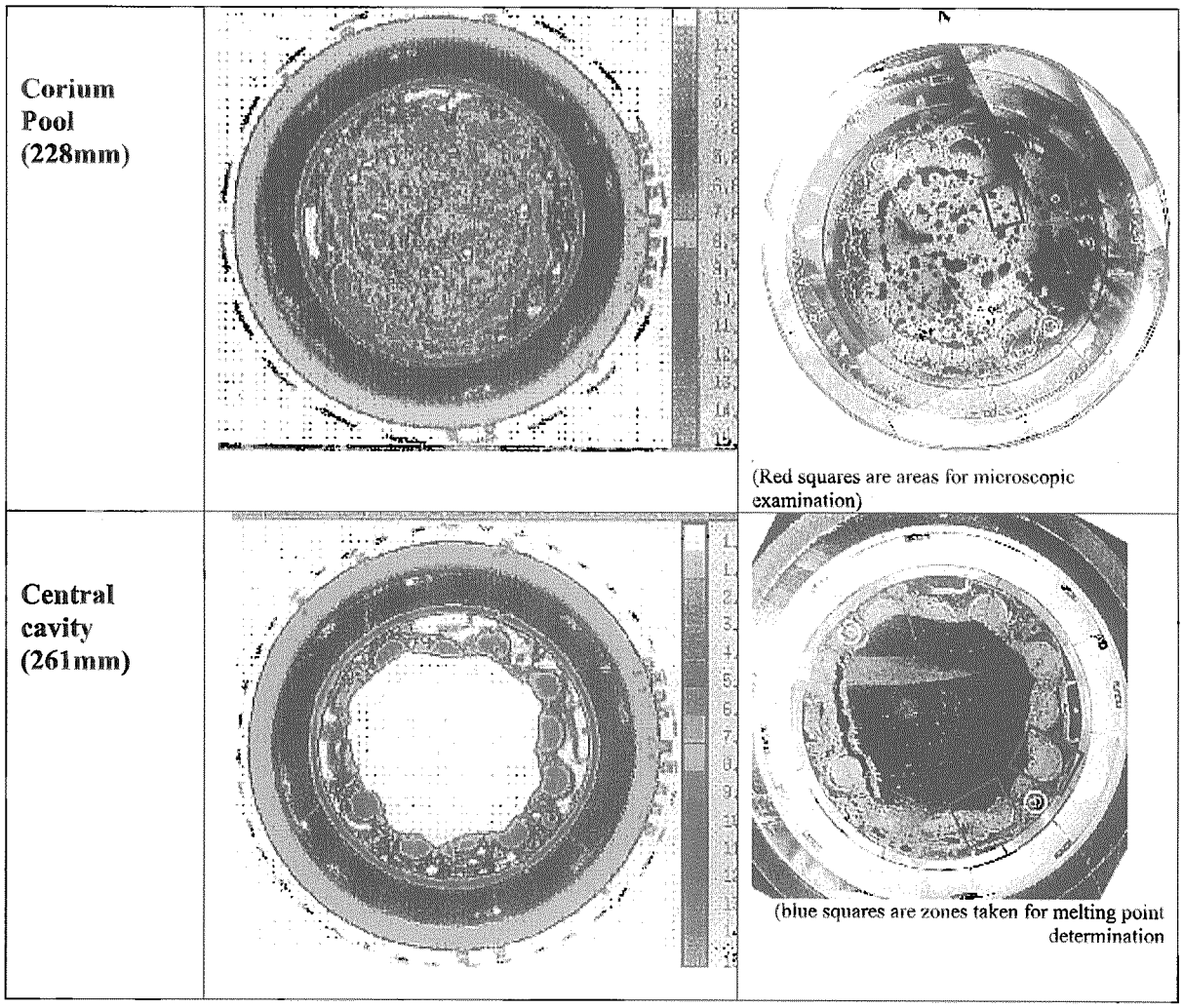


Fig.2 Comparison of tomographic sections of the bundle with the macrographic sections. (mag. 0.6x).

In the central cavity the form is confirmed and it is accurate in displaying the less dense structures such as oxidised zircaloy spacers (ZrO_2 density ca. 5.4 $g.cm^{-3}$). The rods have red central zones and orange edges or around cracks. Again the shading of the rods is confirmed by the ceramography to correspond to the fuel's porosity. In the upper degraded zone (not shown in Fig. 2) the distorted form of the fuel and the oxidised cladding was accurately depicted in the tomography, even for small isolated remnants of porous fuel or cladding [4].

2.2 Microscopic Structure

Selected zones (see red squares in the macro-photos of Fig.2) were cut, embedded, polished and examined by optical microscopy and the phases analysed by a shielded electron microprobe [5,6].

2.2.1 Corium of Pool (+228 mm)

The sample contained both crust and central porous corium as well as remnants of non-irradiated and irradiated fuel rods (Fig.3). The optical microscopy showed the corium was a uniform, large-grained ceramic with small amounts of secondary phases (Fig. 4) and these were often sited at the grain boundary. They were analysed by the electron microprobe to be mostly oxides and containing either Ni, Fe, Cr, Zn, that is structural materials, or metallic phases that had precipitated out during the degradation (eg. Ru, Pd, Rh, Zr, Tc –the 5-metal precipitates found in irradiated fuel of higher burn-ups). The corium pool was very uniform although residual pieces of fuel or structural materials were seen at the edges of the pool.

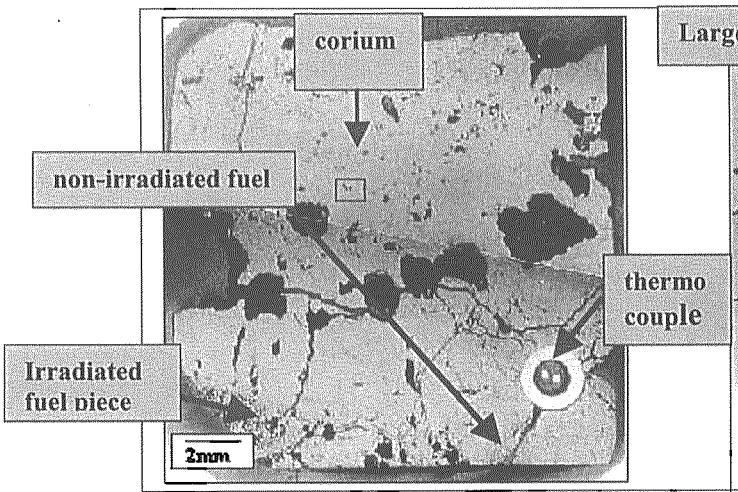


Fig.3 low power photo of the corium containing fuel remnants (mag. ~5x) - red square is zone used for x-ray diffraction

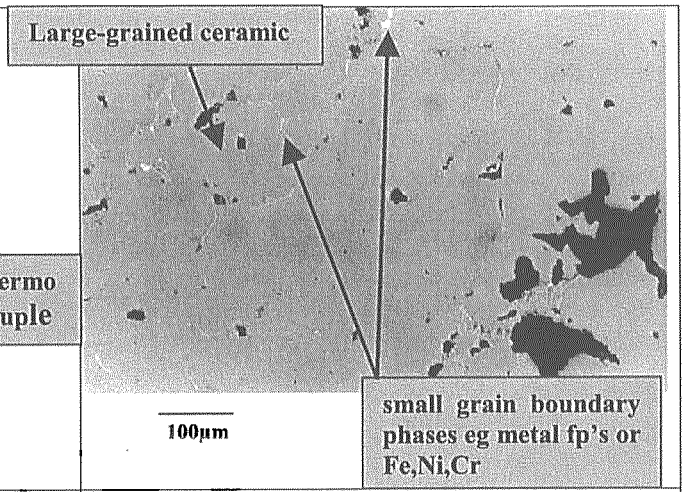


Fig.4 Micrograph showing the major ceramic phase of the corium with minor grain boundary phases (mag. ~150x)

The electron microprobe analysis (EMPA) of the corium showed it to be essentially a mixed zirconium -uranium oxide with impurities. An average of 10 point analyses of the upper corium pool at +228 mm gave the following result: $(U_{0.52}Zr_{0.44}Fe_{0.03}Cr_{0.005}Nd_{0.004}Pu_{0.003}Ce_{0.002})O_{2\pm x}$ [3]
In addition to the principal UO_2 fuel and oxidised cladding (ZrO_2) components, the corium ceramic contains fission products (eg. Nd) and irradiation products (Pu) as well as dissolving Ce from the coating of the thermal shroud and some of the structural materials (Fe, Cr). In addition the corium appeared to have oxygen present in close to a stoichiometric ratio with the metal atoms (O/M ratio) of $2 \pm x$ where $x < 0.1$. There was no evidence of higher oxides in the melt such as U_4O_9. This compares with the composition of the FPT0 melt composition which was analysed by EMPA to be $(U_{0.50}Zr_{0.47}Fe_{0.02}Y_{0.01})O_{2\pm x}$ [4] where no fission or irradiation products were detected and yttria (Y_2O_3) was used as the lining for the thermal shroud.

2.2.2 Melted Fuel in Cavity (+261 mm)

The half-melted fuel is seen from the edge of the cavity (Fig. 5). The highly porous edge with elongated pores indicates a sharp temperature gradient at the cavity border. Further, fully oxidised cladding with large grains remains attached to the fuel and surrounded with melt. EMPA analysis of this melt shows considerable Zr concentration gradients rising towards the contact point with the cladding (varying from 10wt % to 40 wt % Zr). This implied that the cladding was still undergoing dissolution by the melt at the time of the reactor shutdown. Also Zr was also observed to have diffused inward into the UO_2 fuel.

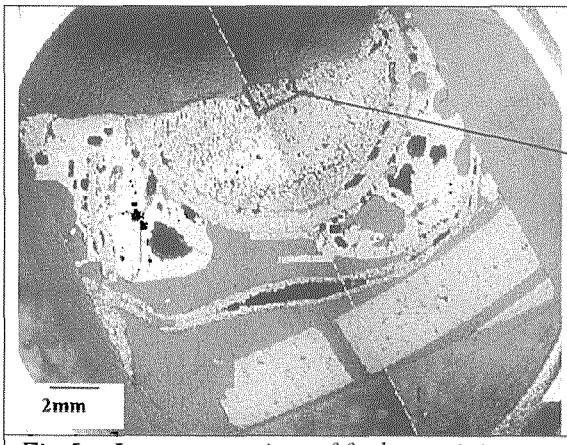


Fig.5 Low power view of fuel remaining at the edge of the cavity showing thickened cladding and porous fuel (mag. ~5x)

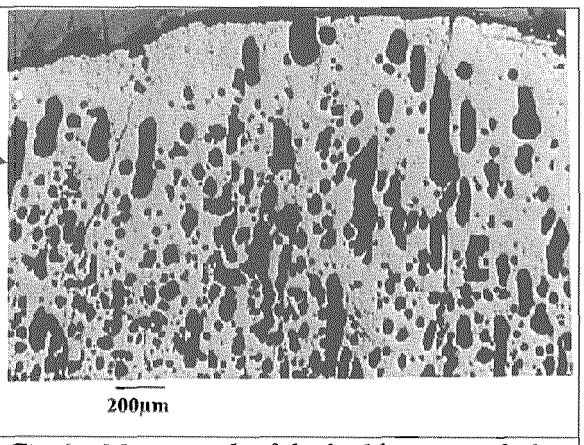


Fig.6 Micrograph of the highly porous fuel with elongated bubbles at the edge indicative of a high temperature gradient and near melting temperatures. (mag. 50x)

2.2.3 Degraded fuel in upper zone (+ 473 mm)

There are only fuel fragments that remain and these are highly porous with thickened and fully oxidised and distorted cladding. The symmetrical oxidation (Fig. 7a) indicates that the cladding had broken open and was oxidising from both sides. The very large grains indicate the rapidity of the double-sided attack. The second feature to notice is that the fuel is very porous and reaches 80 % locally (Fig.7b). This is due to the fission gas release during the degradation through bubble growth, coalescence. The elongated bubbles suggest that the fuel deformed plastically during the degradation and implies that it spent prolonged time at temperatures above 2500°C. A further observation is that there has been no corium, melted cladding or steel structures retained at this level to interact with, or dissolve the fuel. The remaining cladding has been completely oxidised. Thus the higher melting point, oxidised structures have remained at this height, and suffered longer times at such high temperatures. EMPA also shows how the oxidised cladding and fuel interact with U diffusing into the cladding along ZrO_2 grain boundaries (containing approx. 4wt% U).

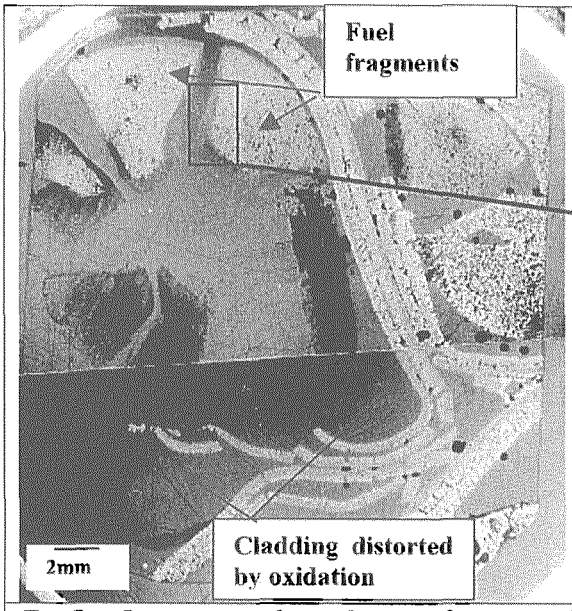


Fig.7a Low power photo showing fragmented fuel and completely oxidised & deformed cladding (mag. ~5x)

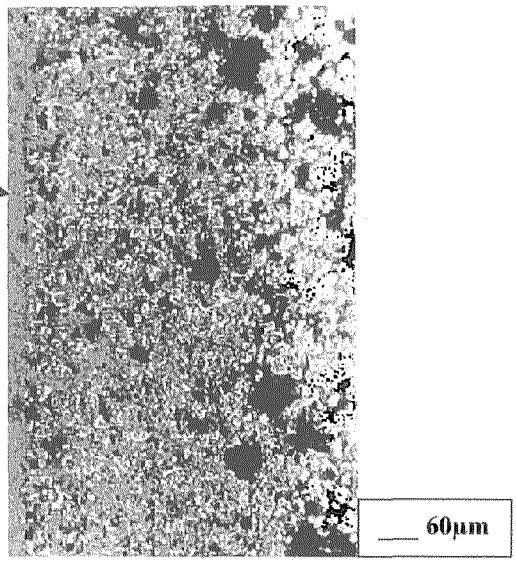


Fig.7b Micrograph of the very porous edge of the fuel (due to fission gas release) (mag. 170x)

2.2.4 Degraded fuel at uppermost area (+607 mm)

At this height where the upper bundle was badly degraded with fractured fuel pieces and cladding and had relatively small amounts of corium or melted material remaining. Badly degraded fuel fragments were observed after specimen polishing, but these included samples of corium and fuel (Fig. 8). Again the fuel pieces were highly porous with remnants of thickened, oxidised cladding (Fig. 9).

EMPA analysis revealed two sorts of fuel samples: one of irradiated fuel (with e.g. Pu) and one of non-irradiated fuel (no irradiation products: Pu or Nd) belonging to an instrumented fuel rod in the bundle). Non-irradiated fuel appears to have interacted with cladding less than irradiated fuel: less Zr having diffused into the fuel. The interaction thickness between corium and oxidised cladding was about 150 μm and so was similar to the interactions taking place at the mid–cavity height (+473mm).

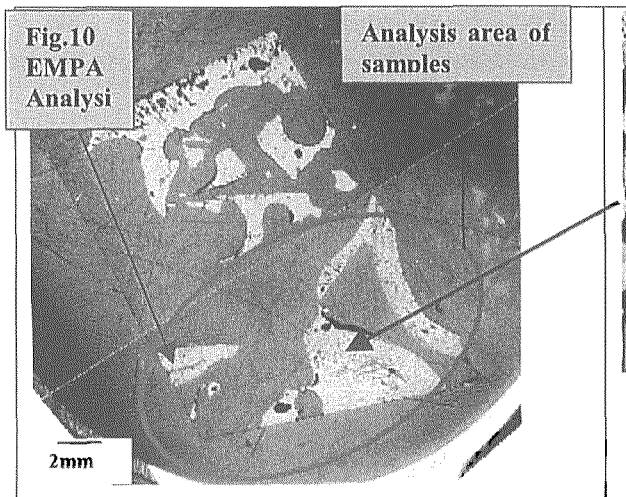


Fig.8 Macrograph showing the fuel fragments and cladding remaining in the upper bundle (mag. ~5x)

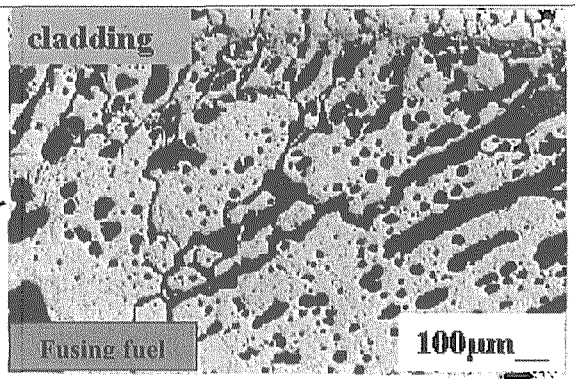


Fig.9 Micrograph of fuel close to fusion with elongated bubbles of fission gas release (mag. 40x)

A minute piece of corium was also found attached to some cladding. The analysis showed that it to be very similar to that of the corium pool (Fig. 10).

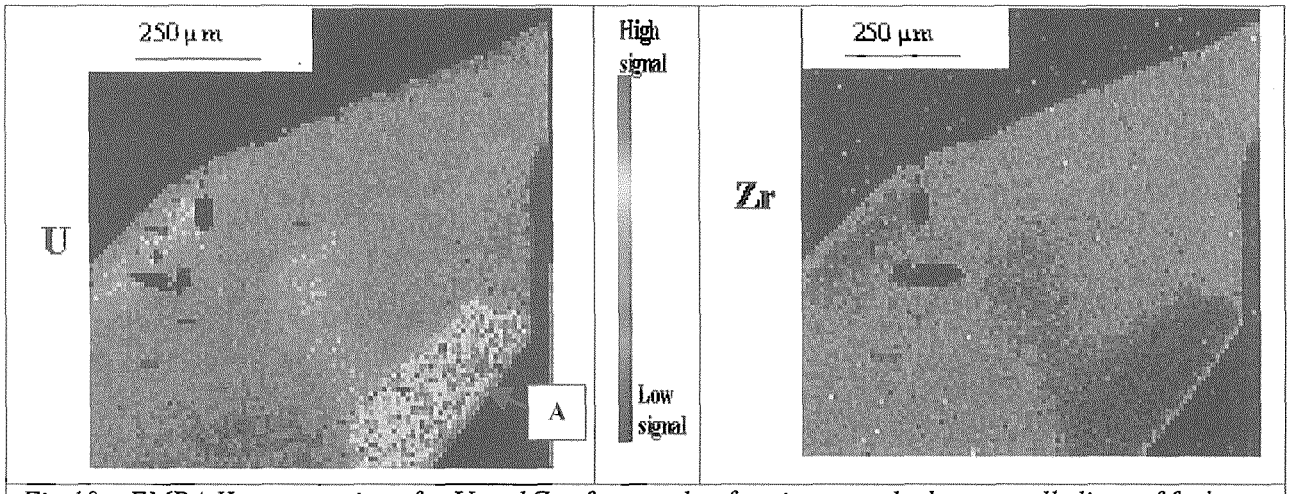


Fig. 10 EMPA X-ray mappings for U and Zr of a sample of corium attached to a small sliver of fuel (area A) (see Fig. 8 for location of sample) (mag. ~80x)

The fuel was found to be superstoichiometric (irradiated fuel O/M =2.42 and non-irradiated O/M = 2.32 and is in stark contrast to the corium (+228mm) with its stoichiometric composition [2.3] (see Table 1 below). The Zr-rich corium found close to the cladding in the cavity at +261mm was also practically stoichiometric.

Table 1 EMPA analyses of both irradiated and non-irradiated fuel fragments & corium piece found in the upper part of the degraded bundle +(607mm height) and compared with the corium pool sample (+228mm height). (s.e. of the oxygen stoichiometry is: irrad. UO_2 ±0.06, non-irradiated UO_2 ±0.03, Corium ±0.075)

Irradiated UO_2	$(U_{0.86}Zr_{0.12}Fe_{0.006}Nd_{0.006}Pu_{0.005}Ce_{0.005})O_{2.42}$
Non-irradiated UO_2	$(U_{0.95}Zr_{0.04}Fe_{0.002})O_{2.32}$
Corium piece	$(U_{0.45}Zr_{0.51}Fe_{0.021}Cr_{0.003}Nd_{0.003}Pu_{0.002}Ce_{0.002})O_{2.01}$
Corium pool	$(U_{0.52}Zr_{0.44}Fe_{0.03}Cr_{0.005}Nd_{0.004}Pu_{0.003}Ce_{0.002})O_{2\pm x}$ ($x \leq 0.1$)

3 Supplementary tests

3.1 melting points of corium and fuel

Melting point determinations of the corium and of the degraded fuel were also carried out as these are important to model their behaviour. This was performed by laser pulse heating of a thin sample until it was completely molten; then multiple wavelength optical pyrometry of the cooling molten sample was used to observe the 'arrest' on solidification and obtain an estimate of the solidus temperature of that composition [7].

This was done on a corium sample (+228 mm) and on a degraded fuel sample adjacent to the cavity (+261 mm). These are the blue squares marked in the macrographs in Fig. 2. The samples were remounted in an alumina cement and ground to remove debris and make a flat surface. The laser pulse profile was shaped to slow the cooling of the molten sample and extend the freezing plateau. The medium power (350W) YAG laser had a spot size of 4mm and was centred on the fuel or corium to avoid surrounding resin or cement. Two pyrometer systems were used: a rapid (10μs rise time) monochromatic pyrometer recorded the brightness temperature at 650±10 mm

while a spectrometer recorded the range 500-900mm every 4ms. These had a smaller spot size of approx. 0.3mm which was centred on the laser spot on the fuel or corium. Initial laser shots resulted in relatively unstable cooling curves and also soot on the glass (due to vapourised resin left in the sample). Later shots (3rd shot for the corium & 5th shot for the degraded fuel) gave stable and reproducible cooling curves as the material was fully melted and uniform in composition. The final cooling curve for degraded fuel is given in Fig. 11.

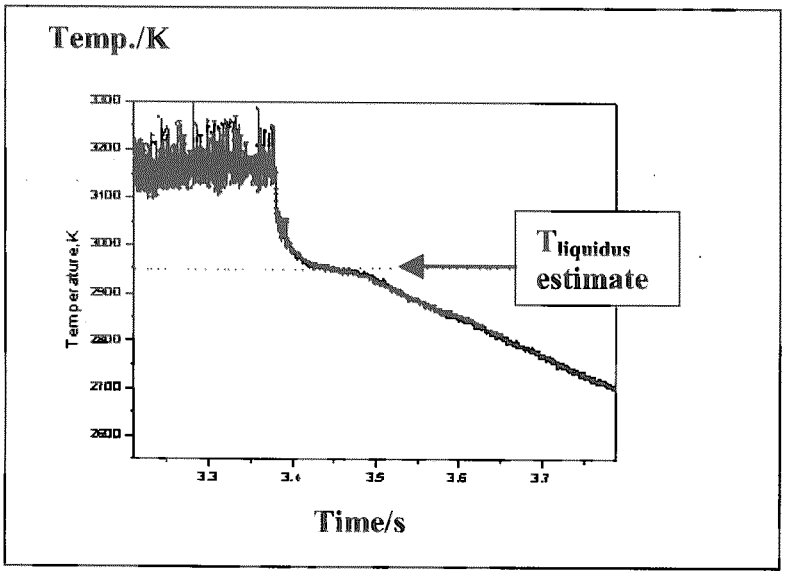


Fig.11
Thermogram or temperature profile of damaged fuel sample from cavity level (+261 mm) of FPT 1. The thermal arrest on cooling gives an estimate of the liquidus temperature of 2950K

The melt area of the sample was also examined by SEM-EDAX. Analysis showed that there was considerable Zr content in the fuel (between 11and 17wt% as well as structural material impurities- see Table 2 below) presumably due to the liquid phase interactions or solid phase Zr diffusion into the fuel during degradation.

Table 2 Analyses of damaged fuel sample for melting point determination (FPT1-5-2) from the outer ring at +261 mm height

Location in fuel	**Element(w/o) without oxygen**							**Atomic Ratio U/Zr**	**Approx. U/Zr Formula (as oxides)**
	U	Zr	Al	Si	Ba	Fe	Cr		
Inner (corium) side	74.0	17.1	1.2	3.7	1.6	1.0	1.4	1.87	$(U_{0.63}Zr_{0.37})O_2$
Centre of fuel	44.6	11.9	9.6	2.5	19.3	8.8	3.3	1.88	$(U_{0.59}Zr_{0.41})O_2$
Outer edge of fuel	93.9	5.0	0.1	0.7	-	-	0.3	8.4	$(U_{0.98}Zr_{0.11})O_2$

EMPA analyses of an adjacent fuel rod showed lower Zr contents of approx. 3-7 wt% Zr (ie $(U_{0.92}Zr_{0.08})O_2$ to $(U_{0.83}Zr_{0.17})O_2$) [3], but confirm the penetration of Zr into the fuel during degradation. The liquidus temperature estimates for the laser flash pyrometry are given in Table 3 below.

Table 3 Estimates of the liquidus temperatures yielded by laser flash pyrometry of the corium pool and degraded fuel from the cavity above and compared with non-irradiated UO_2 [8].

Sample (height)	**Estimate of $T_{liquidus}$/K (°C)**	**Accuracy**
Corium (+228mm)	2760K (2487°C)	± 30 K
Degraded UO_2 fuel (+261mm)	2950K (2677°C)	± 30 K
Non-irradiated UO_2	3083K (2810°C)	± 20 K

Thus the degraded fuel in the cavity gave an estimate of 2950K (2677°C) with an average Zr content of 12 wt%, while the corium from the pool (+228mm) gave a liquidus value of 2950K. Both these lie below that of the non-irradiated UO_2. For the corium pool that is approximately an equimolar $(U,Zr)O_2$ composition, the Zr is seen to cause a drop of over 220K. This is however still more than expected from the ZrO_2-UO_2 phase diagram by 30-40K [9].
The degraded fuel is 170K below the UO_2 fuel and still 30 –40K below the composition anticipated from the phase diagram. Given the accuracy of the estimate the difference could still be attributed to the Zr content of the fuel, caused by the interdiffusion of Zr & U at sustained high temperatures during the final stages of degradation. Nevertheless, it is still possible that additional effects due to fuel irradiation could be further lowering the liquidus temperature, for example fission gas release or pre-existing fuel cracks.

3.2 X-ray diffraction of corium

A slice of the upper corium pool sample (+228 mm) was taken for X-ray diffraction from the inner corium zone marked as 'corium' in Fig. 3. The Cu $_{K\alpha 1}$ line (of 1.540598 Å) was used for the analysis on a $\theta - \theta$ X-ray diffractometer for θ going from 5° to 80°. This was followed by a peak-fitting and an automatic evaluation of the peaks; the resulting spectrum is given in Fig. 14.

The spectrum indicated a distorted cubic fluorite-type lattice of parameter a_o = 5.2984 Å and confirmed the single-phase structure. Moreover the value of a_o lies between pure UO_2 and pure ZrO_2 [10] and, using an experimental correlation for the influence of other cations [11], a composition of approx. $(U_{0.5}Zr_{0.5})O_2$ was estimated. Other effects such as α-irradiation damage to the lattice are not believed to be significant [12]. Assuming that the corium hasn't significantly oxidised (ie. is roughly stoichiometric as most evidence suggests) then the lattice parameter supports the microprobe measurements. Similar measurements with degraded fuel however did not give reliable results, as the sample was too small.

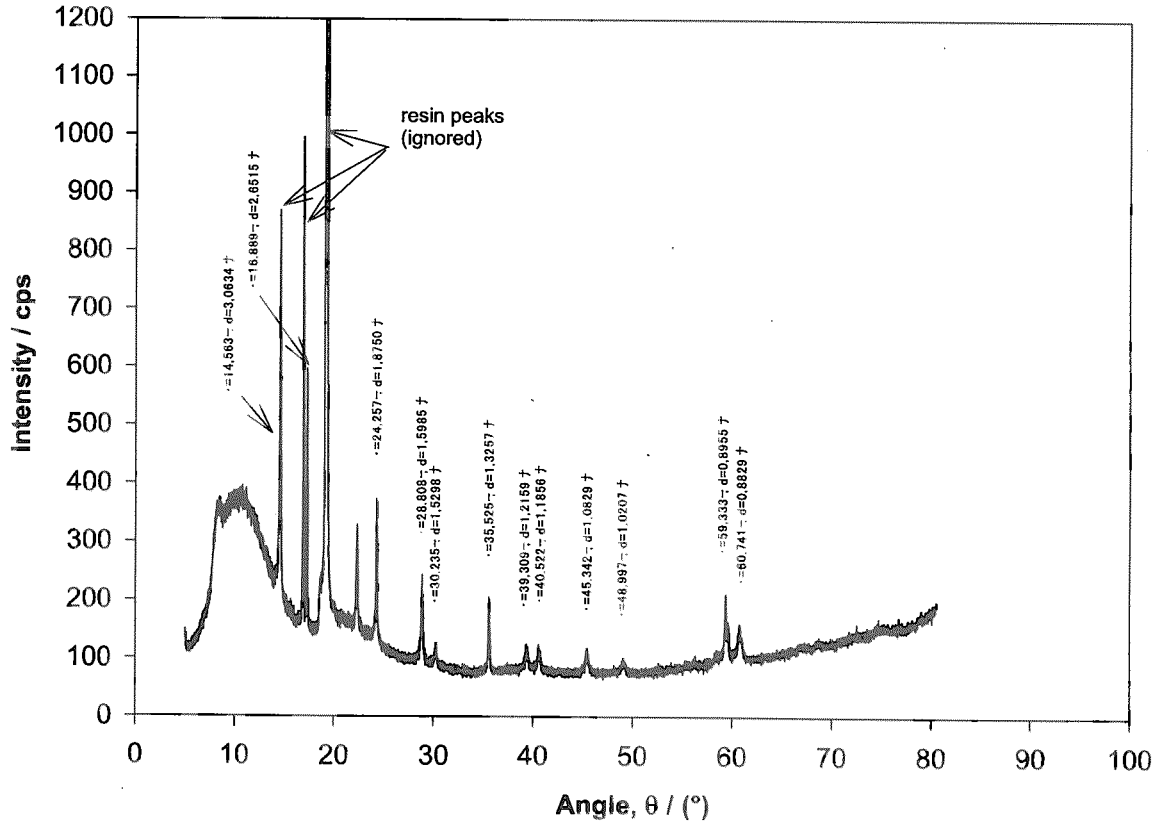


Fig.14 X-ray diffractrogram of the corium sample taken from the upper pool of FPT1 at +228mm height

4 Examination and analysis of FPT1 filters

4.1 Description of filters

The deposits from selected filters of the simulated primary circuit were also examined at ITU. The filters were porous Inconel (Ni-16 Cr-8 Fe) of 80 mm diameter and 3 mm thickness. Samples were examined from both the hotter part of the circuit (at 700°C), and from the cooler part (150°C) after the steam generator. They were exposed during the oxidation phase (about 11.000s) and after shutdown (at 17.000s) with sampling times of 300s or 160s depending on aerosol densities. The samples were cut and mounted for examination by cross-sectional optical microscopy, SEM - EDX, Auger spectroscopy and inductively coupled plasma - mass spectroscopy (ICP-MS).

4.2 Deposit on filters

The amorphous deposit was generally concentrated in the centre, where the largest particles (or agglomerates) impacted. The optical microscopy of the cross-section however shows a heterogeneous deposit – with metallic and non-metallic phases. The shiny metallic phases could be molten metallic silver entrained in the gas flow. The SEM-EDX showed the agglomerated aerosol to have 10-15 μm size range with individual particles of 1-3 μm diameters. (see Fig.15)

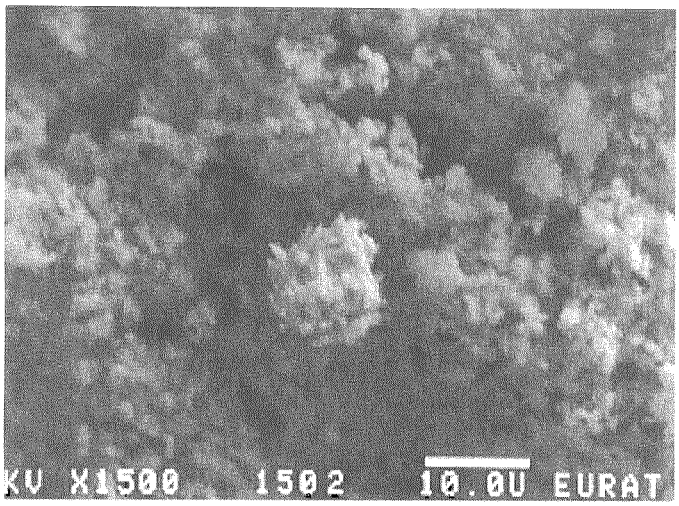


Fig. 15 Photo of U & In rich particle with Ag, Sn and Re (Analysis: U 39.5 a/o, Re 1.5 a/o, In 52 a/o – remainder is Inconel substrate and Si, Cl impurities)

The main elements were Ag, Re and In. The In was sometimes present as feather or needle-like crystals that appeared to have condensed from the vapour phase on the pre-existing particles. Also U & Zr–rich particles of fuel or melt were occasionally seen. Cl was often seen in large quantities and was an impurity. The sources of this is unknown, but was thought to have come from traces of Cl left in the ZrO_2 thermal shroud. γ-spectroscopy showed Cs-137, Cs-134, Sb-125, Eu-154 and Ag-110m on the filters. The caesium provided the major part of the activity.

4.3 Inductively-Coupled Plasma-Mass Spectroscopy (ICP-MS)

The sample of the hot (700°C) point C filter and the deposits of the other back-up and cooler filters were immersed for 1h in distilled water, 0.4M NaOH, & 7M HNO_3 in succession. For the hot point C filter a final deposit dissolution in 7 M-HNO_3 + 0.1M HF was carried out. γ-spectroscopy was then carried out to check the completeness of this deposits' dissolution. In the ICP-MS analysis (Fig. 16) the main elements were structural materials Ag, Sn, Re as well as fission products. Mo, Rb, Cs and also fuel and cladding U, Zr were seen.
More deposit was observed on the upstream hotter filters e.g. Mo, Sn, Ag, Re, Cs and very little on the back-up filter. Cd was concentrated on an early low temp. (150°C) back-up filter. Thus it is deduced that it is easily volatilised, and is vapour at 700°C but condensate at 150°C.

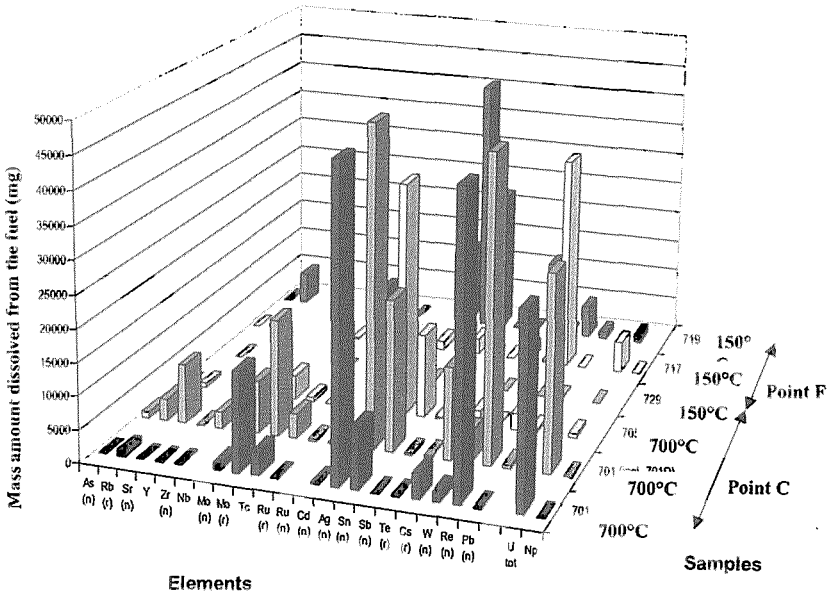


Fig. 16 ICP-MS Analysis of FPT1 filters for the water, 0.4 M NaOH, 7M HNO_3 rinses (and digestion for Point C 700°C filter).

The hot point C filter shows considerable Cs+Sn is 'baked' onto 700°C filter, since filter dissolution was required for 100% removal. By contrast it is water-soluble on the cooler 150°C filter, and seems to remain on the surface. The insolubility at higher temperatures may be due to diffusion of the CsOH into the surface oxide layer, while at low temperatures it remains on the surface. This shows that the deposition temperature affects its subsequent properties.

4.4 Auger Spectroscopy

The sample (10 mm x 5 mm) from a hot (700°C) point C sample (filter 701) was analysed in a special Auger spectrometer designed for active samples.
The analysis was made in a depth-profiling mode. A series of 5 spectra were taken after 0, 10, 30, 90 and 150 minutes of sputtering with Ar^+ ions at $1x10^{-4}$ Torr and 3 kV accelerating voltage.
(The sputtering rate was approx. 3 atomic layers/min - see Fig. 17).

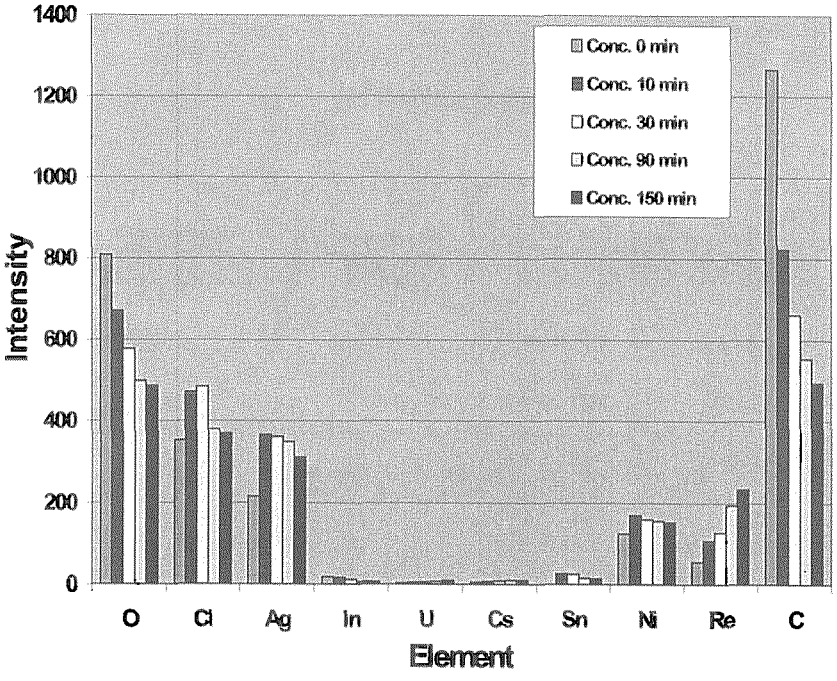


Fig.17 XPS analysis of filter 701 deposit at different sputtering times

Both anions O, Cl as well as cations Ag, In, U, Cs, Sn, Ni, Re, C were detected. C and O are considered to be surface contaminants of the samples; Cl is also a contaminant from the thermal shroud.

The main signals were observed (in descending order) from Ag, Ni, Re, Sn, with small amounts of Cs, In & U. Most signals were oxidic in nature except for Ag & Ni from substrate. The Ag in the top 240 surface layers (80mins sputtering) was oxidic thereafter the peak shift shows it to be metallic within the deposit. The surface Ni was oxidic and was probably oxidation products from the vertical line upstream or from the (Inconel) substrate. The deposit generally had a uniform composition except for an increasing amount of Re (in oxidic form) with depth, implying higher aerosol concentrations in an early phase that is an early release. The Cl shows a shift in parallel with the Ag and this is interpreted as combined deposits of Ag with AgCl within the deposit and AgO and silver oxychloride (AgOCl) on the surface.
The information from the Auger supports the results from the ICP-MS and SEM-EDX analyses but in addition gives useful information on their chemical state, confirming that silver is transported in a metallic state as vapour or droplets, whereas the other major species are usually transported in an oxidic state.

4.5 Vertical line revaporisation tests

It is known that volatile fission products such as Cs could be remobilised under certain circumstances during the later stages of a reactor accident [13]. Thus samples were cut from the vertical line above the bundle for revaporisation testing. These deposits were laid down during the test at about 700°C. A γ-scan of the vertical line revealed strong Cs-137 and Cs-134 lines as the main source of activity.
The tests were carried out under flowing steam atmosphere with 1cm x 1cm samples, cut from the vertical tube. The ramp rate was 3°C/min, from 300°C up to 1000°C (up to 300°C the sample was kept under N_2). It was maintained at 1000°C for 1 hour before descending at 10°C/min to 300°C under steam before switching back to N_2 atmosphere and descending to room temperature at 10°C/min. A γ-spectrometer measured the Cs activity during the ramping under steam. It was seen that Cs activity loss started at 590°C and was completed by 950 °C with only 3 % residual activity at the end (see Fig. 18).

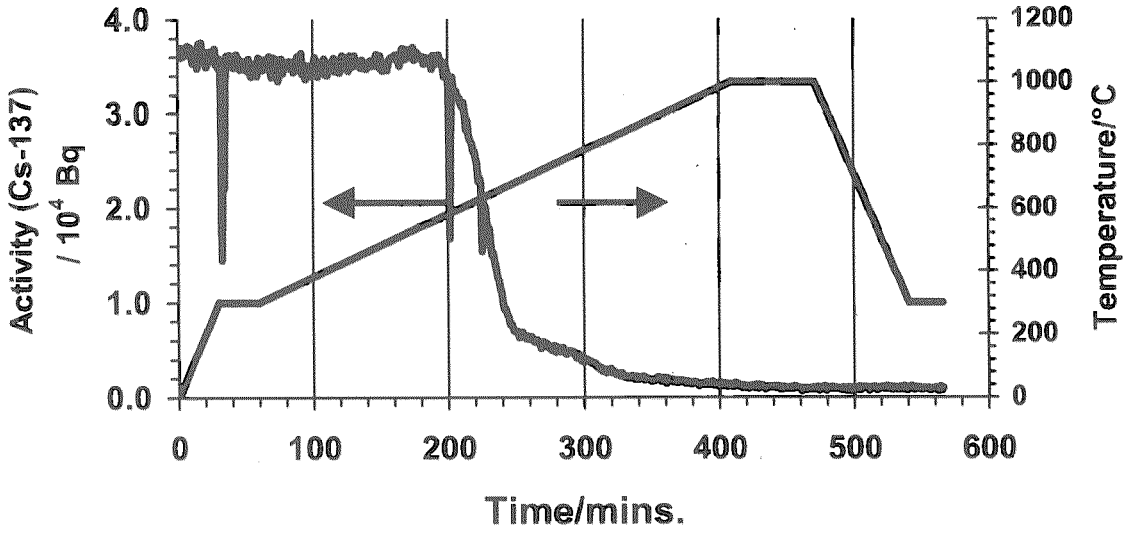


Fig.18 Cs-137 γ-activity of the upper vertical line sample during slow ramping to 1000°C under a steam atmosphere

Steam flow was cooled and diluted with N_2 and then passed through a high flow filter to trap the condensed aerosol particles. Most of the sample's activity loss was collected in the filter.

Further ICP-MS analysis of the filter showed that other fission products also volatilised from the sample and were caught as aerosol on the filter. In addition to Cs, these were Sr, Te, Mo, Rb, as well as fuel and structural materials.
Single effect tests carried out under the SCA revaporisation project [14] also show that pure caesium oxides or hydroxides also revolatilise in the same range. This implies that Cs behaves the same in steam atmospheres whether it is pure or mixed with other products.
These results also give a possible explanation for the 'Cs wave' entering the containment at the end of the Phébus FPT1 test. The increased flow of pure steam over the vertical line at 600-700 °C during the FPT1 shutdown is thought to have enabled Cs compounds in the deposit to revaporise and pass downstream to the containment.

5 Conclusions

FPT1 degradation reproduced features seen in FPT0 such as the pool of melted material (corium) beneath a cavity with an upper region of 'dry' degraded rods.
The corium is a ceramic of approximate composition $(U_{0.5}Zr_{0.5})O_2$ containing fission products with structural material or metallic fission products as small boundary phases. FPT1 corium composition is similar to FPT0. Microprobe analysis is confirmed by X-ray diffraction and they indicate corium appears to be stoichiometric (O/M = 2) and not easily oxidised.
Degraded fuel that is not melted usually has distorted, thick cladding that has undergone double-sided oxidation. Interdiffusion of Zr and U between fuel and cladding is observed, and oxidised cladding is only slowly attacked by any melt.
Porosity from fission gas release reaches 80 % in the upper degraded regions, where the least melt is observed.
The degraded fuel appears oxidise in steam to a considerable degree (~O/M = 2.30) although no higher oxide phases have been observed.
The FPT1 filters show the various fission product, fuel, and structural material aerosols that have flowed down the simulated primary circuit (dominated by Ag, Re & In). The back-up filters have negligible deposit except for Cd that is a vapour at 700°C and condenses at 150°C on the back-up filters. In-rich crystallites on the surface of the aerosols suggest It is condensing out along the circuit. Cs on 700°C filters appears to penetrate into the scale.
Tests on vertical line samples show Cs (and other fission products) will revaporise rapidly in steam atmosphere (Cs above 550°C). The extent may depend on deposition temperature.
Auger spectroscopy confirms the chemical analyses and indicates most deposits, (In, Sn, Cs, U) are oxides except for Ag. However surface oxidation of Ag and Ni (from the substrate) is seen.

6 References

[1] M. Schwarz, B. Clément,C. Ktorza, M. Maegey, R.Zeyen, 4th Technical Seminar on the Phébus FP Programme, Marseille, 20-22 March 2000.

[2] P.D.W.Bottomley, S.Brémier, J-P.Glatz, & C.T.Walker, Mikrochim. Acta **132**, p391-400 (2000)

[3] P.D.W.Bottomley, S.Brémier, D. Papaioannou, & C.T.Walker, Mikrochim. Acta **139**, p27-38 (2002)

[4] P.D.W.Bottomley, A.D. Stalios, J-P.Glatz, B. Sätmark & C.T.Walker, J. Nucl. Mat. **278**, p136 (2000)

[5] C.T.Walker, J. Anal. At. Spectrom., **14**, p477 (1999)

[6] J.L. Pouchou, F. Pichoir, La recherche aérospatiale, **5**, p167 (1984)

[7] C. Ronchi, M. Sheindlin, International Journal of Thermophysics **23**, No 1, p293, (Jan. 2002)

[8] K.A. Romberger, C.F. Baes, Jr., and H.H. Stone, J. Inorg. Nucl. Chem. **29**, p1617 (1967)

[9] W.A. Lambertson, M.H. Müller, J. Am. Chem. Soc. **36**, p365 (1952)

[10] K.H. Hellwege, A.M. Hellwege, (Eds) Landolt-Börnstein; Zahlenwete und Funktionen aus Naturwissenschaften und Technik NS III/7/b1, Berlin, p324 (1975)

[11] F. Schleifer, A. Noumadis, H. Nickel, H. Speltmann, Proc. 5th German-Yugoslav Meeting in Materials Science and Development on Contemporary Inorganic Materials. Simerath-Rurberg, Germany. Kernforschungsanlage Jülich, p61 (1987)

[12] J. Spino, D. Papaioannou, J. Nucl. Mat. **281**, p146 (2000)

[13] A.L. Wright (Ed) - Primary Fission Product Release and Transport: A State of the Art Report to the CSNI, NUREG/CR 6193 (1994)

[14] A.B. Anderson, A. Auvinen, P.D.W. Bottomley, C.J. Bryan, N.E. Freemantle, J-P. Hiernaut, J.K. Jokiniemi, A.F. Kingsbury and A.T. Tuson, - Revaporisation Tests on Samples from Phébus Fission Products - Summary Final Report (ST: RVP(00)-P30), (2000).

EUROPEAN COMMISSION
DIRECTORATE GENERAL JRC
Institute for Transuranium Elements
Hot Cells Technology

Fuel Safety Research Specialists' Meeting
JAERI, Tokai, Japan 4-5 March 2002

Analysis of Phebus FPT1 samples carried out at ITU, Karlsruhe

D. Bottomley, C.T. Walker, J-P. Glatz,
M. Cheindlin, & D. Papaioannou

European Commission
Institute for Transuranium Elements,
Postfach 2340
D-76125 Karlsruhe, Germany

EUROPEAN COMMISSION
DIRECTORATE GENERAL JRC
Institute for Transuranium Elements
Hot Cells Technology

Fuel Safety Research Specialists Meeting JAERI, Japan 4-5 March 2002

Analysis of Phebus FPT1 Samples carried out at ITU Karlsruhe

D. Bottomley , C.T. Walker, J.-P. Glatz, Sheindlin, D. Papaioannou

Outline of Talk

1. Introduction
2. Macroscopic and Microscopic Examination of the bundle and corium
3. Examination and analysis of filters
4. Supplementary tests
5. Conclusions

EUROPEAN COMMISSION
DIRECTORATE GENERAL JRC
for Transuranium Elements
Hot Cells Technology

Analysis of Phebus FPT1 Samples at ITU Karlsruhe

Introduction

Phebus pf is an international severe accident project lead by IPSN Cadarache and the European Commission
- supported by other national institutes
- other non-EU countries : Japan, Korea, Canada, USA, Switzerland.

A 20-rod bundle is heated with to cause severe overheating, degradation and fission product release.

The fp release is monitored along the simulated primary circuit by coupons, impactors and γ-spectroscopy.
The FPT1 bundle was examined by X-ray tomography and cut up to confirm its structure.

ITU received a) bundle, b) filters from the simulated primary circuit &c) vertical line samples for analysis

Test Progress to date

Time	Test	Test	Fuel	Burn-up
Dec 1993	FPT0	1st (baseline) test	trace-irradiated fuel	---
July 1996	FPT1	2nd test	BR3 irradiated fuel	23 GWd/tU
July 1999	FPT4	3rd test (debris bed)	EdF irradiated fuel debris	~30 GWd/tU
Oct. 2000	FPT2	4th test-reducing condn.	BR3 irradiated fuel	32 GWd/tU

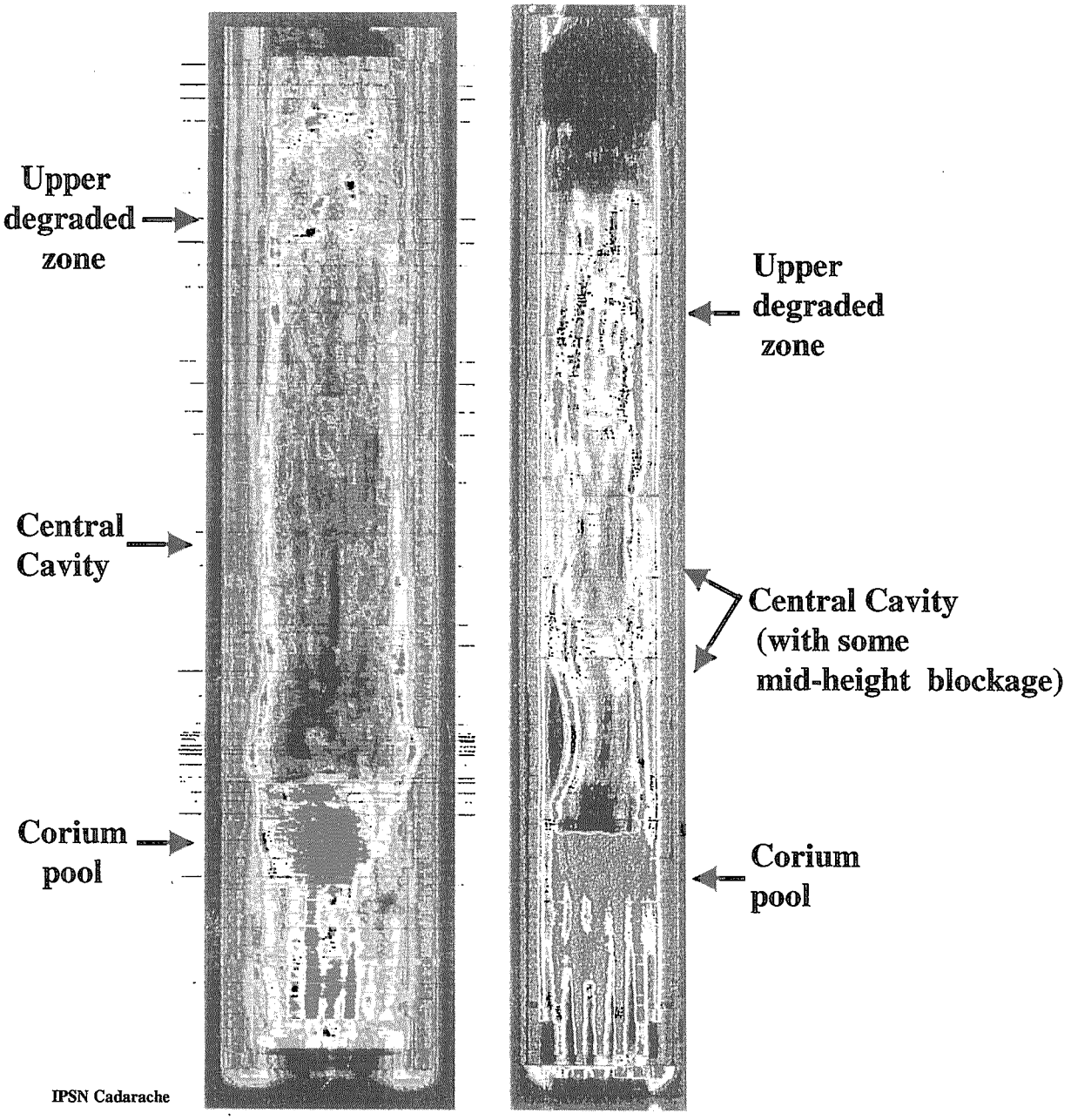
This is a blank page.

EUROPEAN COMMISSION
DIRECTORATE GENERAL JRC

Institute for Transuranium Elements
Hot Cells Technology

Phebus FPT1

Bundle Tomography



FPT0 **FPT1**

A similar structure is seen in both tests
downward movement of material and accumulation
in a pool at 1/3 -1/4 height

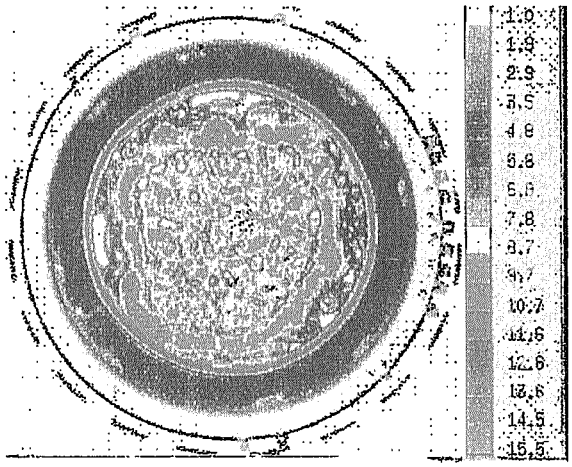
This is a blank page.

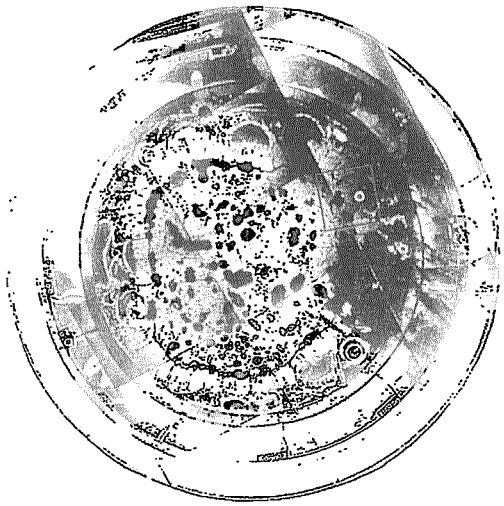
EUROPEAN COMMISSION
DIRECTORATE GENERAL JRC
Institute for Transuranium Elements
Hot Cells Technology

Phebus FPT1 Macrography

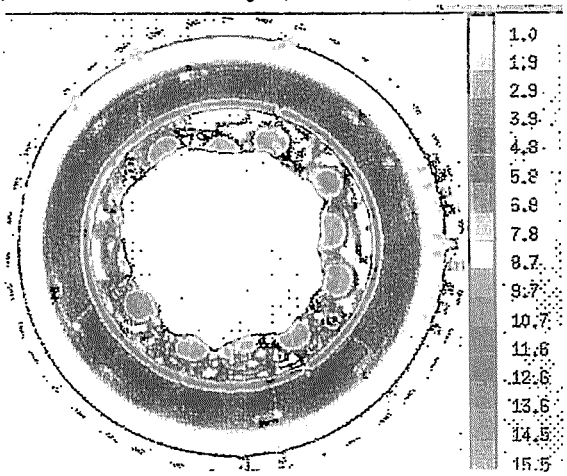
Micro.examⁿ. areas

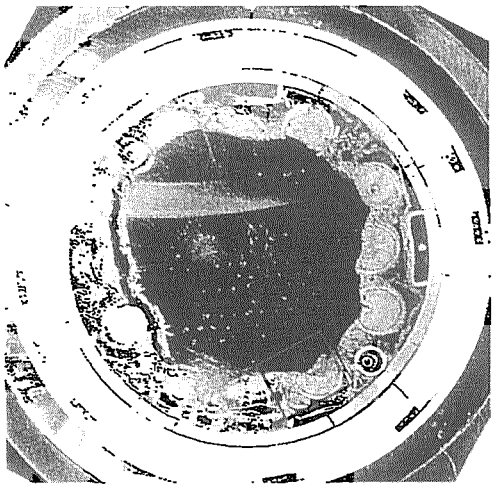
A) Corium pool (228mm)



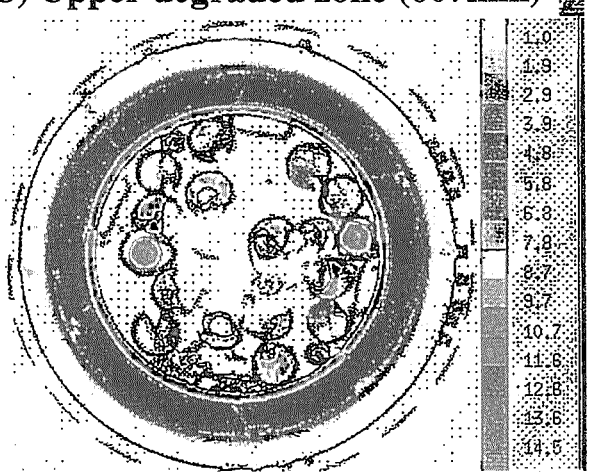


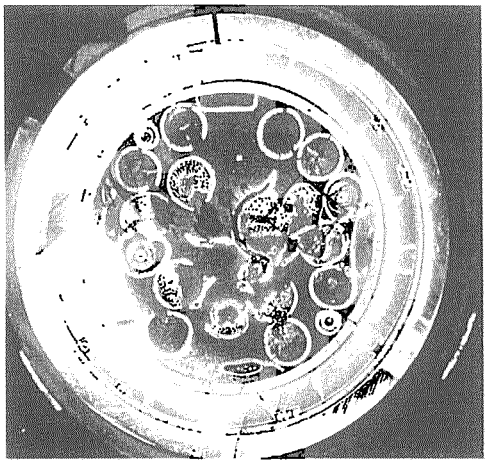
B) Central Cavity (261mm)





C) Upper degraded zone (607mm)





Good agreement of macros with tomography sections is seen.

This is a blank page.

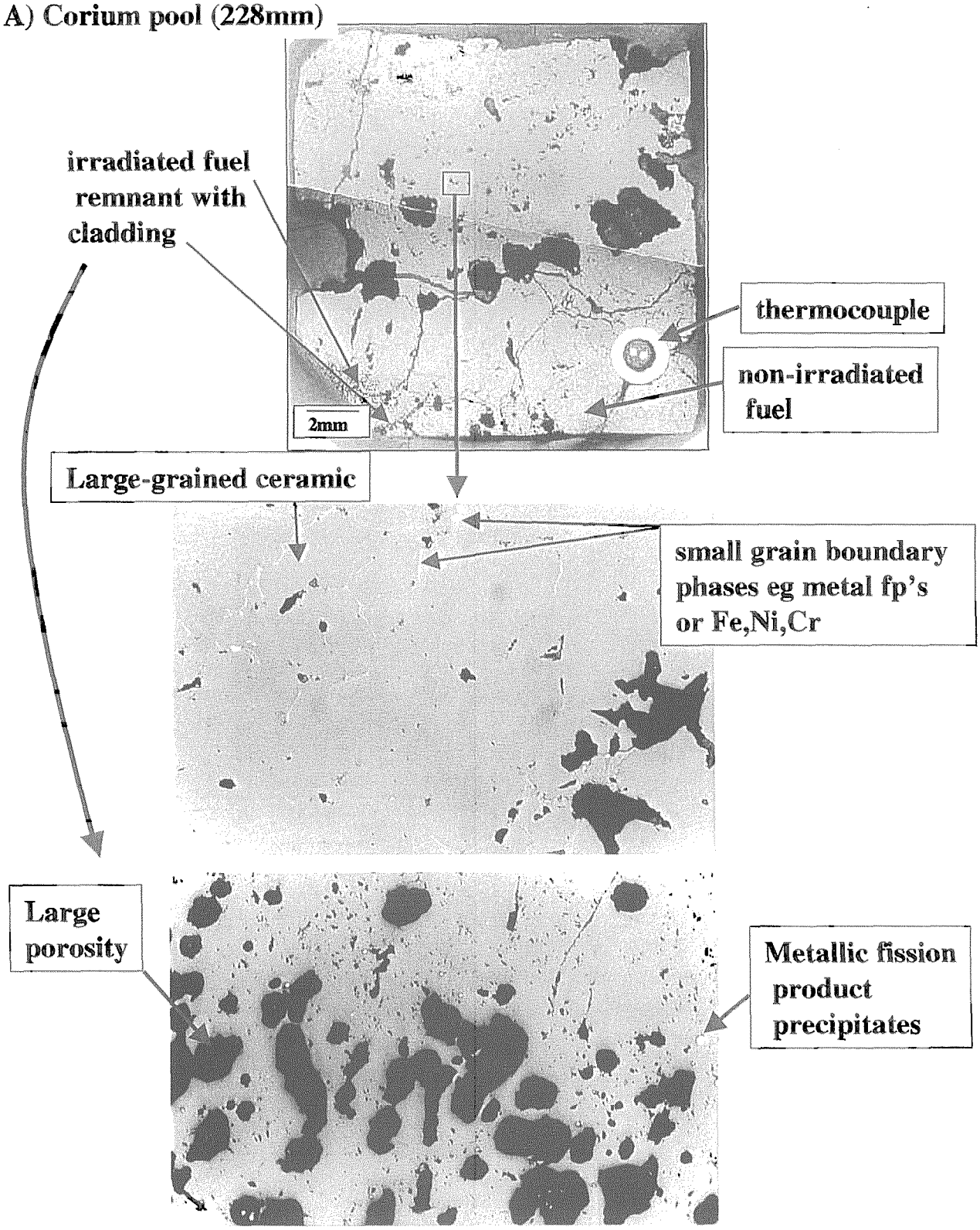
EUROPEAN COMMISSION
DIRECTORATE GENERAL JRC

Institute for Transuranium Elements
Hot Cells Technology

Phebus FPT1

Microscopic structure

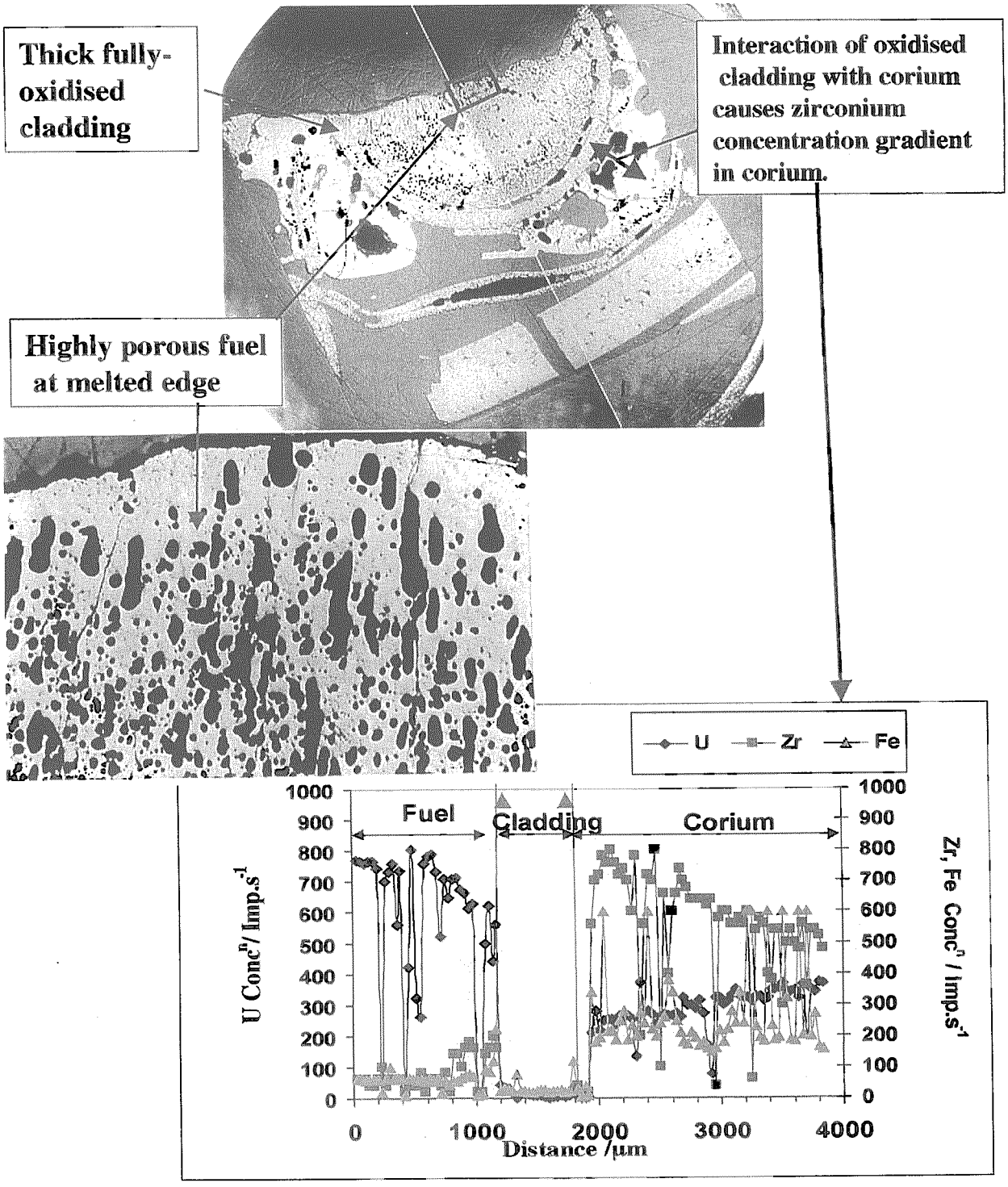
A) Corium pool (228mm)



EUROPEAN COMMISSION
DIRECTORATE GENERAL JRC
Institute for Transuranium Elements
Hot Cells Technology

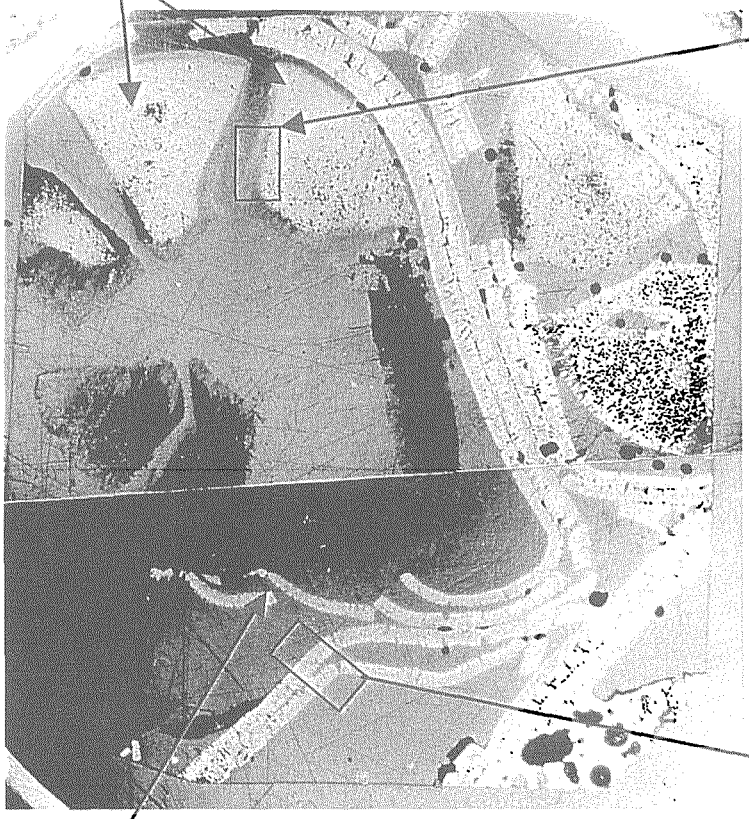
Phebus FPT1 Microscopic structure

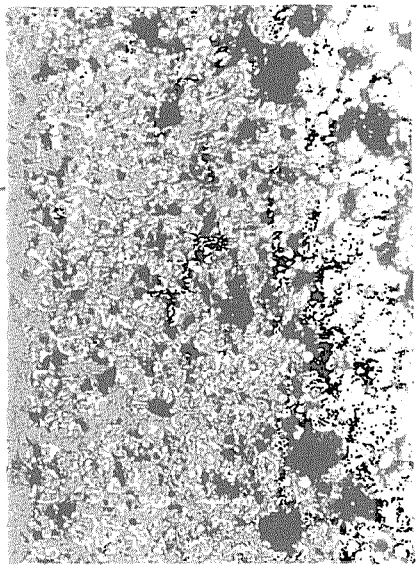
B) Melted Fuel at Cavity (261mm)



Phebus FPT1

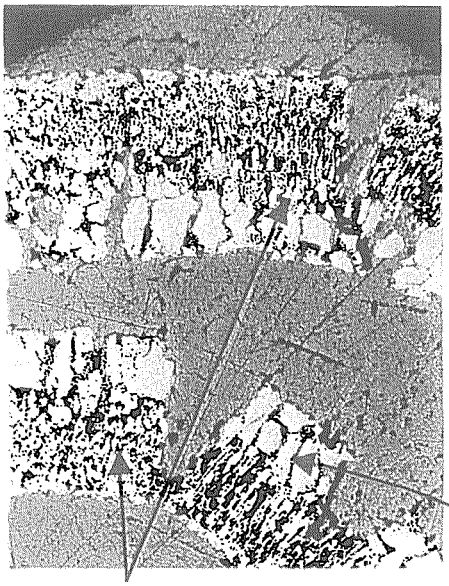
Microscopy: Upper zone (473mm)





Highly porous fuel -upto 80% porosity observed

Cladding distorted ('flowered') by oxidation



Double-sided oxidation -large-grained oxide

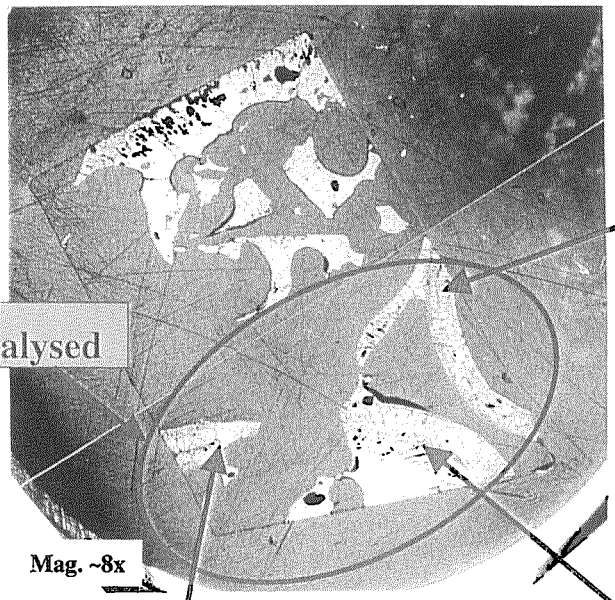
This is a blank page.

EUROPEAN COMMISSION
DIRECTORATE GENERAL JRC

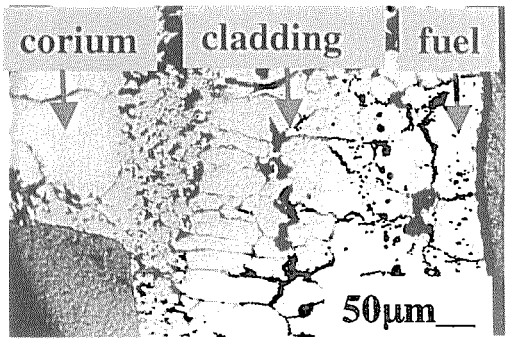
Institute for Transuranium Elements
Hot Cells Technology

Phebus FPT1

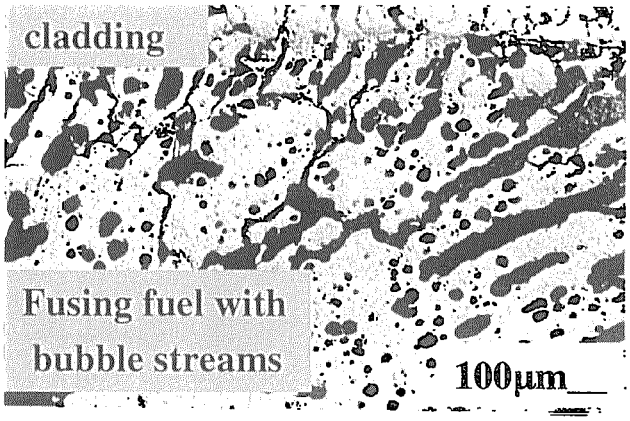
Microscopy: Upper zone (607mm)



1) Cladding with inner layer of un-irradiated fuel

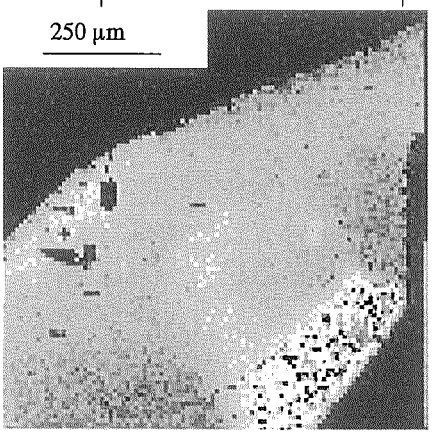


2) Fuel with oxidised cladding

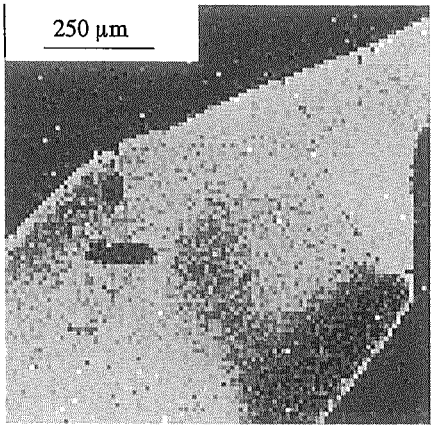


3) corium fused with cladding

U



Zr



High signal

Low signal

EMPA analyses

irradiated fuel composition:

$(U_{0.86}Zr_{0.12}Fe_{0.006}Nd_{0.006}Pu_{0.005}Ce_{0.005})O_{2.42}$

Fuel is superstoichiometric:

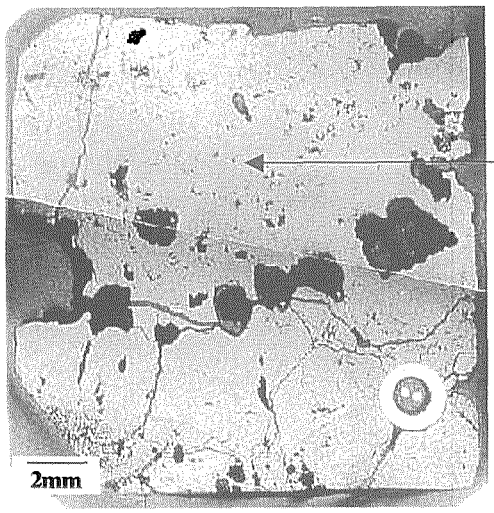
irradiated fuel O/M =2.42,

non-irradiated O/M = 2.32

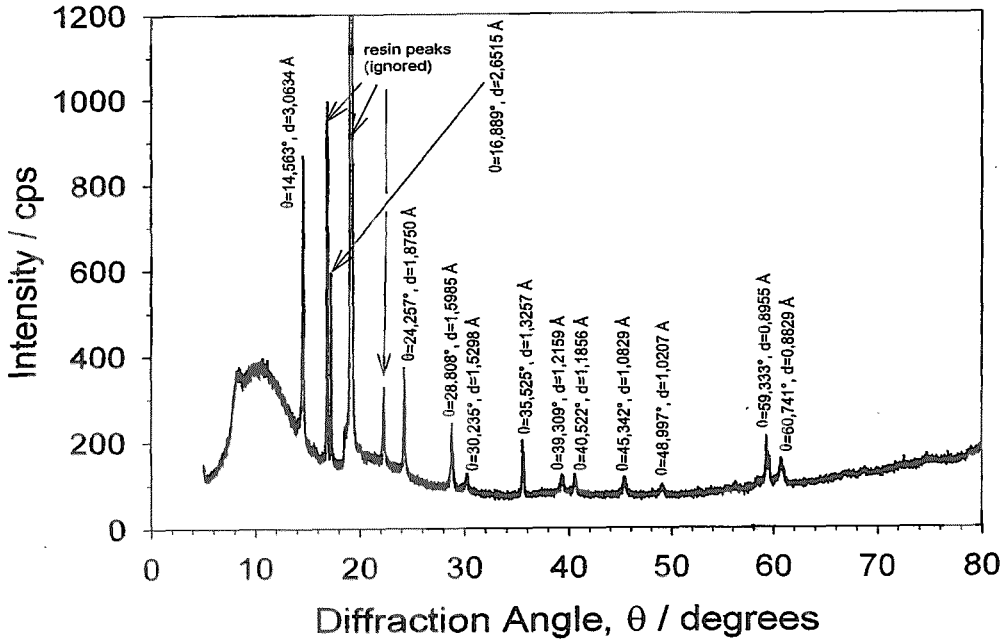
This is a blank page.

Phebus FPT1

X-ray Diffraction



Corium area from upper pool (228mm) examined by XRD



→ $a = 5.2984$ Å

The spectrum indicates a single cubic fluorite-type lattice.
The value of the lattice parameter a
lies between that of pure UO_2 and pure ZrO_2, &
implies a single phase with composition of ~ $(U_{0.5}Zr_{0.5})O_2$

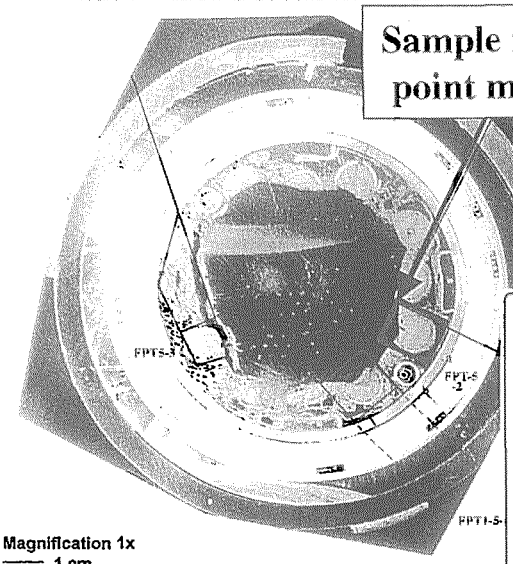
EUROPEAN COMMISSION
DIRECTORATE GENERAL JRC

Institute for Transuranium Elements
Hot Cells Technology

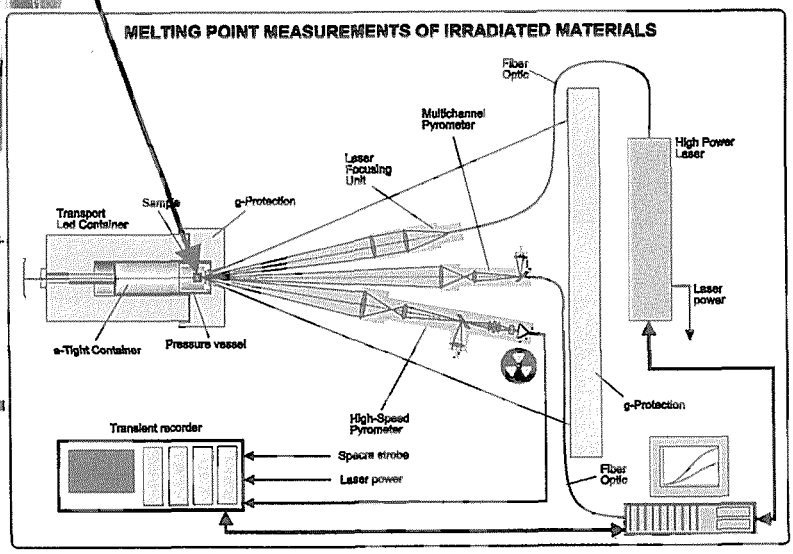
Phebus FPT1

Melting point measurement

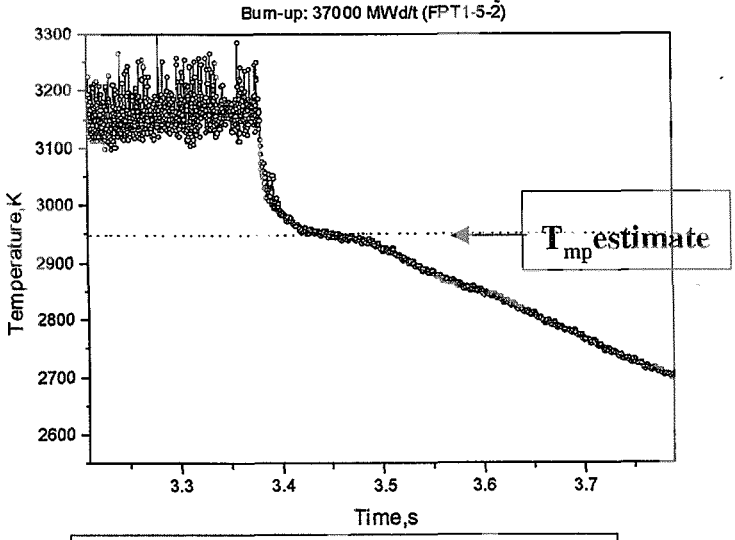
Sample for melting point measᵗ.



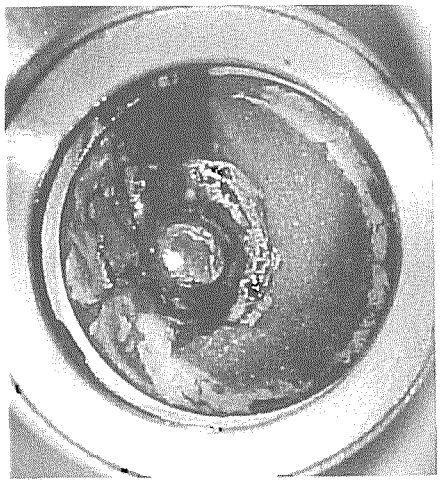
Magnification 1x
—— 1 cm



Thermogram of laser pulse melted FPT1 UO_2 at +261 mm
Burn-up: 37000 MWd/t (FPT1-5-2)



Melting point determined from arrest in cooling curve



Sample after 4 laser shots

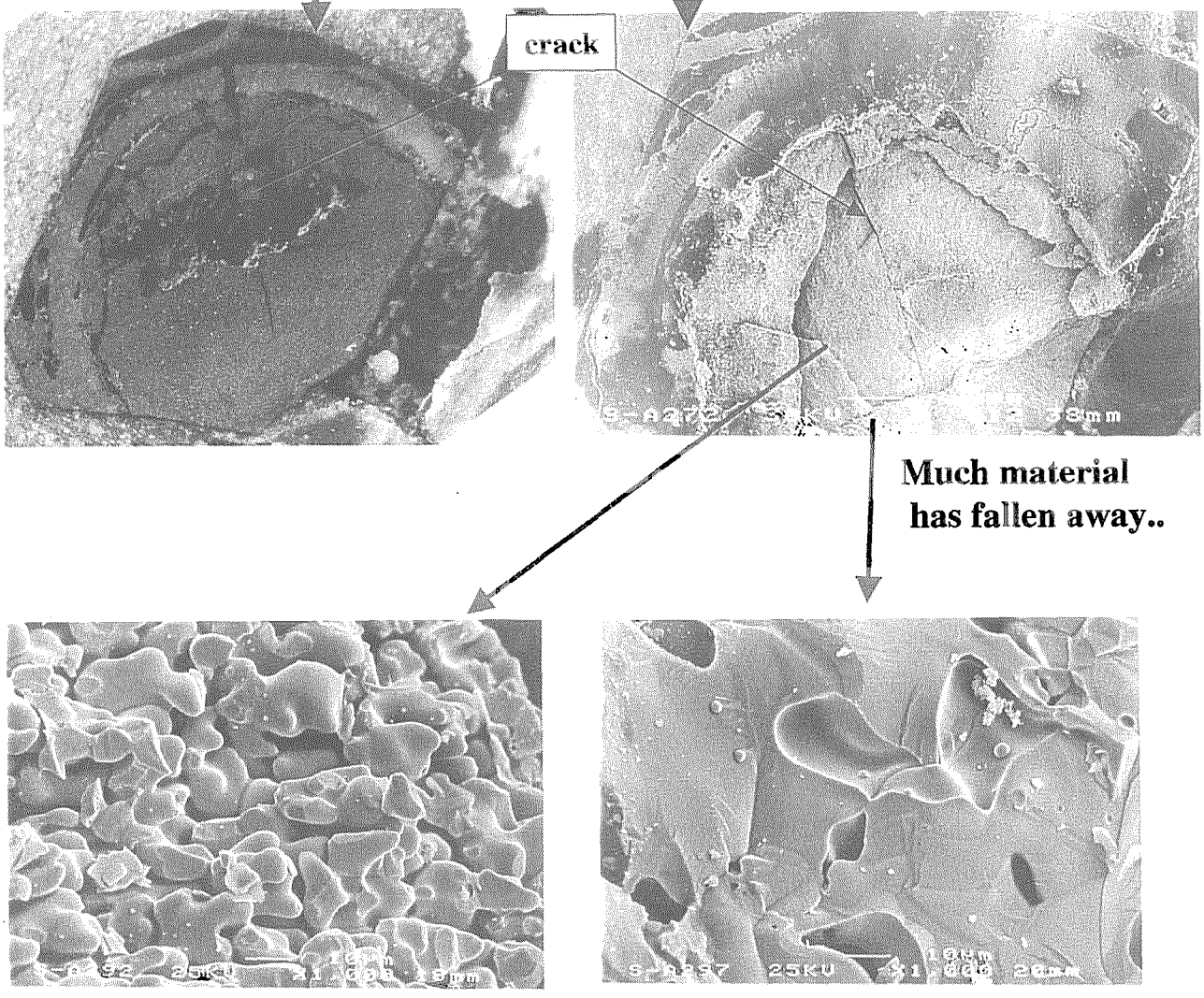
EUROPEAN COMMISSION
DIRECTORATE GENERAL JRC

Institute for Transuranium Elements
Hot Cells Technology

Phebus FPT1

Melting point measurement - 2

Sample before (OM) and after (SEM) laser shots



..but the remaining material shows that it had melted or fused

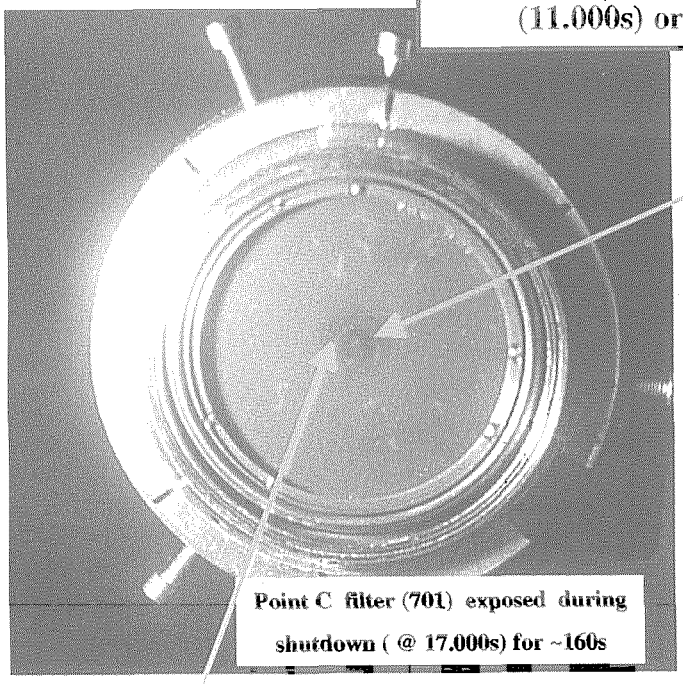
SEM-EDX showed upto 17wt% of ZrO_2 at points in this degraded fuel sample therefore thus the T_{mp} of 2950K $\pm$30K which is over 150°C below the expected value of UO_2 (~3083K) may be due to cladding interaction with fuel

EUROPEAN COMMISSION
DIRECTORATE GENERAL JRC

Institute for Transuranium Elements
Hot Cells Technology

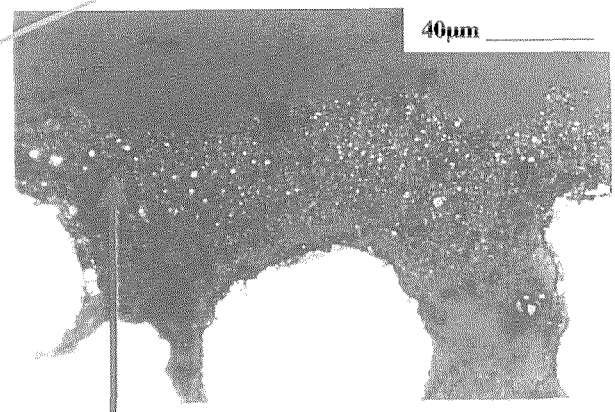
Phebus FPT1 PTA -filter examⁿ

From Points C (700°C) & G (150°C) exposed at oxidation (11.000s) or shutdown (17.000s) for 300s or 160s



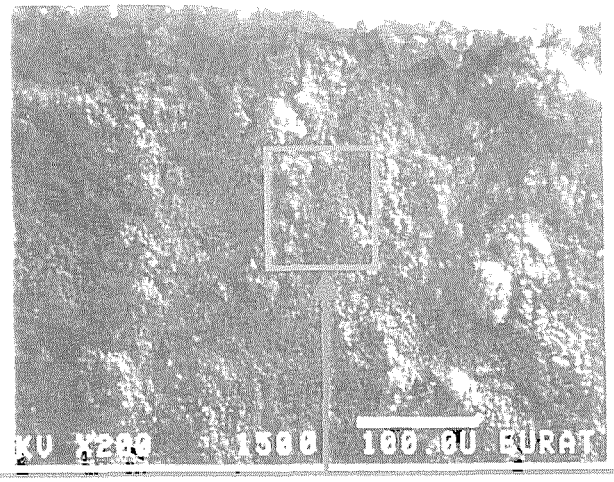
Point C filter (701) exposed during shutdown (@ 17.000s) for ~160s

Optical microscopy

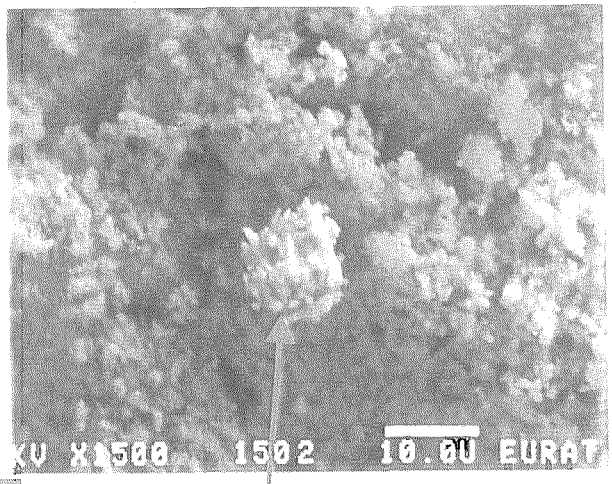


Heterogeneous deposit with metallic phases

SEM-EDX



Particulate deposit of agglomerated aerosols:
Major element is Ag (31at%), next Re, Zr (14at%), U (9at%), & then In (2at%)
(Cl impurity excluded from calc.)



U-rich sphere coated with In crystals
U(40at%), In (39at%) next Ag (8at%), Sn (5at%).
(Cl impurity excluded from calc.)

EUROPEAN COMMISSION
DIRECTORATE GENERAL JRC

Institute for Transuranium Elements
Hot Cells Technology

Phebus FPT1 PTA -filter examⁿ-2

ICP-MS Analysis of Deposits

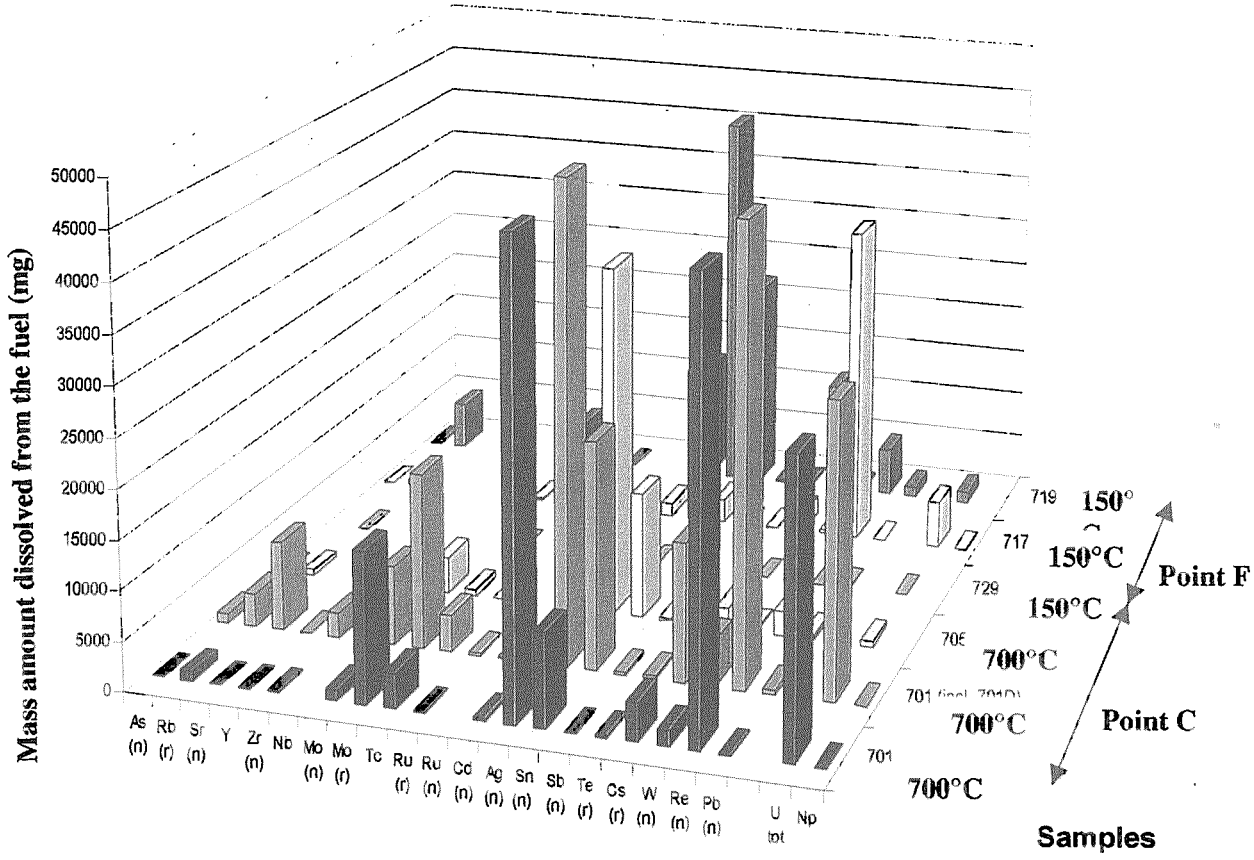
Composition

mainly structural materials Ag, Sn, Re
some fission products (Mo, Rn, Cs) seen, as well as fuel cladding U, Zr.

More deposit on upstream hotter filters
Cd seen on early low temp. (150°C) back-up filter
(is vapour at 700°C, & condensate at 150°C)

considerable Cs+Sn is 'baked' onto 700°C filter, but soluble on 150°C filter.
(700°C filter require digestion for 100% retrieval),

ICPMS Analysis of Point C and G Filters
Total Weights (mg)



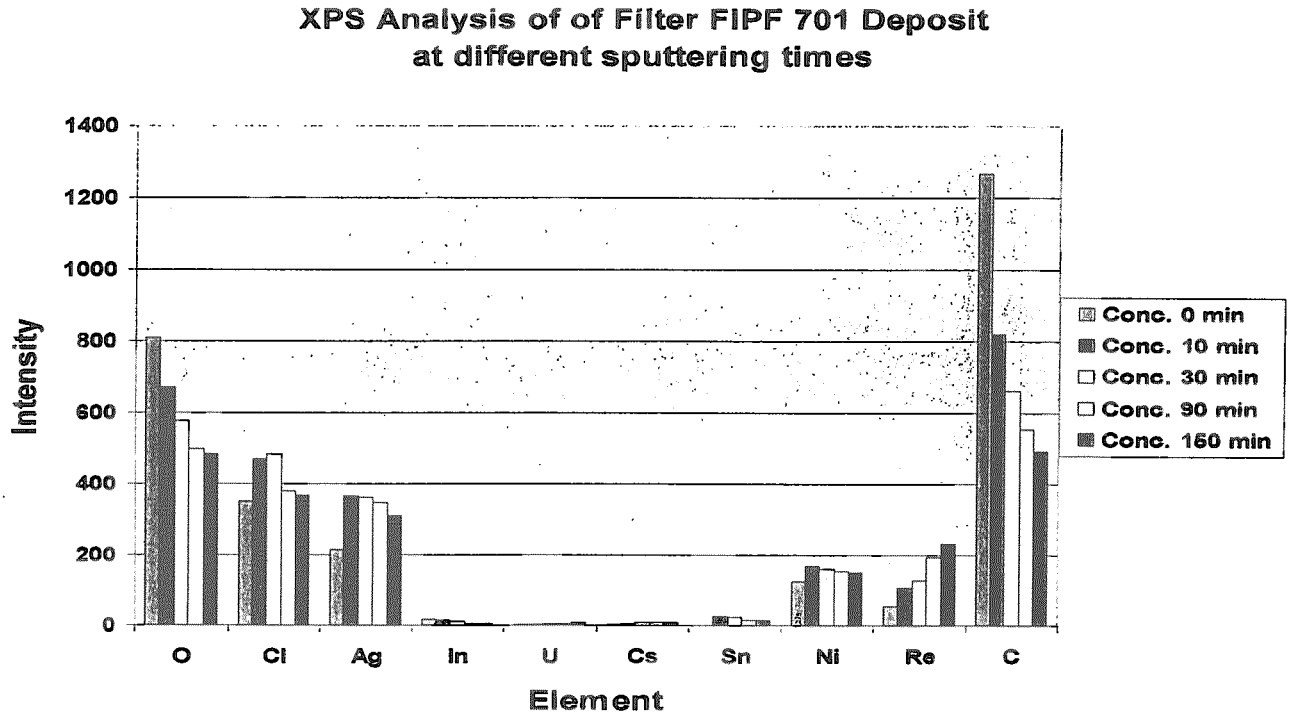
Gamma-spectroscopy also shows the presence of Cs-137,Cs-134, Sb-125, Eu-154, & Ag 110m

EUROPEAN COMMISSION
DIRECTORATE GENERAL JRC

Institute for Transuranium Elements
Hot Cells Technology

Phebus FPT1 PTA -filter examination-3

Auger (XPS) Analysis of Deposit Surfaces



Main elements: are Cs, Ag, In, Re, Sn, Ni (substrate)+ U

oxide: U, Cs, In, Re, Sn
metallic: Ag

notes: Ag oxidised at surface
Ni also oxidised at surface.
oxidic Re found below surface

→ **Auger supports ICP-MS & SEM results**

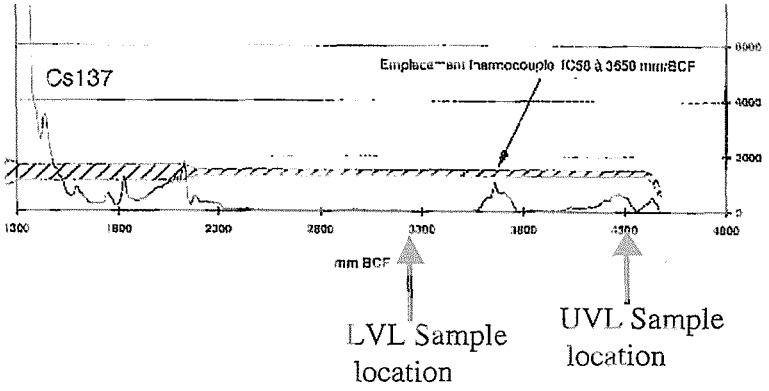
EUROPEAN COMMISSION
DIRECTORATE GENERAL JRC

Institute for Transuranium Elements
Hot Cells Technology

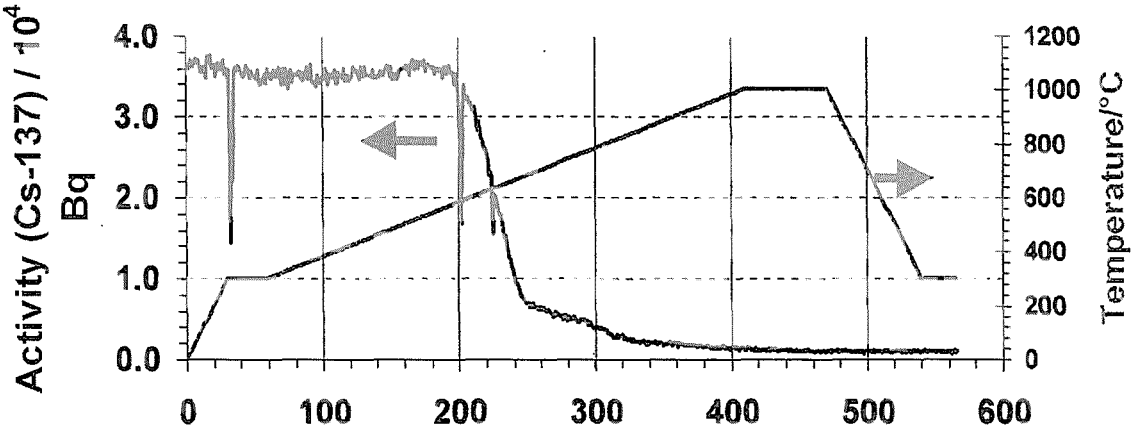
Phebus FPT1 PTA -vertical line examn

Revaporisation testing of Deposits

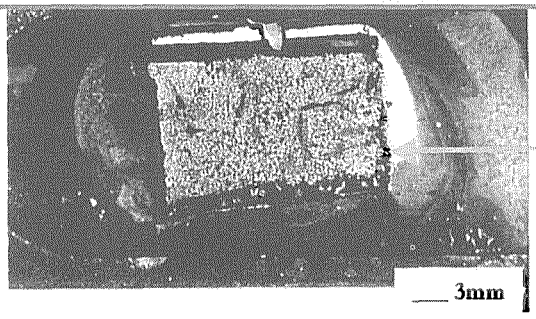
Samples were cut at 2 points that were at ~ 700°C during FPT1, γ-scans showed they had considerable Cs-137



Cs-137 γ Activity of the Upper Vertical Line Sample during Slow Ramping to 1000°C under a Steam in Steam Atmosphere



Considerable Cs loss: starting at 590°C , completed by 950°C - most has been caught on the filter downstream



Upper Vertical Line sample deposit after revaporisation testing to 1000°C in steam.(note corrosion of holder & sample surface) (3.3x)

EUROPEAN COMMISSION
DIRECTORATE GENERAL JRC
Institute for Transuranium Elements
Hot Cells Technology

Phebus FPT1

Conclusions

1. FPT0 & FPT1 degradation show features such as a molten pool (corium) beneath a cavity with an upper region of 'dry' degraded rods.

2. The corium is a ceramic of approx. composition $(U_{0.5}Zr_{0.5})O_2$ containing fission products, structural material or metallic fp's as small boundary phases. Microprobe analysis, XRD indicates stoichiometric corium and not easily oxidised.

3. Degraded fuel that is not melted has distorted fully oxidised cladding. There is interdiffusion of Zr and U between fuel and cladding, oxidised cladding is only slowly attacked by melt.

4. Porosity from fission gas release reaches 80 % in the upper degraded regions, where the least melt is retained.

5. Degraded fuel appears oxidise in steam to a considerable degree (~O/M = 2.30) although no higher oxide phases have been observed. (significance in difference between irradiated & non-irradiated fuel.

6. FPT1 filters show various fission product, fuel, and structural material aerosols flow down the circuit (dominated by Re, In, & Ag. In may condense along the circuit , while Cd is a vapour at 700°C. Cs on 700°C filters penetrates into the scale (Sn has similar behaviour)

7. Tests on vertical line samples show Cs (and other fission products) will revaporise rapidly in steam atmosphere (Cs above 550°C).

8. Auger confirms the ICP-MS & SEM-EDX . It indicates most deposits, (In, Sn, Cs, U) are oxides except for Ag. However surface oxidation of Ag+Ni (from substrate) is seen.

Discussion:

Q: (P. Tempest)
The XRD data on the corium sample is not inconsistent with a hyper-stoichiometric phase. Conclusion 2 would be strengthened / confirmed if the EPMA data confirming O/M of 2.0 had been included in the presentation.

A: Yes, I completely agree. I will add the EPMA analysis.

Q: (M. Zabiego)
You mention that cesium revaporization occurs below 600C in your test. I would think that the vertical line temperature was higher than 600C through the test. If this is right, where does the cesium you measure come from ?

A: Good question. In fact after this revaporization test had been performed, the FPT-1 test data was re-examined and one of the conclusions was that the vertical line probably was not being maintained at 700C, but was perhaps about 600C.

JP0250421

6. Session 5a : Fuel Behavior under Normal Operation Condition

Session 5a-1

NOK High Burn-up Fuel Surveillance Programme

SFRSM Meeting, Tokai 3-4 March 2002

Dr. Christophe Ott, NOK Baden,
Section Head of Fuel Procurement and In-Core fuel Management

Abstract

In 1998 NOK modified Beznau Nuclear Power plants operating strategy for a cycle concept with an annual reload batch of 20 Fuel Assemblies (1/6 of the core). This approach has a significant benefit for back-end cost but is faced with two current licensed limits, fuel burn-up level and enrichment.

A surveillance programme has been proposed on a series of lead test fuel Assemblies, UO2 and MOX, having an enrichment of up to 4.55 w/o ^{235}U and 4.75 w/o Pu_{fiss} respectively. The fuel enrichment limit had to be raised on basis of acceptable calculations for the matrix of stored fuel in the pools having sufficient conservatism, both in the assumptions made and the methodologies applied.

An overview of the surveillance programme estimated to run up to 2007, and the Burn-up credit approach used to increase the enrichment limits in Beznau pool facilities are presented in this paper.

Nordostschweizerische Kraftwerke NOK

NOK High Burn-up Fuel Surveillance Program

Dr. Christophe Ott, NOK Baden,
Section Head of Fuel Procurement and In-Core Fuel Management

Abstract

In 1998 NOK modified Beznau Nuclear Power plants operating strategy for a cycle concept with an annual reload batch of 20 Fuel Assemblies (1/6 of the core). This approach has a significant benefit for back-end cost but is faced with two current licensed limits, fuel burn-up level and enrichment. A surveillance programme has been proposed on a series of lead-test-fuel-assemblies, UO2 and MOX, having an enrichment of up to 4.55 w/o ^{235}U and 4.75 w/o Pu_{fiss} respectively. The fuel enrichment limit had to be raised on basis of acceptable calculations for the matrix of stored fuel in the pools having sufficient conservatism, both in the assumptions made and the methodologies applied. An overview of the surveillance programme estimated to run up to 2007, and the Burn-up credit approach used to increase the enrichment limits in Beznau pool facilities are presented in this paper.

1. Introduction

In March 1998 the NOK management approved a change in Beznau operating strategy for a cycle concept with annual fuel reloading. It was also agreed to aim for a reduction in the reload batch size from an annual 24, to 20 fresh assemblies. This has a significant benefit for back-end fuel cycle costs.

The new reload strategy is faced with two current licensed limits, the ***fuel burn-up*** and ***enrichment.***

Changing 1/6 of the fuel assemblies from the core each year means that the assembly life is 6 years in reactor. From the reactor physical conditions, it can be calculated that the burn-up in the average assembly at discharge will reach around 60 MWd/kg HM which is 10 MWd/kg HM higher than the present licensed level. Based on a Framatone-ANP (formerly Siemens) fuel design, with 322 kg fuel per assembly, an enrichment of 4.55 % U^{235} is required (ref. 1) Here the limit is set by the allowed enrichment in the storage pools (4.28 w/o U^{235} for UO_2 and 5.3 w/o Pu_{fiss} for MOX fuel).

The proposed approach to licensing fuels for target burn-ups up to 60 MWd/kg HM (assembly average) in Beznau is therefore to use several lead test assemblies to verify trouble free operation in the burn-up range 50 to 60 MWd/kg HM . A surveillance programme has been proposed for measurements and examinations on a series of uranium and MOX fuel test assemblies, at intervals throughout their life, to provide the necessary reassurances for reliable and safe performance over six cycles of irradiation.

It is likely that the fuel enrichment limit have been raised on the basis of acceptable calculations for the matrix of stored fuel in the pools having sufficient conservatism, both in the assumptions made and the methodologies applied.

2. NOK High Burn-up Surveillance Program

On current knowledge, the effects having seemingly the greatest potential for limiting the exposure time and burn-up are corrosion, assembly growth, rod internal pressure and materials property degradation which could affect both steady-state and transient behaviour. All of these may have a burn-up or exposure-dependent factor, which needs to be investigated. Of these, the first two effects (corrosion and assembly growth) may be reactor-specific, the other effects are more generic. The lead test assemblies are to be used for measurement of corrosion and assembly growth. In addition to the Surveillance program, NOK and the fuel supplier will draw on experience, experiments and model studies from international or bi-lateral programmes having a high burn-up component which may also involve transient behaviour and materials property measurements (non-destructive and destructive testing). (ref. 2)

2.1 Design and Performance Parameters.

The material characteristics of the uranium fuel rod/assembly design for the high burn-up regime are given in the Tables 1 and 2. A particular characteristic of these fuel assemblies is the use of DUPLEX cladding for improved corrosion resistance. This cladding type has been first used in region 77 (4.25w/o U^{235}), four assemblies of which were loaded in Unit 1 in spring 1999.

MOX assemblies with a content of 4.75 w/o Pu_{fiss} (which is below the equivalent of 4.55 w/o U^{235} of the uranium assemblies) and DUPLEX cladding have been loaded in 2000.

Fuel Assemblies with an enrichment of 4.55 w/o U^{235} have been loaded for the first time in 2001.

2.2 Provisional Surveillance Programme for High Burn-up Assemblies

In a first phase, in April 1999, already spent Fuel Assemblies from Unit 2 were visually inspected and length and oxide thickness measurements carried out in the storage pool, using staff, techniques and equipment supplied by Framatome-ANP.(ref. 3)

Secondly, visual inspections of four Fuel Assemblies Region 77 from unit 1 were made in 2000 and one each of Region 77 and S1 from unit 2 (Lead Use Assembly Inspection) with no negative findings.[1]

The third phase will begin in 2002 with the first of a series of measurements on 4 Fuel Assemblies from Region 77 and 2 MOX (Region S1) at the end of their 3rd and 2nd cycle of exposure respectively. Measurements will be repeated in 2004 at between 47 and 53 MWd/kg HM. Visual, oxide and length measurements will be made in each campaign.

As an interim examination, four assemblies from the high burn-up design Region 78 will be first fully examined from unit 2 in 2003 after two cycles of irradiation

In a fifth phase beginning in 2004, approximately four high burn-up fuel assemblies with 4.55% enrichment or equivalent, will undergo a similar regime of inspection starting at around 36 MWd/kg HM and three years later, at EOL with 59 MWd/kgHM.

The measurement regime may be modified at any time according to the findings of each series of inspections. In particular the 2007 series of measurements at EOL could be brought forward by one year depending on the earlier results. Alternatively assemblies of Region 78 from unit 2 can also be included in the final exams in 2007. This later planning remains open to discussion. (Figure 1). An example of the inspection programme foreseen during the next outage of Beznau 1 is shown Table 3 and a detailed test matrix is shown in Tables 4 and 5.

The results will be reported regularly following each campaign and analysed in conjunction with data from other relevant programmes, aimed to verify the performance of the Beznau fuel up to burn-ups reaching 60 MWd/kg HM (Fuel assembly average).

No special measurements will be made on the un-irradiated fuel. Framatome-ANP considers the data collected during fuel and assembly fabrication is sufficiently accurate for comparison purposes. In addition, no destructive (hot cell) exams are currently planned. Since findings from such exams (e.g fission gas release, chemical burn-up measurements, ceramography) are not reactor-specific there is no reason to use the Beznau Fuel Assemblies for providing such information. This data, in particular including materials properties and transient behaviour, could be more easily derived from other Framatome-ANP and International programmes on high burn-up fuel behaviour (e.g. the Halden programme).

3. Enrichment limits and Burn-up credit

The approved change in Beznau operating strategy required as mentioned an increase of the fresh fuel assembly enrichment (4.55 w/o U^{235}) above the licensed limits (4.28 w/o U^{235} UO_2 and 5.3 w/o Pu_{fiss} for MOX fuel) as defined in the KKB Tech Spec documents. To clear up this difficulty, criticality calculations of Beznau storage facilities (the boron pool, the stainless steel pool and the dry storage capacity) had to be carried out. The calculations were carried out by the Paul Scherrer Institute in Switzerland with the help of the 2D validated code BOXER.(ref. 4 &5)

The Computation consists of determining the maximum UO_2 and MOX fuel assembly enrichments assuming that each storage facility remains sub-critical. The approach used followed the standard NRC criteria (i.e a k_{eff} limit of 0.9235, ref. 6). Based on Framatome-ANP fuel assembly design, the maximum enrichment value found was 4.40 w/o U^{235} for UO_2 fuel.

To overcome the enrichment limit of 4.40 w/o U^{235} a more realistic approach has been considered. As allowed by the NRC procedure, we have taken into account a so called "burn-up credit" for the non fresh fuel assemblies. For the propose of the calculation, the fuel storage facility was considered divided in two zones. A central zone (block) with fresh fuel assemblies surrounded by a zone of once burned fuel assemblies. The burn-up value of the once burned fuel assembly was established by considering only the upper part (100 cm) of a typical axial burn-up distribution obtained after a first insertion of a 12 month equilibrium cycle (Figure 2). This is the most conservative arrangement when considering a two zone set up. The corresponding calculation results showed that the maximum enrichment values are the following:

- 4.57 w/o U^{235} for not more than 72 fresh UO_2 fuel assemblies in one or more connected blocks
- 4.89 w/o U^{235} for not more than 24 fresh UO_2 fuel assemblies in one or more connected blocks
- 8.17 w/o Pu_{fiss} for an unlimited number of MOX fuel assemblies.

These limits have been accepted by the Safety Authorities and included (in July 2000) in the Tech Spec documents of Beznau.

4. Conclusion

The proposal approach to licensing fuels for target burn-ups up to 60 MWd/kg HM (assembly average) in Beznau is performed using selected lead test assemblies to verify trouble free operation in the burn-up range 50 to 60 MWd/kg HM. A series of measurements, visual inspections, length measurements and oxide layer thickness measurements have been carried out since 1999 and should be completed in 2007.

The surveillance program includes also MOX fuel assemblies. But the future operating life of the two Beznau plants is uncertain due to forthcoming referenda asking for a rapid or less rapid abandonment of nuclear power which could lead to a shutdown of Unit 1 in 2009 if the referenda were accepted. This would mean that high burn-up may not be achieved in these MOX assemblies which need a longer cooling time at end of life, before interim dry storage and therefore may be removed at burn-ups below the maximum achievable. In case of a positive decision for nuclear power, of course the situation would be different with a possible life extension to 50 years or 2019.

The change in Beznau operating strategy (annual reload of twenty fuel assemblies) required an increase of the fresh fuel assembly enrichment (4.55 w/o U^{235}) above the then licensed limits. A rise in these limits, taking advantage of the "burn-up credit" concept of the spent fuel has been applied and accepted by the safety Authorities.

5. References

Ref. 1/ Paratte et al. *"Maximal zülassige Anreicherung der UO2-Brennelemente in Kompaktlager des KKW Beznau unter Berücksichtigung des Abbrandes"*. PSI Bericht TM-41-98-35

Ref. 2/ Letter to HSK *"Strategie für die Erstellung einer genehmingungsfähigen Grundlage zu Hochabbrand"* NOK, 10/09/01

Ref. 3/ Siemens Inspektionsbericht *"Brennelementinspektion und Oxidschichtdickenmessung an Brennstäben."* A1C-1305909-0, 30/04/1999

Ref: 4/ Maximal zulässige Anreicherunng der UO_2 und MOX Brennelemente im Kompaktlager des KKW NOK-Beznau, PSI Bericht: TM-41-98-19.

Ref: 5/ Maximal zulässige Anreicherunng der UO_2 Brennelemente im Kompaktlager des KKW NOK-Beznau, unter Berücksichtigung des Abbrandes, PSI Bericht: TM-41-98-35.

Ref: 6/ Spent Fuel Storage Facility Design Basis, U.S. Nuclear Regulatory Commission, December 1981, Appendix A.

Table 1. Fuel Rod Data

Characteristic	Unit	Value
Active Length	[mm]	3050
Fuel Rod Length	[mm]	3210
Rod Outer Diameter	[mm]	10.75
Clad Inner Diameter	[mm]	9.30
Clad Material		Duplex: (Zr-4/ ZrO,0.8Sn) (R 77, S1/S2) Duplex: (Zr-4/D4) (R.78)
Initial Internal Pressure	[bar at 25°C]	22.5 ± 1 abs
Plenum Volume	[cm^3]	7.6

Table 2. UO_2 (MOX) Fuel Data

Characteristic	Unit	Value
Material		UO_2 (UO2/PuO2)
Density	[gm/cm^3]	10.40 (10.45)
Melting Point	[°C]	2837
Fuel Enrichment	[w/o U^{235}]	up to 4.55 (MOX: 4.75% Pu_{fiss})
Pellet Diameter.	[mm]	9.11
Pellet Height	[mm]	11.0
Dishing Volume	[mm^3]	7.0

Table 3: Inspection Program foreseen in July 2002

Region	FA Identification	Core position	EOC burn-up (MWd/kg HM)	Visual	Length	Oxide
77[3]	7701	G-11	39.3	X	X	X
	7702	K-07	39.3	X	X	X
	7703	G-03	39.3	X	X	X
	7704	C-07	39.3	X	X	X
S1[2]	S101	E-10	25.9			
	S102	J-09	25.9	X	X	X
	S103	I-04	25.9			
	S104	D-05	25.9	X		X
	S105	J-05	25.7			
	S106	E-04	25.7			
	S107	D-09	25.7	X		X
	S108	I-10	25.7	X	X	X
78[1]	7801	H-12	12.3	X		
	7802	L-06	12.3	X		
	7803	F-02	12.3	X		
	7804	B-08	12.3	X		

[3] third cycle
[2] second cycle
[1] first cycle

Table 4. Provisional Test Matrix Beznau Unit 1

Year	Nominal Burnup [MWd/kg HM]			No of Fuel Assemblies		
Region U^{235}	R77 U-4.25%	S1 MOX	R78 U-4.55 %	Visual	Length	Oxide
1999	⊗			See Table 3		
2000	**18.0**	⊗		4		
2001	31.0	20.0	⊗			
2002	**43.0**	**32.0**	**11.7**	6	6	4
2003	50.0	40.0	24.5			
2004	**53.0**	**47.0**	**36.7**	6	8	6
2005		52.0	46.0			
2006		55.0	55.8			
2007		**55.0**	**59.0**	4	6	4

Shaded = Long outage, Bold = Measurement Campaign, ⊗ Year of first loading

TABLE 5 Additional Back-Up Test Matrix, Beznau Unit 2

Year	Nominal Burnup [MWd/kg HM]			No of Fuel Assemblies		
Region U-235	R 77 U-4.25%	S1 MOX	R 78 U-4.55%	Visual	Length	Oxide
1999	⊗	⊗				
2000	**9.3**	**10.7**		2		
2001	23.1	25.1	⊗			
2002	34.1	35.8	12.5			
2003	**45.8**	42.3	**26.8**	4	4	4
2004	51.5	48.6	39.5			
2005			49.5	*	*	*
2006			54.2			
2007			**58.0**	4	4	4

* if required

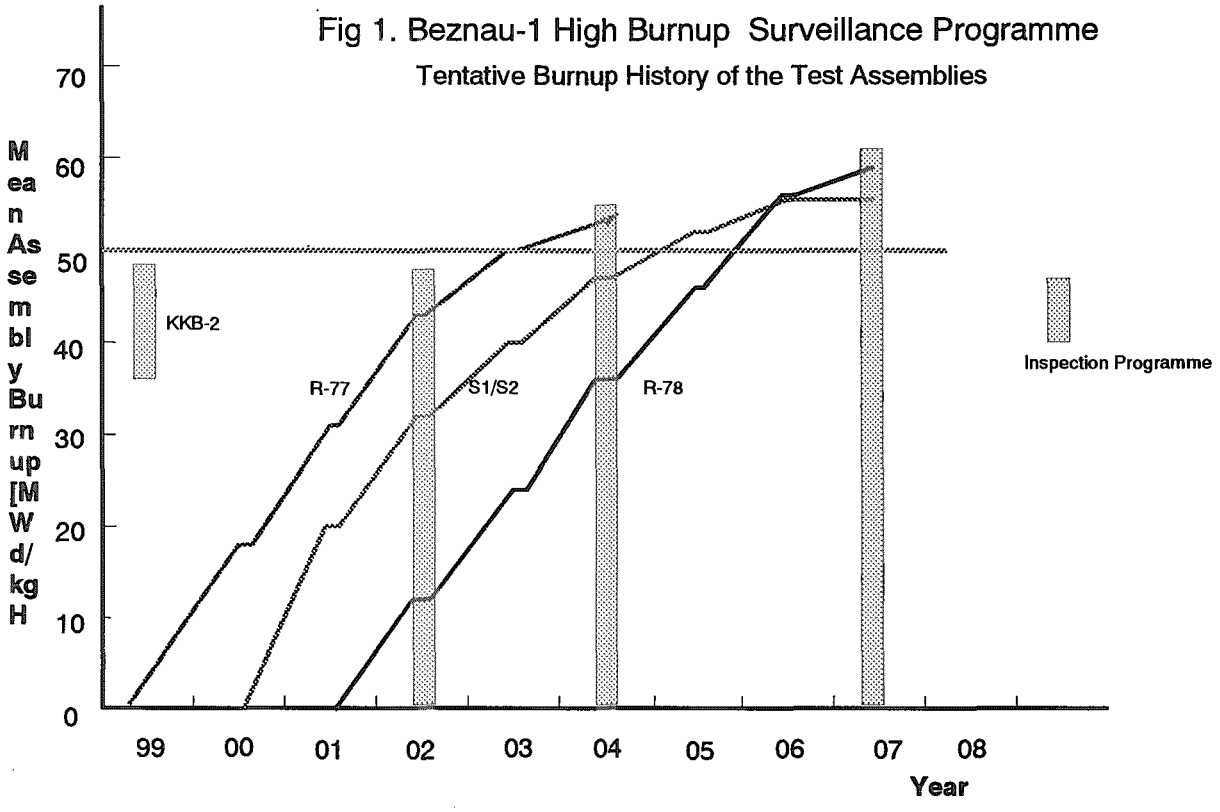
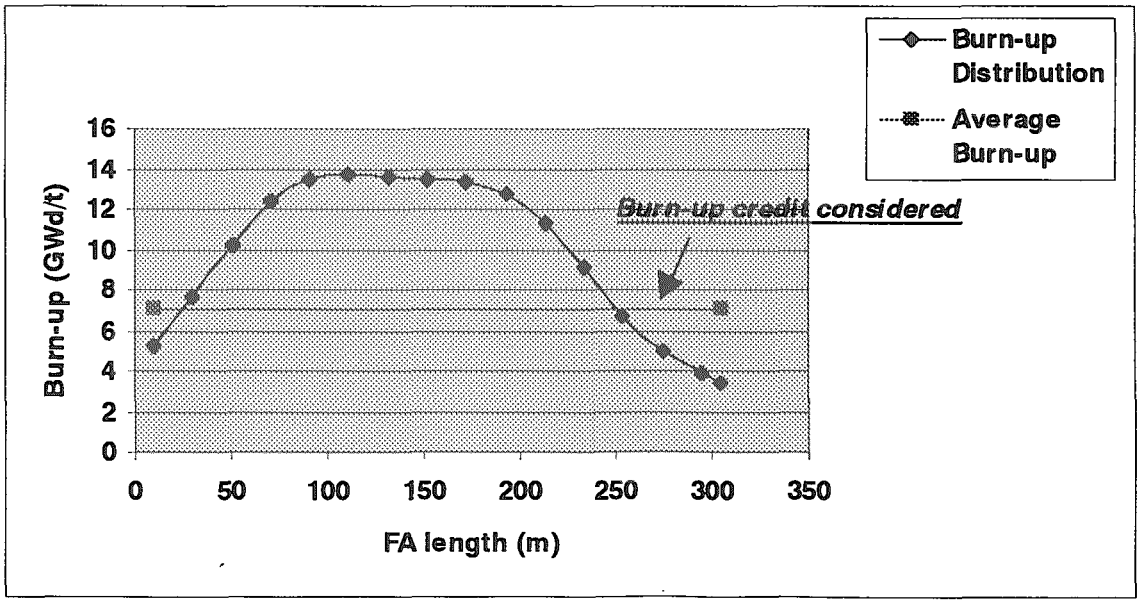

Fig 1. Beznau-1 High Burnup Surveillance Programme
Tentative Burnup History of the Test Assemblies
Mean Assembly Burnup [MWd/kgH
70
60
50
40
30
20
10
0
KKB-2
R-77
S1/S2
R-78
Inspection Programme
99
00
01
02
03
04
05
06
07
08
Year

Figure 2


Burn-up Distribution
Average Burn-up
Burn-up credit considered
Burn-up (GWd/t)
16
14
12
10
8
6
4
2
0
0
50
100
150
200
250
300
350
FA length (m)

Discussion:

Q: Why Beznau 1&2 plants want to go from present 18 months cycle to 12 months cycle?

A: It is for economic reasons. For small reactors like Beznau 1 & 2, 12 months cycle is more economical than the 18 months cycle.

Session 5a-2

BWR-fuel performance at high burn-up

Guido Ledergerber*, Kernkraftwerk Leibstadt AG, CH-5325 Leibstadt, Switzerland
Magnus Limbäck, Westinghouse Atom AB, SE-721 63 Västerås, Sweden
Wolfgang Hoffelner, Paul Scherrer Institut, CH-5232 Villigen, Switzerland

Abstract

In order to optimise fuel cycle costs, Swiss utilities tend to minimise reload batch sizes by utilising advanced fuel types reaching a high discharge burn-up. Eight assemblies were designed for a discharge burn-up well above 50 MWd/kgU and have been inserted into the core of the Leibstadt Nuclear Power plant (KKL) in 1994. Continued operation during seven cycles a bundle average of more than 60 MWd/kgU has been reached.

The fuel was designed and fabricated by Westinghouse Atom (WA) with a Zircaloy-2 cladding material fabricated by Sandvik Steel under the designation LK3. The irradiation took place in a normal water chemistry with Zinc injection at a power rating of 250 W/cm in the first cycle down to 100 W/cm in the last cycle.

Detailed poolside inspections have been carried out and selected rods have been extracted for hot cell examinations at intermediate stage as well as at the end of irradiation. An oxide thickness of less than 50 micron was measured with a new multi-frequency Eddy current technique qualified by destructive examinations.

Destructive examinations focusing on the integral fuel rod behaviour as well as on the cladding material after three, five, six and seven cycle are performed in the hot cells of the Paul Scherrer Institut (PSI) confirmed an excellent behaviour. The fuel after seven cycle with peak pellet burn-up of 73 MWd/kg (rod average 63 MWd/kg) will be characterised with regard of axial (gamma measurements) and radial nuclide distribution by secondary ion mass spectrometry, chemical composition and distribution of fission products. The chemical burn-up will be determined by the neodymium-148 method.

Selected segments from this fuel will be provided to the OECD Halden Reactor Project the be used for LOCA tests, for the study of fission gas release and cladding lift off. Five rods have been extracted form one fuel assembly after six cycles and inserted into a assembly after its second irradiation cycle. Oxide thickness are generally below 25 microns with peak values of 45 micron. Irradiation of the second life started in 2001 and aims on a peak pellet burn-up of 85 – 90 MWd/kg.

Fuel segments of the material which has reached peak pellet burn-up of 73=MWd/kg and material from the two life rods are offered for dedicated RIA and LOCA-tests in the ALPS programme carried out by JAERI.

* presenting author, email: Guido.Ledergerber@KKL.ch,
FAX: +41 56 247 1437, Phone +41 56 267 7111

G. Ledergerber, Leibstadt NPP, CH-5325 Leibstadt guido.ledergerber@KKL.ch

Kernkraftwerk Leibstadt

BWR-fuel performance at high burn-up

Fuel Performance Program
Westinghouse Atom - KKL -PSI

G. Ledergerber, Leibstadt NPP, CH 5325 Leibstadt, Switzerland
M. Limbäck, Westinghouse, SE 721 63 Västerås, Sweden
W. Hoffelner, PSI, CH 5232 Villigen PSI, Switzerland

Kernkraftwerk Leibstadt

Aims and goals

- **To demonstrate the performance of SVEA-96 type fuel to an assembly average burn-up well above 60 MWd/kg Uranium**
- **To complement poolside inspections with NDT and DT results from hot-cell examinations**
- **To generate nuclide specific experimental data for verification and improvement of neutronic and fuel performance codes**
- **to provide well characterised fuel for safety related tests**

G. Ledergerber, Leibstadt NPP, CH-5325 Leibstadt guido.ledergerber@KKL.ch

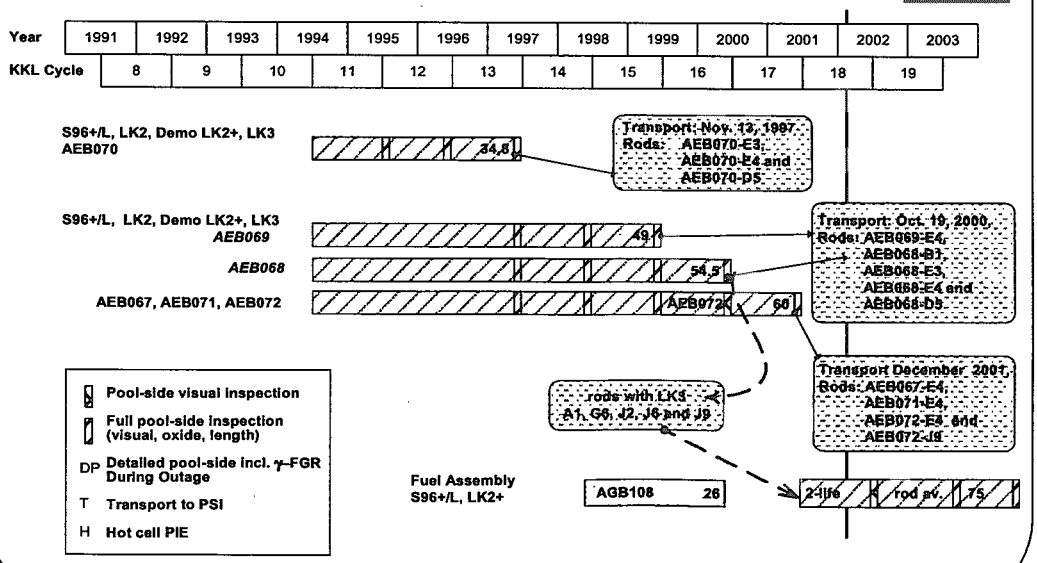
Kernkraftwerk Leibstadt

Fuel irradiated in Leibstadt Nuclear Power Plant

- Reactor data : GE BWR-6 up-rated to 3600 MW thermal power with 648 Fuel Assemblies (32 kW/kg Uranium, 62 kW/dm^3)
- Westinghouse Atom SVEA96+, 10x10 FA with four sub-bundles
- Lead Test Assemblies (LTA) with:
  - ✲ Zircaloy-2 cladding (type LK3, Fe+Cr+Ni 3300 ppm) with 0,63 mm thickness and a inside liner with an Iron content of 200 ppm
  - ✲ Rod diameter 9,62 mm, length 4152 mm with 7 spacers
  - ✲ Inserted in pile cycle 11 (1994), irradiated for 3, 5, 6 and 7 cycles
  - ✲ Peak rod burn-up reached 73.5 MWd/kg U in a bundle with an av. burn-up of 60 MWd/kg U and a peak linear heat rate of 250 W/cm

Kernkraftwerk Leibstadt

Irradiation programme for LTA assemblies with LK3



G. Ledergerber, Leibstadt NPP, CH-5325 Leibstadt guido.ledergerber@KKL.ch

Kernkraftwerk Leibstadt

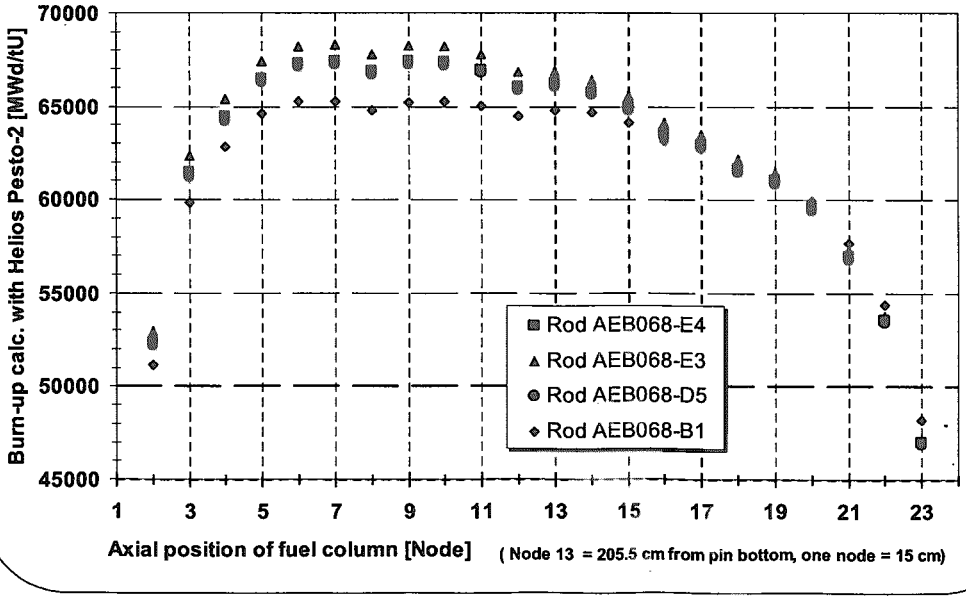
Fuel data for LTA Programme

Assembly – Rod	Initial enrichment [% U-235]	Av. Rod / Local Burn-up [MWd/kgU]	Numb. of cycles in core	Cladding material	Unloaded cycle - year
AEB070 - E4	4.46	36.1 / 44.9	3	LK3/L	13 - 1997
AEB069 - E4	4.46	51.4 / 59.7	5	LK3/L	15 - 1999
AEB068 - E4	4.46	57.6 / 67.1	6	LK3/L	16 - 2000
AEB067 – E4	4.46	57.3 / 67.6	7	LK3/L	17 - 2001
AEB071 – E4	4.46	57.6 / 67.8	7	LK3/L	17 - 2001
AEB072 – E4	4.46	63.1 / 73.5	7	LK3/L	17 - 2001
AEB072 – J9	3.71	63.1 / 72.3	7	LK3/L	17 - 2001

BWR-fuel performance at high burn-up Page 6

Kernkraftwerk Leibstadt

Fuel Assembly AEB068
Nodal burn-up at EOC versus axial position

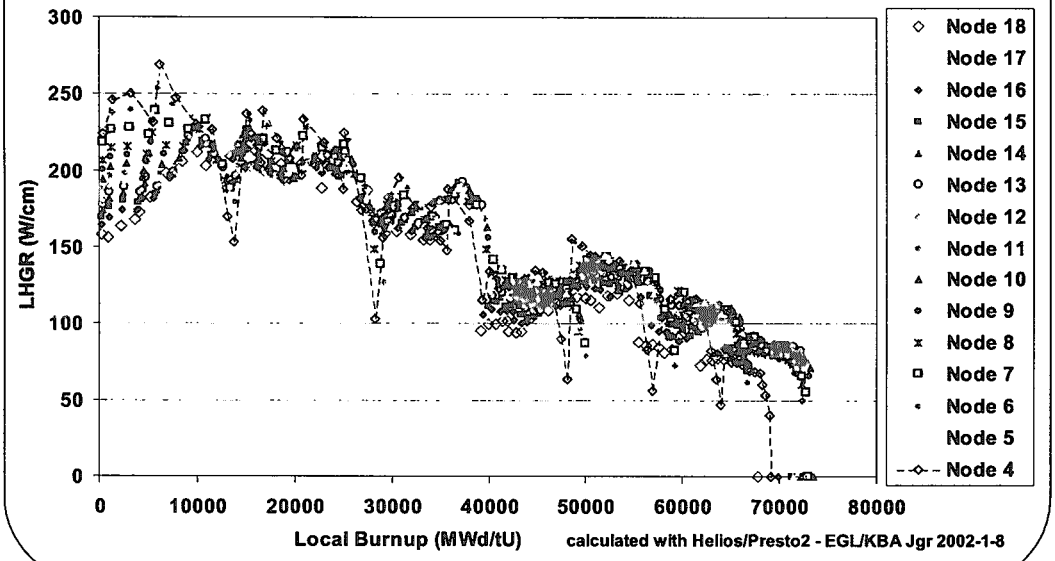


BWR-fuel performance at high burn-up Page 7

G. Ledergerber, Leibstadt NPP, CH-5325 Leibstadt guido.ledergerber@KKL.ch

Kernkraftwerk Leibstadt

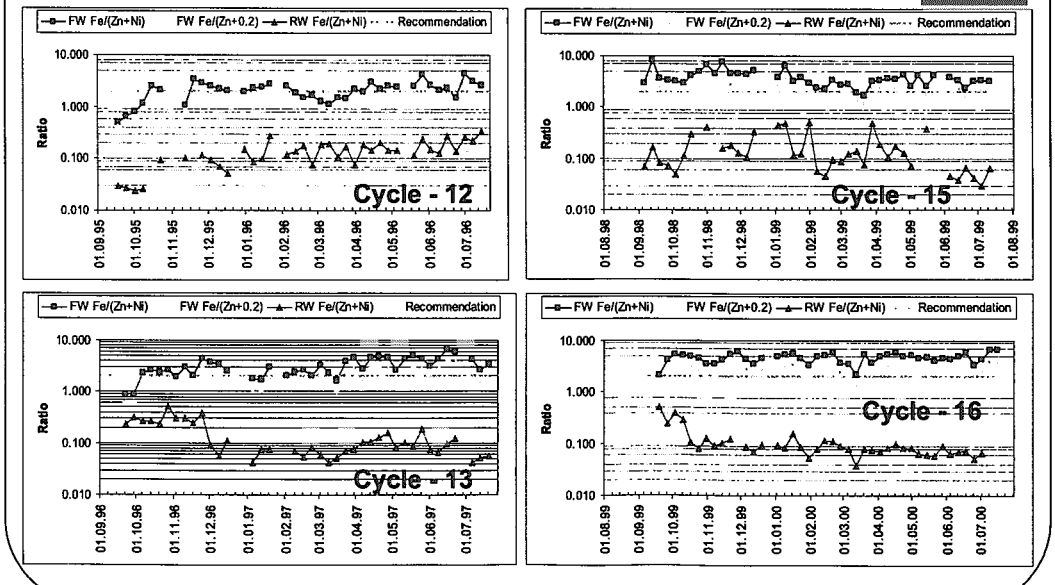
Fuel Assembly AEB072 - Rod E4, Cladding Material LK3/L
Linear heat rate versus burn-up calc. with Helios/Presto-2



BWR-fuel performance at high burn-up Page 8

Kernkraftwerk Leibstadt

Normal water chemistry with Zinc injection
Typical Reactor Water Impurities

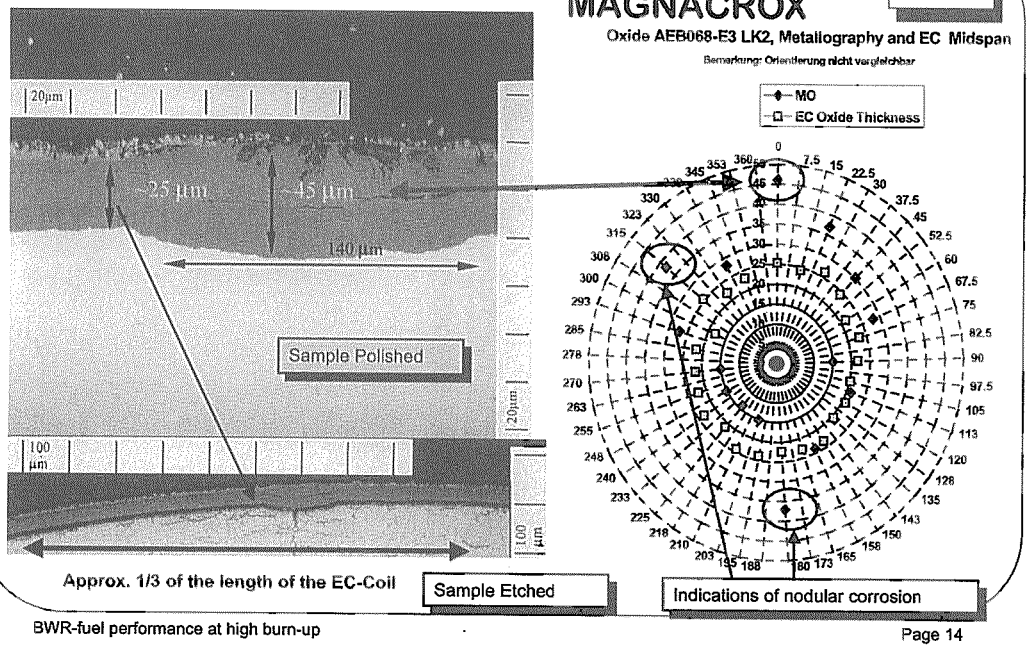


BWR-fuel performance at high burn-up Page 9

G. Ledergerber, Leibstadt NPP, CH-5325 Leibstadt guido.ledergerber@KKL.ch

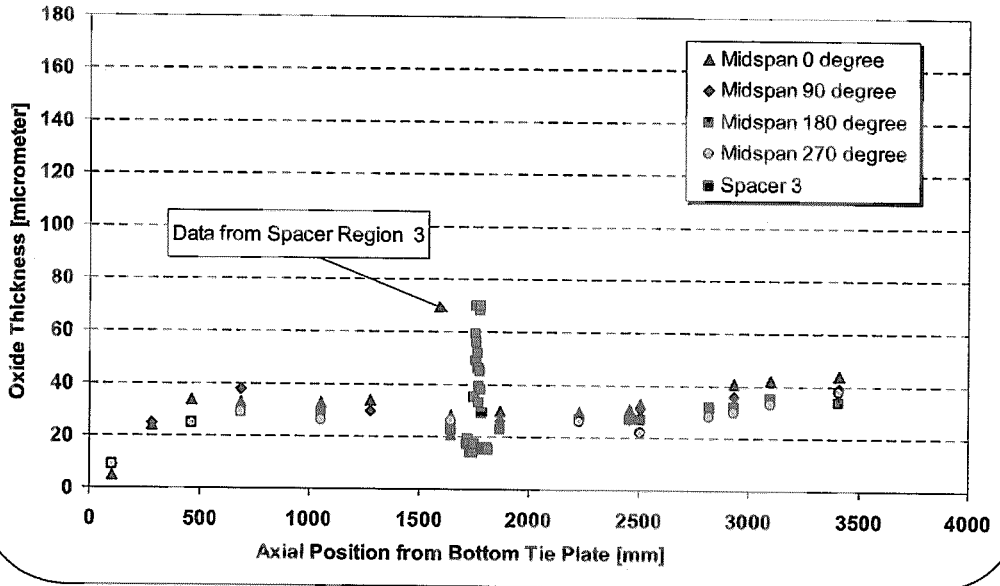
Kernkraftwerk Leibstadt

Qualification of Oxide Thickness Measurements MAGNACROX



Kernkraftwerk Leibstadt

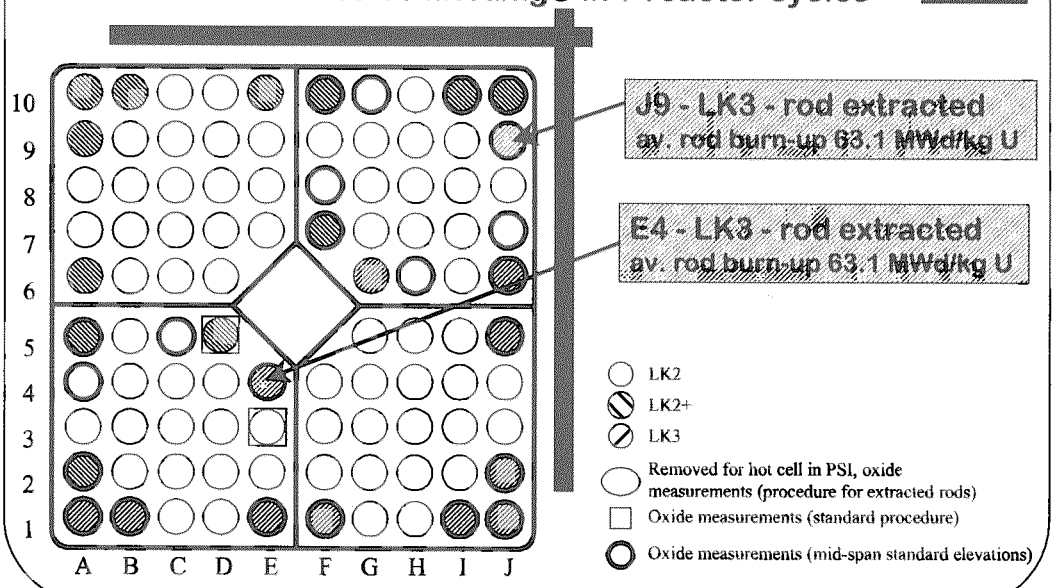
Fuel Assembly AEB069 - Rod E4, Cladding Material LK3/L
Poolside oxide measurements (MAGNACROX)



G. Ledergerber, Leibstadt NPP, CH-5325 Leibstadt guido.ledergerber@KKL.ch

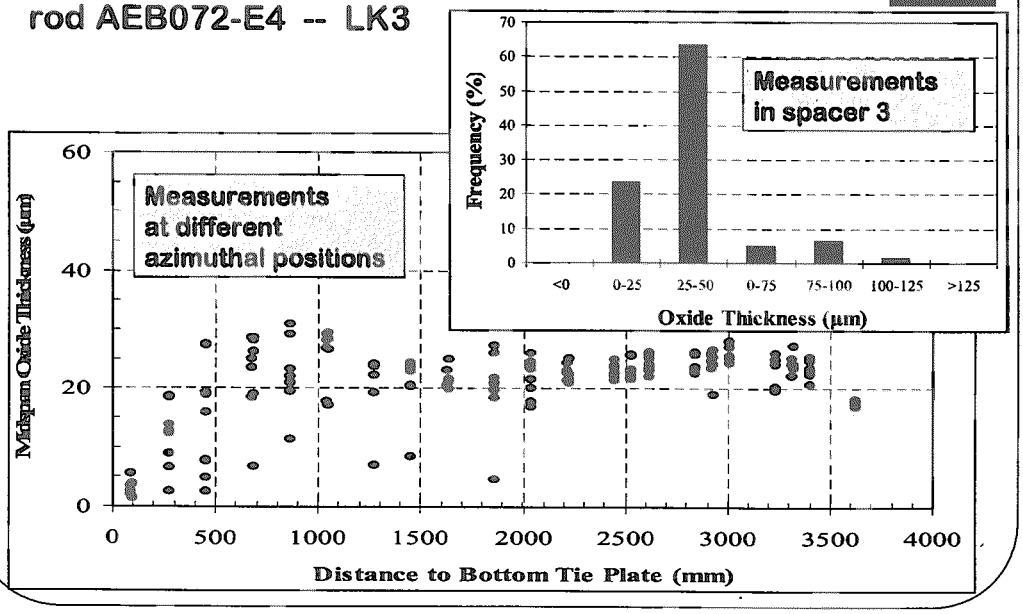
Kernkraftwerk Leibstadt

AEB072 - LTA irradiated to 60 MWd/kgU in 7 reactor cycles



Kernkraftwerk Leibstadt

Oxide thickness pool side measurements rod AEB072-E4 -- LK3



G. Ledergerber, Leibstadt NPP, CH-5325 Leibstadt guido.ledergerber@KKL.ch

Kernkraftwerk Leibstadt

Examinations in PSI on selected rods

- Visual inspection on all
- Length measurement and profilometry (rod thickness) on all
- Gamma spectrometry (axial distribution of fission products) only E4
- Oxide thickness with new W-Atom method on all
  (confirmation of pool side measurements)
- Fission gas release (free volume of rod, composition and release fraction) on all and chemical burn-up (average comp. Pu, U, Nd, Cs) on E4 rods
- Cladding characterisation on all
  [metalography, Hydrogen content, SPP, micro-hardness]
- Fuel characterisation on E4 rods
  [ceramography, density, distribution of selected fission products (EPMA), distribution of selected isotopes (SIMS)]

BWR-fuel performance at high burn-up Page 20

Kernkraftwerk Leibstadt

Fuel Performance Program Westinghouse Atom - KKL -PSI

Support of fuel to other fuel test programmes

- Halden - LOCA (IFA-650), fission gas release (IFA-629), cladding creep (IFA-663) and cladding lift-off (IFA-610) experiments
  [OECD Halden Reactor Project]
- ALPS - Advanced LWR fuel Performance and Safety research programme - LOCA and RIA testing
  [JAERI / NSRR - Japan]
- Studsvik anticipated operational occurrences (AOO) ramp test on three, five, six and seven cycle LK3 material, mechanical tests on three and seven cycle LK3 material
  as well as RIA simulation tests on seven cycle LK3 material
  [Westinghouse Atom Fuel Technology Programme]

BWR-fuel performance at high burn-up Page 22

G. Ledergerber, Leibstadt NPP, CH-5325 Leibstadt guido.ledergerber@KKL.ch

Kernkraftwerk Leibstadt

Fuel for Halden tests

IFA-650 - LOCA-Tests with BWR fuel
two segments of 50 cm from AEB070-E4
two segments of 50 cm from AEB072-E4

IFA-629 - Fission gas release of BWR fuel
one segment of 50 cm from AEB068-E4

IFA-610 - BWR Cladding lift off
two segments of 50 cm from AEB069-E4

IFA-633 - BWR Cladding creep
one segment of 50 cm from AEB068-E4

Fuel data

Assembly – Rod	Initial enrichment [% U-235]	Av. Rod / Local Burn-up [MWd/kgU]	Numb. of cycles in core	Cladding material	Unloaded cycle - year
AEB070 - E4	4.46	36.1 / 44.9	3	LK3/L	13 - 1997
AEB069 - E4	4.46	51.4 / 59.7	5	LK3/L	15 - 1999
AEB068 - E4	4.46	57.6 / 67.1	6	LK3/L	16 - 2000
AEB072 - E4	4.46	63.1 / 73.5	7	LK3/L	17 - 2001

BWR-fuel performance at high burn-up Page 23

Kernkraftwerk Leibstadt

Fuel for ALPS -
Advanced LWR fuel Performance and Safety

- **Seven (7) fuel segments shall be removed from midspan of the high power nodes of the fuel rods E4 and J9 from AEB072 and E4 of AEB071.**
- **Cladding LK3/L, Initial enrichment 4.46 % U-235 (J9 = 3.72%)**
- **Burn-up: 73 [MWd/kgU] max. local after 7 cycles in core**

Proposed test program at JAERI/NSRR and in the Halden BWR

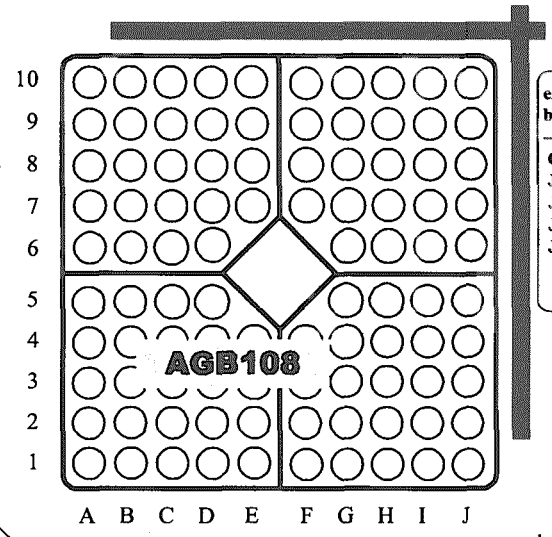
- **One segment for two tests in NSRR (RT and somewhat lower than operation conditions)**
- **Two segments will be used for integral thermal shock tests and for cladding oxidation tests (behaviour under LOCA conditions)**
- **Four re-fabricated and instrumented segments will be ramp tested in the Halden material test reactor.**

BWR-fuel performance at high burn-up Page 24

G. Ledergerber, Leibstadt NPP, CH-5325 Leibstadt guido.ledergerber@KKL.ch

Kernkraftwerk Leibstadt

Two life rods with high burn-up and up to 9 cycles residence time



expected av. rod burn-up for EOC		18	19	20
G6	(AEB068-G 6)	63	71	75
J6	(AEB068-J 6)	61	69	73
J 8	(AEB068-J 2)	61	68	72
J 9	(AEB-068-J 9)	61	69	73
J10	(AEB068-A1)	54	62	67

All data in [MWd/kg]

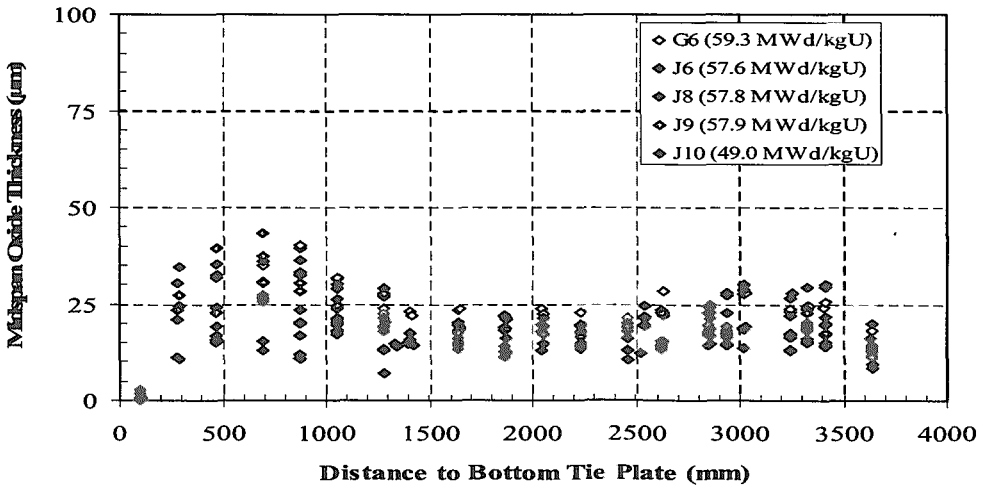
○ replaced rods

burnup calculated by Westinghouse Atom (16.2.01)

BWR-fuel performance at high burn-up Page 25

Kernkraftwerk Leibstadt

Midspan oxide thickness -- 2-Life Rods in AGB108

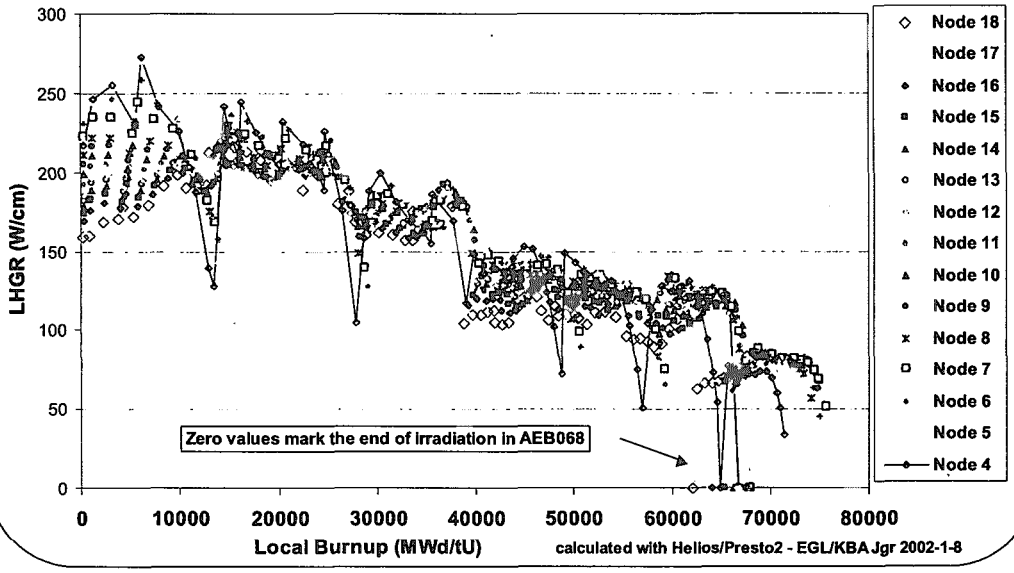


BWR-fuel performance at high burn-up Page 27

G. Ledergerber, Leibstadt NPP, CH-5325 Leibstadt guido.ledergerber@KKL.ch

Kernkraftwerk Leibstadt

Fuel rod AEB068-G6 / AGB108-G6, Cladding Material LK3/L
Linear heat rate versus burn-up calc. with Helios/Presto-2



BWR-fuel performance at high burn-up Page 28

Kernkraftwerk Leibstadt

Conclusion

- **The effort of the Fuel Performance Programme shall provide the material property data for a burn-up derived from the enrichment of 5% U-235.**
- **An extension of the programme with the two-life rods seems to be feasible. The irradiation is ongoing.**
- **The ALPS programme of JAERI, the OECD-Halden Project and the Fuel Technology Programme of European BWR-Utilities are supported with fuel deliveries.**
- **Material deliveries into international programmes are supported by compilation of fabrication and irradiation data, pool side measurements and hot cell examinations.**

BWR-fuel performance at high burn-up Page 30

Discussion:

Q: (H.Uetsuka)

How is the effect of hard crud formed on oxide surface on EC measurement?

Will you give information about new W-A method of oxide thickness measurement, please?

A: The hardness of the crud is not affecting the measurement. It is rather the magnetic properties which distort the signal. The eight frequencies measured are analyzed by a multi-layers model. Similar models have been developed for the interpretation of rock and sediment layers from geophone data in geological explorations.

Session 5a-3

Fuel Irradiation Experiments for An Advanced PWR Fuel Development in the HANARO

Young-Hwan Kang, Bong-Goo Kim and Man-Soon Cho
Korea Atomic Energy Research Institute
P.O. Box 105, Yusong
Taejon, 305-600, Korea

ABSTRACT

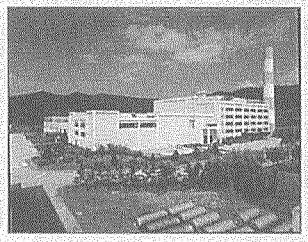
The development program of advanced nuclear fuel pellets includes the evaluation of irradiated fuel materials exposed to irradiation environments, and the in-pile tests using the instrumented capsule. The tests will be performed in the in-core test holes of OR of HANARO and provide the essential information for the developm ent of the advanced nuclear fuel materials and the superior ability of the candidate fuels t o the conventional power reactor fuel.

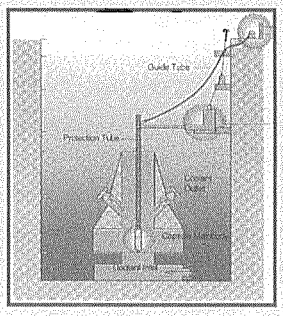
A fuel capsule for the irradiation test of the advanced fuel pellet has been designed a nd fabricated partly, which could be used in HANARO. A series of out-pile tests such as a pressure drop test and compatibility test to HANARO were done by u sing an instrumented mockup capsule.

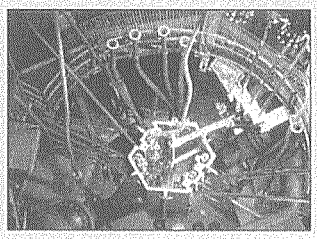
This paper describes the present status and future plans of these R&D activities for the development of the instrumented capsule.

HANARO

Fuel Irradiation Experiments for Advanced PWR Fuel Development in the HANARO







Young-Hwan KANG
Korea Atomic Energy Research Institute

FSSM2002

하나로
HANARO

Outline of Presentation

- Introduction
- User Requirements
- Capsule Design and Mockup Fabrication
- Temperature Control System
- Temperature Controllability Test
- Out-pile Verification Tests
  - Pressure drop
  - Endurance test
- Future Works

INTRODUCTION

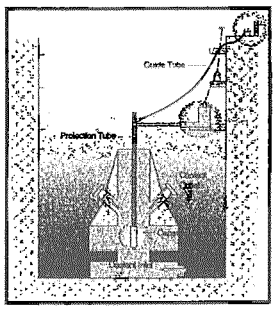
- In Korea, 16 Nuclear Power Reactors are Now in Commercial Operation
  - 12 PWR reactors and 4 PHWR
  - First Commercial Operation of Kori Unit 1 in 1978
  - Nuclear Power Share; 43% in Total Electricity Generation
- As a Part of Adv. Nuclear Fuel Development Program, a Series of In-pile Tests are also Progressing to Examine Performance of Advanced Fuel Compared to Conventional Standard Fuel
- HANARO can Perform Irradiations Needed to Confirm Their Pellet Manufacturing Process and Product Characteristics
  - One of these types entails in capsule.
  - Fuel test loop are not currently available
- Most of Separate Tests for Development of Advanced PWR Fuel, DUPIC Fuel and Metallic Fuel has been Going Using a Non-instrumented Capsule since 1998
- Hence, New Irradiation Technology Development Using an Instrumented Capsule is Highly Needed to Provide Well-qualified Data to Fuel Designers since 2000

In Korea, 16 nuclear power reactors(12 PWR reactors and 4 PHWR reactors) are now in commercial operation

3

USER REQUIREMENT

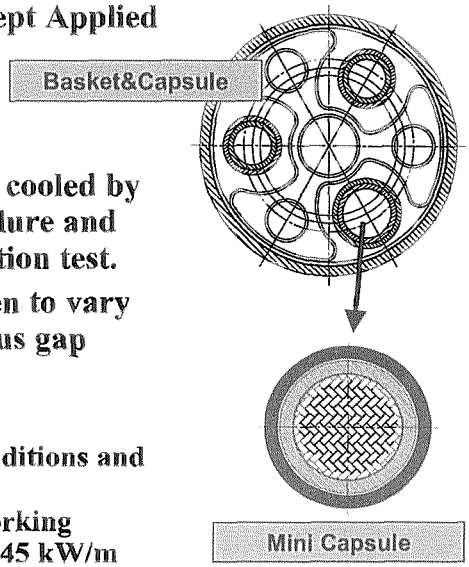
- Experimental Requirement; Thermal Behavior of New Type UO_2
  - Linear heat rate; < 450 W/cm
  - Fuel surface temperature; 600~800 °C
- Instrumentation Requirement During Irradiation in HANARO
  - Fuel temperature monitoring
  - Fission product monitoring
  - Internal pressure of fuel
- Advanced Fuel;
  - Target burnup; >70MWD/kgU
  - Microstructure controlled pellet
  - New Zircaloy cladding



하나로 HANARO

CAPSULE DESIGN

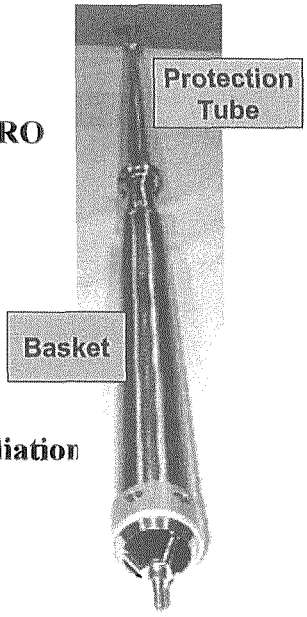
- Design Concept; Double Containment Concept Applied
- Main Composition;
  - Bracket
  - Mini-Capsule loaded with fuel pin
  - Protection Tube welded to basket
- Parts designed for specimen to be effectively cooled by reactor coolant, monitored indication of fuel failure and exposed in neutron environment during irradiation test.
- Main means of temperature control are taken to vary the thermal conductivity of the gas in the annulus gap between capsule tube and fuel cladding
- Design criteria of the capsule;
  - Selected considering HANARO operating conditions and fuel test objectives
  - Structural integrity should be sustained at working conditions of <800 °C and linear heat rating of <45 kW/m



하나로 HANARO

FABRICATION OF MOCKUP

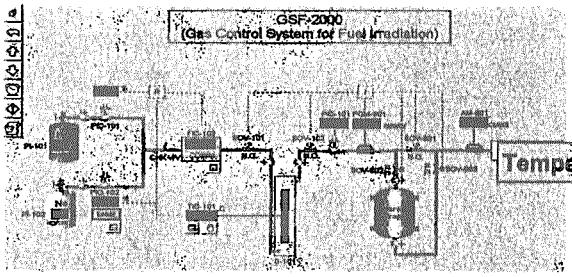
- Mockup Capsule Design and Fabrication;
  - Able to perform pressure drop test
  - Optimize the capsule geometry compatible to HANARO hydraulic conditions
- Basket(Fig. 1)
  - 56mm OD, 2.5mm T, 730mmL
- Mini Capsules Manufacturing
  - Continuous flow of sweep gas to keep const. Temp.
  - Monitor effectively fuel-cladding failure during irradiation
  - Dimension; 11.7mm OD and about 23cmL
  - Loaded with fuel pin of about 20cm in length



HANARO

TEMPERATURE CONTROL SYSTEM

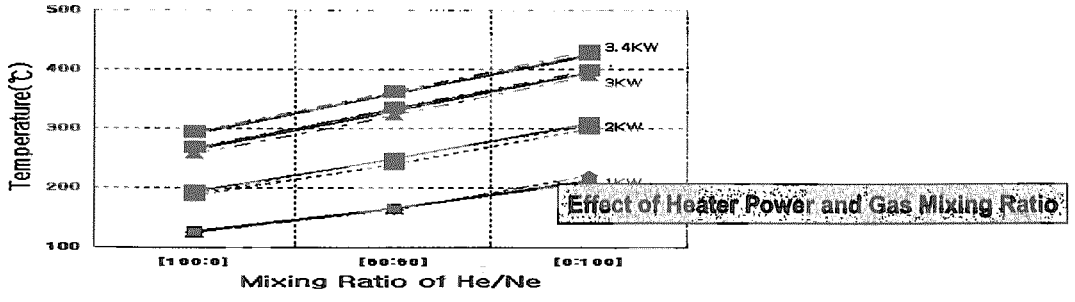
- Composition;
  - Temperature control system; controls the surface temperature of specimens by adjusting the mixing ratio of the gas in annular gas space
  - Fuel failure monitoring system; detects fission products in the annulus gap due to fuel cladding failure in each capsule separately mounted inside of basket
- Several Subsidiary Functions; Data acquisition and storage function, self-diagnosis function, and an alarm-indicating function
- Hardware Configuration; Vacuum controller, Fission product monitor and trap, Gas mixing ratio controller, and Personnel computer
- Has Three Operational Modes: Manual , auto , and computer-aided mode



HANARO

TEMPERATURE CONTROLLABILITY TEST

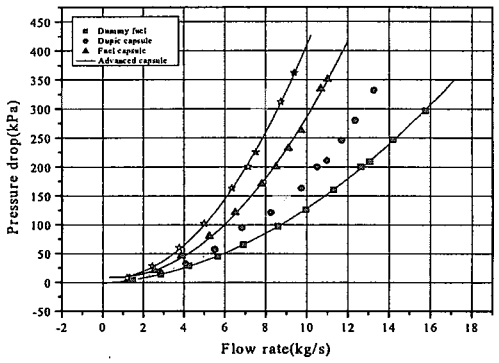
- Methodology Applied;
  - Important for user requirements
  - Confirm for applicability of this technique to HANARO
- Instrumented with a Thermocouple for Monitoring and Controlling Cladding Temperature and a Heater of 3.4kW
- Done to Investigate Thermal Response of Gas Mixing System under HANARO Hydraulic Condition; 40°C and 12.7 kg/s.
- Main Parameters; Mass flow rate of 50 & 100 cc/min of He/Ne gas, gas pressure, heater power of 1 to 3.4kW and gas mixing ratio
- Effects of Power&Mixing Ratio found to be Changed Noticeably



하나로 HANARO

OUT-PILE VERIFICATION TEST

- Out-pile Verification Tests ;
  - Pressure drop & endurance test
  - Performed at the same condition as in normal operation of HANARO
- Loading/unloading Tests ;
- Pressure Drop Test;
  - Measured flow rate inducing 200kPa ; 8.5kg/s
  - Stable vibration observed
- Endurance Test;
  - 30 days in condition of 40℃, 110% of normal flow rate(8.5kg/s) for 1 year test in HANARO
  - Not show any changes in the dimensions, weight and any wear



Pressure Drop Test Data

하나로 HANARO

FUTURE WORKS

Future Works can be Summarized into Two Tasks;

- Improvement of Current Design and Manufacturing Technology;
  From thermal analysis the following parameters should be optimized
  - Irradiation position relative to the core of HANARO
  - Fuel enrichment
  - Solid screen such as boral plate, Hf plate
  - Geometry optimization after consideration of fabric ability
- Design Verification of Capsule at HANARO ;
  - Capsule mockup be designed and fabricated, which is more compatible to the HANARO operation conditions and well matched with user requirements
  - Loaded in in-core of HANARO in 2004
  - Main parameters; control rod position, temperature distribution with reactor power level, capsule temperature controllability under automatic control mode and effects of gas mixing ratio of He/Ne.
  - In-situ measuring technology using sensors(such as pressure transducer, LVDT etc.) also developed
- Essential and Reliable Information on Development of Nuclear Fuels can be Provided for Users

Discussion:

Q: (W.Wiesenack)

What is the pressure of the gas mixture in the capsule temperature control system? Did you consider using pressure control (low temperature of He gas) instead of gas composition for controlling the temperature?

A: In the temperature controllability test, the pressure range we controlled is 1 to 3 bars. The effect of gas pressure was found to be negligible.

For the material irradiation test, the method you suggest was applied to the capsule temperature control system. Another role of the capsule temperature control system for fuel test is to monitor the fuel cladding failure continuously during irradiation.

Q: (M.Kinoshita)

What is the maximum achievable linear heat rating at the device in HANARO, especially for high burnup fuel (with lowered enrichment) ?

A: The requirement of the maximum LHR is from fuel melting condition. Based on flux in HANARO, LHR can be more than 450W/cm, depending on the enrichment.

Session 5a-4

Development of PIE apparatuses and techniques in RFEF

YASUDA Ryou, HARADA Katsuya, NAKATA Masahito, KUSHIDA Teruo,
MITA Naoaki, NISHINO Yasuharu and AMANO Hidetoshi

Dept. of Hot Laboratories, Japan Atomic Energy Research Institute

ABSTRACT

Main works of Reactor Fuel Examination Facility (RFEF) in JAERI are Post Irradiation Examinations (PIEs) of various nuclear fuels and materials including the fuel-assemblies irradiated in commercial reactors. Accumulation of PIE data on the extended burn-up fuels is recently required to evaluate the integrity of the fuels and to confirm criteria of a safety level of the extended burn-up. Especially, knowledge on thermo-physical properties of the extended burn-up fuel pellets and on hydrogen behavior in the Zircaloy tube has been required. In RFEF, various PIE apparatuses and techniques have been developing to satisfy these demands and to supply the PIE data. In this paper, two apparatuses and one technique in them are explained.

Pellet Melting Temperature measurement apparatus (PMT) with around 3000℃ in maximum temperature was installed to investigate the melting temperature of irradiated fuel pellets. The melting temperature is determined by thermal arrest method. High temperature heating system is required in PMT because of high melting temperature of UO_2 pellet. In order to keep stable operation in high temperature atmosphere, high frequency heater with water-cooled type working Cu-coil is used in the system. Structural materials in the most heated parts such as suscepter and heat reflectors in the system are made of tungsten with high melting temperature. The arrangement of the heating system is illustrated in slide 8 and 9. PMT has already introduced a series of irradiated commercial UO_2 pellets with different burn-up. It is clarified that there is no appreciable dependence of burn-up up to 45Gwd/t on the measured melting temperatures of the pellets as shown in slide 2.

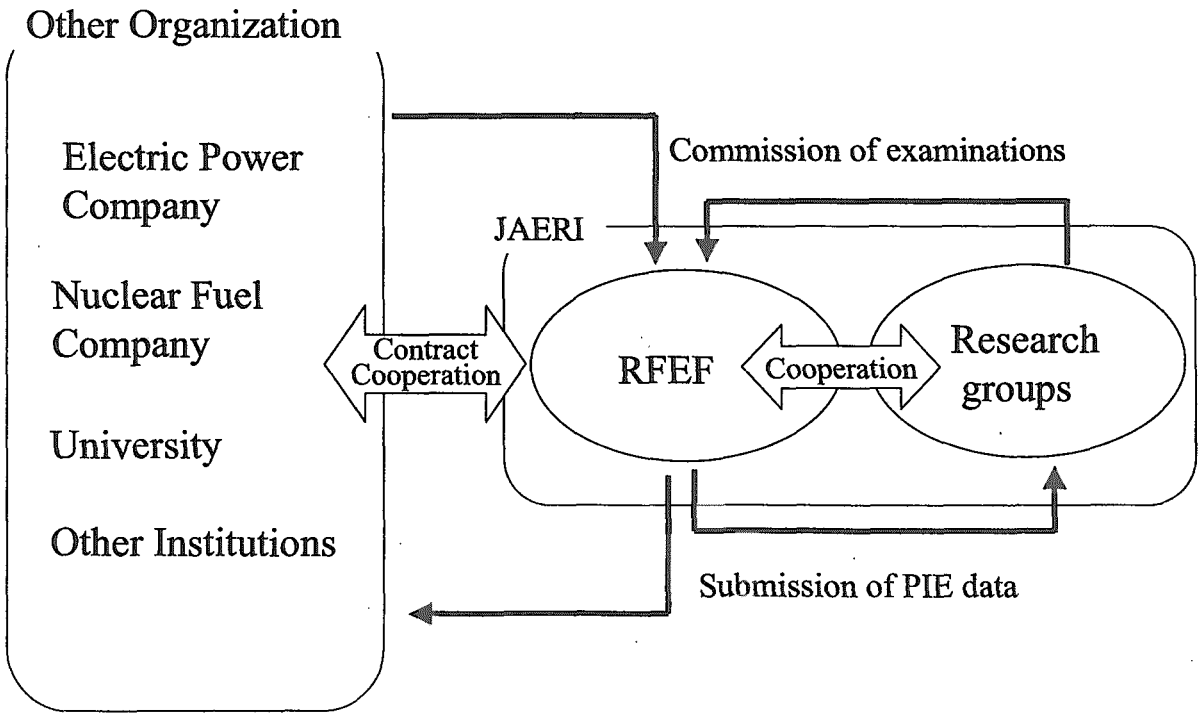
Pellets Thermal Capacity measurement apparatus (PTC) for measuring the specific heat of irradiated fuel pellets is under development. Specific heat is measured by a differential scanning calorimeter (DSC). PTC apparatus is installed in a shielding box made up with iron plates with 100mm in thickness. Reasonable remote handling system and lead glass are equipped in the shielding box as shown in slide 14. The machine characterization has been performed using standard samples such as platinum metal. Slide 15 shows the results of characterization test. Good reproducibility and reasonable agreement with literature data are recognized.

Practicability of advanced neutron radiography techniques such as Neutron Imaging Plate (NIP) to PIE has been investigated. Neutron radiography has been a useful technique for determining the hydrogen distribution in Zircaloy cladding tubes. Some mock-up tests using hydrided Zircaloy tubes are carried out to confirm effectiveness of NIP to PIE. Two kinds of hydrided tubes were used. One with is called as standard sample of which hydrides are uniformly distributed over the sample. The other is called as segregation samples with hydrides segregated at periphery region as shown in slide 18. Slide 19 shows NIP image of standard samples and the figure of the relationship between PSL (Photo-Simulated Luminescence) and hydrogen concentration. PSL corresponds with image brightness level in the NIP image. The standard sample images are getting black with increasing hydrogen concentration. The figure also shows that PSL linearly decreases with increasing the hydrogen concentration. The linear relationship between PSL and hydrogen concentrations in the standard sample images is used to estimate the local hydrogen concentrations in the segregation samples. Slide 20 shows the NIP images and the local hydrogen concentration diagrams of the segregation tubes.

Development of PIE apparatuses and techniques in RFEF

YASUDA Ryou, HARADA Katsuya, NAKATA Masahito, KUSHIDA Teruo, MITA Naoaki, NISHINO Yasuharu, and AMANO Hidetoshi

Roll of RFEF (Reactor Fuel Examination Facility)



Specification of RFEF

Useable fuels :

(1) LWR(PWR, BWR) and MOX(ATR) Fuel Assemblies

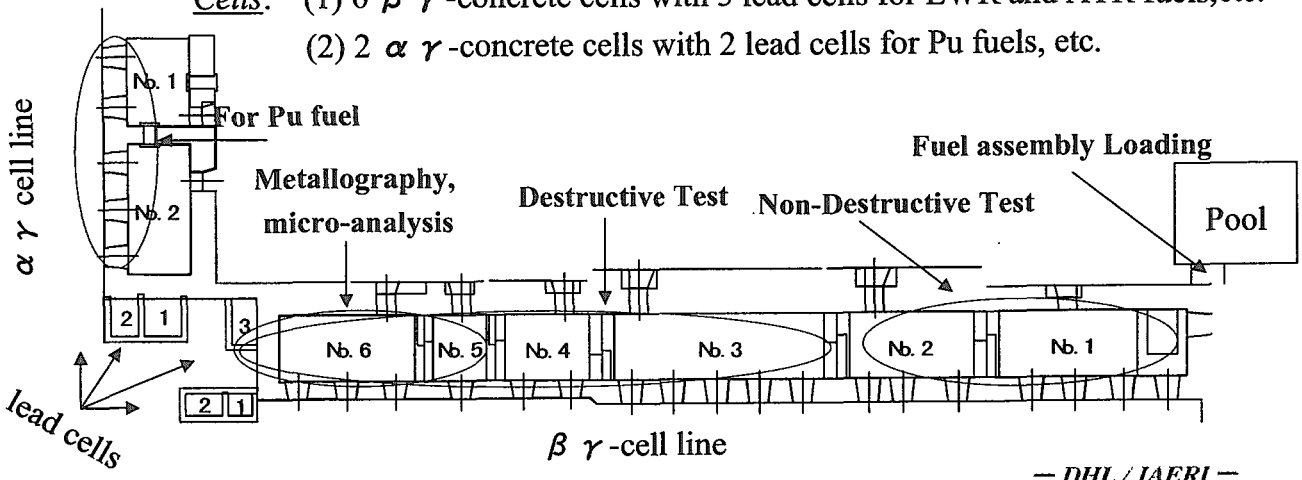
(2) $(U,Pu)O_2$, (U,Pu)C and (U,Pu)N

(3) High Burn-up LWR Fuel

(4) Rock-like Fuels (ROX)

Cells: (1) 6 β γ-concrete cells with 3 lead cells for LWR and ATR fuels,etc.

(2) 2 α γ-concrete cells with 2 lead cells for Pu fuels, etc.



Layout of cell lines in RFEF

Main works of RFEF

1. Non-destructive examinations

- Visual inspection, Dimensional and Profile measurement, X-ray radiography, γ - scanning, Eddy current test, and Puncture test, etc.

2. *Destructive examinations*

- Cladding tensile test, Cladding burst test, Metallography, SEM, EPMA, X-ray diffraction, Out gas analysis, Densitometer, etc.

3. Re-fabrication of fuel rods for pulse irradiation at NSRR

4. Development of PIE apparatuses and techniques

Development of PIE apparatuses in RFEF

Needs of data accumulation for safety evaluation extended burn-up fuels

(1) Thermo-physical properties of the fuel pellet
Melting temperature, Specific heat,
Thermal conductivity, Thermal diffusivity

(2) Hydrogen behavior in Zircaloy tube
Distribution of Hydrogen Concentration

⇩

Apparatuses and Techniques

(1)Pellet Melting Temperature measurement apparatus(PMT)→*Melting temperature*
(2)Pellet Thermal Capacity measurement apparatus(PMC) → *Specific heat*
(3)Pellet Thermal Diffusivity measurement apparatus → *Thermal diffusivity*
(4)Ion Micro-Probe Mass Analyzer → *Distribution of Hydrogen Concentration*
(5)Neutron RadioGraphy (NRG)→ *Distribution of Hydrogen Concentration*

— DHL / JAERI — 5

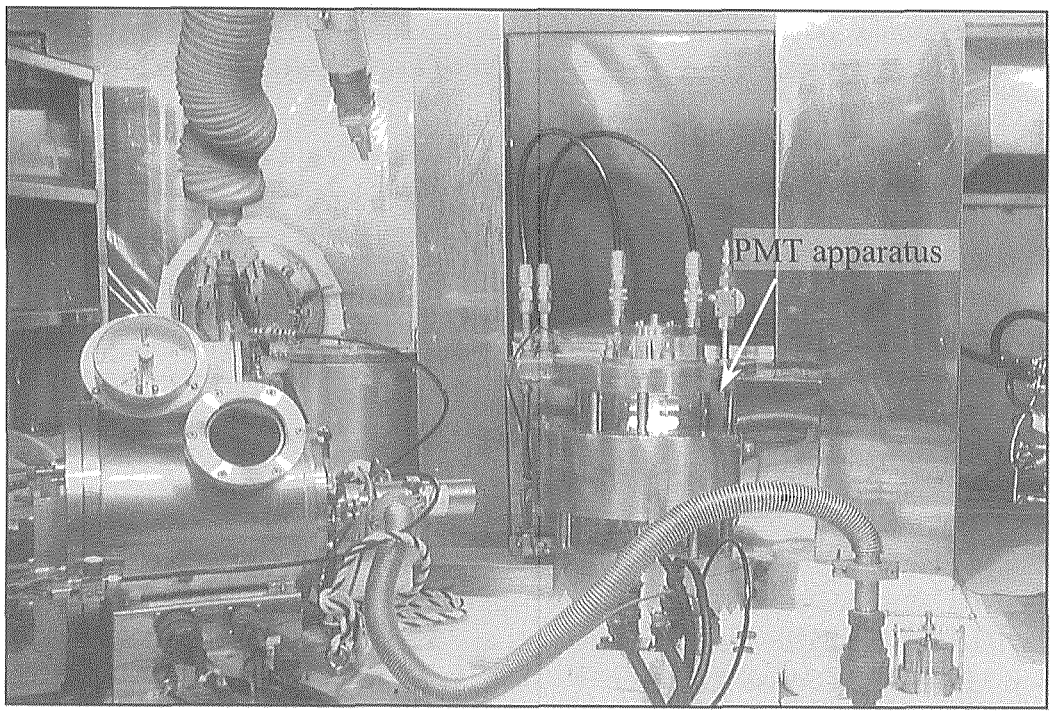
Pellet Melting Temperature measurement apparatus(PMT)

Content

- Outline of PMT apparatus
- Results of measuring the melting temperature of irradiated UO_2 fuel pellets with various burn-up level.

— DHL / JAERI — 6

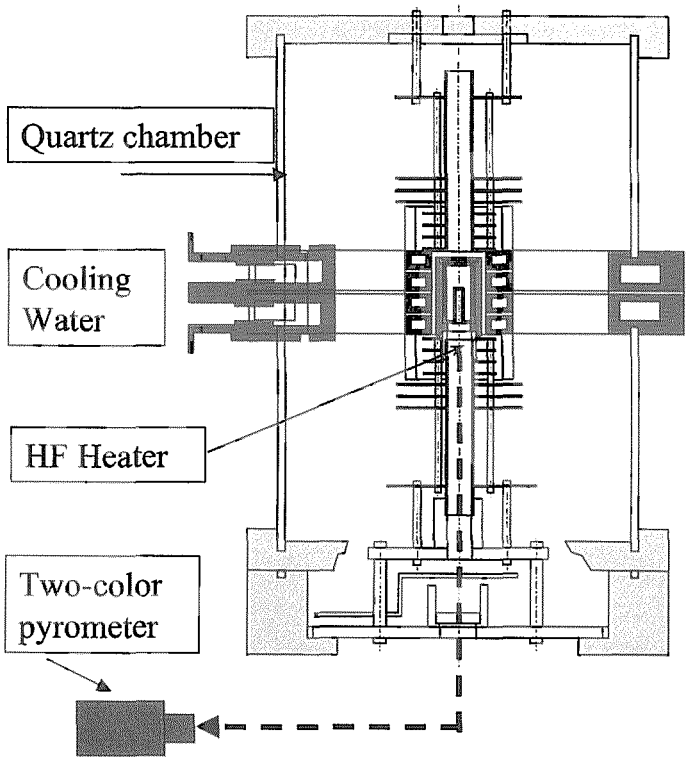
Photograph of PMT apparatus under measurement



— DHL / JAERI —

7

Schematic drawing of heating system in PMT apparatus



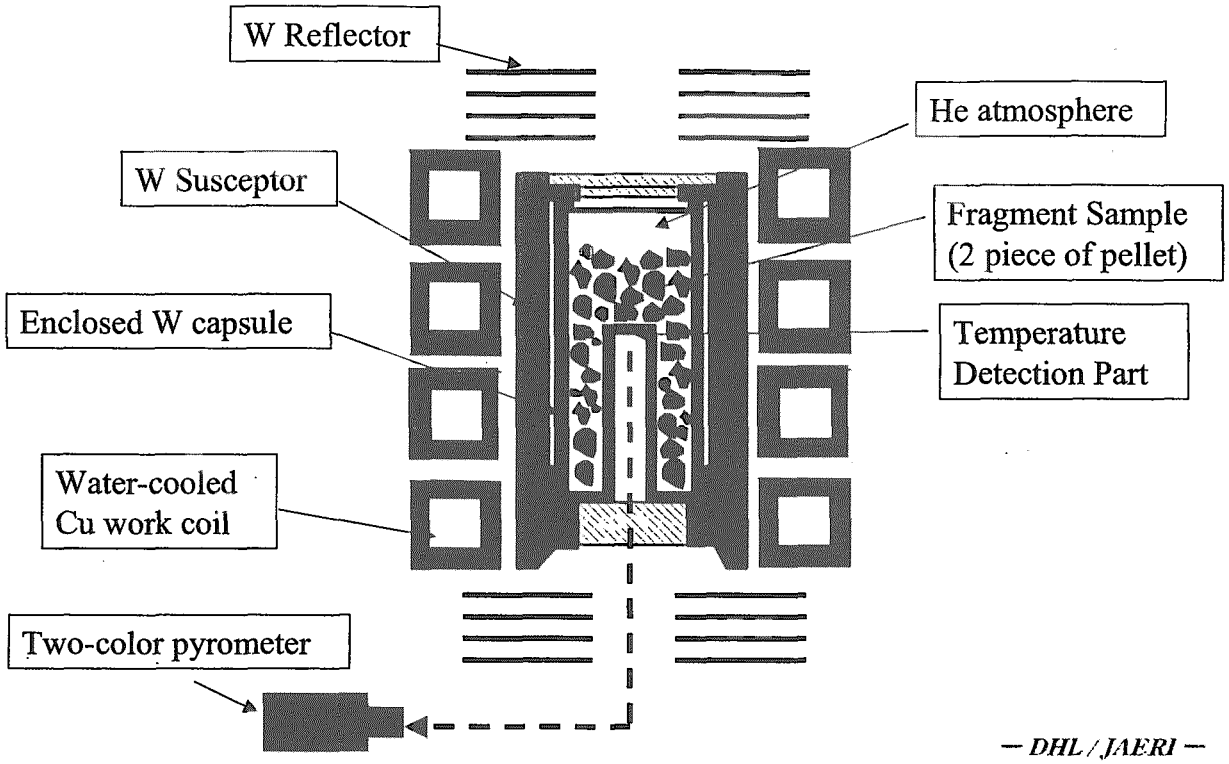
Specification

Method	Thermal Arrest Method
Heating System	High Frequency induction Heating (Voltage control)
Temp. Detector	Fiberglass Two-color Pyrometer
Measurable Range	1500℃～3100℃
Atmosphere	Vacuum (<1.3×10^{-4}Pa)

— DHL / JAERI —

8

Installed sample at heating system in PMT apparatus



— DHL / JAERI —

9

Conditions of melting temperature measurement on UO_2 fuel pellets

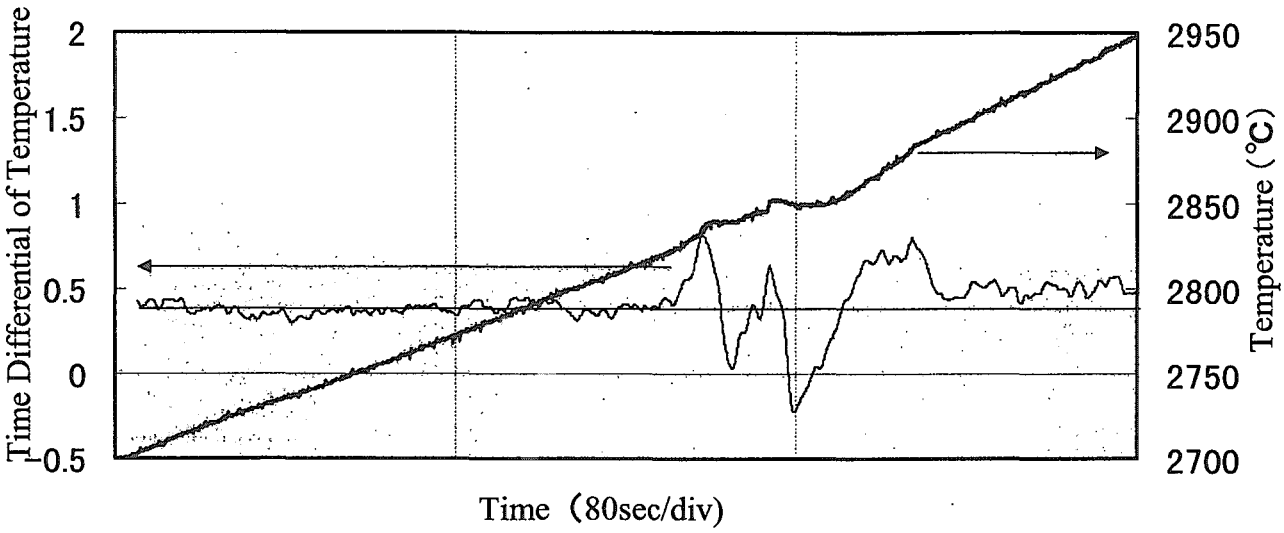
Sample condition

Composition	Burn-up (GWd/t)	Reactor
UO_2	0	---
UO_2	30	PWR
UO_2	45	PWR
UO_2	41	Halden reactor (IFA-535.2 rod 208)
UO_2	63	Halden reactor (IFA-408.3 rod 202)

— DHL / JAERI —

10

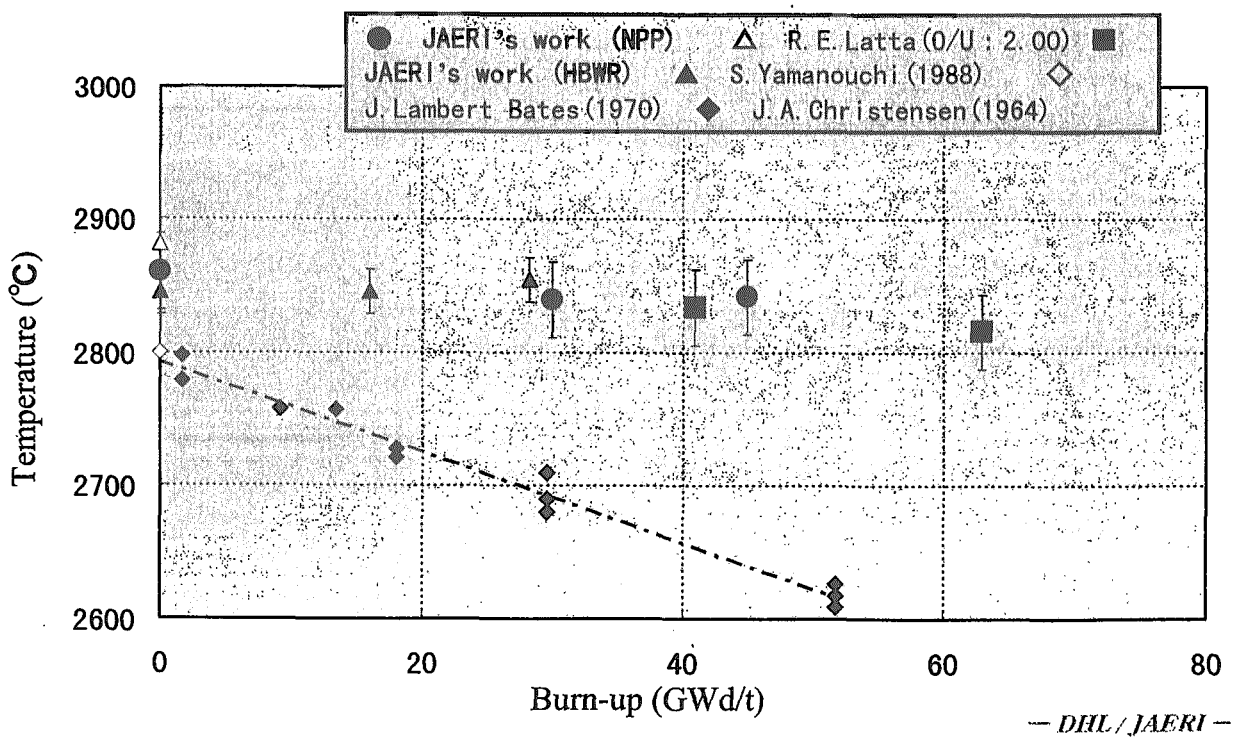
Time-temperature curve on UO_2 pellet (Burn-up level 30GWd/t)



— DHL / JAERI —

11

Comparison of melting temperature on UO_2 pellets



— DHL / JAERI —

12

Pellet Thermal Capacity measurement apparatus(PMC)

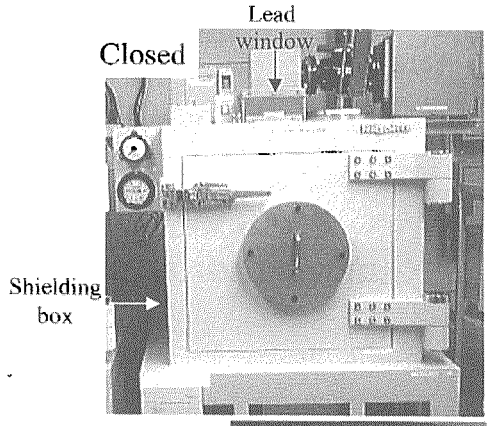
Contents

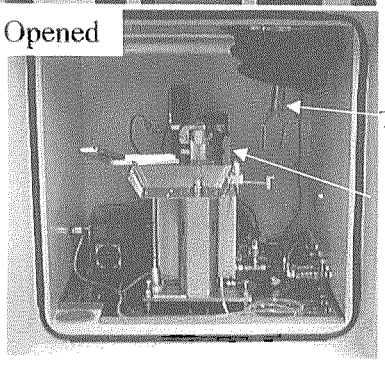
- Outline of PMC apparatus
- Results of characterization test

Thermal capacity measurement apparatus

Specification

Method	**Heat-flux type DSC***
Temp. range	**R.T. ～ 1723 K**
Sample holder	**5mm ϕ × 2.5mmt**
Atmosphere	**Inert gas (Ar)**



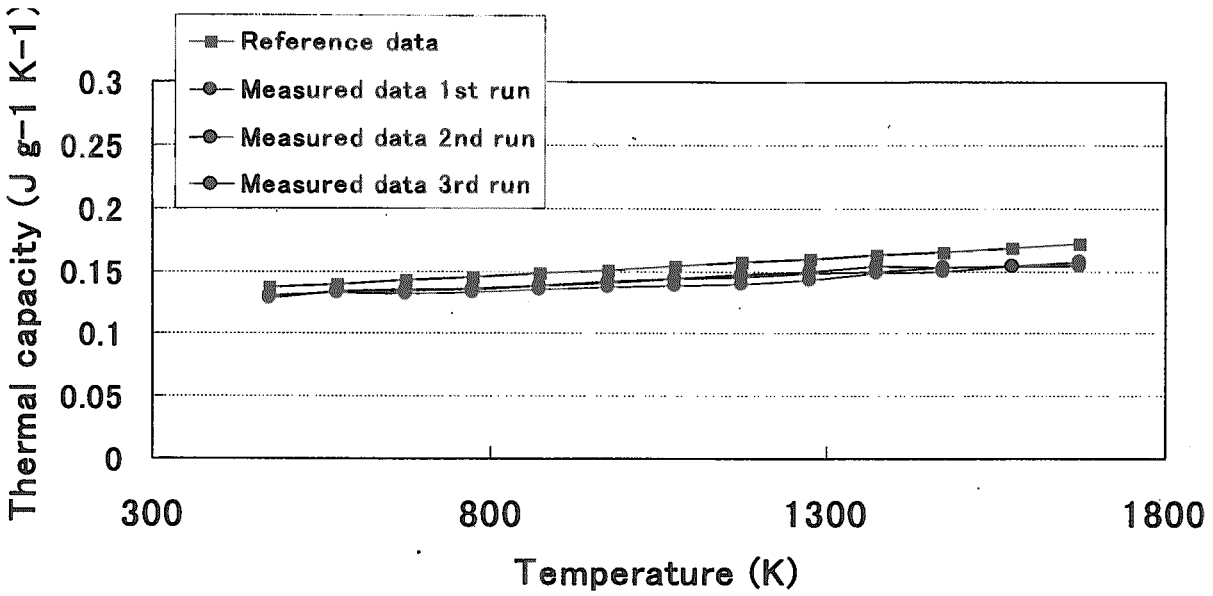


Equipment

Shielding box
Automatic sample mounting system
Tong
Lead window

*DSC = Differential Scanning Calorimeter

Measurement of Specific heat of Pt



— DHL / JAERI —

15

Neutron radiography for hydrogen analysis

— DHL / JAERI —

16

Background and Objective

Background

Neutron radiography is an effective tool for estimating hydrogen distribution.
Cross-section for thermal neutron: H>>Zr

⇩

Hydrogen distribution is qualitatively confirmed by difference in image contrast. By conventional X-ray film method, however, quantitative estimation of hydrogen concentration is difficult because of its narrow dynamic range.

Neutron Imaging Plate(NIP): wide dynamic range, high sensitivity

⇩

Possibility of quantitative estimation of distribution of hydrogen concentration

Objective

To investigate the practicability of NIP method to the quantitative hydrogen Analysis in Zircaloy cladding tube.

— *DHL / JAERI* —

17

Experimental

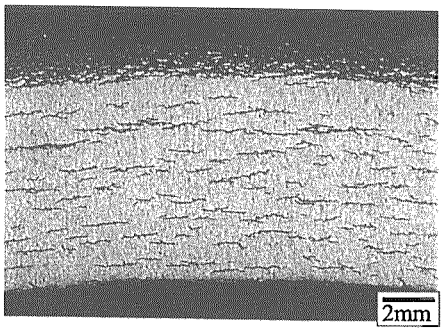
Hydrided samples

(1) Standard samples: Hydrides are uniformed.
(2) Segregation samples: Hydrides are segregated at periphery region

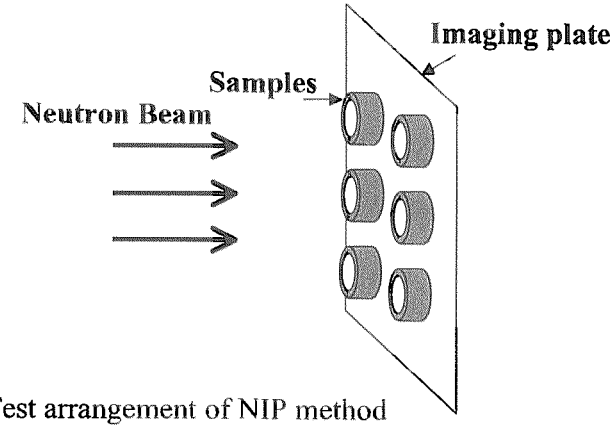
Ring samples; cut from Zircaloy-4 tube 5mm in length

Radiography test

2nd Thermal neutron radiography facility (TNRF-2) in JRR-3M



Micrograph of segregation sample



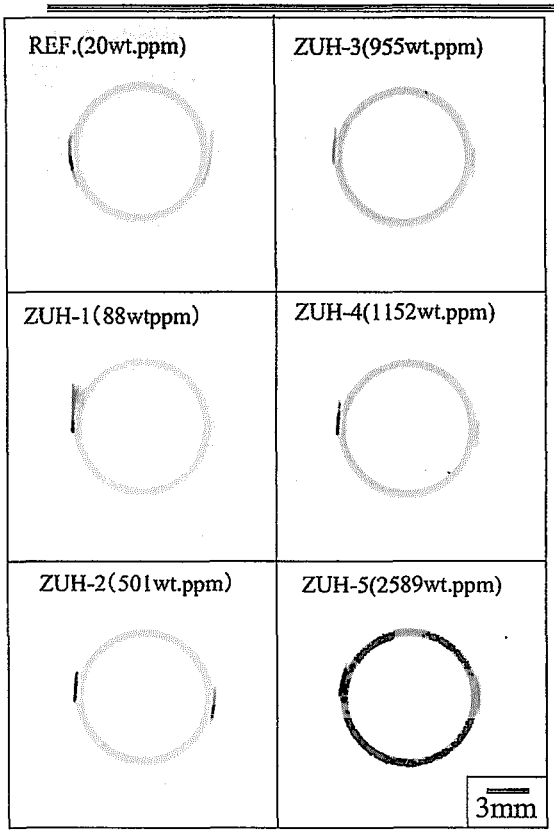
Test arrangement of NIP method

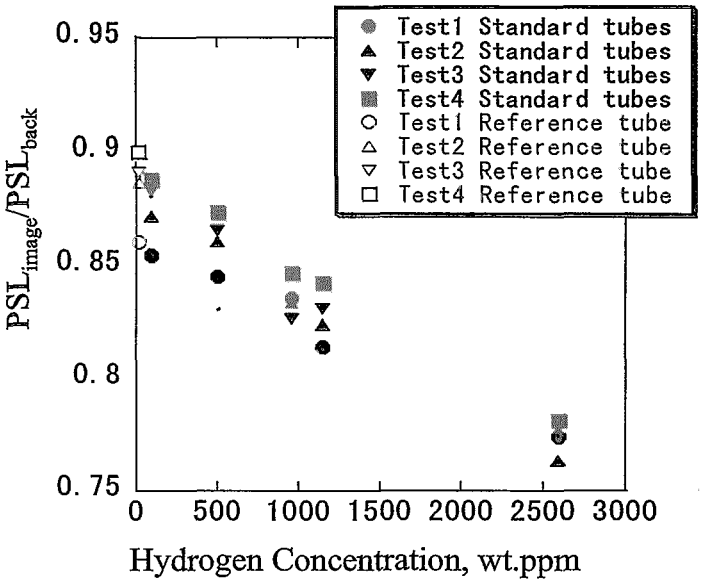
— *DHL / JAERI* —

18

This is a blank page.

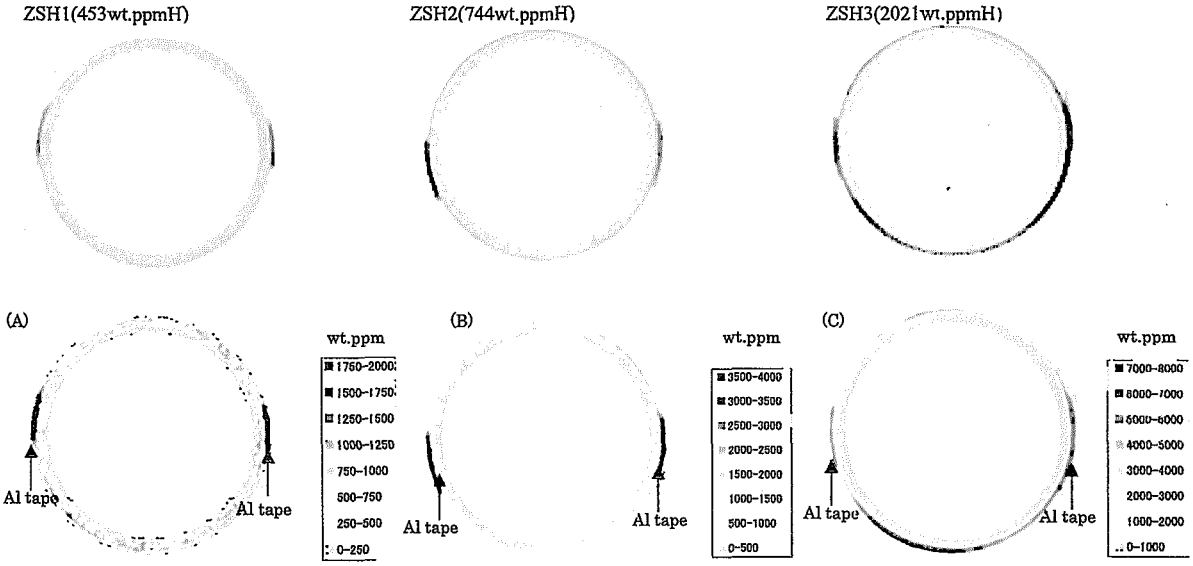
Results of standard samples





*PSL=Degree of image level

Maps of local hydrogen concentration in measured samples



This is a blank page.

Summary-1

Melting temperature measurement apparatus

- Thermal arrest is obviously confirmed in measurement of irradiated UO_2 pellets. However, change of temperature in the thermal arrest period is irregularity.
- By curve of dT/dt , it is easier to determine the melting temperature.
- In the results of these measurements, melting temperature of UO_2 fuel slightly decrease with increasing burn-up level up to 63 GWd/t.

Thermal capacity measurement apparatus

- Thermal capacity measurement apparatus is installed to investigate the specific heat of irradiated fuel pellets.
- Good reproducibility is shown in the characterization tests.
- Hot mock-up test will be performed using irradiated fuels in near future.

Summary-2

Neutron Radiography

- Relationship between image contrast and hydrogen concentration of the tubes is obtained using standard samples with known hydrogen concentration.
- Local hydrogen concentration in the measured samples is quantitatively estimated by the results of standard samples.

Discussion:

Q: (K.Nissen)
Do you plan to measure 1) MOX fuel melting temperature? 2) Gd_2O_3/UO_2 fuel melting temperature?

A: Yes, we plan to measure the melting temperatures of these fuels.

Q: (YH.Kang)
Do you have any plans to measure the density of your samples?

A: A densitometer for PIE is under development. We will measure the density upon the completion of the device.

Q: (P.Bottomley)
What is the limit of spacial resolution of the hydrogen mapping by neutron radiography?

A: The special resolution corresponds to the picture element size in NIP image. In this case, the size of picture element is around 100 μm.

JP0250422

JAERI－Conf 2002－009

7. Session 5b : Fuel Behavior Modelling under Normal Operation Condition

Session 5b-1

Fission Gas Release Modelling at High Burnup

P. Brohan and P.A. Tempest
British Energy Generation Ltd.
paul.tempest@british-energy.com
February 2002

ABSTRACT

A large quantity of experimental data on fission gas release is now available in the public domain. It covers a wide variety of fuel types and burnups of up to more than 70 GWd/tU. This data, together with gas release measurements from British Energy's AGRs, has been used to build a comprehensive validation database for the fuel performance code ENIGMA.

Validation of ENIGMA version 5.11 against this database has identified a requirement for model development to improve predictions at high burnup. A modified gas release model has been produced and tested.

1 Introduction

Prediction of fission gas release in both normal operation and fault transients is a key task for fuel performance codes. Current models for predicting gas release were largely derived from measurements on fuel with burnups of less than 30 GWd/tU — low by modern standards.

A large quantity of experimental data on fission gas release is now available in the public domain. It covers a wide variety of fuel types and burnups of up to more than 70 GWd/tU. This offers an opportunity to re-visit the validation of fission gas release models and identify any areas in which further development is necessary.

This paper outlines the gas release model incorporated into the ENIGMA code, and describes the construction of a new validation database for fission gas release. Validation of ENIGMA against the database demonstrates that performance is poor under some conditions at high burnup, and modifications to the model to improve predictions are described.

2 The ENIGMA gas release model

The ENIGMA model for gas release from the fuel grains considers thermally activated diffusion of gas atoms with irradiation induced re-solution from the grain boundaries. This model was originally formulated by Speight [1] as:

$$\frac{\partial C}{\partial t} = D\nabla^2 C + \beta \tag{1}$$

subject to the boundary condition

$$C = \frac{b\lambda N_g}{2D} \tag{2}$$

on the grain faces.

In the above equations C is the gas atom concentration, D is the fission gas diffusion coefficient, β is the gas atom generation rate, N_g is the number of gas atoms per unit area on the grain boundary, b is the rate at which gas atoms are returned to the matrix at an average distance λ and t is time.

The value of β is well established, so in solving the above equations the key parameters are D and the product $b\lambda$ (known as the re-solution parameter).

2.1 The predicted release threshold

Fission gases will build up on grain boundaries, eventually causing release, whenever the diffusion rate exceeds the re-solution rate. These conditions depend on the fuel temperature and the fuel fission gas inventory (i.e. burnup).

To explore the conditions under which the ENIGMA 5.11 model predicts gas release, the model has been used to simulate isothermal irradiations of fuel samples at a range of temperatures and so determine the temperature and burnup conditions

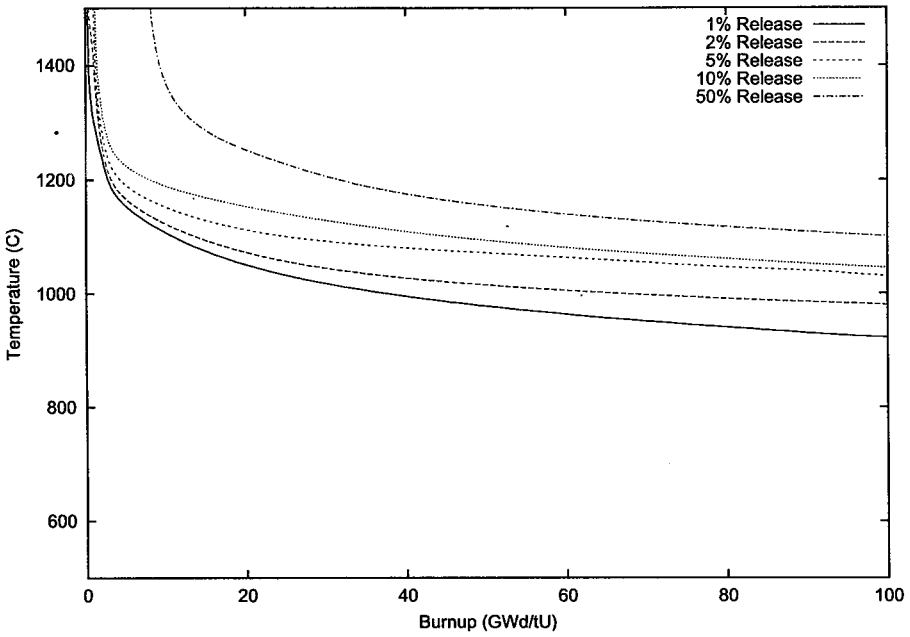


Figure 1: Predicted gas release as a function of temperature and burnup

under which release will occur. Figure 1 is a contour plot showing the burnup and local temperature conditions required for gas release to be predicted by the ENIGMA 5.11 gas release model.

It is clear from figure 1 that negligible gas release is predicted for temperatures below about 950°C, even at high burnup.

3 Building a validation database

To test the accuracy of a model, it has to be validated by comparing predictions of fission gas release with measured release from fuel pins. As the model is general, it should be possible to predict releases from fuel with any irradiation history.

To test the ENIGMA model, a validation database has been built using data from as wide a range of UO_2 fuelled pins as possible. The principal sources of validation cases are British Energy's Advanced Gas-cooled Reactors (AGRs), Halden experiments, and cases from the OECD/NEA sponsored International Fuel Performance Experiments (IFPE) database [2].

3.1 The IFPE database

The IFPE database [2] is the result of cooperation between the OECD/NEA, the IAEA and the IFE/OECD Halden Reactor Project. Their aim is to provide a com-

prehensive and well qualified public domain database on Zircaloy clad UO_2 for model development and code validation.

The IFPE project is still incomplete, and not all the data collected is relevant to FGR validation, but the data available is still extremely useful. Fuel pin power histories were taken from IFPE for Halden IFA-535 [3], Studsvik Inter-Ramp [4], Over-Ramp [5] and Super-Ramp [6] projects, the Risø Transient Fission Gas Project [7], the Third Risø Fission Gas Project [8], some AECL CANDU tests, some VVER irradiations in Kola-3 [9], the SOFIT program [10], some SPC PWR test irradiations [11] and the Tribulation program [12].

3.2 Range of cases covered

The validation cases cover the following range of parameters:

- Gas reactor and water reactor fuel,
- AGR, PWR, BWR, VVER and CANDU fuel pins,
- Typical power reactor and ramp irradiations,
- Burn-ups of up to 75 GWd/tU,
- Ratings of up to 64 kW/m.

The full database contains ENIGMA inputs and measured releases for 236 fuel pins.

3.3 Quality Assurance

It is now standard practice to develop and maintain fuel performance codes under stringent software control [13], where source code is subjected to verification and inspection, and changes are tracked through version control.

If code validation is to support the use of the code for safety analysis, it is equally necessary to verify and control the validation cases. So each validation case, after being created, was independently inspected and checked against the original source of the data. The resulting cases are now maintained under version control.

4 Validation of the ENIGMA model

All the cases in the validation database have been run using the latest version of ENIGMA (release 5.11). Figure 2 plots predictions versus measurement (P/M) for all the cases.

It is clear from figure 2 that predictions are mostly good — most of the points fall in the $\times/2$ bands shown by dotted lines on the figure, and that the good predictions cover all the fuel types studied and the entire range of measured releases from $< 0.1\%$ to $> 50\%$.

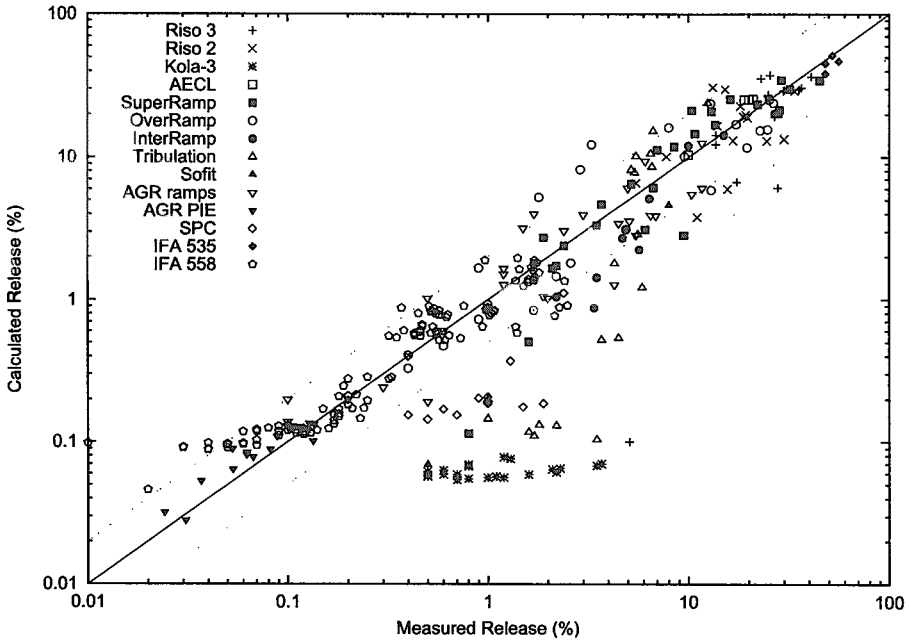


Figure 2: Predicted versus measured gas releases using ENIGMA 5.11

Despite the generally good predictions, a cluster of cases are seriously underpredicted. This cluster consists mostly of the Kola-3, SPC and Tribulation cases; where the measured releases are modest (up to about 5%), but the predicted releases are low (about 0.1%).

4.1 Parameter studies

To get more information on the reason some cases are underpredicted, it is useful to look at the variation of the prediction quality with various properties of the case. Figure 3 is a plot of P/M against burnup, and figure 4 shows P/M versus peak fuel temperature.

It is clear from figures 3 and 4 that the underpredicted cases share the common properties that they have a high burnup and a low peak fuel temperature.

4.2 High burnup, low temperature underprediction

The ENIGMA model for fission gas release, based on equations 1 and 2, was developed using data from low burnup fuel, and has proved very successful over a wide range of fuel operating conditions. However, the validation has demonstrated that it has a deficiency for high burnup, low temperature fuel.

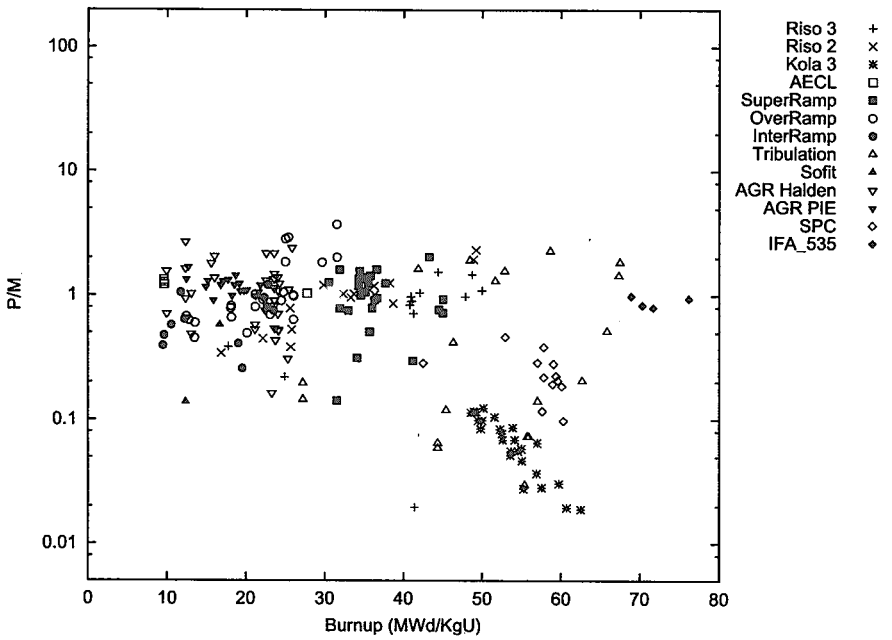


Figure 3: ENIGMA 5.11 P/Ms as a function of burnup

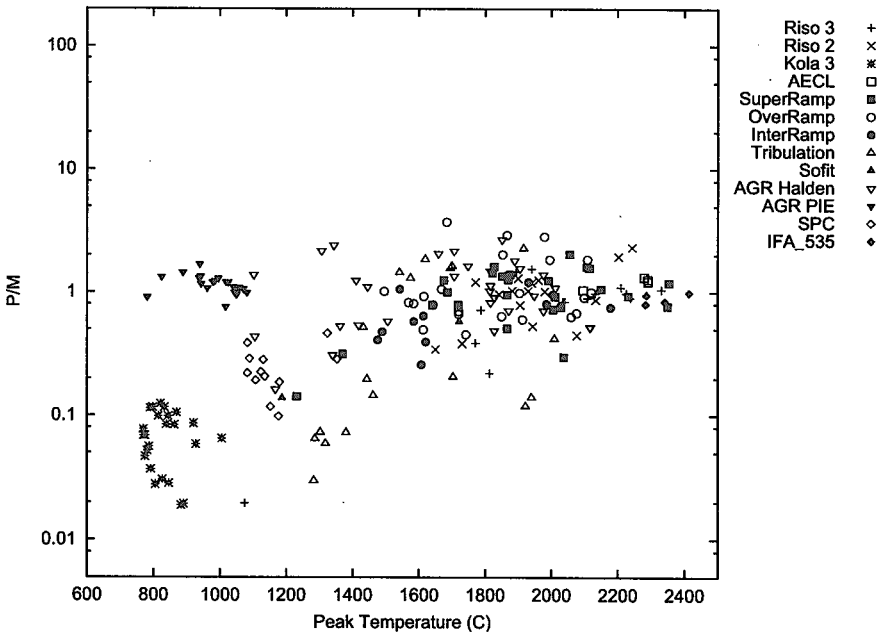


Figure 4: ENIGMA 5.11 P/Ms as a function of peak fuel temperature

Note that high burnup alone is not sufficient to cause problems. High burnup, high temperature cases are well predicted.

5 Measurements on high burnup, low temperature FGR

Changes in fuel behaviour at high burnup are not unexpected. Gas release measurements on fuel pins irradiated to enhanced burnups in PWRs have shown sharp increases in release at burnups above about 45 GWd/tU, and recent Halden experiments have confirmed the effect.

A considerable amount of gas release data from high burnup, un-ramped fuel has been published:

- A high burn-up fuel validation test was run in the Kola-3 VVER [9]. Fuel pins were irradiated at low ratings to a peak rod burnup of above 55 GWd/tU; fuel temperatures were low, but FGR in the peak pins exceeded 3%.
- A lead test assembly (LTA) program was run by SPC in the R.E. Ginna PWR [11]. Peak rod burnups were up to 59 GWd/tU. Fuel temperatures varied, but significant FGR was seen even in the colder rods.
- The TRIBULATION program [12] was an international program jointly managed by Belgonuclaire and CEN/SCK. Fuel rods were irradiated in the experimental PWR BR3 to rod burn-ups of up to 55 GWd/tU. Most of the fuel rods were high rated or ramp tested, but data from low temperature fuel is also available and does show gas release.
- A collaboration between EdF, CEA and Framatome has produced PIE data from 5-cycle PWR fuel at burnups of up to 55 GWd/tU [14]. Fuel centre temperatures were around 700°C and 900°C, with the hotter fuel producing much more FGR.
- Siemens (now Framatome-ANP) have run a considerable program of LTA irradiations producing FGR data from un-ramped PWR fuel rods at burnups of up to 100 GWd/tU [15]. These data show an exponential increase in fractional FGR as burnup increases, reaching values of about 25% at 100 GWD/tU.
- British Energy have measured gas releases in AGR pilot stringers irradiated to pin burnups of up to 42 GWd/tU in Hinkley Point B, and have seen a sharp increase in measured FGR at burnups greater than about 35 GWd/tU [16]. At the same burnup, the hotter element 6 pins released more than element 4 pins.

Figure 5 shows measured gas releases from many of these pins as a function of burnup.

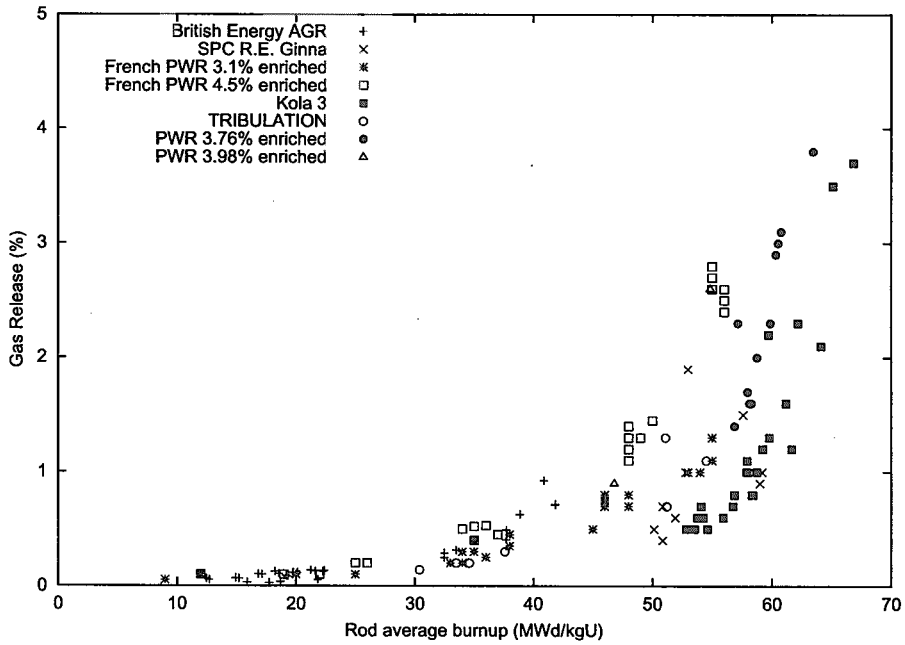


Figure 5: Measured FGR in un-ramped power reactor fuel pins

More detailed information on the gas release behaviour is available from metallographic examination, or Electron Probe Micro-Analysis (EPMA) of fuel pellets. In particular these measurements give information on the radial distribution of release through the fuel pellet.

Metallography on the highest burnup AGR fuel pins [17] showed both intra- and inter-granular fission gas porosity over the inner half of the pellet. This showed that gas release was from the hot pellet centre.

EPMA measurements on the 55 GWD/tU French fuel [14] tell a similar story. EPMA shows loss of xenon from the central parts of the fuel, with the radial extent and depth of xenon loss being larger in the higher temperature fuel type. Xenon loss is also seen in the high burnup pellet rim region.

EPMA on the Siemens fuel [15] demonstrates that at higher burn-ups the xenon loss extends outwards across the whole pellet.

5.1 Conclusions from the measurements

Early analysis of enhanced gas release at high burnup concentrated on the possibility that the enhanced release was related to the well known 'rim effect', but the more recent data has demonstrated the inaccuracy of this hypothesis — gas release is definitely from the fuel centre not the rim and measurements do not indicate any large, rim induced, temperature increases.

Comparison of the results from the cases where fuel has been irradiated at different temperatures to the same burnup (the different PWR enrichments and AGR elements 4 and 6) show that in all cases the hotter fuel produces significantly more release. Therefore the release mechanism is thermally driven.

The German data on fuel samples up to burnups of over 100 GWd/tU demonstrate that the fractional release continues to increase up to very high burnup. EPMA measurements on this fuel show that the release zone extends almost to the pellet edge; implying that the temperature threshold for release drops to below 400°C by 80–100 GWd/tU.

These results suggest that, apart from the low temperatures involved, high burnup gas release is similar in nature to low burnup release, for which the ENIGMA 5.11 model is very successful. This suggests that in modelling high burnup release it will be more productive to explore variations on the existing ENIGMA model than to try to develop completely new release mechanisms.

6 Model developments to improve predictions

From the discussion in section 2, the obvious parameters to alter in the gas release model are the diffusion coefficient and the resolution parameter $b\lambda$.

6.1 The diffusion coefficient

The diffusion coefficient used in ENIGMA 5.11 is based on analysis of data from three sources: the original diffusion rate experiments of Turnbull et al. [18], the Halden gas flow rigs [19] and post-irradiation annealing experiments [20].

The diffusion coefficient used is:

$$\begin{aligned} D &= 1.14 \times 10^{-8} \times e^{\frac{-35000}{T}} \\ &\quad +1.5 \times 10^{-17} \times \sqrt{R} \times e^{\frac{-10600}{T}}. \end{aligned} \tag{3}$$

where T is the temperature in kelvin and R is the rating in W/gU.

6.2 The re-solution parameter

As re-solution is irradiation driven the re-solution parameter is proportional to the rating. In ENIGMA 5.11 λ is 1.0E-8 and b is 3E-5 at a rating of 20 W/gU.

6.3 Model changes and the release threshold

From consideration of figures 1, 2 and 5. It is apparent that to improve the ENIGMA model it must be modified in such a way as to preserve the current behaviour at high temperature, and at low temperature for burnups < 35 GWd/tU, but reduce the release threshold temperature at higher burnups.

At high temperature diffusion dominates over re-solution so the release is determined by the value of the diffusion coefficient. So any modifications to the model

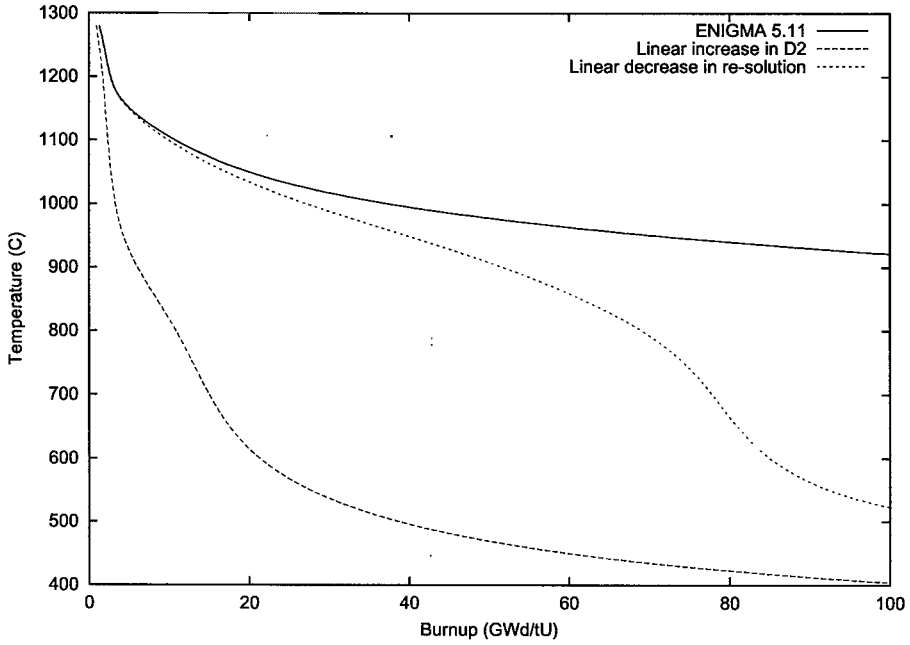


Figure 6: Effect on the 1% release contours of changes in the diffusion coefficient and the re-solution parameter — introduced linearly with burnup

must preserve the value of the diffusion coefficient at high temperature. So changes to the diffusion coefficient must be restricted to its low temperature component — the second term in equation 3, known as D2.

To reduce the release threshold to 400°C at 80 GWd/tU it is necessary either to increase D2 by a factor of about 10^3 or to remove re-solution completely. Following the approach suggested in [21], figure 6 shows the effects of increasing D2 and of decreasing re-solution linearly with burnup.

The validation evidence (figure 2) shows that the ENIGMA model is accurate at burnups below about 40 GWd/tU, but that the predicted release threshold needs to be reduced at higher burnups. Changing D2 produces a large change at low burnups, and so is not a suitable change, but the linear change in re-solution gives a promising effect.

6.3.1 Optimising the model changes

The reduction in release threshold actually occurs at a burnup of about 45-50 GWd/tU (figure 5), and calculations on a sample of high burnup PWR cases indicate that reducing the re-solution parameter to zero at 50 GWd/tU gives the increase in release with burnup shown in figure 5.

Reducing the re-solution parameter linearly to zero at 50 GWd/tU causes a

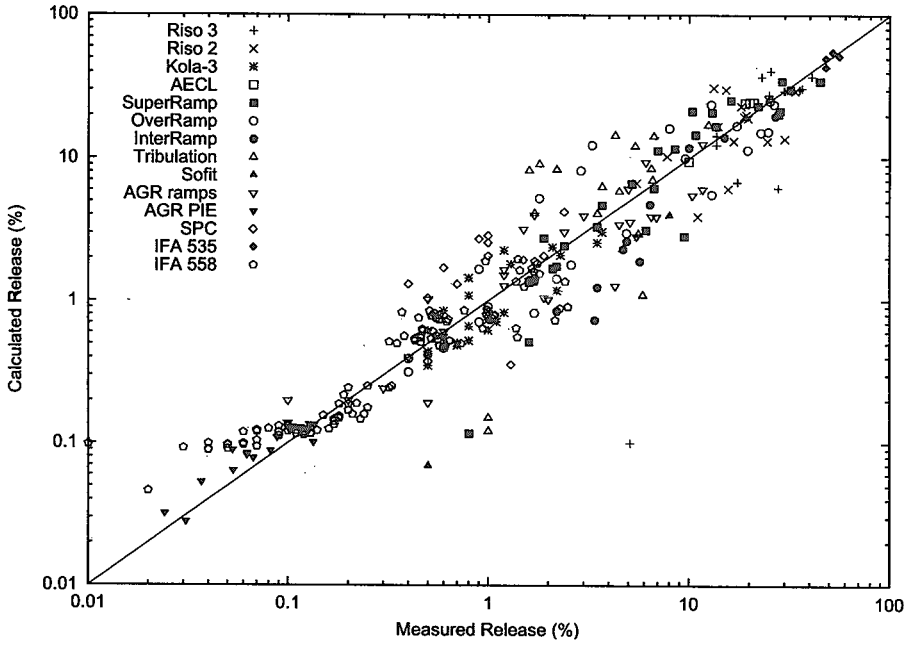


Figure 7: Predicted versus measured gas releases using the revised ENIGMA gas release model

noticeable reduction in the release threshold at lower burnups down to about 25 GWd/tU. Measured gas releases in fuel irradiated in BE's AGRs [16] show that the threshold should not be reduced at these burnups. Calculations with a selection of high burnup AGR and PWR calculations show that doubling the re-solution parameter at zero burnup from its value in ENIGMA 5.11 (section 6.2) and reducing it linearly to zero at 50 GWd/tU give good results at all burnups.

7 Validating the revised model

The real test of the revised release model is its performance against the full database described in section 3. Figure 7 is a P/M plot for all the cases in the new database using the new release model.

It is clear from figure 7 that the cluster of underpredicted cases seen in figure 2 have been eliminated by the model change, and that predictions are now accurate across the whole burnup and temperature range. Figure 8 shows the distribution of P/Ms from the full database; also shown is a log-normal distribution with a standard deviation of $\times/\ 1.6$ — equivalent to a 1σ uncertainty on the fuel pin ratings of about $\pm 3\%$. Figure 8 demonstrates that the remaining errors in the validation database are now dominated by the inevitable rating uncertainties in the validation cases.

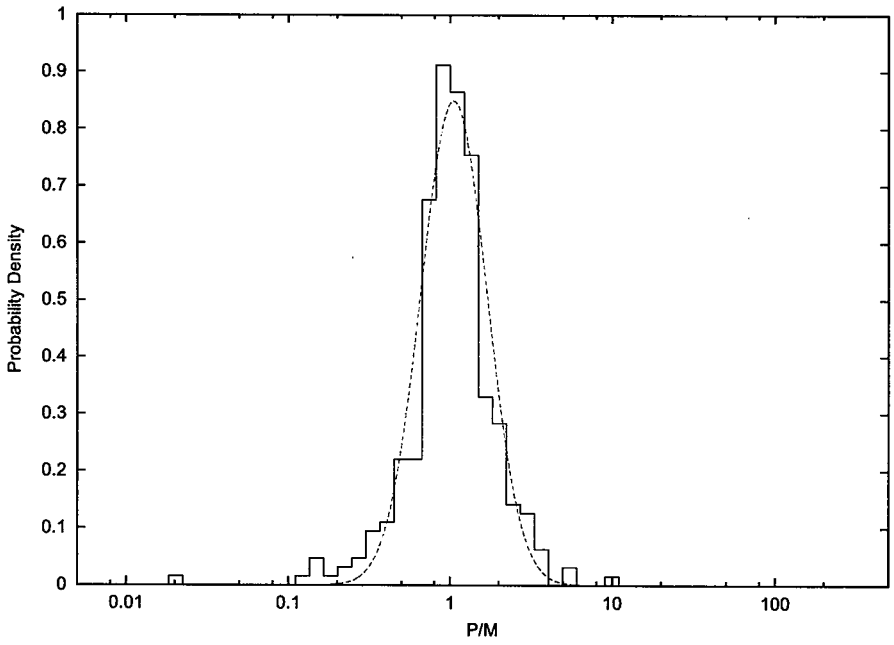


Figure 8: Distribution of P/Ms in the validation database using the revised ENIGMA model

8 Conclusions

- A new validation database for the prediction of fission gas release using the fuel performance code ENIGMA has been constructed. This database contains measured releases and ENIGMA input histories for 236 fuel pins, and covers normal operation and ramp irradiations for AGR, PWR, BWR, VVER and CANDU fuel pins.
- Validation of ENIGMA 5.11 against this database shows that the ENIGMA gas release model, based on Speight's diffusion/re-solution model, accurately predicts gas release from all fuel types, except that release from high burnup (> 45 GWd/tU), low temperature (< 1000°C) fuel is underpredicted.
- Modification of the re-solution parameter in the release model so that re-solution became unimportant at burnups above 50 GWd/tU improved predictions for high burnup, low temperature fuel; eliminating the underpredictions.
- Testing a version of ENIGMA containing the improved release model against the validation database demonstrated that predictions were consistently good. No systematic errors were found, and the random scatter in the results was consistent with an uncertainty in the fuel pin ratings of ± 3%.

9 Acknowledgements

This work was funded by the U.K. Industry Management Committee (IMC) as part of project FC/GNSR/5059.

This work was made possible by the Production of the OECD/NEA International Fuel Performance Experiments Database (IFPED). Both the work of those maintaining the database, and the generosity of those who contributed experimental data, are gratefully acknowledged.

References

[1] Speight, M. V. *Nucl. Sci. and Engineering*, (37):180, 1969.

[2] Menut, P., Sartori, E., and Turnbull, J. A. *The Public Domain Database On Nuclear Fuel Performance Experiments (IFPE) For The Purpose Of Code Development And Validation.* In *International Topical Meeting on Light Water Reactor Fuel Performance*, Park City, Utah, U.S.A., April 2000.

[3] Tosi, V. *The Effect of Pre-Pressurisation on Fission Gas Release in High Burnup BWR-Type Fuel Rods (IFA-535.5 - 6).* Halden report, HWR 198, April 1987.

[4] *Final Report of the Inter–Ramp Project.* Studsvik report, STIR-53, August 1979.

[5] *The Over–Ramp Project, Final Report.* Studsvik report, STOR-37, May 1981.

[6] Djurle, S. *Final Report of the Super–Ramp Project.* Studsvik report, STSR-32, December 1984.

[7] Knudsen, P., Bagger, C., Carlsen, H., Johansen, B. S., Misfeldt, I., and Morgensen, M. *Final Report on the Risø Transient Fission Gas Release Project.* Risø report, RISØ-TFGP-R29, December 1986.

[8] *The Third Risø Fission Gas Project, Final Report: The Project.* Risø report, RISØ-FGP3-FINAL, March 1991.

[9] Lemehov, S. E., Smirnov, A. V., and Tisbulya, V. A. *Kola-3 High Burn-up Fuel Validation Tests FA-198 and FA-222.* In *Enlarged HPG Meeting on High Burn-up Fuel Performance, Safety and Reliability and Degredation of In-Core Materials and Water Chemistry Effects and Man-Machine Systems Research*, Loen, Norway, May 1996.

[10] Yakovlev, V., Moshajev, A., Strizhov, P., Johansson, J., Liuhto, P., Hyvarinen, P., and Terasvirta, R. *SOFIT: A Joint Experimental Programme Between the USSR and Finland on VVER Fuel Performance.* In *IAEA International Symposium on the Utilization of Multi-purpose Research Reactors and Related International Co-operation*, Grenoble, France, October 1987.

[11] Sofer, G. A. and van Swam, L. F. P. *Annular-Pellet Barrier-Clad Fuel Assemblies at the R.E. Ginna PWR: Hotcell Examinations.* SPC report, ESEERCO Project EP 80-17, April 1997.

[12] Lippens, M. and Boulanger, D. *Tribulation Final Report.* Belgonucleaire report, TR 89/79, September 1989.

[13] Gates, G. A. *The ENIGMA Software Control System.* NEL report, EPD/REP/0006/96, 1996.

[14] Noirot, J., Desgranges, L., and Marimbeau, P. *Contribution of the Rim to the Overall Fission Gas Release: What do isotopic analyses Reveal.* In *Inter. Seminar on Fission Gas Behaviour in Water Reactor Fuels: Les Journées de Caderache*, Caderache, France, September 2000.

[15] Brémier, S., Manzel, R., and Walker, C. T. *Fission Gas Release and Fuel Swelling at Burn-ups Higher than 50 MWd/kgU.* In *Inter. Seminar on Fission Gas Behaviour in Water Reactor Fuels: Les Journées de Caderache*, Caderache, France, September 2000.

[16] Clay, B. D. and Gonzales, M. D. U. *PIE Progress Report No. 107.* BNFL Magnox report, TE/EXT/REP/0292/97, November 1997.

[17] Gilmour, T. C. *The Examination of Advanced Gas Cooled Reactor Fuel. Berkeley Centre Metallography Report No. 92 (January–March 1997).* BNFL Magnox report, TE/EXT/REP/0088/97, June 1997.

[18] Turnbull, J. A., Friskney, C. A., Findlay, J. R., Johnson, F. A., and Walter, A. J. *The Diffusion Coefficients of Gaseous and Volatile Species During the Irradiation of Uranium Dioxide.* CEGB report, RD/B/N4892, 1980.

[19] White, R. J. and Turnbull, J. A. *The Measurement of Fission Product Release Using the Gas Flow Rigs: A Review of Experiments, Methodology and Results from 1980–1997.* Halden report, HWR 553, 1998.

[20] White, R. J. *Fission Gas Release and Swelling in Irradiated Uranium Dioxide.* NE report, EPD/GEN/REP/0166/96, January 1998.

[21] Turnbull, J. A. *An Assessment Of Fission Gas Release And The Effect Of Microstructure At High Burn-up.* Halden report, HWR-604, March 1999.

Fuel Safety Research Specialists' Meeting, 4-5 March 2002, JAERI, Tokai, Japan

Fission Gas Release Modelling at High Burn-up

P Brohan and P A Tempest
British Energy

British Energy Generation

- **One modern PWR, Sizewell B, (1188 MW, operational 1995)**
- **Seven twin Advanced Gas Cooled Reactors (2 x ~600MW each, operational 1976 - 1988)**

British Energy: Other Generation Activities

- **U. K.**
  - **Eggborough, Coal fired, 4 x 490 MW**
  - **Wind Power, planning stage**
- **North America**
  - **AmerGen: TMI-1, Clinton, Oyster Creek**
  - **Bruce Power: Bruce A, B, CANDU, 8 x ~ 780 MW**
    Wind power, planning stage

British Energy

Introduction

- FGR prediction in normal operation and faults is a key task for fuel performance codes.
- Current models of the FGR process were derived from data on low burnup fuel
- Lots of experimental data on FGR is now available in the public domain - IFPE - opportunity to expand code validation
- This presentation:

1. Outlines the FGR model in BE's ENIGMA code
2. Describes the construction of a new validation database for FGR
3. Describes modifications to the ENIGMA FGR model to improve predictions where validation results are poor.

British Energy

- The ENIGMA FGR model is based on Speight's equations:

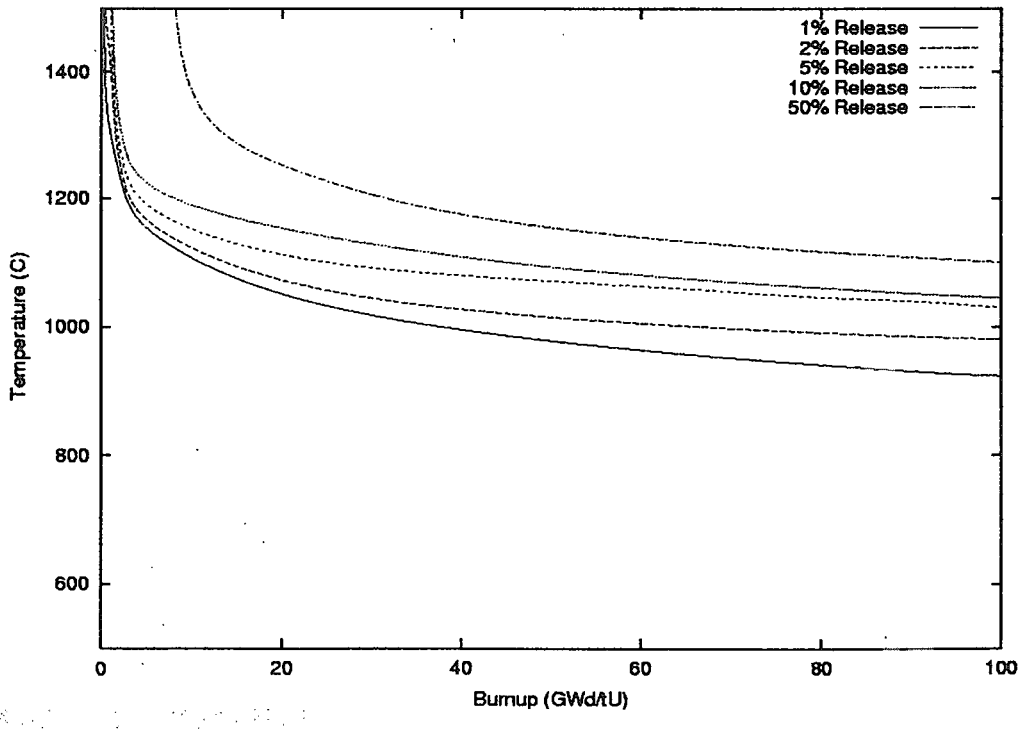
$$\frac{\partial C}{\partial t} = D\nabla^2 C + \beta$$

subject to the boundary condition

$$C = \frac{b\lambda N_g}{2D}$$

on the grain faces.

- The key parameters are the diffusion coefficient (D) and the re-solution parameter (b).



British Energy

The Predicted Release Threshold

- Fission gases will build up on grain boundaries leading to release whenever the diffusion rate exceeds the re-solution rate.
- Conditions for release depend on the fuel temperature and the fuel fission gas inventory.
- Model calculations can determine the range of temperature and burnup conditions where release is predicted.
- Negligible gas release is predicted for temperatures less than about 950°C.

British Energy

Building a Validation Database

- Validate the model against measured releases from the widest possible range of UO_2 fuel pins.
- Principal data sources were BE's AGRs and the OECD/NEA International Fuel Performance Experiments (IFPE) database.
- AGR fuel data: Base irradiated and ramp rested pins - data from condition monitoring and Halden experiments.
- IFPE database:

1. Experimental programmes - Risø 2 & 3, Studsvik Inter-, Over- and Super-Ramp, tribulation and Sofit.
2. LTA programmes - Kola-3, SPC R.E. Ginna.
3. Halden and AECL experiments.

British Energy

Range of Cases Covered

- Gas reactor and water reactor fuel.
- AGR, PWR, BWR, VVER and CANDU fuel pins.
- Typical power reactor and ramp irradiations.
- Burn-ups of up to 75 GWd/tU.
- Ratings of up to 64 kW/m.

- The full database contains ENIGMA inputs and measured releases for 236 fuel pins.

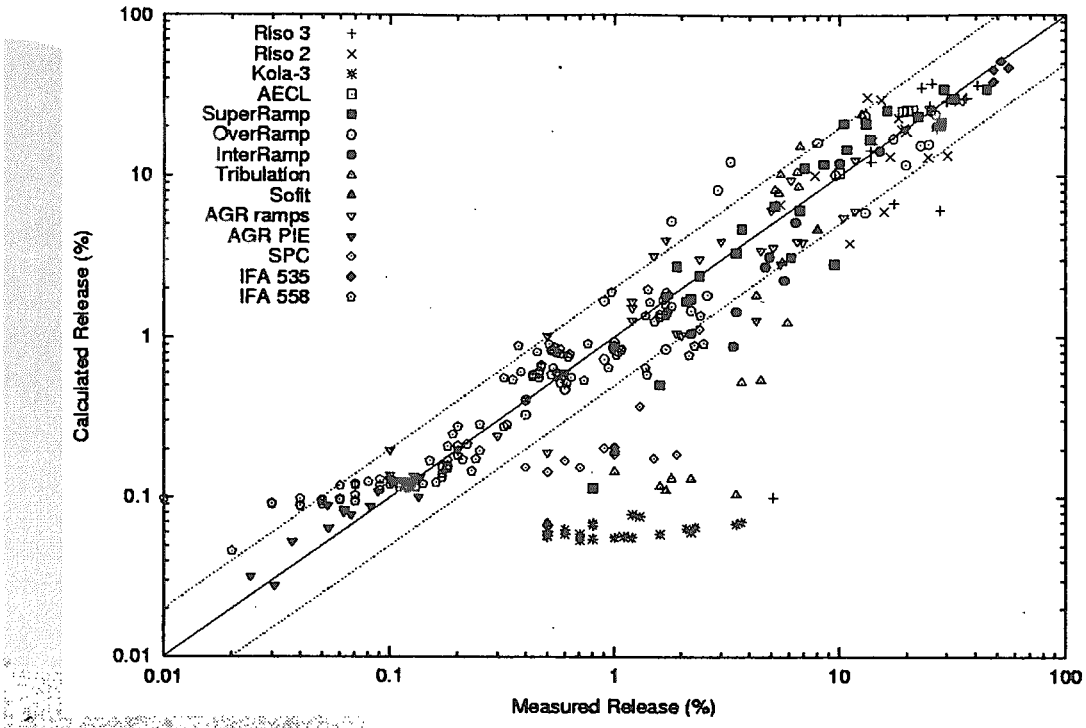
British Energy

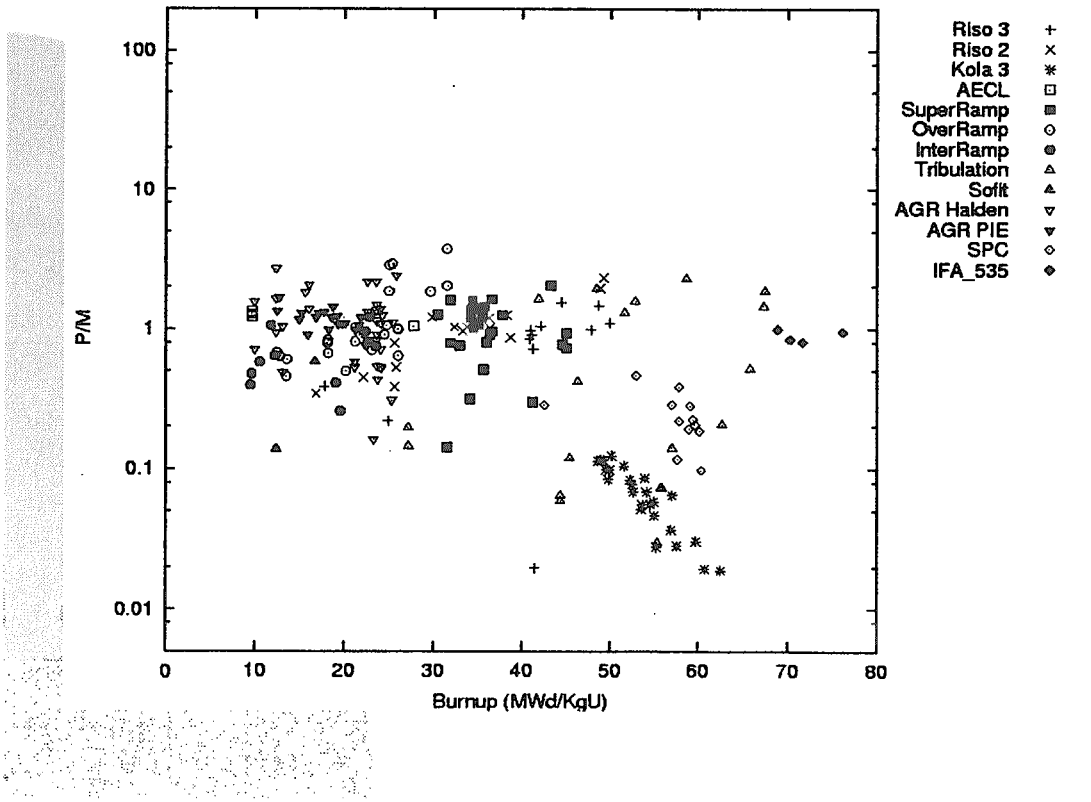
Validation of the ENIGMA Model

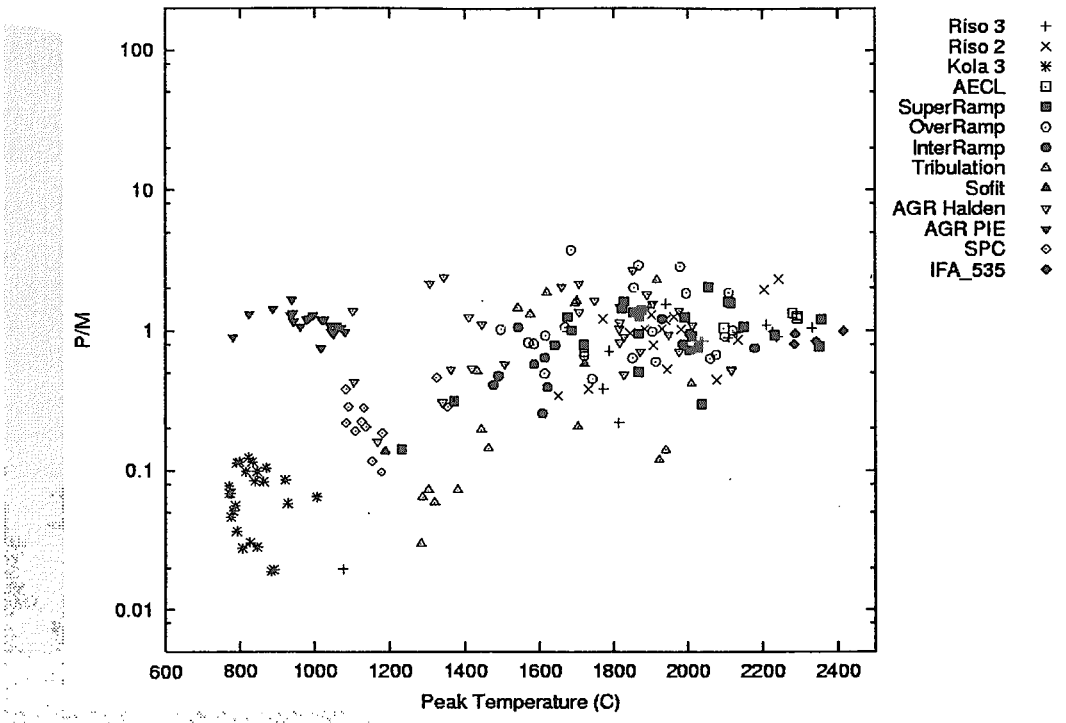
- Predictions are generally good - for most cases P/M falls within the x/2 bands.
- Good predictions cover all the fuel types studied and the whole range of measured releases from <0.1% to >50%.

- A cluster of cases are seriously underpredicted:

- Mostly the Kola-3, SPC and Tribulation cases
- Have a high burnup (45 GWd/tU) and a low peak fuel temperature (<1000°C).


Riso 3
Riso 2
Kola-3
AECL
SuperRamp
OverRamp
InterRamp
Tribulation
Sofit
AGR ramps
AGR PIE
SPC
IFA 535
IFA 558
Calculated Release (%)
Measured Release (%)
100
10
1
0.1
0.01
0.01
0.1
1
10
100


Riso 3
Riso 2
Kola 3
AECL
SuperRamp
OverRamp
InterRamp
Tribulation
Sofit
AGR Halden
AGR PIE
SPC
IFA_535
P/M
Burnup (MWd/KgU)
100
10
1
0.1
0.01
0
10
20
30
40
50
60
70
80

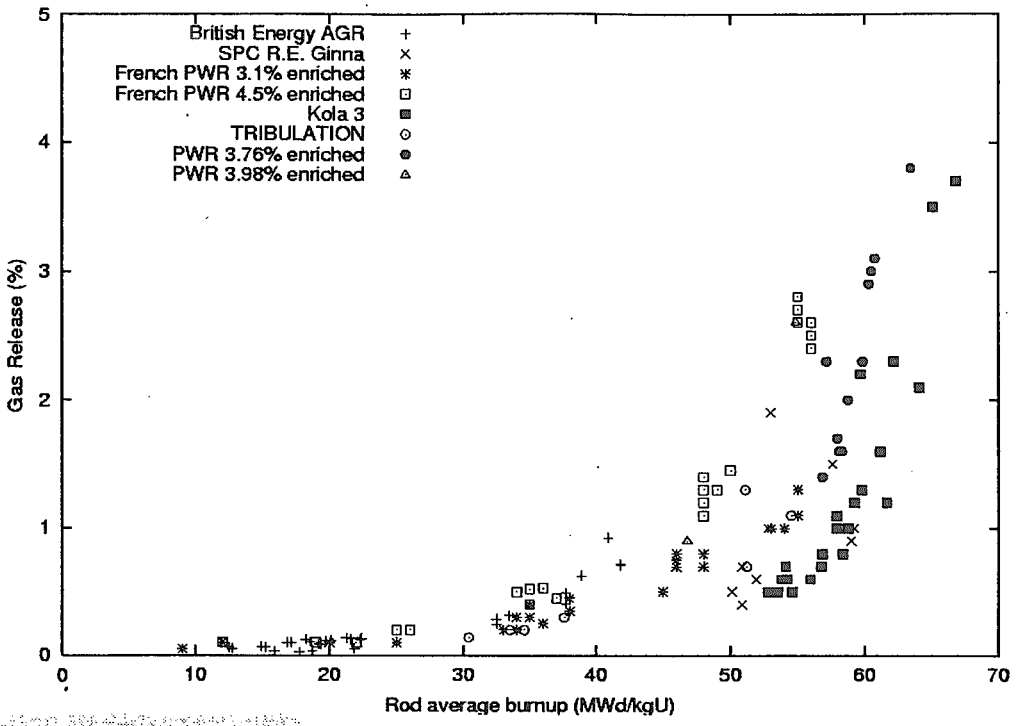


British Energy

Measurements of High Burnup, Low Temperature FGR

- Look at FGR in un-ramped high burnup fuel from power reactors.

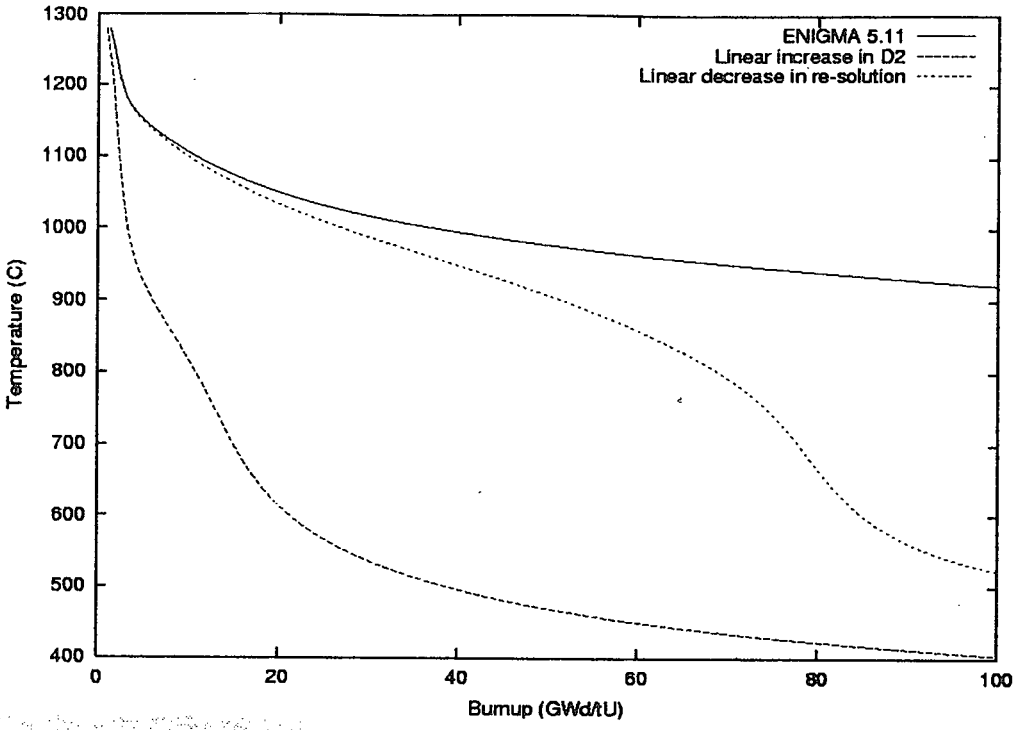
- Release increases exponentially with burnup.
- Higher enrichment (hotter) fuel produces more release.
- EPMA confirms that the release is from the fuel centre - i.e not from the rim.
- As the burnup increases the release zone spreads outwards from the pellet centre, so the release threshold temperature falls with burnup.



British Energy

Model Developments to Improve Predictions

- Obvious parameters to alter in the FGR model are the diffusion coefficient (D) and the re-solution parameter ($b\beta$).
- Need to keep predictions the same at low burnup and high burnup, and at high temperature, but increase predictions at high burnup and low temperature.
- Try introducing a linear burnup dependence into D or $b\beta$.
- Result - Increasing the re-solution parameter has the desired effect: little change at low burnup, whilst the threshold temperature reduces at high burnup.



British Energy

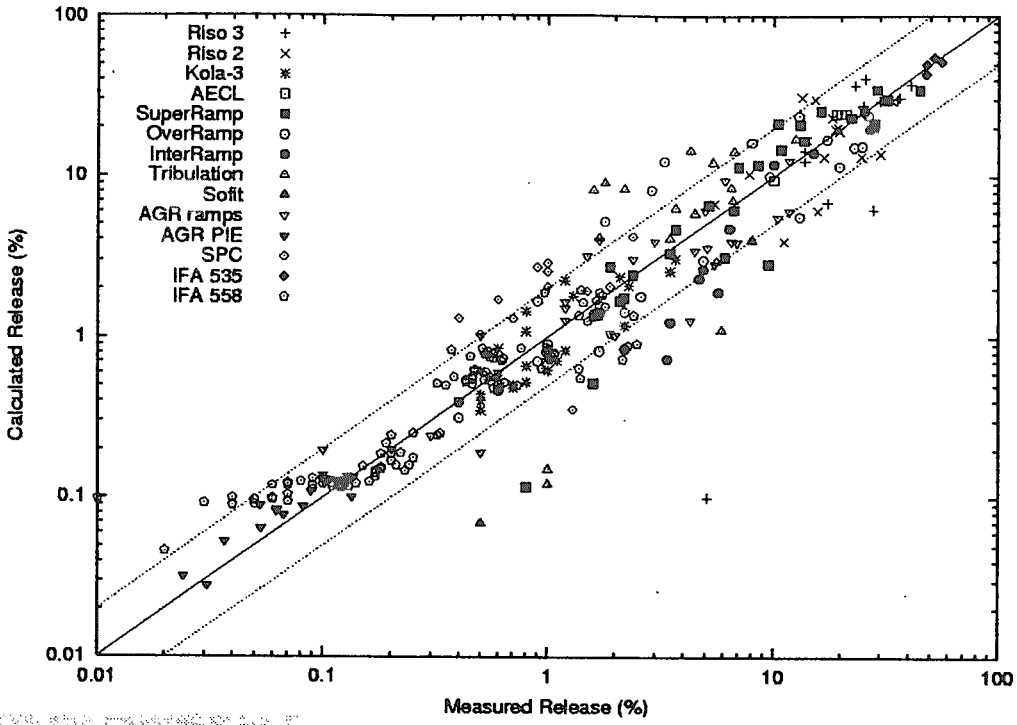
Optimising the Model Changes

- Investigation shows that doubling the re-solution parameter at zero burnup from the constant value used in ENIGMA 5.11 and reducing it linearly to zero at 50 GWd/tU give good results at all burnups.
  That is

$$b\lambda(B) = b\lambda_{5.11} \times 2\left(1 - \frac{B}{50}\right)$$

  for B ≤ 50 and b = 0 for B >50, where B is the burnup in MWd/kgU.

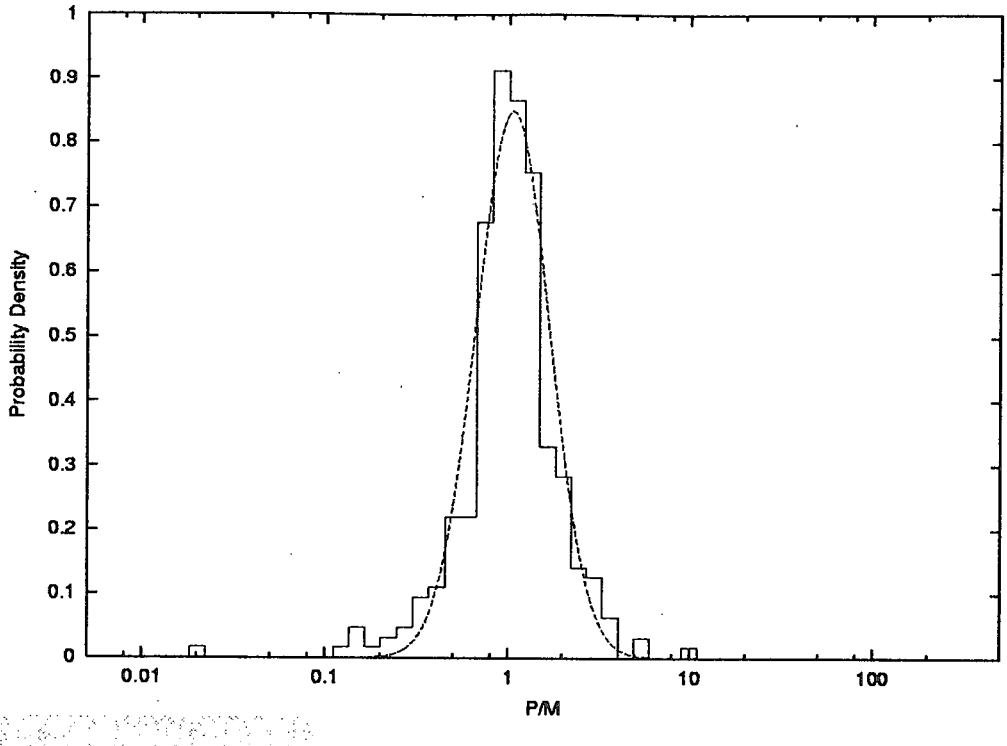
- Validating this revised model gave good results in all conditions.



British Energy

Validating the Revised Model

- The underpredicted cases seen in the original validation have been eliminated by the model change.
- Predictions are now accurate across the whole burnup and temperature range.
- P/Ms are well modelled by a log-normal distribution with 1σ errors of x/ 1.6 - equivalent to the effect of ±3% rating uncertainty.
- The remaining scatter in P/Ms is now dominated by the inevitable rating uncertainties in the validation cases.



British Energy

Conclusions

- An extensive and well qualified FGR validation database has been constructed for the fuel performance code ENIGMA.
- Validation of ENIGMA 5.11 against this database shows that predictions are good, except that releases from high burnup, low temperature fuel are underpredicted.
- Modifying the re-solution parameter in the release model so that re-solution became unimportant at burnups above 50 GWd/tU eliminated these underpredictions.
- Validating the new model gave consistently good results. No systematic errors were found, and the remaining random errors are consistent with an uncertainty in the pin ratings of ±3%.

British Energy

Acknowledgements

- This work was funded by the U.K Industry Management Committee (BE, BNFL and HSE).
- This work was made possible by the production of the OECD/NEA International Fuel Performance Database (IFPD).

Discussion:

Q: (P.Bottomley)

One reason for the decrease of the re-solution parameter at higher burnups may be the increasing levels of fission products in the lattice hindering various phase transformations.

A: I agree that the re-solution probability would be reduced by the mechanism you suggest, i.e. the re-solution of fission gas atoms requires acceptable lattice defect sites which are reduced in number when the lattice has a high concentration of fission products.

C: (M.Kinoshita)

1: Low temperature fission gas release (FGR) could be partly from the rim structure.

2: Another factor of the low temperature FGR could be "time effect" (formation of tunnels by creep). These could be additional to the athermal release, which is due to mechanical cracking/fracturing process.

Session 5b-2

Development of Fuel Analysis Codes FEMAXI-6 and FURBEL

SUZUKI Motoe, NAGASE Fumihisa, KUSAGAYA Kazuyuki and UETSUKA Hirosi

Dept. of Reactor Safety Research

JAERI

ABSTRACT

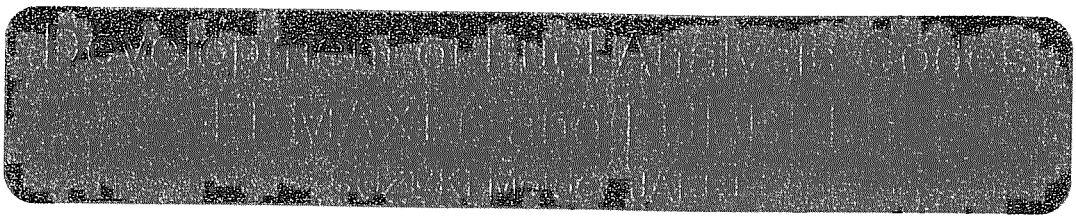
FEMAXI-6 code has been developed to analyze LWR fuel rod behavior in normal and transient conditions. The code will be a cross-check tool for Japanese safety licenser of fuel design. It can incorporate a fuel burnup profile which is calculated by an advanced burning analysis code PLUTON. Two new models for swelling and high burnup structure (HBS) have been installed.

In the swelling model, the equilibrium FP gas bubble radius is determined by simultaneous solution of number density of bubbles, the state equation of gas and the fission gas atom diffusion equation to give a gas-bubble portion of fuel swelling. This model can predict a remarkable diameter increase in the high burnup fuel rod subjected to power ramp.

The HBS model predicts the rim structure fraction increase and related property changes in fuel by the "effective burnup" which is defined with both burnup and temperature. Fission gas release from the rim structure and porosity increase are predicted by the use of the rim structure fraction, the effective burnup, and reported empirical models. Local swelling and thermal conductivity change of fuel are modified by the rim structure fraction and porosity increase. FEMAXI-6 code is being verified with data of test rods and commercial rods.

Development of a new code, FURBEL, is in progress for the experimental analysis and evaluation of failure-bearing capability of cladding in LOCA. The FURBEL code performs thermal shock response analysis and evaluates axial restraint effect, either loading or displacement limitation, on the cladding failure-bearing capability. It performs stress-strain calculation, including alpha-beta phase transformation, in the cladding with varying mechanical properties in the radial direction.

Development of RIA analysis code is at conceptual design stage to predict the mechanical force generation and PCMI inside high burnup fuel rod.



Contents

- Objective and Status of FEMAXI-6 Code
- Development and Evolution of Code System
- Features of FEMAXI-6:
  1. Swelling model and Demo
  2. HBS (rim) model and Demo
- FURBEL code for LOCA analysis
  + RIA analysis code
- Summary and Future Plan

1

◆Objective of FEMAXI Code

Analysis of LWR fuel rod behavior in normal and transient conditions.

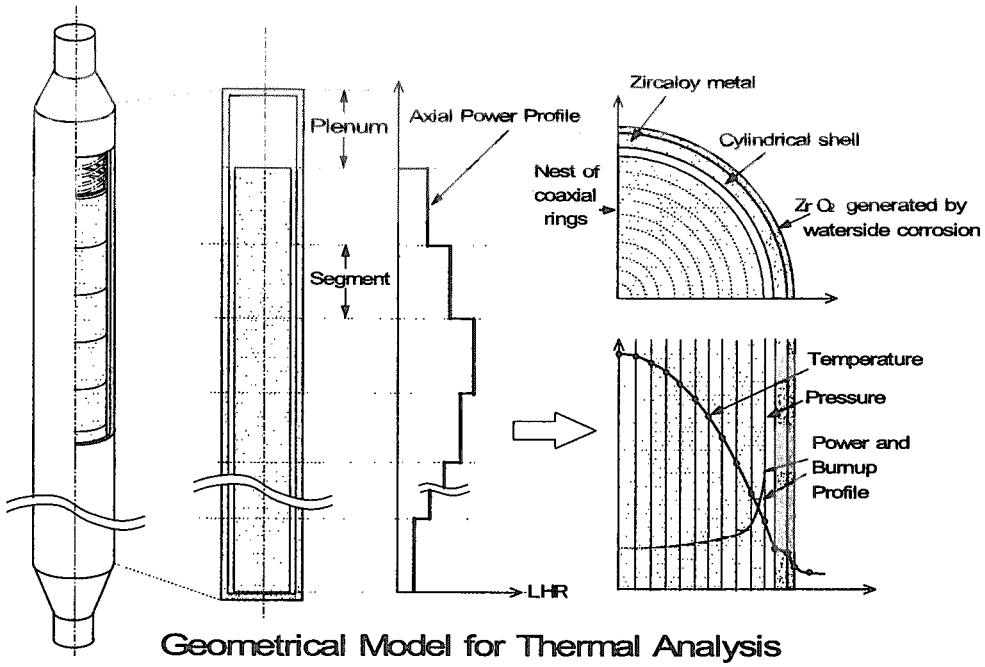
Status of FEMAXI-6

✧Will be a cross-check tool for Japanese safety licenser of fuel design.

✧ Versatile tool for experimental analysis and evaluation of new models.

✧ Basis for the development of accident analysis codes.

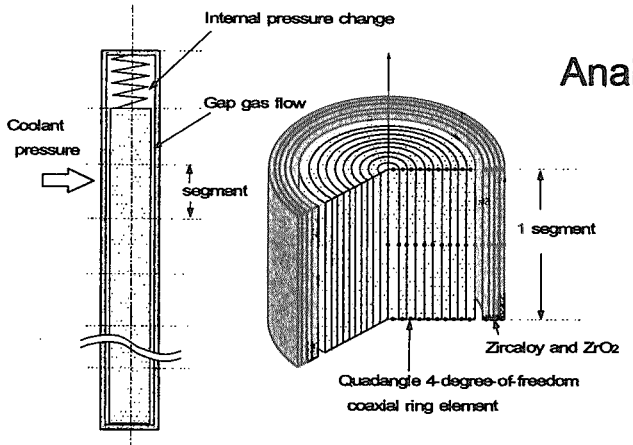
2



Geometrical Model for Thermal Analysis with Simple Mechanical Analysis

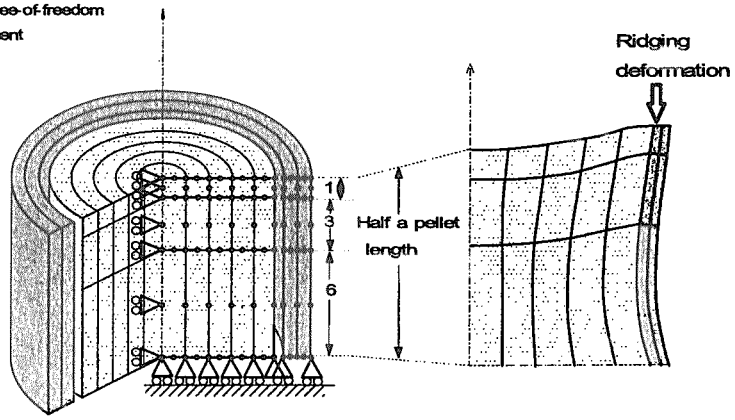
Analytical System of FEMAXI -1-

3



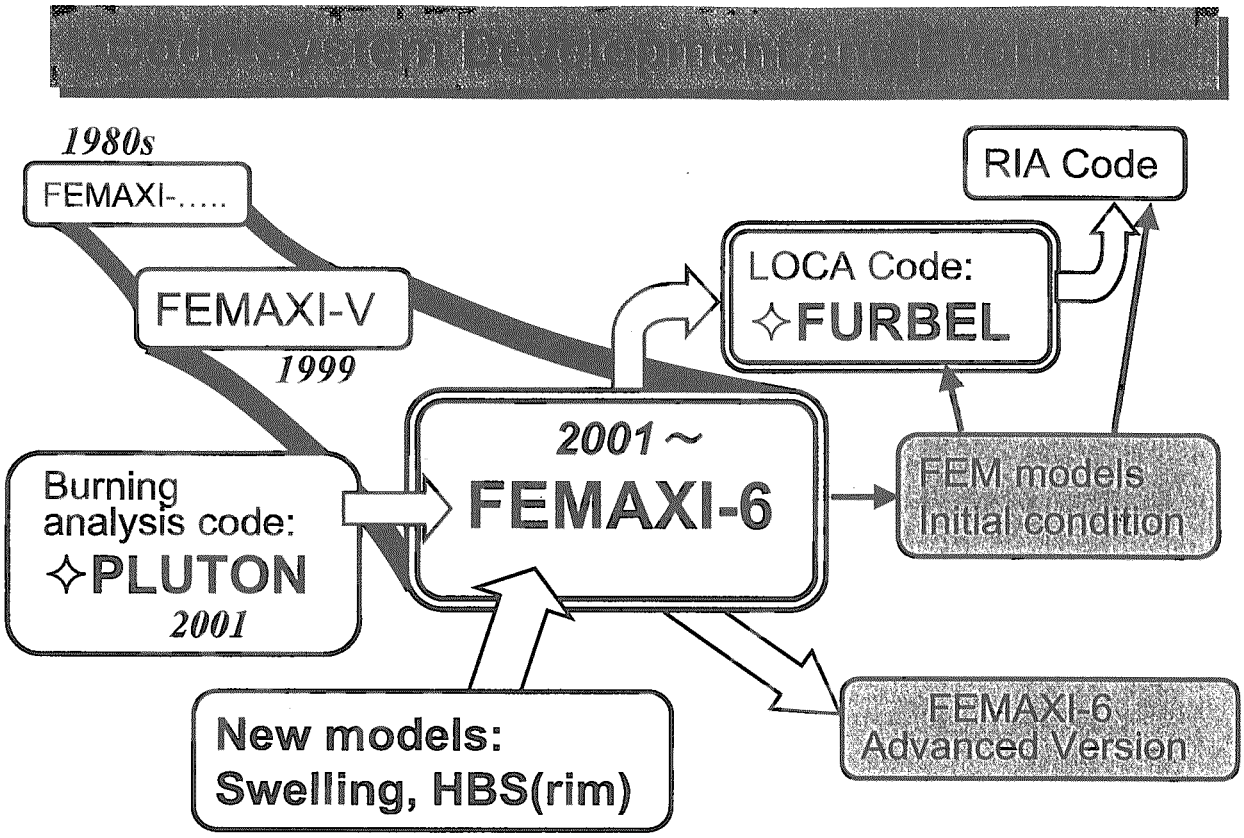
Analytical System of FEMAXI -2-

Geometry of entire-rod-length 2-D mechanical analysis of FEMAXI



Geometry of 2-D FEM for Local PCMI Analysis

4



5

Features of FEMAXI-6

- **A new swelling model on the basis of fission gas bubble growth.**
- **Semi-empirical model for high burnup structure (rim) in pellet.**

6

New Swelling Model (1)

◆**Fuel Swelling induced by FP gas bubble growth is taken into consideration.**

1. Equilibrium bubble radius is determined by simultaneous solution of number density of bubbles, the state equation of gas, and the fission gas atom diffusion equation.

2. Solution of the diffusion equation is based on White & Tucker + Speight models, including trapping and re-solution.

7

New Swelling Model (2)

◆**Fuel Swelling induced by FP gas bubble growth is taken into consideration.**

3. Swelling is the sum of

S1=Grain-boundary gas bubble growth.

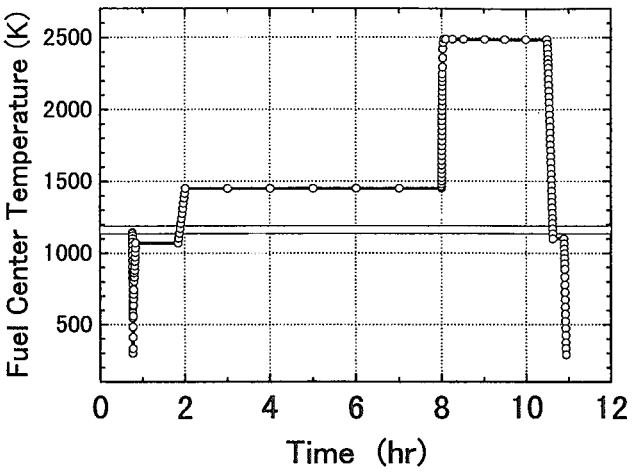
S2=Intra-granular gas bubble growth.

S3 =Solid-FP swelling.

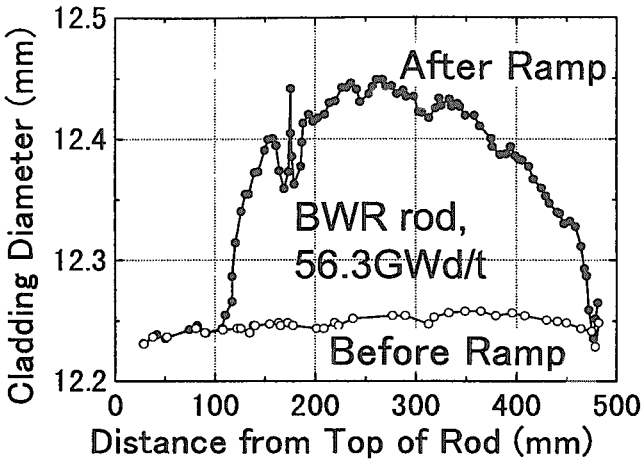
$$\sim 0.0025\%\ per\ 10^{20}\ fissions/cm^3$$

8

New Swelling model (3)



Fuel center temperature rise in power-ramp of high burnup BWR fuel.

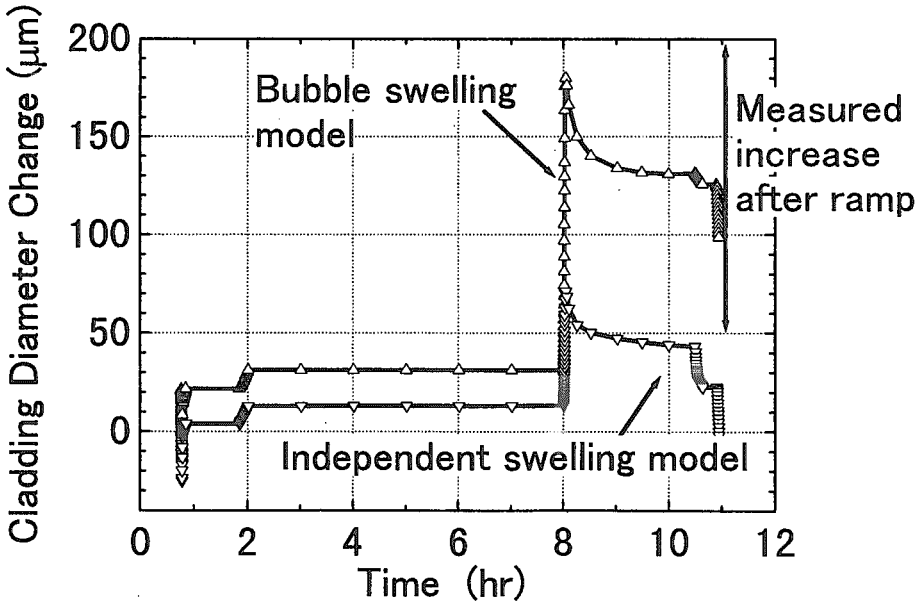


Cladding diameter increase due to fuel swelling during power-ramp.

Reproduced from Fig.13: H.Sakurai, K.Ito, Y.Tukada et al., Irradiation Characteristics of High Burnup BWR Fuels, ANS Topical Meeting, Park City (2000), by courtesy of NUPEC.

9

New Swelling model (4)



Comparison of calculated cladding diameter increase induced by fuel swelling during power-ramp.

10

HBS(rim) model (1)

- *Burnup dependence* ➔Rim structure is generated in the high burnup matrix having intensive strain energy.
- *Temperature dependence* ➔ Strain-energy relieving effect can retard rim structure formation.
- *Effective Burnup* ⬅ burnup level and temperature.

$$B_{eff}^{n} = B_{eff}^{n-1} \cdot \exp\left\{-k_1 (T_n - T_0) \cdot \Delta t\right\} + \Delta B_n$$

Burnup increment is calculated by the **PLUTON** code.

11

HBS(rim) model (2)

- *FP gas release* from rim ➔Empirical model, with *Beff.*
- *Porosity increase* in rim ➔Empirical model, with *Beff.*
- *Local swelling* and *thermal conductivity change*
  ⬅ "*Rim structure fraction*" + "*Porosity increase*"

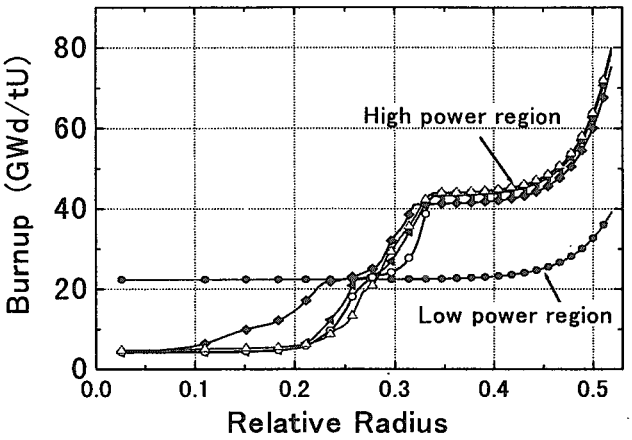
Rim structure fraction increase,
i.e. growth of rim structure ➔ by K-J-M-A model.

$$x_v = 1 - \exp\left\{-k_2 \left(\frac{B_{eff} - B_A}{B_B}\right)^3\right\}$$

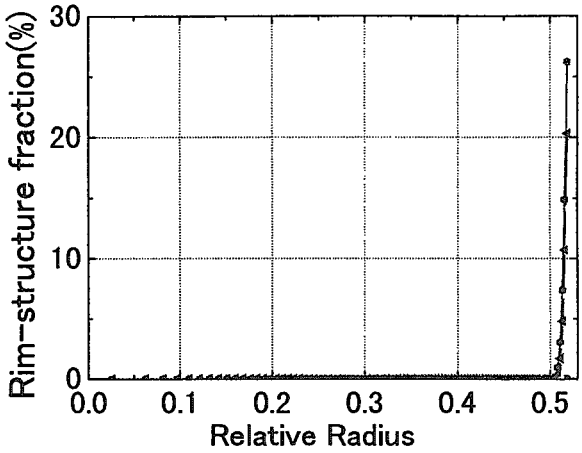
12

HBS (rim) model (3)

Analysis on a BWR rod with average burnup=45GWd/t



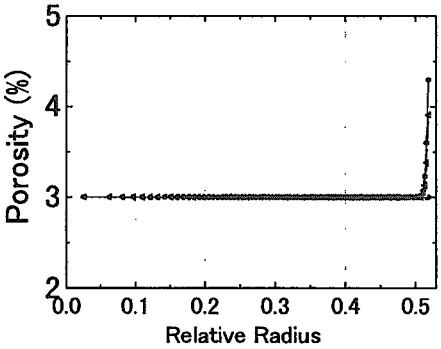
"Effective burnup" profile.



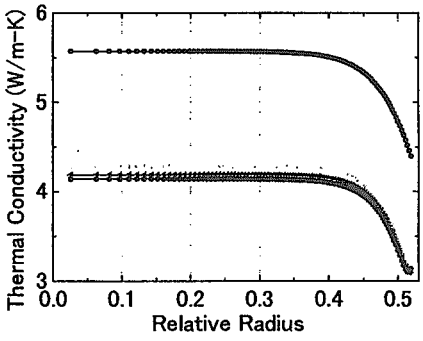
"Rim" structure generation at peripheral region.

13

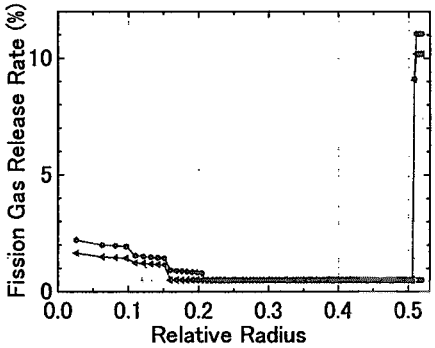
HBS (rim) model (4)



Porosity profile



Thermal conductivity profile



Profile of fission gas release rate

14

FURBEL Code for LOCA Analysis (1)

Objective: Experimental Analysis and Evaluation Tool for Failure-bearing Capability.

1) Proven method and basic structure of FEMAXI.

2) FEMAXI can give the Initial Condition of fuel.

3) **Cladding mechanical analysis:**

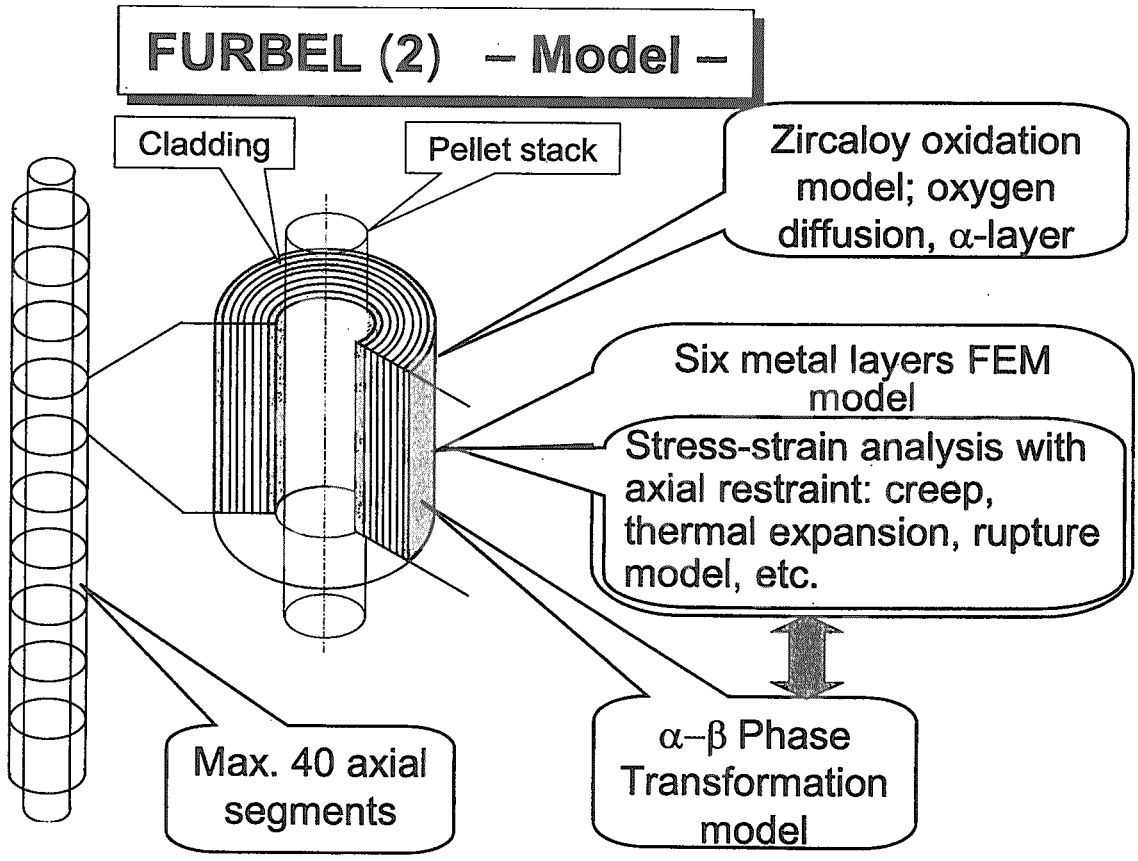
⇨ **Application of 2-D FEM to the deformation analysis of cladding with varying mechanical property.**

⇨ **Thermal shock response analysis. 【Axial restraint】**
➔ ***Failure-bearing capability***

⇨ **Single rod model for experimental analysis**
➔ ***Assembly effect analysis.***

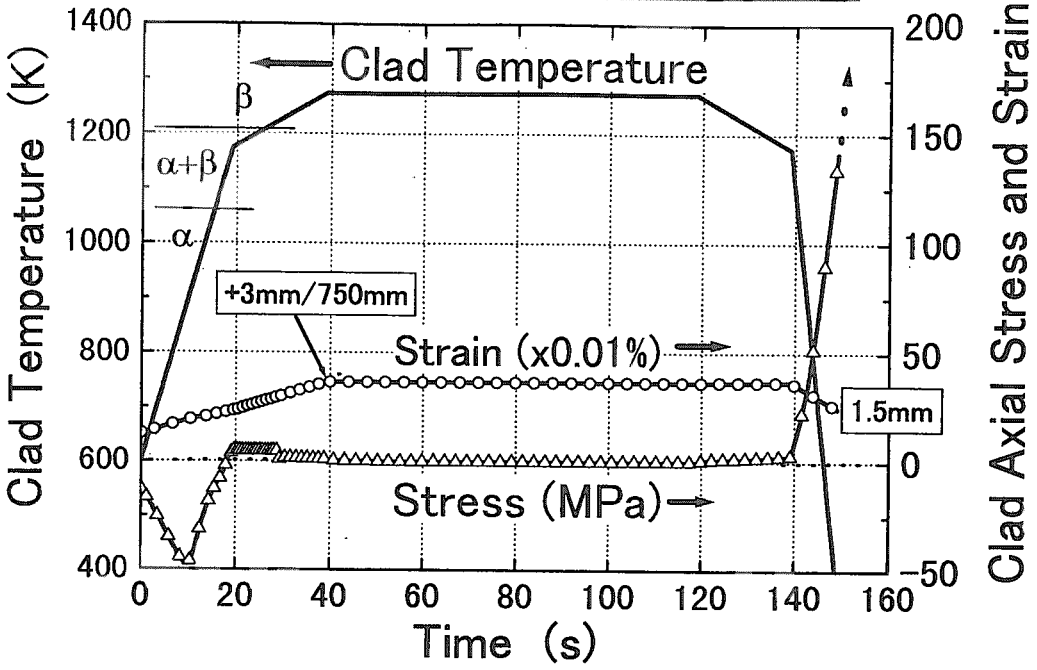
15

FURBEL (2) – Model –



16

FURBEL (3) － Demo －



Test-run results of cladding stress and strain in the axial direction with given temperature history.

17

Development of RIA Analysis Code

- ✧ **PCMI and rupture analysis of fuel rod in RIA.**
- ✧ Under Conceptual Designing.
- ✧ Based on FURBEL code experiences.
  ⇨ Application of 2-D FEM deformation analysis of FURBEL to the behavior of cladding with varying mechanical property in the radial direction.
- ✧ New model for mechanical force generation by gas bubbles.

18

Summary and Future Plan

-- Normal Operation and Transient Condition --

- ➢ **FEMAXI-6** ➔ Verification by the data of test rods and commercial rods.
- ✧ Swelling model + HBS(rim) model
- ✧ Extended version ➔model refinement, various aspects of MOX fuel;

--- LOCA ---

- ➢**FURBEL** ➔ Experimental analysis:
- ✧ Axial force generation and failure-bearing capability of high-burnup fuel cladding will be evaluated.

◆ RIA analysis code: Development of basic structure.

19

Discussion:

Q: (C.Hellwig)
Do you also take into account possible bubble coagulation in your bubble swelling model?

A: No. In my model, I consider an independent bubbles only.

Q: (M.Valach)
Will you explain your bonding model?

A: In mechanical analysis, the bonding model assumes that the pellet stack and cladding are forced to move with the same displacement simultaneously in the axial direction.

Q: (M.Valach)
Do you have any special treatment in your (FEM) mechanical model (FEMAXI-6) for bonding layer in case of very highly burnup fuel? Did you perform parameter or validation calculation varying properties of this layer?

A: For the moment, I have no special treatment for my bonding layer model. My model has specified no particular finite element for the bonding layer. Therefore, I cannot perform a validation calculation for the mechanical properties of this layer.

Q: (R.Montgomery)
What data have you used to develop the material constitutive law for the mechanical models of the prior-beta, oxygen stabilized alpha layer and the oxide layer?
Is fuel-clad bonding considered in your FURBEL code?

A: I will collect those mechanical properties data from open literatures. In my FURBEL code, fuel-clad bonding is not considered, because I think the bonding is easily destroyed by deformation of rod in LOCA.

JP0250423

Session 5b-3

UO_2 Fuel Rod Performance Analysis Code, INFRA Development

Chan Bock Lee, Yong Sik Yang, Je Geun Bang, Dae Ho Kim, Young Min Kim, Youn Ho Jung
Korea Atomic Energy Research Institute
Yusung P.O. Box 105, Daejon, Korea, 305-600

ABSTRACT

UO_2 fuel rod performance analysis code, INFRA (INtegrated Fuel Rod Analysis) has been being developed since 1997.

Fuel performance models such as the prediction of rim microstructure formation, thermal conductivity degradation in the rim microstructure region, radial power and burnup distribution inside the pellet, mechanistic fission gas release model, fission gas bubble swelling, cladding corrosion and creep-out models, and finite element analysis model for pellet cladding mechanical interaction were developed to predict UO_2 fuel behavior which occurs or becomes more important at high burnup.

INFRA code was verified by comparison with the in-pile fuel test data for both the specific models and the integral parameters such as fuel temperature and fission gas release. It showed that INFRA code could predict the UO_2 fuel behavior quite well up to the burnup higher than 60 MWD/kgU-rod avg..

Fuel Safety Research Specialists' Meeting
March 4-5, 2002, JAERI, Tokai, Japan

UO_2 Fuel Rod Performance Analysis Code, INFRA Development

Chan Bock Lee, Yong Sik Yang, Je Geun Bang, Dae Ho Kim, Young Min Kim, Youn Ho Jung
Korea Atomic Energy Research Institute
Yusung P.O. Box 105, Daejon, Korea, 305-600

Abstract

UO_2 fuel rod performance analysis code, INFRA has been developed since 1997. Fuel performance models such as the prediction of rim microstructure formation, radial power and burnup distribution inside the pellet, thermal conductivity degradation in the rim microstructure region, mechanistic fission gas release model, cladding corrosion and creep-out models, and finite element analysis model for pellet cladding mechanical interaction were developed to predict UO_2 fuel behavior which occurs or becomes more important at high burnup. INFRA code was verified by comparison with the in-pile fuel performance date base for both the specific models and the integral parameters such as fuel temperature and fission gas release. It showed that INFRA code could predict the UO_2 fuel behavior up to the burnup higher than 70 MWD/kgU-rod avg..

1. Introduction

As UO_2 fuel rod is irradiated in the reactor, changes in thermal and mechanical properties and dimensions occur inside the fuel rod. Since many phenomena are involved and influenced each other, a computer code with all the fuel performance models together is essential to the analysis of the fuel rod behavior during irradiation. Fuel performance models in the code are mainly based upon the fuel irradiation data base with the burnup. Therefore, fuel rod performance analysis code has been developed and updated as the fuel burnup increases. Currently, UO_2 fuel rod burnup in LWR is about 60 ~ 62 MWD/kgU-rod avg. And for the better economy and reduction of spent fuel production, fuel burnup extension will be pursued continuously. However, It has been found that as the fuel rod burnup increases over 50 - 60 MWD/kgU-rod avg., new phenomena such as rim microstructure formation, enhanced fission gas release and pellet cladding interaction have emerged and become important while the existing fuel rod analysis model and code can not correctly predict those phenomena. Therefore, UO_2 fuel rod performance code, INFRA(INtegrated Fuel Rod Analysis) has been developed specially to focus on the fuel behavior at high burnup.

2. Fuel performance models in INFRA code

- Rim microstructure formation

Rim microstructure formation in the periphery region of UO_2 fuel at high burnup has long been studied[1]. Very small intragranular bubbles with diameters of ~10^{-9} m nucleate along the tracks of fission fragments due to displacement and re-structuring of the atoms[2]. Based upon that, a model to explain the rim microstructure formation mechanism was proposed[3]. The fission gas bubbles in the rim microstructure region are nucleated and stabilized at the critical concentration of gas atoms inside the grain with the help of fission fragment movements. Therefore, rim microstructure formation depends upon not the local burnup but the fission gas concentration inside the grain. Figure 1 shows the threshold local burnup for rim microstructure formation as a function of temperature, grain size and fission rate for the 4 w/o ^{235}U fuel under the assumption that rim microstructure forms at the critical gas concentration of 5.1 x 10^{26} atoms/m^3. The

burnup at which the critical fission gas concentration is achieved inside the grain would increase with temperature due to the diffusional release of gas atoms to the grain boundaries. Therefore, based upon the above mechanism, extent of rim microstructure can be predicted as a function of local burnup and temperature, showing that rim microstructure formation would be limited only to the pellet outer region of low temperature even at the pellet average burnup higher than 70 MWD/kgU.

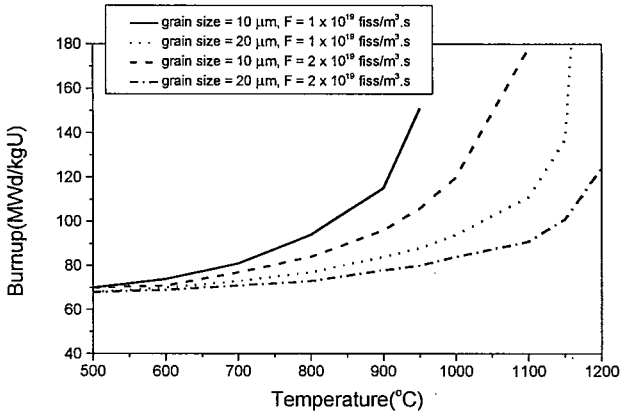


Figure 1. Threshold local burnup for rim microstructure formation

- Radial power and burnup distribution

The RAPID(RAdial power and burnup Prediction by following fissile Isotope Distribution in the pellet) model was developed to predict the radial distribution of power, burnup and fissionable nuclide densities inside the UO_2 pellet[4]. It is based upon and validated by the reactor physics code, HELIOS[5]. RAPID model considers the specific radial variations of the neutron reactions of all the fissionable nuclides such as U-235, U-238, Pu-239, Pu-240, Pu-241 and Pu-242 with burnup so that it should be more accurate than other programs with the simplified model, specially in the high burnup region. Comparison of RAPID prediction with the measured data of the irradiated fuels showed good agreement as shown in Figure 2. RAPID can be used to calculate the local variations of the fissionable nuclide concentrations as well as the local power and burnup inside the UO_2 pellet as a function of burnup up to 10 w/o U-235 enrichment and 150 MWD/kgU pellet average burnup under the PWR environment.

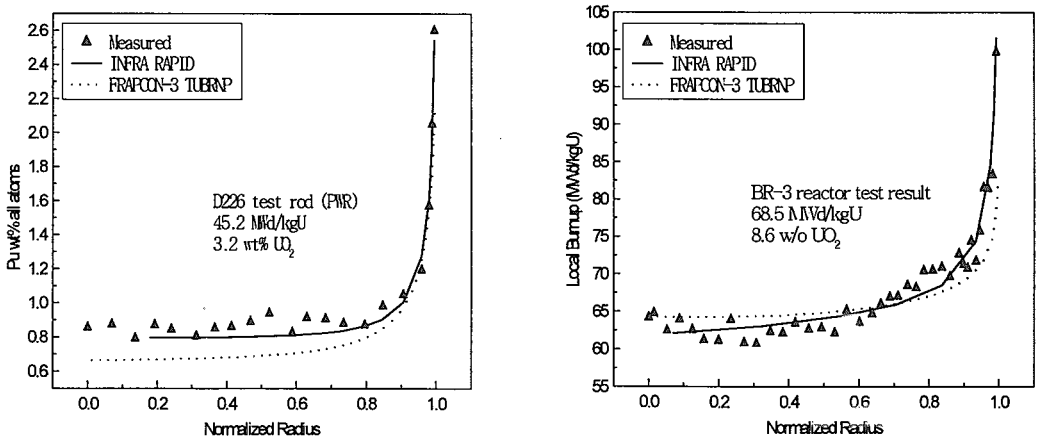


Figure 2. Local plutonium isotopes and burnup distribution inside the UO_2 pellet

- Thermal conductivity of irradiated UO_2

Thermal conductivity model of the irradiated UO_2 pellet was developed, based upon the thermal diffusivity data of the irradiated UO_2 pellet measured during thermal cycling under the NFIR program[6]. The model predicts the thermal conductivity by multiplying such separate correction factors as solid fission products, gaseous fission products, radiation damage and porosity as follows.

$$\lambda = f_{sfp} f_{fg} f_{rd} f_p \lambda_0$$

$$f_{sfp} = \frac{10.152 + 0.0762T}{10.152 - 4.8054BU^{0.5} + 1.563BU + (0.0762 + 4.724\times10^{-3} BU^{0.5} - 8.624\times10^{-4} BU)\cdot T}$$

$$f_{fg} = \frac{10.152 - 4.8054BU^{0.5} + 1.563BU + (0.0762 + 4.724\times10^{-3} BU^{0.5} - 8.624\times10^{-4} BU)\cdot T}{10.152 - 1.423BU^{0.5} + 1.6072BU + (0.0762 + 3.043\times10^{-3} BU^{0.5} - 8.066\times10^{-4} BU)\cdot T}$$

$$f_{rd} = \frac{1}{4.0413\exp(31.598/T) - 3.1186}$$

$$\lambda_0 = \frac{1}{(0.0375 + 2.165\times10^{-4}\cdot T)} + \frac{4.715\times10^9}{T^2}\exp(-\frac{16361}{T})$$

where,

λ = thermal conductivity of irradiated UO_2
λ_0 = thermal conductivity of unirradiated 100 % dense UO_2
f_{sfp} = factor for solid fission products
f_{fg} = factor for gaseous fission products
f_{rd} = factor for radiation damage
f_p = factor for porosity
T = temperature(K)
B = burnup(MWD/kgU)

Since the developed model considers the effect of gaseous fission products as a separate factor, it can predict the thermal conductivity in the rim region of high burnup UO_2 pellet where the fission gases in the matrix are precipitated into bubbles, such that

$$\lambda_{rim} = f_{sfp}^{rim} f_{rd} f_p^{rim} \lambda_0.$$

Application of the above equation to the rim microstructure region indicates that a decrease of thermal conductivity due to the bubble porosity in the rim region would be significantly compensated for by the enhancing effect of fission gas depletion in the UO_2 matrix[6].

- Fission gas release

Mechanistic fission gas release model was developed. Fission gas atoms generated by fission inside a UO_2 grain diffuse to the grain boundary to form bubbles. Bubbles formed at grain boundary surfaces have a lenticular shape, and they grow and interconnect with each other. The fission gases in the grain face bubbles move to the grain edge to form the more stable bubbles in the grain edges. The bubbles in the grain edges can interconnect with each other and ultimately become open to the external surface. When the bubbles in the grain edge and grain face become open to the external surface, the fission gases in the open bubbles are released instantaneously. Then, the open bubbles act as an open channel for the release of fission gases which diffuse to the open bubbles at the grain boundary later. The open bubbles increases with the burnup. Therefore, fission gas release is accelerated at the high burnup due to the increase of open bubbles or channels at the grain boundary. The model was developed

based upon those mechanisms and verification of fission gas model is explained in Section 3.

- Cladding corrosion

Corrosion model of Zircaloy cladding was developed by analyzing the corrosion mechanisms and parameters such as the chemical composition and manufacturing characteristics of the cladding, coolant chemistry, hydride formation in the cladding, and fast neutron flux as follows[7].

$$ds^3/dt = C_1 \exp(-Q_1/RT)$$

$$ds/dt = C_2 F_{Mat} F_{Flux} F_H \exp(Q^*(C_{Li})/RT)$$

where C_1 and C_2 are the corrosion constant; Q_1 is the activation energy in the pre-transition region; R is gas constant; T is the cladding metal-oxide interface temperature; F_i is the enhancement factor, and subscripts, i means the factors influencing corrosion; $Q^*(C_{Li})$ is the activation energy in the post-transition region.

Manufacturing characteristics such as tin content, heat treatment and cold work may depend upon the manufacturer of the cladding. Effect of those parameter upon the corrosion may not be independent. Therefore, material factor, F_{Mat} was defined as a single parameter. The effect of cladding hydride on the corrosion rate was considered by the enhancement factor, F_H which takes effect when hydrogen content in the cladding is high.

Based upon the mechanism that Li in the coolant is incorporated into the oxide layer of the cladding and diffusion coefficient of the oxygen is increased, the effect of Li on corrosion is expressed by changing the activation energy such that

$$Q^*(C_{Li}) = 28200 - A\,(C_{Li} - 0.5)$$

where C_{Li} represents the Li concentration and A is the constant.

Figure 3 illustrates the effect of lithium concentration on the cladding corrosion.

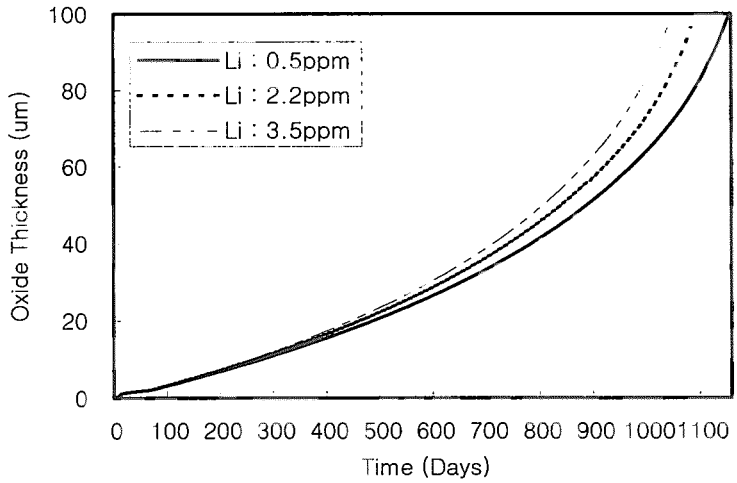


Figure 3. Oxide thickness variation with Li concentration

- Cladding creep-out

Cladding creep-out model was derived by changing the creep constants and the exponents for fast neutron flux and stress in the creep-down model based on Halden in-pile creep-out test data which indicate that under the same irradiation condition, cladding creep-out

rate is about 20 – 30 % higher than creep-down rate[7]. Cladding creep rate consists of the thermal creep and the irradiation creep, and each creep is divided into primary and secondary creep. Primary and secondary creep are described by,

$$\varepsilon_1 = C \cdot \dot{\varepsilon} \cdot (1 - e^{-k\sqrt{t}})$$
$$\varepsilon_2 = \dot{\varepsilon} \cdot t$$

where C is a primary creep constant(2800 h^{-1}), t: irradiation period, k: 5.5 exp(-1460.2/Tc) , and creep rate, $\dot{\varepsilon}$, represents the thermal creep rate or the irradiation creep rate and is expressed as follows, respectively,

$$\dot{\varepsilon}_{th} = \frac{1}{2} A_{th} \cdot \exp(-26116/T_c) \cdot \sigma_{eff}^{1.57} \cdot sign(\sigma_{eq})$$
$$\dot{\varepsilon}_{irr} = \frac{1}{2} A_{irr} \cdot \Phi^{0.86} \cdot \sigma_{eff} \cdot sign(\sigma_{eq})$$

where A_{th}: thermal creep rate factor, T_c: cladding average temperature (K), A_{irr}: irradiation creep rate factor, ϕ : fast neutron flux (E>0.821MeV), σ_{eff}: effective stress, σ_{eq}: equivalent stress.

The irradiation creep rate factor, A_{irr} is obtained by $A_{irr}=C_{irr} \cdot f_{mat}(R_{p0.2})$, where irradiation creep constant for creep-out, C_{irr} was determined to be 1.7×10^{-20} $(n/cm^2\text{-}s)^{-0.86}$ $(N/mm^2)^{-1}$ h^{-1} , and f_{mat} is a material factor varying with yield strength, $R_{p0.2}$.

Figure 4 shows good agreement of cladding creep-out prediction with the Halden test data.

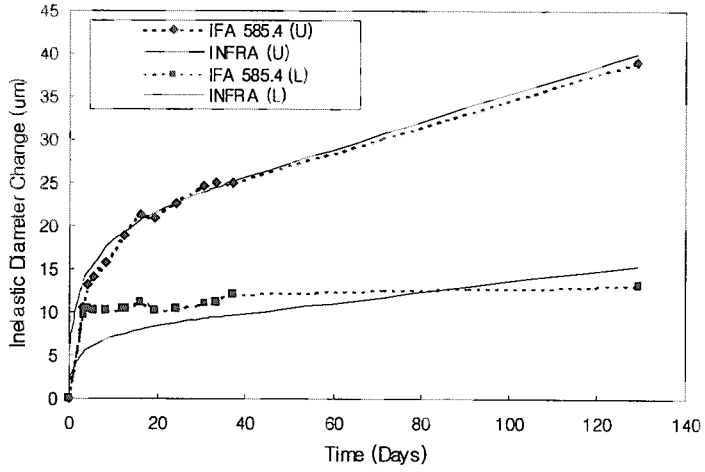


Figure 4. Comparison of cladding creep-out predictions with measured data

- Finite element analysis model

To analyze the local stress and strain inside the fuel rod, finite element analysis module was developed and connected to INFRA code. Half pellet length of fuel rod is modeled locally. Material properties and fuel temperature are exported to the finite element module. Through the finite element mechanical analysis, local variation of stress and strain in the fuel rod can be predicted. Finite element analysis model was verified by comparison with the ABAQUS code[8]. Figure 5 shows that INFRA code could correctly predict the local stress distribution in the fuel rod. Due to the temperature gradient during the irradiation, there occurs a compressive stress at

the center of the pellet while there occurs a tensile stress in the pellet periphery region, which could result in the pellet cracking at high power. Tensile stress is applied on the cladding by thermal expansion of the pellet after fuel gap closure.

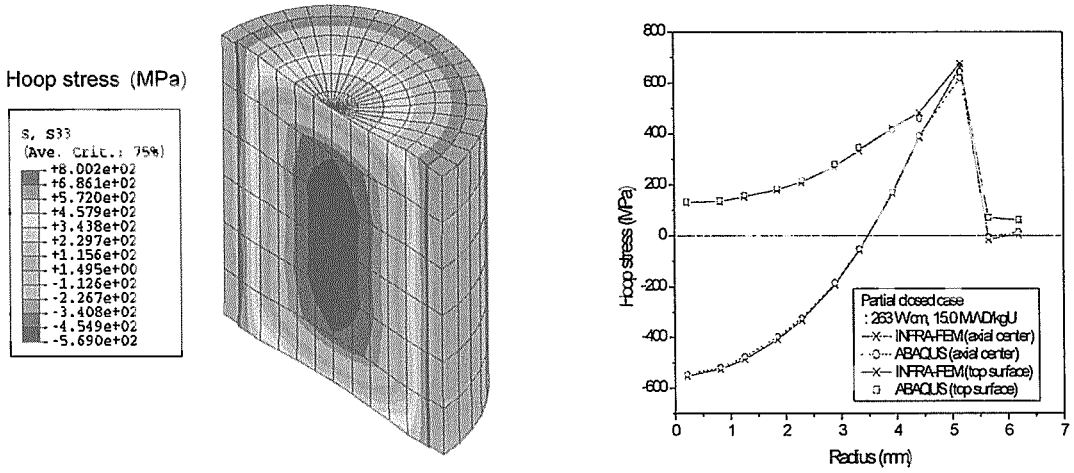


Figure 5. Hoop stress distribution in the fuel rod

3. INFRA Code Verification

- Fuel temperature

Fuel temperature depends upon the fuel performance models such as UO_2 thermal conductivity, fuel gap conductance which is mainly influenced by the gap width, and UO_2 relocation. Fuel gap width depends upon densification and swelling of the UO_2 pellet, and cladding creep-down. Therefore, fuel temperature prediction can represent the overall fuel rod performance analysis capability. Fuel temperature prediction of INFRA code was compared with the in-pile measured data from the Halden reactor as shown in Figure 6. UO_2 thermal conductivity model proposed by Halden Reactor Project was used in the calculation[9]. It shows that INFRA code could predict the fuel temperature reliably in the whole burnup range.

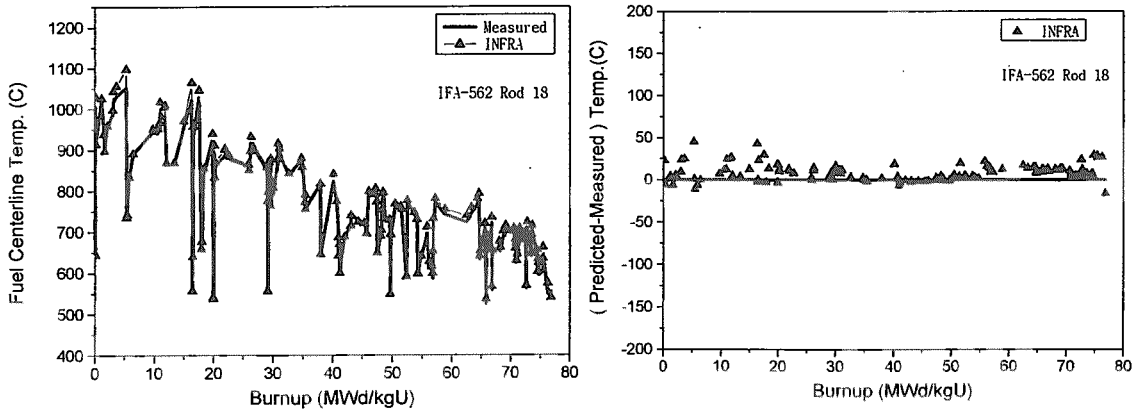


Figure 6. Fuel temperature prediction with burnup

- Fission gas release

Fission gas release prediction capability of the INFRA code was tested by comparison with the measured data. Figure 7 shows that INFRA code could predict the enhanced fission gas release at high burnup without any burnup enhancement in the diffusion coefficient[10], and it also could predict the effect of UO_2 grain size on the fission gas release such that fission gas release decreases with the grain size. Figure 8 shows the result of comparison with fission gas release data base, showing that INFRA code could reliably predict the fission gas release up to the burnup of 102 MWD/kgU.

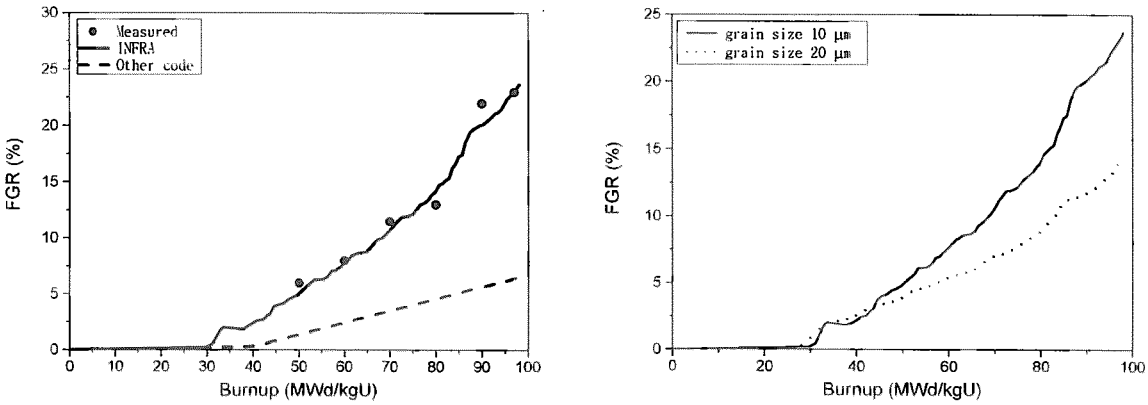


Figure 7. Fission gas release with burnup and UO_2 grain size

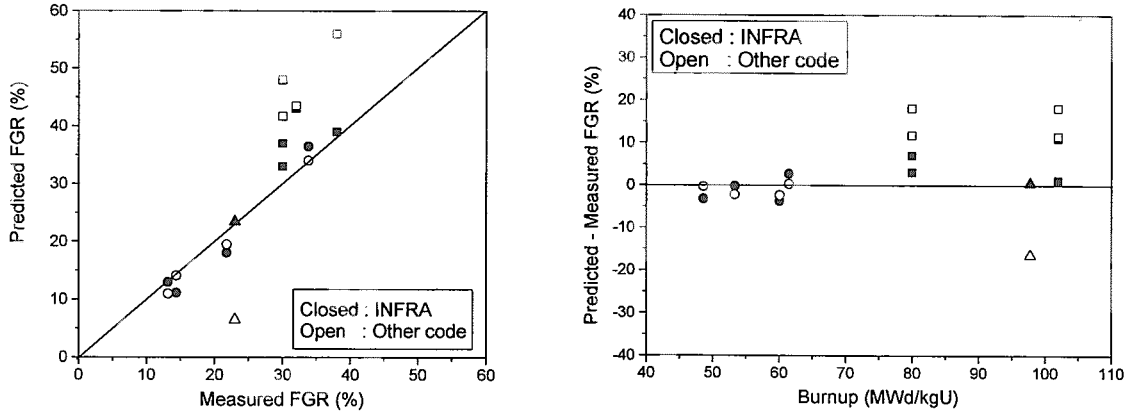


Figure 8. Comparison with the measured fission gas release data base

4. Conclusion

UO_2 fuel rod performance analysis code, INFRA(INtegrated Fuel Rod Analysis) has been developed since 1997. Fuel performance models such as the prediction of rim microstructure formation, radial power and burnup distribution inside the pellet, thermal conductivity of irradiated UO_2 including the rim microstructure region, mechanistic fission gas release model, cladding corrosion and creep-out, and finite element analysis for pellet-cladding mechanical

interaction which occurs or becomes more important at high burnup were developed. INFRA code was verified by comparison with the in-pile fuel test data for both the specific models and the integral parameters such as fuel temperature and fission gas release. It showed that INFRA code could predict the UO_2 fuel rod behavior up to the burnup higher than 70 MWD/kgU-rod avg..

Acknowledgement

This work has been carried out under the Nuclear R&D Program supported by Ministry of Science and Technology in Korea.

References

(1) J. Spino, K. Vennix, M. Coquerelle, J. Nucl. Mater. 231 (1996) 179.
(2) J.A. Turnbull, J. Nucl. Mater. 38 (1971) 203.
(3) C.B. Lee and Y.H. Jung, J. Nucl. Mater. 279 (2000) 207.
(4) C.B. Lee, et al, J. Nucl. Mater. 282 (2000) 196.
(5) F.D. Guist, "Release notes HELIOS system 1.5", TN36/41.16.15, Studsvik Scanpower, 1998.
(6) C.B. Lee, et al, "Development of Irradiated UO_2 Thermal Conductivity Model", IAEA Technical Committee Meeting on Nuclear Fuel Behavior Modelling at High Burnup and its Experimental Support, Windmere, UK, 2000.
(7) J. G Bang, et al, "Modelling of Zircaloy-4 Cladding Behavior at High Burnup", IAEA Technical Committee Meeting on Nuclear Fuel Behavior Modelling at High Burnup and its Experimental Support, Windmere, UK, 2000.
(8) H.D. Hibbitt, G.I. Karlsson and E.P. Sorensen, ABAQUS User's Manual, ver. 6.2, HKS Inc., 2001.
(9) W. Wiesenack and T. Tverberg, "Thermal performance of high burnup fuel in-pile temperature data and analysis", Proc. Of Intl. Top. Meeting on LWR Fuel Performance, Utah, April, 2000.
(10) R. Manzel and C.T. Walker, "High burnup fuel microstructure and its effect on fuel performance", Proc. Of Intl. Top. Meeting on LWR Fuel Performance, Utah, April, 2000.

Fuel Safety Research Specialists' Meeting
March 4-5, 2002, JAERI, Tokai, Japan

UO_2 Fuel Rod Performance Analysis Code, INFRA Development

2002. 3. 5

Chan Bock Lee, Yong Sik Yang, Je Geun Bang,
Dae Ho Kim, Young Min Kim, Youn Ho Jung
Korea Atomic Energy Research Institute

1. Introduction

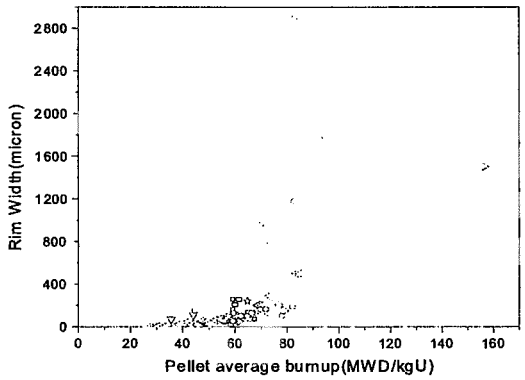
- INFRA (INtegrated Fuel Rod Analysis) Code Development
  - Development started in 1997.
  - Objectives
    - High burnup UO_2 fuel rod performance analysis under normal operation condition and operational transient
      - Fuel rod burnup higher than 70 MWD/kgU-rod avg.
      - U-235 enrichment higher than 5 w/o
    - Model development for high burnup application

2. INFRA Code Development

Contents of Presentation

- ❑ Fuel Performance Model Development
  - Rim microstructure formation prediction
  - Radial power and burnup distribution
  - Thermal conductivity of irradiated UO_2
  - Fission gas release
  - Cladding corrosion
  - Cladding creep-out
  - Finite element analysis module
- ❑ Verification of Integral Fuel Rod Behavior
  - Fuel temperature
  - Fission gas release

Rim Microstructure Formation



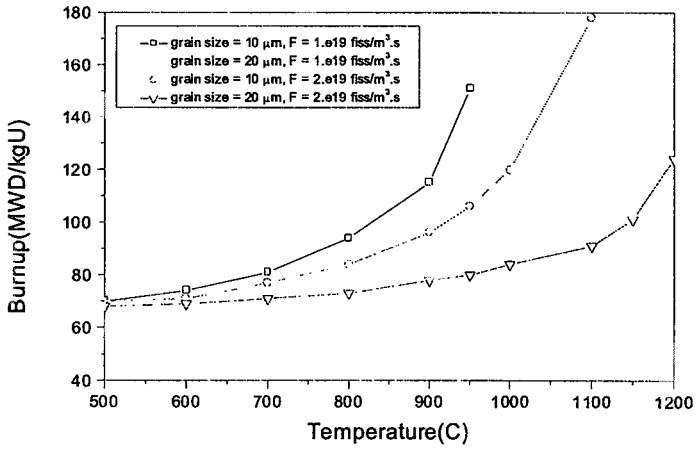
Rim microstructure width vs. burnup

- Dependence of rim width upon fuel rod burnup shows large scattering.
- Variables
  - local burnup
  - radiation damage
  - fission gas concentration
  - power or fission density
  - temperature
  - grain size, etc.

- A Model for Rim Microstructure Formation Mechanism
  - Bubble nucleation along the track of the fission fragments inside the grain
  - Bubble stabilization at the critical concentration of gas atoms in the matrix
    - Gas atom concentration is ~ 5.1 x 10^{26} atoms /m^3 at 70 MWD/kgU
    - Bubble nucleation and **stabilization at the critical gas atom concentration** through gas diffusion and interconnection of smaller bubbles by collision with fission fragments and fast neutrons.
    - Bubble over-pressurization -- > grain sub-division
    - Enhanced diffusion through the new grain boundaries.
    - Bubble over-pressurization -- > grain sub-division (feedback !)

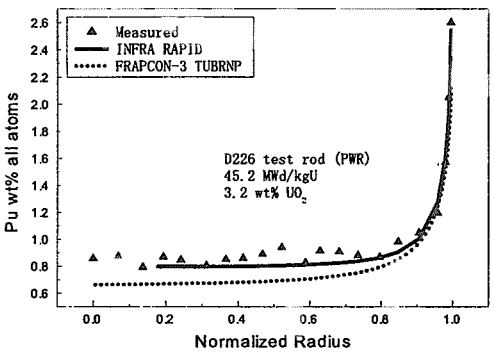
Rim microstructure formation depends upon not just the local burnup, but the fission gas atom concentration inside the grain.

Threshold local burnup of rim microstructure formation as a function of temperature

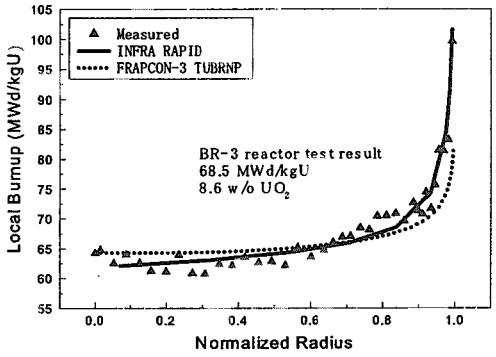


Radial power and burnup distribution prediction(RAPID program)

- Prediction of radial distributions of power and burnup inside the pellet, depending upon the pellet burnup and U-235 enrichment
- Calculation of all the fissionable nuclides by one group neutronics model based on HELIOS neutronics code
- Applicable range : U-235 enrichment up to 10 w/o, Pellet average burnup up to 150 MWD/kgU
  - **Consideration of the effect of U-235 enrichment**
  - **Prediction of the variations of Pu-239, Pu-240, Pu-241 and Pu-242 concentrations.**

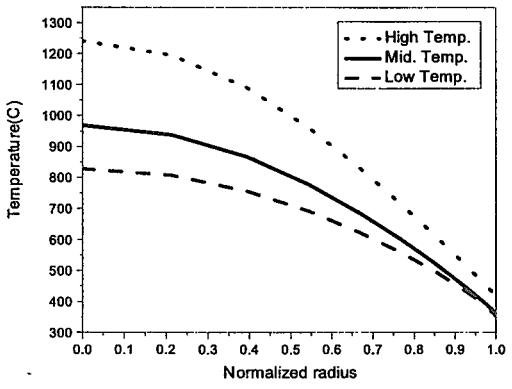


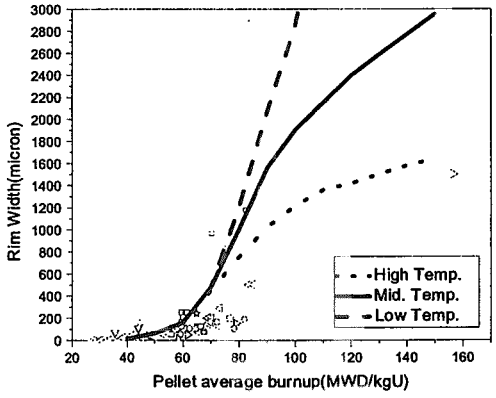
Pu Isotopes



Local Burnup

Prediction of rim width with burnup and temperature



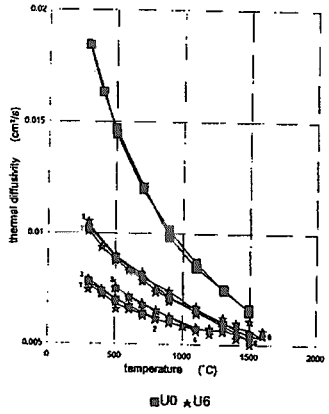


➢Even at the burnup higher than 70 MWD/kgU, rim microstructure would be limited only to outer low temperature region.

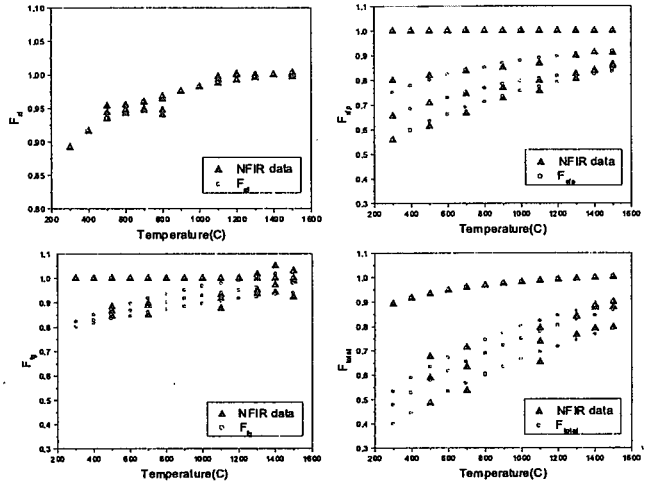
Thermal Conductivity of Irradiated UO_2

- Derivation of thermal conductivity model based upon EPRI-NFIR thermal diffusivity data of irradiated UO_2

$$\lambda = f_{sfp} f_{fg} f_{rd} f_p \lambda_0$$



NFIR TD data
(25, 36 and 60 MWD/kgU)



Thermal Conductivity of Irradiated UO_2

$$\lambda = f_{sfp} f_{fg} f_{rd} f_p \lambda_0 \quad \Rightarrow \quad \lambda_{rim} = f_{sfp}^{rim} f_{rd} f_p^{rim} \lambda_0$$

$$f_{sfp} = \frac{10.152 + 0.0762T}{10.152 - 4.8054BU^{0.5} + 1.563BU + (0.0762 + 4.724\times10^{-3}BU^{0.5} - 8.624\times10^{-4}BU)\cdot T}$$

$$f_{fg} = \frac{10.152 - 4.8054BU^{0.5} + 1.563BU + (0.0762 + 4.724\times10^{-3}BU^{0.5} - 8.624\times10^{-4}BU)\cdot T}{10.152 - 1.423BU^{0.5} + 1.6072BU + (0.0762 + 3.043\times10^{-3}BU^{0.5} - 8.066\times10^{-4}BU)\cdot T}$$

$$f_{rd} = \frac{1}{4.0413\exp(31.598/T) - 3.1186}$$

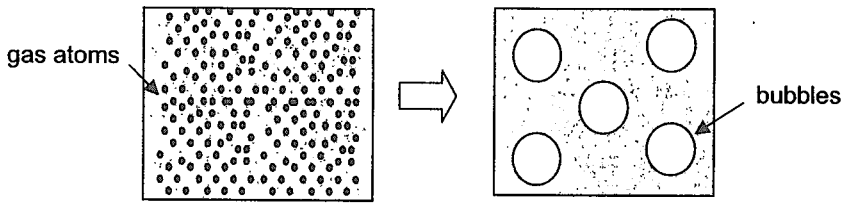
$$\lambda_0 = \frac{1}{(0.0375 + 2.165\times10^{-4}\cdot T)} + \frac{4.715\times10^{9}}{T^2}\exp(-\frac{16361}{T})$$

λ = thermal conductivity of irradiated UO_2
λ_0 = thermal conductivity of unirradiated 100 % dense UO_2
f_{sfp} = factor for solid fission products
f_{fg} = factor for gaseous fission products
f_{rd} = factor for radiation damage
f_p = factor for porosity

❑ Estimation of Thermal Conductivity in Rim Region

- Ex. : Rim microstructure of 80 MWD/kgU local burnup at 600 °C
  - fission gas bubbles : porosity 16 %, sphere shape and uniform distribution
  - Xenon depletion inside the grain
- Ref. : Irradiated UO_2 of same burnup with no fission gas bubble precipitation
  - Decrease of thermal conductivity by bubble porosity factor : 23 %
  - Increase of thermal conductivity by fission gas depletion : 18 %

➔Net decrease of thermal conductivity in rim region : 9 %



Irradiated UO_2 Rim Microstructure

➢Degradation of thermal conductivity by bubble porosity buildup in rim region is significantly compensated by fission gas depletion inside the grain.

Fission Gas Release Model

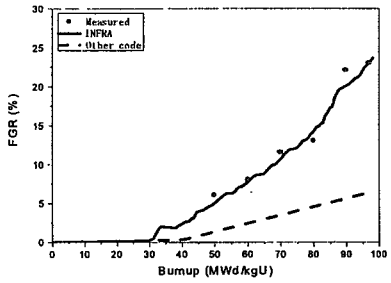
❑ 2-Stage Mechanistic Model : Grain Inside→ Grain Boundary → Fuel Gap

- fission gas generation inside the grain
- diffusion to grain boundary to form the surface bubbles
- diffusion to grain edge to form the edge bubbles
- bubble interconnection to be open to the external space(open bubble)
- instantaneous release of fission gases in the open bubble
- open channel for release of the fission gases diffused to the open bubbles later
- **open channels or bubbles are accumulated and increases with burnup.**

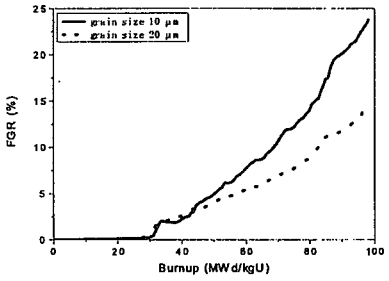
❑ Characteristics of Fission Gas Release Model

- Burnup-independent diffusion coefficient of fission gas is used.
- Enhanced fission gas release at high burnup is predicted without any burnup enhancement factor.
- Effects of grain size is predicted.

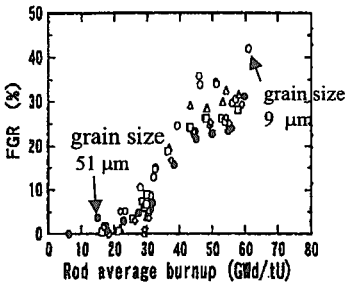
Fission gas release prediction



High power and burnup rod
(R. Manzel, 2000)



Effect of grain size



Fission Gas Release
(M. Hirai, 1997)

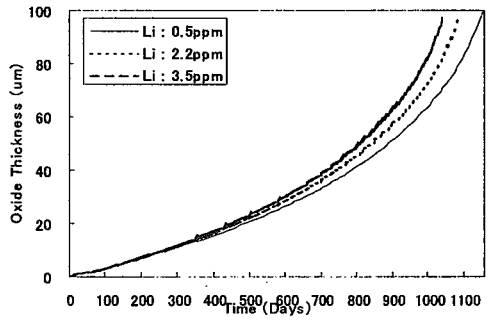
➢Enhanced fission gas release at high burnup is not due to rim effects but the inherent characteristics, considering fission gas release mechanisms.

Cladding Corrosion Model

❑ Corrosion model

- Pre-transition : $ds^3/dt = C_1 \exp(-Q_1/RT)$
- Post-transition : $ds/dt = C_2 F_{mat} F_{flux} F_h \exp(-Q^*(C_{Li})/RT)$

.Manufacturing parameters : F_{mat} = f(Tin content. Heat treatment, Cold work, etc.)
.Lithium in the coolant : $Q^*(C_{Li}) = 28200 - A(C_{Li} - 0.5)$
.Fast neutron fluence : $F_{flux} = C_F f^{0.24}$ ($C_F = 1.4 \times 10^{13}$ n/cm²-s)
.Hydride formation : $F_h = 1$ $C_{H2} \leq 400$ ppm
$F_h = 1 + 0.699 \log(C_{H2}/400)$ $C_{H2} > 400$ ppm



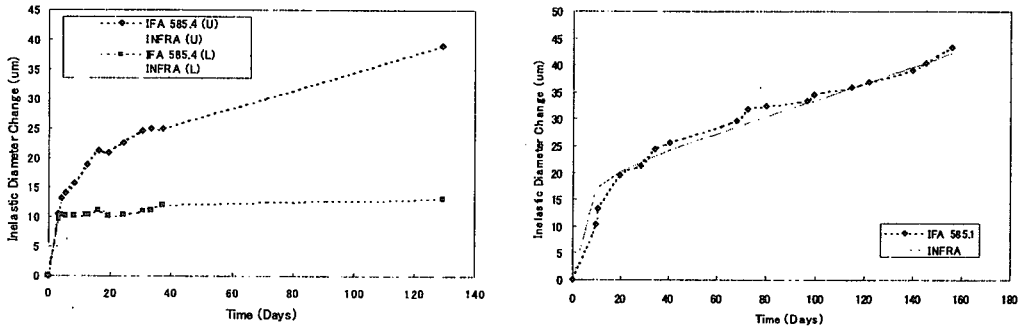
Oxide thickness variation with Li concentration

Cladding Creep-out Model

- To predict the cladding creep-out behavior when the rod internal pressure is higher than coolant system pressure.
  - Cladding creep-out rate is 20-30 % higher than the cladding creep-down rate.
  - Derivation of creep constant and exponent for creep-out behavior.

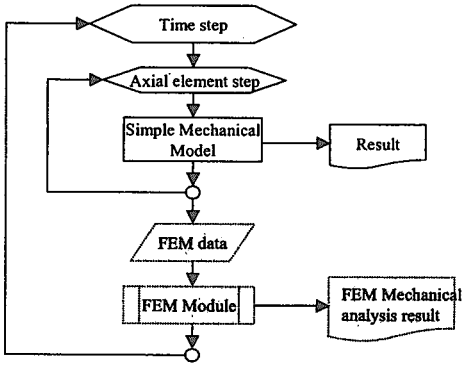
$$\varepsilon_{th} = \sqrt{3}/2 \cdot A_{th} \cdot \exp(-26116/Tc) \cdot \sigma_{eff}^{1.57} \cdot \mathrm{sign}(\sigma_{eq})$$

$$\varepsilon_{irr} = \sqrt{3}/2 \cdot A_{irr} \cdot \varphi^{0.86} \cdot \sigma_{eff} \cdot \mathrm{sign}(\sigma_{eq})$$

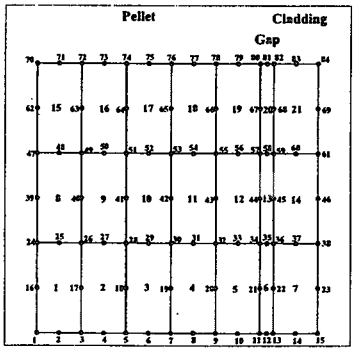


Comparison with Halden Creep-out Test Data

Finite Element Analysis Module



FEM in INFRA Code

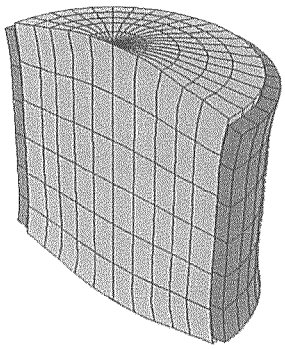


Half pellet length nodalization

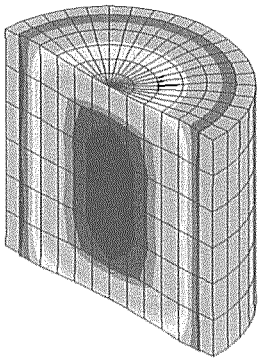
Models in FEM

- Geometric model : 2-D Axisymmetric
- Contact Analysis : Lagrange multiplier method
- Displacement Analysis : Load incremental method

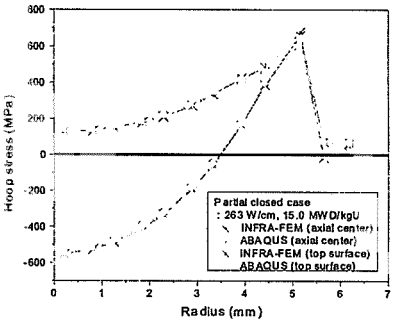
Comparison of INFRA-FEM and ABAQUS



Deformation
(ABAQUS)



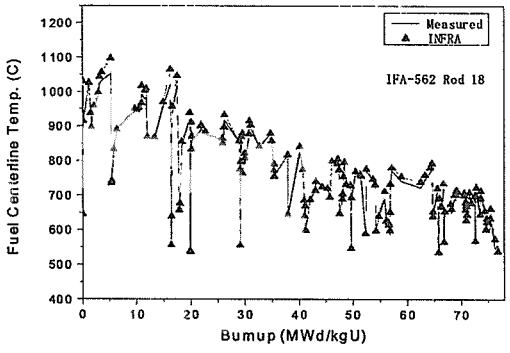
Hoop stress
(ABAQUS)

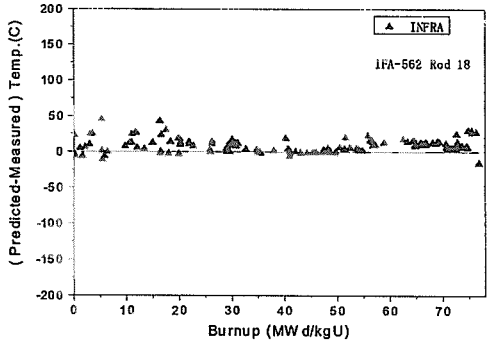


Hoop stress distribution
(INFRA and ABAQUS)

Fuel Centerline Temperature Prediction

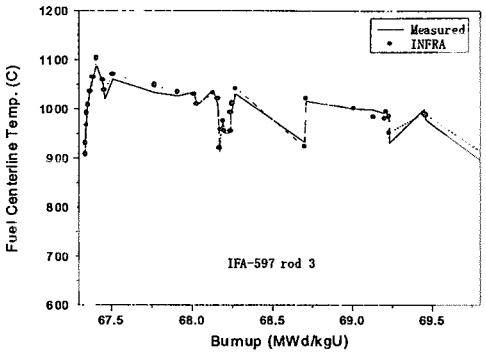
HRP IFA-562 rod 18

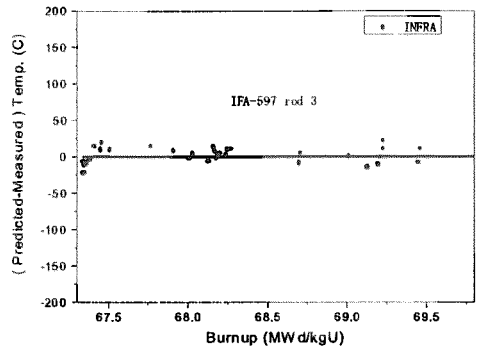




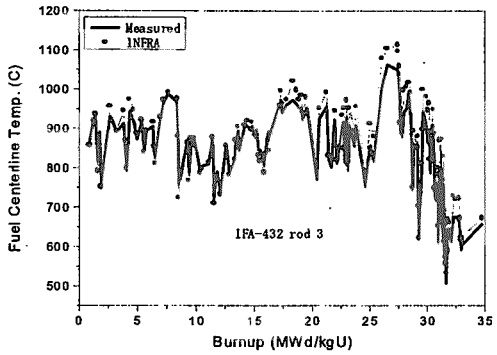
- Good agreement in the whole burnup range
  - Low power and low temperature irradiation : low fission gas release
  - Halden UO_2 thermal conductivity model is used.

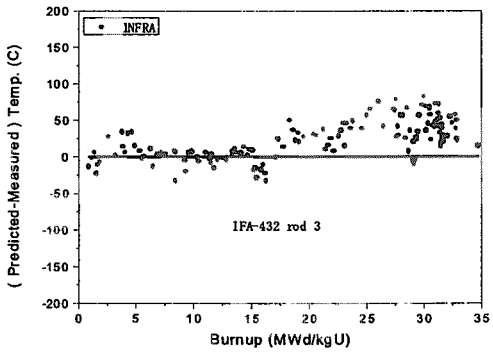
HRP IFA-597 rod 3





- Good agreement with the measured data
  - Re-instrumented rod after irradiation in commercial reactor up to 67 MWd/kgU
  - Early fuel gap closure is expected.
  - Halden UO_2 thermal conductivity model is used.

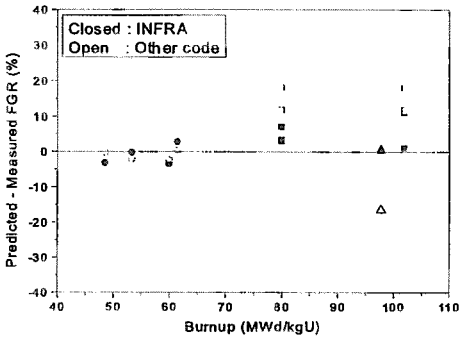


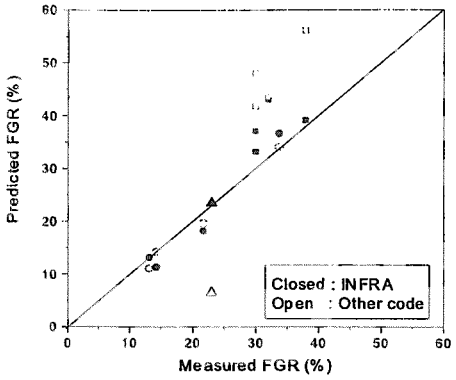


- Reasonable agreement with the measured data
  - Small initial fuel gap width resulted in early fuel gap closure around 17 MWD/kgU.
  - Halden UO_2 thermal conductivity model is used.

Fission Gas Release Prediction

Rod number	Burnup (MWd/kgU)	Measured FGR (%)
BR3 24-I-6	60.1	21.8
BR3 28-I-6	53.3	13.2
BR3 36-I-8	61.5	33.8
BR3 111-I-5	48.6	14.4
IFA-519-DH	80	30
	102	32
IFA-519-DK	80	30
	102	38
Siemens	98	23





- Good agreement for the fuel rod burnup up to 102 MWD/kgU

3. Conclusions

- Development of UO_2 fuel rod performance analysis code, INFRA
  - Application Targets
    - Fuel rod burnup higher than 70 MWD/kg-rod avg.
    - U-235 enrichment higher than 5 w/o.
  - Models for high burnup UO_2 fuel rod were developed.
  - Materials properties are based upon MATPRO.
  - Predictions of integral fuel rod behavior such as fuel centerline temperature and fission gas release show good agreement with the measured data base.

Discussion:

Q: (C.Hellwig)

The fission gas release model: Is intra-granular porosity as perfect and imperfect sinks taken into account in detail in the model or is it taken into account in a generalized form by using an "effective" diffusion coefficient?

A: Yes. To solve the diffusion equation of fission gas from inside of grain to grain boundary, it also assumed that grain boundary plays as a perfect sink for fission gas, and re-solution of fission gas bubbles at grain boundary into grain is not considered.

Q: (G.Ledergerber)

Why did you use the Halden conductivity model instead of the model of the INFRA model?

A: So far, verification calculation of INGRA code by using Halden in-pile temperature data base (in total 6 sets) gives most reliable prediction in the fuel temperature. For the NFIR thermal conductivity case, it gives lower thermal conductivity than Halden thermal conductivity model.

8. Session 6 : Discussion on JAERI's Future Program

Session 6

Outline of ALPS Program

Takehiko NAKAMURA, Fumihisa NAGASE, Jinichi NAKAMURA
Hideo SASAJIMA, and Hiroshi UETSUKA,
JAERI

ABSTRACT

In order to improve economic competitiveness of nuclear power and reduce the amount of spent fuels, burn-up extension of UO_2 fuel is progressing step by step in many countries. The trends would also be applied to mixed oxide (MOX) fuel, which is going to be used in light water reactors (LWRs) in Japan and currently has lower burn-up limit than that of UO_2 fuel. The MOX fuel has potential for high burn-up use, since it could have higher initial fissile content and its burn-up extension could bring larger benefits in economy.

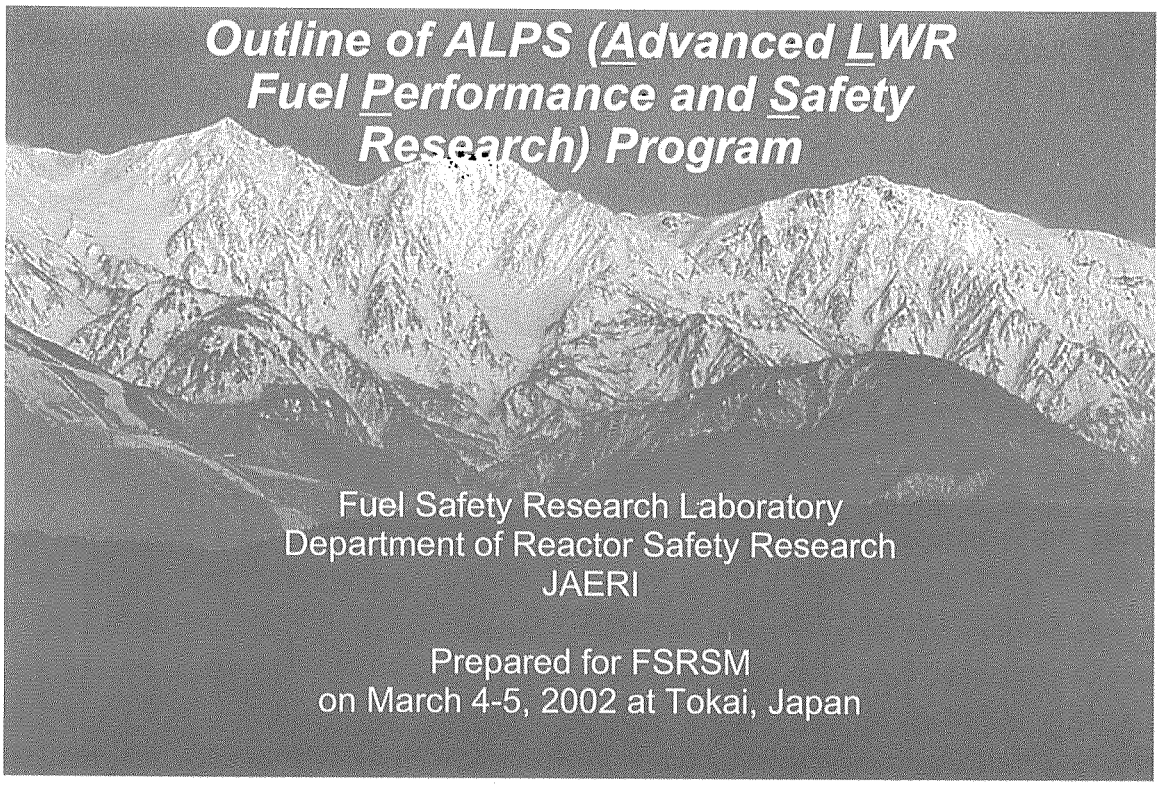
Recent research on high burn-up fuel behavior under accident conditions simulating RIA and LOCA indicated that the behavior could be significantly different from those of fresh and low burn-up fuels and it could depend on the fuel design and materials.

Fuel venders and utilities are trying to improve LWR fuels by changing its design and materials for getting better performance and reliability. High burn-up fuel to 55GWd/t is now in practical use in Japanese BWRs. For PWRs, new Zr-based alloys, MDA, NDA and ZIRLO, might be used as cladding material in the so-called step-II fuel designed for 55GWd/t use, which is expected to be loaded in a couple of years. The extensive fuel development for the next target burn-up level is progressing in some countries including Japan. The performance of such design fuel under normal operation condition is confirmed by industry side. However, investigating the fuel reliability and safety under accident conditions needs special types of facilities like NSRR.

JAERI is strongly expected to provide technical basis for future regulation on LWR fuels in Japan. Thus, a research program ALPS, i.e. Advanced LWR Fuel Performance and Safety Research, is started in full-scale in FY-2002. High burn-up fuels including MOX irradiated to very high burn-up levels in LWRs in Europe will be transported to Japan in FY-2003. Pulse irradiation tests under simulated RIA conditions in the NSRR and integral thermal shock/oxidation tests of the cladding under simulated LOCA conditions are planned in addition to comprehensive PIEs to characterize fuels. Performance of these fuels at rated powers and power ramp conditions will also be investigated in the HBWR at Halden in order to obtain comprehensive views at extended burn-up level up to about 100GWd/t.

Outline and current status of the ALPS program are presented as a base for discussions on needs and perspectives in the field of fuel safety research.

JAERI



1

JAERI

ALPS Program

- *To provide wide range data base of UOX & MOX fuel behavior at very high burn-up level for regulatory requirements*
- *For better understanding of fuel behavior*

➢ RIA simulation experiment at JAERI

Determine failure threshold & investigate fuel behavior using NSRR
- *High temperature & high pressure capsule Test*
- *FP gas release and mechanical energy generation measurements*

➢ LOCA simulation experiment at JAERI

Evaluate failure-bearing capability on quenching
- *Integral thermal shock test*
- *Oxidation rate measurement*

➢ Irradiation & Ramp test at Halden

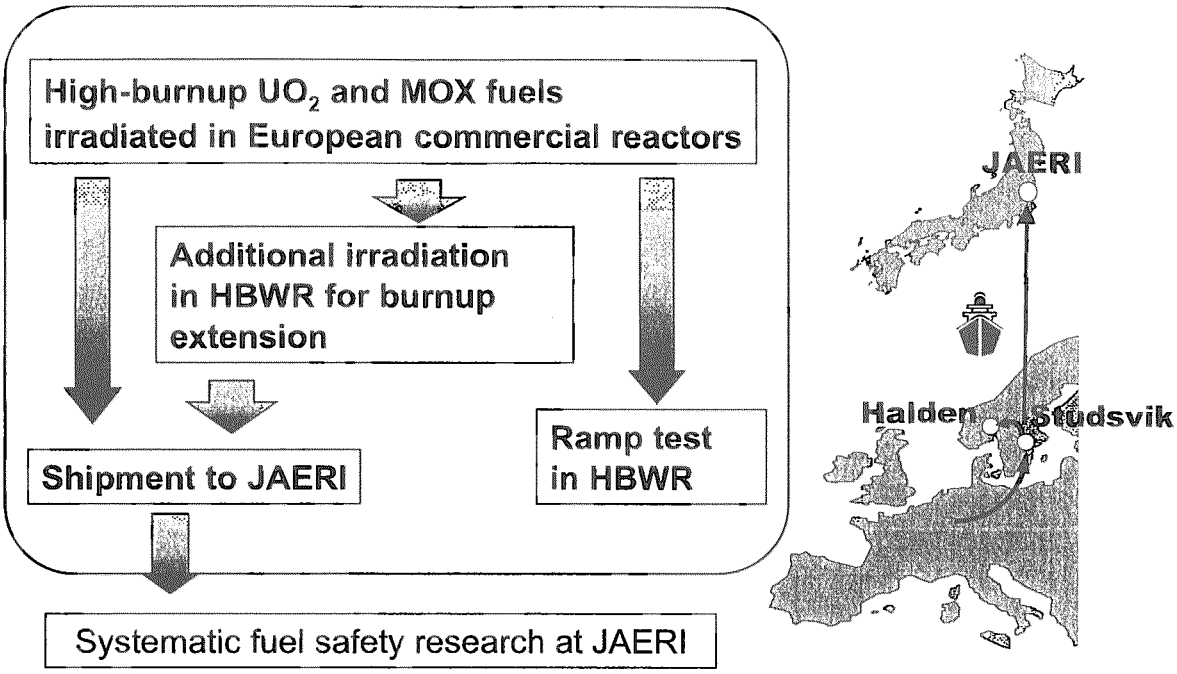
Burn-up extension to very high level to obtain samples for Phase-Ⅱ
Investigate fuel behavior during ramp
- *Additional irradiation in high temperature & high pressure loop*

➢ FP release experiment at JAERI
- *VEGA Program*

2

JAERI

Transportation of candidate fuel in ALPS program



3

JAERI

Schedule of ALPS program

Items \ Fiscal year	2002	2003	2004	2005	2006	2007	2008	2009	2010	2011
	Phase I					Phase II				
a) Transportation *High Burnup UO_2 & MOX*	PSI, MOL → Studsvik, Halden									
• In Europe										
• To Japan		Studsvik to JAERI					Halden to JAERI			
b) Irradiation at Halden reactor			UO_2: 75→100GWd/t							
• Burnup extension			MOX: 76→100GWd/t							
• Ramp test										
c) NSRR/RIA test	NSRR modification		Pulse irradiation					Pulse irradiation		
d) LOCA test			Integral thermal shock test							
		Post pulse irradiation test					Post pulse irradiation test			
e) PIE		Separate effect test					Separate effect test			
f) Analysis & Evaluation	Transient Calculation, Fuel behavior analysis, etc.									

4

JAERI

Candidate Fuel to Ship to JAERI for ALPS Program

Fuel type		Irradiation Reactor	Cladding type	Burnup in Reactor GWd/t	1st Shipment No. of rods	Additional irradiation in Halden GWd/t	2nd Shipment No. of rods
PWR	UO_2	Vandellos	17x17 Zirlo	70	4	85 – 95	1
			17x17 MDA	74	3	90 – 100	2
		North Anna	17x17 Zirlo	72	2	-	0
	MOX	Beznau	14x14 Zry-4	59	1	80	2(20cm)
BWR	UO_2	Leibstadt	10x10 Zry-2	75	3	95	2
	MOX	Dodewaard	8x8 Zry-2	49	1	-	0
		Gundre-mmingen	9x9 Zry-2	65,76	2	96-100	4

Note : listed fuels are just those of candidate as of March 2002

5

JAERI

Current status and on going activities in ALPS program

Present status and on going activities

- Negotiation with European, American and Japanese organizations for fuel supply and information exchange (in progress).
- Arrangements of fuel transportation in Europe and to Japan (in progress).
- Design and safety analysis of a cask, NR-10F, for shipment to Japan (finished).
- Basic design of HTHP capsule, strength examination tests with explosives (in progress).
- Basic design of NSRR facility and safety assessment (in progress).
- Development and set up of LOCA test apparatus in hot-cells (mostly finished).
- Basic design of irradiation rigs for burn-up extension in the HBWR (finished).

Work plan in FY 2002

- Fuel transportation from MOL, PSI to Studsvik and to Halden
- Preparation for shipment to Japan in FY 2003
  - Encapsulation
  - Cask modification (NR-10F) and licensing
  - Shipping arrangement (BNFL/PNTL)
  - Export/Import permits
- Licensing and modification of NSRR facility (by FY 2003).
- Detailed design and fabrication of burnup extension rig.

6

What we want to discuss in the ALPS session

★*Importance or meaning of program*

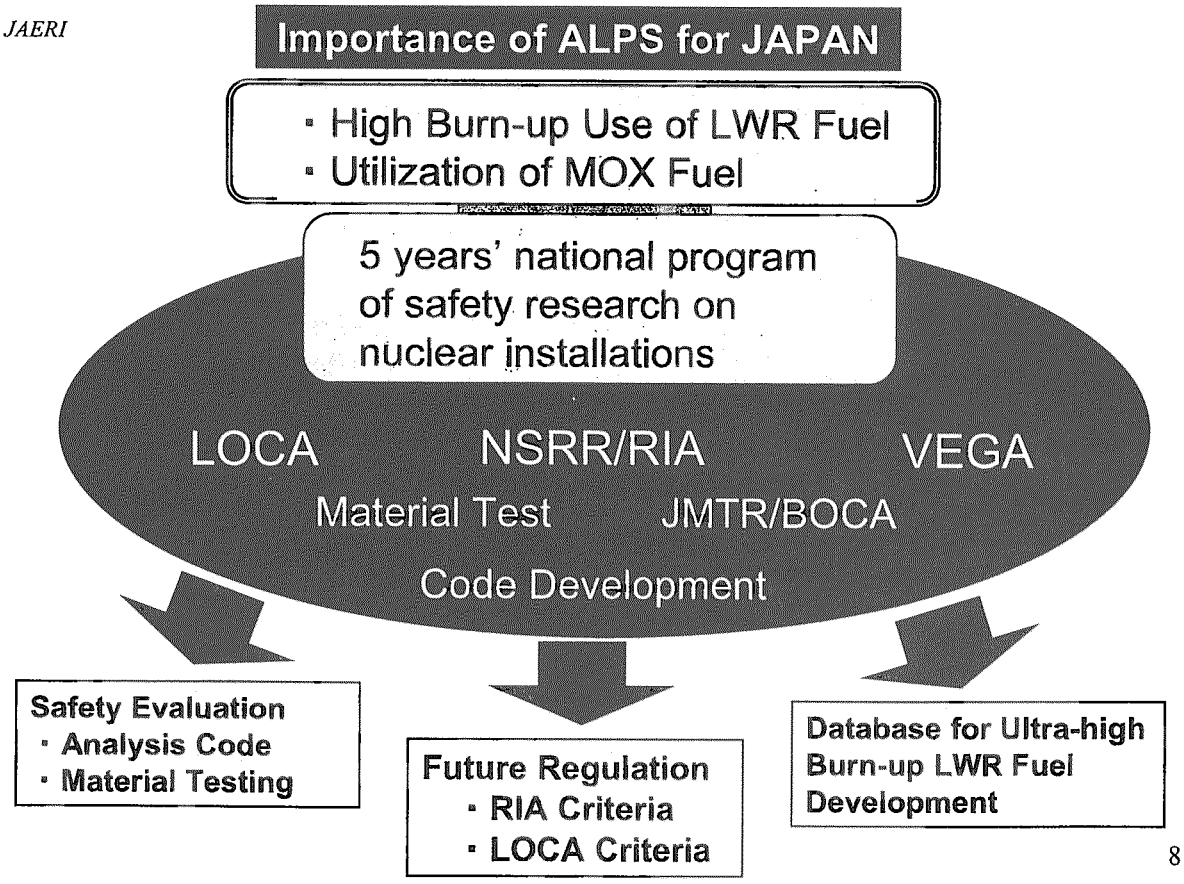
1. for Japan
2. for partners

★*The target of ALPS program is appropriate ?*

1. Fuel burn-up
2. Experimental program of RIA& LOCA Test at JAERI and Ramp Irradiation at Halden

★*Possible cooperation with other international or national program*

JAERI



8

JAERI

Status of BU limit in Japan

	Current	Next step (expected)
UO_2	55GWd/t (70-75GWd/t)	60-65GWd/t (75-85GWd/t)
MOX	40-45GWd/t (55-60GWd/t)	55-65GWd/t (70-85GWd/t)

Assembly average burnup
(Pellet average burnup)

Target BU level in ALPS is appropriate ?

9

JAERI

Phenomena to be clarified in ALPS/RIA Test

Failure threshold

Source terms

Coolability

Mechanical energy generation

Related parameters etc.

☆**Fuel burnup**

☆**Fuel design**

- PWR 14x14, 17x17
- BWR 8x8, 9x9, 10x10
- UO_2, MOX
- Cladding material
  Zry-2, Zry-4, Zirlo, MDA

☆ **Initial temperature**

☆ **Others** **(Related to base irradiation conditions)**

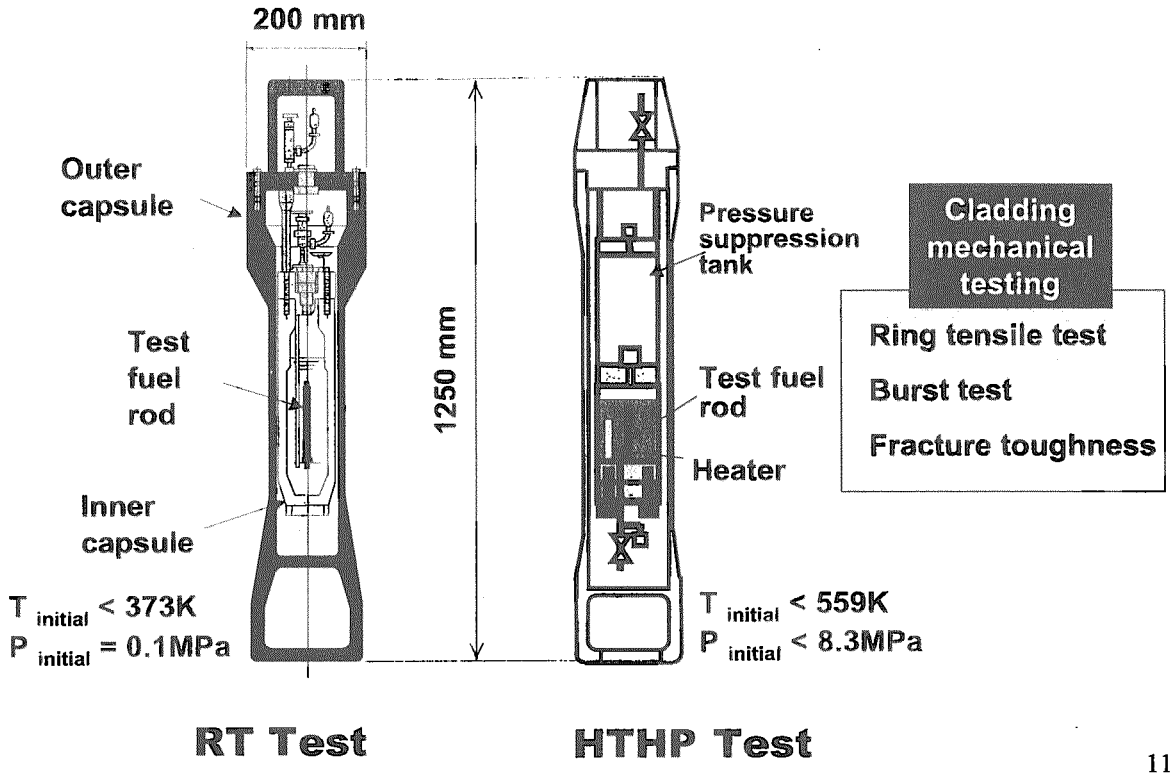
- Cladding corrosion
- Pellet-cladding bonding
- Status of fission gases

MOX effects ?

10

JAERI

ALPS/RIA Tests



11

JAERI

ALPS/RIA Test Matrix (Phase I)

Fuel type	Cladding	BU GWd/t	Number of tests	
			RT	HTHP
PWR UO_2 fuel	ZIRLO (EU)	70	1	1
	ZIRLO (USA)	72	1	1
	MDA	74	1	1
PWR MOX	14x14	59	1	1
BWR UO_2 fuel	10x10	75	1	1
BWR/MOX fuel	8x8	49	1	
	9x9	65-76	2	1

RT: Room temperature test

HTHP: High temperature high pressure test

12

JAERI

Parameters to be covered in ALPS/RIA tests

	Phase I	Phase II
☆ Fuel burnup	75GWd/t (≒Current limit)	100GWd/t (>Next step)
☆ Fuel type	PWR, BWR, MOX 14x14, 17x17, 8x8, 9x9, 10x10 Zry-2, Zry-4, Zirlo, MDA	+α?
☆ Initial temperature	Cold start-up Hot stand-by	ditto
☆ Others (Related to steady state irradiation conditions)	Variation in test fuels	+α?

Need to cover others?

13

JAERI

Subjects and effective parameters to be clarified in ALPS/LOCA test

Subjects

- Failure-bearing capability of cladding on quenching
- Burst behavior
- Oxidation rate

Effective parameters with burnup extension

- Corrosion
- Hydrogen uptake
- Neutron irradiation
- (Total effect)

+ New cladding alloys
+ Fuel and bundle design

14

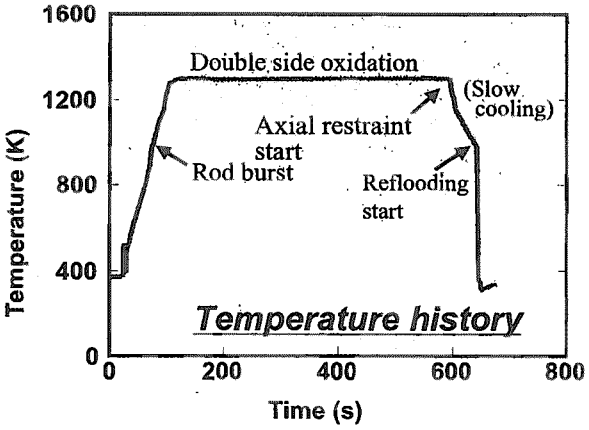
JAERI

ALPS/LOCA test matrix

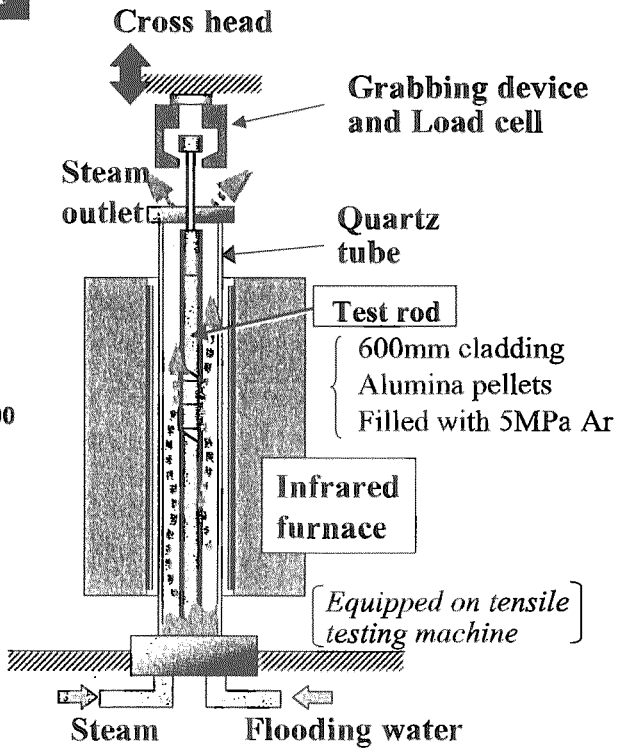
Fuel type	Cladding	Burnup GWd/t	Number of tests	
			Thermal shock test	Oxidation tests
PWR UO_2	Zirlo (EU)	70	2	
	Zirlo (USA)	75	2	
	MDA	74	3	15
BWR UO_2	10x10	75	2	15

15

Integral thermal shock test



- ***Isothermal oxidation***
  - -Temperature:
    1223 - 1523 K
  - -Time:
    30 - 5500s



Schematic drawing of test apparatus

16

JAERI

Burnup extension at HBWR in ALPS program

- Irradiation condition :*PWR/BWR conditions*
- Rod power : *about 20kW/m*
- Burnup increment : *20-30GWd/t during 4 years irradiation*
- Stack length : *300mm(about 200mm for PWR MOX)*

⬇

➢Burnup extension to obtain samples for ALPS-Phase II.
➢FGR and PCMI data during normal operation up to 75-100GWd/tU
➢Basic fuel behavior data to investigate the initial conditions of the accidents such as RIA and LOCA

17

JAERI

ALPS/Ramp tests at HBWR

➢ *PWR UO_2 17x17type*	*70-74GWd/t*	*4 rods*
➢ *BWR UO_2 10x10type*	*65-75GWd/t*	*4 rods*
➢ *BWR MOX 9x9 Type*	*70GWd/t*	*4 rods*

- Irradiation condition :*PWR/BWR conditions*
- Ramp Max power :*40-45kW/m*
- Conditioning power:*about 20kW/m*
- Instrumentation : - *Diameter gauge,*
  - *Cladding elongation and/or*
  - *Rod Inner pressure gauge*

⇩

PCMI data
FGR data
} ➡ Code verification

Failure threshold ➡ Confirmation of fuel safety margin at very high burn-up

18

Discussion:

Presenter: H. Uetsuka

Q: (J. Papin)

The presented program shows complementary aspects to the CABRI program; effect of coolant temperature, BWR conditions, possibility of separate effect tests.

1: How are the tests defined? Are they defined with all the partners?

2: Do you envisage to test waterlogged rods at high burnup? This is of interest.

A: We will decide the test condition after discussion with partners. We will not test waterlogged rods.

Q: (P. Blanpain) I would like to ask about the representatives of the high burnup fuel (mainly, concerning the 2nd shipment in the test matrix) with regard to fuel initial enrichment and cladding material.

A: Answer will be made by T. Nakamura in his presentation. We are using what in available. We are looking for other candidates.

Q: (I. Sato) Fuel swelling in RIA is not well understood. Separate effect tests in NSRR seem a powerful tool to understand the mechanism. No presentation was available during this meeting on this point and it was not included in the ALPS scope. I would like to stress importance of the separate effect tests.

A: The separate effect tests are on-going and will continue in parallel to the ALPS program.

Presenter: J. Nakamura

Q: (I. Sato) Please give me a rough image of power history in the HBWR tetst.

A: The power ramp consists of several power plateaus and step-wise increases. The plateaus continue for about an hour. The increases take place within some minutes.

This is a blank page.

9. Poster Session

This is a blank page.

RIA-Related Studies at JAERI:
NSRR/High-burnup PWR Fuel Test Results

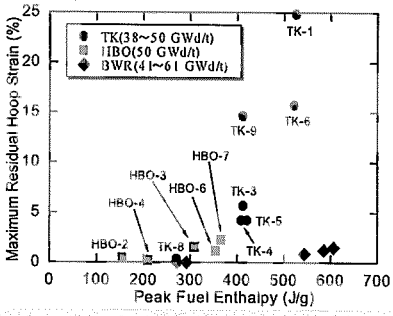
Summary

PWR fuel behavior under RIA conditions was systematically investigated with high-burnup (38-50 GWd/tU) PWR fuels. Important information on fuel failure mechanism, failure threshold and influence of failure was obtained, which was used as a technical basis when NSC decided the PCMI failure threshold.

Test Matrix

Test ID	Span No.	Fuel Burnup (GWd/tU)	Peak Enthalpy (J/g)	Result
HBO-1	3	50.4	306	Failed at 251 J/g
HBO-2	4	50.4	155	No failure
HBO-3	5	50.4	310	No failure
HBO-4	6	50.4	209	No failure
HBO-5	2	44	335	Failed at 322 J/g
HBO-6	4	49	356	No failure
HBO-7	3	49	368	No failure
TK-1	5	38	527	No failure
TK-2	2	48	448	Failed at 251 J/g
TK-3	4	50	414	No failure
TK-4	3	50	410	No failure
TK-5	2	48	423	No failure
TK-6	3	38	523	No failure
TK-7	3	50	397	Failed at 360 J/g
TK-8	4	50	273	No failure
TK-9	5	50	414	No failure
TK-10	8	46	360	No failure

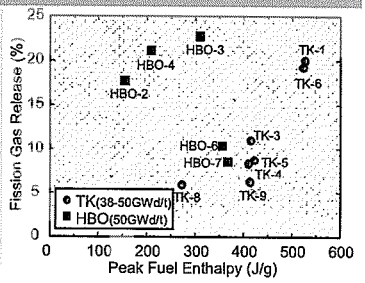
Cladding Deformation



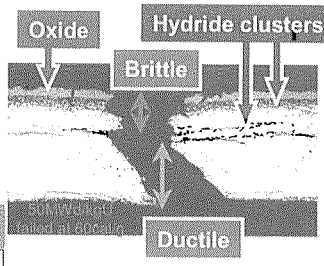
Large cladding deformation, which can not be explained by the fuel pellet thermal expansion, indicates a role of accumulated FP gas. Such large deformation was observed in the tests where the test rod survived prompt PCMI loading and cladding temperature was escalated.

Fission Gas Release

Considerable fission gas release up to 23% was observed in the tests. Such amount of release corresponds to fission gases accumulated in grain boundaries during base irradiation.



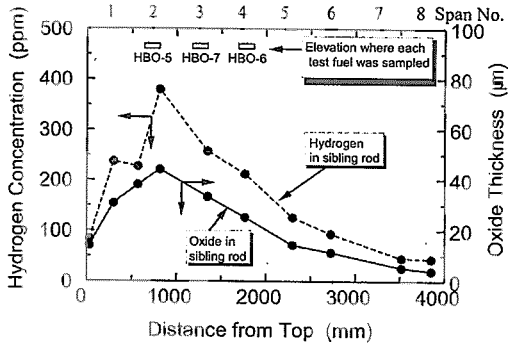
Fuel Failure



Cladding failure occurred in early stage of transient before the escalation of cladding temperature. The brittle cracking was initiated at the cladding outer surface, where dense hydrides were locally precipitated. The crack, then penetrated through ductile inner part of the cladding.

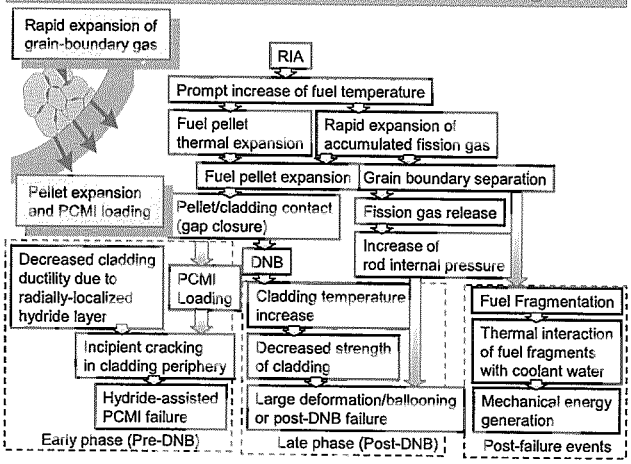
Appearance of the test fuel after pulse (TK-7)





Fuel failure was observed only for the test rods obtained from high axial elevations of spent fuel. Relatively thick oxide layer and high hydrogen concentration at higher elevation correlates well to the occurrence of the failure, suggesting that cladding embitterment due to corrosion has a primary importance in the failure.

Anticipated Process of Fuel Behavior during RIA



Hideo Sasajima / sasa@nsrr.tokai.jaeri.go.jp

RIA-Related Studies at JAERI : NSRR/High-burnup BWR Fuel Test Results

Objective

To investigate
- failure condition (e.g. threshold)
- failure mechanism
- failure consequence (e.g. FGR)

of high-burnup BWR fuel rod under RIA conditions.

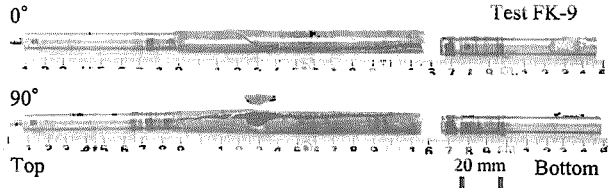
Test Matrix

simulating cold start-up RIA conditions

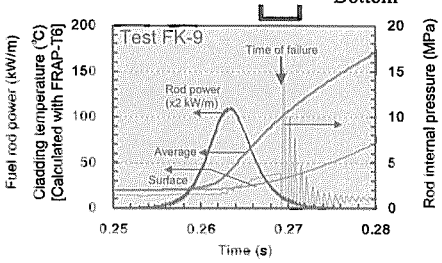
Test No.	TS-1~5	FK-1	FK-2	FK-3	FK-4	FK-5	FK-6	FK-7	FK-8	FK-9
BWR Fuel type	7x7	STEP I (8x8)			STEP II (8x8)					
Fuel burnup, GWd/tU	26	45		41	56		61			
Hydrogen in cladding, ppm	37	45~49			72~107		153~220		141~160	
Peak fuel enthalpy, J/g (cal/g)	230~410 (55~98)	544 (130)	293 (70)	607 (148)	586 (140)	293 (70)	548 (131)	540 (129)	272 (65)	377 (90)
Cladding failure (enthalpy at failure, cal/g)	No	No	No	No	No	No	Yes (70)	Yes (62)	No	Yes (86)

Fuel Failure

Cladding failure occurred in the tests with fuel at a burnup of 61 GWd/tU, in which the peak hydrogen content in the cladding exceeded 150 ppm.

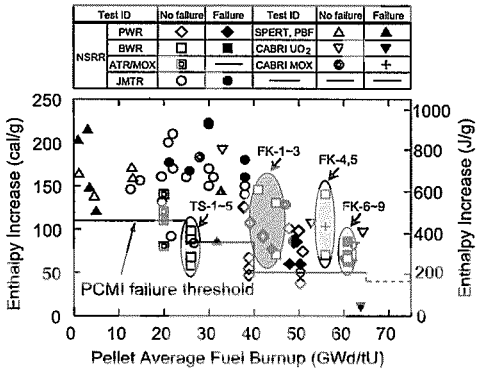


The cladding failed at early timing in pulse irradiation when the cladding average temperature remained about 50 ~ 100℃.



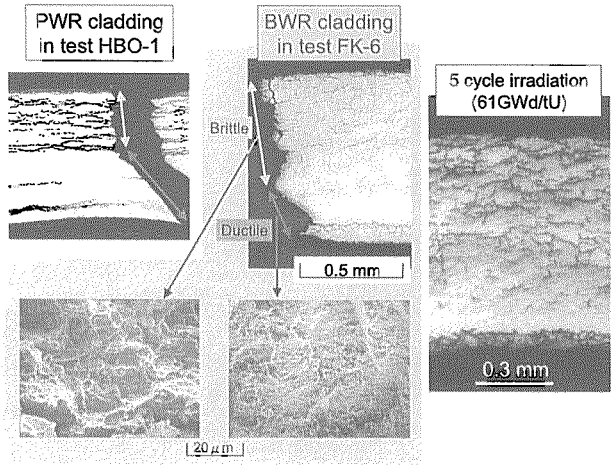
Failure Threshold

The failure occurred at fuel enthalpies of 260 ~ 360 J/g (62 ~ 86 cal/g), which are consistent with the PCMI failure thresholds decided by the Japanese Nuclear Safety Commission.

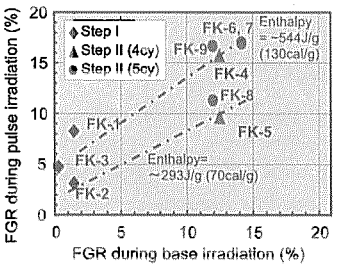


Failure Mechanism

The crack in the BWR cladding progressed in a manner different from the one in PWR cladding, owing to its more randomly oriented hydride distribution.



Fission Gas Release (FGR)



FGR during pulse irradiation tends to increase with that during base irradiation as well as with peak fuel enthalpy during the transients. These gases released are considered those accumulated in grain boundaries during base irradiation.

Summary

BWR fuel behavior under cold start-up RIA conditions was systematically investigated using the NSRR from low to high burnup region. Fuel failure threshold was confirmed by the recent test results for high-burnup fuels. Fission gas release data would be utilized for evaluating source terms in RIAs.

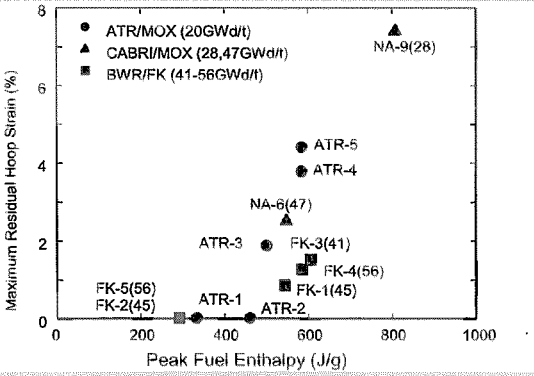
Takehiko Nakamura / take@nsrr.tokai.jaeri.go.jp

RIA-Related Studies at JAERI:
NSRR/MOX Fuel Test Results

Test Matrix

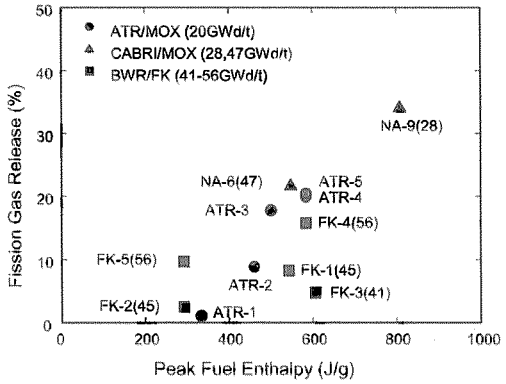
Test ID	Fuel Burnup (GWd/tHM)	Fill Gas at Pulse (MPa)	Peak Fuel Enthalpy (J/g)
ATR-1	20	0.3	335
ATR-2	20	0.3	461
ATR-3	20	0.3	502
ATR-4	20	0.3	586
ATR-5	20	0.3	586

Cladding Deformation



Relatively large radial deformation of the fuel rods due to pellet-cladding mechanical interaction occurred in the experiments with peak fuel enthalpy above 500 J/g.

Fission Gas Release during the Pulse Irradiation

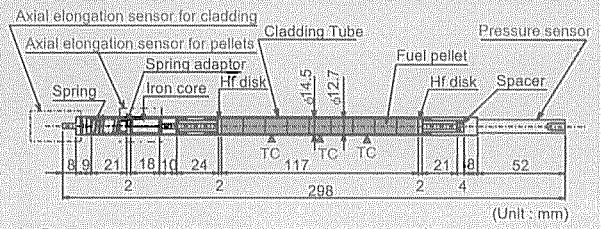


The higher peak fuel enthalpy brought the higher value of fission gas release for the MOX fuel rods. In the tests ATR-3 -5, about 20% fission gas release were measured. These value is higher than that of BWR/FK in spite of lower burnup at comparable enthalpy. The results of French CABRI/MOX tests also shows higher FGR.

Summary

As for the plutonium utilization in Japan, MOX fuel is planned to use in the commercial light water reactors to realize its effective consumption. However, the technical knowledge of high burn-up MOX fuel behavior is rather limited, especially for accident conditions. Therefore, a series of the NSRR experiments with 20 GWd/tHM ATR/MOX fuel rod have been conducted as a 1st step. Higher burn-up MOX fuels will be tested in a couple of years.

Test Fuel

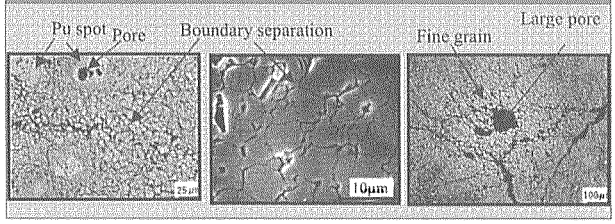


- Reactor: ATR/ Fugen
- Fuel: PuO_2/UO_2
- Initial plutonium enrichment: 2.98wt% ($^{239}Pu+^{241}Pu$)
- Fuel burnup: 20 GWd/tHM
- Linear heat generation rate: 24.0 kW/m at maximum
- Fission gas release: < 0.2% (base-irradiation)
- Radial P/C gap after base-irradiation: 75 - 80 μm

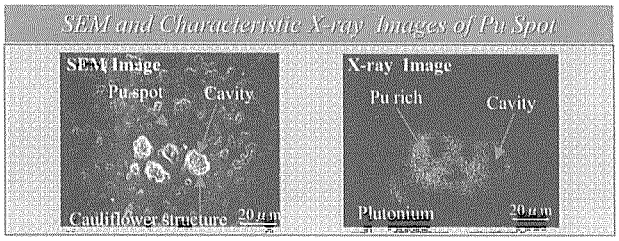
ATR-5: 586 J/g, 4.4%-Radial Deformation

Five pulse irradiation experiments were performed with peak fuel enthalpy ranging from 335 J/g to 586 J/g, resulted in no failure of fuel rods.

Microstructure Change of Fuel Pellet



SEM and Characteristic X-ray Images of Pu Spot



These microstructure changes might contribute to the swelling of fuel pellets during the pulse irradiation. This could cause the large radial deformation of fuel rod and high fission gas release when the pulse irradiation conducted at relatively high peak fuel enthalpy.

Hideo Sasajima / sasa@nsrr.tokai.jaeri.go.jp

RIA-Related Studies at JAERI : NSRR/Rock-like Oxide Fuel Test Results

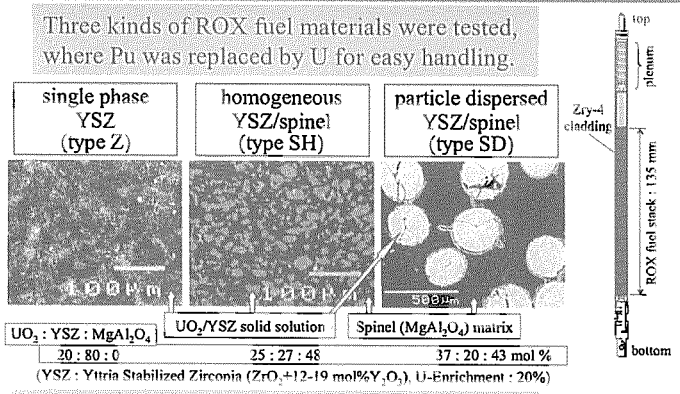
Background and Objective

Rock-like oxide (ROX) fuel, a kind of inert-matrix fuel, has been developed in JAERI as an optional method for burning excess Pu in LWRs. Fuel behavior under RIAs is one of the key to the application, because its extremely small Doppler feedback will cause high energy deposition to the fuel.

The objective is to investigate the fuel behavior under RIA conditions, especially the failure threshold in fuel enthalpy and the failure mechanism.

Test Fuel

Three kinds of ROX fuel materials were tested, where Pu was replaced by U for easy handling.

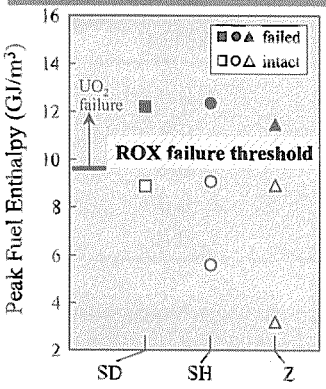


Short 17x17 PWR type fuel rods with the ROX pellets were pulse irradiated in the NSRR.

Pulse Test Matrix

ROX fuel type	Test ID	Peak fuel enthalpy (GJ/m³)	Peak fuel enthalpy (kJ/g)	Fuel Failure
Z	945-1	3.2	0.5	No
	945-2	9.0	1.5	No
	945-3	11.5	1.9	Yes
SH	943-1	5.6	1.0	No
	943-2	9.1	1.6	No
	943-3	12.4	2.2	Yes
SD	947-1	8.9	1.6	No
	947-2	12.2	2.2	Yes

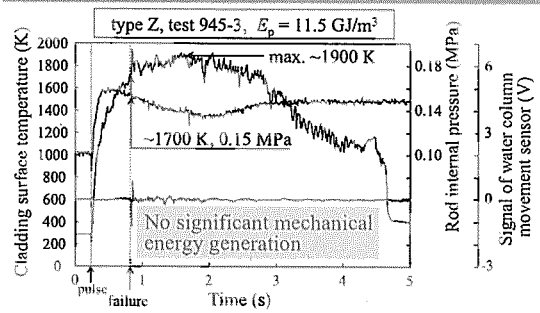
Failure Threshold



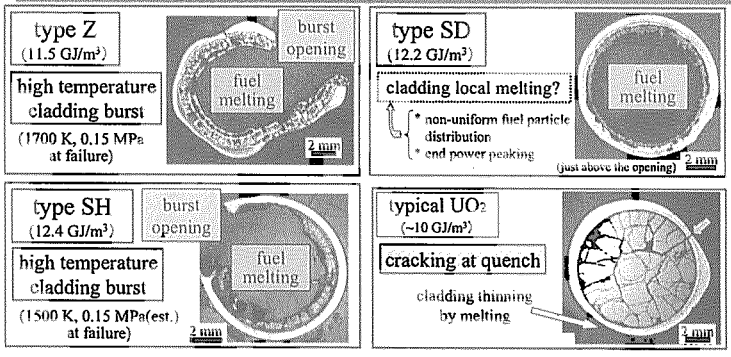
The threshold is ~10 GJ/m³, which is comparable to that of UO_2 fuel.

No apparent difference among the three kinds of ROX fuel.

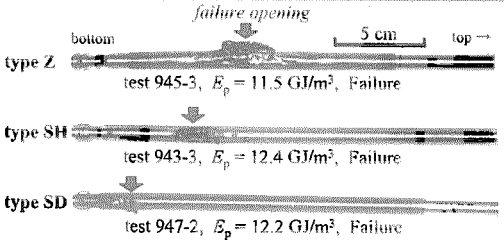
Transient Behavior



Failure Mechanism



Fuel Rod Failure



Summary

ROX fuel failure threshold is ~10 GJ/m³, which is comparable to that of UO_2 fuel.
Failure mechanism is high temperature cladding burst for type Z and SH.
No significant mechanical energy was generated in spite of molten fuel release into coolant.

Fresh ROX fuel can survive under current RIA limit.
(Peak fuel enthalpy can be suppressed to below the threshold by some remedies such as resonant nuclide addition.)

Kazuyuki Kusagaya / kusagaya@nsrr.tokai.jaeri.go.jp, Takehiko Nakamura / take@nsrr.tokai.jaeri.go.jp

NSRR Test Results under Simulated Power Oscillation Conditions of BWRs

Background

- Power oscillation can occur in BWRs due to the void fraction fluctuation at low flow and high power conditions.The probability of this event is much higher than that of RIA. It can affect the performance of high burnup fuel.

Objective

To clarify the fuel behavior during power oscillation of BWRs

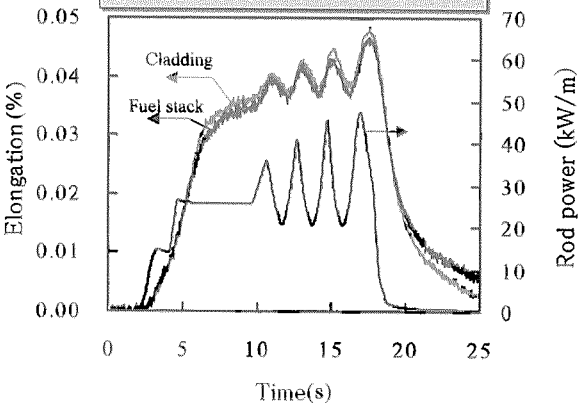
Development of operational method

- Reactor control system modification to achieve high power transient(1985)
- Development of high accuracy simulator for the best use of the capability of the NSRR safely

Test fuel

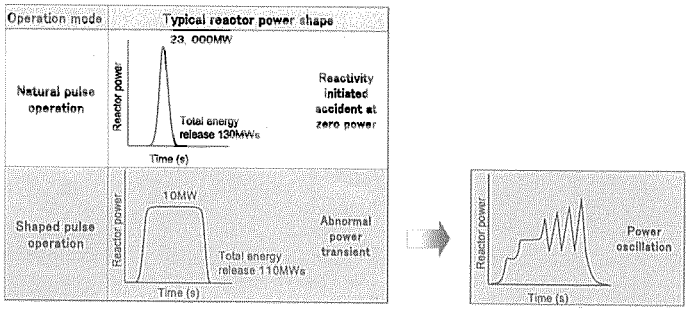
- High burnup BWR fuel(56GWd/tU)
- JMTR pre-irradiated high enriched (20%) fuel (25GWd/tU)
- Un-irradiated fuel with fuel center thermo couples

High burnup BWR rod results

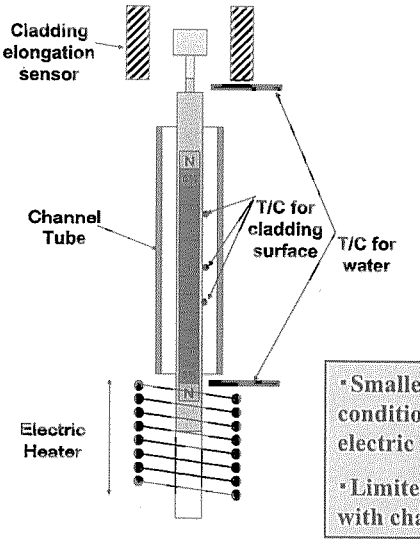


No residual axial strain of cladding

NSRR operation modes and reactor power shapes

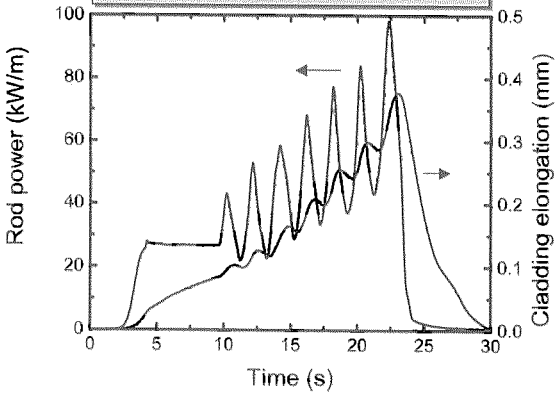


Configuration around fuel rod (JMH-6)



- Smaller subcooling condition with electric heater
- Limited coolant with channel tube

Result of JMTR fuel test



No residual axial strain of cladding

Summary

- Fuel irradiation tests under simulated power oscillation conditions of BWRs were conducted in the NSRR for the first time. Oscillation frequency was about 0.5 Hz and the maximum power was 48-95 kW/m.
- PCMI was observed through cladding elongation and fuel stack elongation, but the residual strain of the cladding was very small.
- It is suggested that the PCMI during power oscillation remained relatively mild as long as DNB does not occur.

Jinichi Nakamura / Jinichi@popsvr.tokai.jaeri.go.jp

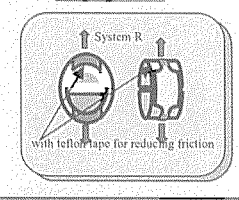
RIA-related studies at JAERI: Studies on fracture behavior and mechanical properties of cladding

Modified Ring Tensile Test

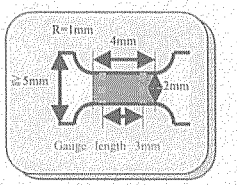
Test Procedure

JAERI determined specimen geometry and tensile method, proper to obtain mechanical properties in hoop direction, by using **FEM analysis** and **experiment**

tensile method

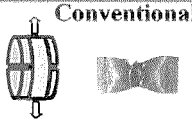


specimen geometry

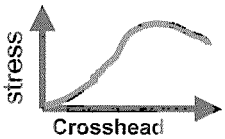


Advantage of modified ring test

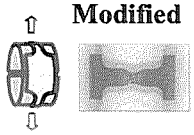
Conventional



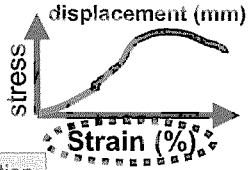
Deformation range is unknown



Modified



Deformation is limited in gauge section



Uniform hoop strain in the gauge section

Quantitative evaluation of ductility

Tests with artificially hydrided cladding tubes

- Quantitative evaluation of influence of hydrogen concentration & temperature

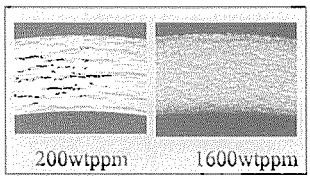
Test condition

Hydrogen concentration

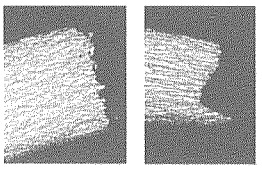
10～1600wtppm

Temperature

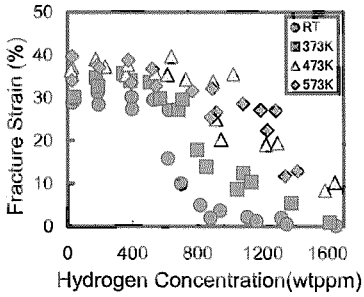
Room temperature ～573K



Results



816wtppm (RT)　912wtppm (473K)



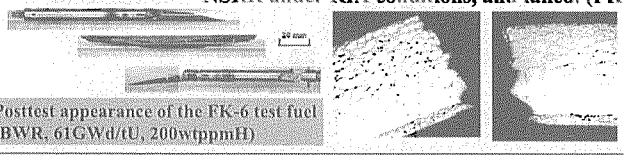
Summary

- Mechanical properties of hydrided cladding tubes were evaluated as functions of hydrogen concentration and temperature by modified ring tensile tests.

Influence of radial hydride on fracture behavior of Zry-2 fuel cladding tube

Background

High burnup BWR fuel were pulse irradiated in NSRR under RIA conditions, and failed. (FK-6,7,9)



Posttest appearance of the FK-6 test fuel (BWR, 61GWd/tU, 200wtppmH)

The crack progressed owing to its more randomly oriented hydride distribution. This type of failure was observed for the first time in BWR fuels.

Objective

To evaluate the effects of hydrogen absorption on burst behavior. (e.g. long axial crack propagation)

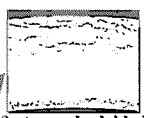
- **orientation of hydride** (circumferential, radial)
- **hydrogen concentration (5wtppm, 200～650wtppm)**

Materials

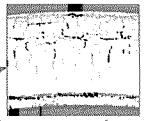
as received
BWR 9×9 type fuel cladding

hydrided
Hydrogen absorption treatment
・200～650wtppm

re-oriented
Heat treatment for hydride re-orientation
・hoop stress :150MPa
・cooling rate :100K/hr

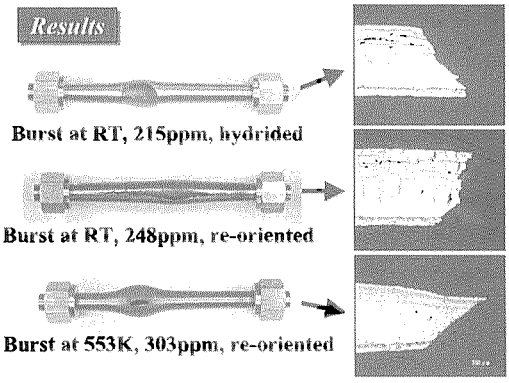


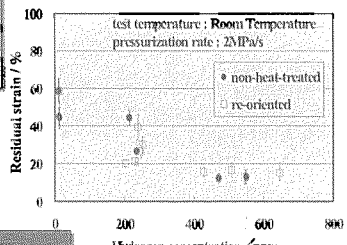
200wtppm, hydrided

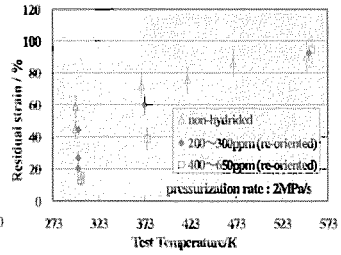


200wtppm,re-oriented

Results







Summary

- Long axial crack propagation which observed in FK-tests could be simulated by this test method.
- Residual strain decreased with the hydrogen concentration increase.
- Effects of hydrogen absorption to the fracture behavior vanished at 553K.

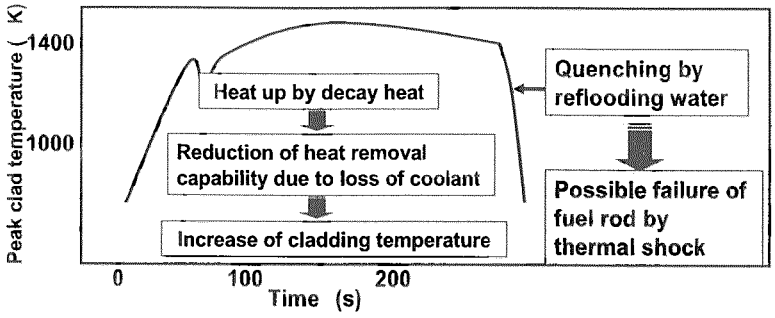
Toru Takeda / takeda@nsrr.tokai.jaeri.go.jp, Sadayuki Uchikawa / uchikawa@nsrr.tokai.jaeri.go.jp

LOCA-related studies at JAERI

- Overview of the research program -

Background

Extension of fuel burnup
- ▶ Changes in pellet and cladding
- ▶ Significant corrosion, hydrogen pickup and increase in fast neutron dose
- ▶ Degradation of cladding ductility



Safety criteria:
Maximum cladding temperature and maximum oxidation defined for preserving a coolable geometry

Objective

To evaluate the influence of further burnup extension on fuel behavior under LOCA conditions and obtain database necessary for regulatory judgment

Failure boundary condition upon quenching of high burnup fuel rod ?

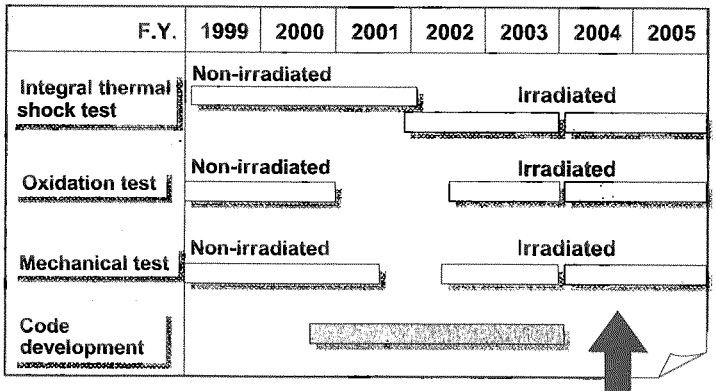
Research items

- Failure-bearing capability of oxidized cladding
- High temperature oxidation of cladding
- Burst behavior
- Mechanical property of cladding

Test samples

- 'Simulated high burnup fuel cladding'(pre-oxidized, pre-hydrided, and/or irradiated at research reactor)
  —*Key factor, Separate effect*
- Cladding from spent fuels(PWR & BWR)
  —*Total evaluation*

Schedule



Performed in ALPS program with higher burnup fuels

Current status
- Test with non-irradiated samples nearly completed by the end of FY 2001
- Preparation for tests with irradiated samples

Future tests

Tests for irradiated claddings (Pre-hydrided and irradiated at research reactor, PWR & BWR high burnup, new type cladding alloy)

Fumihisa Nagase / nagase@popsvr.tokai.jaeri.go.jp

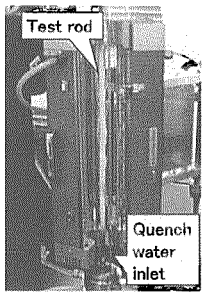
LOCA-related studies at JAERI
- Integral thermal shock test -

Background

- The current Japanese LOCA criteria are based on failure boundary condition upon quenching determined by integral thermal shock tests.
- However, these data are obtained with non-irradiated Zry cladding.
- Failure boundary condition may be reduced for high burn-up fuel rod .

Objective

To obtain the basic data to evaluate failure boundary condition of high burn-up fuel cladding under well simulated LOCA condition (rod-burst oxidation and quench by reflooding) .



Key parameter

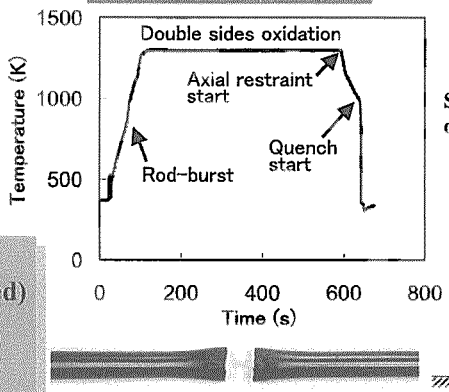
1.Reduction of cladding ductility
- Water-side corrosion
- Hydrogen absorption
- Fast neutron irradiation

2.Mechanical loading due to fuel rod restraint

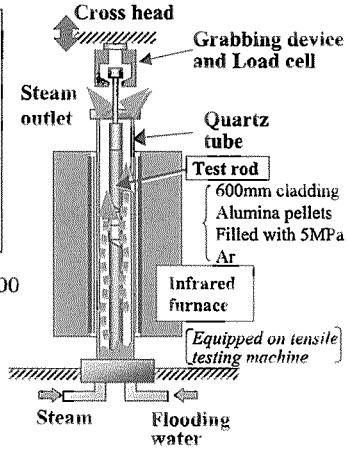
Test for
- Pre-hydrided cladding (Non-irradiated)
- Pre-hydrided & Irradiated cladding
- High burn-up fuel cladding

under various axial load conditions

Test procedure



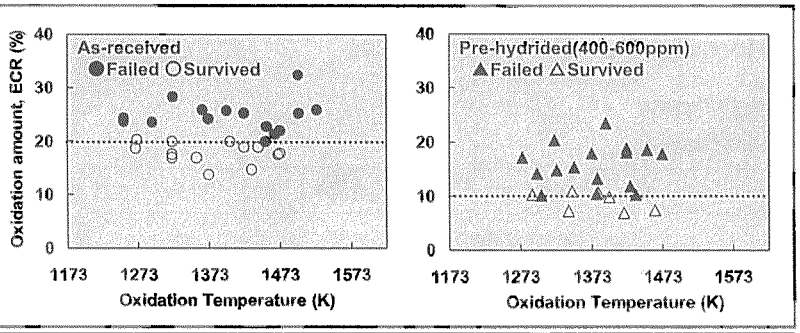
Post-test appearance of cladding tube failed during quenching



Results

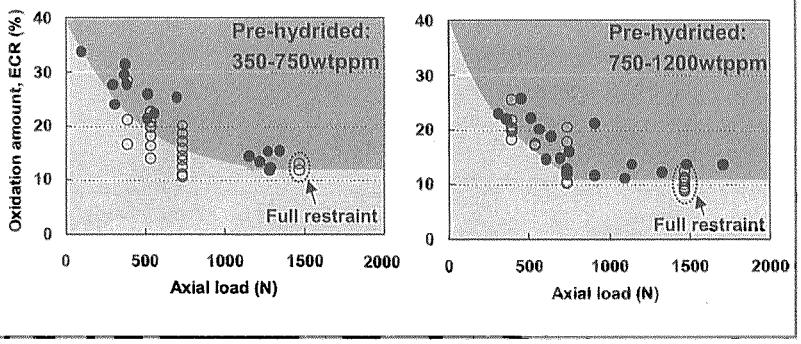
Phase Ⅰ : 1999～2000
- Non-irradiated
- Pre-hydrided 400～600ppm
- Full restraint condition

Remarkable reduction of failure threshold by pre-hydriding under full restraint condition.



Phase Ⅱ : 2001
- Non-irradiated
- Pre-hydrided 100～1200ppm
- Intermediate axial load

Variations of the failure threshold were evaluated as functions of hydrogen concentration and restrained condition during quenching.



Fumihisa Nagase / nagase@popsvr.tokai.jaeri.go.jp

LOCA-related studies at JAERI
- High temperature oxidation of cladding tube -

●Objective

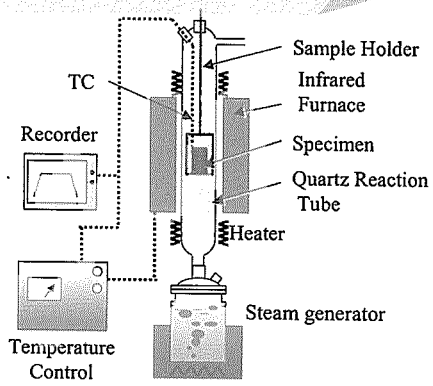
- To examine effect of outer oxide layer and absorbed hydrogen on the oxidation kinetics
- To evaluate oxidation rate of high burnup fuel cladding

●Test conditions

- Heat up rate: 10K/s
- Temperature : 773K to 1573K
- Oxidation time : 120 to 2.16×10^6s
- Atmosphere : flowing steam

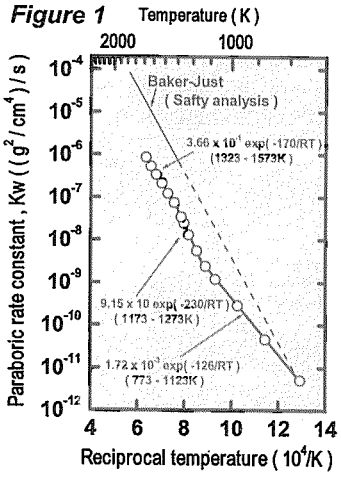
●Sample

- Non-irradiated low-Sn Zircaloy-4 tubes (PWR 17x17 type)
  1. Pre-oxidized sample (oxidized at 703 K in steam or 728K in O_2)
  2. Pre-hydrided sample (200 to 1600 wtppm , hydrided at 673K in H+He)
- Cladding from spent fuel (planned)



●Kinetics evaluation for a wide temperature range for best estimate

Figure 1



●Pre-oxidation effect

Figure 2

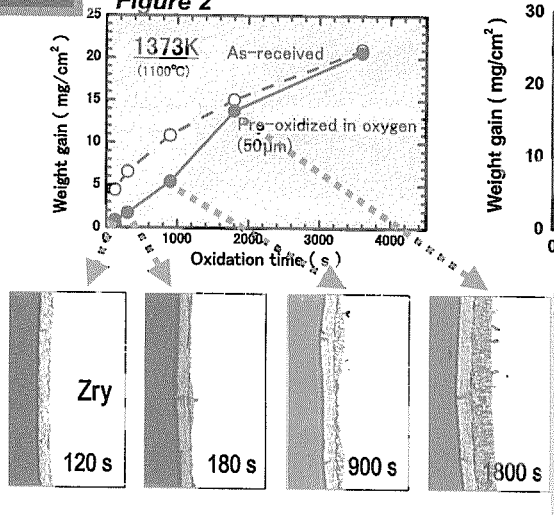
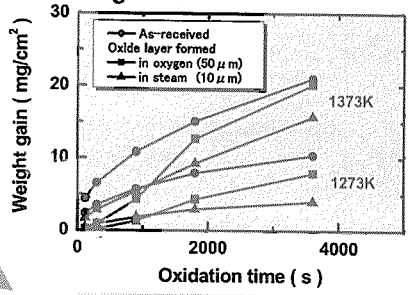


Figure 3

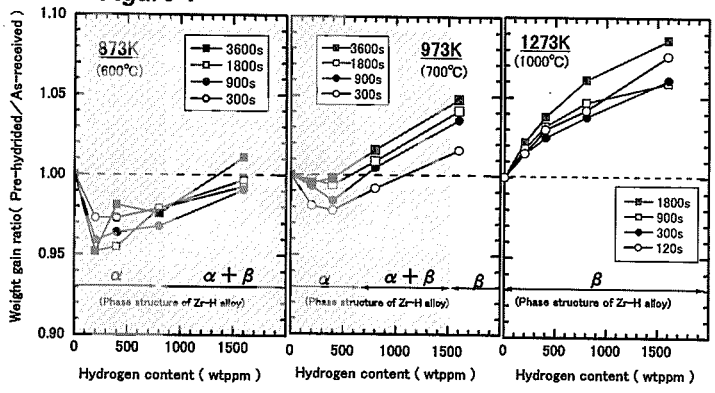


- Retarding effect of pre-oxidation on the oxidation rate for a relatively short oxidation time (Fig.2)
- Different effects of oxide layer formed under different conditions (Fig.3)

●Hydrogen effect

- Variation in the influence of absorbed hydrogen on the Zircaloy oxidation rate depending on the temperature and hydrogen concentration
- Insignificant influence within the condition of postulated LOCA and hydrogen concentration range in high burnup fuel cladding

Figure 4



Fumihisa Nagase / nagase@popsvr.tokai.jaeri.go.jp

LOCA-related studies at JAERI
- Mechanical property of cladding -

High burnup fuel cladding
(Hydrogen absorption, Hydride precipitation)

↓

Temperature transient during accidents

↓

Changes of hydride morphology, hydride distribution and Zircaloy microstructure

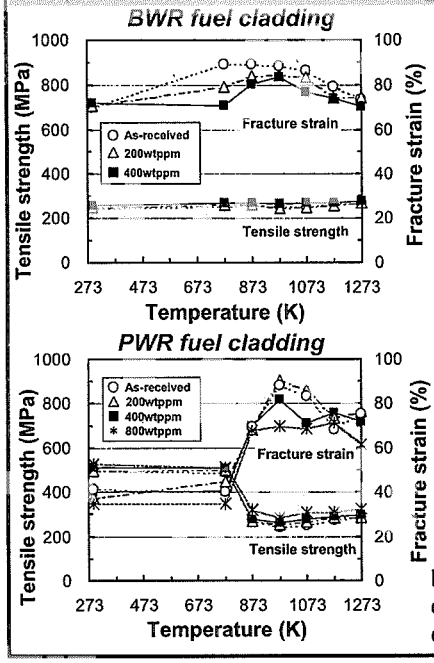
↓

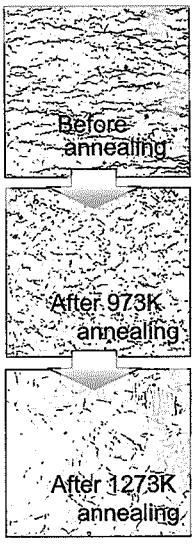
Mechanical property of fuel cladding after temperature transient ?

Annealing tests of *irradiated* cladding tubes	**Annealing tests of *artificially hydrided* cladding tubes for examining separate effect and obtaining wide range of database**

→ Tensile tested at RT after annealing

Tests of artificially hydrided cladding tubes
(tested with *modified* ring tensile test)



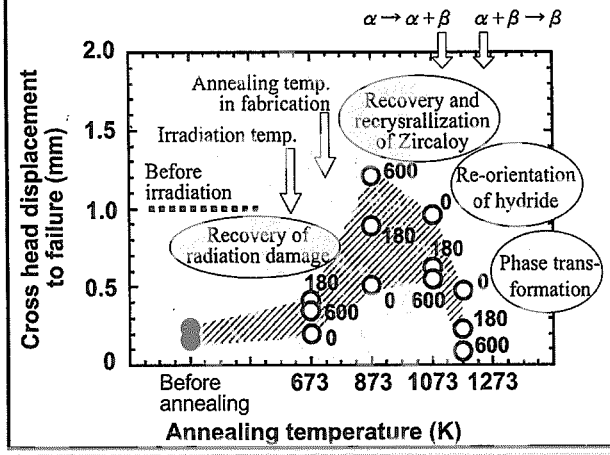


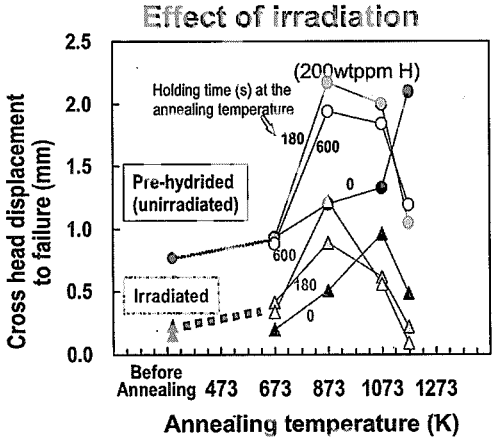
Hydride morphology change in PWR cladding tube

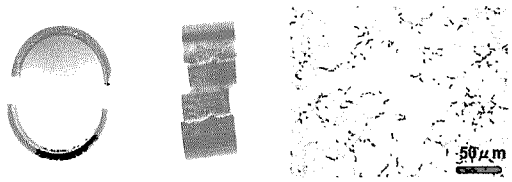
Tests of irradiated cladding tubes
(tested with *conventional* ring tensile test)

Irradiated PWR fuel cladding (provided by KEPCO)

1.5wt%-Sn Zircaloy-4, 9×10^{25}n/m^2 (E>1MeV),
20 to 25 μ m thick oxide, about 210wtppm H,
Ring specimen (without gauge section)







Specimen tested after the annealing at 1173 K for 600 s

- Mechanical property changes corresponding to recovery of radiation defect, recrystallization of the Zircaloy, phase transformations, and associated change of the hydride distribution and morphology
- Differences between BWR and PWR cladding tubes and between irradiated and non-irradiated cladding tubes

Fumihisa Nagase / nagase@popsvr.tokai.jaeri.go.jp

Fuel behavior study during normal operation

Background

・Burnup extension of LWR fuel

・Accumulation of fission gas and degradation of thermal properties of fuel at high burnup

・Fission gas release and thermal property change affect fuel behavior significantly, especially at high burnup.

Objective

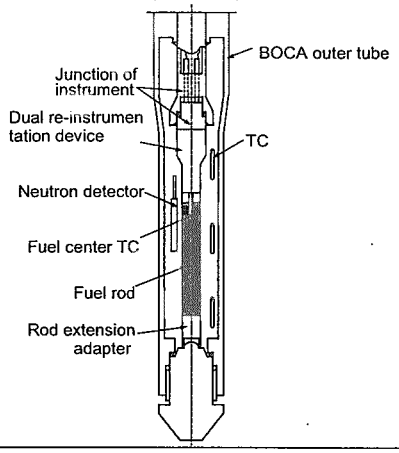
To study the fuel behavior during normal operation especially thermal property change at high burnup and fission gas release during power change

Method

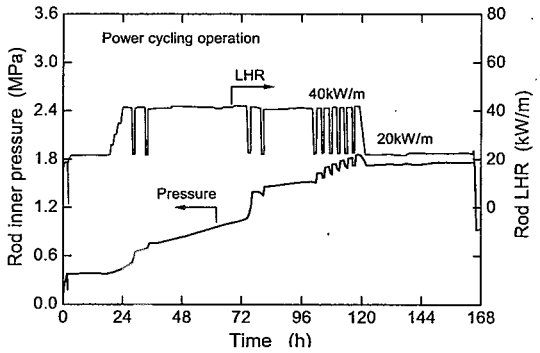
Re-irradiation test by BOCA capsule at JMTR using re-instrumentation technique.

Thermal diffusivity measurement at PIE

Schematic drawing of BOCA capsule with dual re-instrumented rod



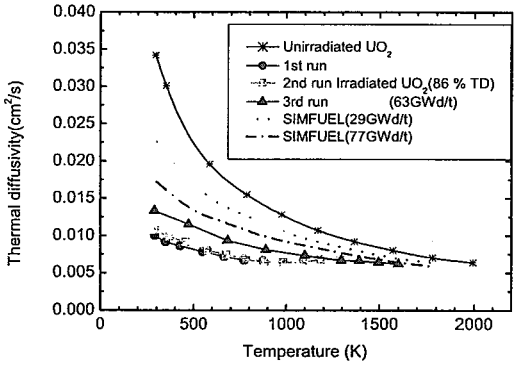
Fission gas release during power change



・Fission gas release during power reduction

・Gas release from grain boundary bubbles affected by thermal stress change

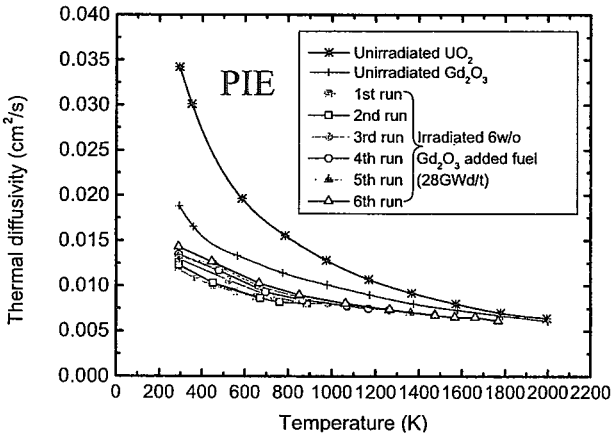
Thermal diffusivity of high burnup UO_2(63GWd/t)

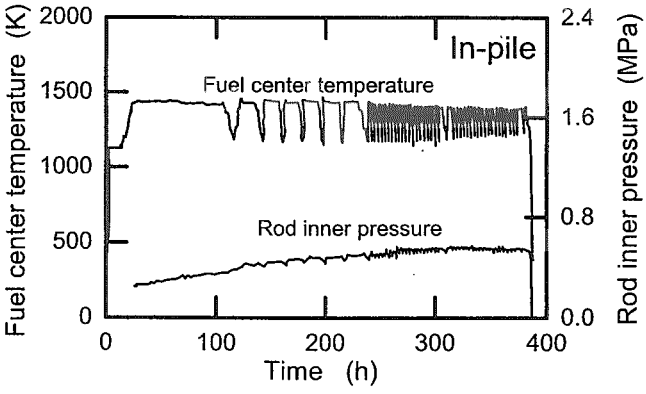


・Thermal diffusivity decreases with burnup due to radiation defects and FP accumulation.

・Recovery of thermal diffusivity due to the recovery of radiation damage

Thermal property of gadolinia added fuel





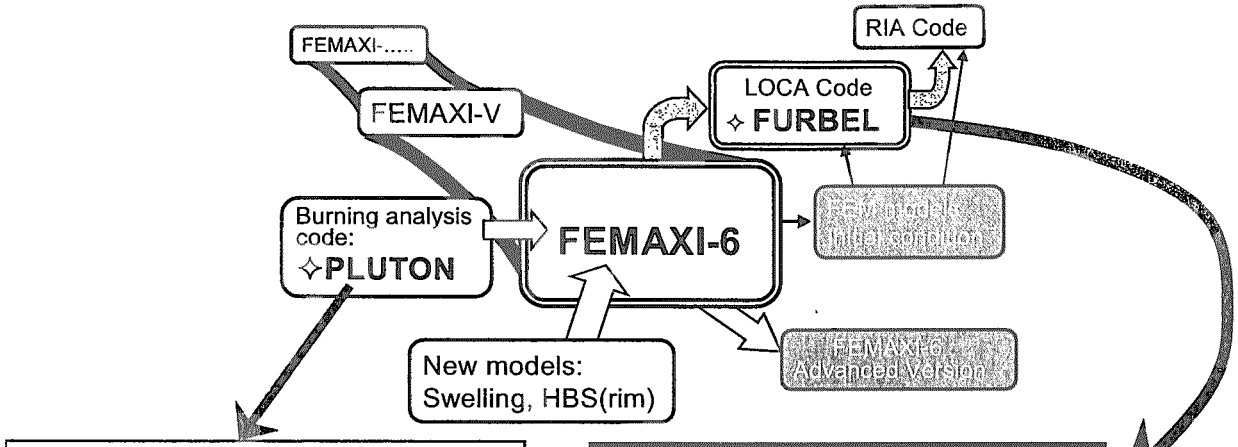
・The thermal diffusivity of irradiated gadolina added fuel is lower than that of irradiated UO_2.

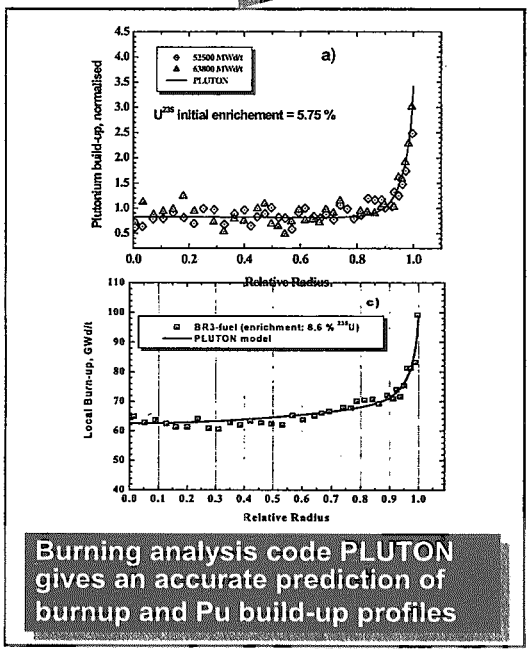
・The relative decrease of thermal diffusivity due to irradiation is smaller for gadolina added fuel than for UO_2.

・Fuel center temperature from in-pile test was a little higher than the evaluated value from thermal diffusivity data at PIE.

Jinichi Nakamura / Jinichi@popsvr.tokai.jaeri.go.jp

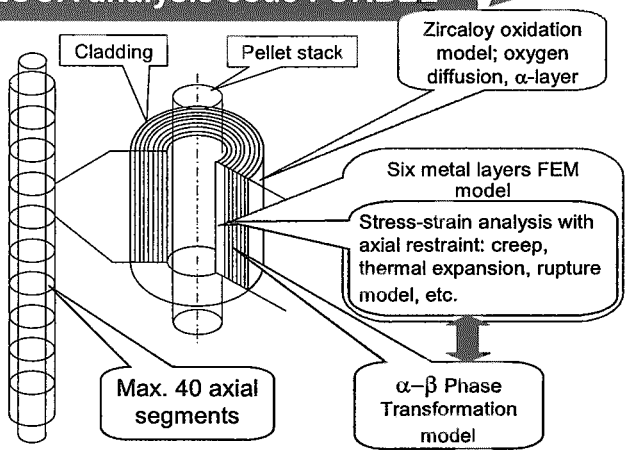
Development of Fuel Analysis Code

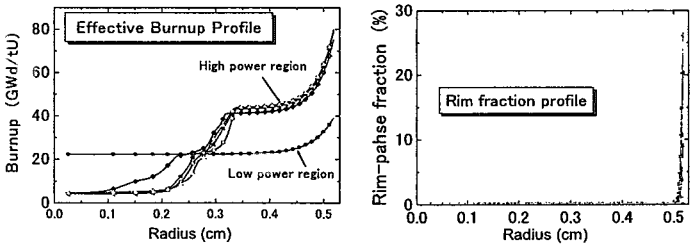




Burning analysis code PLUTON gives an accurate prediction of burnup and Pu build-up profiles

LOCA analysis code FURBEL

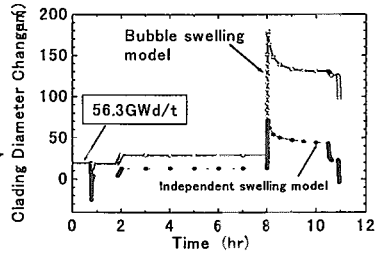




Semi-empirical model of rim structure fraction in BWR type rod with average burnup of 45 GWd/t.

Features of FEMAXI-6

1. Coupled solution of the thermal analysis and entire-rod-length FEM mechanical analysis.
2. Incorporation of results of the advanced burning calculation code PLUTON.
3. Empirical model of bonding layer effect on gap thermal conductance.
4. Bonded gap calculation is possible.
5. Semi-empirical model for high burnup structure (rim) in pellet.
6. A new swelling model on the basis of FP gas bubble growth.



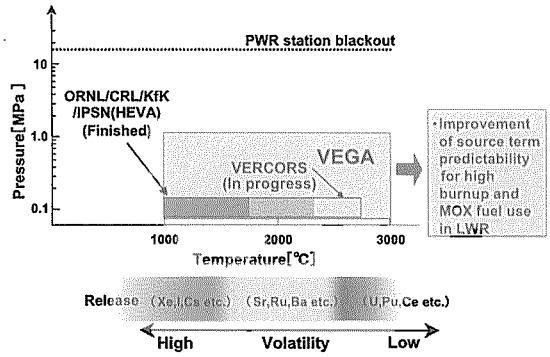
FP gas bubble swelling model predicts diameter increase of BWR test rod during power ramp.

Motoe Suzuki / motoe@popsvr.tokai.jaeri.go.jp

Verification Experiments of Radionuclides Gas/Aerosol Release

Fuel Safety Research Laboratory

Scope and Target



VEGA Facility

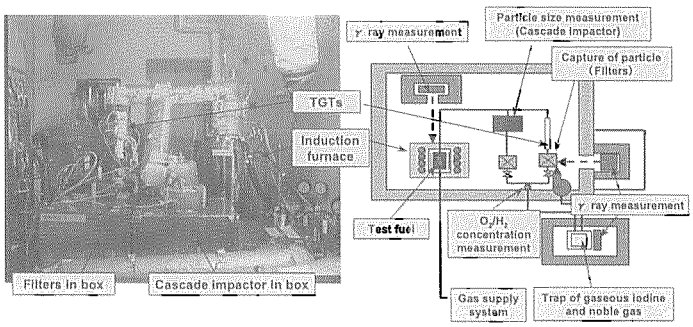
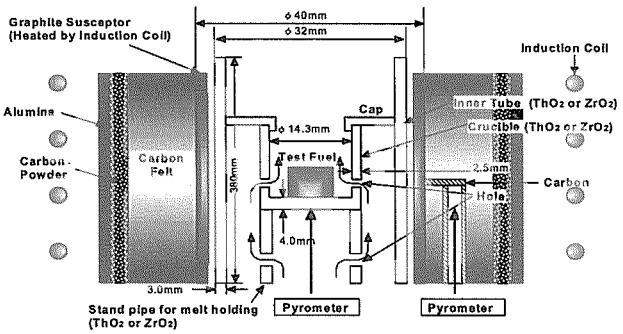


Photo. of VEGA Facility　　Outline of Facility

VEGA Furnace for Oxidizing Condition



Fabrication of ThO_2 Tube

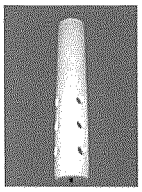
■ Requirement for Furnace Material
– Stable under high temperature > 3000℃ and oxidizing conditions

	M.P. > 3000℃	Stability under oxidizing condition
ThO_2	○ (3370℃)	○
W	○ (3382℃)	×
ZrO_2	× (2677℃)	○

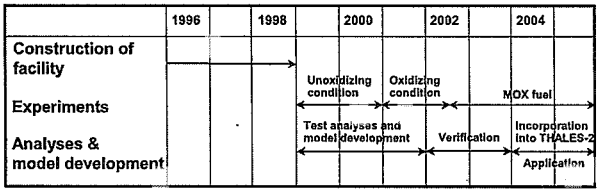
● Method for ThO_2 Tube Fabrication
– Powder size adjustment by heating to improve mold strength
– Slip preparation by changing masses of water and dispersant
– Casting of tube and crucible
* (Centrifugal) slip and drain casting
– Sintering at 1700℃ after drying up of casted tube

◐ Heat up test in progress

Photo. of Sintered ThO_2 Crucible



VEGA Test Schedule (2 tests/year)



Summary of VEGA Tests

●Test Fuel
-PWR 47GWd/tU
-6 years cooling
●He atmosphere,
●No-reirradiation

●VEGA-1 Test (Sep. ,'99)
-Max. 2500℃, 0.1MPa
-Basic release data and facility capability
-Cs:90%, Eu:No release

●VEGA-2 Test (April ,2000)
-Max. 2500℃, 1.0MPa
-Release data under high pressure
-Cs:70%, Eu:No release

●VEGA-3 Test (Oct. 3 ,2000)
-Max. 2850℃, 0.1MPa
-Release data under high temp.
-Cs:100%, Eu:No release

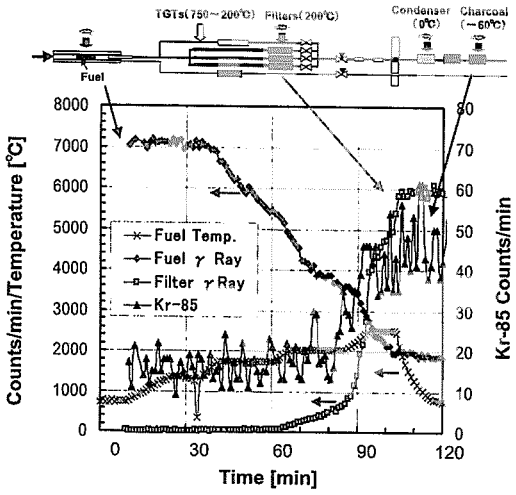
Pressure effect
Temperature effect

Flowchart of VEGA Post-Test Analyses

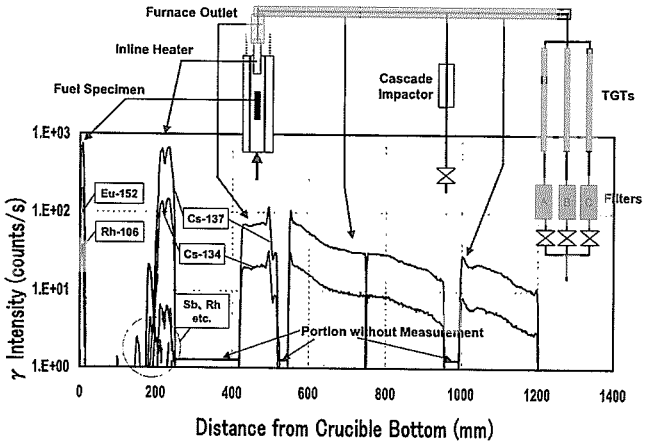
Heat up test (On-line γ measurement) → Pipe cutting → Off-line γ measurement for piping (FP distribution) → Nitric acid leaching (FP mass balance) → SEM/EPMA

Akihide Hidaka / hidaka@sarl.tokai.jaeri.go.jp

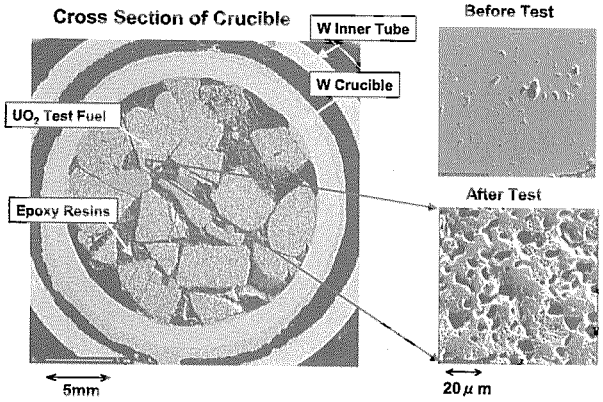
On-line γ Ray Measurements of VEGA-1 Test



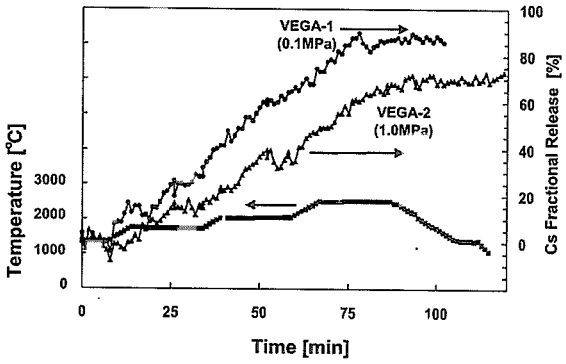
Distribution of γ Intensity in VEGA-1 Facility



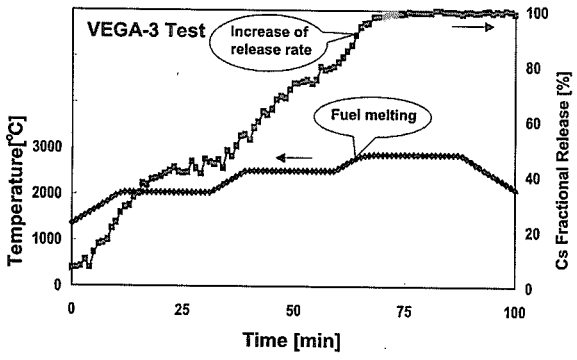
Microphotograph of VEGA-1 Test Fuel



Effect of Pressure on Fractional Release



Effect of Temperature on Fractional Release



Fractional Release Estimated from Intensity Changes of γ Peaks

(Assuming no release of Eu-154)

Nuclide	γ Energy [keV]	VEGA-1 (2500℃,0.1MPa) Release[%]	VEGA-1 (2500℃,0.1MPa) Error[%]	VEGA-2 (2500℃,1.0MPa) Release[%]	VEGA-2 (2500℃,1.0MPa) Error[%]	VEGA-3 (2850℃,0.1MPa) Release[%]	VEGA-3 (2850℃,0.1MPa) Error[%]	VI-3* Release[%]
Cs-134	605	86	0.1	74	1.40	100	0.06	99.9
Cs-137	662	85	0.1	70	0.50	100	0.02	
Ru-106	622	18	5.5	31	13.7	32	5.4	5
Ce-144	696	31	36.0	7	47.2	8	55.0	<0.2
Eu-154	724	0	4.4	0	5.0	0	5.0	<0.01
	1275	0	3.0	0	2.0	0	2.0	

*ORNL Test VI-3 : 2427℃(20min) in steam

Tamotsu Kudo / kudo@sarl.tokai.jaeri.go.jp

Appendix 1

Fuel Safety Research Specialists' Meeting
Program

Monday, March 4 — Hotel to JAERI by Bus

9:30		Opening Address by Director Abe	Chairmen
		Session 1: General Report of Activities	Uetsuka and Wiesenack
9:45	–	Outline of Fuel Safety Research at JAERI	H.Uetsuka (JAERI)
10:05	–	Fuel Research at the OECD Halden Reactor Project	W.Wiesenack (Halden)
10:40	–	The CABRI International Program for RIA Research and Development Studies	J.C.Melis (IPSN)
11:10	–	Fuel Safety Research Activities in Spain	J.Conde (CSN)
11:40	–	IPSN Future Programs in the Phebus Facility	A.Mailliat (IPSN)
12:00	–	Lunch (Lunch Box is sold in the lobby)	
		Session 2a : RIA Experimental Research on High Burnup Fuel	Nakamura and Grigoriev
13:00	–	NSRR RIA tests on PWR, BWR and MOX fuels	T.Nakamura (JAERI)
13:25	–	NSRR test results under simulated power oscillation conditions of BWRs	J.Nakamura (JAERI)
13:50	–	Temperature effect on BWR cladding failure under mechanically simulated RIA conditions	V.Grigoriev (Studsvik)
14:15	–	Fracture behavior and mechanical properties of cladding Part1: Influence of radial hydride on fracture behavior of Zry-2 fuel cladding tube Part2: Modified ring tensile test	T.Takeda (JAERI) S.Uchikawa (JAERI)
14:40	–	Influence of hydrogen on the integrity of Zircaloy cladding under accidental conditions	S.Yamanaka(Osaka Univ.)
15:05	–	Coffee Break	
		Session 2b : RIA Analytical Code and Modelling	Nakamura and Grigoriev
15:20	–	Numerical simulation of the expansion-due-to-compression test	A.Varias (Malmo Univ.)
15:45	–	Three dimensional analysis of RIA in PWR and BWR with high burnup fuel	T.Nakajima (NUPEC)
16:10	–	RIA Modelling- a comparison between TRANSURANUS and FREY	C.Hellwig (PSI)
		Session 3: LOCA-related Research on High Burnup Fuel	Nagase and Billone
16:35	–	Thermo-mechanical behavior of irradiated Zr-1%Nb alloy claddings in LOCA simulating conditions	L.Andreeva (VNIINM)
17:00	–	Status of LOCA research in the high burnup cladding performance program	M.Billone (ANL)
17:25	–	Results from JAERI research program on high burnup fuel behavior under LOCA conditions	F.Nagase (JAERI)
18:00–20:30		Reception (Akogi-ga-ura Club, by Bus)	Club to Hotel by Bus

Tuesday, March 5			Hotel to JAERI by Bus
		Session 4: FP Release from Fuel under Severe Accident	Hidaka and Kissane
9:30	–	Overview of VEGA program on radio-nuclide release from fuel under severe accident conditions and effect of pressure on release behavior	A.Hidaka (JAERI)
9:55	–	Effect of temperature and atmosphere on release of nuclides including short-life FPs –Results of recent VEGA- 3 through-5 tests –	T.Kudo (JAERI)
10:20	–	Fission product release from CANDU fuel at 1650C: the HCE4 experiment	R.Dickson (AECL)
10:45	–	Fission-product release and transport analysis in severe accident conditions: strategy and illustrations	M.Kissane (IPSN)
11:10	–	Overview of the fission products behavior in the Phebus FP tests, including latest experimental results on the FPT2 test	M.Zabiego (IPSN)
11:35	–	Analysis of Phebus FPT1 samples carried out at IUT, Karlsruhe	P.D.W.Bottomley (ITU)
12:00	–	Lunch (Lunch Box is sold in the lobby)	
		Session 5a: Fuel Behavior under Normal Operation Condition	Suzuki and Ledergerber
13:00	–	NOK high burnup fuel surveillance program	C.Ott (NOK)
13:25	–	BWR-fuel performance at high-burnup	G.Ledergerber (KKL)
13:50	–	Fuel irradiation experiments for an advanced PWR fuel development in the HANARO	YH.Kang (KAERI)
14:15	–	Development of PIE apparatuses and techniques in RFEF in JAERI	R.Yasuda (JAERI)
14:40		Coffee Break	
		Session 5b: Fuel Behavior Modelling under Normal Operation Condition	Suzuki and Ledergerber
14:55	–	Fission gas release modelling at high burn-up	P.Tempest (BritishEnergy)
15:20	–	Development of fuel analysis codes FEMAXI and FURBEL	M.Suzuki (JAERI)
15:45	–	UO_2 fuel rod performance analysis code, INFRA development	CB.Lee (KAERI)
		Session 6 : Discussion on JAERI's Future Program	Uetsuka and Conde
16:10		Outline of ALPS Program	T.Nakamura and H.Uetsuka (JAERI)
16:30		Comments from Partners	CSN, ENUSA, NOK, KKL, Halden, Studsvik, etc.
17:10	–	Closing Remarks by Deputy Director Ishijima	
			JAERI to Hotel by Bus

Appendix 2

List of Participants

Participants from Overseas		
Jose Alonso	ENUSA	Spain
Liudmila A. Andrievskaya	FSUE A.A.Bochvar VNIINM	Russia
Geun-Sun Auh	Korea Institute of Nuclear Safety (KINS)	Korea
Pedro Gonzalez Arjona	ENDESA	Spain
Daniel Baron	Electricite de France (EdF)	France
Patrick Blanpain	Framatome-ANP Nuclear Fuel	France
Paul David William Bottomley	Institute for Transuranuin Elements (ITU)	Germany
Michael Billone	Argonne National Laboratory (ANL)	U.S.A.
Jin-Sik Cheon	Korea Atomic Energy Research Institute	Korea
Jose M. Conde	CSN (Consejo de Seguridad Nuclear)	Spain
Raymond Dickson	Atomic Energy of Canada Limited (AECL)	Canada
Gerard Ducros	CEA Cadarache-DEN	France
Viatcheslav Grigoriev	Studsvik Nuclear AB	Sweden
Christian Hellwig	Paul Scherrer Institut (PSI)	Switzerland
Young-Hwan Kang	Korea Atomic Energy Research Institute	Korea
Seppo Kelppe	VTT	Finland
Martin Kissane	Institut de Radioprotection et de Sûreté Nucléaire (IRSN)	France
E. Kolstad	Halden Project	Norway
T.M. Karlsen	Halden Project	Norway
Chan Bock Lee	Korea Atomic Energy Research Institute	Korea
Byung-Ho Lee	Korea Atomic Energy Research Institute	Korea
K. Lunde	IFE/Kjeller	Norway
Alain Mailliat	IRSN	France
Jean-Claude Melis	IRSN	France
Joelle Papin	IRSN	France
Guido Ledergerber	Kernkraftwerk Leibstadt (KKL)	Switzerland
Reiner Manzel	Framatome-ANP GmbH	Germany
Robert Montgomery,	EPRI	USA
Klaus Nissen	Framatome-ANP GmbH	Germany
Christophe Ott	Nordostschweizerische Kraftwerke (NOK)	Switzerland
Manuel Quecedo	ENUSA	Spain
David Schrire	Studsvik Nuclear AB	Sweden
Paul Tempest	British Energy	UK
S. Vaidyanathan	Global Nuclear Fuel /USA	USA
Mojmir Valach	Nuclear Research Institute Rez plc	Czech
Andrew Varias	Malmo University	Sweden
Eric van Welle	CSK/CEN	Belgium
Pascal Yvon	CEA/Saclay	France
Wolfgang Wiesenack	Halden Project	Norway
Maxime Zabiego	IRSN	France

Japanese Participants from outside JAERI	
Katsuhiro Abe	Kobe Special Tube Co., LTD.
Sadaaki Abeta	Mitsubishi Heavy Industries, LTD.
Takafumi Anegawa	Tokyo Electric Power Company, LTD.
Tosikazu Baba	Mitsubishi Heavy Industries, LTD.
Toshio Fujishiro	Research Organization for Information Science & Technology
Hirotaka Furuya	Nuclear Safety Technology Center
Hiroshi Hayashi	Nuclear Power Engineering Corporation
Kouzou Honma	Mitsubishi Heavy Industries, LTD.
Hisasi Ikehata	Nuclear Development, Ltd.
Siori Ishino	Tokai University
Noboru Itagaki	Nuclear Fuel Industries, LTD.
Shouichi Kitajima	Central Research Institute of Electric Power Industry
Motoyasu Kinoshita	Central Research Institute of Electric Power Industry
Kennji Konasi	Tohoku University
Sinsuke Matumoto	Nuclear Fuel Industries, LTD.
Tosio Matumoto	Global Nuclear Fuel, LTD.
Keizou Matuura	Nuclear Fuel Industries, LTD.
Sinnya Miyahara	Japan Nuclear Cycle Development Institute (JNC), O-arai Engineering Center
Tomoyasu Mizuno	JNC, O-arai Engineering Center
Tamotu Murata	Nuclear Fuel Industries, LTD.
Tetsuo Nakajima,	Nuclear Power Engineering Corporation
Masafumi Nakatsukasa	Global Nuclear Fuel, LTD.
Hiroshi Ohashi	Econics Co., LTD.
Takesi Ohta	Tokyo Electric Power Company, LTD.
Ikken Sato	JNC, O-arai Engineering Center
Takasi Sawada	Mitsubishi Heavy Industries, LTD.
Yu Shirai	TEPCO Systems, LTD.
Youjirou Suzawa	TEPCO Systems, LTD.
Yosihiro Takagawa	Global Nuclear Fuel, LTD.
Katumi Une	Global Nuclear Fuel, LTD.
Sigeru Urata	Kansai Electric Power Company, LTD.
Sinsuke Yamanaka	Osaka University
Michio Yamawaki	Tokyo University

JAERI Participants

Kiyoharu Abe
Keiichi Aizawa
Hidetosi Amano
Misao Fujita
Toyosi Fuketa
Akihide Hidaka
Michio Ichikawa
Kiyomi Ishijima
Masumi Kajiyama
Fumio Kanaitsuka
Tooru Kanazawa
Tsuneo Kodaira
Tamotsu Kudo
Kazuyuki Kusagaya
Ayako Motoishi
Nobuya Nagai
Fumihisa Nagase
Jinichi Nakamura
Takehiko Nakamura
Tsutomu Nakamura
Masahiro Nishi
Takashi Otomo
Reiko Sakamoto
Hideo Sasajima
Yukio Sasajima
Jun Sugimoto
Motoe Suzuki
Hidetake Takahashi
Tooru Takeda
Masataka Tanimoto
Yosifumi Terakado
Sadayuki Uchikawa
Hiroshi Uetsuka
Chieko Yamashita
Ryo Yasuda
Tosiyuki Yoshida
Makio Yoshinaga

This is a blank page.

国際単位系 (SI) と換算表

表1　SI基本単位および補助単位

量	名称	記号
長さ	メートル	m
質量	キログラム	kg
時間	秒	s
電流	アンペア	A
熱力学温度	ケルビン	K
物質量	モル	mol
光度	カンデラ	cd
平面角	ラジアン	rad
立体角	ステラジアン	sr

表2　SIと併用される単位

名称	記号
分，時，日	min，h，d
度，分，秒	°，′，″
リットル	l，L
トン	t
電子ボルト	eV
原子質量単位	u

1 eV=1.60218×10^{-19} J

1 u=1.66054×10^{-27} kg

表5　SI接頭語

倍数	接頭語	記号
10^{18}	エクサ	E
10^{15}	ペタ	P
10^{12}	テラ	T
10^{9}	ギガ	G
10^{6}	メガ	M
10^{3}	キロ	k
10^{2}	ヘクト	h
10^{1}	デカ	da
10^{-1}	デシ	d
10^{-2}	センチ	c
10^{-3}	ミリ	m
10^{-6}	マイクロ	μ
10^{-9}	ナノ	n
10^{-12}	ピコ	p
10^{-15}	フェムト	f
10^{-18}	アト	a

表3　固有の名称をもつSI組立単位

量	名称	記号	他のSI単位による表現
周波数	ヘルツ	Hz	s^{-1}
力	ニュートン	N	m·kg/s^2
圧力，応力	パスカル	Pa	N/m^2
エネルギー，仕事，熱量	ジュール	J	N·m
工率，放射束	ワット	W	J/s
電気量，電荷	クーロン	C	A·s
電位，電圧，起電力	ボルト	V	W/A
静電容量	ファラド	F	C/V
電気抵抗	オーム	Ω	V/A
コンダクタンス	ジーメンス	S	A/V
磁束	ウェーバ	Wb	V·s
磁束密度	テスラ	T	Wb/m^2
インダクタンス	ヘンリー	H	Wb/A
セルシウス温度	セルシウス度	℃	
光束	ルーメン	lm	cd·sr
照度	ルクス	lx	lm/m^2
放射能	ベクレル	Bq	s^{-1}
吸収線量	グレイ	Gy	J/kg
線量当量	シーベルト	Sv	J/kg

表4　SIと共に暫定的に維持される単位

名称	記号
オングストローム	Å
バーン	b
バール	bar
ガル	Gal
キュリー	Ci
レントゲン	R
ラド	rad
レム	rem

1 Å=0.1 nm=10^{-10} m

1 b=100 fm^2=10^{-28} m^2

1 bar=0.1 MPa=10^5 Pa

1 Gal=1 cm/s^2=10^{-2} m/s^2

1 Ci=3.7×10^{10} Bq

1 R=2.58×10^{-4} C/kg

1 rad=1 cGy=10^{-2} Gy

1 rem=1 cSv=10^{-2} Sv

(注)

1. 表1－5は「国際単位系」第5版，国際度量衡局 1985年刊行による。ただし，1 eVおよび1 uの値はCODATAの1986年推奨値によった。
2. 表4には海里，ノット，アール，ヘクタールも含まれているが日常の単位なのでここでは省略した。
3. barは，JISでは流体の圧力を表わす場合に限り表2のカテゴリーに分類されている。
4. EC閣僚理事会指令ではbar，barnおよび「血圧の単位」mmHgを表2のカテゴリーに入れている。

換　算　表

力	N(=10^{5}dyn)	kgf	lbf
	1	0.101972	0.224809
	9.80665	1	2.20462
	4.44822	0.453592	1

粘度　1 Pa·s(N·s/m^2)=10 P(ポアズ)(g/(cm·s))

動粘度　1 m^2/s=10^{4}St(ストークス)(cm^2/s)

圧力	MPa(=10 bar)	kgf/cm^2	atm	mmHg(Torr)	lbf/in^2(psi)
	1	10.1972	9.86923	7.50062×10^3	145.038
	0.0980665	1	0.967841	735.559	14.2233
	0.101325	1.03323	1	760	14.6959
	1.33322×10^{-4}	1.35951×10^{-3}	1.31579×10^{-3}	1	1.93368×10^{-2}
	6.89476×10^{-3}	7.03070×10^{-2}	6.80460×10^{-2}	51.7149	1

エネルギー・仕事・熱量	J(=10^{7}erg)	kgf·m	kW·h	cal(計量法)	Btu	ft·lbf	eV
	1	0.101972	2.77778×10^{-7}	0.238889	9.47813×10^{-4}	0.737562	6.24150×10^{18}
	9.80665	1	2.72407×10^{-6}	2.34270	9.29487×10^{-3}	7.23301	6.12082×10^{19}
	3.6×10^6	3.67098×10^5	1	8.59999×10^5	3412.13	2.65522×10^6	2.24694×10^{25}
	4.18605	0.426858	1.16279×10^{-6}	1	3.96759×10^{-3}	3.08747	2.61272×10^{19}
	1055.06	107.586	2.93072×10^{-4}	252.042	1	778.172	6.58515×10^{21}
	1.35582	0.138255	3.76616×10^{-7}	0.323890	1.28506×10^{-3}	1	8.46233×10^{18}
	1.60218×10^{-19}	1.63377×10^{-20}	4.45050×10^{-26}	3.82743×10^{-20}	1.51857×10^{-22}	1.18171×10^{-19}	1

1 cal = 4.18605 J (計量法)

= 4.184 J (熱化学)

= 4.1855 J (15 °C)

= 4.1868 J (国際蒸気表)

仕事率　1 PS (仏馬力)

= 75 kgf·m/s

= 735.499 W

放射能	Bq	Ci
	1	2.70270×10^{-11}
	3.7×10^{10}	1

吸収線量	Gy	rad
	1	100
	0.01	1

照射線量	C/kg	R
	1	3876
	2.58×10^{-4}	1

線量当量	Sv	rem
	1	100
	0.01	1

(86年12月26日現在)